



University
of Glasgow

<https://theses.gla.ac.uk/>

Theses Digitisation:

<https://www.gla.ac.uk/myglasgow/research/enlighten/theses/digitisation/>

This is a digitised version of the original print thesis.

Copyright and moral rights for this work are retained by the author

A copy can be downloaded for personal non-commercial research or study,
without prior permission or charge

This work cannot be reproduced or quoted extensively from without first
obtaining permission in writing from the author

The content must not be changed in any way or sold commercially in any
format or medium without the formal permission of the author

When referring to this work, full bibliographic details including the author,
title, awarding institution and date of the thesis must be given

Enlighten: Theses

<https://theses.gla.ac.uk/>
research-enlighten@glasgow.ac.uk

**Effects of allometric growth and toe pad morphology
on adhesion in hylid tree frogs**

Joanna McLellan Smith

Presented in candidature for the degree of Doctor of Philosophy, to the
Institute of Biomedical and Life Sciences, University of Glasgow

September 2003

ProQuest Number: 10753974

All rights reserved

INFORMATION TO ALL USERS

The quality of this reproduction is dependent upon the quality of the copy submitted.

In the unlikely event that the author did not send a complete manuscript and there are missing pages, these will be noted. Also, if material had to be removed, a note will indicate the deletion.



ProQuest 10753974

Published by ProQuest LLC (2018). Copyright of the Dissertation is held by the Author.

All rights reserved.

This work is protected against unauthorized copying under Title 17, United States Code
Microform Edition © ProQuest LLC.

ProQuest LLC.
789 East Eisenhower Parkway
P.O. Box 1346
Ann Arbor, MI 48106 – 1346

GLASGOW
UNIVERSITY
LIBRARY:

13287

COPY 1

Candidates declaration

I declare that the work reported in this thesis has been carried out by myself, unless otherwise acknowledged and that it is of my own composition. No part of this work has been submitted for any other degree.

A handwritten signature in black ink, appearing to read 'Joanna McLellan Smith', with a stylized, cursive script.

Joanna McLellan Smith

September 2003

ACKNOWLEDGEMENTS

Thanks to my family and Dan for maintaining faintly credible levels of interest in sticky frogs and very credible levels of support throughout.

At Glasgow University I would like to thank my supervisors, Jon Barnes, Roger Downie and Graeme Ruxton. Also thanks to everyone else that worked with me, in particular Jen Ward and Beth Mouat who have always had shoulders broad enough for my troubles as well as their own. At the S.E.M. unit, thanks to Laurence Tetley, Eoin Robertson and particularly Margaret Mullin. My frogs would like to thank Maggie Reilly, John Laurie and Graham Adam for looking after them so well when I was away on field work.

For help in the field I owe thanks to all of the members of Glasgow University Expeditions to Trinidad 1999, 2000 and 2001 but in particular Claire Craig, Ann-Marie McMaster, John McQueen, Barry Nicholls (1999); Gary Mason, Christine Oines (2000); Carrie-Ann McCulloch, Rebecca Johnson, James McVeigh (2001) and Dan Thornham (2000 & 2001) all of whom frogged above and beyond the call of duty. Also to Andrew Barnes and the Leeds University Guppers (Beth Arrowsmith, Jon Bielby, Darren Croft, Kirsten Skinner, Liz White) for extra-curricular nocturnal forages into mud for my benefit.

At the University of the West Indies I would like to acknowledge the help and support of the late Peter Bacon, Karen Duhn, Mary Alkins-Koo, and Mike Oatham. For permission to work in and around Simla Research Station thanks to the Asa Wright Nature Centre and in particular to Ronnie Hernandez without whom I may well have ground to a halt some days. Also in Trinidad, special thanks to Ryan Flemming and Tony Dougdeen for keeping me supplied with rum and friendship!

All studies were carried out with funding from N.E.R.C. (Grant no: GT0499TS99) with additional funding for field assistance provided by the Blodwen Llloyd Binns Trust, managed by the Glasgow Natural History Society.

Table of Contents

Candidate's declaration.....	1
Acknowledgements.....	2
Table of contents.....	3
Table of figures.....	7
Summary.....	18
 Chapter 1: Adhesion in the animal kingdom	 22
1.1. Biological adhesion.....	22
1.2. Adhesion in invertebrates.....	29
1.2.1. Adhesion in arthropods	29
1.2.2. Adhesion in cephalopods.....	35
1.2.3. Adhesion in gastropods	38
1.2.4. Adhesion in echinoderms	41
1.2.5. Duo-gland adhesion in various marine invertebrate phyla.....	43
1.3. Adhesion in vertebrates.....	45
1.3.1. Adhesion in fish	45
1.3.2. Adhesion in lizards.....	46
1.3.3. Adhesion in mammals.....	49
1.3.4. Adhesion in amphibians	53
 Chapter 2: Adhesion in adult tree frogs.....	 56
2.1. Introduction.....	56
2.2. Methods.....	65
2.2.1. Experimental animals.....	65
2.2.2. Measurement of sticking ability	67
2.2.3. Calculating adhesive force	70
2.2.4. Statistics	70
2.3. Results.....	71
2.3.1. Morphometric analyses	71
2.3.2. Size Effects on Adhesion	74
2.3.3. Effects of Surface Wettability on Adhesion.....	79
2.4. Discussion	82

Chapter 3: Morphology of adhesive structures in adult tree frogs	91
3.1. Introduction.....	91
3.2. Methods.....	98
3.2.1. Scanning electron microscopy.....	98
3.2.2. Image analyses	98
3.2.4. Statistics	99
3.3. Results.....	100
3.3.1. Toe pad morphology	100
3.2.2. Toe pad cells.....	103
3.3.3. Intercellular channels	108
3.3.4. Mucosal pores	109
3.3.5. Specialised cells on accessory adhesive areas.....	116
3.4. Discussion	120
 Chapter 4: Adhesion in small Hyliid tree frogs.....	 133
4.1. Introduction.....	133
4.2. Methods.....	138
4.2.1. Experimental animals.....	138
4.2.2. Measurement of sticking ability.....	144
4.2.3. Calculating adhesive force	146
4.2.4. Toe pad morphology	146
4.2.5. Statistics	146
4.3. Results.....	147
4.3.1. Morphometric analyses.....	147
4.3.2. Size effects on adhesion.....	153
4.3.3. Toe pad morphology	161
4.3.4. Accessory adhesive areas.....	185
4.3.5. Effects of size on toe pad morphology.....	195
4.3.6. Integrating pad morphology and adhesion.....	199
4.4. Discussion	203

Chapter 5: Adhesion in medium hyliid tree frogs	210
5.1. Introduction.....	210
5.2. Methods.....	212
5.2.1. Experimental animals	212
5.2.2. Measurement of sticking ability	215
5.2.3. Calculating adhesive force.....	217
5.2.4. Toe pad morphology.....	217
5.2.5. Statistics	217
5.3. Results.....	218
5.3.1. Morphometrics.....	218
5.3.2. Size effects on adhesion.....	223
5.3.3. Toe pad morphology.....	233
5.3.4. Accessory adhesive areas	249
5.3.5. Effects of size on toe pad morphology	254
5.3.6. Integrating pad morphology and adhesion	257
5.4. Discussion	260
 Chapter 6: Adhesion in large hyliid frogs.....	 268
6.1. Introduction.....	268
6.2. Methods.....	270
6.2.1. Experimental animals.....	270
6.2.2. Measurement of sticking ability.....	275
6.2.3. Calculating adhesive forces	277
6.2.4. Toe pad morphology	277
6.2.5. Statistics	277
6.3. Results.....	278
6.3.1. Morphometrics.....	278
6.3.2. Size effects on adhesion.....	287
6.3.3. Toe pad morphology	297
6.3.4. Accessory adhesive areas.....	321
6.3.5. Effects of size on toe pad morphology.....	333
6.3.6. Integrating pad morphology and adhesion.....	337
6.4. Discussion	342

Chapter 7: General discussion	352
7.1. Allometry and adhesion	352
7.2. Adhesion and toe pad morphology	359
7.2.1. Cell size	361
7.2.3. Cell shape	370
7.2.3. Pad curvature.....	377
7.2.4. Extra-accessory areas	381
7.3. Adhesion and mucosal properties	387
7.4. Conclusions.....	403
 APPENDICES	 410
APPENDIX 1: Literature values for adhesion forces from a variety of organisms ...	410
APPENDIX 2: Maps of study and collection sites.....	413
APPENDIX 3: Sex effects on adhesion in adult frogs.....	416
APPENDIX 4: Species average slip and detachment angles on different materials..	418
APPENDIX 5: Arboreality and toe pad morphology.....	419
APPENDIX 6: Behavioural observations of juvenile frogs	420
 REFERENCES	 436

Table of Figures

Chapter 2

Figure 2.1: Photograph illustrating presence of meniscus around adherent toe pads in juvenile <i>P. venulosa</i>	57
Figure 2.2: Diagram of rotation equipment used for determination of adhesive abilities of tree frogs.....	68
Figure 2.3: Diagram of geometric elements used in adhesive force calculations.....	70
Figure 2.4 a: Log:log plot of species average weight vs. snout-vent length in adult frogs from twelve hylid species.....	73
Figure 2.4 b: Log:log plot of species average toe pad areas vs. snout-vent length in adult frogs from twelve hylid species.....	73
Figure 2.5 a: Scatter plot of species average values for slip angle vs. snout-vent length in adult frogs from ten hylid species.....	77
Figure 2.5 b: Scatter plot of species average values for detachment angles vs. snout-vent length in adult frogs from twelve hylid species.....	77
Figure 2.5 c: Log:log plot of species average adhesive force vs. snout-vent length in adult frogs from twelve hylid species.....	78
Figure 2.5 d: Scatter plot of species average adhesive force per unit area of toe pad vs. snout-vent length in adult frogs from twelve hylid species.....	78
Figure 2.6: Scatter plot of average angles of detachment in three species on seven substrates according to increasing contact angle of water droplets on their surface.....	81
Figure 2.7: Scatter plot of species average values for theoretical meniscal heights calculated from frogs adhering on Perspex vs. snout-vent length in adults from twelve hylid species.....	88

Chapter 3

Figure 3.1. Diagram of digital morphology in typical adult tree frog.....	94
Figure 3.2 a – l: Scanning electron micrograph (S.E.M.) images of toe pad structure in adult frogs from twelve Hylid species.....	101-102
Figure 3.3: S.E.M. image of cell structure in (a) <i>H. minuta</i> and (b) <i>S. lacteus</i>	103
Figure 3.4: Scatter plot of species average values for toe pad cell area vs. snout-vent length in adult frogs from twelve Hylid species.....	105
Figure 3.5: Scatter plot of species average values for toe pad cell density vs. snout-vent length in adult frogs from twelve Hylid species.....	105
Figure 3.6 a - l: S.E.M. images of toe pad cells in adult frogs from twelve Hylid species.....	106-107

Figure 3.7 a - l: S.E.M. images of mucosal pore structure in adult frogs from twelve Hylid species.....	114-115
Figure 3.8 a - f: S.E.M. images of subarticular tubercle cells in adult frogs from six Hylid species.....	118
Figure 3.9 a - f: S.E.M. images of proximal margin cells in adult frogs from six Hylid species.....	119
Figure 3.10: S.E.M. image illustrating distribution of different cell shapes on the front toe pad of a juvenile <i>Hyla crepitans</i>	121
Figure 3.11: Scatter plot of species average adhesive force per unit area of toe pad vs. average toe pad cell area in adult frogs from twelve Hylid species.....	123
Figure 3.12: Scatter plot of species average adhesive force per unit area of toe pad vs. average cell density in adult frogs from twelve Hylid species.....	123
Figure 3.13: Scatter plot of species average adhesive force per unit area of toe pad vs. average channel density in adult frogs from twelve Hylid species.....	125
Figure 3.14: Photograph illustrating the distribution of mucosal layer along ventral surface of the toe in adult <i>Hyla geographica</i>	129
Figure 3.15: Scatter plot of species average adhesive force per unit area of toe pad vs. average pad elevation score in adult frogs from twelve Hylid species.....	130
 Chapter 4	
Figure 4.1: Photograph of adult male <i>Hyla minuscula</i>	138
Figure 4.2: Photograph of ‘pregnant’ female <i>Flectonotus fitzgeraldi</i>	140
Figure 4.3: Photograph of adult <i>Scinax rubra</i>	141
Figure 4.4: Photograph of adult <i>Hyla punctata</i>	143
Figure 4.5: Log:log plot of weight vs. snout-vent length in juvenile and adult frogs of the small Hylid species, <i>Scinax rubra</i>	149
Figure 4.6: Log:log plot of toe pad area increase vs. snout-vent length in juvenile and adult frogs of the small Hylid species, <i>Scinax rubra</i>	149
Figure 4.7: Log:log plot of weight increase vs. snout-vent length in juvenile and adult frogs of three small Hylid species; <i>H. minuscula</i> , <i>F. fitzgeraldi</i> and <i>H.punctata</i>	152
Figure 4.8: Log:log plot of toe pad area increase vs. snout-vent length in juvenile and adult frogs in three small Hylid species; <i>H. minuscula</i> , <i>F. fitzgeraldi</i> and <i>H. punctata</i>	152
Figure 4.9: Scatter plot of detachment angles on Perspex vs. snout-vent length in juvenile and adult frogs of the small Hylid species, <i>Scinax rubra</i>	155
Figure 4.10: Log:log plot of adhesive forces vs. snout-vent length in juvenile and adult frogs of the small Hylid species, <i>Scinax rubra</i>	155

Figure 4.11: Scatter plot of detachment angles on Perspex vs. SVL in juvenile and adult frogs of three small Hylid species; <i>H. minuscula</i> , <i>F. fitzgeraldi</i> and <i>H. punctata</i>	157
Figure 4.12: Log:log plot of adhesive forces vs. snout-vent length in juvenile and adult frogs of three small Hylid species; <i>Hyla minuscula</i> , <i>Flectonotus fitzgeraldi</i> and <i>Hyla punctata</i> ...	157
Figure 4.13: Scatter plot of adhesive force per unit area of toe pad vs. snout-vent length in juvenile and adult frogs of four small Hylid species; <i>Hyla minuscula</i> , <i>Flectonotus fitzgeraldi</i> , <i>Scinax rubra</i> and <i>Hyla punctata</i>	160
Figure 4.14: Detachment angles in adult frogs from two small species of Hylid frog on seven substrates according to contact angle of water droplets on their surface.....	160
Figure 4.15: S.E.M. image illustrating distribution of different cell shapes on front toe pad of juvenile <i>Scinax rubra</i>	161
Figure 4.16 a - d: S.E.M. images of toe pad cells in juvenile and adult frogs of the small Hylid species, <i>Scinax rubra</i>	162
Figure 4.17 a - d: S.E.M. images of mucosal pore structure in juvenile frogs of the small Hylid species, <i>Scinax rubra</i>	164
Figure 4.18 a - d: S.E.M. images of mucosal pore structure in adult frogs of the small Hylid species, <i>Scinax rubra</i>	165
Figure 4.19 a - f: S.E.M. images of toe pad structure in juvenile and adult frogs of the small Hylid species, <i>Scinax rubra</i>	167
Figure 4.20 a - d: S.E.M. images of circumferal grooves and marginal cells in juvenile and adult frogs of the small Hylid species, <i>Scinax rubra</i>	168
Figure 4.21 a - d: S.E.M. images of proximal margins and sub-marginal cells in juvenile and adult frogs of the small Hylid species, <i>Scinax rubra</i>	169
Figure 4.22 a - b: S.E.M. image illustrating distribution of different cell shapes on front toe pad of juvenile and adult <i>Flectonotus fitzgeraldi</i>	171
Figure 4.23 a - d: S.E.M. images of toe pad cells in juvenile and adult frogs of the small Hylid species, <i>Flectonotus fitzgeraldi</i>	172
Figure 4.24 a - d: S.E.M. images of mucosal pore structure in juvenile and adult frogs of the small Hylid species, <i>Flectonotus fitzgeraldi</i>	174
Figure 4.25 a - f: S.E.M. images of toe pads in juvenile and adult frogs of the small Hylid species, <i>Flectonotus fitzgeraldi</i>	176
Figure 4.26 a - d: S.E.M. images of circumferal grooves and margins in juvenile and adult frogs of the small Hylid species, <i>Flectonotus fitzgeraldi</i>	177
Figure 4.27 a -b: S.E.M. images of proximal marginal areas in juvenile and adult frogs of the small Hylid species, <i>Flectonotus fitzgeraldi</i>	178
Figure 4.28 a - d: S.E.M. images of toe pad cell structure in juvenile and adult frogs of the small Hylid species, <i>Hyla punctata</i>	180

Figure 4.29 a - f: S.E.M. images of mucosal pore structure in juvenile and adult frogs of the small Hylid species, <i>Hyla punctata</i>	181
Figure 4.30 a - d: S.E.M. images of toe pad structure in juvenile and adult frogs of the small Hylid species, <i>Hyla punctata</i>	182
Figure 4.31 a - d: S.E.M. images of circumferal groove and marginal cells in juvenile and adult frogs of the small Hylid species, <i>Hyla punctata</i>	183
Figure 4.32 a - b: S.E.M. images of proximal margin and sub-marginal cells in adult frogs of the small Hylid species, <i>Hyla punctata</i>	183
Figure 4.33 a - d: S.E.M. images of hand and foot morphology in juvenile and adult frogs of the small Hylid species, <i>Scinax rubra</i>	186
Figure 4.34: Diagram of typical hand and foot morphology in adult frogs of the small Hylid species, <i>Scinax rubra</i> . (Duellman, 2001)	186
Figure 4.35 a - d: S.E.M. images of subarticular tubercles in juvenile and adult frogs of the small Hylid species, <i>Scinax rubra</i>	188
Figure 4.36 a - b: S.E.M. images of inner metatarsal tubercle in juvenile frogs of the small Hylid species, <i>Scinax rubra</i>	188
Figure 4.37 a - d: S.E.M. images of hand and foot morphology in juvenile and adult frogs of the small Hylid species, <i>Flectonotus fitzgeraldi</i>	189
Figure 4.38 a - b: S.E.M. images of subarticular tubercles in adult frogs of the small Hylid species, <i>Flectonotus fitzgeraldi</i>	191
Figure 4.39 a - b: S.E.M. images of supernumerary tubercles in adult frogs of the small Hylid species, <i>Flectonotus fitzgeraldi</i>	191
Figure 4.40 a - b: S.E.M. images of inner metatarsal tubercle in adult frogs of the small Hylid species, <i>Flectonotus fitzgeraldi</i>	191
Figure 4.41 a - d: S.E.M. images of hand and foot morphology in juvenile and adult frogs of the small Hylid species, <i>Hyla punctata</i>	192
Figure 4.42 a - d: S.E.M. images of subarticular tubercles in juvenile and adult frogs of the small Hylid species, <i>Hyla punctata</i>	194
Figure 4.43: S.E.M. images of supernumerary tubercles in juvenile frogs of the small Hylid species, <i>Hyla punctata</i>	194
Figure 4.44: Scatter plot of average mucosal pore densities vs. snout-vent length in juvenile and adult frogs from four small Hylid species: <i>Flectonotus fitzgeraldi</i> , <i>Hyla minuscula</i> , <i>Scinax rubra</i> and <i>Hyla punctata</i>	198
Figure 4.45: Scatter plot of subarticular tubercle cell size vs. snout-vent length in juvenile and adult frogs from four small Hylid species: <i>Flectonotus fitzgeraldi</i> , <i>Hyla minuscula</i> , <i>Scinax rubra</i> and <i>Hyla punctata</i>	198

Figure 4.46: Scatter plot of adhesive force per mm ² vs. cell densities on toe pad in juvenile and adults from four small Hylid species; <i>Flectonotus fitzgeraldi</i> , <i>Hyla minuscula</i> , <i>Scinax rubra</i> and <i>Hyla punctata</i>	202
Figure 4.47: Scatter plot of adhesive force per unit area vs. pore densities in juvenile and adults from four small Hylid species; <i>Flectonotus fitzgeraldi</i> , <i>Hyla minuscula</i> , <i>Scinax rubra</i> and <i>Hyla punctata</i>	202

Chapter 5

Figure 5.1: Photographs of dorsal and ventral views of an adult male of the medium Hylid species, <i>Hyla geographica</i>	212
Figure 5.3: Photographs of juvenile and adult frogs of the medium Hylid species, <i>Hyla crepitans</i>	214
Figure 5.3: Photograph of the abdominal skin of an adult <i>Hyla geographica</i>	216
Figure 5.4: Log:log plot of weight vs. snout-vent length in juvenile and adult frogs from the medium Hylid species, <i>Hyla geographica</i>	219
Figure 5.5: Log:log plot of toe pad area vs. snout-vent length in juvenile and adult frogs of the medium Hylid species, <i>Hyla geographica</i>	219
Figure 5.6: Log:log plot of weight vs. snout-vent length in juvenile and adult frogs of the medium Hylid species, <i>Hyla crepitans</i>	222
Figure 5.7: Log:log plot of toe pad area vs. snout-vent length in juvenile and adult frogs of the medium Hylid species, <i>Hyla crepitans</i>	222
Figure 5.8: Scatter plot of detachment angles on Perspex vs. snout-vent length in juvenile and adult frogs of the medium Hylid species, <i>Hyla geographica</i>	225
Figure 5.9: Log:log plot of adhesive force vs. snout-vent length in juvenile and adult frogs of the medium Hylid species, <i>Hyla geographica</i>	225
Figure 5.10: Average detachment angles and 95% c.i. error bars for monthly age cohorts of the medium Hylid species, <i>Hyla crepitans</i>	226
Figure 5.11: Scatter plot of detachment angles on Perspex vs. snout-vent length in juvenile and adult frogs of the medium Hylid species, <i>Hyla crepitans</i>	227
Figure 5.12 a - b: Log:log plots of adhesive force vs. snout-vent length in juvenile and adult frogs of the medium Hylid species, <i>Hyla crepitans</i> : (regression lines calculated for populations both with and without outliers)	228
Figure 5.13: Scatter plot of adhesive force per unit area of toe pad vs. snout-vent length in juvenile and adult frogs of two medium Hylid species, <i>Hyla geographica</i> and <i>Hyla crepitans</i>	232

Figure 5.14: Detachment angles in on seven substrates according to contact angle of water droplets on their surface of adult frogs belonging to two medium-sized species of Hylid; <i>Hyla geographica</i> and <i>Hyla crepitans</i>	232
Figure 5.15 a – d: S.E.M. images of toe pad cells in juvenile and adult frogs of the medium Hylid species, <i>Hyla geographica</i>	233
Figure 5.16 a – f: S.E.M. images of mucosal pore structure in juvenile and adult frogs of the medium Hylid species, <i>Hyla geographica</i>	236
Figure 5.17 a - f: S.E.M. images of toe pad morphology in juvenile and adult frogs of the medium Hylid species, <i>Hyla geographica</i>	238
Figure 5.18 a - b: S.E.M. images of cells on proximal margin of the pad in juvenile and adult frogs of the medium Hylid species, <i>Hyla geographica</i>	239
Figure 5.19 a – b: S.E.M. images of toe pad cells in juvenile and adult frogs of the medium Hylid species, <i>Hyla crepitans</i>	241
Figure 5.20 a – f: S.E.M. images of toe pad cells in juvenile and adult frogs of the medium Hylid species, <i>Hyla crepitans</i>	242
Figure 5.21 a - f: S.E.M. images of mucosal pore structures toe pad cells in juvenile and adult frogs of the medium Hylid species, <i>Hyla crepitans</i>	244
Figure 5.22 a – d: S.E.M. images of toe pad structure in juvenile and adult frogs of the medium Hylid species, <i>Hyla crepitans</i>	246
Figure 5.23: S.E.M. images of circumferal margin cells n adult <i>Hyla crepitans</i>	247
Figure 5.24 a - b: S.E.M. images of circumferal grooves and margins in juvenile and adult frogs of the medium Hylid species, <i>Hyla crepitans</i>	248
Figure 5.25 a – d: S.E.M. images of proximal margin in juvenile and adult frogs of the medium Hylid species, <i>Hyla crepitans</i>	248
Figure 5.26 a – b: S.E.M. images of hand and foot morphology in juvenile frogs of the medium Hylid species, <i>Hyla geographica</i>	249
Figure 5.27 a – d: S.E.M. images of subarticular tubercles in juvenile and adult frogs of the medium Hylid species, <i>Hyla geographica</i>	250
Figure 5.28: S.E.M. images of hand and foot morphology in juvenile frogs of the medium Hylid species, <i>Hyla crepitans</i>	252
Figure 5.29: Diagram of hand and foot morphology in adult <i>Hyla crepitans</i>	252
Figure 5.30 a – d: S.E.M. images of subarticular tubercles in juvenile and adult frogs of the medium Hylid species, <i>Hyla crepitans</i>	253
Figure 5.31 a - b: S.E.M. images of inner metatarsal tubercle in adult frogs of the medium Hylid species, <i>Hyla crepitans</i>	253
Figure 5.32: Scatter plot of average mucosal pore size vs. snout-vent length in juvenile and adult frogs of the two medium Hylid species: <i>Hyla geographica</i> and <i>Hyla crepitans</i>	256

Figure 5.33: Scatter plot of average lateral groove score vs. snout-vent length in juvenile and adult frogs of two medium Hylid species: <i>Hyla geographica</i> and <i>Hyla crepitans</i>	256
Figure 5.34: Scatter plot of average lateral groove score vs. adhesive force per mm ² of toe pad in juvenile and adult frogs belonging to two medium-sized species of Hylid: <i>Hyla geographica</i> and <i>Hyla crepitans</i>	258

Chapter 6

Figure 6.1: Photograph of adult male <i>Phrynohyas venulosa</i>	270
Figure 6.2: Photograph of amplexant pair of <i>Phyllomedusa trinitatis</i>	272
Figure 6.3: Photograph of adult male <i>Hyla boans</i>	273
Figure 6.4: Log:log plot of weight vs. snout-vent length in juvenile and adult frogs of the large Hylid species, <i>Phrynohyas venulosa</i>	280
Figure 6.5: Log:log plot of toe pad area vs. snout-vent length in juvenile and adult frogs of the large Hylid species, <i>Phrynohyas venulosa</i>	280
Figure 6.6 a: Log:log plots of weight vs. snout-vent length in juvenile and adult frogs of the large Hylid species, <i>Phyllomedusa trinitatis</i>	282
Figure 6.6 b: Log:log plots of weight vs. snout-vent length in adult male and adult female frogs of the large Hylid species, <i>Phyllomedusa trinitatis</i>	282
Figure 6.7: Log:log plot of toe pad area vs. snout-vent length in juvenile and adult frogs of the large Hylid species, <i>Phyllomedusa trinitatis</i>	284
Figure 6.8: Log:log plot of weight vs. snout-vent length in juvenile and adult frogs of the large Hylid species, <i>Hyla boans</i>	286
Figure 6.9: Log:log plot of toe pad area vs. snout-vent length in juvenile and adult frogs of the large Hylid species, <i>Hyla boans</i>	286
Figure 6.10: Scatter plot of detachment angles on Perspex vs. snout-vent length in juvenile and adult frogs of the large Hylid species, <i>Phrynohyas venulosa</i>	288
Figure 6.11: Log:log plot of adhesive force vs. snout-vent length in juvenile and adult frogs of the large Hylid species, <i>Phrynohyas venulosa</i>	288
Figure 6.12: Scatter plot of detachment angles on Perspex vs. snout-vent length in juvenile and adult frogs of the large Hylid species, <i>Phyllomedusa trinitatis</i>	291
Figure 6.13: Log:log plot of adhesive force vs. snout-vent length in juvenile and adult frogs of the large Hylid species, <i>Phyllomedusa trinitatis</i>	291
Figure 6.14: Scatter plot of detachment angles on Perspex vs. snout-vent length in juvenile and adult frogs of the large Hylid species, <i>Hyla boans</i>	293
Figure 6.15: Log:log plot of adhesive force vs. snout-vent length in juvenile and adult frogs of the large Hylid species, <i>Hyla boans</i>	293

Figure 6.16: Scatter plot of adhesive force per unit area of toe pad vs. snout-vent length in juvenile and adult frogs of three large Hyloid species: <i>Phrynohyas venulosa</i> ; <i>Phyllomedusa trinitatis</i> and <i>Hyla boans</i>	296
Figure 6.17: Scatter plot of average detachment angles recorded from adult frogs belonging to three large species of hyloid frog on seven substrates of differing wettability (as defined by the contact angle of water droplet).	296
Figure 6.18: S.E.M. images of toe pad cell structure in juvenile <i>Phrynohyas venulosa</i>	297
Figure 6.19: S.E.M. images of toe pad cells in juvenile and adult frogs of the large Hyloid species, <i>Phrynohyas venulosa</i>	298
Figure 6.20 a - d: S.E.M. images of mucosal pores in juvenile frogs of the large Hyloid species, <i>Phrynohyas venulosa</i>	299
Figure 6.21 a - d: S.E.M. images of mucosal pores in adult frogs of the large Hyloid species, <i>Phrynohyas venulosa</i>	300
Figure 6.22 a - f: S.E.M. images of toe pad structure in juvenile and adult frogs of the large Hyloid species, <i>Phrynohyas venulosa</i>	302
Figure 6.23: S.E.M. images of groove on toe pad in adult <i>Phrynohyas venulosa</i>	303
Figure 6.24 a – d: S.E.M. images of circumferal grooves and marginal cells in juvenile and adult frogs of the large Hyloid species, <i>Phrynohyas venulosa</i>	304
Figure 6.25 a - d: S.E.M. images of proximal margins in juvenile and adult frogs of the large Hyloid species, <i>Phrynohyas venulosa</i>	306
Figure 6.26 a - b: S.E.M. images of cells along mid line of ventral surface of toe in adult <i>Phrynohyas venulosa</i>	306
Figure 6.27 a - d: S.E.M. images of toe pad cells in juvenile and adult frogs of the large Hyloid species, <i>Phyllomedusa trinitatis</i>	307
Figure 6.28 a – f: S.E.M. images of mucosal pore structure in juvenile frogs of the large Hyloid species, <i>Phyllomedusa trinitatis</i>	310
Figure 6.29 a - d: S.E.M. images of mucosal pore structure in juvenile and adult frogs of the large Hyloid species, <i>Phyllomedusa trinitatis</i>	311
Figure 6.30 a - d: S.E.M. images of toe pad structure in juvenile and adult frogs of the large Hyloid species, <i>Phyllomedusa trinitatis</i>	312
Figure 6.31 a - b: S.E.M. images of circumferal marginal areas in juvenile and adult frogs of the large Hyloid species, <i>Phyllomedusa trinitatis</i>	314
Figure 6.32 a - d: S.E.M. images of proximal margins and sub-marginal cells in juvenile and adult frogs of the large Hyloid species, <i>Phyllomedusa trinitatis</i>	314
Figure 6.33: S.E.M. image of ventral surface and lateral margins of the toe in adult <i>Phyllomedusa trinitatis</i>	315

Figure 6.34 a - b: S.E.M. images of cells on ventral surface of the toe in juvenile and adult frogs of the large Hyliid species, <i>Phyllomedusa trinitatis</i> .	315
Figure 6.35: S.E.M. image of toe pad cells in juvenile <i>Hyla boans</i> .	316
Figure 6.36 a - d: S.E.M. images of toe pad cells in juvenile and adult frogs of the large Hyliid species, <i>Hyla boans</i> .	317
Figure 6.37 a - b: S.E.M. images of mucosal pore structure in adult frogs of the large Hyliid species, <i>Hyla boans</i> .	317
Figure 6.38 a - d: S.E.M. images of toe pad structure in juvenile and adult frogs of the large Hyliid species, <i>Hyla boans</i> .	320
Figure 6.39 a: S.E.M. image of proximal margin in adult <i>Hyla boans</i>	320
Figure 6.39 b: S.E.M. image of dimples in pad in adult <i>H. boans</i> .	320
Figure 6.40: S.E.M. images of hand and foot morphology in juvenile <i>P. venulosa</i> .	322
Figure 6.41: Diagram of typical hand and foot morphology in adult <i>P. venulosa</i> .	322
Figure 6.42: S.E.M. image of cells on the inner metatarsal in juvenile <i>P. venulosa</i> .	323
Figure 6.43 a - d: S.E.M. images of distal subarticular tubercles in juvenile and adult frogs of the large Hyliid species, <i>Phrynohyas venulosa</i> .	324
Figure 6.44 a - b: S.E.M. images of proximal subarticular tubercle in adult <i>Phrynohyas venulosa</i> .	324
Figure 6.45: S.E.M. images of hand and foot morphology in juvenile <i>P. trinitatis</i> .	326
Figure 6.46: Diagram of typical hand and foot morphology in the closely related Phyllomedusine species, <i>P. venusta</i> .	326
Figure 6.47 a - f: S.E.M. images of subarticular tubercles in juvenile and adult frogs of the large Hyliid species, <i>Phyllomedusa trinitatis</i> .	327
Figure 6.48 a - d: S.E.M. images of supernumerary tubercles in juvenile and adult frogs of the large Hyliid species, <i>Phyllomedusa trinitatis</i> .	329
Figure 6.49 a - b: S.E.M. images of prepollex in adult <i>Phyllomedusa trinitatis</i> .	329
Figure 6.50: S.E.M. images of hand and foot morphology in juvenile <i>Hyla boans</i> .	331
Figure 6.51: Diagram of typical hand and foot morphology in adult <i>Hyla boans</i> .	331
Figure 6.52 a - b: S.E.M. images of subarticular tubercles in juvenile <i>Hyla boans</i> .	332
Figure 6.53 a - b: S.E.M. images of subarticular tubercles in adult <i>Hyla boans</i> .	332
Figure 6.54: Scatter plot of average mucosal pore size vs. snout-vent length in juvenile and adult frogs of three large Hyliid species: <i>Phrynohyas venulosa</i> , <i>Phyllomedusa trinitatis</i> and <i>Hyla boans</i> .	336
Figure 6.55: Scatter plot of average lateral groove score vs. snout-vent length in juvenile and adult frogs of three large Hyliid species: <i>Phrynohyas venulosa</i> , <i>Phyllomedusa trinitatis</i> and <i>Hyla boan</i> .	336

Figure 6.56: Scatter plot of force per unit area vs. average mucosal pore size in juvenile and adult frogs of three large Hyliid species: <i>P. venulosa</i> , <i>P. trinitatis</i> and <i>H. boans</i>	339
Figure 6.57: Scatter plot of force per unit area vs. average lateral groove score in juvenile and adult frogs of three large Hyliid species: <i>P. venulosa</i> , <i>P. trinitatis</i> and <i>H. boans</i>	340
Figure 6.58: Scatter plot of force per unit area vs. circumferal groove score in juvenile and adult frogs of three large Hyliid species: <i>P. venulosa</i> ; <i>P.trinitatis</i> and <i>Hyla boans</i>	341

Chapter 7

Figure 7.1: Scatter plot of slopes of lines of best fit in log:log relationships between SVL and weight increase relative to the linear dimension in six hylid species.....	357
Figure 7.2: : Scatter plot of slopes of lines of best fit in log:log relationships between SVL and weight increase relative to the tibia to snout-vent length ratios in six hylid species.....	357
Figure 7.3: Bar chart illustrating trends in average cell size in hylid species according to haploid number.....	365
Figure 7.4: (a) Slip angles and (b) Detachment angles vs. average cell size in adult Hylids sampled for S.E.M. analysis belonging to three size classes.....	368
Figure 7.5: Bar chart of average cell areas from adult frogs sampled from twelve species of Trinidadian Hyliid according to degrees of arboreality.....	369
Figure 7.6: S.E.M. images of hexagonal cells on the adhesive pads of (a) the green bush cricket, <i>T.viridissima</i> (b) the Hyliid tree frog, <i>P.trinitatis</i>	370
Figure 7.7: S.E.M. images of epidermal cells on the (a) stomach and (b) thighs of juvenile <i>F. fitzgeraldi</i>	371
Figure 7.8: Images illustrating the hexagonal elements found in (a) bee honeycomb (b) the compound eye of an ant (c) the human retina.....	372
Figure 7.9: S.E.M. showing irregularly shaped cells on the compound eye of an ant.....	373
Figure 7.10: Patterns in distribution of cells across (a) the human retina and on (b) the toe pad of <i>H.crepitans</i>	375
Figure 7.11: Bar chart illustrating trends in average pad elevation in adult frogs belonging to twelve species of Trinidadian Hyliid according to special degrees of arboreality.	377
Figure 7.12: Scatter plot of average pad elevation scores in juvenile and adult frogs belonging to twelve species of Hyliid vs. snout-vent length.	380
Figure 7.13: Scatter plot of average values for angle of slip on Perspex vs. score for pad elevation in adults from ten species of Hyliid frog.....	380
Figure 7.14: S.E.M. images of Subarticular tubercle cells in (a) Adult <i>H. punctata</i> (b) Adult <i>H. crepitans</i> . (c) Juvenile <i>P. venulosa</i> (d) Adult <i>P. venulosa</i>	382
Figure 7.15: Cells on the circumferal groove in (a) Juvenile <i>S. rubra</i> (b) Adult <i>H.crepitans</i> . (c) Juvenile <i>H. punctata</i> . (d) Adult <i>F. fitzgeraldi</i>	383

Figure 7.16: Photograph of adhering toe pads of adult <i>O. septentrionalis</i> adhering to Perspex oriented at 90° with water, (stained with vegetable dye), flowing over the surface at a rate of 150ml min ⁻¹ .	385
Figure 7.17: S.E.M. images of ventral epidermis cells of <i>H. arborea</i>	386
Figure 7.18: Scatter plot illustrating the relationship between theoretical values for h and the effect on capillary adhesion and Stefan adhesion.	390
Figure 7.19: Log:log plot of theoretical forces produced by different models of adhesion for a range of meniscal heights assuming mucosal properties similar to water.	390
Figure 7.20: Scatter plot of frictional coefficients vs. SVL in ten species of hylid from three size classes.	394
Figure 7.21: Scatter plot of frictional coefficient calculated from angles recorded from <i>S.lacteus</i> on seven different substrates of differing wettability.	394
Figure 7.22 S.E.M. images showing bacterial clusters around the (a) mucous pores and (b) intercellular channels on the toe pads of two juvenile <i>Hyla crepitans</i> .	398
Figure 7.23 Cell apices of <i>Litoria caerulea</i> in close contact at (a) beginning and (b) end of hour long interference microscopy experiment.	401

Appendices

Figure A2.1: Collection sites in Northern range.	414
Figure A2.2: Collection and study sites on Southwest Peninsula.	415
Figure A2.3: Collection site on east coast.	416
Figure A5.1: Box plots illustrating medians and upper and lower ranges in toe pad cell size according to degree of arboreality in Trinidadian Hylids.	424
Figure A5.2: Box plots illustrating medians and upper and lower ranges in cell densities on toe pads according to degree of arboreality in Trinidadian Hylids.	424
Figure A5.3: Box plots illustrating medians and upper and lower ranges in channel densities on toe pads according to degree of arboreality in Trinidadian Hylids.	424
Figure A6.1: Bar charts illustrating distribution of activity observations of juvenile frogs from three different species of hylid according to their orientation from the horizontal.	428
Figure A6.2: Percentage of sleeping frogs found on various substrata in (a) <i>H.crepitans</i> (b) <i>H. geographica</i> (c) <i>P. trinitatis</i> .	429
Figure A6.3: Degree of orientation from horizontal of sleeping juvenile <i>H.crepitans</i> on leaf surfaces relative to increasing temperature.	433
Figure A6.4: Daytime temperatures vs. humidity in enclosures in Glasgow and Trinidad.	435
Figure A6.5: Temperature effects on average perch heights in groups of <i>H. geographica</i> and <i>H. crepitans</i> within enclosures in Glasgow and Trinidad.	436

Summary

Many species of arboreal frog, over a wide range of taxa, possess specialised expanded digital pads which are remarkable similar in structure. It has long been accepted that the function for which these toe pads have evolved is to facilitate the ability seen in 'tree frogs' to adhere to smooth, vertical surfaces. Recent consensus is that tree frogs adhere through wet adhesion, with the forces produced by this mechanism scaling directly with pad area. If frogs are geometrically similar and scale following isometric predictions, with weight increasing with the linear dimension cubed and toe pad area with the linear dimension squared, then the problem arises as to how an area dependent adhesive mechanism is able to cope with the pressures of increasing size?

Adhesive forces recorded in adult frogs from twelve species of Trinidadian hylid support earlier studies, scaling directly with toe pad area. Weight increases at a lesser rate than that expected through isometry, but not sufficiently to be matched by toe pad area, which increases as the linear dimension squared. The ability to adhere is thus affected so that large species are not able as small species to maintain angles significantly beyond the vertical on smooth surfaces. Nevertheless, force per unit area increases with the linear dimension, suggesting that the pads of larger species are able to adhere more efficiently. Toe pad morphology and epidermal structure are roughly similar but there are small interspecific differences; particularly in the delineation of grooves separating the pad from the ventral surface of the toe and in cell size, which have significant effects on the adhesive efficiency of the pad. In large species there is

an extension in the distribution of specialised pad cells to include subarticular tubercles, perhaps increasing the area available for wet adhesion.

The increase in size in the period of growth from metamorphosis to adulthood is substantial for most species of frog. With similar metamorphic sizes in all species in this study, the degree to which growth will put pressure on the adhesive mechanism was dependent on the adult size and so species were considered separately according to their eventual size:

In four small-sized species of hylid, there is a lowered rate of weight increase to that expected with isometric growth, though the degree to which this is the case is not sufficient to be matched by the equivalent increase in pad area, which increases with the linear dimension squared. There is, nevertheless, a greater increase in adhesive force with growth than can be explained by the equivalent increase in toe pad area and adhesive ability is not affected by growth, with no significant differences in detachment angles recorded in adults and juveniles. Furthermore, all four small species show an improvement in toe pad efficiency as adults. There are changes in pad morphology that might be expected to facilitate in this; particularly significant being the inverse correlation between the reduced pore density seen in larger frogs and increasing adhesive force.

In two medium-sized species of hylid, there is evidence of a greater increase in adhesive force than can be explained by toe pad area, which scales as expected through isometry. In both the rate of weight increase is reduced; in the smaller species, *Hyla geographica*, the extent to which this is the case is sufficient for the

equivalent toe pad area to match so that adults are as able as juveniles to adhere to smooth surfaces at orientations beyond the vertical. This is not the case in the larger *Hyla crepitans*, where adults detach from smooth surfaces at a lower angle than do juveniles. There are few demonstrable correlative relationships between aspects of pad morphology and adhesion in *H. geographica*. In *H. crepitans* there is some evidence of an increase in adhesive force with the delineation of the grooves that run down the lateral margins of the toe. There is also evidence of changes in the structure of the cells on the subarticular tubercles that suggests that the function of these structures has altered in adults, perhaps increasing the area available for wet adhesion.

The three large species of tree frog found in Trinidad are from two separate subfamilies within the Hylidae, the Hylinae and the Phyllomedusinae. All three species show a reduced rate of weight gain to the expected. All show trends towards a greater rate of increase in pad area than expected through isometry but *Phyllomedusa trinitatis* is the only species in which this trend is significant. This species, is the only one of the large species of Trinidadian hylid in which adhesion is able to cope with the increase in size between metamorphosis and maturation so that adults are as able to adhere to smooth surfaces as are juveniles. Alterations in growth rates seen in the other two large species are not sufficient for the adhesive mechanism to compensate, leading to the significant decrease in the average detachment angles attained by adult frogs on smooth substrates. This is in spite of tendencies seen in all three large species towards increased pad efficiency in adult frogs, related to changes in pad cell size and other aspects of toe pad morphology seen in smaller size classes.

Overall, this study suggests that the area dependent adhesive mechanism used by tree frogs is able to cope to varying degrees to the pressures of changing size with growth, through a combination of alterations to allometry and morphology seen between small and large frogs. The changes in pad morphology and the extent to differences in growth patterns vary according to the adult size of the frogs. This study has also demonstrated links between toe pad morphology and adhesive ability that have not been taken into account in previous studies. However, as certain morphological characteristics also differ according to ecological considerations it is important for future studies that the specific influence of features such as cell size and shape, mucosal pore density and subarticular tubercles on adhesive abilities are better understood.

Chapter 1: Adhesion in the animal kingdom

1.1. Biological adhesion

Animals that live in habitats in which their risk of dislodgement from their positions is enhanced by the actions of the external environment have evolved a variety of ingenious mechanisms to counteract the adverse effects that these external influences may exert. Marine organisms and torrential fauna, subject to continual exposure to the actions of waves and water currents, and arboreal animals, subject to sudden and prolonged winds, show a particular prevalence in the development of adhesion promoting strategies. Many of the animals that inhabit these environments have evolved highly specialised organs of attachment to maintain a hold upon substrates, which has allowed them to expand their range into habitat that may otherwise be inaccessible. Specialised structures promoting increased adhesion have also evolved separately to fulfil other functions: for prey capture and handling, such as the suctorial tongue pad in the chameleons (Herrel *et al.* 2000) and the maxillar setae in malachiid beetles (Stork, 1983b); in reproduction, the males of many species of fly (Walker *et al.* 1985), beetle (Stork, 1980a) and frog (Kurabuchi 1993, 1994) have developed adhesion promoting structures which allow a maintained hold upon the female during mating; as anti-predator devices, such as the Cuvierian tubules of Holothuroid echinoderms (Flammang *et al.* 2002) and for brood protection, one peculiar example of which is the hook seen on the forehead of the nursery fish, *Kurtus gulliveri*, which is covered in adhesive epithelium which holds egg masses in place (Berra and Humphrey, 2002). Although the parameters of this study are most concerned with the use of adhesion in the maintenance of a hold upon substrates

within the animals' environment, many of the structures that promote attachment and locomotion are multifunctional and this is of some importance when considering the evolution of the functional morphology of adhesive organs. The solutions seen within animals responding to environmental pressures that induce this need for sticking abilities confer levels of attachment to substrates that can be considered in three broad categories: permanent attachment, temporary attachment and dynamic attachment (*sensu* Alberch, 1981).

Permanent attachment to a substrate usually results from the production, in specialised 'cement' glands, of a gluing secretion that anchors the animal permanently to a substrate, such as is seen in barnacles (Denny, 1993), or by surface replication at a microscopic scale, seen in protruding cellular elements produced by the eggs of many teleost fish (Scherge and Gorb, 2001). The advantages to the animal of utilising this type of attachment relies on the immovability of the substrate upon which the animal has chosen to settle and therefore can often present a risky strategy. If the substrate itself is dislodged or the environment altered so that, for example, the sea no longer inundates a rock, then the attached organism may find itself exposed to increased predation risk or an inability to feed. Temporary attachment mechanisms, such as seen in many species of echinoderm (Flammang *et al.* 1994) and in sea anemones (Davenport and Thorsteinsson, 1990), solve this problem to some extent, allowing organisms to adhere strongly to a substrate but detach quickly when necessary. This means that the animal has some degree of flexibility should its settlement site alter in some way that will detrimentally affect its survival. Dynamic attachment increases this degree of flexibility by permitting simultaneous attachment and movement along a substrate (Scherge and Gorb, 2001) but this greater degree of

flexibility may come at an increased cost to the animal's ability to maintain a hold upon a substrate; the tenacity of a motile limpet is significantly reduced from the maximal tenacity when stationary (Miller, 1974; Smith, 1991).

Dynamic attachment requires a more complex solution to the problems of counteracting dislodgement effects than is seen in the other two forms of adhesive response. Many of the organisms that employ adhesive mechanisms that allow a degree of dynamic attachment also exhibit some use of temporary attachment; in the previous example of limpets, there is some evidence that there are changes in the chemical composition of the pedal mucus in motile and stationary limpets and winkles (Smith *et al.* 1999; Smith and Morin, 2002) and that there is a graduated response in behaviour according to the degree of wave exposure that the limpet is exposed to (Denny *et al.*, 2000). There is also a degree of flexibility evident within the system in response to the degree of threat that dislodgement will present under different conditions. Ellem *et al.* (2002) found significant differences in the adhesive strength promoted by 'clamping' behaviour in limpets responding to wave action when compared to those being attacked by a 'predator' that reflects a degree of flexibility within the adhesive system under natural conditions. Additionally, where there is a multipurpose function of the adhesive organs, such as is the case in many species of echinoderm and cephalopod, this will require that there is adaptability inherent in the design of the mechanism that will facilitate adhesion whilst not detrimentally affecting any other function that the organ fulfils. This makes it difficult to attribute the adhesive abilities of an organism to any one mechanism, as there is usually some degree of mixed response to the challenges of the environment involved in the evolution of adhesion in that animal, though in most organisms exhibiting

adhesive abilities there is one mechanism that predominates. Both temporary and dynamic attachment in biological adhesion are based on a variety of mechanisms, with the most common utilising forces produced by intermolecular adhesion, mechanical interlocking, friction, suction and wet adhesion (Alberch, 1981).

Intermolecular adhesion occurs when two closely contiguous surfaces are closely juxtaposed at a sufficiently small distance that Van der Waal's forces are induced between the atoms and molecules of the two contacting materials (Nachtigall, 1974). These forces can be extremely strong and limited only by the breaking strain of the structures of the adhesive organs that are involved in their production (Autumn *et al.* 2000; Dai *et al.* 2002). Their effectiveness is, however limited to a very narrow range, only being significantly operational over very short distances, with the strength of the forces produced by intermolecular forces being directly related to the inverse seventh power of the distance between the two adherent surfaces (Baier *et al.* 1968). The implications of this are that it is a difficult mechanism for animals to utilise, as it requires the extremely close conformation of adhesive structures to substrates within the environment. Very few surfaces present the idealised, uncontaminated planar smoothness that will maximise the forces produced by this mechanism (Baier, *et al.* 1968). Even the presence of a monolayer of water may impede the setting up of intermolecular forces between substrate and attachment structures in organisms utilising this mode of adhesion (Denny, 1993).

In practice, many natural surfaces have irregularities that will lead to a reduction in the total area of contact between the attachment structure and the substrate and which will not allow the degree of conformation to the surface that is required for functional

intermolecular forces to be initiated. In many circumstances, organisms have adapted to take advantage of these surface asperities by developing structures that maximise frictional forces when they come into contact with a rough substrate. These frictional forces measured, for example, in beetles walking across sandpaper are particularly high when surface asperities measure between 12 – 50 μm in diameter but become limiting when the animal walks across smooth surfaces without surface asperities (Dai *et al.* 2002). Frictional forces depend on normal forces holding the adherent surfaces together. These are provided in biological systems by the action of gravity upon the weight of the animal, and thus tend to be negative at surfaces oriented beyond 90° so that friction has a limited functionality where animals find themselves upon smooth and vertical surfaces (Riskin and Fenton, 2001). Animals that depend on frictional forces as they walk upon inclined surfaces often utilise other mechanisms to supplement adhesion on vertical surfaces, usually interlocking mechanisms which, like frictional mechanisms, are highly dependent on surface roughness but, unlike frictional mechanisms, do not require a force normal to the surface in order to function. These forces are usually limited by the mechanical breaking strain of the structures, most commonly claws, that allow this interlocking. Claws were long thought to have only a minimal contribution to the total adhesive forces that an animal is able to produce (Cartmill, 1985), but recent work in insects show that the forces produced when the claws are in use can represent a significant percentage of the attachment forces recorded in beetles (Dai *et al.* 2002) and in aphids walking on rough substrates (Lees and Hardie, 1988).

In the aphids, the adhesive mechanism being supplemented by interlocking with claws is not a friction-dependent system but one dependent on wet adhesion. This

type of adhesion occurs when two contiguous substrates are held together by an intervening liquid layer (Nachtigall, 1974) and is capable of producing powerful adhesive forces; Budgett (1911) demonstrated that two smooth polished discs of only an inch in diameter held together by thin layers of various liquids required over 20 N of force to separate them. There are two main modes of wet adhesion; Stefan adhesion and capillarity. These are discussed in further detail in following chapters, but the features common to both are the dependence on the surface area of contact between the two substrates (Emerson and Diehl, 1980). The two types are defined by differences in the influence of properties of the intervening liquid layer to the adhesive forces produced. Stefan adhesion forces are highly dependent on the viscosity of the intervening fluid, while capillarity is dependent on surface tension. The definition of the edges of the contact area gives a clue to the type of wet adhesion that is being utilised in that Stefan adhesion occurs when the liquid is present both outside and inside the adhesive joint, whilst capillarity is restricted to instances where the intervening liquid is not present outside the joint. Adhesive structures that implement capillarity often have morphological elements that allow the containment of the meniscus to an area below the adhesive organ, such as the t-shaped bones seen at the terminal ends of the phalanges in arboreal salamanders (see **1.3.4**).

In neither type of wet adhesion is muscular exertion necessary to implement the adhesive process, with the efficacy of the system being chiefly dependent on the tendencies of a fluid layer to wet the two adherent surfaces. When adhesion utilising a liquid layer is combined with muscular exertion that acts to increase the volume of a sealed system below an attachment structure, the resultant decrease in the pressure beneath the adhesive organ allows the animal to adhere to a substrate by suction. This

mode of adhesion is particularly prevalent in marine organisms (Davenport and Thorsteinsson, 1990), due chiefly to differences in the cohesive properties of air and water. As water is highly cohesive, relatively small increases in the volume of the sealed vacuum below a water-filled sucker will produce decreases in pressure that if produced within an air-filled sucker would require a substantially greater increase in the volume beneath the sucker (Kier and Smith, 1990). Thus animals operating suctorial adhesion out of the water require a far greater degree of muscular exertion for an equivalent adhesive force to that seen in aquatic animals, and this may explain the fact that animals that utilise this form of adhesion in non-aquatic conditions usually supplement suction with additional mechanisms, such as interlocking with claws (bats) or wet adhesion (salamanders).

Although the scope of this particular study is primarily concerned with the mode of adhesion that is utilised by arboreal frogs (**Chapter 2**), it is important to compare the solutions seen within tree frogs in response to the threat that dislodgement presents, with those of other organisms faced with similar challenges in their environment, in order to understand fully the implications and reasons for the mode of adhesion utilised in tree frogs. As tree frogs do not show any form of permanent attachment to surfaces, the consideration of adhesion in other organisms will focus chiefly on temporary and dynamic attachment mechanisms.

Other than the amphibians, which include the tree frogs, the vertebrate classes that utilise adhesion under natural conditions include fish, reptiles and mammals. The mechanisms employed within these diverse groups range from suction in fish (Green and Barber, 1988; Davenport and Thorsteinsson, 1990) to molecular adhesion in

geckos and other lizards (Irschick *et al.* 1996; Autumn *et al.* 2000, 2002; Autumn and Peattie, 2002; Macrini *et al.* 2003). The invertebrate phyla represent a diversity of organisms inhabiting a wide variety of ecological niches and have evolved attachment organs allowing them to utilise most forms of adhesion to exploit their environment. The majority of research into adhesion in the invertebrates focuses on the temporary adhesion seen in the molluscs, echinoderms and, particularly in recent years, on adhesive abilities seen in the insects. This chapter will outline in brief the growing body of literature that is concerned with the adhesive abilities of a wide range of species, with the diversity in the organisms in which they are seen reflected in a wide variety of adhesive mechanisms and attachment organs seen both between and within different phyla. Comparative forces in the variety of organisms in which adhesion is seen are outlined in **Appendix 1**.

1.2. Adhesion in invertebrates

1.2.1. Adhesion in arthropods

The bulk of recent research work into adhesion within the animal kingdom has focused strongly on the insect class of the arthropods, with adhesion prevalent in: flies, (Walker *et al.* 1985; Gorb, 1998; Gorb *et al.* 2001; Niederegger *et al.* 2002); beetles, (Stork, 1980a; 1980b; 1983a; 1983b; Attygalle *et al.* 2000; Eisner and Aneshansley, 2000; Dai *et al.* 2002; Eigenbröde and Jetter, 2002; Betz, 2002, 2003); bees and ants, (Federle *et al.* 1997; 2000; 2001; 2002); crickets (Gorb and Scherge, 2000; Vötsch *et al.* 2002); aphids, (Lees and Hardie, 1988; Dixon *et al.* 1990); bugs, (Gillett and Wigglesworth, 1932) and cockroaches (Roth and Willis, 1952). In general work has focused on attachment and climbing, but many insects also have additional

adhesive structures that are utilised in reproduction (Stork, 1980a; Walker *et al.* 1985; Aiken and Khan, 1992) and in feeding (Stork, 1983b; Aiken and Khan, 1992).

Most climbing insects have well-developed tarsal claws to give them purchase on substrata through friction and interlocking (Lees and Hardie, 1988; Federle *et al.* 1997; Betz, 2002). These are capable of producing substantial adhesive ability on rough surfaces: for example, the tarsal claws of the beetle *Pachnoda marginata* allows the animals to resist detachment forces equivalent to up to thirty-eight times their own body weight (Dai *et al.* 2002). However, many insects living on plants regularly require to move across smooth surfaces such as the waxy leaves and stems of a host-plant (Stork, 1983a; Federle, 1997; Eigenbrode and Jetter, 2002) and the lack of irregularities on such substrata means that the tarsal claws are largely non-functional. This has led to the development of complementary adhesive strategies in many of these insects. The widespread occurrence of plant dwelling lifestyles seen in diverse groups of insects means that there is considerable diversity in the morphology of the attachment organs (Lees and Hardie, 1988; Federle *et al.* 1997; Beutel and Gorb, 2001; Beutel *et al.* 2002; Ober, 2003). However, in general the adhesive pads can be regarded as falling into two distinct categories defined by their morphological appearance as being either ‘smooth’ or ‘hairy’ (Scherge and Gorb, 2001). Extensive variety is seen within these categories; Stork’s (1980a) extensive scanning electron microscopy study of the adhesive structures seen on the ‘hairy’ pads of the Coleoptera describes seventy-five distinct types of setae in eighty-four species.

‘Smooth’ pads are found in cockroaches, grasshoppers, bees, ants and in the true bugs (Hemiptera). These are devoid of any of the hair-like structures seen in the beetles

and flies and are formed by eversible sacs of soft flexible cuticle, called arolia, pulvilli or euplantulae (Beutel and Gorb, 2001). There are differences in the biomechanics of these organs between classes. In leafhoppers and aphids pliable pouch-like structures on the pre-tarsus and tarso-tibial articulation become everted passively when the foot is extended, acting to supplement the action of the tarsal claws (Lees and Hardie, 1988; Dixon *et al.* 1990). In the Hymenoptera the adhesive structures are called arolia, and are soft cuticular sacs located between the claws (Federle *et al.* 2001). Many smooth pads are actively moved and unfolded using increased haemolymph pressure, with the mechanism of unfolding on smooth surfaces being triggered by the retraction of the tarsal claws when the insects fail to get a purchase upon a substrate (Federle *et al.* 1997, 2000, 2001; Dai *et al.* 2002; Federle *et al.* 2002; Frantsevich and Gorb, 2002). One unusual form of smooth pad is seen in the grasshopper *Tettigonia viridissima*, hemispherical in cross-section and covered with hexagonal outgrowths formed by closely packed rods (dendrites) of a highly flexible cuticular material (Gorb and Scherge, 2000; Jiao *et al.* 2001; Gorb *et al.* 2002).

‘Hairy’ pads are seen most commonly in beetles and flies (Stork, 1980a; Walker *et al.* 1985; Gorb, 1996; Gorb *et al.* 2002; Betz, 2002, 2003) and are formed by discrete cushions of integument at the ends of the tarsi covered in thousands of long, deformable adhesive ‘hairs’ or setae (Lees and Hardie, 1988; Jiao *et al.* 2000; Scherge and Gorb, 2001). These differ between the Coleoptera and the Diptera in which they are most commonly found, inserting to a multicellular ‘socket’ on the ventral surface of the tarsus in the case of the beetles and originating from a single cell in the flies (Gorb *et al.* 2001). The functionality of these setae in adhesion also

appears to be strongly directionally dependent, both in beetles (Stork, 1980a; 1983a; 1983b) and flies (Gorb, 1998; Gorb *et al.* 2001; Niederegger *et al.* 2002), adhesion is facilitated by a drawing of the foot towards the body of the animal; if the force is directed away from the body then the pads automatically detach (Gorb, 1998). The drawing of the foot towards the body is hypothesised to facilitate adhesion in two ways; firstly by changing the orientation of the spatulate and discoid terminal ends to maximise the setal area in contact with the substrate (Stork, 1983a; 1983b), and secondly through the initiation of the mechanical release and spreading of a fluid secretion implicated in the adhesive abilities of the dipterans in particular (Gorb, 1998; Niederegger *et al.* 2002). The similarities of the morphology of these setae together with the positional dependency of adhesion makes the mechanism seen in beetles superficially similar to that seen in climbing lizards (Stork, 1983b). The convergent evolution of setal structures with such remarkable geometrical similarity suggests that the structure of the adhesive setae is critical to the adhesive function.

However, from some of the earliest research into insect adhesion a liquid layer present beneath the pads of many insects has been noted; ‘the fly had a fuzzy kind of substance like little sponges, with which she hath lined the soles of her feet, which substance is always repleated with a whitish liquor which she can at pleasure squeeze out, and so sodder and be-glew herself to the plain she walks on, which otherways her gravity would hinder (were it not for this contrivance) especially when she walks in those inverted positions’ (Power, 1664; quoted in Stork, 1983a). More recent research has also noted fluid secretions seen beneath the pads of beetles (Attygalle *et al.* 2000; Eigenbrode and Jetter, 2002) and flies (Walker *et al.* 1985; Gorb, 1998; Gorb *et al.* 2001; Niederegger *et al.* 2002), which would be detrimental to the adhesive

mechanism used by the lizards (see 1.3.3). Adhesion is also supplemented by the presence of fluid secretions where insects have the smooth type of attachment pad and these are shown to be essential in their attachment to smooth surfaces (Gillett and Wigglesworth, 1932; Stork, 1980b; Dixon *et al.* 1990; Jiao *et al.* 2000; Eisner and Aneshansley, 2000; Scherge and Gorb, 2001; Federle *et al.* 2002; Dai *et al.* 2002; Eigenbrode and Jetter, 2002). If these fluids are removed by washing the pads with solvents (Edwards and Tarkanian, 1970) or by walking the animal across drying agents (Dixon *et al.* 1990; Gorb, 1998), then the insects lose their ability to attach to smooth and vertical surfaces. The tarsal secretions largely remain uncharacterised but it appears that many of them are oily mixtures of hydrocarbons, likely to be similar to those covering the cuticles of the insects (Attygalle *et al.* 2000; Jiao *et al.* 2000; Eigenbröde and Jetter, 2002; Vötsch *et al.* 2002; Betz, 2003). Chemical extracts of tarsal footprints of the palmetto tortoise beetle (*Hemisphaerota cyanea*) and of the migratory locust (*Locusta migratoria*) yield oily mixtures of saturated and unsaturated linear hydrocarbons of between C₁₆ to C₂₈ chain length (Attygalle *et al.* 2000, Vötsch *et al.* 2002). The secretory fluid beneath the tarsal pads of Staphylinid beetles, the rove beetles, is a two-phase liquid consisting of a lipid and a proteinaceous fraction; gas chromatography and infrared spectroscopy reveals that the lipid fraction of the secretion is a mixture of unsaturated fatty acid glycerides and hydrocarbons similar to extractions of the superficial lipid coating of the chitinous body surface (Betz, 2003). The spreading tendencies of the fluid droplets left in the footprints of the weaver ant (*Oecophylla smaragdana*) also suggest that the secretion utilised in adhesion is largely hydrophobic in nature, but interference microscopy studies indicate that there is a presence of a second hydrophilic fluid beneath the pad that is highly volatile in nature (Federle *et al.* 2002). It seems likely that a ‘two-phase

fluid' is present under the smooth pads of other insects; the chemical composition of the locust footprint secretions certainly indicates the presence of a second volatile portion within the secretory fluid (Vötsch *et al.* 2002). Many insects with the smooth type of pad are often able to adhere equally well to both hydrophobic and hydrophilic substrates (Roth and Willis, 1953; Lees and Hardie, 1988; Dixon *et al.* 1990). An insect adhering to plants is likely to encounter many types of substrate as it moves through its environment (Gorb and Gorb, 2002), so the production of an 'emulsion' with two phases is likely to be of considerable advantage (Vötsch *et al.* 2002).

Preliminary assessments of the nature of the secretory fluids in both *T. viridissima* and *O. smaragdina* suggest that the adhesion effected by these secretions is not sufficient to explain the magnitude of the forces seen in either (Jiao *et al.* 2000; Federle *et al.* 2002). Both studies suggest that the deformability of the pad is key to the adhesive abilities of both insects, through the enhanced ability to conform to the substrate through the increase in the contribution of 'rubber' friction to the overall forces (Jiao *et al.* 2000; Scherge and Gorb, 2001; Federle *et al.* 2002). Gorb *et al.* (2001) and Niederegger *et al.* (2002) found that friction forces in syrphid flies, with setose pads, also substantially contribute to the overall adhesive forces. The cuticular materials that form both the 'hairy' setose pads and the smooth 'hairless' pads in insects are naturally friction-active and elastic (Scherge and Gorb, 2001).

Gorb (1998), considering the design of the fly adhesive pad, quotes Tuffen West, who writes as early as 1862 that 'the structure and action of the fly's foot have been so frequently treated of, and are so generally considered to be fully understood, that it may appear, at the first glance, as if nothing further could be done with so hackneyed

a subject'. The wealth of new research in recent years, using novel and sensitive techniques of force determination and microscopy, clearly demonstrates that, over a hundred years later, there is still a lot to be learned within the field of insect adhesion.

1.2.2. Adhesion in cephalopods

Adhesion in the cephalopod molluscs is rather complicated by the multifunctional nature of the tentacles that effect adhesion via various structures on their ventral surfaces. Kier and Smith (1990) identify six distinct functions of the suckers on octopod tentacles, contributing to aspects of locomotion, anchorage during prey capture, object manipulation, chemotactile recognition, display behaviours and cleaning. These functions are also performed by the tentacles of squids (Smith, 1996), cuttlefish (von Boletzky and Roeleveld, 2000) and nautilids (Muntz and Wentworth, 1995).

The latter, the most primitive of the cephalopods, provide a deviation from the norm in terms of the structure of the adhesive ventral surfaces of the tentacles. Rather than the disc-like structures that cover the tentacles in coleoid cephalopods the tentacles of nautilid species have distinct transverse ridges of thickened epithelium along their length (Muntz and Wentworth, 1995). These have numerous glands present on their vertical sides that produce a secretion of mucopolysaccharides, and it is this mucosal secretion that is proposed as the main contributory factor in the nautilids' ability to adhere. Using such a gluing mechanism might be expected to lead to problems for the organism in terms of the forces required to remove the tentacle. The need for an unpeeling mechanism to effect this will explain the presence of powerful radial and longitudinal muscles within the tentacle (Muntz and Wentworth, 1995). The

hypotheses about both adhesive and detachment abilities in the nautilids are, however, based only on the morphological and histological studies of the tentacles. Behavioural studies of these animals are problematic due to their highly benthic nature, poorly understood ecology and the general scarcity of observations in the wild (Muntz and Wentworth, 1995).

Ventral discs are seen in both octopod and decapod groups of the Cephalopoda. The morphology in the two are substantially different, being chitinous cylinders with internal 'muscular pistons' in the case of squids (Smith, 1996) and flatter double-chambered suckers with internal volumes controlled by muscular sphincters in the octopi (Kier and Smith, 1990). In spite of these differences, the function of both types in adhesion is broadly similar, relying on the production of suction forces when brought into contact with a substrate. Though the stalked structures seen in the decapod cephalopods are capable of producing suction forces up to four times the strength of equivalently sized octopod suckers this increased strength comes at a cost to the dexterity of the suckers (Smith, 1996). Suckers in both the decapod and octopod cephalopods have the edges ridged with chitin to allow a degree of frictional resistance to the shear forces that may dislodge the animal from a substrate (Kier and Smith, 1990). Similar structures are seen on the surfaces of suctorial discs in fish and tadpoles living in torrential streams and in rough coastal conditions (Hora, 1923; Gradwell, 1973; Daugherty and Sheldon, 1982) suggesting that there may well be an adaptive significance implied by the convergent evolution of these suckers in diverse species. That the close conformation the chitinous structures facilitate is likely to be most influential at the rim of the sucker is particularly telling, as such a sealing at the edges as this would promote, is key to the efficiency of suction (Kier and Smith,

1990; Smith, 1991; Denny, 1993; Scherge and Gorb, 2001). After the sucker is brought into close contact with the substrate the internal musculature will contract to increase the volume enclosed beneath it: this occurs through the retraction of the central muscular column in the decapod cephalopods or through the opening of the muscular sphincter separating the inner 'acetabulum' from the external 'infundibulum' in the two-chambered structure beneath the sucker in the octopi. In both instances this causes a negative pressure differential between the internal and external environment that holds the tentacles to the substrate by suction. This decrease in pressure accounts for 100% of the attachment forces recorded in *Octopus vulgaris* adhering to glass substrates at sea level (Smith, 1991), suggesting that suction forces are the key mechanism by which the cephalopods are able to maintain a hold upon smooth substrates.

At sea level the maximum tenacity of the suckers in all cephalopods is limited to between 100-200 mN/mm² by the cavitation threshold of water (Smith, 1996). This value relates to the lowest pressure that a fluid can sustain before gas bubbles form within the fluid (Smith, 1991; Denny, 1993), which has a significantly detrimental effect on the continuing functionality of a system dependent on suction forces (Kier and Smith, 1990). However, the cavitation threshold of water is highly dependent on depth, increasing by 100 kPa every ten metres (Kier and Smith, 1990; Smith, 1996). Therefore a theoretical cephalopod with suckers of 1 mm² in area can increase the forces produced by suction by around 100% from that recorded at sea level simply by descending through ten metres.

Attachment forces generated by suction are a product of the contact area of the sucker and the pressure differential between the external and internal environment (Kier and Smith, 1990). Perhaps as a compensatory response to their smaller size, suckers below 7.5mm in diameter are often capable of producing much higher pressure differentials than larger suckers. Indeed, in four octopus species with differently sized suckers, there were no significant differences in the attachment forces between species (Smith, 1996). In the case of pelagic octopi and squid it may be an advantage to have larger suctorial discs as the cavitation threshold of the seawater limits the pressure differential. As this ceases to be a consideration with increasing depth, so benthic cephalopods need not have such large suckers, which may well be an advantage for functions such as the manipulation of small objects. This prediction is borne out amongst different octopus species, which exhibit an inverse correlation between sucker size and the depth of habitual occurrence (Kier and Smith, 1990).

1.2.3. Adhesion in gastropods

The sticking abilities of the gastropod molluscs include what is perhaps one of the more familiar incidences of animal adhesion, that seen in the slugs and snails. In spite of this familiarity, remarkably little detailed knowledge exists as to the nature of the adhesive mechanism in terrestrial slugs and snails. These animals move across substrata using muscular podia covered with cilia; small species are able to move by the beating of the cilia within the mucosal secretions produced beneath the foot but in larger species forward movement is facilitated by transverse waves of muscular contraction (Rudman, 2001). Evidence is that the key to locomotory abilities in terrestrial slugs and snails is in large part due to the viscoelastic properties of the mucus, which behaves as a fluid friction-reducing lubricant at the slow velocities at which these animals usually move (Scherge and Gorb, 2001; Smith, 2002). Mucus in

the slugs is, in fact, multifunctional. In addition to locomotory considerations it plays a role in attachment to vertical surfaces, reproduction, hydroregulation, antibacterial defence and in navigation (Viney, 2002). This has led to the evolution of polymorphic mucus, the nature of which is affected by the behaviour of the animals. Mucus sampled from resting slugs and motile slugs has significant differences in protein composition that appear to affect both viscosity and tensile strength (Viney, 2002). Maximum values of tenacities extrapolated from the viscoelastic properties of mucus from the banana slug, *Ariolimax columbianus*, are around 2 mN/mm² (Denny and Gosline, 1983). This is, in comparison to a number of marine snails and limpets, a fairly low tenacity value; many marine gastropods are capable of forming far stronger attachments, also utilising viscoelastic mucus secretion (Smith, 2002). The limpet, *Patella vulgata*, has been particularly well studied (Grenon and Walker, 1981; Smith, 1991b; Denny, 1993; Denny, 2000; Ellem *et al.* 2002). Mean tenacities depend on whether the organisms have been recently active, ranging from 40 mN/mm² in recently motile limpets to 690 mN/mm² in long-term stationary limpets (Denny, 2000). The changes in tenacity that this represents is, in large part, due to changes in the protein composition and subsequently the nature of the mucosal 'gel' (*sensu* Smith, 2002) beneath the feet of these molluscs. In the limpet, *Lottia limatula*, and the marsh periwinkle, *Littorina irrorata*, there are significant increases in the total volume in proteinaceous elements of the mucus used for attachment compared to that used for locomotion (Smith *et al.* 1999; Smith and Morin, 2002). Additionally, specific proteins are seen only in the attachment mucus that is presumed to be responsible for the change from 'gel' to 'glue' in these species (Smith, 2002). However the tensile strength of the mucosal layer in such species is not sufficient to

be the sole mechanism by which these animals are adhering to the substrata within their environment, (Holmes *et al.* 2002).

There is evidence from both field and laboratory studies of limpets adhering to smooth plates, that limpets additionally utilise suction as an attachment mechanism (Smith, 1991b; 1992). Pressure measurements taken from beneath the muscular foot of three species of limpet indicate that they are able to actively decrease the pressure beneath the foot, (Smith, 1991b). The suctorial mechanism that this suggests is confirmed by the detrimental effect of decreased atmospheric pressure on the sticking abilities seen in the limpets (Smith, 1991b). In laboratory conditions, the forces produced through suction account for almost all of the tenacity recorded under the foot. However, in adherent limpets in the field suction accounts for only 90 mN/mm^2 of the total adhesive force production, equivalent to 30% of the maximal adhesive forces that would be possible using gluing (Smith, 1992). Limpets vary their adhesive mechanism according to tidal influences and utilise suction most often at high tide and ‘gluing’ during low tide, presumably linked to foraging requirements (Smith, 1992) for if limpets were too firmly attached then the large detachment forces required to overcome the adhesive mechanism would make it energetically impossible to forage efficiently. Many species also respond to increased wave action with a clamping behaviour which generates an additional resistance to dislodgement by shear through the generation of friction at the site of closer juxtaposition of the shell edge to the substratum; in the limpet, *Cellana tramoserica*, this behaviour can contribute over a third of the maximal force recorded from beneath the foot (Ellem *et al.* 2002).

1.2.4. Adhesion in echinoderms

All members of the Echinodermata bear tube feet or podia which adhere and release from substrates, and which are used in a variety of functions, including locomotion, anchorage, feeding and in anti-predation (Flammang, 1994; Flammang, 2002). There are slight morphological differences in the morphology of these different types of podia, though the basic general structure remains roughly similar, consisting of a long flexible stem with a distal attachment, usually disc-shaped, that is the main site of attachment during adhesion (Thomas and Hermans, 1985; Flammang, 1994; Vickery and McClintock, 2000; Scherge and Gorb, 2001).

The concave nature of these discs in the best-studied of the echinoderm classes, the Asteroidea (starfish), led to suction being hypothesised as the chief mechanism by which the podia function in adhesion. Morphological studies of the podia describe a powerful levator muscle inserting to the podial disc which suggests that there is certainly some likelihood that suction plays an important role in allowing the echinoderms to adhere to smooth solid substrates within their environment (Flammang, 1996; Vickery and McClintock, 2000). However, there is some evidence that starfish (*Leptasterias hexactus*: Thomas and Hermans, 1985) are able to adhere to porous substrates with higher mesh density than the diameter of the podia, where suction would be non-functional. The extent to which they are able to do this appears to be limited only by the mechanical breaking strain of the podial stems (Thomas and Hermans, 1985).

These findings, together with evidence of secretions remaining on substrates post-detachment, have led to the opinion that suction is in fact an accessory mechanism,

with the majority of adhesive force conferred by the presence of strong adhesive secretions (Thomas and Hermans, 1985; Smith, 1991; Flammang, 1994, 1996; Vickery and McClintock, 2000). The Cuvierian tubules in the Holothuroidea (sea cucumbers), which function to entangle attacking predators do not appear to have a suctional capability and are therefore dependent on the production of a 'sticky' secretion for their functionality (Flammang *et al.* 2002). These are produced within secretory glands, distributed across the whole of the surface of the distal attachment disc. In the Asteroidea these consist of two types of secretory cell; one producing an adhesive and the other a de-adhesive. In the Ophiuroidea (brittle-stars) and the Holothuroidea there are two types of adhesive producing cell (Flammang, 1996; Flammang *et al.* 2002). Although the adhesive secretions have been found to be highly variable protein-polysaccharide complex, the nature of the de-adhesive secretions are as yet unidentified, due to a lack of staining response to any standard histological dyes (Scherge and Gorb, 2001). The dependence of the adhesive mechanism in the Echinoderms on these two separately induced secretions means that podial adhesion is roughly analogous in its function to the duo-gland adhesive system seen in small, largely marine invertebrates inhabiting interstitial environments (Flammang, 1994), see **1.2.5**.

The actions of both the adhesive and de-adhesive secretions are still under debate, though most studies agree that there is some degree of chemical interaction between the secretions and the natural substrata. There is some evidence that these are dependent on the dielectric nature of the adherent substrates as podia do not adhere to all surfaces equally and do not attach at all to uncharged surfaces. This is particularly relevant for adhesion in a marine environment, where immersed surfaces become

quickly coated with negatively charged microbial films (Thomas and Hermans, 1985; Callow and Callow, 2002). The relative positioning and grouping of the secretory cells, both in relation to one another and in relation to other epidermal cell types, in particular sensory cells, has a significant effect on the functionality of the podial structure. In handling podia, secretory cells are always found in close association with sensory cells, forming discrete sensory-secretory complexes distributed across the disc. This appears to be more efficient for the handling of small substrate particles (Flammang, 1996; Scherge and Gorb, 2001) or the manipulation of eggs and larvae (Thomas and Hermans, 1985). In locomotory podia, sensory and secretory cells form a continuous layer across the surface of the distal disc, allowing the whole structure to adhere when required to withstand strong dislodgement forces (Flammang, 1994; Scherge and Gorb, 2001). Thomas and Hermans (1985) hypothesise that the adhesive strengths of the podia are variable through the relative control of the secretions of the adhesive and de-adhesive secretory cells, thus allowing the starfish to regulate adhesion on different substrates in its environment. The properties of the adhesive mechanism, effected by changes in the relative amounts of two separately induced secretions, makes it flexible enough for one mechanism to aid in attachment, locomotion, feeding and in object manipulation.

1.2.5. Duo-gland adhesion in various marine invertebrate phyla

There are a number of invertebrate phyla, including a number of species of the Platyhelminthes, Annelidae and Hirudinae that utilise a form of adhesion that is intermediary in its nature, between being transitory and temporary, which is known as duo-gland adhesion (Scherge and Gorb, 2001). Organisms utilising this form of adhesion often live in interstitial environments or as ectosymbionts or parasites on

other organisms (Hermans, 1983; Whittington *et al.* 2000; Buchmann and Lindenstrom, 2002). Many have two separate attachment sites, one of which is in contact with the substrate/host at any one time allowing the organism to move along a substrate without being dislodged. In the branchiobdellid annelid worms, which live exclusively as ectosymbionts of freshwater crustaceans, these attachment structures take the form of a large anterior-ventral attachment pad and a smaller posterior disc located on the terminal body segment, reminiscent of the arrangement seen in leeches (Scherge and Gorb, 2001). These attachment organs are characterised by the presence of at least two secretory cell types, one producing an adhesive secretion and the other producing a de-adhesive (c.f. echinoderm adhesive mechanism in 1.2.4). The nature of these remains largely unknown, though it is suggested that the adhesion is caused by the setting up of intermolecular bonds, promoted by the secretion of polycationic substances that bind to anionic sites. This is particularly important when considering the negatively charged nature of the biofilms which coat the surfaces of most marine substrata (Thomas and Hermans, 1985; Callow and Callow, 2002). The mechanism of adhesion is therefore highly dependent on the chemistry of the adhesive secretions in organisms utilising this duo-gland adhesive system. In the case of monogenean platyhelminth fish parasites, histochemistry has shown that the adhesive is proteinaceous (Hamwood *et al.* 2002). Properties of the adhesive show similarities to those seen in the temporary adhesive secretions in starfish and limpets though there are a number of differences in the specific amino acid compositions which may reflect the fact that monogeneans attach to living tissue (Hamwood *et al.* 2002): there is some evidence that the specific amino acid composition of the adhesive secretion plays a role in host-specificity (Buchmann and Lindenstrom, 2002).

1.3. Adhesion in vertebrates

1.3.1. Adhesion in fish

Fish living on the bottom of the ocean and in torrential hill streams have evolved modified attachment organs which act to counter the dislodgement effects of the strong currents acting upon them in their natural environments. The best studied of these are muscular disc-shaped structures on the mouth and thorax (Scherge and Gorb, 2001). The morphology of these suggests that they may have evolved to act principally as suction organs (Davenport and Thorsteinsson, 1990), but the heavy degree of mucilation of the surfaces of these suckers (Green and Barber, 1988; Davenport and Thorsteinsson, 1990) together with prominent ridges and papillae in many (Hora, 1923; Green and Barber, 1988; Davenport and Thorsteinsson, 1990) suggests an additional contribution of other mechanisms to the overall adhesive forces seen in these fish. The extent to which the suction discs are ridged and papillated has led to the suggestion that in some hill stream species friction and interlocking may well be the predominant forces (Hora, 1923; Scherge and Gorb, 2001).

Experimental studies on the biomechanics of these attachment forces are scarce, with most of the conclusions about the function of the structures based chiefly on morphological studies (Green and Barber, 1988). Davenport and Thorsteinsson's (1990) study of the lumpsucker, *Cyclopterus lumpus*, shows that the sucker is formed by modified pectoral fins with fin rays extending to form a skeletal structure within the sucker. Muscles act upon these fin rays to spread and flatten the sucker onto the substrate prior to attachment, allowing the close conformation of the sucker to the

substrate, particularly at the outer edges where the surface is significantly smoother than elsewhere.

Adhesive mucus seals the edges of the sucker and allows the fish to withstand shear forces of up to 5 N before the central portion of the sucker is raised by the action of a horizontal pair of muscles to produce a negative pressure below the pad, thus increasing the adhesive forces holding the fish to the substrate. These negative pressures are transitory and decay with time, requiring to be periodically renewed to maintain adhesion (Davenport and Thorsteinsson, 1990; Scherge and Gorb, 2001). In torrential fauna, the action of water flowing over the top of the attached fish allows the initial pressing down phase of the attachment to be constantly renewed without the need for repeated muscular exertion. In the lumpsucker the replenishment of the initial attachment phase is antagonised by the action of the five pairs of muscles that insert to the modified fin rays. The forces that are produced beneath the sucker of this fish can be considerable, able to withstand detachment forces of over 100 mN/mm².

1.3.2. Adhesion in lizards

Most lizards are able to climb up rough and inclined surfaces by using claws, and in most species the excising of the claws removes the ability to cling on rough surfaces (Zani, 2000). However, sub-digital toe pads composed of expanded scales (lamellae) have evolved independently in three lineages of lizard: the anoles, geckos and praesinohaemid skinks (Ruibal and Ernst, 1965). In most species these scales are covered with microscopic keratinised projections called setae, though in some of the Scincidae the scales have modified surfaces that appear to be covered in closely packed 'ruffled' ridges (Williams and Peterson, 1982). Carphodactyline geckos from

New Caledonia and Australia have extended the locations of these specialised setae-covered scales, to include the underside of their prehensile tails. Setal structure and function on the tail 'pads' are exactly as found on the sub digital pads of the same species (Bauer, 1998). These modified sub-digital pads allow many lizards to climb on surfaces that are so smooth that claws are non-functional, up vertical glass surfaces and even upside down on a ceiling (Scherge and Gorb, 2001).

The evolution of these subdigital pads has been invoked in several morphological studies as an important adaptation that allows the lizards to exploit arboreal habitats (Hora, 1923; Maderson, 1964; Ruibal and Ernst, 1965; Russell, 1975, 1979; Williams and Peterson, 1982; Stork, 1983b; Lauff *et al.* 1993). In theory the pads can provide functional capabilities in two ways; the lamellae may enhance the flexibility of the toe to allow the pad to be more closely moulded to narrow or irregular surfaces (Macrini *et al.* 2003) and/or the thousands of microscopic keratinised setae may enhance the adhesive abilities by contacting and forming bonds with the surface of the substrate (Russell, 2002). There is some evidence that there is a significant relationship between the number of lamellae and the perch height chosen by arboreal anoles (Irshick *et al.* 1996; Glossip and Losos, 1997), reinforcing the likelihood that these pads have evolved as a response to the pressures of arboreality. There is no correlation with perch diameter (Glossip and Losos, 1997), which might be expected should the increase in lamellar number facilitate an improved gripping ability. Studies have demonstrated a positive correlation between setal number and the clinging abilities both within the anoles (Irschick *et al.*, 1996) and across lizard genera (Zani, 2000), suggesting that it is these structures that are responsible for the production of adhesive abilities in these animals.

Setal function in the geckos has been extensively studied in recent years by Kellar Autumn and colleagues (Autumn *et al.* 2000, 2002; Autumn and Peattie, 2002) and these studies have dramatically increased our understanding of their highly developed toe pads. Their remarkable ability to climb rapidly up vertical surfaces was noted as early as the 4th century B.C. when Aristotle noted that the ‘gecko-lizard’ is able to ‘run up and down a tree in any way, even with the head downwards’ (in Autumn *et al.* 2002). Microscopic studies have found that lizards have between ten thousand and a million setae on the lamellae of their feet which are in their turn subdivided at their tips up to a hundred times (Ruibal and Ernst, 1965). The Tokay gecko (*Gekko gekko*) has about five thousand setae per mm², up to about 100 μ m in length, each of which terminates in hundreds of flattened spatulate ends (Autumn *et al.* 2000). A gecko adhering to glass can produce forces of around 100 mN/mm² (Irschick *et al.* 1996), so that it might be predicted that each seta will produce an average force of 20 μ N. Autumn *et al.* (2000) found that individual setae are nearly ten times more effective than this, each producing on average 194 μ N of force. These measurements support models of adhesion by intermolecular bonding using van der Waal’s forces (Autumn *et al.* 2000, 2002).

If all the setae of a 50 g gecko were in contact with a surface at any one time then the system could theoretically generate over 1,000 N of adhesive force; enough to support the weight of two adult humans (Autumn and Peattie, 2002). Measurements of the forces produced by a single seta in Autumn *et al.* (2000, 2002) therefore suggest that a gecko need only attach 3% of its total setae to generate the greatest forces recorded in the whole animal and 0.04 % in order to support its own weight (Autumn and Peattie, 2002). It appears from these studies that a gecko’s feet are

vastly over-designed for their function and that if all setae are in contact with a surface simultaneously the forces required to remove the foot are likely to be so great as to make the system impractical for functional locomotion. However, setal force is highly dependent on their three-dimensional orientation to the contact surface; if the active spatular region is not facing the surface, the forces recorded from single setae are reduced significantly with forces of only $0.3 \mu\text{N}$ (Autumn *et al.* 2000) and automatically detach at angles of 30° to the surface. As it is unlikely that all setae will achieve the same orientation simultaneously, particularly on roughened surfaces, the proportion of spatulae in close enough contact with the substrate to allow the formation of intermolecular forces is likely to be greatly reduced. This helps to explain the high densities of setae seen on the lamellar scales of most species.

The directionality of setal function may also explain the mechanics of the complex toe uncurling behaviour seen in many species (Russell, 1975; Lauff *et al.* 1993; Russell, 2002). This is facilitated by a controlled increase in the volume of blood circulated to the toe tips (Bauer, 1998), and is likely to change the orientation of the setae covering the sub-digital pads through the key detachment angle, thus allowing the lizards to detach their pads without needing to exert the kinds of forces required in the experimental conditions every time they move their feet (Autumn *et al.* 2000).

1.3.3. Adhesion in mammals

Mammals commonly inhabiting environments that require movement over inclined and vertical surfaces most commonly use claws to climb substrates (Cartmill, 1985). Arboreal rodents, marsupials and primates also have large cushioned volar pads, which exhibit high frictional coefficients as the pads deform on contact with the

surface (Cartmill, 1979; Häffner, 1998; Rosenberg and Rose, 1999; Hamrick, 2001). Galagos have a fine network of blood vessels that allow the continual maintenance of a grip through a swelling of these pads, they also coat on their hands frequently with sugary, sticky urine that is believed to enhance their grip as well as functioning in trail-marking (Attenborough, 2002). Most climbing mammals also have additional features of the pads that increase the frictional properties of the skin, including increased numbers of eccrine glands across the pads that produce oily sebaceous secretions (Cartmill, 1979; Häffner, 1998; Stumpf and Welsch, 2002) and the degree of development of ridges, with these analogous to our own fingerprints (Hamrick, 1998, 2001). The function of these features in aiding climbing is illustrated by considering the positive correlation between the degree of development in these epidermal ridges with increasing frequency of small branch foraging (Scherge and Gorb, 2001) and with arboreality (Hamrick, 2001). The number of glands seen across the pad also correlates with the degree of arboreality seen in climbing rodents (Häffner, 1998).

These trends have been taken to extremes in the highly arboreal possum, *Acrobates pygmaeus*, in which the epidermis of the volar pads has become arranged into distinct transverse ridges separated by deep grooves into which numerous sweat glands empty (Rosenberg and Rose, 1999). The surface tension of the sweat that covers the epidermal ridges on the hands and feet of this species is sufficient to hold the animals in place on vertically inclined glass surfaces, where claws are non-functional. The contact surfaces of each epidermal ridge on each pad act as separate narrow adhesive strips, separated by the deep grooves that confer flexibility to the pad, allowing it to

conform closely to the substrate, thus maximising the contact area for wet adhesion (Rosenberg and Rose, 1999).

One interesting incidence of adhesion in the mammals is the case of the rock and tree hyraxes of the order Hyracoidea, whose closest living relatives are the elephants (Dorst and Dandelot, 1980). These largely desert-dwelling species exhibit climbing abilities that are due to musculature that raises the central portion of their pads which, together with the secretions from the numerous eccrine glands on the surface (Stumpf and Welsch, 2002), induces the formation of a poorly sealed suction cup which, apparently, allows these animals to ‘run up almost vertical rock faces’ (Kenmuir and Williams, 1985). There is little evidence from biomechanical studies of the mechanism that suction is actually in effect during climbing in these animals but the degree of development in the pad for the function that is suggested by morphological studies is of particular interest because, although the progressive development of the volar pads is seen in all groups where arboreality is present (Hamrick, 2001), the development of structures specifically evolved for attachment is rare amongst the mammals (Scherge and Gorb, 2001). More highly evolved suction cups are evident as disc-like structures on the wing-tips of bats from several genera including the Vespertilionidae (Thewissen and Etnier, 1995) and the Thyroptera (Riskin and Fenton, 2001) which are presumed to confer the ability of these animals to adhere to the smooth surfaces of furled leaves in which they regularly roost. Although there is a general consensus that these structures facilitate adhesion by acting as suction cups supplemented by gluing or wet adhesion (Thewissen and Etnier, 1995), prior to the study by Riskin and Fenton (2001) on *Thyroptera tricolor* (Spix’s disk-winged bat),

these suppositions were largely based on morphological and histological studies (Scherge and Gorb, 2001).

Riskin and Fenton (2001) tested the adhesive abilities of *Thyroptera tricolor* against 18 other species and found that, whilst most species were able to adhere well to rough surfaces, only *T. tricolor* was able to adhere to the smooth surface presented by glass. In animals adhering to glass, the centrally raised portion of the disc is clearly visible as is the fluid-sealed perimeter around it that led to the conclusion that wet adhesion may play an additional role in the abilities of these bats to stick to smooth surfaces. This is supported by experimental evidence of the sticking abilities of the suction discs on finely perforated aluminium sheets, which, whilst having some detrimental effect on the bats' clinging abilities, did not entirely eliminate the forces being produced by the pads. Riskin and Fenton (2001) propose that wet adhesion serves as a secondary mechanism to allow the animal to stick to some degree without having to constantly replenish the negative pressures beneath the pad through continued muscular exertion. The specific nature of this secondary wet adhesive mechanism is unclear as it has not yet been ascertained whether the intervening layer facilitates adhesion through the influences of viscosity or through surface tension. The former might be expected if the fluid is the 'sticky mucus' secreted by the glands found across the disc surface, the latter if the fluid is replenished by the continual licking of the pads that is seen in this fastidiously grooming species.

1.3.4. Adhesion in amphibians

The best-studied group of arboreal amphibians in terms of their adhesive abilities are the tree frogs with which this study is primarily concerned and which will be discussed in detail in the next chapter. The arboreal habits that have led to the adoption of mechanisms that enhance adhesive abilities are not confined to the anuran class of amphibians, as neotropical salamanders from the genera *Bolitoglossa*, *Pseudoeurycea*, *Ithorius* and *Chiropterotriton* all exhibit high degrees of arboreality (Green and Alberch, 1981). Among these genera, the bolitoglossids are the most diverse and specialised towards arboreality and are characterised by palmate, heavily webbed feet which are believed to be adaptive features that have evolved to allow arboreal salamanders to move on flat, smooth surfaces such as the leaves of the bromeliads that they frequently inhabit (Alberch, 1981; Green and Alberch, 1981).

Morphological studies of the palmar surfaces of the feet of arboreal salamanders (Green and Alberch, 1981; Trauth and Wilhide, 1988) show that there are numerous glands distributed across the whole of the ventral surfaces. These secrete a mucosal substance that coats the entire surface of the foot, reducing the likely mechanisms of adhesive force production to suction and wet adhesion. In fact, morphological studies by Green and Alberch (1981) and experimental studies by Alberch (1981) suggest that in fact both mechanisms are likely to be implicated in adhesive force production in these animals.

Smith (1941), in his study of the herpetofauna of Mexican bromeliads, described a species of salamander (*Oedipus rufescens* = *Bolitoglossa rufescens*) as having 'big, flat, fully webbed feet...the animals move slowly and sedately, lifting their limbs

with seeming care, the great flaring feet displayed fully as they are solemnly placed down heel first, the edges clasping the surface a moment later'. Although this description is somewhat romantic, the biphasic nature of the adhesive mechanism that these observations suggest is confirmed by more recent recordings of forces generated by salamanders from the same species group adhering to glass (Alberch, 1981). These show an initial period of positive force as the animal presses its foot against the surface. The design of the pad then facilitates an effective sealing along the edges, with an increased degree of smoothness in the cell surfaces at the margins (Green and Alberch, 1981; Trauth and Wilhide, 1988) and a development of expanded phalangeal elements (Alberch, 1981), both of which will facilitate a closer conformation of the pad edges to smooth substrates. The central portion of the pad can then be pulled upwards by muscular contraction to allow the formation of a functional suction cup. Negative pressures are recorded below the pad in support of this theory, though these are gradually degraded over time. Whether this occurs by muscular fatigue or by ineffective sealing at the pad edges is unclear, but the implications are that utilising an adhesive mechanism dependent on forces generated by suction alone is likely to limit the salamander's ability to adhere. Further experiments (Alberch, 1981) suggest that a salamander's adhesive abilities in lowered atmospheric conditions or on porous substrates are not significantly affected, suggesting that suction is not the only mechanism in effect. Direct measurements of the suction forces generated below the pad represent a relatively small fraction of those seen overall (Alberch, 1981). When these are removed the total forces scale directly with the increasing surface area of the pad, suggesting that a wet adhesive mechanism dependent on surface tension (**Chapter 2**) is the primary mechanism,

perhaps being supplemented by suction when the surfaces of waxy leaves are hydrophilic.

Arboreal frogs belong to a range of families, but in Trinidad chiefly belong to the family *Hylidae*, which is in part defined by the possession of specialised expanded toe pads which act to increase the adhesive abilities in the species that possess them (Duellman and Trueb, 1997).

This chapter has outlined the fact that biological mechanisms of adhesion utilised by animals are diverse; with friction, interlocking, intermolecular bonding, suction and wet adhesion as the main sources of adhesive abilities in vertebrates. All have been implicated at some stage in the study of tree frog adhesion and proposed as the mechanism by which they stick. There have been a number of studies in previous years to determine the biological adhesive mechanism involved in tree frogs. The following chapter will discuss the evidence for the current consensus opinion of the mechanism involved and the implications of this when taking into consideration aspects of ecology and the effects of increasing body size both between and within species on the adhesive abilities of tree frogs.

Chapter 2: Adhesion in adult tree frogs

2.1. Introduction

Many species of frog, over a wide range of taxa, possess specialised and often expanded digital pads, with this adaptation being particularly prevalent amongst arboreal frogs in the families Hylidae, Microhylidae, Centrolenidae, Rhacophoridae, Hyperolidae, Leptodactylidae and Dendrobatidae (Duellman and Trueb, 1997). In spite of the diversity of taxa in which they are found, the structure and morphology of the toe pads in tree frogs has converged and is remarkably similar between the groups, suggesting their evolution is functionally adaptive (Hertwig and Sinsch, 1995; Green and Simon, 1986; McAllister and Channing, 1983; Green, 1979; Welsch *et al.* 1974). It has long been accepted that the function for which these toe pads have independently evolved in so many groups is the extraordinary ability seen in arboreal frogs to adhere to smooth and vertical surfaces (Hora, 1923). Whilst the way in which the morphology of the toe pads specifically contributes to tree frogs' adhesive abilities is still little understood, there have been a number of studies that seek to determine the biological adhesive mechanism involved.

Early arguments for friction and interlocking being the primary mechanisms involved (Hora, 1923; Noble and Jaekle, 1928) were largely based on light microscope studies of preserved specimens of the toe pads. These identified the extreme specialisation of the epidermal layer resulting in an arrangement of hexagonal tessellating cells covering the pad, with deep intercellular grooves between. The free apices of the cells led to an assumption that the functional purpose of this arrangement was to provide grip through interlocking with surface

irregularities at a cellular level (Hora, 1923). This being the case, tree frogs would be expected to adhere poorly on surfaces with few irregularities whereas, in fact, tree frogs are extremely good at sticking to smooth surfaces. Indeed, a number of species have reduced adhesive abilities on rough surfaces in comparison to smooth surfaces (Emerson and Diehl, 1980; Barnes, 1999; Barnes *et al.* 2002). Additionally, when



Figure 2.1: Meniscus around actively adhering toe pads in *P. venulosa*. Smallest grid = 1 mm.

observing a live tree frog climbing on a sheet of glass, a meniscus is clearly visible around adhering toe pads, (**Figure 2.1**) suggesting the existence of a fluid joint between pad and surface. Friction would be adversely affected by an intermediary liquid layer between adherent surfaces and is therefore unlikely to be the main mechanism involved.

The observation of a liquid layer between pad and surface also means that dry adhesion, as seen in gekkonid lizards (Autumn *et al.* 2000) can also be dismissed as the mechanism involved in tree frog adhesion. This type of adhesion is dependent on two surfaces getting close enough to one another to allow the formation of intermolecular bonding via Van der Waals forces, which become significant at a gap distance of around 0.3 nm (Denny, 1988). As a water molecule is also around 0.3 nm

in diameter (Pellicer *et al.* 2002) even the presence of a monomolecular layer of water between the adjacent surfaces is sufficient to prevent materials from adhering by this mechanism. The presence of the liquid layer beneath the toe pads restricts the possible mechanisms involved in tree frog adhesion to suction or to wet adhesion, as these are the only two mechanisms which are not adversely affected by moisture.

Suction as an adhesive mechanism is certainly seen in other arboreal amphibians. As was discussed in the previous chapter, in salamanders belonging to the genus *Bolitoglossa*, the whole foot acts as the attachment organ (Green, 1981b). The raising of the central portion creates the conditions required for suction, through the formation of a pressure differential between outside air pressure and the pressure beneath the adherent foot (Alberch, 1981). There is no evidence to suggest that there is any musculature in place in tree frog toe pads that would allow the raising of the central portion of the pad (Burton, 1996). Indeed, examining photographs of adhering frogs it is evident that the whole pad is in contact with the surface (**Figure 2.1**). Emerson and Diehl (1980) provide additional experimental evidence against suction, placing a live frog within a depressurisation chamber and monitoring the effect of reducing the external air pressure. The study found that when the air pressure reached the equalisation threshold, and the pressure differential required to support the weight of the frog is eliminated there was no effect on the frogs' position or adhesive ability.

Adhesion in tree frogs has been shown to be highly dependent on the layer of fluid between the pad and the substrate, with dry toe pads unable to stick (Green, 1979) with this suggesting that wet adhesion is the most likely mechanism to be involved in

the tree frogs' ability to adhere to smooth surfaces. Further experimental evidence also suggests that adhesive forces are highly dependent on toe pad area and are velocity-dependent, both of which are features of mechanisms dependent on wet adhesion (Emerson and Diehl, 1980; Green, 1981a; Green and Carson, 1988; Hanna and Barnes, 1991; Barnes, 1997). It has therefore been this mechanism that has been the chief focus in recent considerations of the means by which frogs are able to adhere to smooth surfaces (Barnes, 1999; Barnes *et al.* 2002).

Wet adhesion occurs when a layer of liquid spreads thinly along adjacent surfaces so that a force is required to separate the two (Nachtigall, 1974). The mechanism is dependent on the surfaces being 'wetable'; molecules in the fluid will be more strongly attracted to the molecules of the substrate than they will be to themselves. The resulting tendency of the liquid is to spread along the surfaces, forming an adhesive bond. For a substrate to be wettable, the surface energy must be greater than the surface tension of the liquid; with the value of both of these parameters dictated by the energy required to move a single molecule a set distance through the material in question (Denny, 1993).

The resistance to separation in the meniscus formed if these requirements are met is itself a product of two component forces: capillarity (F_C) and Stefan adhesion (F_{SA}). In a tree frog these are likely to be chiefly influenced in their turn by: the distance between the toe and substrate; the contact area of the meniscus beneath the pad, and the surface tension and viscosity of the intermediate fluid.

The relative contributions of each to the forces generated differ for the two component forces according to the following formulae:

$$(2.1) \quad F_C = \frac{2\pi r^2 \gamma}{h}$$

$$(2.2) \quad F_{SA} = \frac{3\pi r^4 \eta v}{2h^3} \quad (\text{adapted from Denny, 1993})$$

Where: r = radius; η = viscosity; γ = surface tension; h = meniscal height, v = speed of separation of two surfaces.

As tree frogs' toe pads are roughly circular, one might predict that the surface area of the adherent pad will be given by πr^2 , where r = radius of the toe pad. This being the case then these formulae will predict that if the surface tension dependent forces of capillarity dominate the wet adhesion mechanism then adhesive force measured in tree frogs would be expected to scale directly with the contact area, i.e. with toe pad area. If, on the other hand, viscosity dependent Stefan adhesion forces predominate then the measured forces will scale as toe pad area squared.

If the mechanism were to be more strongly dependent on Stefan adhesion forces of viscosity than on capillarity then this might be expected to present a two-fold problem to tree frogs; as well as the problem of the high detachment forces that a mechanism dependent on a high viscosity fluid layer would require, the time dependent nature of these forces will mean that whilst such a mechanism might give the frogs a strong degree of resistance to a rapid detachment force such as might be presented by a sudden gust of wind, it is likely to present a poor defence against the continuous relentless pull of gravity on the mass of the frog.

Adhesive forces from a number of species of tree frog in several studies have in fact been found to scale directly with toe pad area (Emerson and Diehl, 1980; Green, 1981a; Hanna and Barnes, 1991; Barnes, 1997; Barnes, 1999). This suggests that of the two forces that contribute to tree frog adhesion, the surface tension dependent capillarity forces are the most influential. Indeed, if surface tension is lowered by the introduction of a detergent to the system there is a significant detrimental effect on the adhesive ability of the frog (Green, 1981a). Furthermore, the negligible detachment forces recorded in frogs walking across a force platform suggest that the mucus involved in the fluid joint is low in viscosity and so will not produce large Stefan adhesion forces (Hanna and Barnes, 1991).

This however, presents another set of problems: Emerson (1978) comments on the suitability of frogs for studies of allometric effects on locomotion, quoting Inger (1967) who writing on the uniformity of shape seen between species states that ‘ a frog is a frog is a frog’. If hylids do have geometric similarity and scale following isometric predictions then with increasing linear dimensions, mass will increase at a significantly greater rate than the corresponding increase in toe pad area. Specifically, area (and hence adhesive force) would be expected to increase as the square of the linear dimension, whilst mass will increase as the cube. If frogs do adhere by capillarity, as evidence suggests, then large species of frog would be expected to show reduced adhesive ability in comparison to small species, or to show allometric growth characterised by faster than isometric growth in toe pad area.

As well as this, in addition to being highly dependent on contact area, capillary forces are highly dependent on the tendency of the fluid in the meniscal layer to

spread along the adherent surfaces; in this case, between toe and substrate. Tree frogs may be expected to encounter a range of substrates in their natural environment with variability in their wettability properties; indeed, pesticide application studies have found significant differences in leaf surface wettability in closely related plant species (Watanabe, 1991). Unless frogs are able to make short-term compensatory adjustments to their adhesive mechanism, movement across highly variable surfaces may well be expected to present a considerable problem.

Through laboratory and field studies this investigation will consider the various problems that might be expected as a result of the adoption of wet adhesion as the primary sticking mechanism by tree frogs, particularly with respect to the problems presented by increasing size. Trinidad is an ideal place to study the implications of scaling on adhesion in tree frogs as the twelve species of arboreal hylid found there range from amongst the smallest (i.e. *Hyla minuscula*) to the largest (i.e. *Hyla boans*) found in the world. Between adult frogs belonging to the smallest and largest species found in Trinidad a ten-fold increase in linear dimensions is represented. A similar scaling problem is represented by the increase in size that occurs between metamorphosis and adulthood, particularly in larger species of frogs such as *Hyla boans*. The study of Trinidadian hylids therefore presents the opportunity to investigate responses of the adhesive mechanism to the scaling-related problems that might be expected in tree frogs in terms of both development and evolution simply by considering the following questions on both an intraspecific and an interspecific level:

1. Does adhesive force produced in hylid tree frogs from Trinidad increase in direct relation to the toe pad area increase, as might be predicted from results of previous studies?
2. If this is the case then is there any evidence of an impediment to adhesive ability in larger frogs, are large frogs as able as small ones to adhere to smooth surfaces or is there a detrimental effect of increased size on sticking ability?
3. If such an effect is evident is there any evidence of compensatory adjustments to the wet adhesive mechanism that may be an attempt to counter these in larger frogs? These might be detected by considering the following:
 - a) Is there evidence of deviation from isometric scaling in terms of either the mass or area increase relative to the linear dimension that might aid adhesion in larger frogs i.e. does toe pad area increase at a greater rate than the linear dimension squared or mass increase at a lesser rate than the linear dimension cubed?
 - b) Is there evidence of changes in the properties of the intervening fluid layer evident beneath the pads of the tree frogs i.e. such as might be indicated by changes in spreading tendencies on smooth substrates of differing surface energies or alterations in depth of fluid layer?
 - c) Is there any evidence of development of accessory areas or supplementary adhesive mechanisms in larger frogs that may be a response to the pressures of increasing size? This seems likely in view of the fact that in most animals that utilise some form of adhesion, incidences of a single mechanism acting in isolation to others are extremely rare (**Chapter 1**). Most animals have a principle adhesive mechanism that dominates but a complementary secondary

adhesive mechanism that aids sticking ability under conditions that are not ideal for the primary mechanism.

- d) Is there any evidence of changes in toe pad morphology that may enhance the functional efficiency of their 'design' that can be directly related to adhesive ability? There is evidence from earlier studies that a number of aspects of toe pad morphology are influenced by the degree of arboreality typical of the tree frog species so any examination of pad design must also be examined alongside the ecology of each of the species under consideration.

Chapters 2 and 3 will consider these questions in relation to intraspecific trends in allometry and pad morphology in adult frogs from twelve species. Chapters 4, 5 and 6 will discuss interspecific trends in small, medium and large species of frog respectively:

2.2. Methods

2.2.1. Experimental animals

Experiments investigating adhesive abilities have been carried out on adults of twelve of the thirteen species of Hylid frog found in Trinidad (Murphy, 1997); *Flectonotus fitzgeraldi*, *Hyla boans*, *Hyla crepitans*, *Hyla geographica*, *Hyla microcephala*, *Hyla minuscula*, *Hyla minuta*, *Hyla punctata*, *Phrynohyas venulosa*, *Phyllomedusa trinitatis*, *Scinax rubra* and *Sphaenorhynchus lacteus*. The only Hylid tree frog not investigated, *Phyllodytes auratus*, is endemic and is legislatively protected and thus difficult to gain access to. For all species other than *Flectonotus fitzgeraldi*, adult frogs were collected from calling aggregations at breeding sites at various locations in Trinidad. *Flectonotus fitzgeraldi* were collected from searches of smooth-leaved bromeliads in an area of cloud forest in which the frogs were known to be breeding*.

Frogs were taken back to the lab where they were weighed and measured. Using callipers, snout-vent lengths (SVL) were ascertained for use as the comparative linear measurement, against which weight and adhesive forces will be analysed. This measurement from the tip of the nose to the urino-genital opening is the standard one for determining comparative sizes of frogs (Duellman, 2001), though some studies use the end of the backbone, the urostyle, as the posterior endpoint for the body length measurement (SUL). Weights were determined using an electronic balance accurate to 0.01g immediately prior to experiments to determine adhesive ability. In each species, the toe pads of front and back feet of at least one adult frog were

* For collection sites for all species see **Appendix 2**.

photographed through acetate marked with a grid of one millimetre square using a Polaroid MicroSLR camera attached to a binocular microscope. Toe pad area was then determined from these images (see **Figure 2.1**) using a digitiser program (Cherry Digitiser).

Distinctive dorsal and ventral markings were noted on ID sheets to allow for the identification of individual frogs. Sex was noted where possible. In some species there are sex-dependant external features such as horny nuptial pads on the front feet (e.g. *P. trinitatis*, *P. venulosa*) or prominent vocal pouches (*P. venulosa*) seen only in the males. In a number of species, males are the exclusively calling sex. In these, where a frog was known to have been calling at the time of collection, sex could be determined as male. As calling frogs at breeding sites are more easily located, then the ratio of males and females in most species is likely to be heavily skewed in favour of males. Female sex was determinable by external cues only in the cases where a visible egg mass or a brood pouch was present. Separating the sexes using the size dimorphism that is evident in many of these species by considering all frogs below a certain weight as male, is unsafe as juvenile female frogs may well be of comparable sizes to adult male frogs. If no calling behaviour was noted on capture, no egg masses were visible and no obvious physical characteristics other than size could be used as a reliable sex determinant, then the frog was classified as being of unknown sex. This is an important consideration as the assumption that all frogs without breeding male characteristics are female is unsafe, since these may include non-breeding males.

In all cases where a female was determined to be in a gravid state, the frog was measured both prior to and following egg deposition. Females were observed in a number of cases to have been carrying egg clutches equivalent to as much as 50% of their post-deposition weight and the potential effects of this extra mass on comparative allometry considerations necessitated the exclusion of data obtained from gravid females. No statistical differences between adhesive abilities in males and females in a non-gravid state (**Appendix 3.1**) were determined for the twelve species under investigation here, and so data for both were considered together for the purposes of all analyses pertaining to adult frogs.

Frogs were maintained in terraria for a maximum of one week before being released again at their original capture site. Animals were fed every two days on live insects and their weights monitored daily to check for any sudden decreases in weight, which led to an early release for the individual concerned.

2.2.2. Measurement of sticking ability

The adhesive abilities of the frogs were determined following the protocol of Hanna and Barnes (1991) (modified from Emerson and Diehl, 1980). Frogs were weighed immediately prior to use in adhesion experiments. Each frog was placed on a 'rotation platform' consisting of a Perspex sheet clipped to a wooden board which in its turn was attached to a kymograph spindle and smoothly rotated from 0° (horizontal) through 90° (vertical) to 180° (upside down) at an angular velocity of 3° s⁻¹. The angle at which the animal was seen to fall from the platform was recorded from a pointer attached to the platform which shows the angle on a 360° protractor attached to the base of the spindle (**Figure 2.2**). Frogs were caught as they fell from

the platform and rotations

repeated until ten

detachments were

recorded. It is important

to note that there are

limitations in this

methodology in that if

angles of 180° are

regularly recorded within

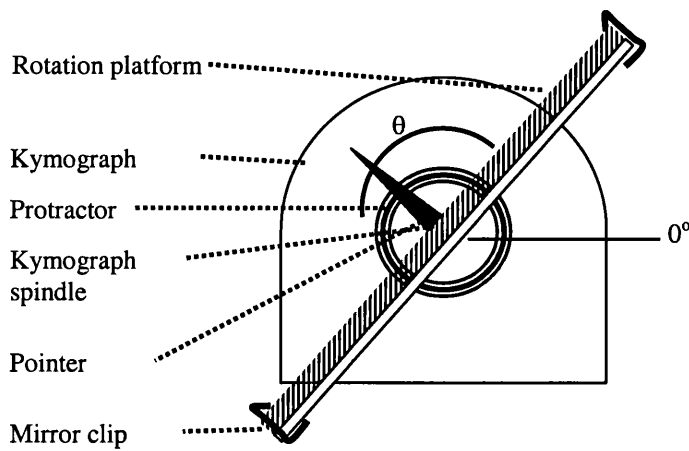


Figure 2.2: Rotation equipment used for determination of adhesive abilities of tree frogs.

a species then the adhesive abilities of such frogs that do regularly achieve maximum rotations are likely to be underestimates of the true ability. Angles of slip were also noted for most species, with this angle being the first at which the toes slid downwards on the substrate or the first at which the frogs were seen to replace their feet as the board rotated.

Perspex was used as the main substrate in these experiments to allow comparisons with earlier studies, (Emerson and Diehl, 1980; Hanna and Barnes, 1991; Tomlinson, 1995; Barnes, 1999). Adults from eight species of frog were also tested on six other surfaces: waxy leaves of the climbing fig, *Ficus nymphaeolia*; wood; glass; rubber and Teflon, to determine the effects of varying wettability properties on the ability of frogs to adhere to a surface. The relative wettabilities of these substrates were comparatively assessed from the mean contact angle formed by ten $50\ \mu\text{l}$ droplets of water on the surfaces, this angle being measured using a binocular microscope with a 360° eyepiece protractor.

Frogs were placed on the rotation platform so that they were facing 'head upwards' as it turned and records were only taken if they maintained this orientation throughout. This precaution was taken because that it has been found in the Cuban tree frog, *O. septentrionalis*, that frogs forced to maintain a downwards-facing orientation have impaired sticking ability (Hanna and Barnes, 1991). Frogs were prevented from jumping by the light cupping of hands around the frog as the platform rotated; this prevented the frog from seeing any objects onto which it might jump to escape and had a calming effect. Any instances where there was any suggestion that the frog jumped from the platform rather than fell were not recorded.

Many frogs also utilise additional areas of skin on the stomach and upper thighs when adhering naturally. Frogs were allowed to adhere as they wished for an initial observation rotation to determine the natural adhesive behaviours of each species (2.3.2). For rotations used in the calculation of adhesive ability, frogs were prevented from using their stomach and thigh skin by gently prodding the hindquarters – an action which causes the frogs to walk up the platform with accessory areas clear of the rotation platform. This means that any detectable differences in adhesive force are directly attributable to the toe pads only.

The bringing of the lower eyelid over the eye followed by the cessation of active attempts to maintain a hold on the surface were noted to be the main indicators that a frog was suffering from stress. When this behaviour was noted then the frog was misted with water and transferred to a darkened tank to calm down for at least half an hour before any experiments were resumed. The effect on frogs of stress, particularly in terms of the reduced effort on the rotation platform to maintain a hold upon the

surface is seldom been taken under consideration in studies where the methodology involves holding the frog in a harness. In the case of those species that are particularly prone to stress then the minimal amount of handling of the frog that is involved in this method makes this more valuable as a means of determining the true adhesive abilities of the frogs under natural conditions.

2.2.3. Calculating adhesive force

The angles at which frogs fall from the rotation platform can be used to calculate the adhesive force that the frog is exerting according to the simple geometry shown in **Figure 2.3**. This gives rise to the following formula for the calculation of adhesive force:

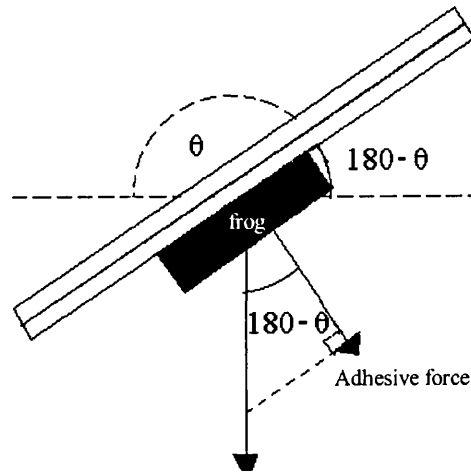


Figure 2.3:Geometric elements used in force calculations, where θ = detachment angle.

$$(2.3) \text{ Force} = \cos(180-\theta) \times \text{mass} \times \text{acceleration due to gravity} \quad (\text{Barnes, 1999})$$

2.2.4. Statistics

As a point of note: All statistics and graphs are generated using SPSS statistics software. This package does not have the functional capability to truncate lines of best fit to confine them to the edges of data sets and the lines of best fit on many graphs extend further than the parameters of the study can predict.

All statistical means are given in the format: $\bar{x} \pm 1 \text{ s.e.}$

2.3. Results

2.3.1. Morphometric analyses

Species	SVL (mm)		Weight (g)		Regression statistics			
	Mean	s.e.	Mean	s.e.	r	Slope	t	n
<i>H. minuscula</i>	17.98	0.69	0.45	0.03	0.97	<i>1.67</i>	9.50	12
<i>F. fitzgeraldi</i>	18.67	1.59	0.52	0.11	0.98	2.36	1.21	3
<i>H. minuta</i>	23.10	0.42	0.93	0.05	0.90	2.73	0.93	22
<i>H. microcephala</i>	23.63	0.76	0.91	0.10	0.94	3.16	0.44	12
<i>S. rubra</i>	30.23	0.60	2.02	0.08	0.66	<i>1.32</i>	3.11	10
<i>H. punctata</i>	33.42	0.24	2.43	0.08	0.49	-	-	12
<i>S. lacteus</i>	37.57	0.46	3.69	0.16	0.63	2.36	0.63	10
<i>H. geographica</i>	57.93	1.69	8.43	0.54	0.95	<i>1.99</i>	5.10	14
<i>H. crepitans</i>	63.35	0.98	14.14	0.67	0.63	1.85	1.60	12
<i>P. trinitatis</i>	74.44	1.86	21.39	2.78	0.89	3.45	0.92	15
<i>P. venulosa</i>	75.90	1.92	24.79	1.87	0.90	2.67	0.85	13
<i>H. boans</i>	94.86	1.15	44.72	2.29	0.86	3.56	0.74	10

Table 2.1: Adult snout-vent lengths (SVL) and weights from individuals collected in Trinidad 2000-2001 and within species regression statistics for the correlation of weight to SVL on a log log plot. Bold type indicates a significant correlative relationship; italics indicate where slope of increasing weight within a species differs significantly from the expected ($p < 0.05$). n = sample size, t = t-statistic for difference observed slope and the expected slope of 3.

Adult sizes in the twelve Trinidadian species of tree frog exhibit a range from the smallest, *H. minuscula*, (mean SVL: 17.98 ± 0.69 mm) to the largest, *Hyla boans* averages (mean SVL: 94.86 ± 1.15 mm) that represents an approximately five-fold increase in linear dimensions. The relationship between linear dimensions and weight in these Hylid tree frogs is illustrated in a log-log plot in **Figure 2.4 a**. There is a strong positive correlation between the two variables in this case with the slope of the line of best fit is significantly less than the slope of 3 that would be predicted by isometry ($t = 5.89$, $p < 0.01$, 10 d.f.) Between species, the ‘design’ of the frog has

become adapted so that the larger species are proportionally lighter than if they were simply directly scaled-up versions of the smaller species.

The area of toe in contact with the surface, between species, is also strongly positively correlated to the size of the frog and increases as expected, with no significant difference in the observed rate of increase in toe pad area with SVL (**Figure 2.4 b**) to the expected slope of 2 ($t = 1.68$, N.S. 10 d.f.). This indicates that larger species of frog do not have proportionally larger toe pads when compared with the smaller species.

If the change in linear measurements between the largest and smallest species is accompanied by an increase in weight as expected then the adhesive system in the largest species, *H. boans*, will need to be able to cope with a weight a hundred and twenty five times that in the smallest species, *H. minuscula*. The rate of weight increase is closer to a hundred-fold; which, whilst not as great an increase as expected, is still a considerable strain to place upon an adhesive system that is dependent chiefly upon surface area. With area increasing isometrically, an approximate twenty-five-fold increase in toe pad area (**Figure 2.4 b**) is all that is in place to counter a hundred-fold increase in weight. It is likely then that there will be a significant detrimental effect on the ability to adhere in larger species of frog.

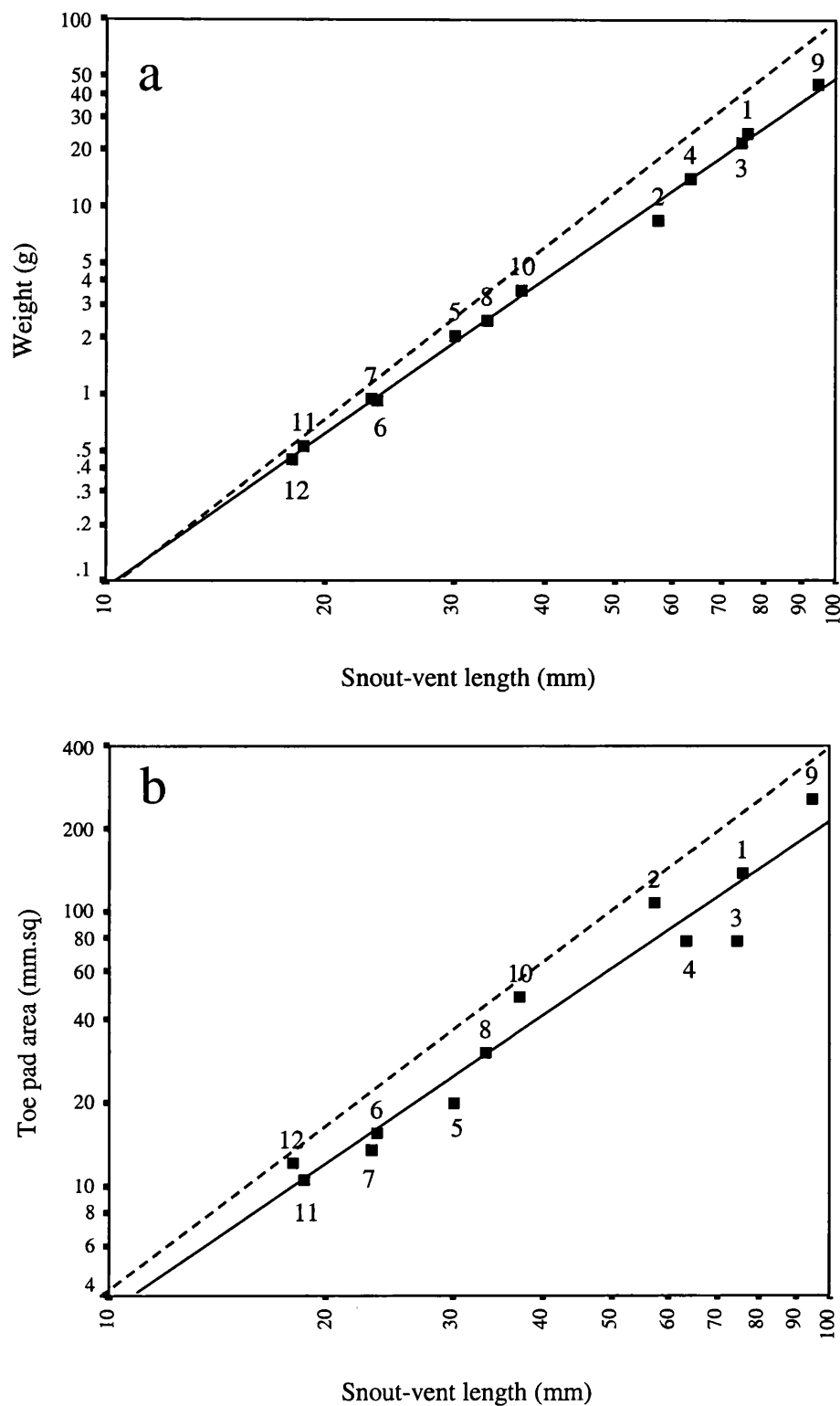


Figure 2.4: Log-log plots of species average values for SVL vs. (a) Weight. Correlative statistics: $r = 0.999$. Line of best fit $y = 2.72x - 3.75$, $t = 57.28$, $p < 0.001$, $n = 12$ (b) Toe pad area. Correlative statistics: $r = 0.97$. Line of best fit $y = 1.78x - 1.23$, $t = 13.61$, $p < 0.001$, $n = 12$. Dotted lines indicate predicted relationships following isometry (slope of 3 in a; slope of 2 in b). Species numbers: 1. *P. venulosa*, 2. *H. geographica*, 3. *P. trinitatis*, 4. *H. crepitans*, 5. *S. rubra*, 6. *H. microcephala*, 7. *H. minuta*, 8. *H. punctata*, 9. *H. boans*, 10. *S. lacteus*, 11. *F. fitzgeraldi*, 12. *H. minuscula*.

2.3.2. Size Effects on Adhesion

Behavioural responses

Behavioural strategies in place for falling avoidance in individual species are outlined in further chapters but in general can be defined by the way in which the frogs replace their feet as they start to slip. In general small frogs are ‘shufflers’ and tuck their feet beneath their body as they rotate whereas large species are ‘spreaders’, extending the limbs away from the body as they begin to fall:

Small species are often active on the rotation platform, walking across the surface on their toe tips, often able to adhere at angles of 180° like this. They make compensatory adjustments to their position on the board by drawing their feet under the body; the angle at which this adjustment is first made is often taken as the point at which shear forces first affect the frogs. All small frogs will attempt to adhere using ventral skin as the angle of the rotation board increases, particularly so *S. lacteus*, a species which has areas of particularly loose skin on the stomach and thighs compared to the other species.

Large frogs, with the exception of *P. trinitatis*, initially stick using accessory skin on the stomach and thighs if allowed to, drawing themselves close to the board. As the surface continues to rotate, this skin begins to slowly peel from the surface and the front feet begin to slip. In response to this, the frogs replace their front feet, often spreading the toes so that the webbing between them also touches the surface thus actively increasing the area of the foot in contact. Frogs will then alter their posture on the board by spreading their back legs wide; stretching them away from the body whilst at the same time holding the posterior end closer to the rotation surface as their situation becomes more precarious.

Slip and detachment angles

Species in order of increasing SVL	Slip angle			Detachment angle		
	Mean	± s.e.	N	Mean	± s.e.	N
<i>H. minuscula</i>	-	-	-	179.24	0.33	12
<i>F. fitzgeraldi</i>	-	-	-	174.66	3.98	3
<i>H. minuta</i>	81.78	2.18	15	157.35	3.78	22
<i>H. microcephala</i>	82.06	1.47	10	144.33	6.83	12
<i>S. rubra</i>	83.30	3.62	10	151.64	4.49	10
<i>H. punctata</i>	80.25	2.60	12	143.21	5.26	12
<i>S. lacteus</i>	87.50	4.61	10	142.53	2.44	10
<i>H. geographica</i>	68.20	-	1	149.52	3.83	14
<i>H. crepitans</i>	71.25	2.07	11	109.53	3.49	12
<i>P. trinitatis</i>	63.02	2.55	13	111.82	2.42	15
<i>P. venulosa</i>	83.38	1.42	12	120.35	4.00	13
<i>H. boans</i>	72.67	9.19	3	113.80	4.67	10

Table 2.2. Species average values for angles of initial slip and detachment on Perspex in adult frogs.

There are no within species effects of increasing size on the angles at which frogs slip or fall, with the one exception being *H. geographica*[†] ($r = 0.53$, $t = -2.19$, $p = 0.05$, $n = 14$). This suggests that strategies being employed within the species under investigation are generally compensating effectively for increasing weight with adult growth in spite of the fact that weight is increasing at a rate not significantly different to that expected through isometry, as $(SVL)^3$, in the majority of species (see **Table 2.1**). The average angles of slip and fall are significantly different between species, (ANOVA: $F_{\text{slip}} = 6.60$, $p = 0.001$, 9 d.f.; $F_{\text{fall}} = 27.93$, $p = 0.001$, 11 d.f.) and, looking at the species average values for the angles of initial slip and detachment on Perspex

[†] In this instance this negative correlative relationship is highly dependent on consistently poor performances of a single large female, the removal of which removes the effect of size seen within the species ($r = 0.27$, N.S., 13 d.f.) see **Chapter 5**.

(Table 2.2), it appears that there is a detrimental effect of species size on the ability to adhere to a rotating surface. There are negative trends in relationships between species for the angles at which the frogs slip and fall, and their size both in terms of the linear dimension (Figures 2.5 a and b) and weight[‡]. Angles of fall are more affected by increasing size between species than are the slip angles ($t = 2.99$, $p < 0.05$, 18 d.f.). It should be noted however that there is also a negative correlation between the percentage of detachment angles of 180° recorded within a species and the average linear dimensions ($r = 0.74$, $y = 6.28 - 0.09x$, $t = -3.43$, $p = 0.001$, $n = 12$). This means that smaller species have higher incidences of full rotations than in large species, making it fairly likely that greater adhesive forces might be recorded using different methodology in smaller species.

Linear dimensions and adhesive forces calculated from detachment angles are highly positively correlated between species (Figure 2.5 c) The line of best fit on this log/log plot has a slope that is not significantly different to the rate of increase in toe pad area seen in Figure 2.4 b ($t = 1.68$, N.S., 20 d.f.). Neither are adhesive abilities are scaling at a sufficient rate to match the corresponding weight increase between species seen in Figure 2.4 a ($t = 5.00$, $p < 0.01$, 20 d.f.). Adhesive forces generated per mm^2 of toe pad show a weakly positive correlation to the linear dimension between species (Figure 2.5 d) and range between 0.36 mN/mm^2 in *H. minuscula* to 1.10 mN/mm^2 in *P. trinitatis*.

[‡] Weight vs. angle of slip: $r = 0.53$, N.S. 9 d.f. Weight vs average detachment angle: $r = 0.76$, $t = -3.72$, $p = 0.004$, 10 d.f.

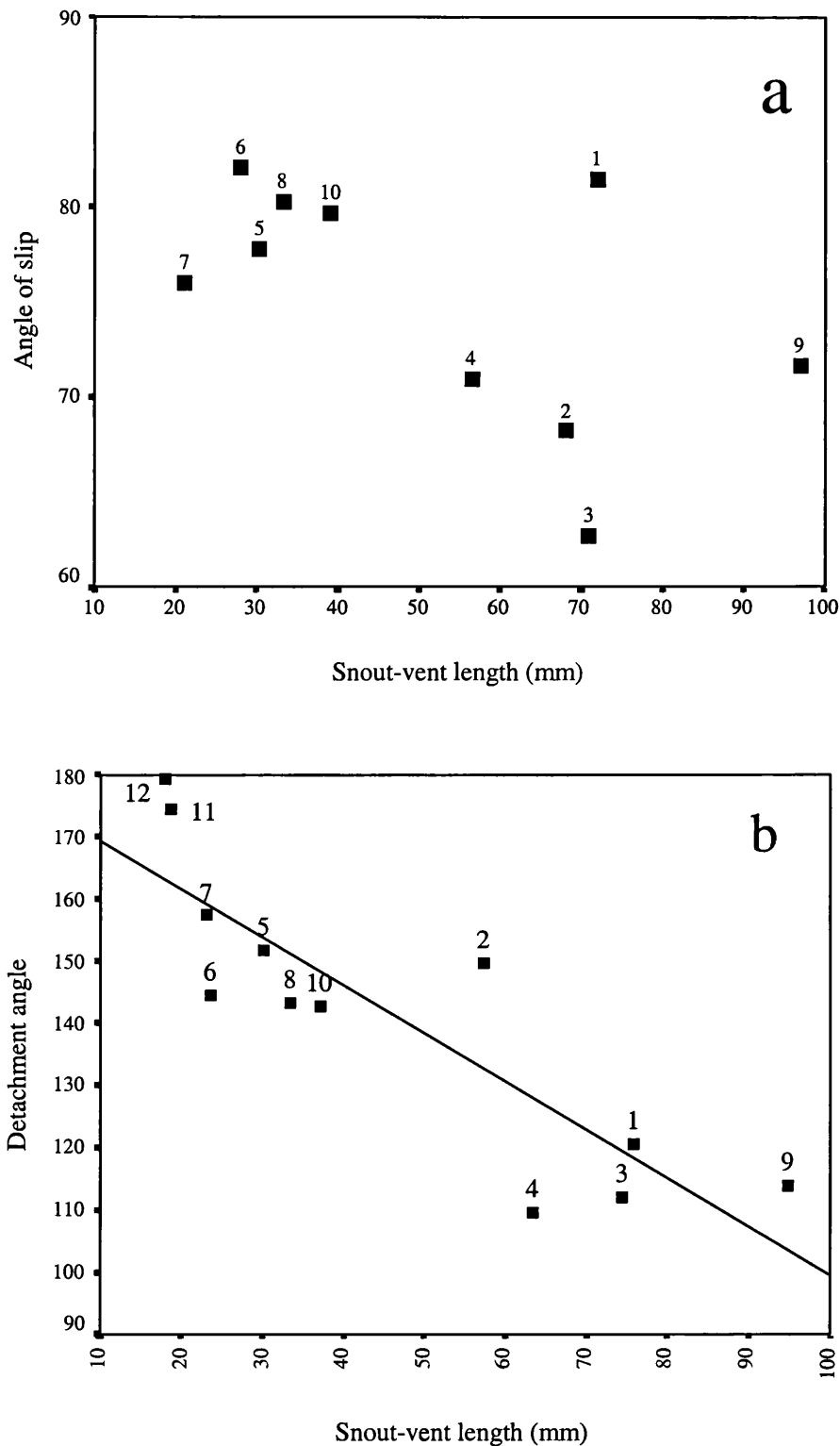


Figure 2.5: Species average values for: (a) Angle of initial slip vs. SVL. Correlative statistics: $r = 0.56$, $p = 0.09$, N.S. 9 d.f. (b) Detachment angle vs. SVL. Correlative statistics: $r = 0.87$, $p < 0.05$, 11 d.f. Line of best fit: $y = 177.11 - 0.78x$, $t = -5.49$, $p = 0.001$, 10 d.f. Numbers indicate species as follows: 1. *P. venulosa*, 2. *H. geographica*, 3. *P. trinitatis*, 4. *H. crepitans*, 5. *S. rubra*, 6. *H. microcephala*, 7. *H. minuta*, 8. *H. punctata*, 9. *H. boans*, 10. *S. lacteus*, 11. *F. fitzgeraldi*, 12. *H. minuscula*

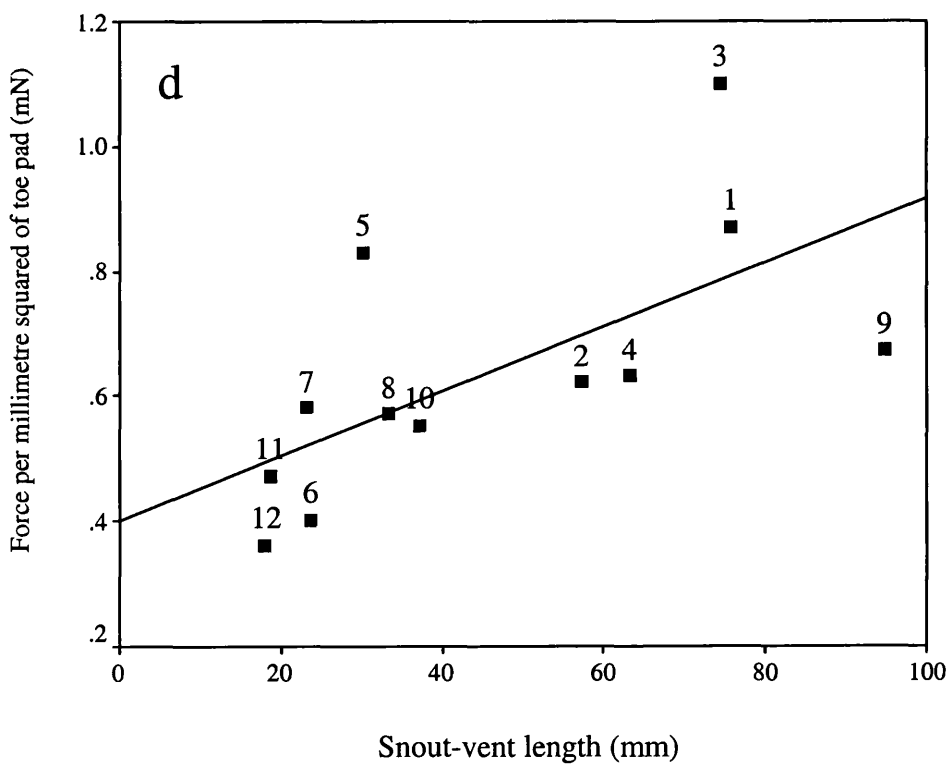
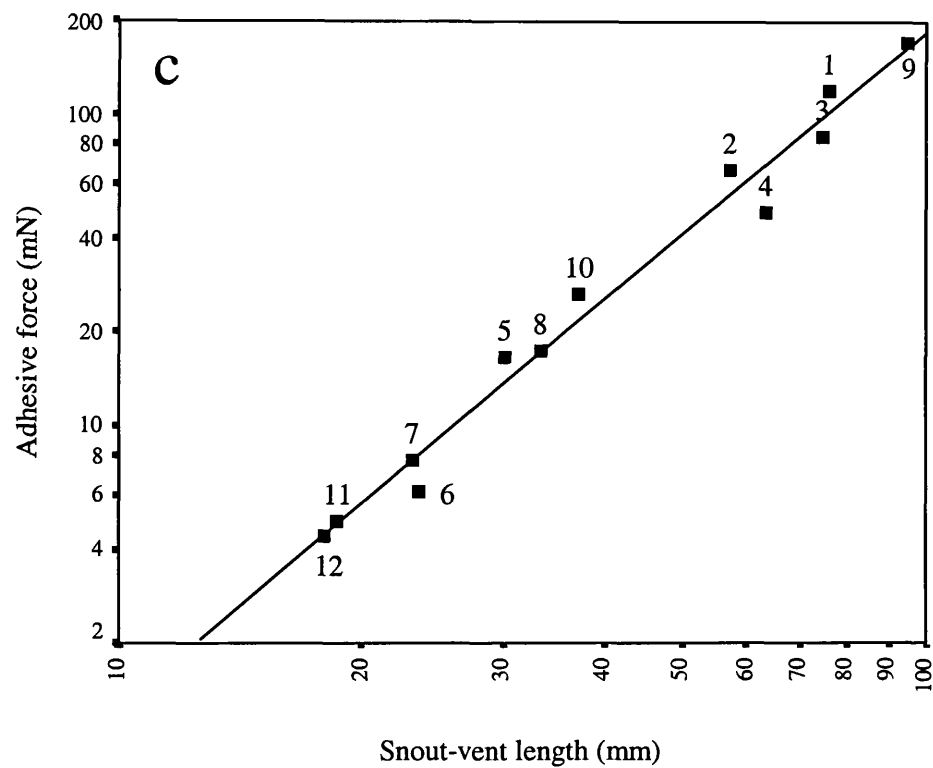


Figure 2.5 cont.: Species average values for (c) Adhesive force vs SVL on a log-log plot. Correlative statistics: $r = 0.99$, $p < 0.05$, 11 d.f. Line of best fit: $y = 2.17x - 2.08$, $t = 22.51$, $p < 0.001$, 10 d.f. (d) Adhesive force per mm² of toe pad vs SVL. Correlative statistics: $r = 0.64$, $p < 0.05$, 11 d.f. Line of best fit: $y = 0.005x + 0.40$, $t = 2.66$, $p = 0.02$, 10 d.f. Numbers indicate species as follows: 1. *P. venulosa*, 2. *H. geographica*, 3. *P. trinitatis*, 4. *H. crepitans*, 5. *S. rubra*, 6. *H. microcephala*, 7. *H. minuta*, 8. *H. punctata*, 9. *H. boans*, 10. *S. lacteus*, 11. *F. fitzgeraldi*, 12. *H. minuscula*.

2.3.3. Effects of Surface Wettability on Adhesion

Eight species of frog were rotated on six surfaces in addition to Perspex: the waxy leaves of the climbing fig (*Ficus nymphaeolia* Mill.), wood, glass, rubber and Teflon. These materials were selected for the likelihood of there being differences in their surface energies (and hence their wettability). To quantify these in a comparative way, values for contact angles of a droplet of water were obtained: as the degree to which water will tend to spread is inversely related to the surface energy of the surface on low

Material	Contact angle	\pm s.e.	n
Glass	1.10	0.31	10
Wood	2.90	0.15	10
Top leaf	17.40	1.49	10
Perspex	36.10	0.71	10
Rubber	44.50	1.45	10
Teflon	73.50	1.83	10
Under leaf	115.40	2.59	10

Table 2.3. Average values for contact angles of water droplets on each surface.

surface energy surfaces droplets will tend to 'bead up', producing droplets with higher contact angles. Contact angles are therefore inversely proportional to the wettability of a surface (Baier, 1970) i.e. the lower the contact angle value, the higher the wettability of a surface.

The average angles of slip and the angles of detachment (**Appendix 4**) in the majority of the species studied are significantly different from one another on the different materials upon which the frogs were tested (**Table 2.4**). However there is no correlative effect of the surface energy of the material, as estimated by the contact angle formed by a droplet of water upon the surface, for any of the species studied (**Table 2.5**). This table shows that in all of the species under consideration there is a negative trend towards lower angles of detachment as a result of decreasing substrate wettability, (i.e. increasing contact angle) but this is only statistically significant in

three of the eight species (**Figure 2.6**), and only marginally non-significant in *H. crepitans*. This suggests that the other four species are able to make short-term adjustments to aspects of their adhesive mechanism to compensate to some extent for the effects of the differences in the wetting properties of the surfaces. That slip angles are not significantly affected by differences in the surface energies of the substrates suggesting that the resistance to shear is not as dependent on capillarity as adhesion.

Species	Slip angles			Fall angles		
	F	Sig	d.f.	F	Sig	d.f.
<i>H.minuta</i>	16.40	0.001	6	4.24	0.001	6
<i>H. microcephala</i>	4.74	0.001	6	3.86	0.004	6
<i>S. rubra</i>	6.71	0.001	6	1.42	0.228	6
<i>H. punctata</i>	12.28	0.001	6	6.95	0.001	6
<i>S. lacteus</i>	9.86	0.001	6	10.55	0.001	6
<i>H.crepitans</i>	32.10	0.001	6	8.37	0.001	6
<i>P. trinitatis</i>	6.55	0.001	6	3.04	0.011	6
<i>H. boans</i>	1.35	0.360	6	1.36	0.279	6

Table 2.4: ANOVA statistics comparing angles on seven surfaces of differing wettability. Significant ($p < 0.05$) results designated by bold type.

Species	Slip vs. contact angle			Fall vs. contact angle		
	R	t	Sig	R	t	Sig
<i>H.minuta</i>	0.71	-2.22	0.10	0.59	-1.62	0.17
<i>H. microcephala</i>	0.66	-1.95	0.11	0.90	-4.64	0.01
<i>S. rubra</i>	0.68	-2.05	0.10	0.40	-0.97	0.38
<i>H. punctata</i>	0.45	-1.13	0.31	0.54	-1.43	0.21
<i>S. lacteus</i>	0.22	-0.50	0.64	0.75	-2.57	0.05
<i>H.crepitans</i>	0.52	-1.35	0.24	<i>0.74</i>	<i>-2.47</i>	<i>0.06</i>
<i>P. trinitatis</i>	0.38	-0.91	0.41	0.82	-3.17	0.03
<i>H. boans</i>	0.26	-0.61	0.57	0.13	-0.30	0.77

Table 2.5: Regression statistics for angles vs wettability on seven surfaces. Statistically significant results ($p < 0.05$) designated by bold type. Marginally non-significant results italicised.

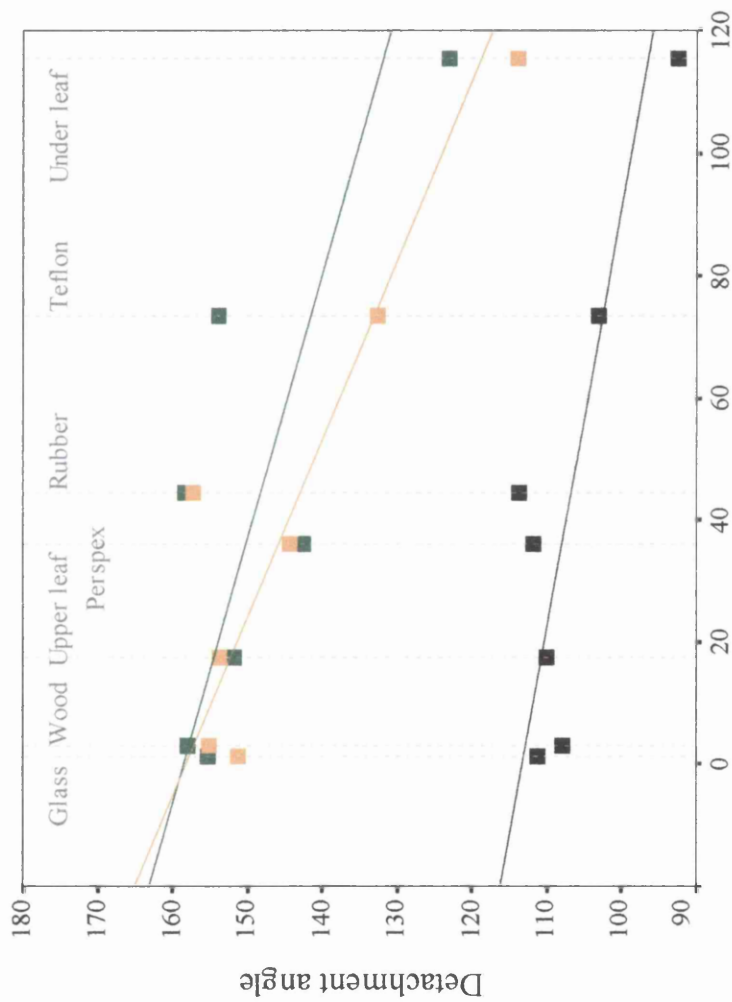


Figure 2.6: Average angles of detachment in three species on seven substrates according to contact angle of water droplets on their surface. Correlative statistics for, *P. trinitatis*: $r = 0.82$, $p < 0.05$, 6 d.f. Line of best fit $y = 113.25 - 0.15x$, $t = -3.17$, $p = 0.03$, 5 d.f. *H. microcephala*: $r = 0.90$, $p < 0.05$, 6 d.f. Line of best fit $y = 158.30 - 0.34x$, $t = -4.64$, $p = 0.006$, 5 d.f. *S. lacteus*: $r = 0.75$, $p < 0.05$, 6 d.f. Line of best fit $y = 158.60 - 0.23x$, $t = -2.57$, $p = 0.05$, 5 d.f.

2.4. Discussion

The adhesive mechanism in a number of species of frog has been found to be strongly dependent on the toe pad area in contact with the surface. This being the case, the question arises as to the efficacy of the adhesive mechanisms being used when the pressure of increasing size is placed upon the system. This study aimed to investigate this and to provide baseline information on the adhesive mechanisms in effect in the adults of the particular species in which the development of adhesion will be discussed in the following chapters.

Looking at a range of different species then, how does the adhesive mechanism cope with an increase in weight between the smallest and largest species that can be as much as twenty times greater than the equivalent increase in toe pad area? Evidence from the twelve species under investigation here suggests that it does not, as the ability to adhere to a surface is detrimentally affected by increasing size between species. The angles to which large frogs are able to maintain a hold are significantly less than the angles attained in the smallest species: indeed, in *H. minuscula* ($0.45\text{g} \pm 0.03$, $n = 12$) 94.20% of all angles recorded were 180° compared with none at all in *H. boans* ($44.72\text{g} \pm 2.29$, $n = 10$). The prevalence of 180° angles recorded in the small species means that when considering the relationship between linear dimensions and adhesive forces in frogs, the slope is likelier to be steeper than if maximal forces were calculable for the smaller species. Notwithstanding, it is clear that adhesive forces are not increasing any faster than the equivalent rate of toe pad area increase between species in these frogs. This is as expected from studies on other species and is as predicted for a system dominated by capillarity forces.

If the effect of area is removed then the force per unit area of toe pad can still be seen to be increasing in larger species (**Figure 2.5 d**). This suggests that the pads of larger species are able in some way to adhere more efficiently than those of smaller species, although ultimately these improvements are not sufficient to compensate for the differences in weight between the largest and smallest species since larger species are not able to achieve such high detachment angles. There is also evidence that, within the majority of species, the frogs are able to increase the efficiency of their toe pads so that although sticking abilities are altered they are not significantly affected by changes in substrate wettability that might be expected to have a detrimental on their adhesive abilities (**Table 2.4 and 2.5**).

How then might this increase in toe pad efficiency be effected? There are a number of possibilities; firstly, changes may be occurring within the adhesive mechanism whereby the properties of the meniscal layer are altered to improve efficiencies and secondly, there may be changes in toe pad morphology that affect toe pad efficiency. For the moment this discussion will concentrate on the first of these possibilities, for consideration of what allows within and between species improvements in toe pad efficiency; there is insufficient evidence to examine whether toe pad morphology is significantly different between individual frogs of the same species and **Chapter 3** examines changes in toe pad morphology between species in relation to the adhesive abilities that the frogs are able to generate.

That the results here suggest that the adhesive system in place in these frogs is likeliest to be predominated by capillarity forces is not to discount entirely the effects of viscosity within the system. Indeed, one feature of capillarity is that there is no

inherent resistance to the application of slow continuous shear force (Denny, 1988; Hanna and Barnes, 1991), so the recording of angles of slip over 90° in a number of individuals in this study suggests that there is at least some influence of viscosity forces on adhesion in tree frogs. Frogs are capable of manufacturing far stronger adhesive secretions than the capillarity model first discussed in Nachtigall (1974) predicts, which suggests that the intermediate liquid layer involved in tree frog adhesion is analogous in properties to water. Evans and Brodie's (1994) study on adhesive secretions produced in a variety of amphibians, found that one of the frogs in this study, *Phrynohyas venulosa*, is capable of producing allergenic mucus as an anti-predator device with a tensile strength of 54 mN/mm². If this species were to produce similarly 'strong' mucus on their toe pads, the area of the toe pads in *P. venulosa* would be capable of supporting a frog of around 750g in weight at 180° from the horizontal. That this is not the case suggests that frogs are not producing mucus to the same degree of stickiness that they are capable of for use in their adhesive mechanism, though this is perhaps not surprising if the effect that having mucus of this strength on the size of detachment forces that would be required on every step is considered. High detachment forces are likely to impede a frog's ability to jump (Hanna and Barnes, 1991), certainly there is some experimental evidence that jumping ability in *Osteopilus septentrionalis* is adversely affected by increasing mucosal viscosity (Barnes, 1999; Barnes *et al.* 2002). As the ability to jump long distances is of particular importance to tree frogs both as a means of moving across gaps between trees and as a predator avoidance strategy, it is therefore likely that the consideration of maintaining this ability is a major limiting factor on the maximum viscosity of the mucus utilised in adhesion.

There is some evidence that, interspecifically, the allometric ‘design’ of the frog for adhesion has become adjusted to attempt to compensate for the fact that weight increases at a far greater rate than the equivalent increase in toe pad area. This is not affected in the hylid frogs studied here as between some others (McAllister and Channing, 1974; Green, 1979) by larger species of frog possessing proportionally larger toe pads than seen in the smaller species. Toe pad area between these species increases as expected through isometry, as the linear dimension squared. Increase in weight, however, does differ from isometric predictions, so that larger species of frog are proportionally lighter than if they were simply scaled up versions of the smaller species. This may well be an adaptive response to the adverse effects of increasing weight on adhesion but it is important to note that trends in allometry cannot be considered in isolation from the effects they may have on other aspects of the frogs’ locomotory abilities. This is particularly the case with respect to aspects of jumping performance in these frogs. There is evidence within several species of frog that although jumping distances are positively correlated with increasing weight, jump acceleration is negatively affected (Emerson, 1978; Wilson *et al.* 2000). At the same time jump distance has been found to positively correlate to increasing hind limb length and musculature (Zug, 1972; Peplowski and Marsh, 1997) and in some species to weight (Emerson, 1978; Choi *et al.* 2000). As relative hind limb lengths do not alter significantly between *Hyla microcephala* and *Hyla boans*, (Tibia:SVL ratios of 0.516 and 0.517 respectively; Duellman, 2001), it would be an advantage to keep weight increases to a minimum if the speed of escape were the prime consideration in the jumping ability of these species. Trends in weight increase may, therefore, reflect differences in the relative advantages of jump distance vs. speed according to the degree of arboreality and predation threat between species (see later chapters).

According to meniscal theory, capillarity forces are a product of the pressure within the meniscus and the surface tension of the intermediate liquid layer according to the following relationship:

$$(2.4) \quad F = \pi r^2 \gamma \left[\frac{1}{r} - (\cos\theta_1 + \cos\theta_2) \cdot \frac{1}{h} \right] + (-2\pi r \gamma) \quad (\text{Zhu, 1999})$$

where F = adhesive force per pad; r = radius of the meniscus; γ = surface tension of the fluid; θ_1 = contact angle of water on substrate; θ_2 = contact angle of water on toe pad and h = meniscus height.

If the size dependent elements of this formula are fixed, as is the case where we consider the force per unit area of toe pad in frogs adhering to the same substrate (**Figure 2.5 d**) then the only factors that may be changing between species are: wettability of the pad surface ($\cos\theta_2$); the height of the meniscal layer (h) and the surface tension of the intermediary liquid layer (γ). Given the high degree of similarity seen in pad morphology between species (Green, 1979), and the assumption that the pads have evolved for their function it seems a fairly likely that the pad will be wettable, with θ_2 tending to zero. Little is known of the specific nature of the mucus so the effects of the changes in composition that would increase the surface tension are not known and it is difficult to predict the effect that this might have on other mucosal properties, such as viscosity. If frogs were effecting changes in properties of the mucus in terms of the surface tension or viscosity as a response to finding themselves on surfaces of differing wettability then this would require a feedback mechanism to elicit these changes and is unlikely to be effected quickly enough to respond to the challenges presented as they encounter surfaces with differing wettability as they move through their environment i.e. in a frog jumping from tree trunk to the upper leaf surfaces of a waxy epiphyte.

The most likely of the elements within this formula to be easily manipulated both within and between species is the meniscal height between the pad and the substrate. Using adhesive forces and the allometric measurements from this study, theoretical active meniscal heights were modelled for adult frogs belonging to each of the twelve species under investigation following the rearrangement of **Formula 2.4**:

$$(2.5) \quad h = \frac{(\cos\theta_1 + \cos\theta_2)}{\frac{1}{r} - \left(\frac{F + 2\pi r\gamma}{\pi r^2\gamma}\right)}$$

where F = adhesive force per mm^2 ; r = radius of the meniscus; γ = surface tension of the fluid; θ_1 = contact angle of water on substrate; θ_2 = contact angle of water on toe pad and h = meniscus height.

All ten species of frogs tested on glass, with a surface energy of 0.17 mN/mm (Denny, 1988), adhere comfortably to angles well beyond the vertical. This suggests that the mucus is able to completely wet the substrate and so must have a lower surface tension value than glass. A number of studies of tree frog adhesion have suggested that the mucus involved in tree frog adhesion is likely to have similar properties to water, as far as viscosity is concerned (Nachtigall, 1974; Green, 1981a; Emerson and Diehl, 1980). If we assume that surface tension properties of the mucus are also similar to those of water at 0.073 mN/mm (Pellicer, 2002), this falls well below the upper limit imposed by the observation that frogs exhibit good adhesive abilities on glass. Using this surface tension value in the model proposed in **Formula 2.5**, resultant meniscal depths proposed beneath the pad range between 0.1 and 1 mm (**Figure 2.7**). Novel fluorescence microscopy techniques are at present being developed by researchers at the University of Glasgow (Riehle and Barnes, in prep.) and are being used to attempt to measure meniscal heights in live frogs. The technique is limited, and can only be used for very small individuals on a horizontal

plane at present so that meniscal heights are likely to be overestimates as frogs sitting on a flat horizontal plane will not need to exert force and may not be have pads pressed as close to the surface as would be necessary during adhesion to more inclined substrates. Notwithstanding, values for juvenile *P. venulosa* obtained using this methodology range between 0.5 and 6 μm (Bausch, 2000), several orders of magnitude lower than those derived from this model. If these parameters are in the correct range then the surface tension of the mucus that effects adhesion would need to be between 3×10^{-5} and 3×10^{-4} mN/mm according to the model in **Formula 2.5**. Typical values for the surface tension of low concentration mucus* provides further evidence of the inadequacy of this model with respect to adhesion in tree frogs.

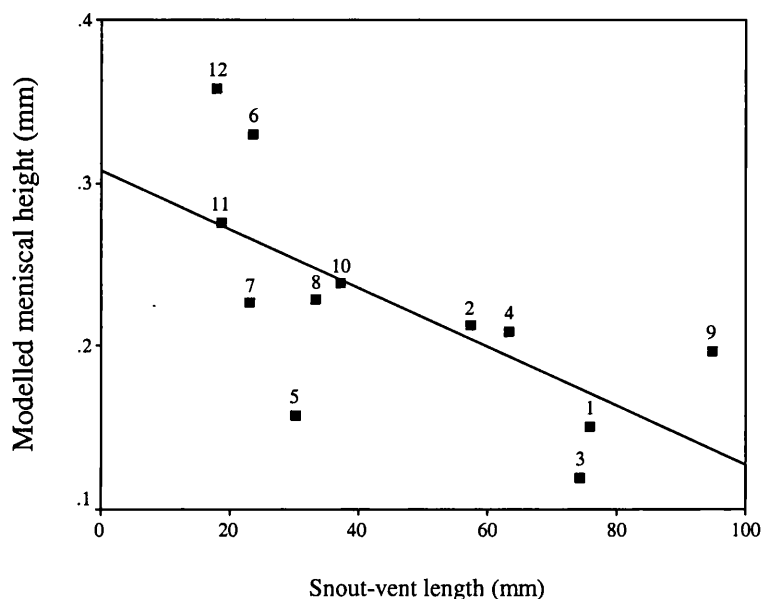


Figure 2.7: Theoretical meniscal heights on Perspex vs. linear dimensions using model based on Zhu, 1999 (assuming fixed mucosal properties similar to water). Correlative statistics: $r = 0.68$, $p < 0.05$, 11 d.f. $y = 3.09 - 0.02x$, $t = -2.91$, $p = 0.016$, 10 d.f. Numbers indicate species as follows: 1. *P. venulosa*, 2. *H. geographica*, 3. *P. trinitatis*, 4. *H. crepitans*, 5. *S. rubra*, 6. *H. microcephala*, 7. *H. minuta*, 8. *H. punctata*, 9. *H. boans*, 10. *S. lacteus*, 11. *F. fitzgeraldi*, 12. *H. minuscula*.

* Values pertain to mucus from vertebrate stomach and lungs where the functional requirements of mucus are very different to those for adhesion. Nevertheless, values for mucus of 95% water content (and therefore 5% mucopolysaccharide content) range from 0.053 to 0.167 mN/mm (DeNeuville *et al.* 1997). Similar surface tension values of 0.058 mN/mm are recorded in rabbit stomach mucus (Mack *et al.* 1994).

The discrepancies between the range of values in meniscal heights suggested by microscopy techniques and those modelled using Zhu (1999) suggests that the model is not sophisticated enough to take into account functional aspects of the adhesive structures in frogs that might be expected to have an effect on the adhesive forces. There are a number of aspects of tree frog adhesion that are not accounted for in this model which assumes that the surfaces being held together by the thin layer of fluid are two flat, rigid continuous plates. The substrates to which the frogs are adhering may fulfil these criteria but the pads have curvature and deformability that means that they do not fit the assumptions of this model. Furthermore, the contact surface of the pad does not present a continuous interface (see **Chapter 3**) but has channels across it, the effects of which will not be accounted for by this model. These parameters may well differ between species and if so might be expected to have an effect on the adhesive abilities of the frogs. We have so far been unable to make quantitative measurements of these in live adhering frogs for the twelve species considered here and it is therefore difficult to predict the relative effects of these on the trends in adhesive ability seen between species in this case. It is of some importance for the development of a more sophisticated predictive model for wet adhesion in tree frogs that future studies develop a better understanding of the degree of deformability inherent in the pad structure, and attempt to make measurements of other aspects of the pad structure in live adhering frogs that will have an effect on functionality. At present, the inability to make such measurements in live frogs means that meniscal heights cannot be easily modelled from forces seen in the species. Predictions about the ability of frogs to effect changes in their adhesive mechanism might be possible through the consideration of aspects of toe pad morphology that may promote a reduction in meniscal height.

If large frogs are able by some mechanism to get their toe pads closer to the substrate than smaller species then this may be a way in which an individual frog may be able to make short-term adjustments to the way in which they are adhering to substrates to compensate for small fluctuations in weight or for changes in the properties of the substrate to which they are attempting to adhere. Controlling the volume of liquid present beneath the pad may effect a change in meniscal height which allows a closer degree of conformation to the substrates. The simplest ways in which this might be effected are likely to be through a proportional reduction in the volume of mucus released onto the pad or by an increased degree of drainage of mucus from the pad or by a combination of both. In either case, changes in the pad structure at a micro structural level may be indicative of ways in which frogs might be able to alter their adhesive mechanism to explain the increase in pad efficiency seen in larger species, i.e. if lower mucus volumes are secreted then a trend towards a reduction in pore densities in larger species might be expected; if there is an increase in the efficiency of removal of excess mucus from beneath the pad then there may be an increased level of development in the drainage channels on and around the pad evident in these frogs. It is of importance to the further elucidation of the frogs' adhesive mechanisms that the morphology of the toe pads in the different species is considered to ascertain whether there are any changes with increasing size that may allow for adjustments to the adhesive mechanism in Hylid frogs. This will be the focus of the next chapter.

Chapter 3: Morphology of adhesive structures in adult tree frogs

3.1. Introduction

The possession of specialised toe pads has become a taxonomic characteristic in many families in which the feature is prevalent, particularly amongst frogs in the families Hylidae, Microhylidae, Centrolenidae, Rhacophoridae, Hyperolidae, Leptodactylidae and Dendrobatidae (Duellman and Trueb, 1997). The family Hylidae is of particular interest in the context of this study, being the family to which the majority of the Trinidadian examples of frogs with toe pads belong.

The high incidence of arboreal lifestyles within the aforementioned families has meant that such frogs are often considered under the common heading of ‘tree frog’, though in actuality this encompasses a number of species with a great degree of variation in their levels of arboreality; the family Hylidae, which are all known under this heading, range from fossorial species such as *Cyclorana brevipes*, specialised for digging and desert life, to complete arboreal specialists such as the Gliding Leaf Frog, *Agalychnis spurelli*.

Digital pads are also found on a number of other species, in particular in the so-called ‘torrent’ and ‘stream’ frogs, which at various stages of their life histories frequent fast-flowing mountain streams and rivers. Specialised toe pads can therefore be demonstrated to have evolved in several lineages, in all of which their presence is a derived characteristic (Lynch, 1974). In view of the range of species in which these toe pads are found, it is perhaps of some surprise that their morphology is remarkably

similar, even between species in which the pads have evolved independently (Hertwig and Sinsch, 1995). The degree of convergence in toe pad structure in the diverse families in which they are found suggests that their evolution has arisen in response to a functional requirement of the species' life histories. In spite of the wide variation in these, common ground does exist between frogs with toe pads; all inhabit environments in which the likelihood of dislodgement from a substrate is heightened due to increased exposure to extreme external factors. This dislodgement may result in the dashing of the frog against rocks or in a fall from a great height, both of which would be likely to be injurious to the animal. It seems reasonable to assume then that the evolution of toe pads is a response to a challenge of the environment that requires the animal to be able to adhere more firmly to the substrates within its habitat.

In the species in which highly evolved toe pads are found, the pad is distinguished from the non-specialised ventral surface of the toe by the presence of specialised epidermal cells covering an expanded disc at the distal end. The epidermis on the pad is substantially thicker than the ordinary epithelium, and can be as much as three times the thickness of the dorsal epithelium (Ba-Omar *et al.* 2000). Typically the pad epidermis consists of six to eight cell layers (Ernst, 1973a; Richards *et al.* 1975; Hertwig and Sinsch, 1995), which differentiate gradually into columnar cells with hexagonal apices, separated from one another by intercellular channels. Surface architecture is usually obscured from view by the presence of a dense cell coat, which gives the apices a smooth appearance at all but the highest magnifications. Tonofilament bundles fill densely packed villus-like processes evident beneath the cell coat in many instances, and run parallel to the longitudinal axes throughout the matrix of the cell, forming a filamentous cytoskeleton which confers rigidity to the

cells and which may act to resist compression (Green, 1979). The cytoskeletal elements are visible on the sides of the cells that form the intercellular channel walls as striations and convoluted ridges running from base to apex, which appear complementary on adjacent cells (Ernst, 1973a).

If Transmission Electron Microscopy (TEM) and Scanning Electron Microscopy (SEM) images of the pad epidermis are compared between species, the intercellular channels can be seen to differ in both depth and width. Of these the former is the least variable and is generally around a third of a lateral cell length, between 10 and 20 μm (values derived from measurements of images in Ernst, 1973a; Welsch *et al.* 1974; Green, 1979; McAllister and Channing, 1983; Hertwig and Sinsch, 1995). The channels are thought to allow the individual cells to find their closest contact with the substrate upon which the pads are placed (Green and Carson, 1988) and act to disperse mucus which is produced in glands that open out onto the surface of the pad (Ernst, 1973b; Emerson and Diehl, 1979).

The mucosal glands on the toe pads of tree frogs empty onto the surface of the pad through a duct that opens to pores that are around 7-8 μm in diameter (Green and Simon, 1986). Ernst (1973b) proposed that the mucosal glands on frog feet are emptied by a combined mechanism of the smooth muscle and collagen bands that surround the dermal glands. Under horizontal conditions, smooth muscle acts on the glands to facilitate mucus secretion but when the frog becomes vertical the glands become fully emptied mechanically as the effect of gravity acting on the weight of the frog pulls together the collagen bands that surround the dermal glands.

The glands fall into two types, classified by differences in the sculpturing of the cell walls facing the pore opening (Green, 1979). Type I glands are defined by the lining of the ducts lined with striations that appear no different to the normal sides of the columnar epithelium of the pad. Type II glands on the other hand have duct linings that are modified in comparison to the cell sides, with a roughened, non-striated appearance conferred by the presence of numerous microvilli on the luminal surface (Ernst, 1973 b). In the species that have so far been investigated, Type I glands are restricted to the 'Old World' non-Hylid tree frogs, being found in the hyperoliid genera (Richards *et al.* 1978; McAllister and Channing, 1983) and in one Rhacophorid species (*Polypedates leucomystax*: Green, 1979). Type II glands are found in all Hylid and Microhylid species investigated in previous studies (Green, 1979; Green and Simon, 1986) and in a number of Rhacophorids (Welsch *et al.* 1974; McAllister and Channing, 1983).

The pad area is further delineated from the non-specialised area of epidermal cells by two grooves around the edges of the pad: at the circumferal and the proximal margins (**Figure 3.1**). Green (1979) suggests that the presence of grooves at the circumferal and proximal margins are an artefactual effect of the meeting of the discontinuous cell types in these regions. However the correlation between the degree of development in

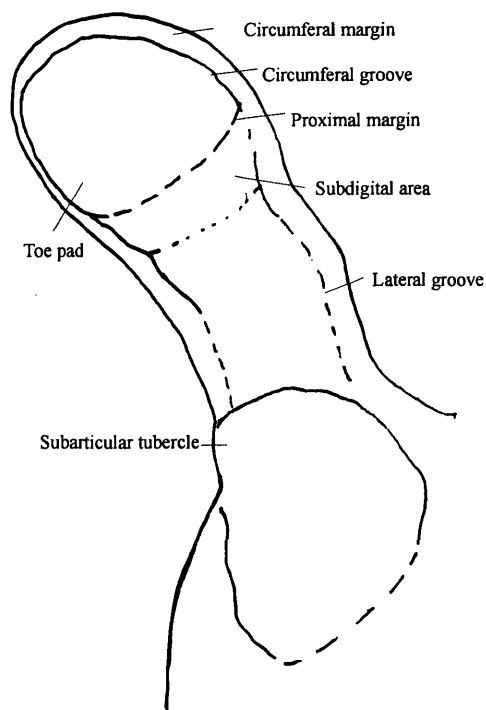


Figure 3.1. Diagrammatic representation of digital morphology in an adult tree frog

both areas and arboreality suggested in later studies (McAllister and Channing, 1983; Green and Simon, 1986) implies an adaptive function of these structural features. McAllister and Channing (1983) found wider circumferal margins and more complete circumferal grooves around the pad in more arboreal species, suggesting that the grooves seen around the pad may function as a reserve for the mucus used in wet adhesion.

A number of comparative studies have explored the relation of the structural development of the digital area to the levels of arboreality seen between species (Welsch *et al.* 1974; Green, 1979; Green, 1980; McAllister and Channing, 1983; Green and Simon, 1986; Hertwig and Sinsch, 1995). One finding upon which these studies agree is that structural complexity, in terms of the extent of specialisation of cell types seen on the terminal phalanx and on the subarticular tubercles, increases according to the degree of arboreality seen in a species. Green and Simon's (1986) study of frogs from the Microhylid genus *Cophixalus*, found demonstrably progressive development in cells that cover the distal end of the digit between species. Semi-fossorial species (active under leaf-litter) possess only non-specialised squamous epithelium with no development of the accessory adhesion areas. In terrestrial species (active in open on ground), both pad and accessory structures are covered with epithelium of a cuboidal nature, intermediary in the degree of their specialisation. This cell type is also found in semi-arboreal species but only on accessory adhesive areas; toe pads were covered with specialised columnar cells of the type described earlier. In the most arboreal of the species studied both toe pads and subarticular tubercles were covered in these highly specialised columnar cells. The exclusively tree-dwelling species, *Rhacophorus reinwardti*, has an additional

specialised cell type with a brush border, strikingly similar in structure to the setae on the digital lamellae of geckos (Welsch *et al.* 1974).

The means by which the specialised structure of the toe pad enhances a frogs' ability to maintain a hold on substrates within their environment has been a source of curiosity since the early twentieth century (Hora, 1923; Noble and Jaeckel, 1928). As discussed in **Chapter 2**, consensus from more recent studies of adhesion in a number of species (Emerson and Diehl, 1980; Green, 1981a; Barnes, 1997; Hanna and Barnes, 1997) suggests that frogs adhere to substrates by the means of wet adhesion, primarily influenced by capillarity forces and thus by contact area. This being the case, it might be expected that larger species would run into particular difficulty in matching adhesive ability to the increase in weight involved as the toe pads will increase in area at a considerably lesser rate than the corresponding increase in mass with linear dimensions. In two of the families investigated previously, the Microhylidae (Green and Simon, 1979) and the Rhacophoridae (McAllister and Channing, 1983), larger species have been found to have proportionally larger toe pads, perhaps in response to the problems imposed by their adhesive mechanism. However, this trend is not exhibited in the hylid species under investigation here (see **Chapter 2**).

If increasing structural complexity of the pad is indeed related to arboreality, it seems reasonable to assume that the development of areas with increasingly specialised cells is a response to increased pressures to counteract falling and to maintain a grip upon leaves and branches and thus confers increased adhesive abilities. Therefore, it may be possible for a large species to counter the detrimental effects on their adhesive

abilities of their lowered surface-volume ratio through the development of increasingly more structurally complex pads. If large species of hylid do not possess proportionally larger pads, as is suggested by the results discussed in **Chapter 2**, do they exhibit a greater structural complexity of the specialised toe pads? Through SEM studies of the toe pads of adults of the twelve species, the link between species size and pad structural complexity can be explored and directly related to the species' adhesive abilities.

3.2. Methods

3.2.1. Scanning electron microscopy

Front and back feet were removed from frogs over-anaesthetised with lethal doses of Benzocaine belonging to twelve of the species of hylid frog found in Trinidad, *Flectonotus fitzgeraldi*, *Hyla boans*, *Hyla crepitans*, *Hyla geographica*, *Hyla microcephala*, *Hyla minuscula*, *Hyla minuta*, *Hyla punctata*, *Phrynohyas venulosa*, *Phyllomedusa trinitatis*, *Scinax rubra* and *Sphaenorhynchus lacteus*. Prior to their death, each frog's adhesive ability and toe pad area was determined according to the methodology in the previous chapter.

Nine toes from each frog, four from the front and five from the back feet were fixed in pH buffered 2.5% glutaraldehyde. The material was then rinsed in 0.1M phosphate-buffered sucrose, followed by immersion in buffered 1% osmium tetroxide for one hour. After washing in distilled water, tissues were taken through to full dehydration in an alcohol series and critical point drying from CO₂. The samples were then mounted on stubs and gold-coated before being viewed under a Philips SEM 500 scanning electron microscope. Images were taken at a range of magnifications.

3.2.2. Image analyses

Cell size for each species was determined from still images made at 1600x magnification, using Cherry Digitiser and Scion Image Analysis Programs. Ten cells per pad were measured, with cells being sampled from a central portion of the pad where curvature of the surface is minimal. Cell densities were calculated from counts within a fixed area of an image taken at 1600x magnification. In the same area the

total length of intercellular channel was measured, using another function of the Cherry Digitising program and densities determined from this measurement.

Mucosal pore size was determined from still images of a number of pores per pad. Where possible, structures of the pores were also assessed using these samples and numbers of cells bordering the cell lumen were noted for each pore measured. Pore counts were made from whole pad images and translated to pore densities using areas obtained from live frogs.

Structural complexity scores (0-3) were recorded for several structural elements from images of whole toe pads. Scores were made to assess the degree of elevation of each pad and the sub marginal area below the pad and the definition of grooves separating the pad from the circumferal margin and along the lateral edges of the toe as follows:

Elevation scores: 0 = completely flat; 1 = slightly raised; 2 = rounded; 3 = globular.

Groove scores: 0 = not present; 1 = shallow; 2 = defined; 3 = prominent.

3.2.4. Statistics

As a point of note: All statistics and graphs are generated using SPSS statistics software. This package does not have the functional capability to truncate lines of best fit to confine them to the edges of data sets and the lines of best fit on many graphs extend further than the parameters of the study can predict.

All statistical mean values are given in the format: $\bar{x} \pm 1 \text{ s.e.}$

3.3. Results

3.3.1. Toe pad morphology

As in hyliid species investigated in previous studies, (Ernst 1973a; Green, 1979, 1980, 1981; Ba-Omar *et al.* 2000), the surface of the toe pad in all twelve species studied here is defined by the characteristic presence of a pavement-like arrangement of specialised cells at the distal end of the toe, (**Figure 3.2 a-l**).

The main source of variation between species is the degree of development of the circumferal and proximal grooves separating the area covered with specialised cells from the rest of the toe, chiefly due to differences in the prominence of the adjacent margin and to the degree to which the groove encircles the pad. For example, *H. minuscula*, the smallest species, has pads that are almost emarginate in appearance (**Figure 3.2 a**) with a shallow circumferal groove extending only around the distal and lateral edges of the pad. In *H. geographica* (**Figure 3.2 h**), the circumferal margin is wider and flush with the pad, forming a deep circumferal groove. This groove extends full-circle around the pad in this species, separating the pad from the ventral surface at the proximal margin.

No correlations were found between frog size and scores for development of circumferal grooves ($r = 0.13$, N.S. 11 d.f.), proximal margin grooves ($r = 0.02$, N.S. 11 d.f.) or pad elevations ($r = 0.39$, N.S. 11 d.f.) between the twelve species nor were any found when considering the frogs according to genera.

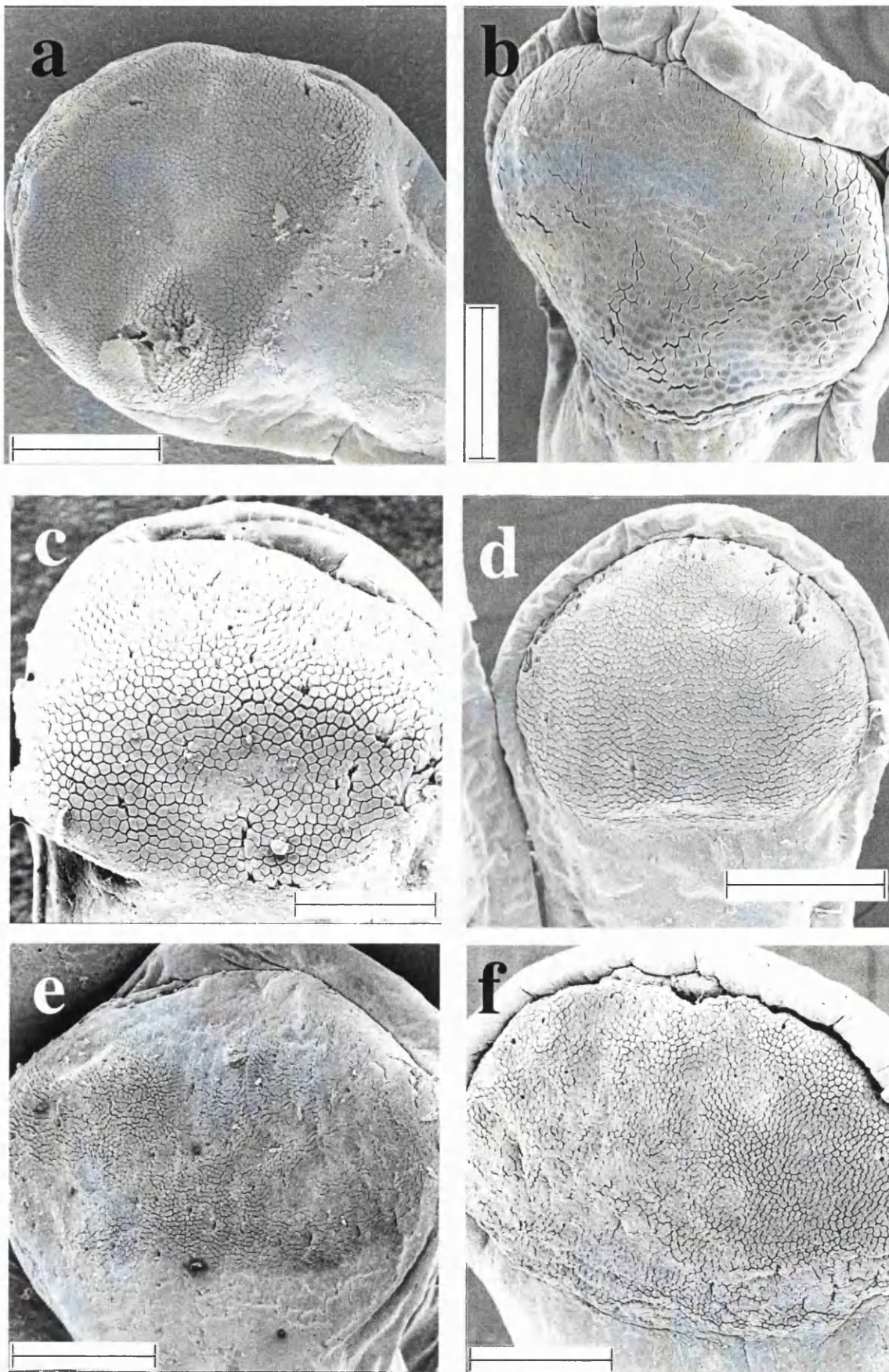


Figure 3.2: S.E.M. images of toe pads in (a) *H. minuscula*; Front 1, Scale bar =300 μm (b) *F. fitzgeraldi*; Front 1, Scale bar =150 μm (c) *H. microcephala*; Back 1, Scale bar =150 μm (d) *H. minuta*; Front 2, Scale bar =150 μm (e) *S. rubra*; Front 4 Scale bar = 300 μm (f) *H. punctata*; Back 1, Scale bar =300 μm .

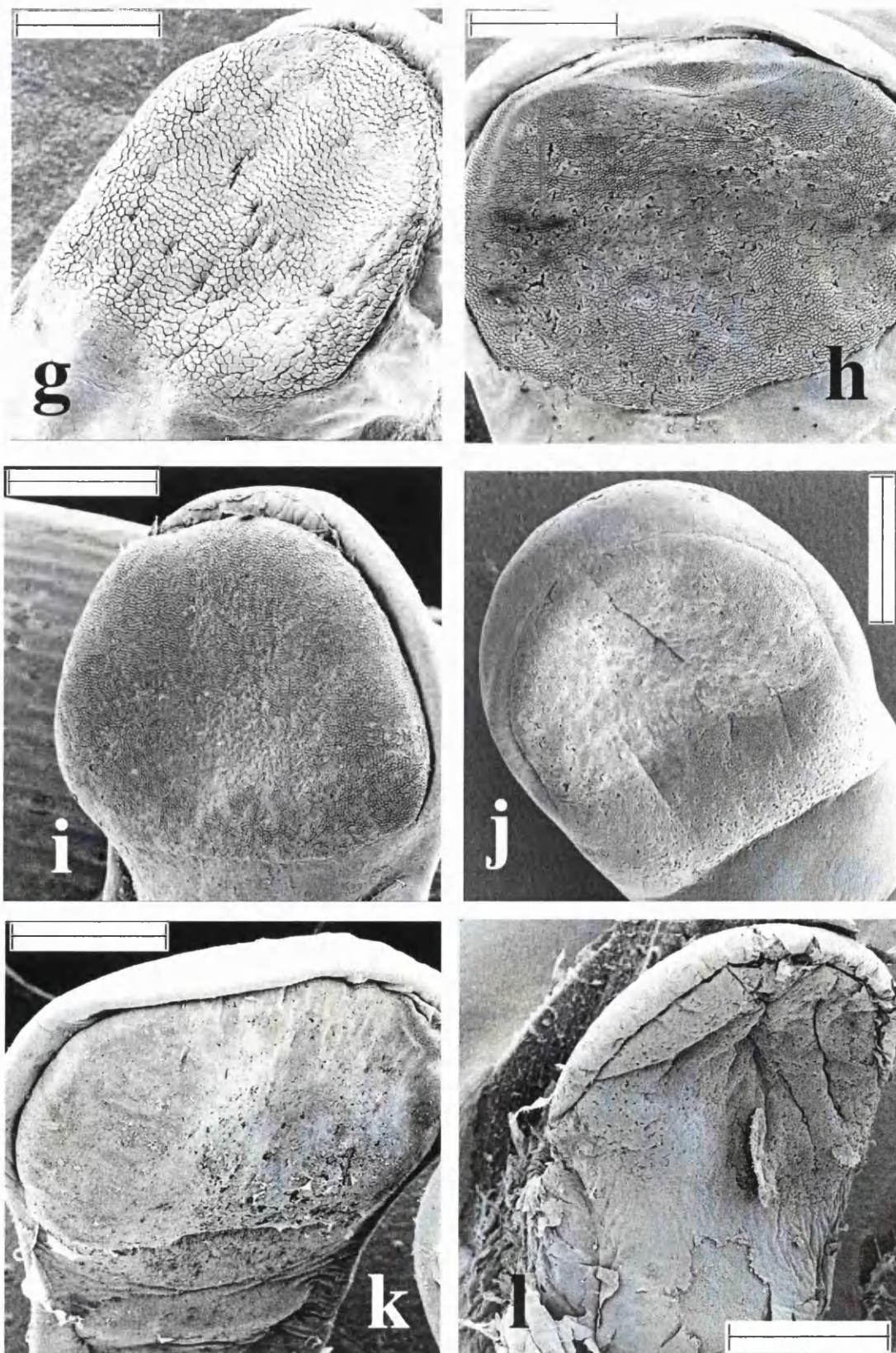


Figure 3.2 cont: S.E.M. images of toe pads in (g) *S. lacteus*; Back 1, Scale bar = 300 μ m (h) *H. geographica*; Back 5, Scale bar = 625 μ m (i) *H. crepitans*; Back 2, Scale bar = 625 μ m (j) *P. trinitatis*; Front 1, Scale bar = 625 μ m (k) *P. venulosa*; Front 3, Scale bar = 1.25 mm (l) *H. boans*; Front 3, Scale bar = 1.25 mm..

3.2.2. Toe pad cells

Cell architecture is also highly conserved between species, with cells being columnar in nature with hexagonal apices and striated sides (**Figure 3.3 b**). In a number of samples tightly packed tonofilament bundles can be clearly seen (**Figure 3.3 a**), though in many cases a cell coat obscures these structures. Cells are virtually indistinguishable between species (**Figure 3.6 a - l**) structurally.

There are significant differences in cell size between species (ANOVA: $F_{11,1405} = 85.68$, $p = 0.0001$) though there is little evidence of directionality in these differences (**Table 3.1**). There is a tendency towards smaller average cell size in smaller species, though there is no statistically significant correlation with the linear dimension ($r = 0.50$, $t = 1.81$, $p = 0.10$, 11 d.f.). However, if the species are examined according to their genera (**Figure 3.4**), those species within the genus *Hyla* do show a positive correlative relationship between cell size and linear dimensions ($r = 0.76$, $t = 2.22$, $p = 0.05$, 6 d.f.)

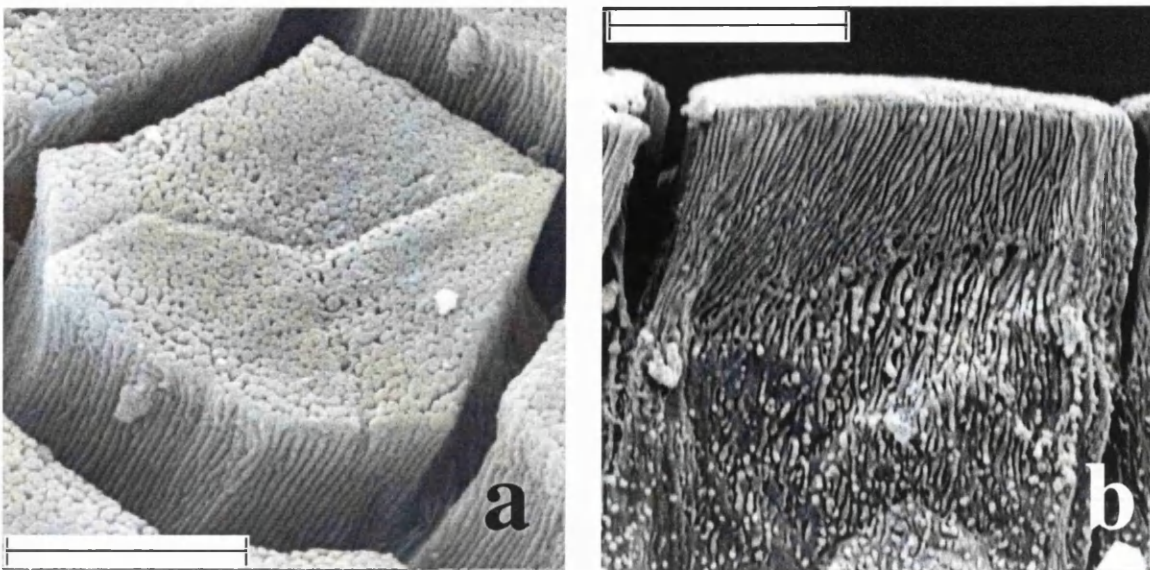


Figure 3.3: S.E.M. images of cell structure in (a) *Hyla minuta* Front 1, Scale bar = 6.25 μm (b) *Sphaenorhynchus lacteus* Back 5, Scale bar = 12.50 μm .

Using average cell area to calculate cell density over the total toe pad area indicates a tendency towards higher density in smaller frogs as might be expected from that towards smaller cell size in these frogs (**Table 3.1**). Cell densities per toe pad in the twelve species are significantly different from one another (ANOVA: $F_{11,148} = 14.70$, $p = 0.001$) though again, there are no statistical differences and no correlative effect of increasing size upon densities across all species ($r = 0.49$, $p = 0.10$, 11 d.f.). There is a significant relationship within the genus *Hyla*, such that the smaller *Hyla* species have lower cell densities than the larger species (*Hyla*: $r = 0.80$, $t = -2.99$, $p = 0.03$, 6 d.f.). This relationship is, perhaps, not surprising as cell density is likely to be highly dependent upon cell size. It is, however, important to remember that the cell density values in **Table 3.1** are likely to be overestimates as the methodology does not take into account the area taken up by the intercellular channels which is likely to be considerable (see **Section 3.2.3**).

Species in order of increasing SVL	Cell area (μm^2)	s.e.	n	Density (no/mm ²)	s.e.	n
<i>H. minuscula</i>	98.02	1.45	179	10730	350	18
<i>F. fitzgeraldi</i>	101.46	1.36	173	10340	520	18
<i>H. microcephala</i>	93.73	1.84	90	12070	850	14
<i>H. minuta</i>	87.06	1.25	164	10910	620	9
<i>S. rubra</i>	65.60	1.45	70	16110	1090	7
<i>H. punctata</i>	110.70	2.41	80	9930	510	14
<i>S. lacteus</i>	144.25	2.24	152	6950	280	17
<i>H. geographica</i>	119.91	2.68	80	8540	480	8
<i>H. crepitans</i>	115.40	3.03	78	8990	590	8
<i>P. trinitatis</i>	105.00	2.14	164	9830	450	17
<i>P. venulosa</i>	133.23	1.61	89	7620	210	9
<i>H. boans</i>	98.02	3.64	87	8540	300	9

Table 3.1: Average cell size and densities in adult frogs from twelve species of hylid.

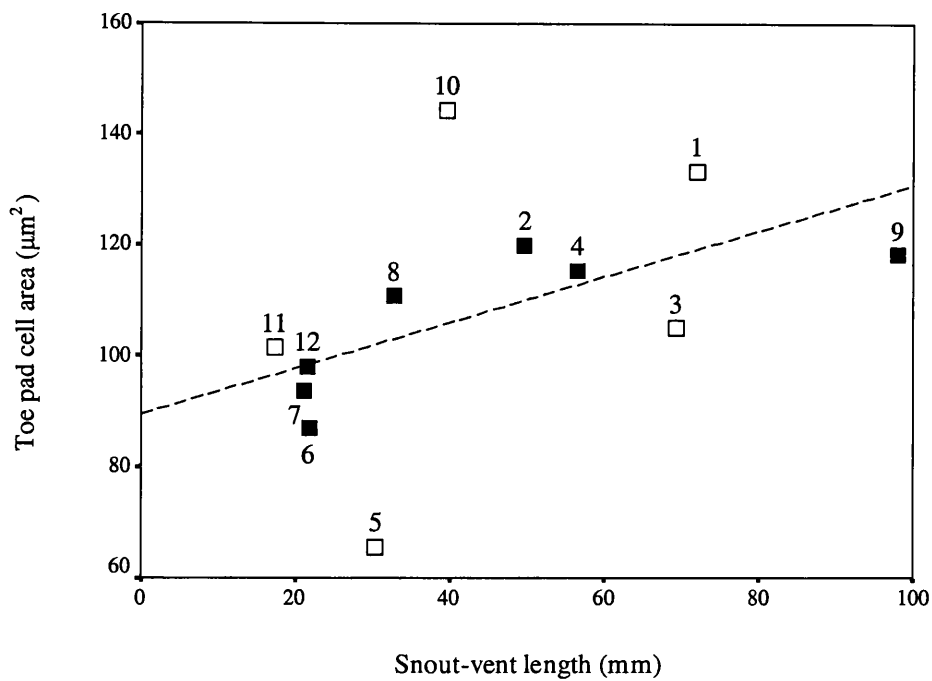


Figure 3.4: Average toe pad cell area in genus *Hyla* (+) and non-*Hyla* genera () vs. SVL. Statistics for *Hyla* species only: Correlative statistics: $r = 0.76$, $p < 0.05$, 6 d.f. Line of best fit $y = 0.36x + 90.85$, $t = 2.65$, $p = 0.05$, 5 d.f.

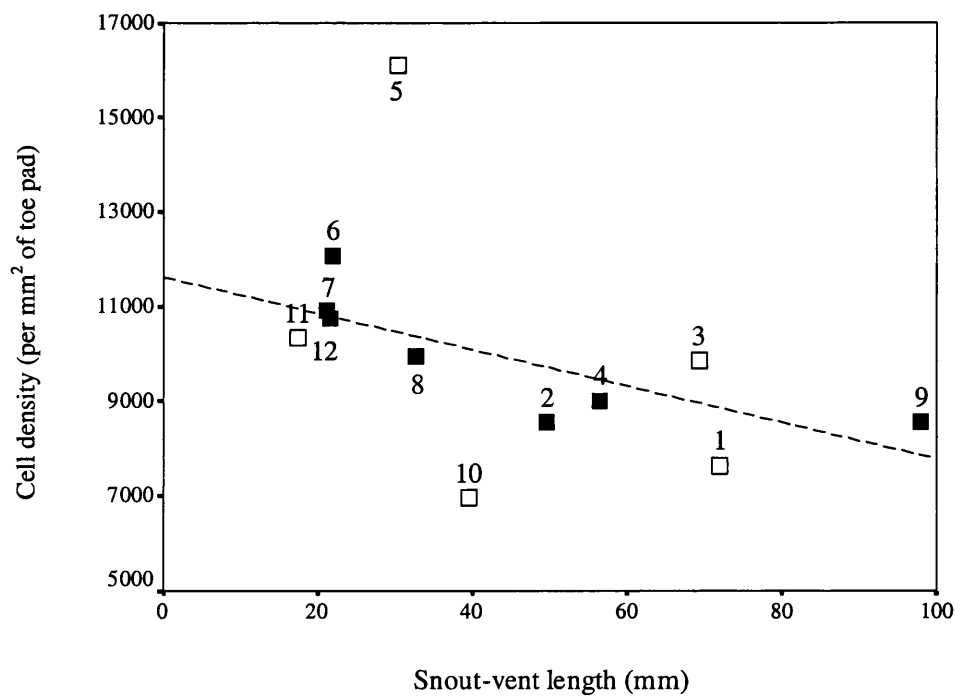


Figure 3.5: Average toe pad cell density in the genus *Hyla* (+) and non-*Hyla* genera () vs. SVL. Statistics for *Hyla* species only: Correlative statistics: $r = 0.80$, $p < 0.05$, 6 d.f. Line of best fit $y = 11620 - 38.50x$, $t = -2.99$, $p = 0.03$, 5 d.f. Numbers in both figures on this page indicate species as follows: 1. *P. venulosa*, 2. *H. geographica*, 3. *P. trinitatis*, 4. *H. crepitans*, 5. *S. rubra*, 6. *H. microcephala*, 7. *H. minuta*, 8. *H. punctata*, 9. *H. boans*, 10. *S. lacteus*, 11. *F. fitzgeraldi*, 12. *H. minuscula*.

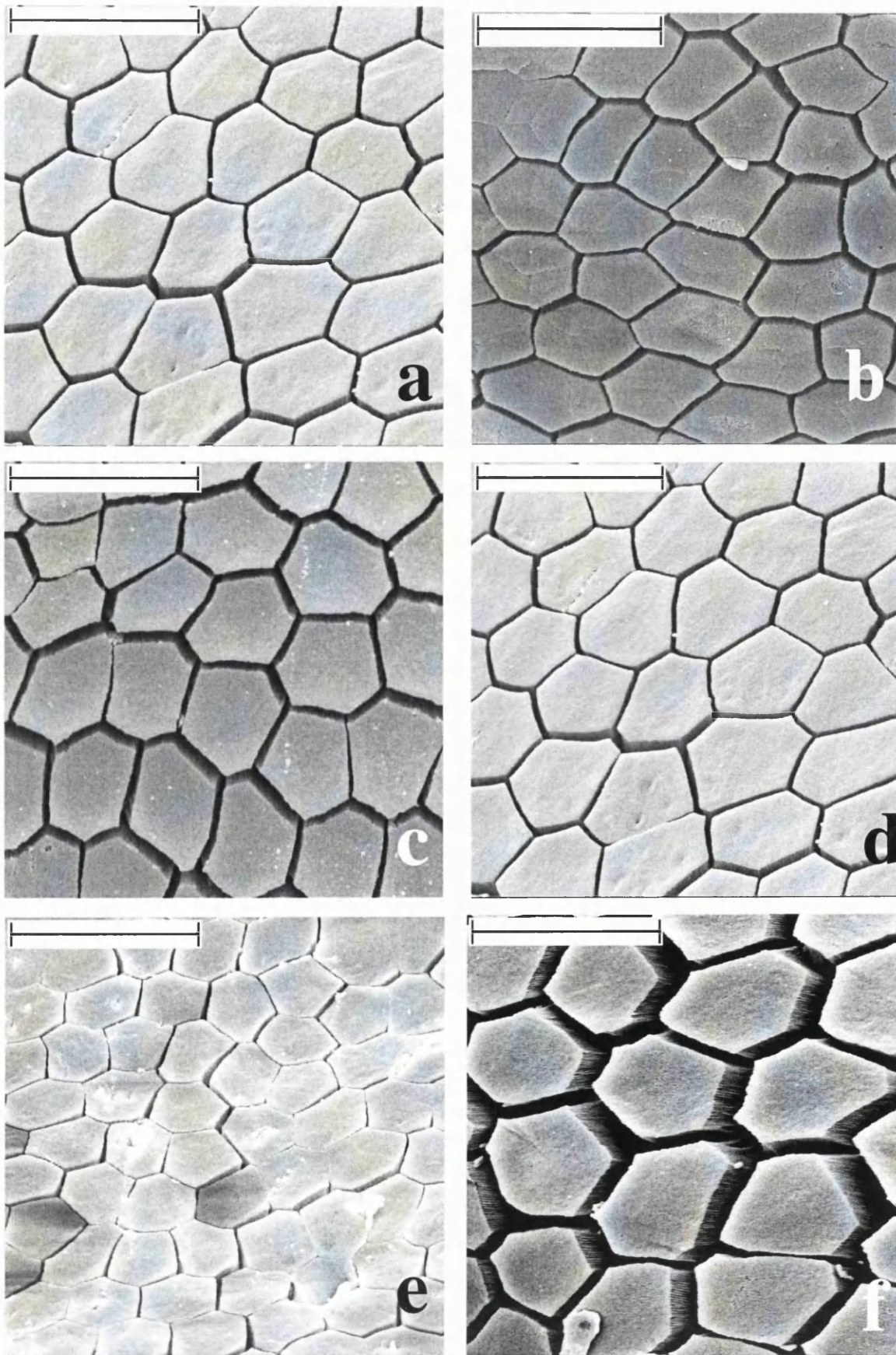


Figure 3.6: S.E.M. images of toe pad cells in (a) *H. minuscula*; Front 3 (b) *F. fitzgeraldi*; Back 1 (c) *H. microcephala*; Front 2 (d) *H. minuta*; Front 3 (e) *S. rubra*; Front 1 (f) *H. punctata*; Back 4. All scale bars in images = 25 μm

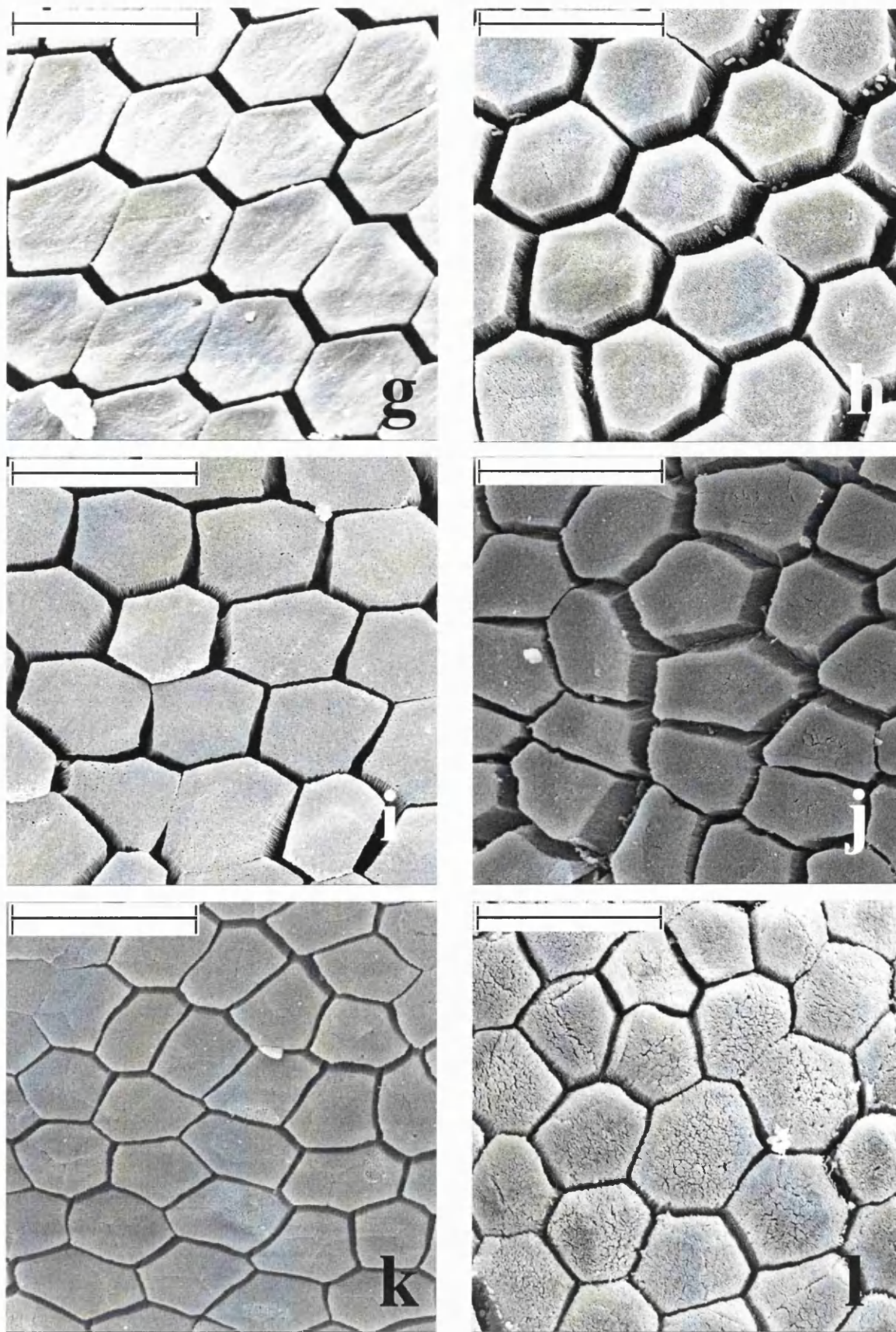


Figure 3.6 cont.: S.E.M. images of toe pad cells in (g) *S. lacteus*, Back 1 (h) *H. geographica*, Back 5 (i) *H. crepitans*, Back 2 (j) *P. trinitatis*, Back 5 (k) *P. venulosa*, Back 3 (l) *H. boans*, Front 4. All scale bars in images = 25 μm .

3.3.3. Inter cellular channels

Channels can be seen to be running between the columnar cells of the toe pad. The width of these channels is highly variable in all species, (**Figure 3.6 a-l**). This is likely to be due in part to distortion effects during sample dehydration for S.E.M. but normal values range from 1-5 μm in width.

Plotting total channel length per toe (y) against toe pad area (x) yields a highly significant positive correlative relationship such that $y = 141.84x + 25.01$ ($r = 1.00$, $t = 45.67$, $p < 0.001$, 22 d.f.). This suggests that the channel densities are relatively

constant between species, and this appears to be confirmed when considering the values derived from the S.E.M. images (**Table 3.2**). There is no correlation between linear dimensions and channel density for all twelve species ($r = 0.51$, N.S. 11 d.f.).

As channel length is dependent on the combined lengths of the cell

perimeters it might be expected that higher channel densities will

correlate to cell densities, which is indeed the case across all twelve species ($r = 0.99$, $y = 0.01x + 68.33$, $T = 19.26$, $p = 0.001$, 11 d.f.) so that the relationships seen within the genus *Hyla* between cell densities and linear dimensions are similar for channel densities (*Hyla*: $r = 0.77$, $y = 171.53 - 0.32x$, $T = -2.70$, $p = 0.04$, 6 d.f.).

Species	Channels mm/mm ²	s.e.	n
<i>H. minuscula</i>	169.07	4.33	18
<i>F. fitzgeraldi</i>	168.60	5.88	18
<i>H. microcephala</i>	176.01	8.53	14
<i>H. minuta</i>	160.10	8.17	9
<i>S. rubra</i>	215.72	7.06	7
<i>H. punctata</i>	157.75	6.58	13
<i>S. lacteus</i>	134.71	3.33	15
<i>H. geographica</i>	145.56	6.20	9
<i>H. crepitans</i>	148.45	6.04	8
<i>P. trinitatis</i>	159.99	2.62	17
<i>P. venulosa</i>	134.06	4.30	9
<i>H. boans</i>	145.88	5.28	8

Table 3.2: Inter cellular channel densities in twelve Trinidadian hylids.

3.3.4. Mucosal pores

All mucosal pores seen in adults of the species studied here (**Figure 3.7 a-l**), are examples of the ‘Type II’ pores, *sensu* Green (1979); i.e. pores in which the sides of the cell facing the lumen are modified in comparison to the normal cell striations. Within and between species, pore size is extremely variable. Minimum, maximum and median pore sizes seen in different species are given in **Table 3.3**. The high variability in the number of pores visible across the toe pad area may well be due to the different opening status of the gland at the point at which the frog was killed and may well have led to an underestimate of pore counts in a number of species here. Pore counts are higher in large species, though as larger species have larger toe pads this is to be expected. Controlling for this by dividing counts by toe pad area gives pore densities for all species (**Table 3.3**) that although they are significantly different from one another (ANOVA: $F_{11,93} = 3.54$, $p = 0.001$) are not significantly correlated with SVL ($r = 0.03$, N.S., 11 d.f.).

Species	Mucosal pore size (μm^2)			Mucosal pores/ mm^2		
	Minimum	Maximum	Median	Value	s.e.	n
<i>H. minuscula</i>	3.23	361.38	36.18	24.14	3.07	13
<i>F. fitzgeraldi</i>	6.13	6.22	6.18	25.31	4.27	15
<i>H. microcephala</i>	58.06	361.38	121.34	28.31	5.02	9
<i>H. minuta</i>	53.63	260.60	87.54	25.32	7.68	7
<i>S. rubra</i>	15.85	249.35	54.32	22.85	1.60	5
<i>H. punctata</i>	49.69	131.92	63.26	7.79	3.98	2
<i>S. lacteus</i>	9.32	75.07	36.49	7.46	1.67	12
<i>H. geographica</i>	137.67	426.61	344.55	34.43	6.89	6
<i>H. crepitans</i>	38.11	296.75	197.31	9.44	1.54	6
<i>P. trinitatis</i>	17.22	221.86	93.81	39.70	12.76	4
<i>P. venulosa</i>	28.76	339.16	118.19	18.98	2.60	9
<i>H. boans</i>	49.69	460.01	128.29	21.03	2.96	5

Table 3.3: Mucosal pore size and densities in twelve study species

There is some interspecific variation in the structures of the mucosal pores seen across the toe pads:

Mucosal pores in *Hyla minuscula* average in size at around $86.52 \mu\text{m}^2 \pm 36.92$ ($n = 11$). The most commonly observed type is a slit-like pore such as that illustrated in **Figure 3.7 a**. These are variable in size and may be bordered by as many as six cells. This image also shows a partial view of a second type of pore seen in this species: long slits formed between the walls of several adjoining cells are found on a number of pads, almost exclusively at the proximal edge. Very small pores are present in *Hyla minuscula* but are few in number. Pore counts are generally low for this species, at 15.00 ± 2.25 ($n = 13$) per pad with pores appearing scattered in an even distribution across the pad.

Flectonotus fitzgeraldi have very small mucosal pores (**Figure 3.7 b**), atypical in structure, with the lumen being formed in many cases by the infolding of the wall of a single cell. Sizes are uniform and small, averaging at $6.18 \mu\text{m}^2 \pm 0.05$ in size. Average pore counts are the lowest for any species at 9.93 ± 1.31 ($n = 15$) per pad, though due to the tiny nature of the pores it is highly likely that this value is an underestimate.

Pores in *Hyla microcephala* (**Figure 3.7 c**) are typified by a simply shaped rounded pore opening which may be bordered by as many as twelve cells, each with a modified wall contributing to a side of the lumen. In this species bordering cells are most commonly six or seven in number with an average size of $129.88 \mu\text{m}^2 \pm 30.90$ ($n = 9$). Pores appear evenly distributed over the pad, with average counts of 19.44 ± 3.72 ($n = 9$) with no evidence of concentration in any particular area.

In *Hyla minuta* (**Figure 3.7 d**), pores are of the simple type described for *Hyla microcephala*, with five cells bordering the lumen being typical. Mean sizes are a little smaller than in the smaller species, at $101.13 \mu\text{m}^2 \pm 18.84$ ($n = 10$). Pore counts are low in this species, at 15.86 ± 4.16 ($n = 7$) per pad, and are principally concentrated around the edges.

Two main pore types are seen in *Scinax rubra*: small geometrical pores of around $50 \mu\text{m}^2$ in area ($41.86 \mu\text{m}^2 \pm 6.20$, $n = 8$), bordered by five to eight cells, make up the majority of the number (**Figure 3.7 e**) scattered in even lines across the central portion of the pad. The sculpturing of the cells that form the luminal walls is unusual, being closer in architecture to the convoluted ridges seen on ‘normal’ columnar cells rather than the microvillar projections seen lining the pores in other species. The second type of pore has a thin slit-like opening, one to two cell-sides in length and with the terminal end inserting into the cell wall of a single cell, these are fewer in number than the first type and are more frequent on the proximal edge of the pad*. These pores are larger in size, being typically 100 to $200 \mu\text{m}^2$ in size ($153.25 \mu\text{m}^2 \pm 34.79$, $n = 4$). Numbers per pad are low, with average counts of 27.41 ± 3.40 ($n = 5$).

Hyla punctata have rounded pores (**Figure 3.7 f**), the majority of which have a simple single opening formed in a gap between modified surrounding cell walls. As in *Hyla minuta*, pores are pentagonal in the main, being bordered in most cases by five cells, though this number can vary between four and seven. Pore counts are less variable than in a number of species, at around 21.13 ± 2.90 ($n = 8$) per pad. Pores appear to be distributed evenly across the pad, though there is a tendency towards slightly

* See **Figure 4.18** in next chapter for more images of pores in adult *S. rubra*.

larger pores being present on the distal margins of the pad. Average pore size is $73.25 \pm 8.36 \mu\text{m}^2$ ($n = 14$).

Similar pore structures are seen in *Sphaenorhynchus lacteus*, although on average these are smaller ($42.82 \mu\text{m}^2 \pm 11.26$, $n = 5$) than those seen in *Hyla punctata*. Pore openings are slightly more complex in shape in a number of cases and can be bounded by as many as eight cells (**Figure 3.7 g**). Pore counts are low, averaging 18.75 ± 3.62 ($n = 12$) per pad.

Mucosal pores in *Hyla geographica* have a greater diversity in lumen structure than seen in the smaller species. The commonest pores have openings shaped by multiples of hexagons, framed by 6 to 11 cells and average $176.71 \mu\text{m}^2 \pm 34.19$ ($n = 3$) in area. The second type have a small pore opening but are embedded in a y-shaped groove around 2-3 cell sides in length, with average areas of the whole structure being $376.64 \mu\text{m}^2 \pm 17.25$ ($n = 5$). The sides of the grooves are distinct from the mucosal channels by modifications to the framing cell walls such as that seen in Type II mucosal pores (**Figure 3.7 h**). Mucosal pore counts are high, at 186.83 ± 28.34 ($n = 6$), with the lower central portion appearing to have a greater concentration of pores than other areas.

Mucosal pores seen in *Hyla crepitans* are smaller than in the similarly sized *H. geographica* ($167.38 \mu\text{m}^2 \pm 20.04$, $n = 17$) and bordered by between six and ten cells, with the openings generally hexagonal, heptagonal (**Figure 3.7 i**) or shapes formed by combinations of the two. Pores are lightly scattered over the pad and are often more visible on the lower central portion with very few seen on the edges of the

pad adjacent to the circumferal margins, pore counts are low at 33.67 ± 6.54 ($n = 6$) per pad.

In *Phyllomedusa trinitatis* are small ($92.16 \mu\text{m}^2 \pm 18.56$, $n = 12$), simple round pores bordered by six to eight cells are again in the majority, scattered across the central portion of the pad in an even distribution. A significant number of pores seen in this species are elongate and bordered by 10-15 cells, (**Figure 3.7 j**), they are found around the outer edges of the pad. Counts average at 106.28 ± 26.77 , ($n = 11$).

Mucosal pores in *Phrynohyas venulosa* are again of the simple type, with pore lumens being generally hexagonal, most commonly bordered by six cells (**Figure 3.7 k**). Areas of pore openings are $140.96 \mu\text{m}^2 \pm 19.12$ ($n = 23$) on average. Pore counts are high, at around 131.11 ± 9.77 ($n = 9$) per pad, with cells scattered over the whole pad and a tendency towards greater densities in the lower half.

Hyla boans have the highest average pore count of the twelve species at 345.81 ± 44.89 ($n = 5$), pores per pad, with the pores evenly distributed across the whole pad. Pores in this species are most often bordered by seven cells (**Figure 3.7 l**), and have an average area of $181.49 \pm 34.06 \mu\text{m}^2$ ($n = 17$).

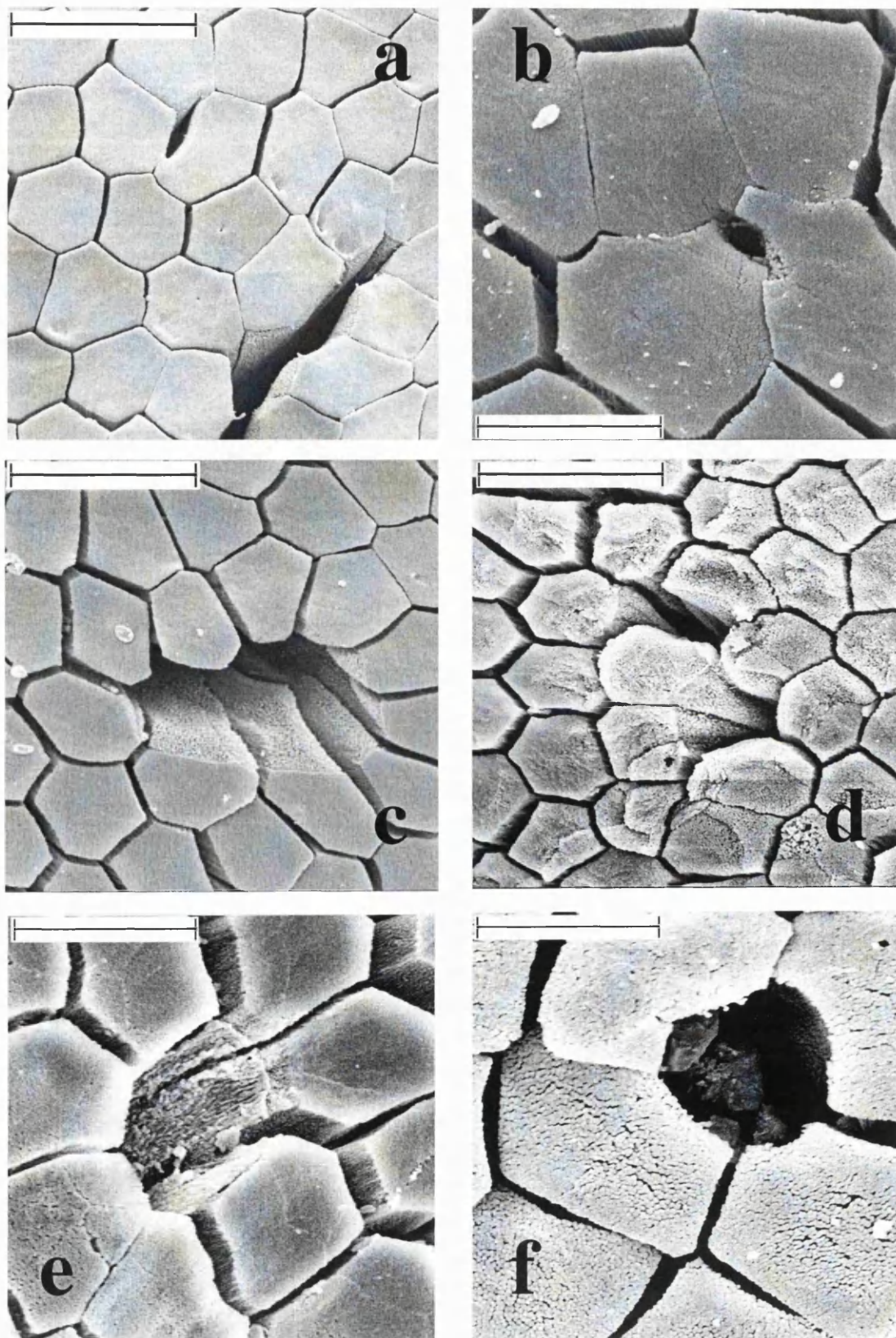


Figure 3.7: S.E.M. images of pores (a) *H. minuscula*; Front 2, Scale bar = 25 μm (b) *F. fitzgeraldi*; Back 1, Scale bar = 12.5 μm (c) *H. microcephala*; Front 1, Scale bar = 25 μm (d) *H. minuta*; Front 1, Scale bar = 25 μm (e) *S. rubra*; Back 3, Scale bar = 12.5 μm (f) *H. punctata*; Front 3, Scale bar = 12.5 μm

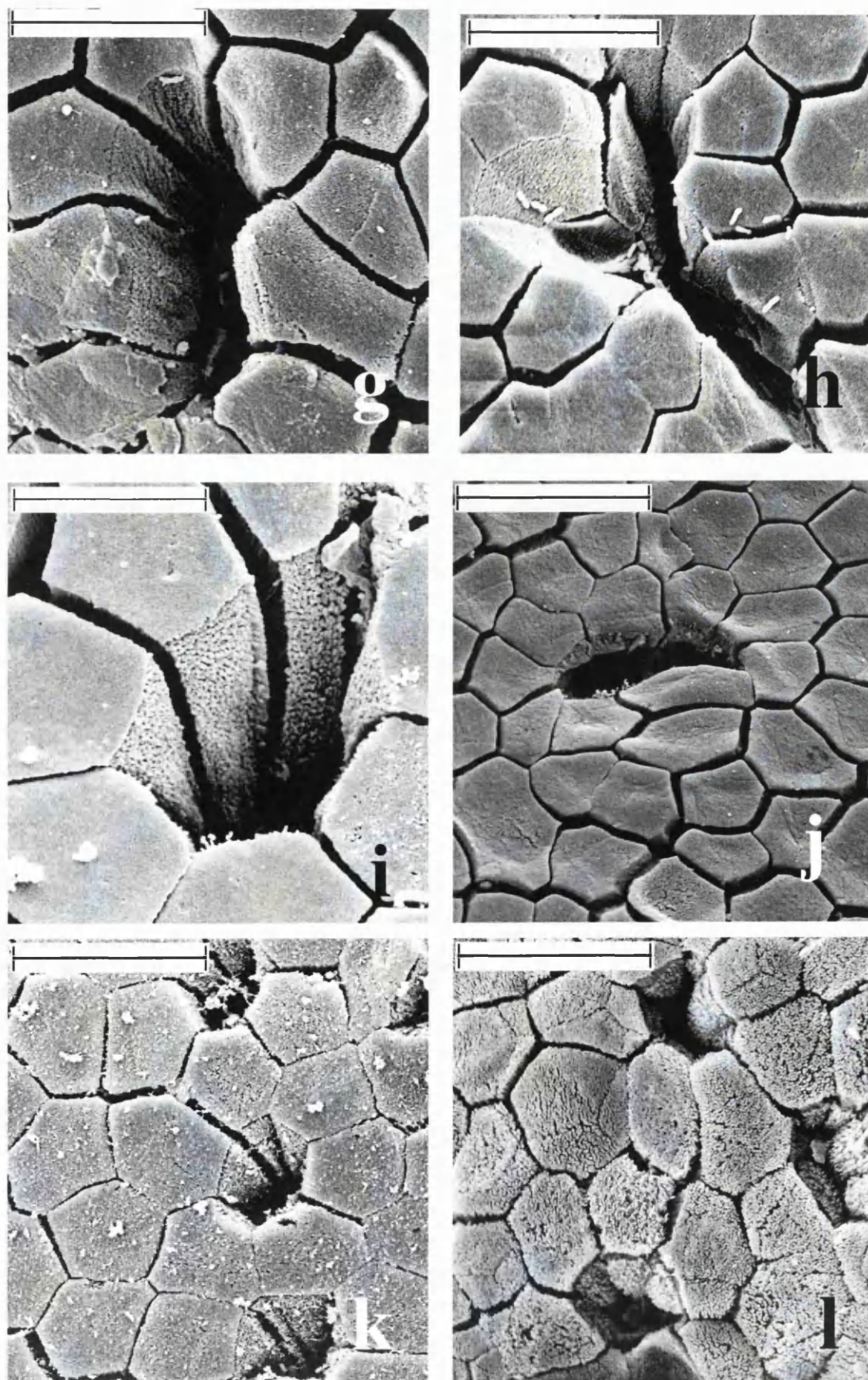


Figure 3.7 cont: S.E.M. images of pores in (g) *S. lacteus*; Back 2, Scale bar = 25 μm (h) *H. geographica*; Back 5, Scale bar = 25 μm (i) *H. crepitans*; Back 3, Scale bar = 12.5 μm (j) *P. trinitatis*; Front 1, Scale bar = 25 μm (k) *P. venulosa*; Front 4, Scale bar = 25 μm (l) *H. boans*; Back 4, Scale bar = 25 μm .

3.3.5. Specialised cells on accessory adhesive areas.

Specialised cells are found elsewhere on the ventral surface of the toe, particularly at the proximal margin of the toe pad and on raised areas on the joints of the fingers and toes, the subarticular tubercles.

Subarticular tubercle cells vary considerably in their degree of specialisation, and they differ significantly in their areas (**Table 3.4.**), ANOVA: $F = 20.03$, $p < 0.01$, 9 d.f. between species though no correlation exists between SVL and cell size ($r = 0.16$, N.S. 9 d.f.). Cells on the subarticular tubercles range from relatively unspecialised cells with ill-defined margins in *F. fitzgeraldi* (**Figure 3.8 a and d**) to cells that are very similar in appearance to toe pad cells in *H. crepitans* and *P. venulosa* (**Figure 3.8 e - f**). In most species though, subarticular tubercle cells are intermediary in appearance (**Figure 3.8 b and c**).

Species in order of increasing SVL	Proximal margin cell size (μm)			Subarticular tubercle cell size (μm)		
	Mean	s.e.	n	Mean	s.e.	n
<i>H. minuscula</i>	112.44	7.83	13	142.37	5.06	52
<i>F. fitzgeraldi</i>	-	-	-	135.49	5.39	33
<i>H. minuta</i>	136.36	4.53	6	148.02	2.37	62
<i>S. rubra</i>	165.9	6.84	13	130.43	9.15	11
<i>H. punctata</i>	-	-	-	138.01	4.97	31
<i>S. lacteus</i>	219.79	15.51	10	174.76	6.62	64
<i>H. geographica</i>	173.37	14.14	8	210.75	10.08	23
<i>H. crepitans</i>	137.49	8.18	25	100.77	2.34	36
<i>P. trinitatis</i>	212.48	18.98	4	141.3	4.71	97
<i>P. venulosa</i>	147.06	5.26	30	111.81	3.92	23

Table 3.4: Average cell sizes on proximal margin and subarticular tubercles in different species. Missing data for proximal margin cells in *F. fitzgeraldi* and *H. punctata* is due to indistinct nature of margins of cells in these species.

The proximal margin of the toe pad is an area defined by the transition of highly modified columnar cells characteristic of the toe pad to less modified irregularly shaped cells. The cells below the proximal margin are often transitional between the specialised columnar cells and normal squamous epithelial cells seen elsewhere on the pad, being similar in appearance to cuboidal cells noted in earlier studies of other species of frog in equivalent areas and on the subarticular tubercles. Sizes are significantly different between species (ANOVA: $F = 10.84$, $p < 0.01$, 7 d.f.) though again there is no correlative relationship between cell size and linear dimensions in a species ($r = 0.35$, N.S. 7 d.f.).

The degree of specialisation of cells on subarticular tubercles in many species may be indicative of an involvement in some way with adhesion. Examining the architecture of the cells on the subarticular tubercles, many have surfaces which appear to be covered in microvilli, with perhaps the most extreme example of this seen in *H. punctata* (**Figure 3.8 d**). Cells on the proximal margins also have a rough cell surface architecture, with microvilli giving the cells an almost 'hairy' appearance. Another feature typical of the cells in this area can be seen in examples from six species (**Figure 3.8 a-f**), where the imprint of cell edges from the sloughed-off layer above them can be seen across the surface of the cells. The surface in proximal margin areas and of the subarticular tubercles is often further specialised in comparison to neighbouring areas, with surface roughness enhanced by liberal scatterings of shallow pits (**Figure 3.9 a**, **Figure 3.9 b-c**) and by numerous areas which appear as if single cells have been removed whole from an upper stratum of skin (**Figure 3.9 c**, **Figure 3.9 f**). There is no evidence in these of ducts that may lead to a mucous gland.

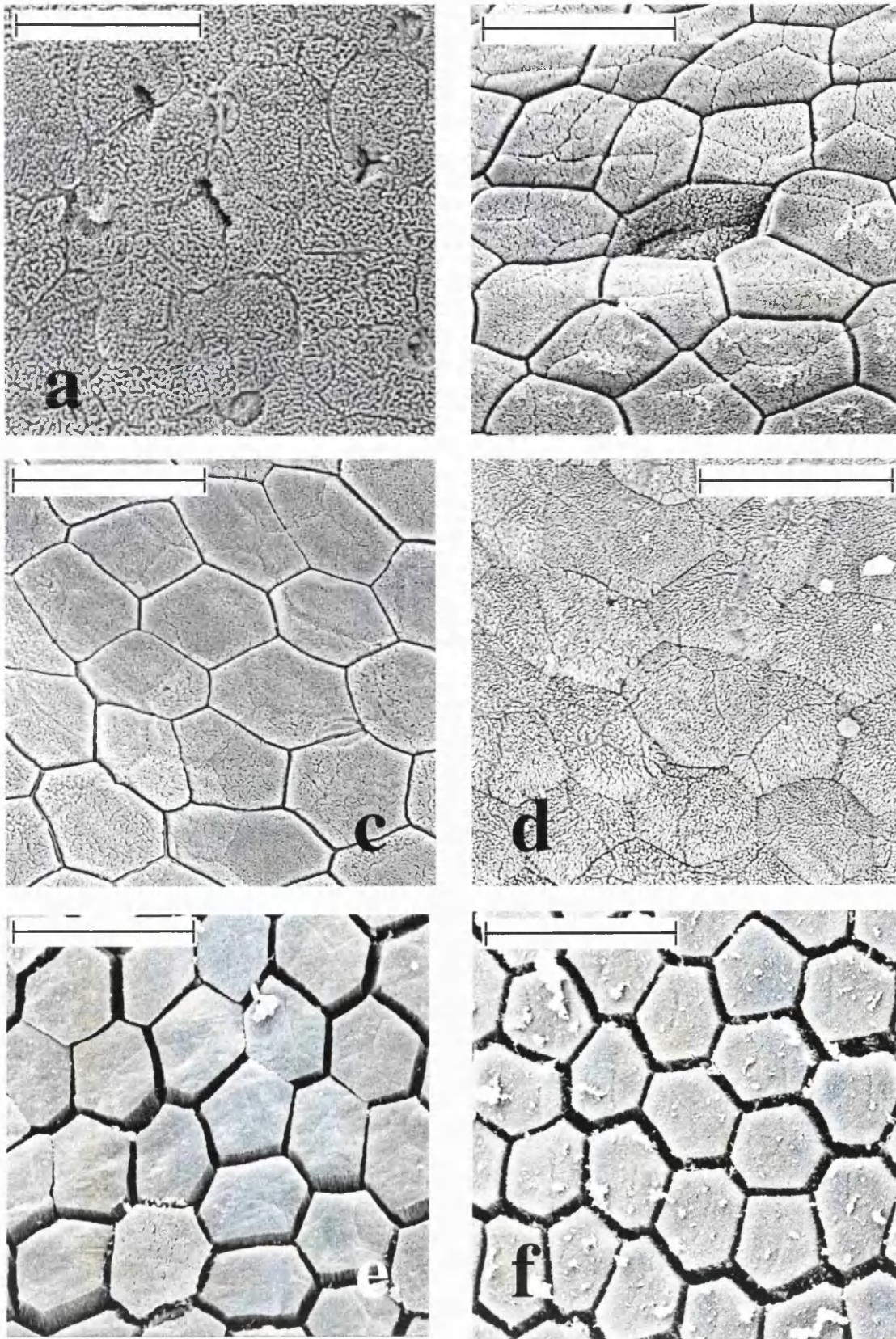


Figure 3.8: S.E.M. images of subarticular tubercle cells in (a) *F. fitzgeraldi*: Front 1 (b) *H. microcephala*: Back 3 (c) *H. minuta*: Back 2 (d) *H. punctata*: Front 3 (e) *H. crepitans*: Back 2 (f) *P. venulosa*: Front 4. All scale bars = 25 μm .

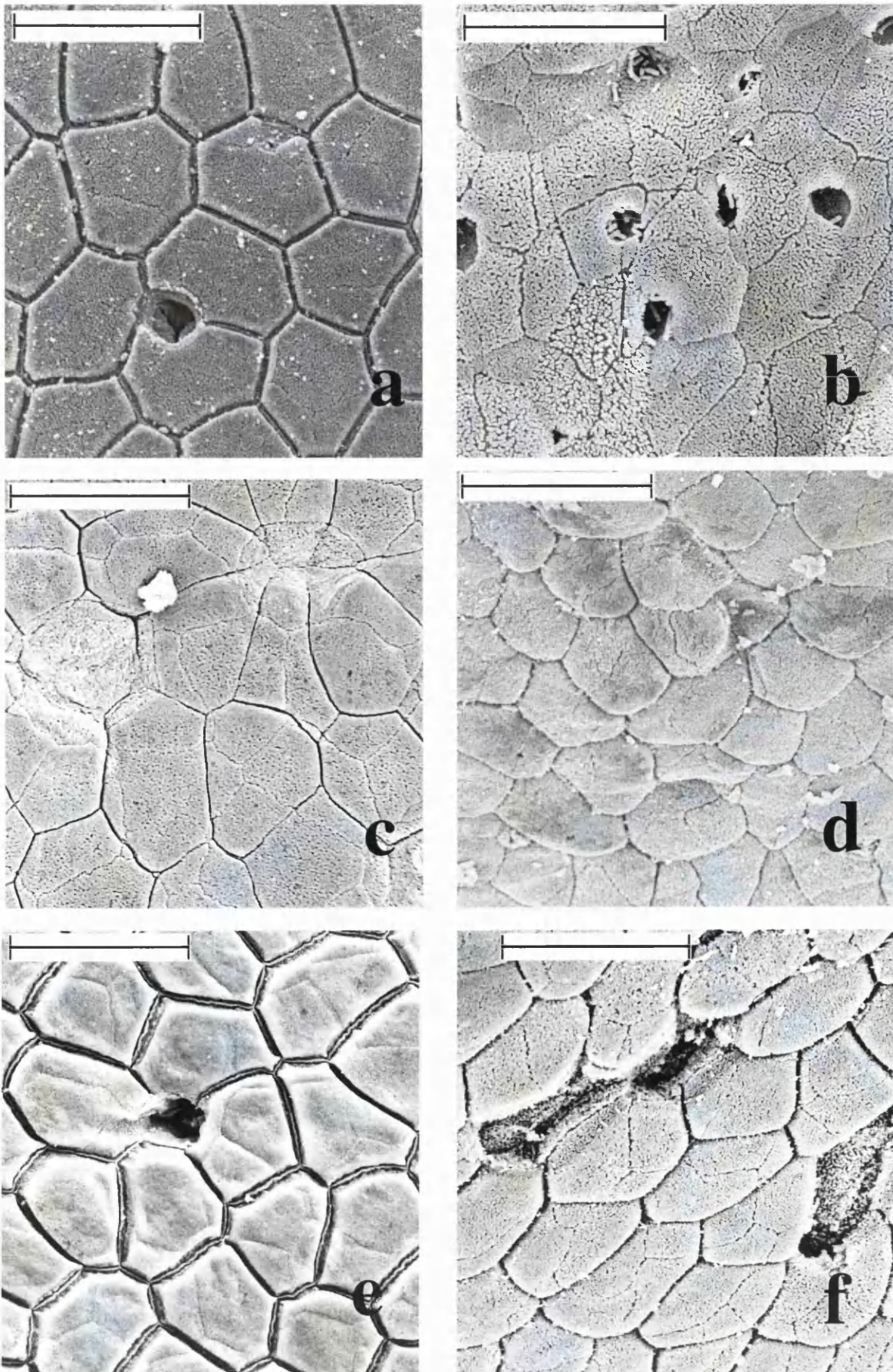


Figure 3.9: S.E.M. images of proximal margin cells in (a) *H. minuscula*; Back 2 (b) *S. rubra*; Front 2 (c) *H. geographica*; Back 3 (d) *H. crepitans*; Back 1 (e) *P. trinitatis*; Front 1 (f) *P. venulosa*; Front 3. All scale bars = 25 μm .

3.4. Discussion

Toe pad morphology and the epidermal structure are highly conserved between the twelve species of Trinidadian investigated, though as all are Hylids and thus from the same phylogenetic (Bufonid) lineage this is as might be expected. However, structures are also very similar to climbing frogs in different families, including the Hyperoliidae, Rhacophoridae and Microhylidae (McAllister & Channing, 1983; Green and Simon, 1986; Hertwig and Sinsch, 1995). These convergent similarities support the theory that the structure of the pad has become highly evolved for a specific adaptive function.

One of the most striking features of the convergence in toe pad design is in the similarities in the architecture of the specialised epidermal layer, characterised by stratified columnar cells with hexagonally shaped free apices. The hexagonal geometry of the apices is highly conserved between species and this, together with the prevalence of similar cells in adhesive structures on the footpads of certain insects (Gorb and Scherge, 2002) suggests that this shape is of some functional significance. As dependent as the tree frog's adhesive abilities are on contact area, it is important that the total cell area in contact with the surface on each pad is maximised; additionally, for a meniscus to spread evenly, a smooth surface is most efficient so cells should have minimal spaces between them. To allow even and close matching to irregular substrates the ability to deform must be equal across the whole of the pad, so that cells that form the continuous pad surface should ideally be uniform in both shape and size. The tessellating nature of the regular hexagon shape fulfils all of these requirements and the high perimeter to area ratio, means the hexagon is the most efficient tessellating shape to maximise both wet adhesion forces and resistance to

shear force along their perimeter length. The obtuse angles of the hexagon also help to resist any area reducing deformation of the cells that may result from the horizontal application of friction forces against the leading edges of the cell through the equality of force distribution that will result from the equi-angular nature of these regular hexagon.

Patterns of lesser-seen cell types with between four and eight sides appear to be distributed randomly across the toe pad (**Figure 3.10**). Irregularly shaped cells are often seen around the lumina of mucosal pores (**Figure 3.7 a-l**). It may be that the clusters of irregular cells seen on the main body of the pad (**Figure 3.10**) are gathered around closed mucosal pores, which are otherwise undetectable. If the presence of a cluster of irregular shaped cells can be proved to correlate to mucosal pore presence, this may well be a useful diagnostic feature for future studies to allow a greater degree of accuracy in pore density assessments for different species. There is also a tendency towards greater densities of these irregularly shaped cells at the distal edges of the pad. This may be due to a greater need for deformation in this area to bring the pad close to the surface at the leading edge. Additionally, cells at this leading edge are generally more elongate in

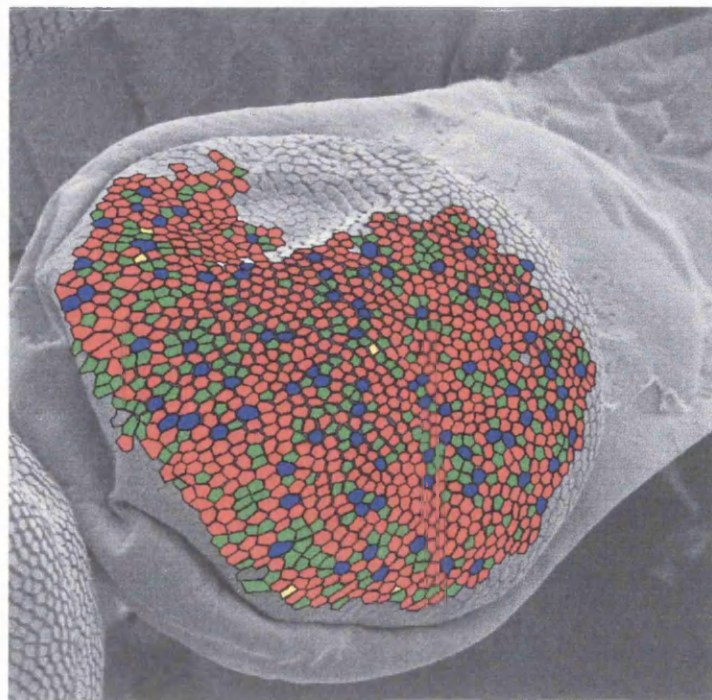


Figure 3.10: Cell distribution on a juvenile *Hyla crepitans* toe pad. Red = hexagonal, green = pentagonal, blue = heptagonal.

shape than on the body of the pad, reminiscent of cells in the ‘torrent’ frogs belonging to the genus *Amolops* (Öhler, 1995), believed to be an adaptation to allow an increase in fluid dispersal from their pads to allow closer conformation between the pad and the substrate. The importance of the pad’s ability to conform to a surface in adhesion is discussed with reference to pad elevation scores in later pages.

Although cells are regular in size, and differ between species, no correlation was found between cell size and adult size for all twelve species. Examining the species according to genera however, demonstrates that there *is* a size effect on the area of the toe pad cell area (**Figure 3.4**) within frogs belonging to the genus *Hyla*. Why then do these frogs exhibit differences in the size of the cells on their pads, and, as larger species tend to have larger cells, are there any advantages that this confers to the frogs in terms of their adhesive abilities?

Green (1981a) discusses the implications of the differences in cell size on adhesive ability within a polyploid complex, due to an observation that the tetraploid *H. versicolor* have larger cells than their diploid sibling species *H. chrysocelis*. This study found that *H. versicolor* were on average 5% ‘stickier’ than *H. chrysocelis*, and, although this was discounted as perhaps being due to ‘experimental error’, the effects of cell size on the adhesive forces being produced within the genus *Hyla* under investigation here support the observation seen in this earlier study. If the influence of area on the forces produced is removed by calculating the force per mm² of toe pad, a significant effect of increasing cell size on the adhesive force produced within species belonging to the genus *Hyla* remains (**Figure 3.11**), suggesting that there is a positive effect of increased pad cell size on the adhesive force seen.

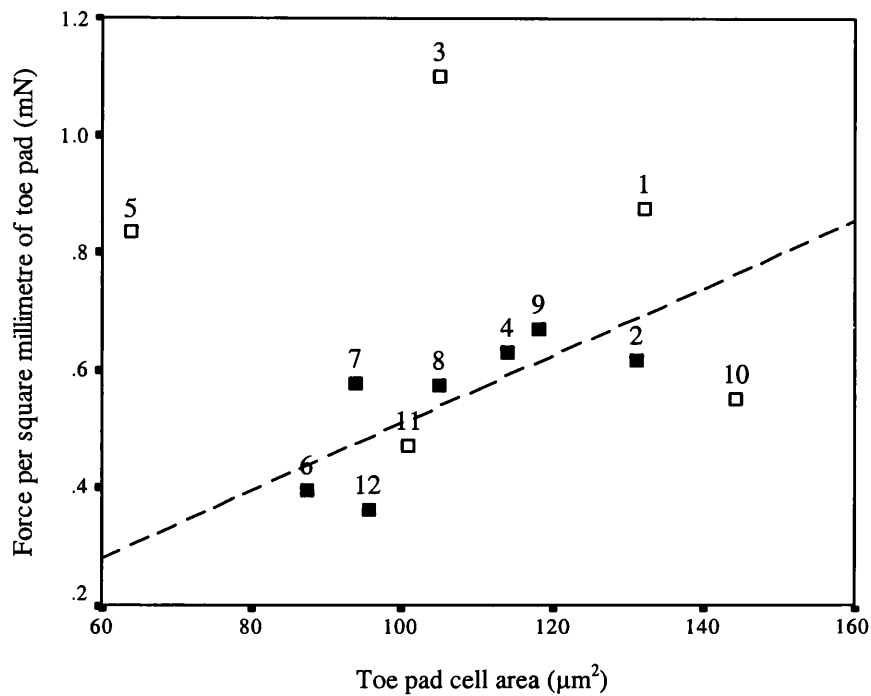


Figure 3.11: Force per mm² on Perspex vs. average toe pad cell area in the genus *Hyla* (+) and in non-*Hyla* genera (). Statistics for *Hyla* species only: $r = 0.75$, $p < 0.05$, 6 d.f. Line of best fit $y = 0.01x - 0.06$, $t = 2.52$, $p = 0.05$, 5 d.f. Numbers indicate species: 1. *P. venulosa*, 2. *H. geographica*, 3. *P. trinitatis*, 4. *H. crepitans*, 5. *S. rubra*, 6. *H. microcephala*, 7. *H. minuta*, 8. *H. punctata*, 9. *H. boans*, 10. *S. lacteus*, 11. *F. fitzgeraldi*, 12. *H. minuscula*.

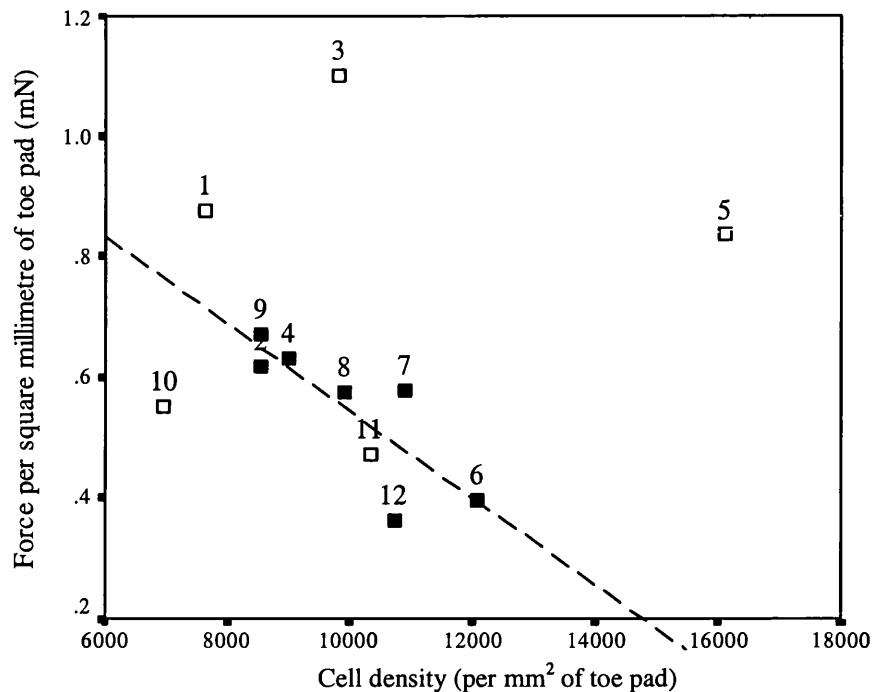


Figure 3.12: Force vs. cell density in genus *Hyla* (+) and non-*Hyla* genera () on Perspex. Statistics for *Hyla* species only: $r = 0.82$, $p < 0.05$, 6 d.f. Line of best fit $y = 1.27 - 0.0001x$, $t = -3.18$, $p = 0.02$, 5 d.f. Species numbers as in Figure 3.11.

Complementary to this finding is the negative relationship between cell density, which is itself inversely proportional to cell size, and force per mm^2 in frogs of the genus *Hyla*. In this case, as cell number per mm^2 is increased, the force generated per mm^2 of pad is substantially reduced (**Figure 3.12**).

One explanation for this, and one touched upon by Green (1981a), is the effect of the size on the ‘tiling’ efficiency of the cell. As the cells get smaller, and there are more of them per square millimetre of toe, there is likely to be an accompanying increase in the area of the intercellular spaces in the same area. These may cause gaps in the even spreading of the meniscus that may be deleterious to the frogs’ adhesive abilities. The increase in intercellular channel area will decrease the actual area of close contact between the cell apices and substrates. Indeed the negative correlative relationship between the adhesive force per mm^2 and the density of the intercellular channels within the species belonging to the genus *Hyla* supports this theory (**Figure 3.13**).

If the only functions of the vast network of intercellular channels that cover the adhesive toe pads in tree frogs are the drainage of excess mucus from the pad, and the supplying of mucus to all parts of the pad, it might be expected that the adhesive forces should increase with increased channel density due to the effects that increased drainage will have upon the height of the fluid layer beneath the pad. It may be that the opposite nature of the trends between intercellular channel density and adhesive force per unit area is due to the effect of increased numbers of intercellular gaps on the even coverage of the pad by the mucosal layer.

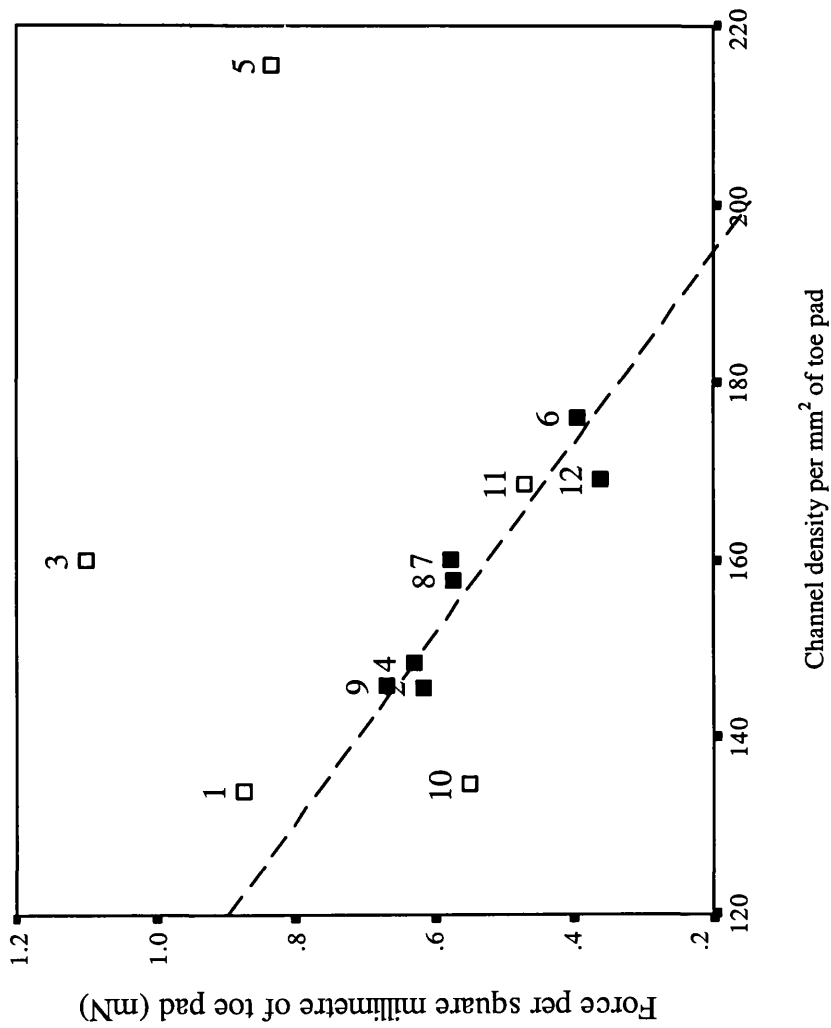


Figure 3.13: Force vs. channel density in genus *Hyla* (+) and non-*Hyla* genera () on Perspex. Statistics for *Hyla* species only: $r = 0.93$, $p < 0.05$, 6 d.f. Line of best fit: $y = 2.02 - 0.01x$, $t = -5.59$, $p = 0.003$, 5 d.f. Numbers indicate species: 1. *P. venulosa*, 2. *H. geographica*, 3. *P. trinitatis*, 4. *H. crepitans*, 5. *S. rubra*, 6. *H. microcephala*, 7. *H. minuta*, 8. *H. punctata*, 9. *H. boans*, 10. *S. lacteus*, 11. *F. fitzgeraldi*, 12. *H. minuscula*.

Higher channel densities may in fact increase the necessity for mucus production, in order to maintain a continuous even spread and functional meniscus in spite of the high density of intercellular ‘gaps’, though there is no correlative relationship demonstrable between the channel densities and mucosal pore densities ($r = 0.27$, N.S. 11 d.f.) that might support this theory.

Alternatively, smaller cell size may be an adaptation to allow species to climb upon rougher surfaces, as they will allow a closer contact, particularly if the surface asperities are smaller in size than the area of the pad will allow for. The differences in cell size between *S. rubra* and *S. lacteus* are of particular interest considering the similarity of their SVL measurements. Differences in the substrata that they regularly encounter in their natural habitats may confirm this hypothesis. The natural behaviour of *S. lacteus* has been difficult to discern in the field as the species is less extensive in its distribution and there is a scarcity of literature about the genus as a whole. The flooded fields that form their habitat in Trinidad (**Appendix 2**), together with the tendency of frogs in laboratory conditions to spend the day immersed entirely beneath the water in burrows in the gravel and the heavily muscled thighs, fully webbed feet and particularly well developed axillary membranes characteristic of the species, may indicate a more aquatic lifestyle in these frogs in comparison to the other more typical ‘tree frogs’ in the study. *S. rubra*, on the other hand, are more terrestrial in their habits (**Appendix 5**) and may have a greater tendency to move on rough substrates than *S. lacteus*, thus explaining the unusually small cell size seen in this species.

The separate consideration of cell size, density and channel density as independent morphological elements of the pad is problematic, as each is directly affected by the

other: channel densities, for example, are strongly correlated to the cell densities between all twelve species, regardless of genera ($r = 0.99$, $y = 0.01x + 68.33$, $T = 19.26$, $p = 0.0001$, 11 d.f.) Given the interdependence of these two variables, it may well be that the relative benefits that increasing the density of the intercellular channel network may confer upon the frogs' sticking ability may be outweighed by the beneficial effects of larger cell size and lowered cell densities on the adhesive forces produced, within the genus *Hyla* (**Figure 3.12**). Additionally, considering a single isolated function of these channels is perhaps to ignore the more complex inter-relationship between pad morphology and functionality. The intercellular gaps may well allow for an even dispersal of mucus through drainage from the pad (Green, 1979) or spreading across the pad (Emerson and Diehl, 1980; Öhler, 1995) but at the same time they also facilitate a closer conformation to a substrate by allowing individual cells to find the best contact with the surface in spite of irregularities.

In all of these trends the positions of two outliers is of particular interest, *Scinax rubra* and *Phyllomedusa trinitatis*. *S. rubra* is capable, in spite of the smaller cell size seen in adults of the species, of producing adhesive forces that are amongst the highest per unit area of pad in any of the species. Jungfer (1987) noted the ability in all seven species of *Scinax* to partially suspend their weight from the first digits alone, with this conferred by the frogs' ability to bend the first finger and first toe with the discs directed posteriorly. He suggests that this is also an adaptation to allow for the 'head-down posture commonly assumed by these frogs on vertical surfaces'. The ability to adhere in this position is highly unusual in tree frogs; the maintenance of low detachment forces is usually effected through an anteriorly-directed peeling mechanism which is passively induced in frogs forced into a head-down orientation

(Hanna and Barnes, 1991). *P. trinitatis*, which although fitting into the trends of cell size increase seen in the genus *Hyla*, produces substantially higher adhesive forces per unit area of toe pad than most species in spite of the low detachment angles recorded. Like other frogs within the genus, *Phyllomedusa trinitatis* are distinctive for the slow deliberate locomotion, described as 'similar to that of a slow loris' (Murphy, 1997). Their hands are specialised for this grasping locomotory mode, unwebbed and with opposable first digits (Duellman, 2001) and it may well be that the adhesive forces being produced within the species have an increased contribution of frictional influences. In both *P. trinitatis* and *S. rubra* there is a substantial decrease in the meniscal heights modelled from the adhesive forces produced on Perspex, suggesting that in both pads conform far more closely to the substrates than is seen in similarly sized species.

The importance of a close conformation between pad and substrate is demonstrable by considering the effect of pad elevation upon the forces produced in frogs adhering to Perspex substrates (**Figure 3.15**). Pad elevation scores range from 0, where the pad lies flush with the ventral surface of the toe as to 3 where the pad is rounded and stands proud of the surface of the toe. If average scores per pad are considered between species then, although there is no effect of frog size on the elevation of the pad, there is a negative correlation between the degree of pad elevation and the force that is being produced per square millimetre of pad (**Figure 3.15**). The observation that the flatter the pad, the better its sticking ability may be due to the effect that an increased pad curvature is likely to have on the even continuous spread of the mucus below the pad. The relationship between pad elevation and the force per unit area may suggest that the rounder pads do not exhibit as close a conformity to the substrate as flat pads.

Images of toes in *Hyla geographica* (Figure 3.14) taken to determine toe pad area (Chapter 2.2.1) suggest that mucosal distribution covers the toe pad proper (tp) and then flows in lines down the lateral edges of the toe towards the subarticular tubercles (sat). There is also a significant mucosal layer covering the area immediately below the proximal margin of the pad in the sub-marginal (sub) areas discussed in 3.2.4.

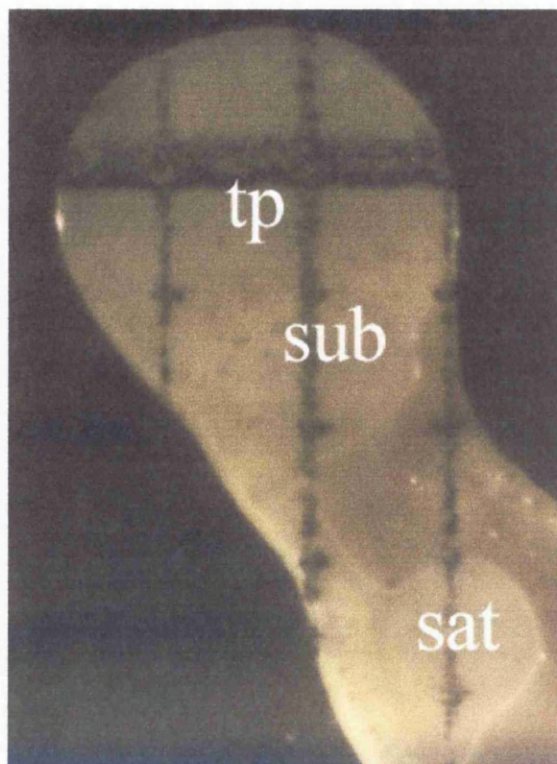


Figure 3.14: Photograph showing the distribution of mucosal layer along ventral surface of the toe in *H.geographica* (Grid = 1 mm).

It may be that the lateral grooves increase the flow of mucus away from the pad and thus aid the maintenance of a thin layer of fluid beneath the pad and the substrate. Alternatively it may be that these grooves carry liquid from the pad to accessory areas including subarticular tubercles along the length of the toe, in either case the distribution of the mucosal layer to areas other than immediately below the pad suggests that the importance of these accessory areas has perhaps been underestimated in previous studies. This last is particularly true if the distribution of specialised cell types along the ventral surface of the toes in different species is taken into consideration.

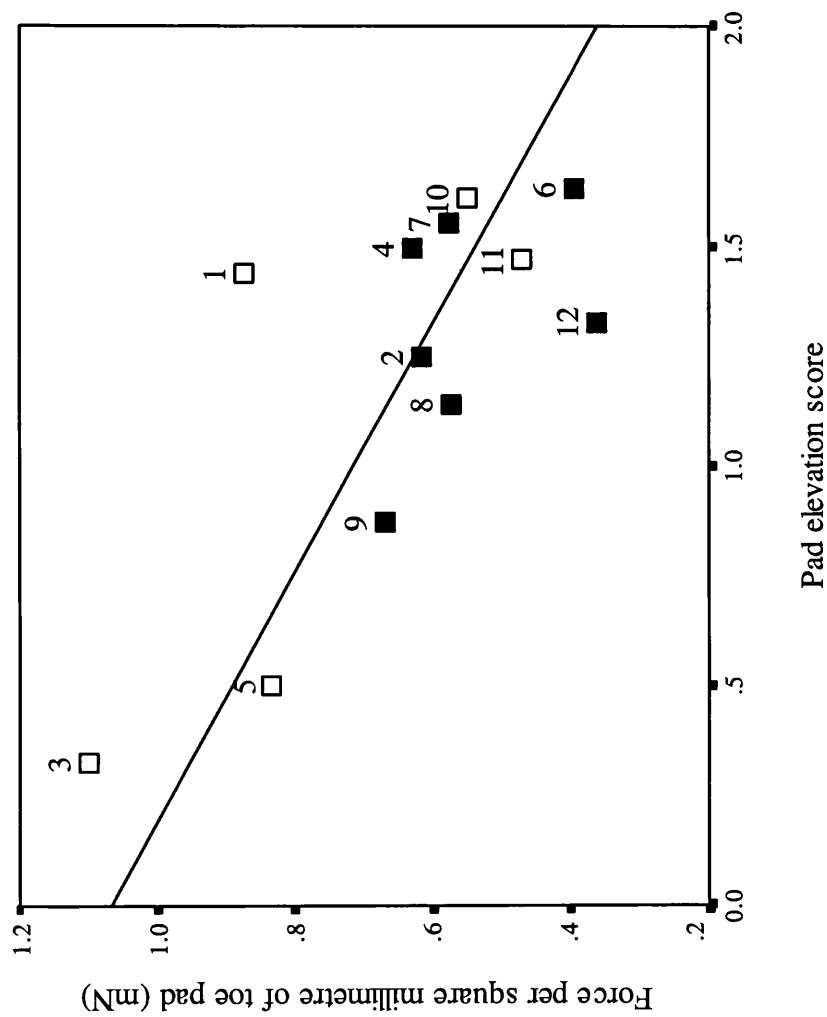


Figure 3.15: Force per unit area vs. pad elevation score in Hylid frogs from the genus *Hyla* (■) and non-*Hyla* genera (□). Statistics for all species: $r = 0.73$, $p < 0.05$, 11 d.f. Line of best fit $y = 1.07 - 0.35x$, $t = -3.40$, $p = 0.006$, 10 d.f. Numbers indicate species: 1. *P. venulosa*, 2. *H. geographica*, 3. *P. trinitatis*, 4. *H. crepitans*, 5. *S. lacteus*, 6. *H. microcephala*, 7. *H. minuta*, 8. *H. punctata*, 9. *H. boans*, 10. *S. latus*, 11. *F. fitzgeraldi*, 12. *H. minuscula*.

Findings in **Chapter 2** suggest that adult frogs belonging to the larger species do not have proportionally larger pads than smaller frogs. However, this S.E.M. study has shown that, in the large species, the areas in which specialised columnar cells occur include the accessory subarticular tubercles as well as the toe pad proper. This suggests that in larger species the area capable of producing forces by wet adhesion is likely to be proportionally greater than in the smaller species which have less specialised cells in these accessory areas (**Figure 3.8**). There is some further evidence of an increasing level of development of the sub-marginal area below the proximal edge of the pad with cells in larger species of frog having more defined intercellular margins.

There is also some evidence that skin in the sub-marginal area is subject to frictional wear; the increased prevalence of impressions of the previous layer of cells upon the surface of the cells on the proximal margin of the pad and on the subarticular tubercles suggests that the skin in these areas is being abraded at a greater rate than elsewhere on the pad. Furthermore, the orientation of the lines indicate that the skin cells in the recently shed layer of skin are arranged above the exposed new skin in a fashion akin to a brick wall, rather than directly on top of the next layer, a feature which would be particularly advantageous in areas particularly prone to mechanical wear and tear during locomotion. The potential for these cell types to function to provide an additional contribution of frictional forces is supported when the increased extent of their distribution to cover the entire ventral surface of the toe is considered for *P.trinitatis* (**Chapter 7.3.5**), as discussed earlier, this species has a locomotory mode that is more dependent on gripping of the substrates than that of other species.

As described in **Appendix 5**, there were, contrary to previous studies, few differences in pad morphology that were directly attributable to the levels of arboreality seen in these species. Indeed, as the four largest species are all highly arboreal, trends in toe pad morphology seen with increasing arboreality are likely to be similar to those seen with linear dimensions.

Overall, this study provides some evidence that changes in adult toe pad morphology between species has a significant effect on the adhesive forces that are produced by the frogs. The differences in pad morphology appear small, but they have significant effects on the efficiency of the pad between species in terms of the force being generated per unit area. Pad morphology has also found to be somewhat variable within adult frogs of a single species (Green, 1979) and it may be that such small differences in the development of grooves and pad elevations may explain how adult frogs within a species are able to maintain adhesive abilities at around a similar level in spite of differences in size (**Chapter 2.3.1**).

Chapter 4: Adhesion in small Hylid tree frogs

4.1. Introduction

From previous chapters it appears that adult frogs belonging to the twelve species of Hylid found in Trinidad are sticking to substrates within their environment utilising a wet adhesive mechanism dominated by area-dependent capillarity forces. This agrees with observations made on an interspecific level in the earlier study by Emerson and Diehl (1980) whereby adhesive forces scale directly with toe pad area. Emerson (1978) notes that as frogs are known to maintain a similar shape over a wide size range, they are particularly useful for the study of allometric effects upon locomotor function. If the Trinidadian Hylids are geometrically similar, as is suggested by looking at the ratios of tibia to SVL in the largest and smallest species (**Chapter 2**), and growth occurs isometrically, then weight will scale with increasing body lengths at a significantly higher rate than the equivalent area (Schmidt-Nielsen, 1993). This might be expected to give an adhesive system dependent on toe pad area a considerable challenge. Although there is a trend between the species in this study towards a reduced rate of weight increase, so that larger species are proportionally lighter than smaller species, the extent of this reduction is not sufficient for the equivalent toe pad area, which does increase isometrically, to compensate effectively for the increasing pressures on the adhesive system imposed by growth. There is therefore a significant decrease in the average angle to which large species are able to maintain a grip upon a surface in comparison to small species on the same substrate.

Conversely, on an intraspecific level an individual adult frog's size seldom has any effect on the average angle to which it is able to maintain a grip upon the rotation platforms. This finding is surprising in view of the fact that, in the majority of species, the rate of weight increase within the adult age class does not show a significant reduction from the expected increase as $(SVL)^3$ (**Table 2.1**). This suggests that, for the changes in weight involved with growth between adult frogs of the same species, there are alterations to the adhesive mechanism that are sufficient to counter the effect that increasing weight may have upon the system. The range of adult sizes that are recorded within a species can represent a substantial difference between the lightest and heaviest individual. For many, the increase in weight can be as much as a hundred per cent, so the fact that the intraspecific adjustments within the adhesive system are able to adequately compensate for this increase is of particular interest. This is especially the case when taking into consideration the effect that gravidity has upon the females of the species (**Appendix 3**). In all cases where a female frog's adhesive abilities were determined both prior to and after egg deposition, a decrease in the average detachment angle was noted in gravid frogs (**Table A3.1.**) As egg-mass burden seldom represents as much as the hundred per cent increase in weight seen between the largest and smallest individuals within a species (**Table A3.2.**), the failure of the adhesive system in gravid females suggests that whatever the compensatory mechanisms being put into effect in adult frogs, these are not effective solutions for relatively short-term large fluctuations in weight and are likely to be being developed with growth over time.

In previous chapters I have discussed the ways in which adult frogs may attempt to adjust variables within the wet adhesive mechanism to attempt to compensate for the

changes in weight between species. The likeliest of the different contributory factors to be readily adjustable, as discussed in the two previous chapters, are likely to be effected by either a proportionally greater increase of toe pad area within a species or changes in the toe pad structure that may facilitate better adhesive ability.

Toe pad area increases as expected interspecifically, so that larger species do not have disproportionately larger pads than small species. Whether this trend is continued on an intraspecific level is difficult to determine from adult data alone as toe pad areas are only known for one to two frogs in each species. However, within the one species *F. fitzgeraldi* for which there is sufficient evidence to carry out such analyses, trends suggest that pad areas intraspecifically may well increase at a greater rate than expected from isometric growth.

There is evidence between species that there are aspects of pad morphology that develop between species that correlate to a greater level of toe pad efficiency (**Chapter 3.3 and 3.4**). Again there is insufficient data to determine whether there are similar intraspecific trends from adult frogs alone, but an S.E.M. study on the development of adhesive toe-pads in one Trinidadian species, *P.trinitatis*, points to a potentially significant within-species trend (Ba-Omar *et al.* 2000) with larger cell sizes obtained from adult toe pads in comparison to those from juveniles. This observation follows extrapolations from adult data as to trends in cell size that might be expected with growth within a species and suggests that the intraspecific development of toe pad structure may well warrant further investigation.

The consideration of the period of growth between metamorphosis and maturation raises an interesting question about how the adhesive system might be able to cope within a species with the size increases involved in attaining adulthood. If typical measurements of new metamorphs belonging to the species under consideration in this study (Downie *et al.* submitted) are considered in relation to adult frogs in **Chapter 2** it can be seen that the increases in size that are involved in growth are substantial (**Table 4.1**). If intraspecific adjustments to the adhesive system, such as proportionally higher rates of increase in toe pad area or development of toe pad morphology with growth, are able to cope with an increase in weight of around a hundred per cent in adult frogs, are such adjustments similarly able to cope with the considerably more substantial weight increase between new metamorph and adult?

Species in order of increasing SVL	Average SVL (mm)			Average weight (g)		
	Juvenile ¹	Adult ²	Increase in size	Juvenile ¹	Adult ²	Increase in size
<i>F. fitzgeraldi</i>	7.40	18.67	x 2.5	0.06	0.52	x 8.7
<i>S. rubra</i>	11.40	30.23	x 2.7	0.17	2.02	x 11.9
<i>H. punctata</i>	13.90	33.42	x 2.4	0.25	2.43	x 9.7
<i>H. geographica</i>	23.28	57.93	x 2.5	0.75	8.43	x 11.2
<i>H. crepitans</i>	18.50	63.35	x 3.4	0.55	14.14	x 25.7
<i>P. trinitatis</i>	15.30	75.90	x 5.0	0.75	21.39	x 28.4
<i>P. venulosa</i>	19.60	74.44	x 3.8	0.39	24.79	x 71.9

Table 4.1: Species average values for snout-vent lengths and weight in juvenile and adult frogs: (1) measurements from new metamorphs in Downie *et al.* (submitted); (2) adult values from **Table 2.1**.

The following chapters describe investigations into the adhesive ability of nine out of the species discussed in the previous chapters during their development from metamorphosis to adulthood. At the same time the changes in toe pad morphology in these species have been studied over the same time period so as to relate structure to function. Since the increase in weight during this period of development is greater in the larger frog species (**Table 4.1**), the pressure put on their area-dependent mechanism will also be greater. Results are thus considered according to the size class of the frog.

Duellman (2001) recognises four size classifications for Hylid frogs, defined by snout-vent length measurements, as follows: Small, < 30 mm SVL; Medium, 30 – 50 mm SVL; Large, 50 – 80 mm SVL and Very large, > 80 mm SVL. Limited data are available for the very smallest and largest of the Trinidadian species so size classes are defined within broader parameters for the purposes of this study: Small < 50 mm SVL; Medium, 50 – 70 mm SVL; and Large, 70 – 100 mm SVL. This chapter will discuss results from studies of adhesive abilities pertaining to species belonging to the ‘small’ size class when adult.

4.2. Methods

4.2.1. Experimental animals

Of the nine study species for which there are both juvenile and adult data available, there are four species that belong to the smaller size class when adult (SVL < 50 mm). In order of increasing average size these are: *Hyla minuscula*, *Flectonotus fitzgeraldi*, *Scinax rubra* and *Hyla punctata*.

Hyla minuscula

The majority of the Hyliid frogs in Trinidad belong to the subfamily Hyliinae, and within that subfamily to the genus *Hyla*. The genus is itself split into over 20 recognised species groups (Duellman, 2001), one of which, the *Hyla microcephala*



Figure 4.1: Male *Hyla minuscula* (Murphy, 1997)

complex, encompasses all three small *Hyla* species found in Trinidad, including the tiny *Hyla minuscula* (**Figure 4.1**) with the sizes recorded in this species being only 12 - 17 mm (Murphy, 1997).

Literature for *Hyla minuscula* is scarce, particularly from Trinidad, where the species is only a very recent discovery (Read 1986, in Murphy, 1997). Duellman (2001) states that the members of the species group exhibit few differences in size and proportion, and all are similar in dorsal colouration. The physical similarity of this species to the more common *Hyla minuta* and *Hyla microcephala*, together with the

range of its distribution in Trinidad, restricted as it is to the Southwest Peninsula (Murphy, 1997), are probably the main contributory factors to its late discovery on the island. The restriction of its range to the Southwest Peninsula also means that it is also possible that *H. minuscula* is amongst species that are believed to be recent arrivals from mainland Venezuela (Kenny, 1977). Frogs of this species were collected from swampy pasturelands at the edge of scrubby forest in the Los Blanquizales marshes, from roadside ditches outside Bonasse and from a drainage ditch in a coconut plantation on the road to Galfa Point. The last of these sites also yielded an unusually small individual (11.25 mm), which was assumed to be a juvenile of the species.

Of the adults collected, ten were male frogs, captured whilst calling or from amplexus. Two gravid female frogs were also collected from amplexing pairs from the Bonasse site. Amplectant pairs were maintained together in tanks with a shallow water film overnight and deposited egg masses that represented 24 % and 29 % of the post-depositional body mass of the two female frogs. Although these hatched into tiny black tadpoles within 72 hours, none survived beyond a few days of hatching.

Flectonotus fitzgeraldi

F. fitzgeraldi is a special case within the size class, belonging as it does to a different sub-family of the Hylidae than the other three, the Hemiphractinae (Mendelson *et al.* 2000). These are commonly known as the 'marsupial' frogs due to the females carrying eggs on their back, often in pouches of varying degrees of development in the dorsal skin (Duellman and Trueb, 1997). *Flectonotus* females have mid-dorsal fleshy folds that entirely cover the eggs (**Figure 4.2**) until late stages of development are reached (Gosner stages 39-41; Duellman and Gray, 1983). Young hatch from the

egg as non-feeding tadpoles and quickly undergo metamorphosis in phytotelmata of bromeliads or other plants (Mendelson *et al.* 2000).

Flectonotus fitzgeraldi is a small agile species, with literature values for SVL measurements placing the species as one of Trinidad's smallest frogs, with average sizes for the species in the locality given as 21 (♂) and 25 (♀) mm SVL (Murphy, 1997; Kenny, 1969). Frogs were collected from the forest floor of humid montane forest on the Morne Bleu ridge, (**Figure A2.1**). At this site, a number of small frogs were seen to be active on the ground during the day but proved extremely difficult to capture, being very active and then cryptic once on the leaf litter. In both of the cases where frogs were captured, one from leaf litter and one from a fallen bromeliad, neither was heard calling on collection and so it was difficult to determine conclusively that these were indeed adult frogs. However, the similarity of the values for SVL in these frogs to combined samples from Trinidad, Tobago and mainland Venezuela in Duellman and Gray (1983) (♂: 17.2 ± 0.26 , $n = 18$) suggests that these frogs are likely to be adult males. Certainly, the size of the single adult female (**Figure 4.2**), collected from a clump of shado beni (*Cilantro* sp.) at the edge of a small pond at Simla in the Arima Valley (**Figure A2.1**), is more comparable to the values in Duellman and Gray (1983) (♀: 21.3 ± 0.44 , $n = 16$).



Figure 4.2: Female *F. fitzgeraldi* from Arima, Trinidad. Photo: J.Smith

Tadpoles were collected from bromeliads sampled from slender tree trunks and branches between 1.5 – 2.5 m from the ground, at a site with only partial canopy

cover. Tadpoles were only found in bromeliads where water was present in the central well, though they were sometimes found in outer crevices formed by overlapping leaves. All bromeliads in which tadpoles were found had smooth-edged leaves and were less than 50cm in diameter; most had spathe-like inflorescences (*Vriesca* sp.). Tadpoles are yolk and delicate and easily crushed if bromeliads are roughly handled, and needed to be transported from study site to laboratory in individual sample tubes to avoid fatal mechanical damage. Once in the lab, most tadpoles transform to fully formed froglets within approximately four days of forelimb emergence. Juveniles were fed on fruit flies but none survived beyond a fortnight of metamorphosis, perhaps having a dietary requirement that was not being met in captivity.

Scinax rubra

This medium-small species belongs to the hylid subfamily Hylinae, as do the majority of the frogs in this study, though it is assigned to the relatively new genus *Scinax*. The genus is characterised by small to moderate-sized elongate frogs



Figure 4.3: *Scinax rubra* (from Murphy, 1997)

(**Figure 4.3**), highly active and scurrying in their locomotion (Murphy, 1997) with these latter tendencies being the derivation of the genus name, from the Greek 'skinos' (nimble) (Duellman, 2001). Previous SVL values for given for this species in Trinidad are given as 33-39 mm (Murphy, 1997) and 31-39mm (Kenny, 1969). Mainland records for this species are smaller on average (Bourne *et al.* 1992: 28-32 mm, Guyana; 28-34 mm, Surinam) and it is worth noting that this species is

known to reach maturity at much smaller sizes in favourable breeding conditions (spermatogenesis at 19 mm; Bourne *et al.* 1992).

The species is highly opportunistic, breeding in open areas under natural conditions and is usually found in disturbed habitat modified by human activity (Kenny, 1969; Murphy, 1997; Duellman, 2001). Collection sites in this instance were typical of this, with frogs sampled from roadside verges and ditches on the East coast (**Figure A2.3**), from tyre ruts at the side of a quarry road near Simla and even from the field station's laundry house (**Figure A2.1**). Frogs were extremely difficult to capture, due to the speed and agility characteristic of the genus but were hardy in captivity, readily feeding and breeding in laboratory conditions.

Tadpoles too were generally hardy, being raised from a clutch of eggs produced in captivity by a pair of frogs sampled in amplexus and from larger tadpoles collected from roadside ditches at Simla and Matura. Metamorphosis occurs around 32-65 days after egg deposition (Bourne, 1992) with metamorphic size in these froglets ranging between 12-15 mm SVL. The small active froglets thrive in captivity, growing quickly on a diet of fruit flies and crickets, achieving full adult size within five months of metamorphosis.

Hyla punctata

Literature is scarce for this medium-small species (**Figure 4.4**), which is from an eponymous species group (Duellman, 2001). The species is not common in Trinidad; Kenny (1969) describes its distribution in isolated pockets across the island as being due to the frogs' dependence on certain habitats, finding the frogs in association with vegetation choked ditches near slow-moving water. The main site of collection in the

Lopinot Valley confirms this theory (Figure A2.1), with the majority of frogs collected from a site used for cultivation of dasheen (*Colocasia esculenta*); these plants were also present at the southern site for the species (Figure A2.2). These large taro-like plants are used in traditional

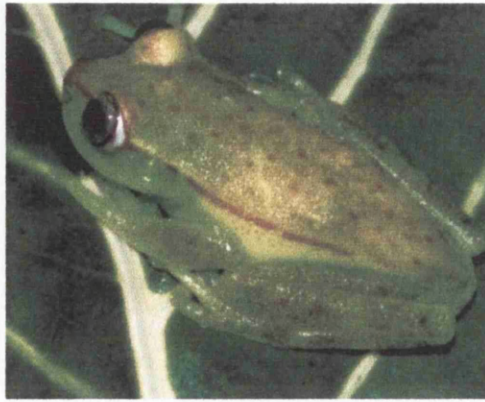


Figure 4.4: Adult *Hyla punctata* (34.2mm).

Photo: J. Smith

Trinidadian cooking and are therefore grown across the island in pits foul with rotted vegetation and often irrigated, as in the instance of the Lopinot site, by slow-flowing diversions of water from nearby rivers and streams. They therefore provide ideal habitat for this frog, both in terms of its growing conditions and in the structure of the plants themselves. In a number of instances, released frogs were seen to take shelter in the hollow bases of the axils of the large heart-shaped leaves.

Large tadpoles were collected from the film of water that lies on the rotted vegetation below these plants where they lie almost motionless on the surface of the mud and transported to the laboratory in a shallow container of clear water. However, maintenance of the tadpoles in the laboratory is difficult and successful metamorphosis of juveniles was achieved on only a few occasions. Froglets show poor post-metamorphic survival so that data are limited for this species.

The most recent literature referring to this species in Trinidad gives SVL measurements of 35 mm in females and 38 mm for male frogs (Murphy, 1997). However, Murphy's values are likely to be an erratum as sexual size dimorphism in anurans favours larger females and instances of reversals, although they do exist, are

unusual and tend to be associated with aggressive male fighting and territoriality (Shine, 1979). Whereas there is no evidence that male-male combat does not occur in this species, earlier studies make no mention of this reversal in sexual dimorphism with values in Kenny (1969) of 30 mm SVL for males and to 35mm SVL in female frogs. Adults of this species do not thrive in captivity and so were released within two days of their capture.

4.2.2. Measurement of sticking ability

All adults were processed prior to determination of sticking abilities as discussed in 2.2.1. Snout-vent lengths, weights and toe pad areas of juvenile frogs were monitored in much the same way at regular intervals after metamorphosis, with these measurements taken prior to the determination of adhesion in the small frogs on each occasion. Sticking ability in adult frogs was determined in the lab in Trinidad, using the methodology outlined in **Chapter 2.2.2**. Juvenile frogs were rotated at least once monthly, again according to this protocol and as with adults weighed and measured immediately prior to experimental use. All experiments were carried out in the room in which the frogs were kept, at temperatures comparable to typical air temperatures in Trinidad.

Species-specific notes on the behaviour of the frogs on rotation platform were also recorded to make sure that detachment angles were an accurate representation of the adhesive performance by toe pad contact alone in all four species:

F. fitzgeraldi are jumpy and active as adults and seldom utilise stomach skin when adhering naturally, scurrying around the platform on their toe tips at angles

significantly greater than the vertical. As juveniles, these frogs tuck their toes beneath the body and press close to the platform with the entire lower ventral surface in contact and need to be 'encouraged' to adhere using only the toe pads.

H. minuscula will also stick with their stomachs if allowed to adhere naturally and often additionally utilise the skin on the postero-ventral surfaces of their thighs. These frogs will tend to adopt a hunched position as the platform continues to rotate from the vertical, bringing the toes and feet under the body as it continues towards 180°.

Scinax rubra are also active on the rotation platform, with an occasional attempt to utilise stomach skin in sticking, though this is not common. Once frogs begin to slip (average angles in adults: $86.1^{\circ} \pm 3.50$, $n=10$) they bring the toes of the front feet together and draw the feet in towards the body. As the platform continues to rotate, any stomach skin in contact peels and they begin to replace their feet continuously, often walking around the board until they fall.

Hyla punctata use both toe pads and stomach skin when adhering naturally. Stomach skin is loose and seems to be quite an important element in natural adhesion for this species as frogs would often stretch their limbs out and walk around the rotation platform with stomach skin sliding across the surface prior to slipping. Specific problems arise from the particular tendency of adults of this species to sit on the platforms with the toe tips curled up from the surface: this is also a feature of behaviour in *S. rubra* though it is less prevalent.

4.2.3. Calculating adhesive force

Adhesive forces were calculated as outlined in **Chapter 2.2.3**.

4.2.4. Toe pad morphology

Toe pads from juvenile and adults were sampled and processed for S.E.M. as described in **Chapter 3.2.1**. Juveniles were sampled immediately following transformation at metamorphosis and thereafter at monthly stages for as long as a significant number of juveniles remained alive for use in adhesion studies. The use of tropical species in this study, only able to be replenished once a year, combined with length of time taken to reach maturity (particularly in the case of the largest species) and the high mortality rates in many species means that the numbers of juvenile samples are less than ideal. Images captured from juvenile and adult frogs were analysed as described in **Chapter 3.2.2**.

4.2.5. Statistics

As a point of note: All statistics and graphs are generated using SPSS statistics software. This package does not have the functional capability to truncate lines of best fit to confine them to the edges of data sets and the lines of best fit on many graphs extend further than the parameters of the study can predict.

All statistical mean values are given in the format: $\bar{x} \pm 1 \text{ s.e.}$

4.3. Results

4.3.1. Morphometric analyses

Scinax rubra

Scinax rubra are a medium-small species of frog. Adults captured at breeding sites ranged in size from 28.3 mm (♂) and 34.8 mm (♀), smaller than previously recorded in Trinidad. As sexes are difficult to determine using external features the average SVL for adult frogs ($29.36 \text{ mm} \pm 0.46$ ($n = 18$)) are likely to include both sexes.

When frogs metamorphose they are around 12-15mm SVL and are a little under 0.2g. Within a year they have attained full adult sizes, with the largest of the frogs raised in Glasgow being 30.9mm SVL and 2.33g, five months after metamorphosis. Investigations of the relationship between linear dimensions and weight increase on a log:log plot for juveniles (**Figure 4.5**) suggest that weight is increasing in these frogs as $(\text{SVL})^{2.73}$. This is significantly lower than the slope of three expected through allometry, ($t = 2.45$, $p < 0.02$, 43 d.f.). The addition of adult data (**Figure 4.5**), increases the rate of weight gain to $(\text{SVL})^{2.86}$, though not to sufficient extent to affect the finding that weight increase is occurring at a lesser rate than three ($t = 2.33$, $p < 0.05$, 61 d.f.). Within the adult data set the tendency to exhibit a lowered rate of weight increase is amplified and at $(\text{SVL})^{1.84}$ is lower than the slope of three expected through allometry, ($t = 3.41$, $p < 0.01$, 16 d.f.) and is lower than seen in the juvenile frogs ($t = 2.49$, $p < 0.02$, 60 d.f.)

The rate of increase in toe pad area with growth (**Figure 4.6**) does not occur at a greater rate than expected in these frogs. In fact the opposite trend is suggested when looking at juvenile data alone (**Figure 4.6**), with area increasing as $(\text{SVL})^{1.53}$, though

this lowered rate is not significantly different to the expected slope of two ($t = 1.18$, N.S. 4 d.f.). The addition of the adult data (**Figure 4.6**) pulls the line upwards to a small degree, to $(SVL)^{1.76}$, though this increase is not statistically significant so that the addition of the adult data does not significantly affect the trends seen (Difference from slope for juveniles only: $t = 0.89$, N.S. 9 d.f. Difference from slope of two: $t = 0.48$, N.S. 5 d.f.).

Across age classes and within the juveniles, the rate at which weight is increasing with growth is occurring a good deal faster than the concurrent increase in toe pad area (Juveniles, $t = 2.89$, $p < 0.01$, 47 d.f.; Total population, $t = 3.98$, $p < 0.01$, 66 d.f.). Within the adult data set alone, weight increase is lowered to such an extent that it is not significantly different to the rate of toe pad area increase seen in the total population ($t = 0.18$, N.S. 21 d.f.). As discussed in **Chapter 2**, evidence is that the total toe pad area in contact with a surface directly influences sticking abilities in tree frogs. Consequently, if the comparative growth trends seen in this species are considered in terms of the effects on the frogs' adhesive abilities, the implications are considerable. In particular, adhesive abilities within the juvenile age class may be expected to be compromised with growth, as weight is increasing at a rate considerably greater than the correspondent increase in area will be able to compensate for. This detrimental effect might be expected to continue across the age groups so that adult frogs are likely to stick less effectively than newly metamorphosed froglets. Within the adults alone, however, the rate at which weight gain with growth occurs is reduced to such an extent that the toe pad area increase will likely be sufficient to allow large and small adults to be able to adhere equally well. The extent to which these predictions are borne out in practice is dealt with in **Section 4.3.2**.

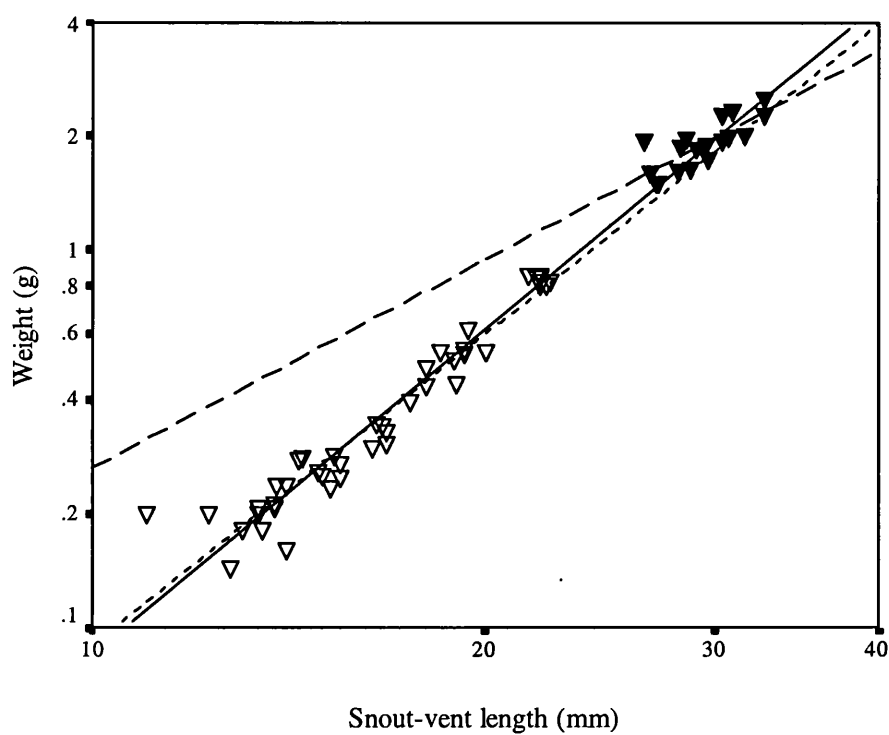


Figure 4.5: Log-log plot of weight vs. linear dimensions in juvenile (▽) and adult (▼) *Scinax rubra*.

Correlation coefficients and lines of best fit in: Total population ____ $r = 0.99$, $y = 2.86x - 3.92$, $t = 50.29$, $p < 0.001$, $n = 63$; Juveniles $r = 0.97$, $y = 2.73x - 3.78$, $t = 24.64$, $p < 0.001$, $n = 45$; Adults___ $r = 0.80$, $y = 1.84x - 2.41$, $t = 5.35$, $p < 0.001$, $n = 18$.

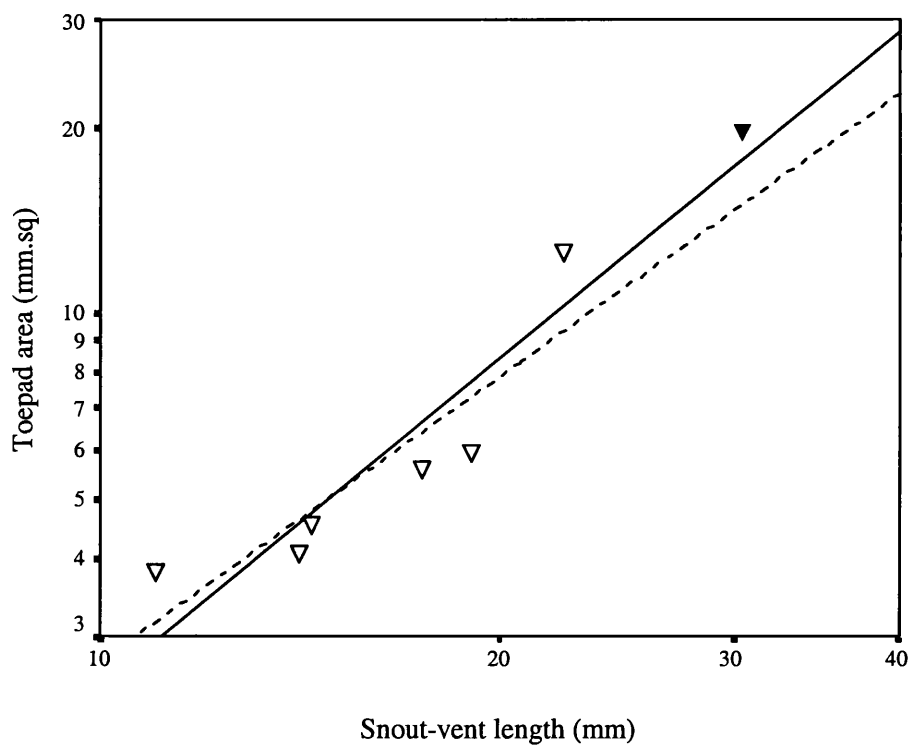


Figure 4.6: Log-log plot of toe pad area increase with linear dimensions in juvenile (▽) and adult (▼) *Scinax rubra*. Correlation coefficients and lines of best fit in: Total population ____ $r = 0.95$, $y = 1.76x - 1.36$, $t = 6.61$, $p < 0.001$, $n = 7$. Juveniles..... $r = 0.88$, $y = 1.53x - 1.09$, $t = 3.79$, $p < 0.02$, $n = 6$.

Flectonotus fitzgeraldi, *Hyla minuscula* and *Hyla punctata*

As an adult, *H. minuscula* is the smallest sized frog of all the species in this study. Snout-vent lengths recorded in calling adult males average at $16.99 \text{ mm} \pm 0.24$ ($n = 10$), with females slightly larger, at $22.90 \text{ mm} \pm 0.10$ ($n = 2$). One particularly small individual was sampled from the field, measuring 11.25 mm SVL; considering the size of the newly metamorphosed froglets of the similarly sized *F. fitzgeraldi*, it seems likely that this juvenile was half-grown and it is difficult to know whether trends here will accurately reflect the typical growth rates seen in this species.

Tadpoles of the marsupial frog, *F. fitzgeraldi*, metamorphose into froglets of $7.93 \text{ mm} \pm 0.13$ ($n = 10$) in length, again at a little less than half of the length of the adult frogs. Frogs sampled from bromeliads on the forest floor averaged in size at 17.30 ± 1.98 ($n = 2$); the single adult female frog found in a gravid state (**Figure 4.1**) measured 21.40 mm in SVL; with this representing a three-fold increase in linear dimensions for growth from juvenile to adult in female frogs, much as is seen in *S. rubra*.

H. punctata is a medium-small species with values for average adult snout-vent lengths of $33.42 \text{ mm} \pm 0.24$ ($n = 12$). As both sexes are known to vocalise at breeding sites (Kenny, 1969) and given the small isolated populations, I did not think killing frogs in order to determine sex was justifiable it seems likely that adults in this study will encompass both male and female frogs. Post-metamorphic survival is low, with the individual froglet sampled measuring 14.70 mm SVL. Growth in this species involves a little over a doubling in the linear dimensions in the period between metamorphosis and adulthood.

If the increase in linear dimensions with growth seen in these three species is accompanied by an isometric increase in weight as expected then there will be an eight-fold increase in weight involved in *H. punctata* and *H. minuscula* and a twenty-seven-fold increase in weight in *F. fitzgeraldi*. In fact, weights recorded for *F. fitzgeraldi*, range from 0.05g to 0.75g, representing a fifteen-fold increase. This suggests that these trends warrant closer scrutiny in all three species.

In the smallest species, *H. minuscula* (**Figure 4.7**), weight can be seen to be increasing as $(SVL)^{1.94}$, considerably less than the expected increase, as $(SVL)^3$ ($t = 8.67$, $p < 0.01$, 11 d.f.). The degree to which weight gain is reduced in this species is greater than in *F. fitzgeraldi* (Difference from slope of 3: $t = 3.36$, $p < 0.01$, 11 d.f.); or *H. punctata* (Difference from slope of 3: $t = 3.42$, $p < 0.01$, 11 d.f.). Rates of weight gain in both *F. fitzgeraldi* (**Figure 4.7**) and *H. punctata* (**Figure 4.7**) increase as $(SVL)^{2.53}$ and $(SVL)^{2.54}$ respectively and are not significantly different from one another ($t = 0.06$, N.S. 22 d.f.).

Toe pad area increase is not significantly different between the species (**Figure 4.8**), and increases at rates no different to those expected; in *H. minuscula* as $(SVL)^{1.94}$ ($t = 0.75$, N.S.) and in *F. fitzgeraldi* as $(SVL)^{2.07}$ ($t = 0.41$, N.S.). Toe pad area is increasing at a significantly lesser rate than is weight in the equivalent time period; *H. minuscula*, $t = 0.14$, N.S. 12 d.f.; *F. fitzgeraldi*, $t = 2.21$, $p < 0.05$, 13 d.f.

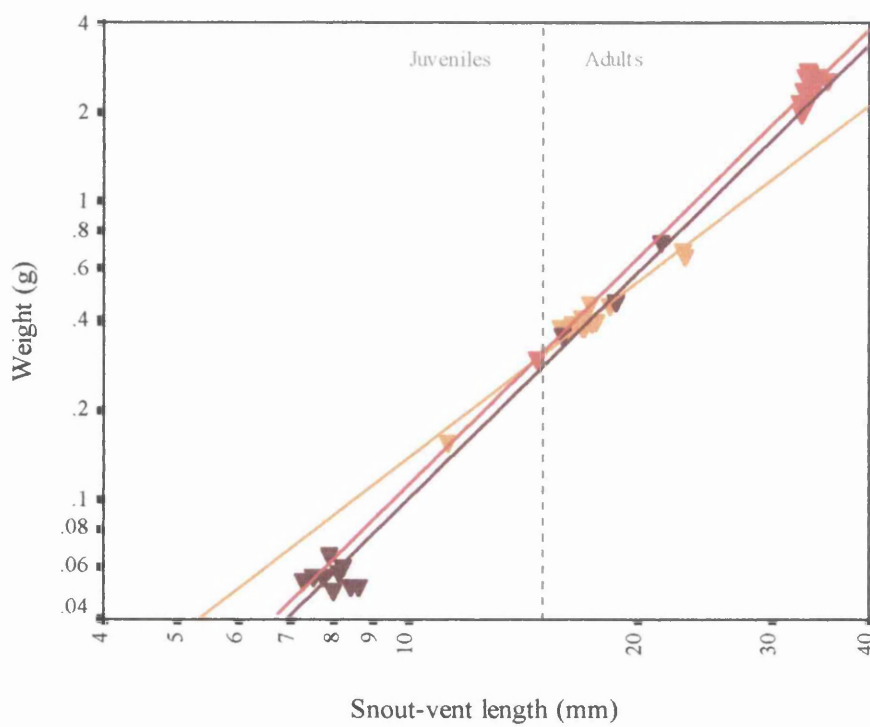


Figure 4.7: Log:log plot of weight increase with linear dimensions in: *H. minuscula* (▼) $r = 0.98$, $y = 1.96x - 2.82$, $t = 16.98$, $p < 0.001$, $n = 13$; *F. fitzgeraldi* (▼) $r = 0.99$, $y = 2.53x - 3.52$, $t = 21.46$, $p < 0.001$, $n = 13$; *H. punctata* (▼) $r = 0.99$, $y = 2.54x - 3.48$, $t = 20.80$, $p < 0.001$, $n = 13$.

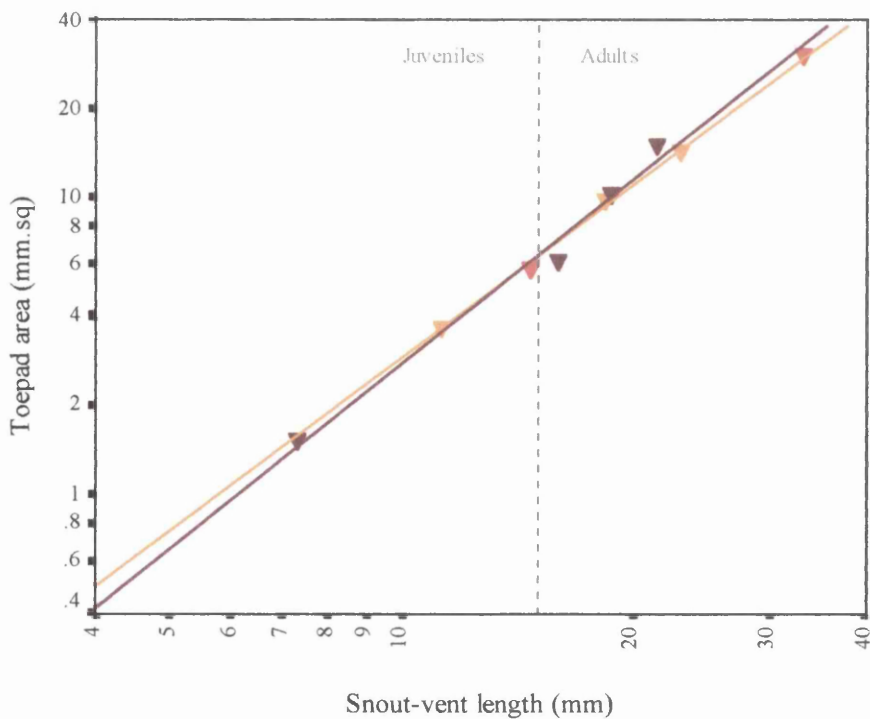


Figure 4.8: Log:log plot of toe pad area increase with linear dimensions in: *H. minuscula* (▼) $r = 0.99$, $y = 1.94x - 1.47$, $t = 25.63$, $p = 0.02$, $n = 3$; *F. fitzgeraldi* (▼) $r = 0.99$, $y = 2.07x - 1.62$, $t = 11.91$, $p = 0.007$, $n = 4$; *H. punctata* (▼) no statistics, $n = 2$.

4.3.2. Size effects on adhesion

Scinax rubra

The adhesive abilities of both juveniles and adults within this species, when considered in terms of the maximal angle of detachment from the experimental platform, are very similar in value and range (**Figure 4.9**). In contradiction to the predictions made considering the effects of comparative allometry, there appears to be no effect of increasing size on the angle to which the frogs are able to maintain a hold, either within or between age classes (**Figure 4.9**).

There is little effect of age on the angle to which the frogs are able to adhere with growth. Average angles in juveniles ($153.68^\circ \pm 2.02$, $n = 45$) are not significantly higher than those recorded from adults ($150.95^\circ \pm 3.46$, $n = 18$); ($t = 0.71$, N.S. 61 d.f.). The percentage of 180° angles recorded within the two age classes was also not significantly different (Juvenile, $1.96\% \pm 0.43$ ($n = 45$); Adult, $1.44\% \pm 0.39$ ($n=18$): $t = 0.71$, $p = 0.48$, N.S. 61 d.f.)

Translating these angles into the adhesive forces required to allow the frogs to maintain a grip at these elevations, makes it clear that the rate at which frogs are increasing the adhesive forces that they are able to produce with increasing size is greater than can be explained by the increase in toe pad area (**Figure 4.10.**), other than within the adults alone (**Figure 4.10**) where adhesive forces scale at a rate no different to linear dimensions squared ($t = 0.60$, N.S. 16 d.f.). Comparing the increase in adhesive force production to the actual increase in toe pad area there is, similarly, no difference between the slopes of the lines of best fit for the increase in pad area and adhesive forces with linear dimensions ($t = 0.20$, N.S. 21 d.f.) but, as pad area

and weight increase at the same rate in adults of this species, then adhesive forces also scale to match weight ($t = 0.31$, N.S. 32 d.f.).

For the total population (**Figure 4.10**) adhesive forces are increasing as $(SVL)^{2.81}$, greater than the expected relationship, which would predict a slope of 2 on a log:log plot of adhesive force vs. SVL ($t = 10.13$, $p < 0.01$, 62 d.f.). Significantly, adhesive force production is also increasing at a greater rate than the observed toe pad area increase in the same frogs ($t = 3.73$, $p < 0.01$, 66 d.f.) but matches the increase in weight over the period of development from new metamorph to adult ($t = 0.50$, N.S. 122 d.f.).

Within the juvenile age class alone (**Figure 4.10**), the rate of adhesive force production is reduced in comparison to that seen across age classes, though the degree to which the slope of the line is affected by the removal of adults from the data under analyses is not significant ($t = 0.71$, N.S. 103 d.f.) The reduction in the elevation of the slope is also not sufficient to affect the observation that adhesive force production is increasing as $(SVL)^{2.69}$, at a significantly higher rate than expected ($t = 4.60$, $p < 0.01$, 43 d.f.). This is higher than the observed rate of increase in toe pad area in juveniles ($t = 2.72$, $p < 0.02$, 47 d.f.) and matches the lowered rate of weight increase seen in these frogs ($t = 0.22$ d.f. N.S. 86 d.f.).

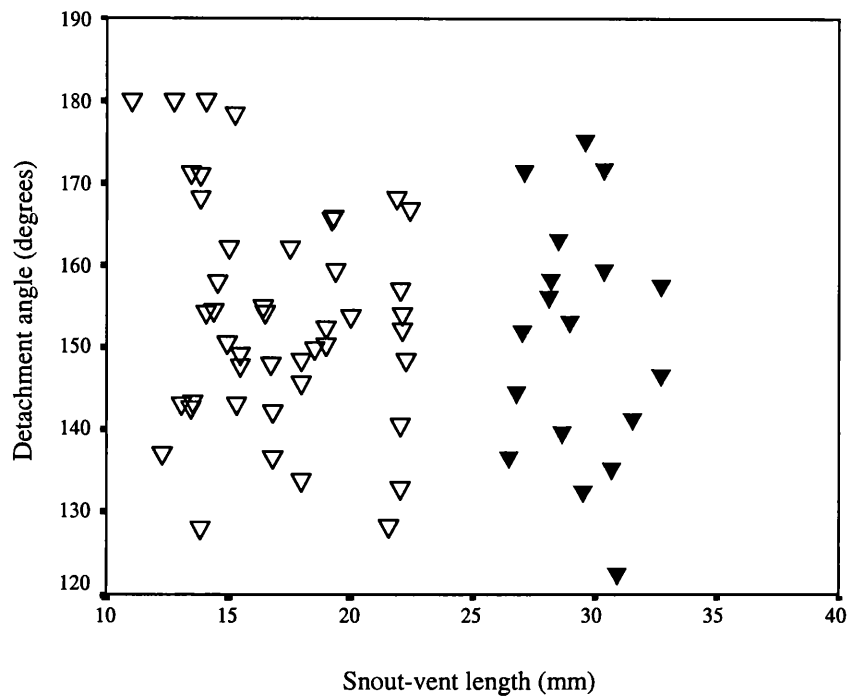


Figure 4.9: Detachment angle relative to linear dimensions in juvenile (∇) and adult (\blacktriangledown) *Scinax rubra*. Correlative statistics for: Total population: $r = 0.16$, N.S., $n = 63$; Juveniles: $r = 0.20$, N.S., $n = 45$; Adults: $r = 0.11$, N.S., $n = 18$.

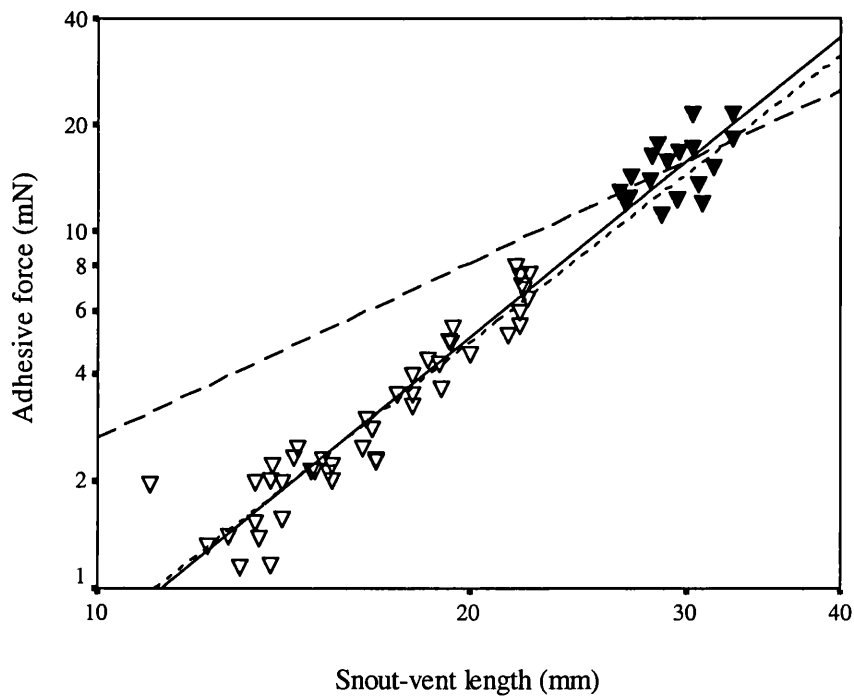


Figure 4.10: Log-log plot of adhesive forces vs. linear dimensions in juvenile (∇) and adult (\blacktriangledown) *Scinax rubra*. Correlation coefficients and lines of best fit in: Total population ____ $r = 0.98$, $y = 2.81x - 2.95$, $t = 35.83$, $p < 0.001$, $n = 63$; Juveniles $r = 0.94$, $y = 2.69x - 2.81$, $t = 18.27$, $p < 0.001$, $n = 45$; Adults ___ $r = 0.54$, $y = 1.62x - 1.19$, $t = 2.55$, $p = 0.02$, $n = 18$.

Flectonotus fitzgeraldi, *Hyla minuscula* and *Hyla punctata*

There is no detrimental effect of growth on sticking ability in *H. minuscula* (**Figure 4.11**) with no significant difference between the average angles recorded in adult and juvenile frogs ($t = 0.64$, N.S. 11 d.f.); when these are translated to adhesive force (**Figure 4.12**) increasing as $(SVL)^{1.96}$, is as expected for an adhesive mechanism dependent on the area of contact ($t = 0.33$, N.S. 11 d.f.). The rate of increase in adhesive force production scales with toe pad area ($t = 0.14$, N.S. 12 d.f.) and, is also able to match the increase in weight in the same growth period ($t = 0.02$, N.S. 22 d.f.)

In *F. fitzgeraldi*, (**Figure 4.11**), there is again no effect of growth on the angle to which the frogs are able to adhere, with average angles in juveniles $179.30^\circ \pm 0.70$ ($n = 10$) and in adults $174.63^\circ \pm 4.03$ ($n = 3$); Difference between means, $t = 1.98$, N.S. 11 d.f. The increase in force production with growth, as $(SVL)^{2.51}$, can also be seen to be occurring at a significantly greater rate to that expected from a mechanism dependent on area ((**Figure 4.12**); Difference from slope of 2: $t = 4.63$, $p < 0.01$, 11 d.f.). The increase in adhesive force production is greater than the equivalent toe pad area ($t = 2.17$, $p < 0.01$, 13 d.f.) and is not significantly different to the lowered rate of increase in weight with growth ($t = 0.12$, N.S. 22 d.f.).

Average angles of $143.21^\circ \pm 5.26$ ($n = 12$) recorded in adult *H. punctata* (**Figure 4.11**) are not significantly different to those seen in the juveniles ($t = 1.94$, N.S. 11 d.f.). When angles are translated to adhesive forces, the relationship with linear dimensions, as $(SVL)^{2.12}$, is much as would be expected in an area dependent system (**Figure 4.12**); Difference from slope of 2, $t = 0.29$, N.S. 22 d.f. However, adhesive force production also matches the weight slope seen in this species ($t = 0.98$, N.S. 22d.f.) so that there is no detrimental effect of growth on adhesion in this species.

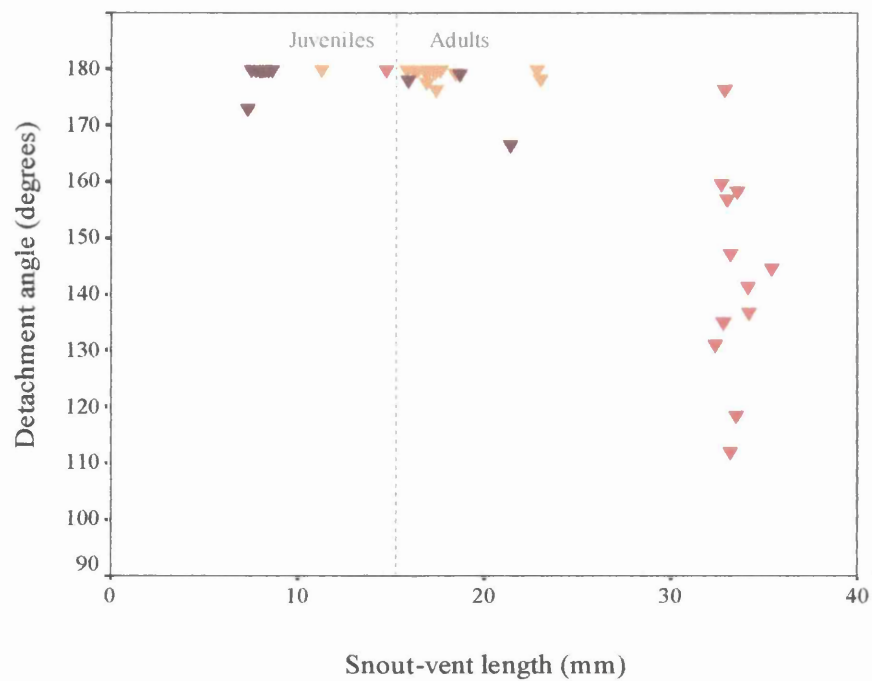


Figure 4.11: Detachment angles on Perspex in: *H. minuscula* (▼) $r = 0.19$, N.S. $n = 13$; *F. fitzgeraldi* (▼) $r = 0.61$, $F = 6.61$, $p = 0.03$, $n = 13$; *H. punctata* (▼) $r = 0.51$, N.S. $n = 13$.

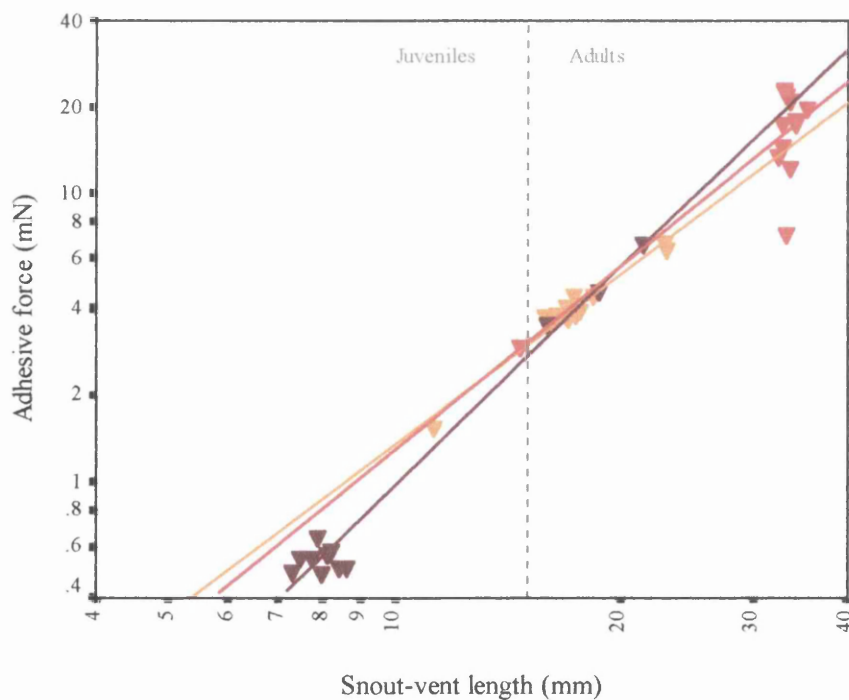


Figure 4.12: Log:log plot of adhesive force increase with linear dimensions in *H. minuscula* (▼) $r = 0.98$, $y = 1.96x - 1.82$, $t = 15.91$, $p < 0.001$, $n = 13$; *F. fitzgeraldi* (▼) $r = 0.99$, $y = 2.51x - 2.51$, $t = 2.27$, $p < 0.001$, $n = 13$; *H. punctata* (▼) $r = 0.84$, $y = 2.12x - 2.01$, $t = 5.12$, $p < 0.001$, $n = 13$.

Small species

The increase in the adhesive forces produced with growth is more than enough to match the increase in weight in the period of development from juvenile to adult both between and within the age classes in all four species discussed here.

In adults this is perhaps largely explained by the fact that the trend seen both across and within the age classes, such that weight gain seen with growth is significantly lower than that expected, is particularly pronounced and is reduced to such an extent that the rate of toe pad area increase matches weight gain with growth. The substantial lowering of weight increase with growth in adults suggests that the pressure to maintain low body weight is greater in this age class, and that this is likely to be the main means by which they are able to maintain sticking ability independent of body size.

Whilst it is also the case that juvenile frogs may also be keeping their weight proportionally low in response to the demands that increasing weight will place upon their adhesive system, particularly in *Hyla minuscula*, the reductions in weight gain with growth are not sufficient to explain how in all cases frogs are able to produce adhesive forces that increase at a greater rate than equivalent area increase can explain.

This is confirmed by considering the effect that removing the contribution of differing areas of pads on the adhesive forces produced by frogs has upon the relationship between SVL and force per mm². By dividing adhesive forces by toe pad area, then there is a positive correlation with the linear dimensions, both across the species and

within the *Scinax* frogs alone (**Figure 4.13**). This, together with the observation that sticking angles are being conserved at the same level regardless of increasing size in these frogs, suggests that increasing adhesive ability in these frogs is due to an ‘improvement’ in some other element within the adhesive system on an interspecific level that allows the frogs to compensate for the pressures of growth.

The ability to adjust aspects of the adhesive mechanism on an intraspecific level is confirmed by considering trends within adult frogs of the two of these smaller species tested on a variety of substrates with differing surface energies (**Figure 4.14**). In spite of the changes between substrates in terms of their wettability, adult *S. rubra* and *H. punctata* are both able to maintain detachment angles on Teflon to around the same degree as they are on glass. The lowered tendency of fluid to spread along the surface of Teflon means that frogs might be expected to be detrimentally affected on this surface were they not able to adjust some property of the meniscus that effects wet adhesion in some way.

If we assume that similar limitations on changes to mucosal properties such as viscosity and surface tension exist for juveniles as they do in adult frogs (see **Chapter 2**) then the likeliest of the variables within the wet adhesion model to change with increasing linear dimensions might again be the depth of mucus below the pad, the meniscal height. There is some evidence of interspecific differences in toe pad structure between twelve species that may have an effect on this parameter in adult frogs. If, as the trends in force per unit area suggest, adult frogs within the four small species of Hylid have more efficient pads (**Figure 4.13**) than the juveniles, it seems reasonable to assume that improvements seen in the adhesive mechanism might be reflected at a fine structural level.

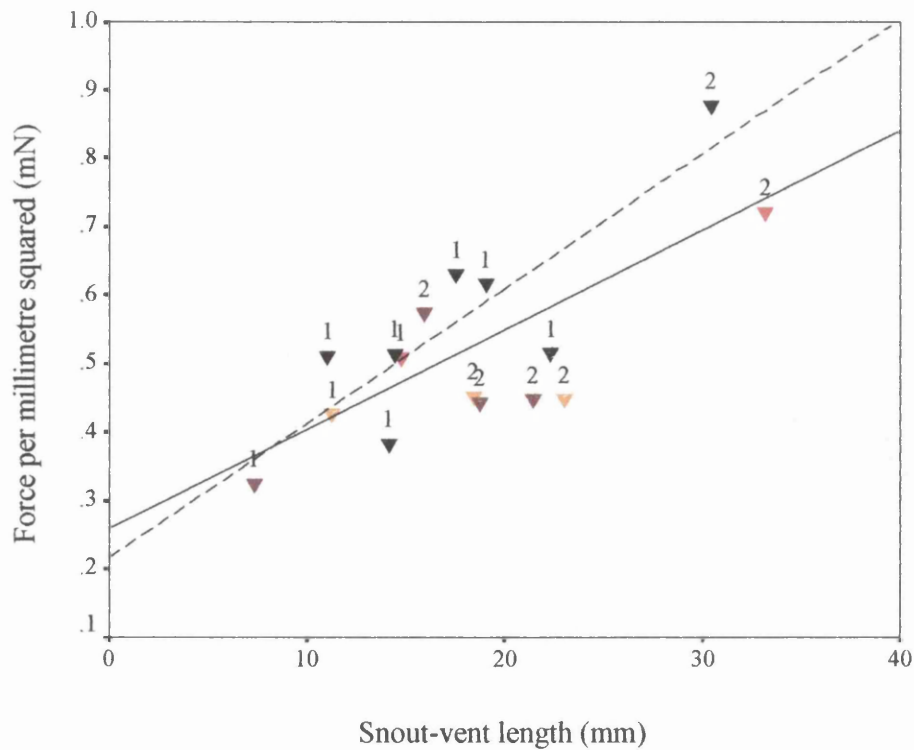


Figure 4.13: SVL vs. adhesive force per mm² of toe pad in juvenile (1) and adult (2) frogs belonging to four small species of Hylid frog; *F. fitzgeraldi* (▼) *H. minuscula* (▼) *S. rubra* (▼) *H. punctata* (▼). Correlative relationships: All frogs, $r = 0.73$, $y = 0.01x - 0.27$, $t = 3.88$, $p = 0.02$, $n = 15$; *S. rubra*, $r = 0.82$, $y = 0.02x - 0.22$, $t = 3.19$, $p = 0.02$, $n = 7$.

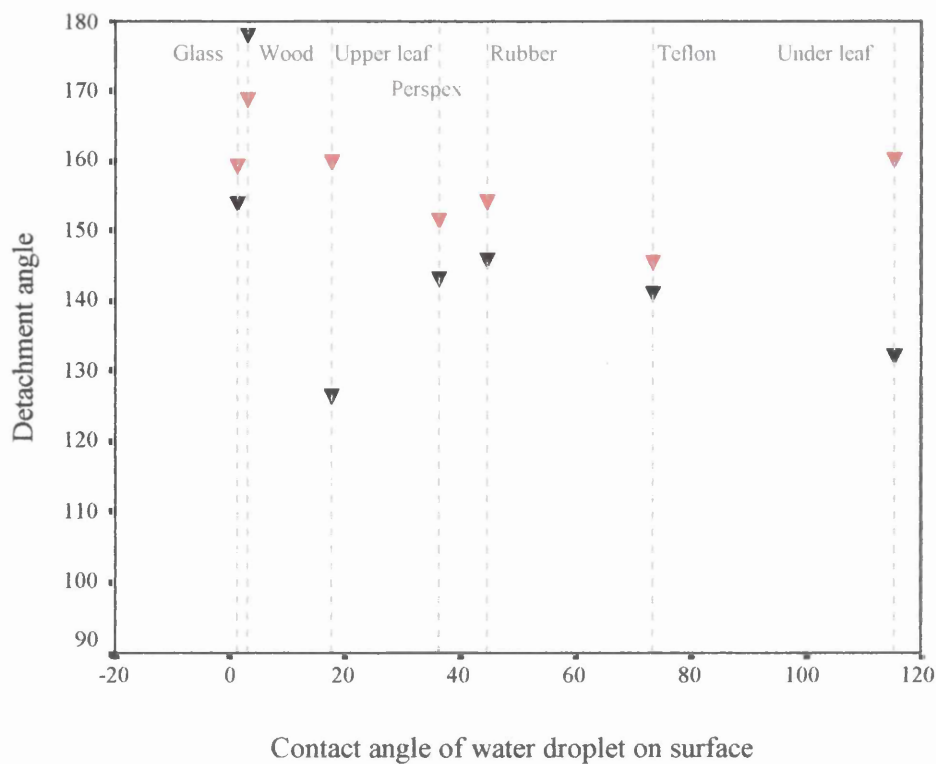


Figure 4.14: Detachment angles in adult frogs from two small species of Hylid frog on seven substrates according to contact angle of water droplets on their surface; *S. rubra* (▼) *H. punctata* (▼). Correlative statistics: All frogs, $r = 0.42$, $t = -1.60$, $p = 0.14$, N.S., $n = 14$; *S. rubra*, $r = 0.40$, $t = -0.97$, $p = 0.39$, N.S., $n = 7$; *H. punctata*, $r = 0.54$, $t = -1.43$, $p = 0.21$, N.S., $n = 7$.

4.3.3. Toe pad morphology

Scinax rubra

Toe pad cells in *Scinax rubra* are visually indistinguishable from any other Hylid species studied here (Chapter 3). The specialised cells that tessellate across the surface of the pad are hexagonal in the main, though towards the proximal margin and around mucosal pores there are a number of pentagonal and heptagonal cells (Figure 4.15).

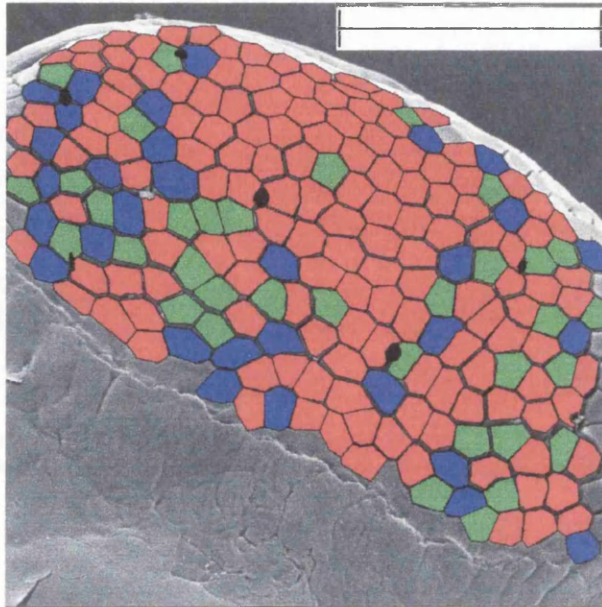


Figure 4.15. Cell shape on toe pad of juvenile *S. rubra*
Scale bar = 150 μm . Colour coding: red = hexagonal; green = pentagonal; blue = heptagonal; black = mucosal pores.

The presence of the alternate geometries in cell apical shapes in these areas is perhaps a product of the need for greater deformability at the edges of the pad to aid in the maintenance of meniscal boundaries.

Although cells are structurally similar between the age classes, there are some differences in the cells seen in adult and juvenile frogs in terms of the apical contact area of each cell. Adult frogs exhibit an average cell size of $65.60 \mu\text{m}^2 \pm 1.95$ ($n=70$), with these dimensions being considerably smaller than those seen in juvenile frogs whose cell areas average around $109.79 \mu\text{m}^2 \pm 1.40$ ($n = 268$). Differences in variances (Levene's test statistic: $F_{69,267} = 18.68$) means that non-parametric tests are necessary, and a Mann-Whitney U test performed on the data ($U_{70,268} = 978$, $p <$

0.01), confirms the observation that the median cell size is statistically significantly different between the two age classes.

One consequence of this is that cell densities are also significantly different in the two age classes. This can be seen by comparing the images of cells in juvenile and adult frogs at the same magnifications in **Figure 4.16 b** and **d** (below), where it is obvious that, in the smaller celled adults, densities appear higher than in juveniles.

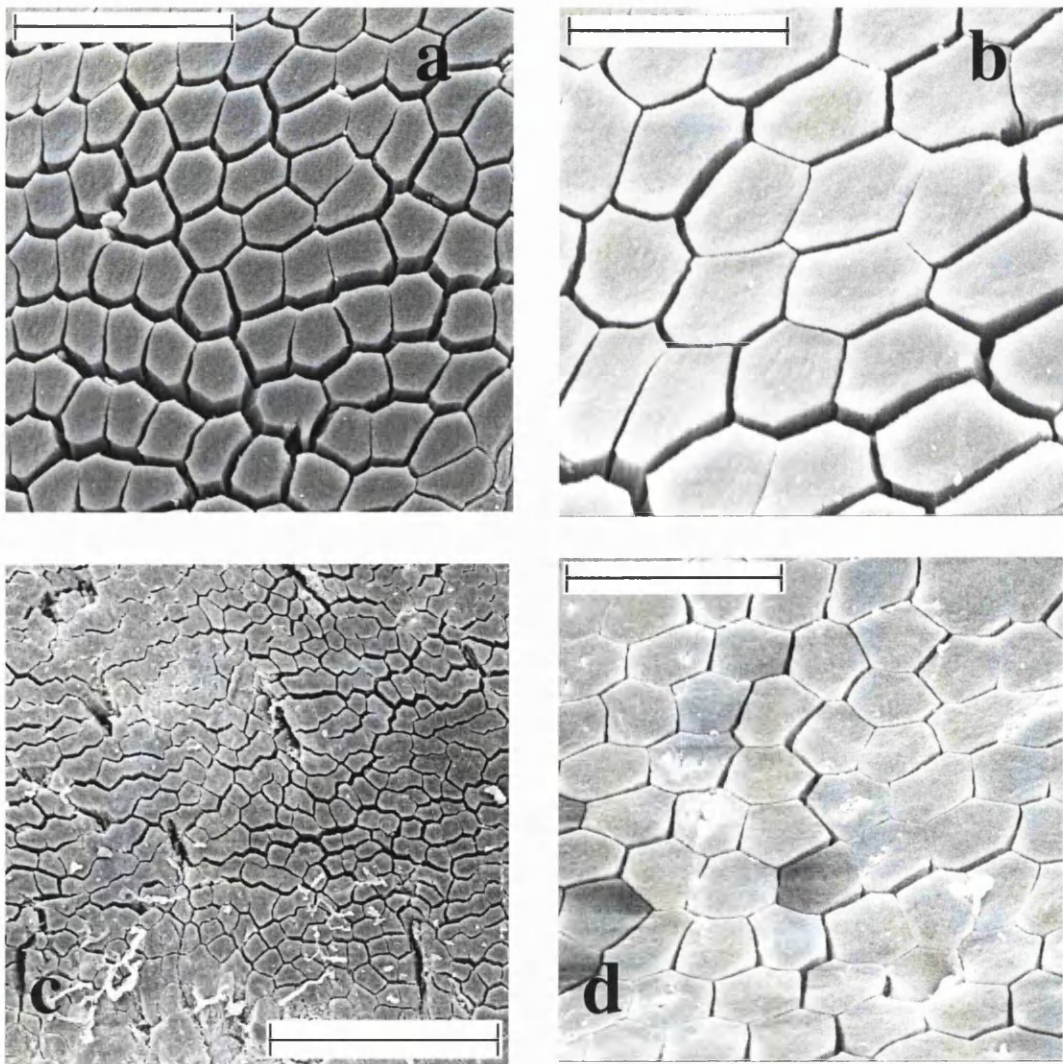


Figure 4.16: S.E.M. images of toe pad cells in *S. rubra* (a) Juvenile 1 (12.25 mm) Front 3, Scale bar = 50 μm (b) Juvenile 1 (12.25 mm) Front 2, Scale bar = 25 μm (c) Adult (30.40 mm) Front 4, Scale bar = 100 μm (d) Adult (30.40 mm) Front 2, Scale bar = 25 μm

This observation is borne out when considering the results of cell counts of comparable areas in the central portion of the pad where the topography of the pads is relatively flat. In juveniles, cell densities per pad have a value of $9451.32 \text{ cells per mm}^2 \pm 353.95$ ($n = 27$), a figure which is considerably less than that seen in adults; $16111.23 \text{ cells per mm}^2 \pm 1094.80$ ($n = 7$). Statistically, average cell densities in adult frogs are significantly higher than seen in juveniles ($F_{6,26} = 1.26$; $t = -7.55$, $p < 0.001$, 32 d.f.) in spite of the high degree of variability seen in adults.

Another consequence of the statistical differences between the cell sizes in the two age classes is the change in the intercellular channel densities between the two age classes, dependent as this parameter is on the cells' perimeter lengths. Each square millimeter of the pad in juveniles is traversed by over 10 cm of channels, with average cell densities of $163.36 \text{ mm/mm}^2 \pm 9.36$ ($n = 27$). This is a value that is comparable with those seen in adults of larger species (**Chapter 3.3.3.**). Adults of *S. rubra* have the highest channel density of all twelve species under investigation (**Table 3.2.**), with densities averaging at $215.72 \text{ mm/mm}^2 \pm 7.06$ ($n = 7$). This is significantly higher than the densities measured in juveniles ($F_{6,26} = 1.21$; $t = -2.77$, $p = 0.009$, 32 d.f.).

Mucosal pores seen across the pads in both juveniles and adults (**Figure 4.17** and **Figure 4.18**) all belong to the Type II (Green, 1979) category of pore, with the cell walls that form the lumen being modified in comparison to the normal striations that are seen on the vertical sides of the columnar cells.

In juveniles, pore size is small; especially so in the two smallest froglets where average pore size is $10.96 \mu\text{m}^2 \pm 1.94$ ($n = 9$). In these frogs the pores are mostly stomata-like, bordered by two cells and formed by 'dents' in the adjacent walls of these two cells (**Figure 4.17a**). There are also a number of more typical small rounded pore openings in juveniles bordered by four to six cells (**Figure 4.17 b**). Pads of the largest juvenile show two further pore types: the first of which have luminal cell walls more horizontally inclined in orientation, forming a shallow roughened depression which slopes into the central pore opening (**Figure 4.17 c**). Cells with roughened surface architecture are also seen framing shallow 'slits' on the pad surface (**Figure 4.17 d**).

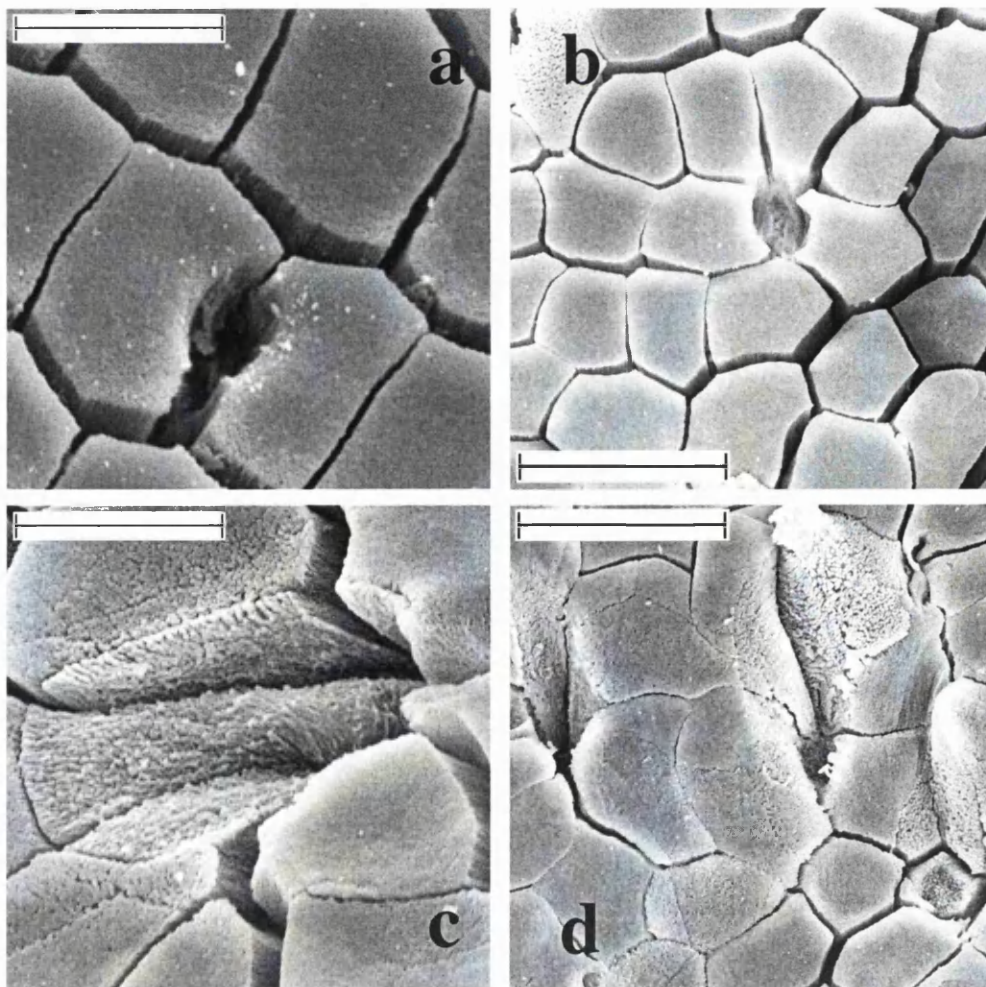


Figure 4.17: S.E.M. images of mucosal pores in juvenile *S. rubra*. (a) Juvenile 1 (12.25 mm) Back 1, Scale bar = $12.50 \mu\text{m}$. (b) Juvenile 3 (14.41 mm) Front 4, Scale bar = $25 \mu\text{m}$. (c) Juvenile 3, Back 1, Scale bar = $12.50 \mu\text{m}$. (d) Juvenile 3, Front 3, Scale bar = $25 \mu\text{m}$.

Typical pore sizes in adults are considerably larger than seen in the two smallest juveniles, at $78.99 \mu\text{m}^2 \pm 19.42$ ($n=12$). The most commonly seen type of mucosal pore seen in adult frogs is of a simple geometrical shape bordered by five to nine cells (**Figure 4.18 a and b**). These are similar to those described from the adults of several species but differ in the extent to which the framing cell sides are modified. In species such as *H. crepitans* (**Figure 3.7. i**), modifications to the lumen walls in Type II pores consist of microvilli-like structuring on the vertical sides of the bordering pad cells; in *S. rubra*, changes in appearance to the normal striations are less extensive with the walls sculpted instead into knobbed and roughened lines (**Figure 4.18 a**).

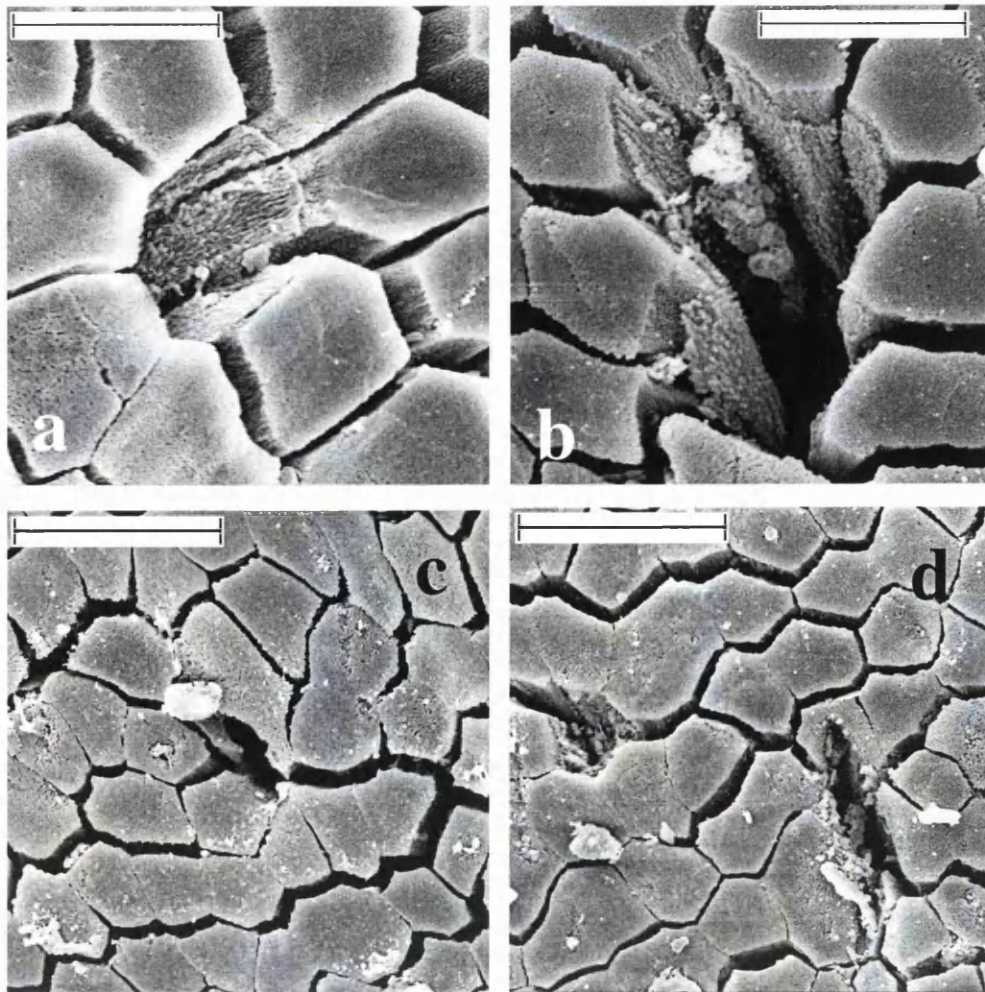


Figure 4.18: S.E.M. images of mucosal pores in adult *S. rubra* (a) Adult (30.4 mm) Back 3, Scale bar = $12.50 \mu\text{m}$. (b) Adult (30.4 mm) Front 4, Scale bar = $12.50 \mu\text{m}$. (c) Adult (30.4 mm) Front 4, Scale bar = $25 \mu\text{m}$ (d) Adult (30.4 mm) Front 4, Scale bar = $25 \mu\text{m}$

Although the stomatal type of pore seen most prevalently in very small juveniles has disappeared from the adult sample, slit-shaped pores are still prevalent in the adult sample as they are in the younger frogs. In adults slit-shaped pores are generally relatively small (**Figure 4.18 c**) with one terminal end imbedded in the cell wall of a framing cell. In a number of cases, especially near the proximal margin of the pad the pores are slightly longer with one to two cell sides forming the longitudinal edges of the slit (**Figure 4.18 d**).

In both age classes pores are distributed in transverse lines across the central portion of the pad (**Figure 4.19**). Values for average densities seen in juveniles, $52.07 \text{ per mm}^2 \pm 4.42$ ($n = 17$), are significantly higher than the values in adults where average pore densities on a pad are around $22.85 \text{ per mm}^2 \pm 1.60$ ($n = 5$) ($F_{4,16} = 3.36$; Difference between means; $t = 3.51$, $p = 0.002$, 20 d.f.).

Other structural changes to toe pad morphology between juvenile and adult can be seen in **Figure 4.19**. In both age classes the elevation of the pad from the ventral surface of the toe is very shallow, though there is a tendency towards a flatter pad in the adults where the crown of the pad is often situated below the ridge of the circumferal margin (**Figure 4.19 f**). The circumferal groove that is bordered by this margin is shallower and less well defined in the juveniles than in the adults (**Figure 4.20 a and c**), with the extension of the groove terminating below the front pad in adults (**Figure 4.19 e**) in comparison to midway down the lateral edge in the smallest juvenile (see **Figure 4.19 a**). The completion of the circumferal groove to form a proximal marginal groove seen in a number of larger species is not noted for any individuals in this species.

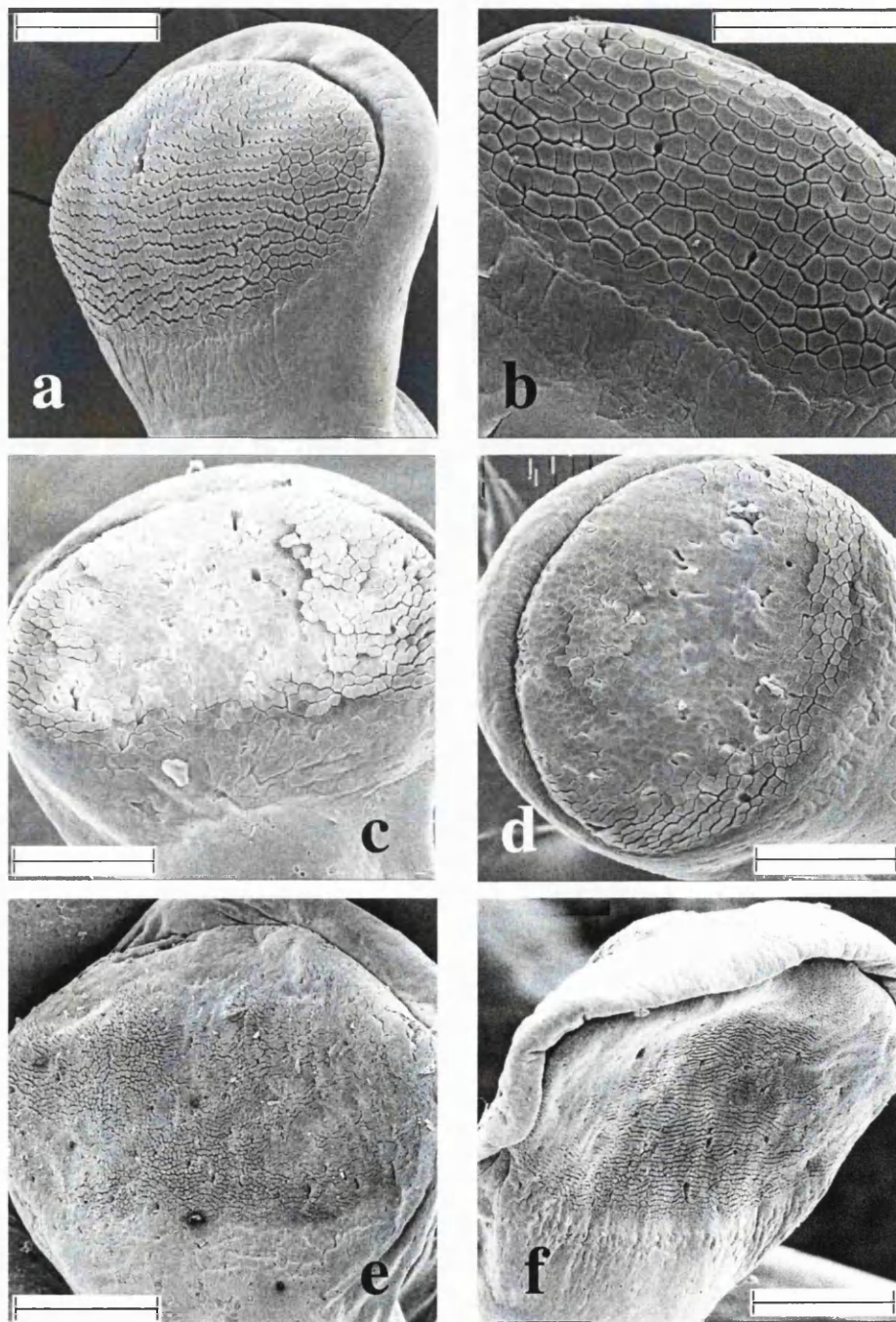


Figure 4.19: S.E.M. images of toe pads in *S. rubra* (a) Juvenile 1 (12.21 mm) Front 3, Scale bar = 150 μm (b) Juvenile 1 (12.21 mm) Back 1, Scale bar = 100 μm (c) Juvenile 3 (14.40 mm) Front 1, Scale bar = 150 μm (d) Juvenile 3 (14.40 mm) Back 4, Scale bar = 150 μm (e) Adult (30.4 mm) Front 2, Scale bar = 300 μm (f) Adult (30.4 mm) Back 4, Scale bar = 300 μm .

The circumferal margin is often set fairly far back from the crown of the pad, particularly in the front toes (**Figure 4.19 a, c and e**) and in the juvenile frogs where the pads appear almost emarginate (**Figure 4.19 b and d**). The cells on these margins in juvenile frogs have a complex surface architecture with knobbed convolutions and rolled margins (**Figure 4.20 b**) with the extent of roughening reduced on the internal wall of the ridge (**Figure 4.20 a**). In adults the separation of the cells on the circumferal margin is less defined, with the finer surface architecture giving the continuous layer of cells a 'spongy' appearance (**Figure 4.20 d**).

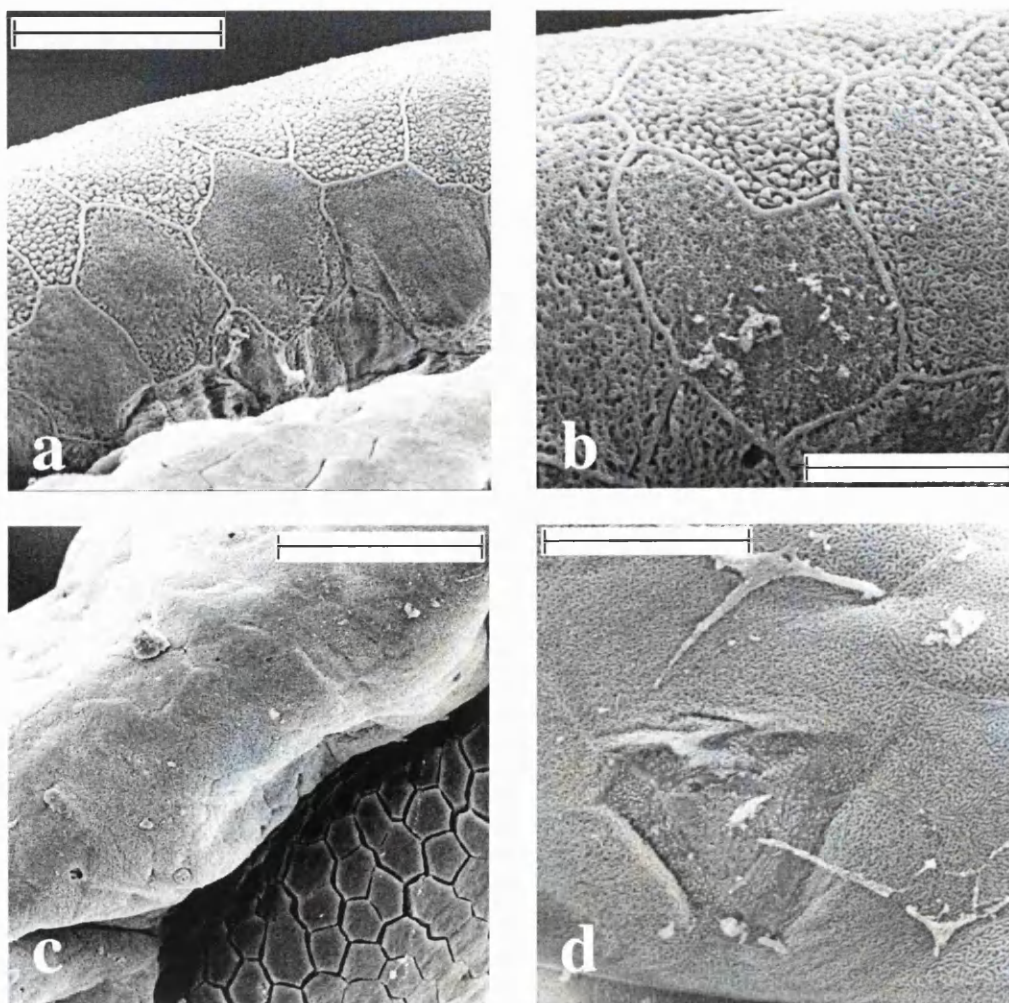


Figure 4.20: S.E.M. images of circumferal grooves and marginal cells in *S. rubra* (a) Juvenile 3 (14.40 mm) Front 3, Scale bar = 25 μm . (b) Juvenile 3 (14.40 mm) Front 3, Scale bar = 12.5 μm (c) Adult (30.40 mm) Front 4, Scale bar = 50 μm (d) Adult (30.40 mm) Front 1, Scale bar = 25 μm .

The definition of the proximal margin is indistinct in this species in juveniles (**Figure 4.21 a**) and in adults (**Figure 4.21 c**), with the area of differentiation of cell types lying flush with one another in both age classes. This is unusual as in most other species the two regions are usually separated by the increased elevation of the pad surface from the ventral surface of the toe. The sub-marginal cells have a micro-villated surface architecture, particularly evident in the adults, and are separated from one another by very shallow intercellular channels (**Figure 4.21 b and d**) with the separation of the individual cells being better defined in the juvenile frogs.

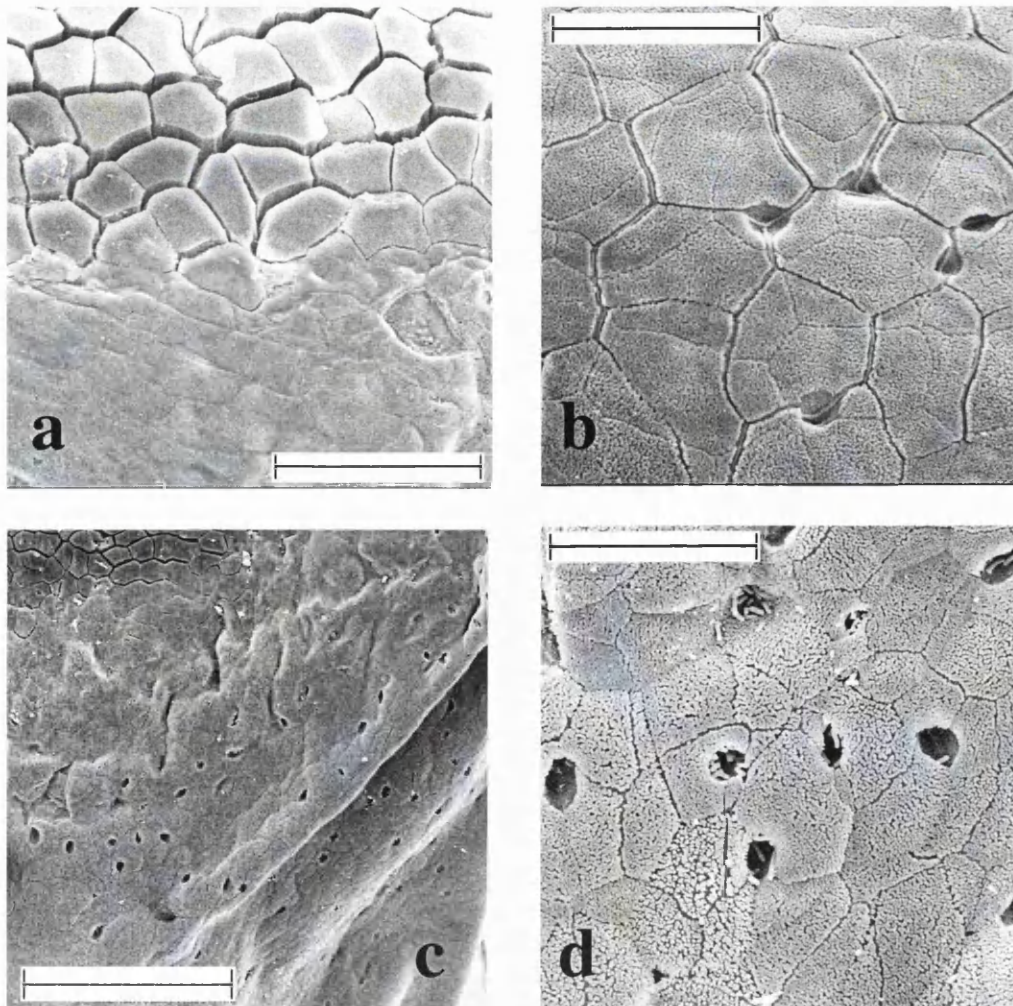


Figure 4.21: S.E.M. images of proximal margins and sub-marginal cells in *S. rubra* (a) Juvenile 3 (14.40 mm) Front 2, Scale bar = 50 μm (b) Juvenile 3 (14.40 mm) Back 1, Scale bar = 25 μm (c) Adult (30.40 mm) Front 2, Scale bar = 100 μm (d) Adult (30.40 mm) Front 2, Scale bar = 25 μm .

Of particular interest in these samples is the evidence of the distinct imprinting of the margins of the cells from the previous epithelial layer over the surface of the sub-marginal cells (**Figure 4.21 b and d**). This is in large part responsible for the observation of the ill-defined cell boundaries in the adult sample, which shows evidence of more than one layer imprinted on the surface. This teamed with the impressions of the underlying large cell nuclei visible on the surface of the sub-marginal cells in the juvenile frog (**Figure 4.21 b**) suggests that the cell layers are thin in this area and frequently shed, features that would suggest that this area was particularly prone to wear. The region also has shallow pits scattered liberally across the surface (**Figure 4.21 c**), particularly found on the margins of the cells (**Figure 4.21 b and d**).

Flectonotus fitzgeraldi

The structure of the toe pad cells in adult *F. fitzgeraldi* are typically as seen in other species, being columnar in nature with striated sides and hexagonal apices, in the main (**Figure 4.23 c**). The tonofilament bundles that underlie the external cell coating are often visible at high magnification (**Figure 4.23 d**), particularly in cells on the distal edge of the pad in juvenile frogs (**Figure 4.23 b**) where, in the most extreme incidence of this, the bundles have become divided and brush-like.

There is a particular prevalence of irregular cell shapes in this species. Comparing the pads shown in **Figure 4.22 a** and **b**, this tendency can be seen to be slightly reduced in adult frogs with the non-hexagonal cell types making up only 33% of the total cells in comparison to the 41% seen on the juvenile pad. The high incidence of non-hexagonal cells on the juvenile pad is likely to be responsible for the higher degree of variability and the greater value of the average cell size in these frogs.

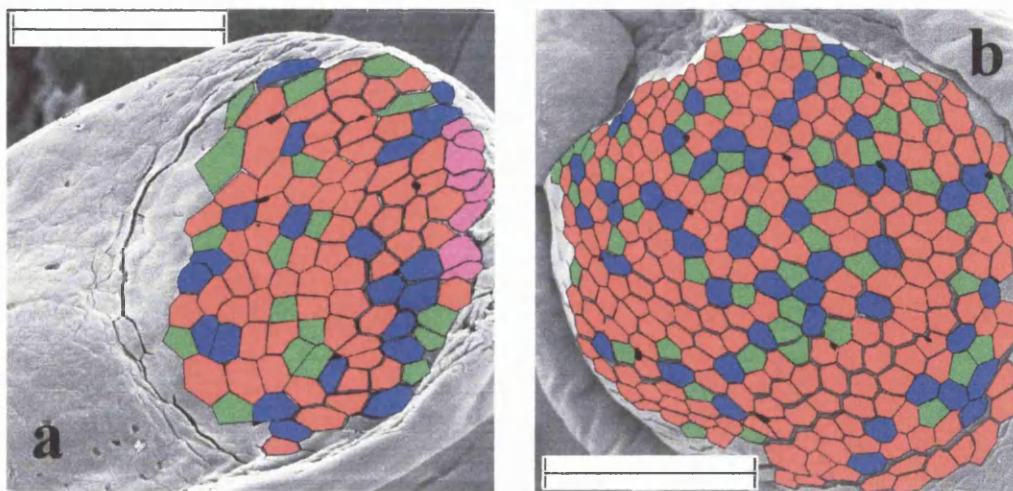


Figure 4.22: Toe pad cell shapes in *F. fitzgeraldi*: (a) Juvenile (7.3mm) Front 2 (b) Adult (15.7mm) Back 3. Scale bars = 100 μ m. Colour coding: red = hexagonal; green = pentagonal; blue = heptagonal; pink = rounded cells; black = mucosal pores.

Nevertheless cell size in juveniles, averaging $116.97 \mu\text{m}^2 \pm 5.01$ ($n = 67$) in area, is not in fact statistically any different to the average value of $101.46 \mu\text{m}^2 \pm 1.94$ ($n = 179$) seen in adult frogs ($F_{66,176} = 9.80$: Difference in medians: $U_{67,179} = 4791.50$, $p = 0.15$, N.S.). Cell densities in juveniles and adults are also not significantly different from one another at $8947.49 \text{ per mm}^2 \pm 917.40$ ($n = 7$) and $10336.45 \text{ per mm}^2 \pm 521.71$ ($n = 18$) respectively ($F_{6,17} = 0.03$, Difference between means: $t = -1.38$, N.S. 23 d.f.).

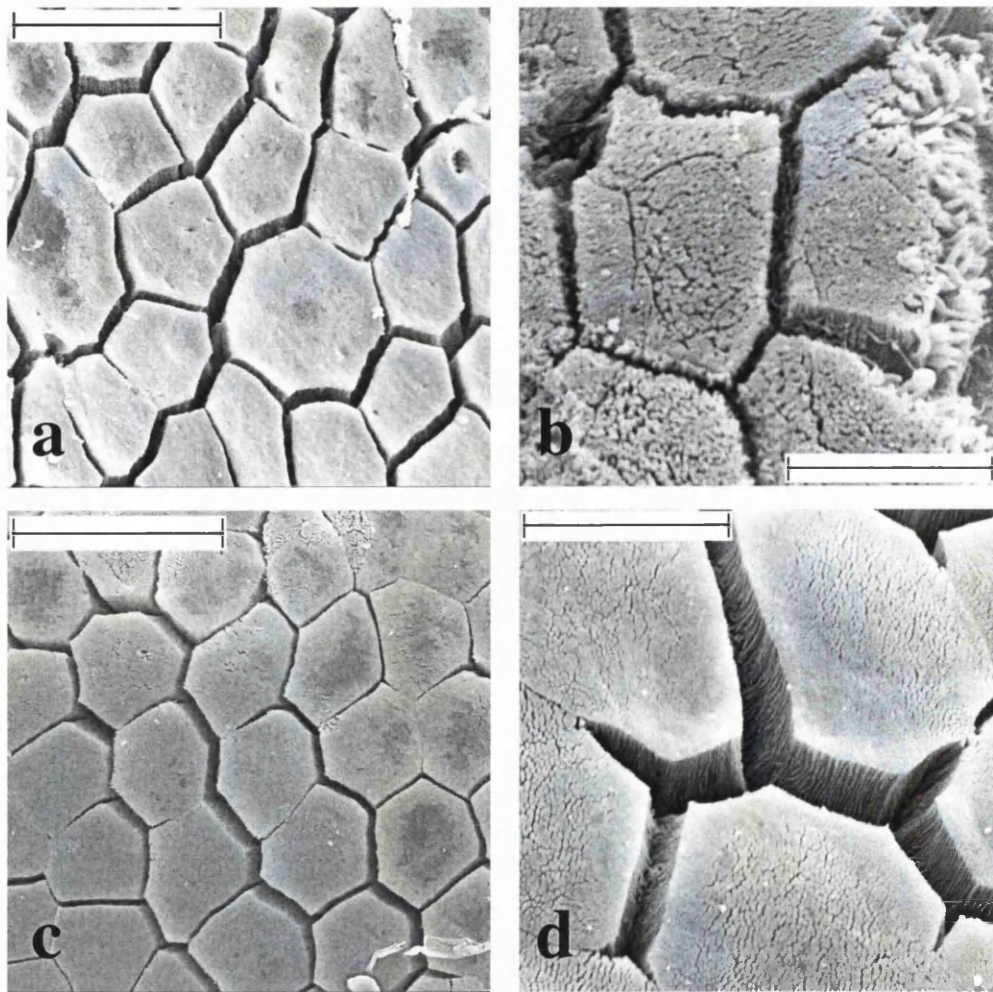


Figure 4.23: S.E.M. images of toe pad cells in *F. fitzgeraldi* (a) Juvenile (7.30 mm) Front 4, Scale bar = $25 \mu\text{m}$. (b) Juvenile (7.30 mm) Front 1, Scale bar = $12.5 \mu\text{m}$ (c) Adult (18.70 mm) Front 2, Scale bar = $12.5 \mu\text{m}$ (d) Adult (18.70 mm) Front 1, Scale bar = $25 \mu\text{m}$.

Channel widths are variable, with this being particularly obvious in juvenile frogs where cells around the proximal marginal edges of the pad are, in many instances, almost fused together (**Figure 4.24 a**). Channel densities, with values of $157.95 \text{ mm/mm}^2 \pm 9.64$ ($n = 7$) on each pad in juveniles and $168.60 \text{ mm/mm}^2 \pm 5.98$ ($n = 18$) in adults, are not significantly different between the two age classes ($F_{6,17} = 0.34$; Difference between means; $t = -0.94$, N.S. 23 d.f.).

The mucosal pores seen in both juvenile and adult *F. fitzgeraldi* are very small, measuring around 5 to $6 \text{ }\mu\text{m}^2$ in area, and with no notable differences either in size or type in the two age classes. As the opening is often too small for the sides of the neighbouring cells to be visible (**Figure 4.24 b**), it is difficult to determine whether pores belong to Green's Type I or II. There are a number of types of small mucosal pore, including a stomatal type (**Figure 4.24 a**) similar in structure to those seen earlier in juvenile *S. rubra*. In the main, the pores are roughly circular in shape (**Figure 4.24 a** and **c**) and bordered by two to four cells. A number are entirely imbedded in a single cell (**Figure 4.24 b**) or are slit-shaped and around a cell-side in length with terminal ends causing invaginations in the cell walls of neighbouring cells (**Figure 4.24 d**).

There is a significant reduction in the pore density seen in the two age classes, from $124.95 \text{ per mm}^2 \pm 13.43$ ($n = 7$) in juveniles to $25.31 \text{ per mm}^2 \pm 4.27$ ($n = 15$) in adults ($F_{6,14} = 6.57$; Difference between medians: $U_{7,15} = 0.00$, $p < 0.001$). Indeed, actual counts of mucosal pores per pad in juveniles (11.71 ± 1.43 , $n = 7$) and adults (9.93 ± 1.13 , $n = 15$) are not significantly different from one another ($F_{6,14} = 1.32$; $t = 0.82$, N.S. 20 d.f.), and their distribution over the pad surface is similar between the

age classes. This suggests that the density differences seen are likely to be due, not to a physical reduction of the number of pores seen on adult pads, but to differences in the sizes of toe pads in juvenile ($0.08 \text{ mm}^2 \pm 0.01$, $n = 9$) and adult frogs ($0.46 \text{ mm}^2 \pm 0.05$, $n = 18$).

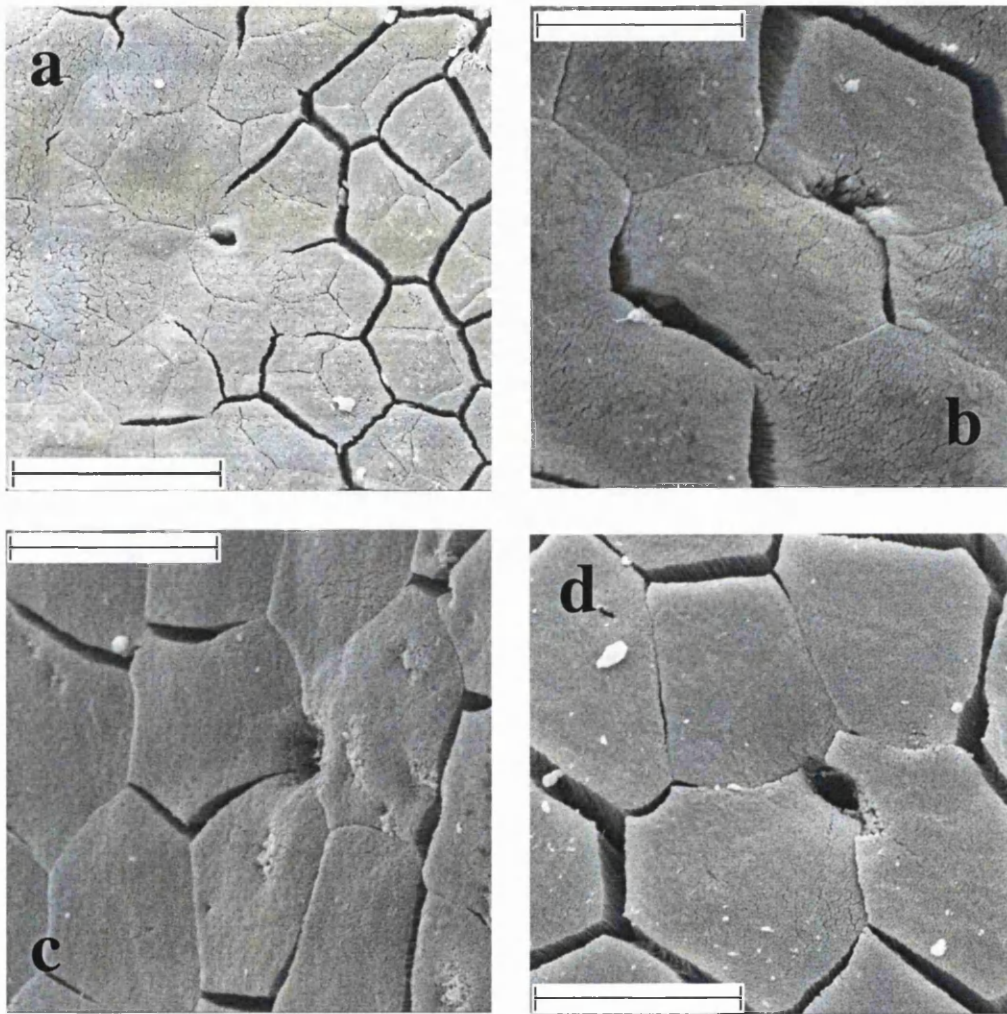


Figure 4.24: S.E.M. images of mucosal pore structures in *F. fitzgeraldi* (a) Juvenile (7.30 mm) Front 1, Scale bar = 25 μm . (b) Adult (18.70 mm) Back 4, 12.5 μm . (c) Adult (18.70 mm) Back 3, Scale bar = 12.5 μm . (d) Adult (18.70 mm) Back 1, Scale bar = 12.5 μm .

Changes in the structure of the toe pads that accompany this size change in *F. fitzgeraldi* (Figure 4.25 a – f) are similar to those seen in *S. rubra*, though in contrast with the trend seen in the larger species the pad elevation in *F. fitzgeraldi* increases

with size. Indeed, juvenile frogs of this species have the flattest pads of any in the study (**Figure 4.25 a and b**), with very little development of the circumferal groove and the adjacent marginal area. This is reduced in a number of pads to such an extent that they appear largely emarginate (**Figure 4.26 a**). There is evidence of cell modification on the pad edge of the circumferal groove, where a number of cells have a knobbed surface architecture and are irregularly shaped to ‘fill’ gaps between the toe pad cells and the margin (**Figure 4.26 b**). The proximal margin is defined, as in other species, by the differentiation in adjacent cell types from the specialised columnar cells on the pad proper to the more squamous cells of the sub-marginal area (**Figure 4.27 a**). In a number of cases, a fissure is visible along the marginal boundary (**4.25 a and b**).

Adult frogs have simply structured toe pads, still shallow in elevation but with a rounder shape (**Figure 4.25 c – f**). The circumferal grooves are not as well developed as in some larger species, and are often shallow enough for the cells at the bottom of the groove to be visible using SEM imaging (**Figure 4.26 c and d**). The cells on the circumferal margin, which has become better defined in adult frogs (**Figure 4.25**), generally have a surface architecture that appears perforated and ‘spongy’ (**Figure 4.26 c**) though a number of smoother cells are also evident in small groupings along the margin (**Figure 4.26 d**). The separate definition of the cells on the margin in adults is less distinct than is seen in the juvenile frogs (**Figure 4.26 b and d**). Proximal margins are again discernible through the change in cell type from columnar to a cell more squamous in appearance with roughened cell architecture (**Figure 4.27 b**), similar to those seen in the same area in *S. rubra*. Again, fissures are present between the pad and the sub-marginal area in a number of samples (**Figure 4.25 b and c, Figure 4.27 b**).

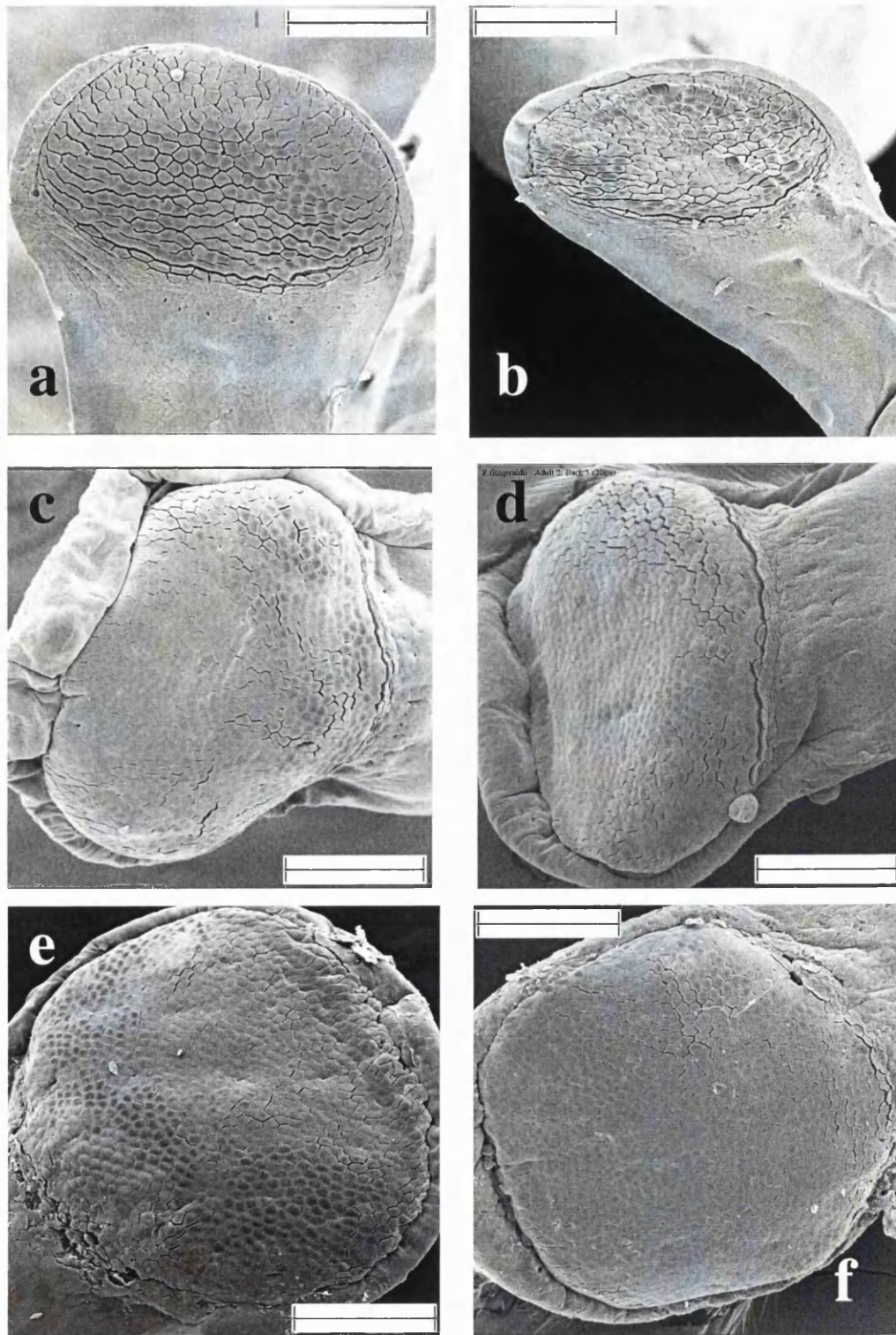


Figure 4.25: S.E.M. images of toe pads in *F. fitzgeraldi* (a) Juvenile (7.3mm) Front 3 (b) Juvenile (7.3mm) Back 4 (c) Adult 2 (15.9mm) Front 1 (d) Adult 2 (15.9mm) Back 3 (e) Adult (18.1mm) Front 2 (f) Adult (18.1mm) Back 2. Scale bars in all images = 150 μ m.

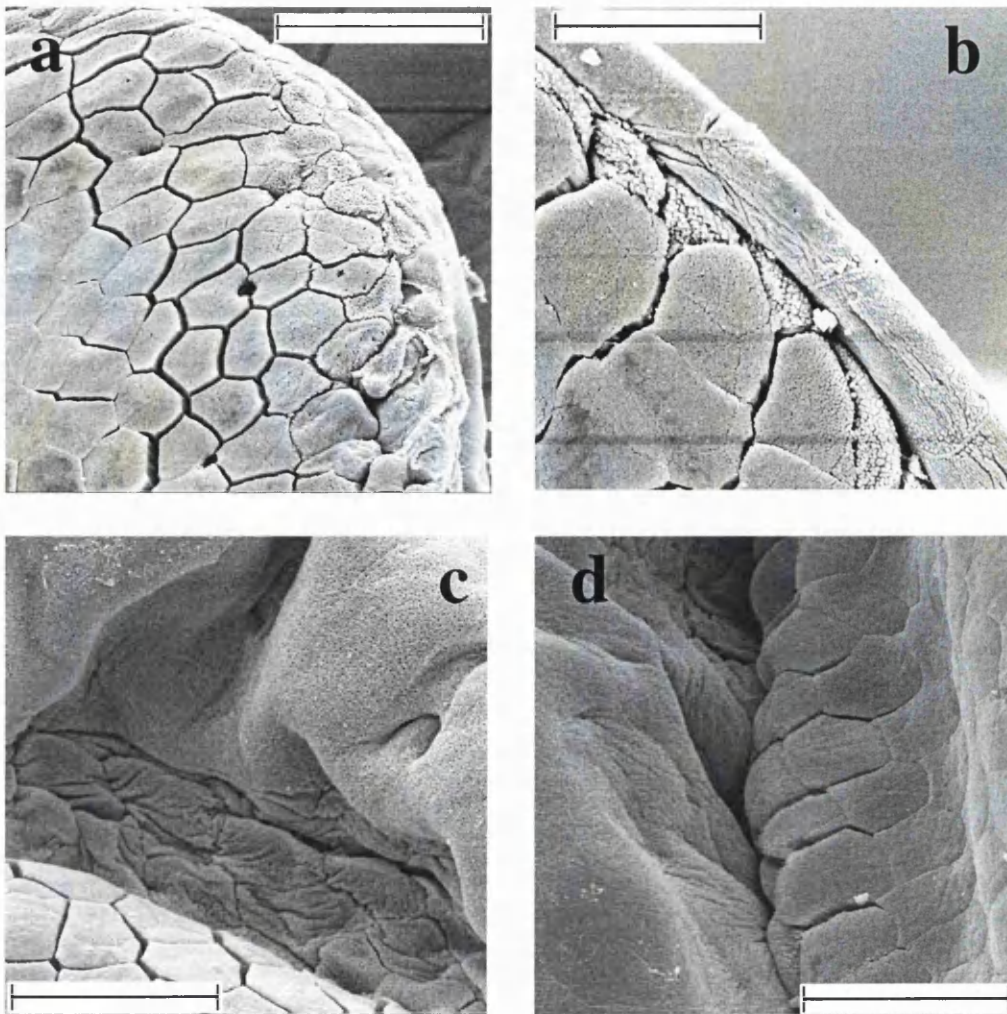


Figure 4.26: S.E.M. images of circumferential grooves and margins in *F. fitzgeraldi*: (a) Juvenile (7.3mm) Front 2, Scale bar = 50 μm . (b) Juvenile, Front 3, Scale bar = 25 μm . (c) Adult (18.1mm) Back 3, Scale bar = 25 μm . (d) Adult (18.1mm) Back 1, Scale bar = 25 μm .

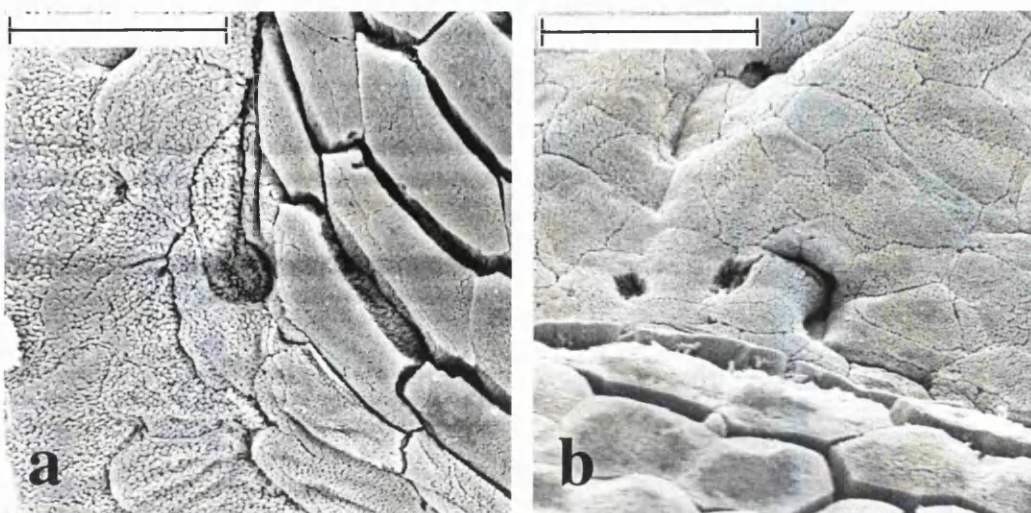


Figure 4.27: S.E.M. images of proximal marginal areas in *F. fitzgeraldi* (a) Juvenile (7.3mm) Front 3 (b) Adult (18.1mm) Back 4. Scale bars in both images = 25 μm .

Hyla punctata

Toe pad cells in *H. punctata* are, again, very similar to those seen in the other species under investigation. The epithelium consists of hexagonal columnar cells (**Figure 4.28**) with striated lateral sides (**Figure 4.28 b**). The underlying tonofilament bundles are often visible in the S.E.M. samples (**Figure 4.28 a** and **d**), and, in a number of instances, the roughened apices show the imprint of the previous cell layer on their surface (**Figure 4.28 a, b** and **d**).

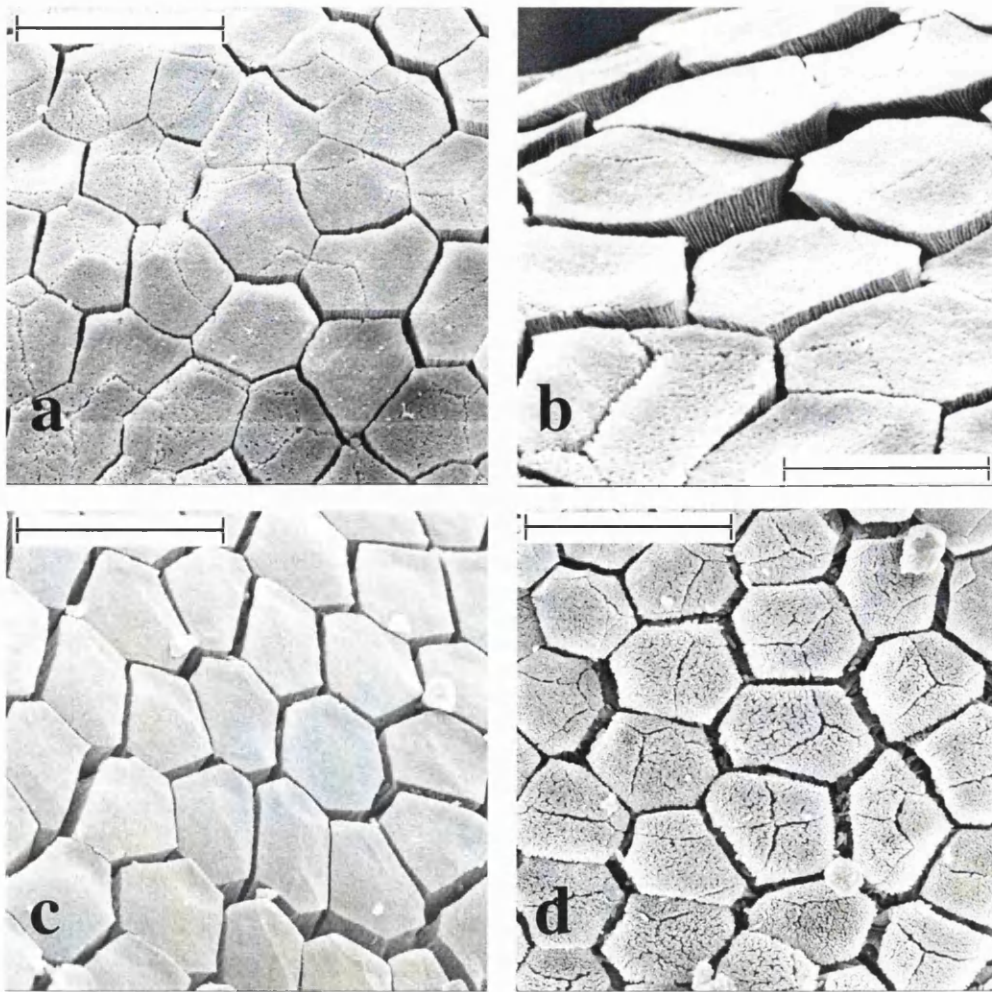


Figure 4.28: S.E.M. images of toe pad cell structure in *H. punctata* (a) Juvenile (14.7mm) Back 2, Scale bar = 25 μm (b) Juvenile (14.7mm) Back 1, Scale bar = 12.5 μm (c) Adult (34.7mm) Back 1, Scale bar = 25 μm (d) Adult (34.7mm) Back 2, Scale bar = 25 μm .

The average cell size in juveniles ($104.97 \mu\text{m}^2 \pm 2.03$, $n = 136$) is not statistically significant to that in adults ($109.52 \mu\text{m}^2 \pm 2.39$, $n = 90$): ANOVA, $F_{135,89} = 0.85$; Difference between means: $t = 1.44$, N.S. 224 d.f. Dependent as cell densities are on the size of the cells, values for these are also not significantly different between the age classes ($F_{8,13} = 1.20$; $t = -0.83$, N.S. 21 d.f.). Cell densities in adult frogs average at $9930.86 \text{ per mm}^2 \pm 511.03$ ($n = 14$); whilst in juveniles this value is slightly less, at $9316.50 \text{ per mm}^2 \pm 468.86$ ($n = 9$). Channel densities are also not significantly different between juvenile and adult frogs ($F_{8,12} = 0.001$: Difference between means: $t = -0.64$, N.S. 20 d.f.), with respective values of $151.49 \text{ mm/mm}^2 \pm 6.99$ ($n = 9$) and $157.75 \text{ mm/mm}^2 \pm 6.59$ ($n = 13$).

Mucosal pores in both juveniles and adults are generally simple and regular in shape (**Figure 4.29 b, c, f**), with modified cell walls that are roughened and micro-villated in appearance (**Figure 4.29 b, c**). Geometrical pore openings are framed by between five and seven cells, though in both cases the pentagonal configurations arising from five bordering cells are the most prevalent (**Figure 4.29 b and f**). More rounded pores are also found in both age classes (**Figure 4.29 a and e**), bordered by three and four cells. Indeed, there is very little difference in the pore types seen in the two age classes, with the only pore type seen in adults that is exclusive to the adults being a slit-like pore, similar to those seen in *S. rubra* (**Figure 4.29 d**).

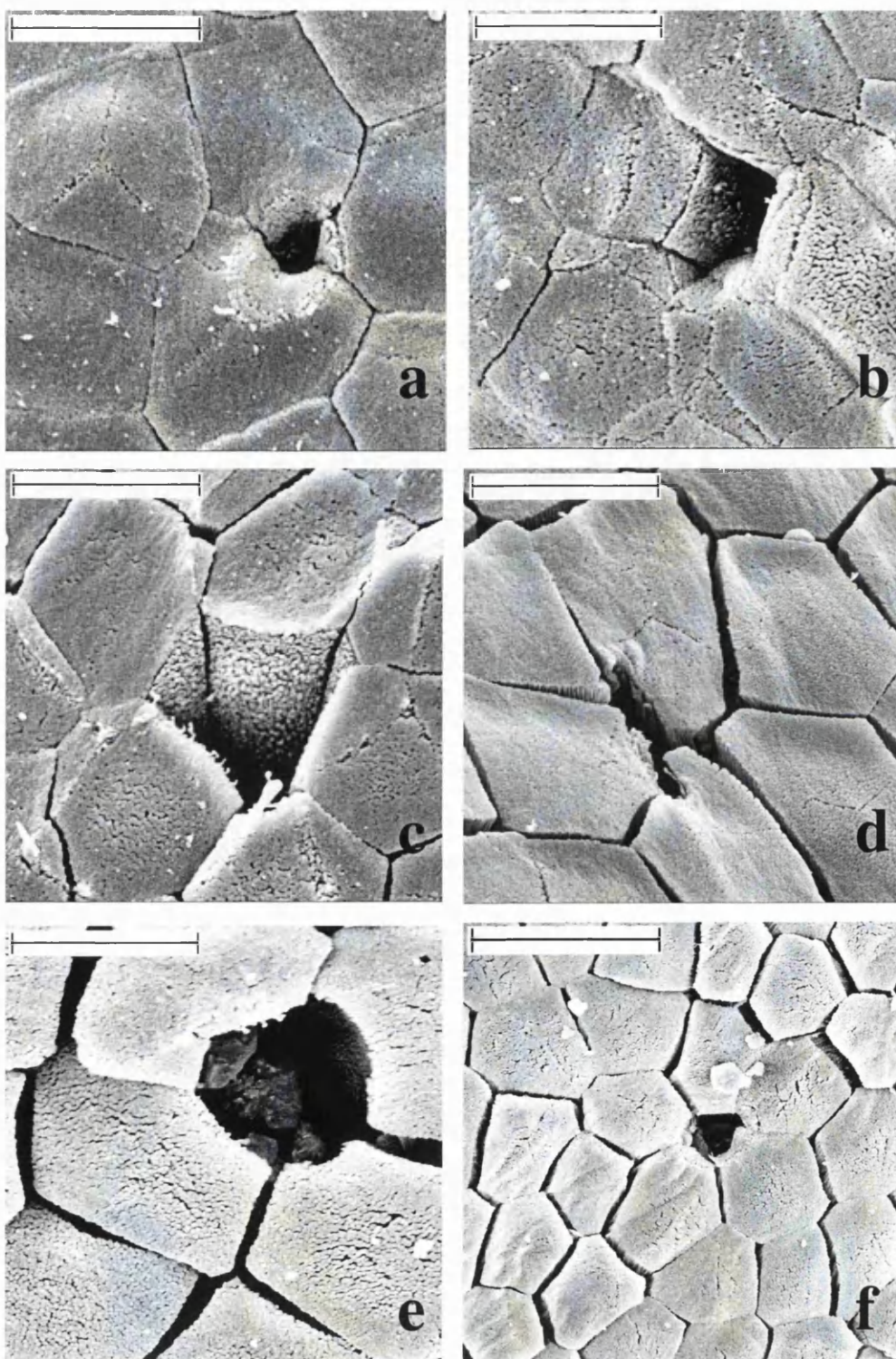


Figure 4.29: S.E.M. images of mucosal pore structure in *H. punctata* (a) Juvenile (14.7mm) Back 3, Scale bar = 12.50 μm (b) Juvenile, Back 5, Scale bar = 12.50 μm . (c) Juvenile, Back 2, Scale bar = 12.50 μm (d) Adult (34.7 mm) Back 1, Scale bar = 12.50 μm . (e) Adult (34.7mm) Front 3, Scale bar = 12.50 μm (f) Adult (34.7mm) Front 1, Scale bar = 25 μm .

This similarity is continued when considering the size of the pores that are seen in juveniles and adults, average sizes being 68.65 ± 10.08 ($n=10$) in juveniles and 73.25 ± 8.36 ($n=14$) in adults (Difference between means; $t = 0.34$, N.S. 22 d.f.).

The numbers of pores per pad increases considerably in adult frogs with average counts of 21.13 ± 8.18 ($n = 8$) rather than 8.13 ± 0.90 ($n = 8$) seen in the juveniles. This is not unexpected, as toe pads in adult frogs are considerably larger than those of the new metamorphs, measuring around 3 mm^2 on average rather than 0.3 mm^2 . This ten-fold increase in toe pad area means that in spite of the increase in mucosal pore numbers, the average value for pore density per mm^2 of pad is reduced in adults (7.79 ± 3.98 ($n = 2$)) in comparison to the juvenile pads (26.42 ± 2.92 ($n = 8$)). Difference in means; $t = 2.96$, $p = 0.02$, 8 d.f.

The distribution of the pores across the pad is difficult to determine in the juvenile sample, due to the low count values (see **Figure 4.30 a and b**) but there does appear to be a concentration on the proximal half of the pad in some samples (i.e. **Figure 4.30 a**). Pore distribution is more even on the adult pads, though the pores at the edges of the pad are generally more visible (**Figure 4.30 c**) and the majority of pores in the upper size ranges in this species (ca. $100\mu\text{m}^2$) were sampled from the proximal regions of the pad.

Other aspects of toe pad structure are also demonstrated in **Figure 4.30 a – d**; with a trend towards a flattening of pad elevation and a development of the definition of the marginal areas with growth. The latter of these trends is particularly marked on the front pads (**Figure 4.30 c**) where the margin is projected forwards to lie flush with the edge of the pad and is separated from it by a defined groove (**Figure 4.31 c**). This level of development is never seen in juvenile frogs where the marginal area is generally set back from the crown of the pad and separated by a shallow partial groove at best (**Figure 4.30 a, b and Figure 4.31 a**).

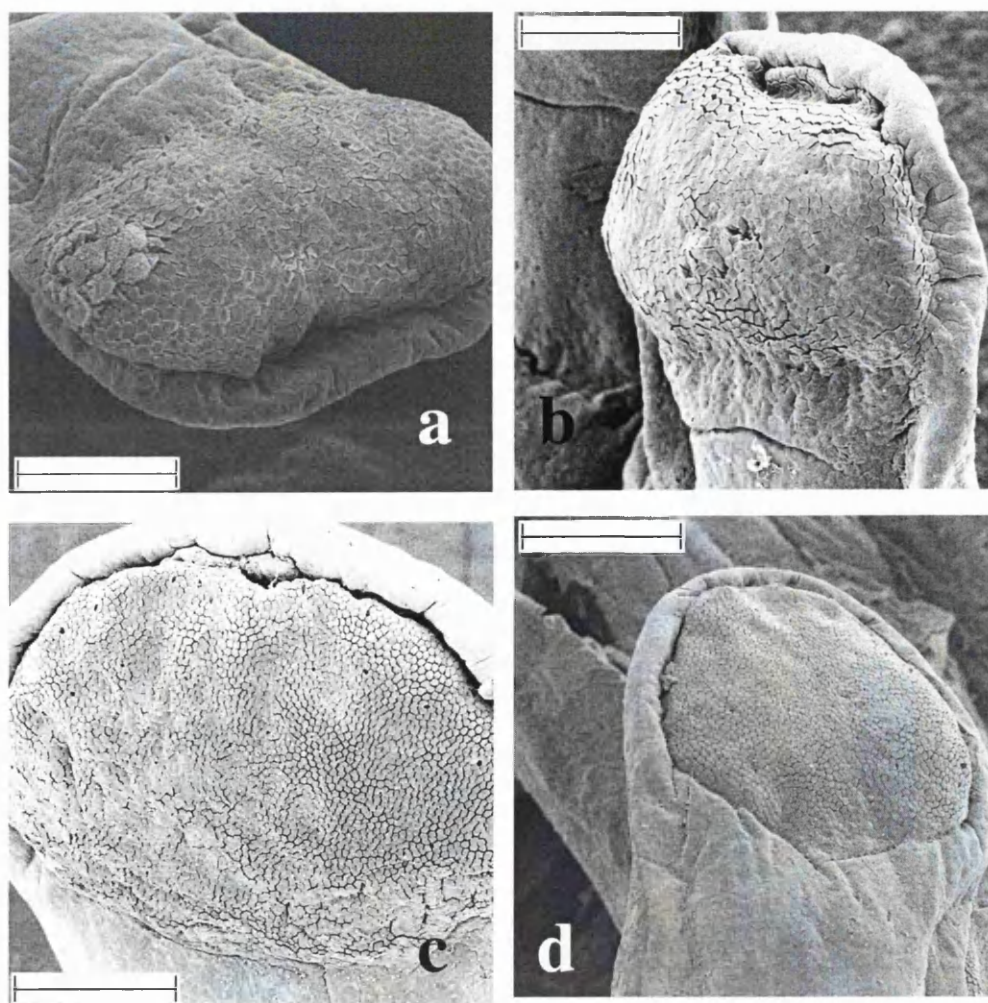


Figure 4.30: S.E.M. images of toe pad structure in *H. punctata*: (a) Juvenile (14.7mm) Front 1, Scale bar = 150 μm . (b) Juvenile (14.7mm) Back 5, Scale bar = 150 μm . (c) Adult (34.8mm) Front 2, Scale bar = 150 μm . (d) Adult (34.8mm) Back 1, Scale bar = 300 μm .

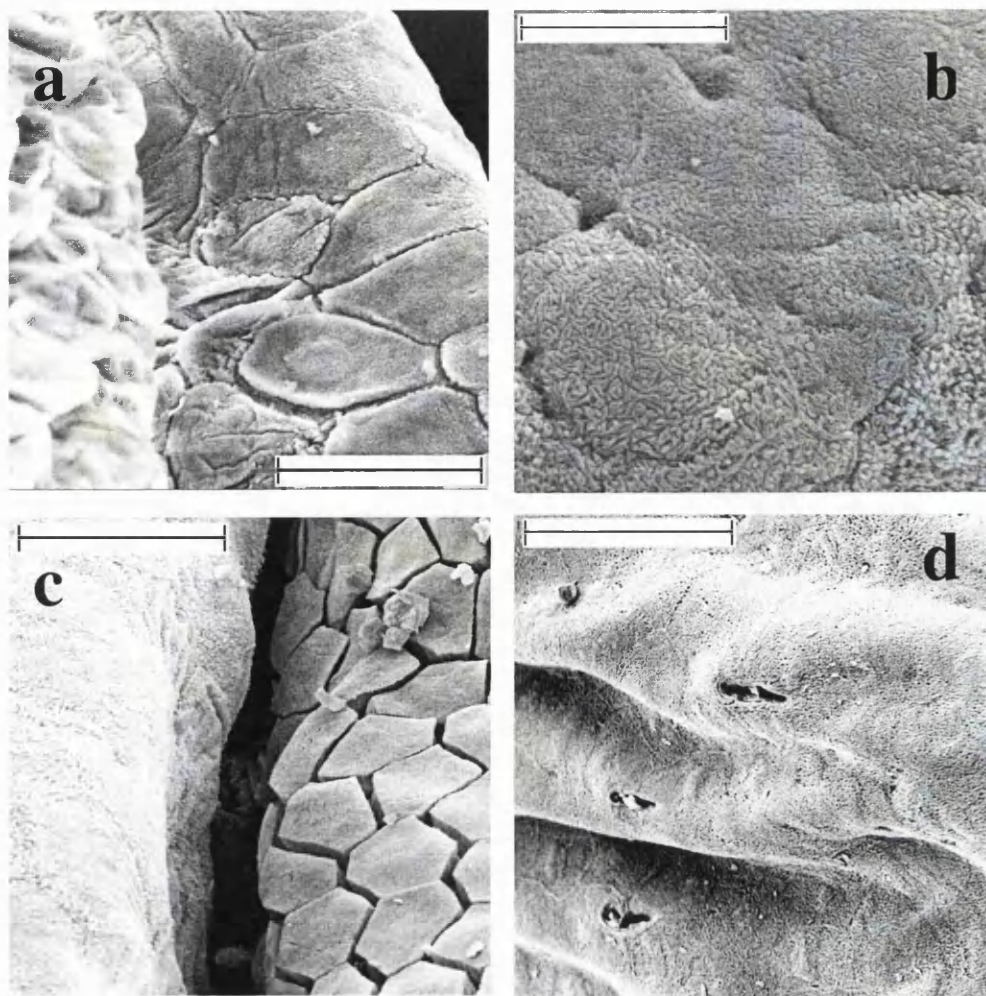


Figure 4.31: S.E.M. images of circumferential groove and marginal cells in *H. punctata*: (a) Juvenile Front 1, Scale bar = 50 μm (b) Juvenile Front 1, Scale bar = 12.5 μm . (c) Adult (34.8mm) Front 2, Scale bar = 25 μm (d) Dorsal surface of toe (adult), Scale bar = 25 μm .

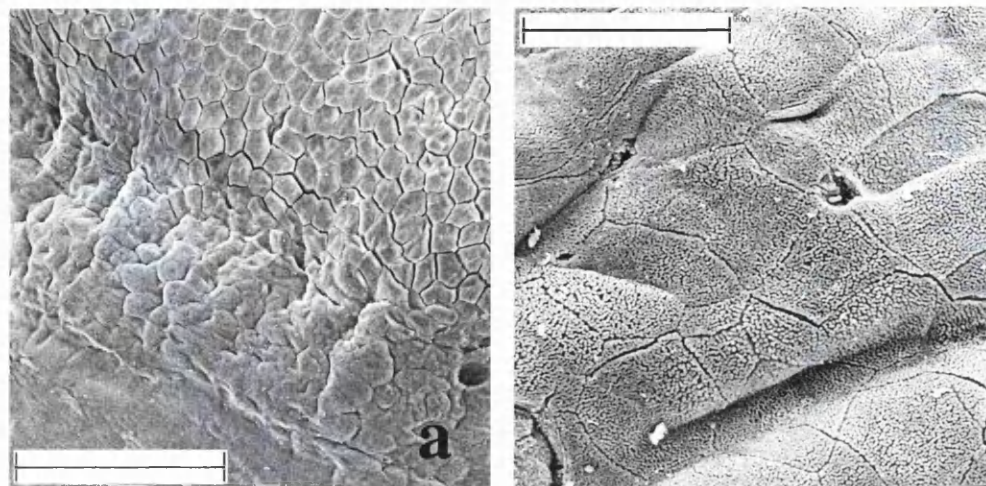


Figure 4.32: S.E.M. images of proximal margin and sub-marginal cells in adult *H. punctata*: (a) Front 4, Scale bar = 100 μm (b) Back 1, Scale bar = 25 μm .

The cells on the marginal circumferal ridge of the pads in both juvenile and adult frogs are large and hexagonal, with individual cells separated by ridged margins (**Figure 4.31 b – c**) or shallow grooves (**Figure 4.31 a**). Cell surface architecture has a convoluted raised surface with ridges and knobs (**Figure 4.31 a - c**) that is distinct in texture from the dorsal skin, which is spongy in appearance (**Figure 4.31 d**).

There are no real differences in the structuring of the proximal margins in juveniles and adults. In both they are defined by the change in appearance of cells on the pad and the sub-marginal area. There is no distinct marginal groove at the proximal edge of the pad, though the change in elevation between the two areas causes a folding and gathering in the cells in the sub-marginal region in both age classes (**Figure 4.30 d** and **Figure 4.32 a**) which helps define the two areas. Sub-marginal cells are much as seen in other species with a surface architecture that gives them a micro-villated appearance with shallow intercellular grooves that separate the individual cells.

Hyla minuscula

Comparisons of toe pad morphology in juvenile and adult frogs are not available for *Hyla minuscula* due to a lack of juvenile availability for this species. S.E.M. images from adult frogs of this species can be seen in **Chapter 3**.

4.3.4. Accessory adhesive areas

The specialised toe pads are not the only areas that contribute to adhesion in these frogs. Most species would, if allowed to do so, utilise areas of skin on the stomach, thighs and chin to aid their adhesion to the rotation platform (see **Section 4.2.2**). Although methodology excludes the use of these areas in these frogs, examination of hand and foot morphology suggests that there is a developed system of accessory adhesive tubercles that can be utilised: subarticular tubercles at the ‘knuckle’ joint; supernumerary tubercles along the digits and toes; and palmar and metatarsal tubercles on the main body of the hands and feet.

Scinax rubra

The accessory tubercular system in juvenile *Scinax rubra* is not significantly different to that described for adult frogs in Duellman (2001) (**Figure 4.33** and **4.34**). Subarticular tubercles on both toes and fingers are small and rounded. There is a tendency towards a slightly lesser elevation of these in the juvenile frogs (**Figure 4.35 a**) in comparison to those in the adult sample (**Figure 4.35 c**), though cells on these areas are not significantly different to one another in their structure. These are roughly hexagonal in shape: in both, the imprint of the previously shed layer of skin on the surface of the cells is clearly visible. There is a slight reduction in cell size with growth, with typical cell areas of around 150-200 μm^2 in juveniles and 100 μm^2 in adults. Numerous rounded shallow pits are scattered liberally across the surface of these structures in both age classes, though there is a tendency towards higher densities of these in adult frogs (**Figure 4.35 b** and **d**).

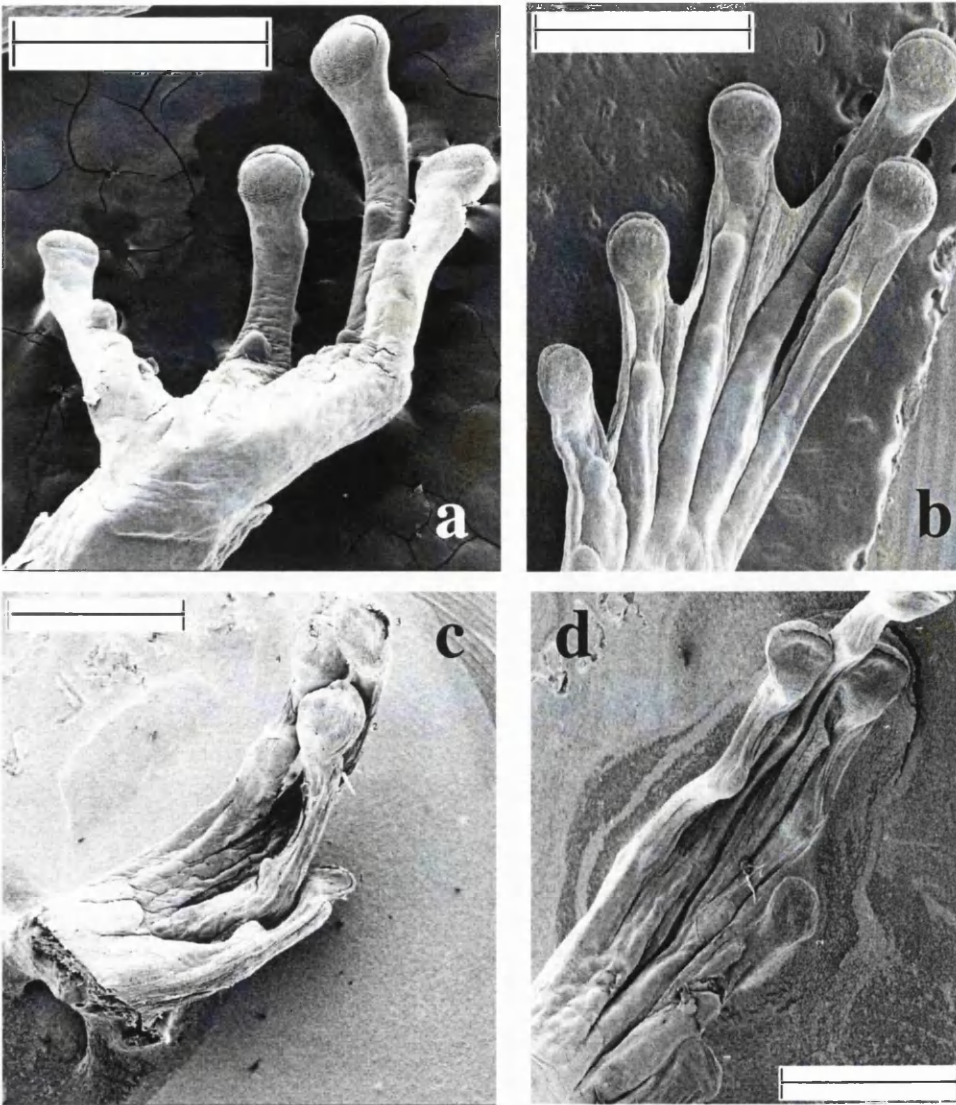


Figure 4.33: S.E.M. images of hand and foot morphology in *S. rubra*: (a) Juvenile, Scale bar = 1.25 mm (b) Juvenile, Scale bar = 1.25 mm (c) Adult, Scale bar = 2.5mm (d) Adult, Scale bar = 2.5mm.

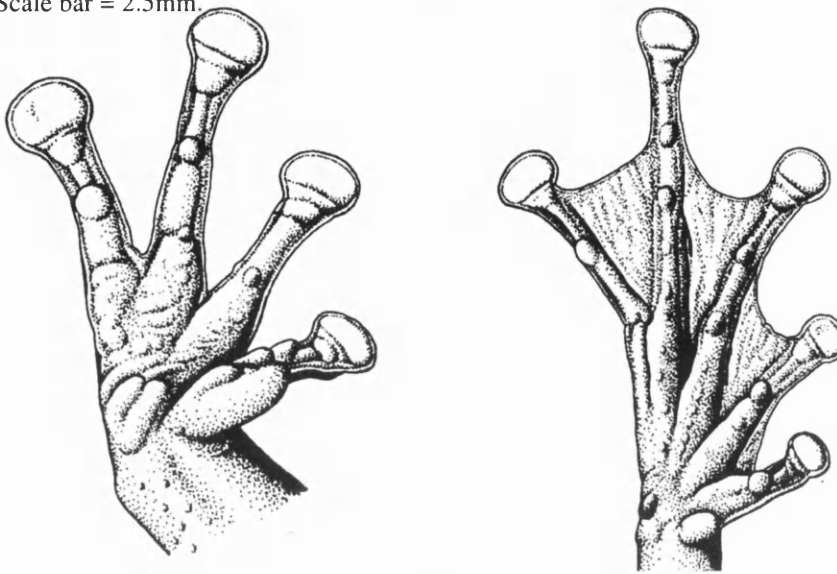


Figure 4.34: Typical hand and foot morphology in adult *S. rubra*. (Duellman, 2001)

The rows of well-defined supernumerary tubercles seen on the proximal segments of the toes on the feet of adult frogs in Duellman (2001) (**Figure 4.34**), are not distinct in any of the samples under examination here (**Figure 4.33**). This is the case in both adult and juvenile frogs, with neither showing detectable levels of tubercle development on the lower portions of the toes or fingers.

Palmar tubercles are much as would be expected from descriptions in Duellman (2001); the former are less evident in juveniles than in the adult example, though this may in part be due to the angle that the hands are fixed on the S.E.M. stubs (**Figure 4.33 a and c**). In contrast, the inner metatarsal tubercle appears better developed in juvenile frogs. Whereas it is described as 'broad, low and flat' in adults (Duellman, 2001), in juveniles there is a distinct rounded elevation of the tubercles found on the distal portion of the inner toe (**Figure 4.36 a**). Furthermore, cell types seen on the metatarsal tubercles are specialised in appearance, being similar to the cuboidal cells seen in the proximal marginal areas and subarticular tubercles. However, the degree to which the surface architecture of these cells is roughened (**Figure 4.36 b**) is more comparable to the texture of adult cells in the aforementioned areas (**Figure 4.35 d**) to that of juvenile frogs.

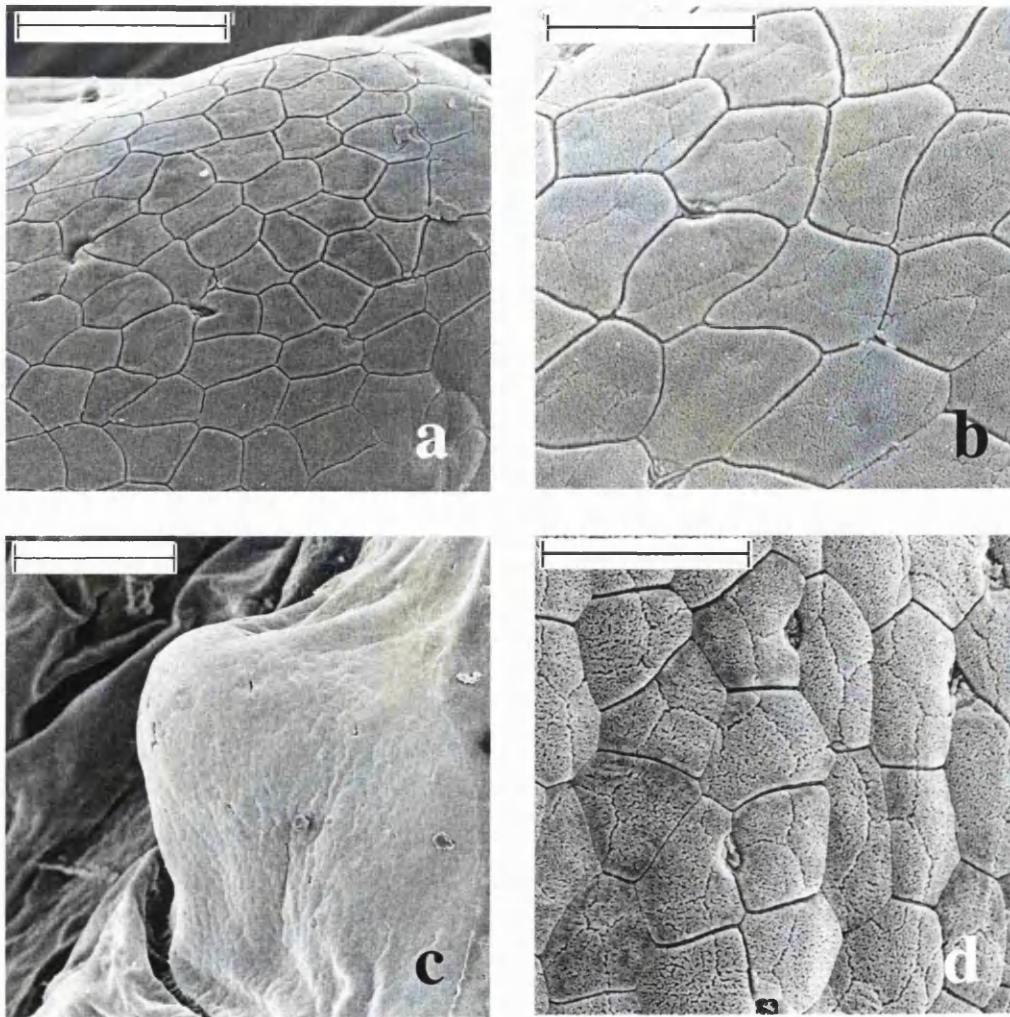


Figure 4.35: S.E.M. images of subarticular tubercles in *S. rubra* (a) Juvenile 1 (12.21 mm) Back 3, Scale bar = 50 μm (b) Juvenile 1 (12.21 mm) Back 2, Scale bar = 25 μm . (c) Adult (30.40 mm) Front 2, Scale bar = 150 μm (d) Adult (30.40 mm) Back 4, Scale bar = 25 μm .

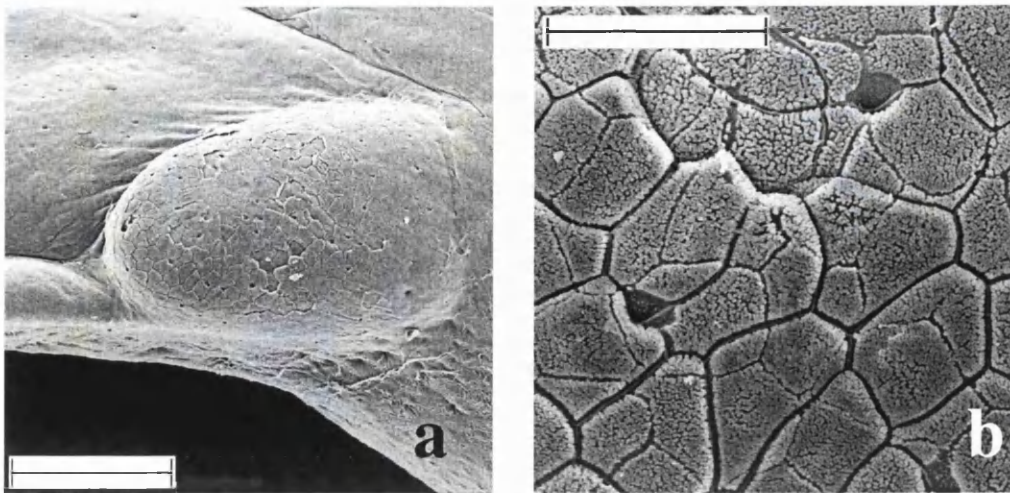


Figure 4.36: S.E.M. images of inner metatarsal tubercle in juvenile *S. rubra* (a) Scale bar = 150 μm (b) Scale bar = 25 μm

Flectonotus fitzgeraldi

Changes in the extent of accessory adhesive structures seen on the hands and feet of *F. fitzgeraldi* are marked between the age classes, with adults exhibiting a considerably more developed tubercular system than seen on juvenile digits (**Figure 4.37**). Subarticular tubercles in juveniles are not well distinguished from the rest of the ventral surface of the digits (**Figure 4.37 a and b**), and there is a lack of specialisation of the cells in these areas that suggests that accessory ares are absent at this stage in *F. fitzgeraldi*.

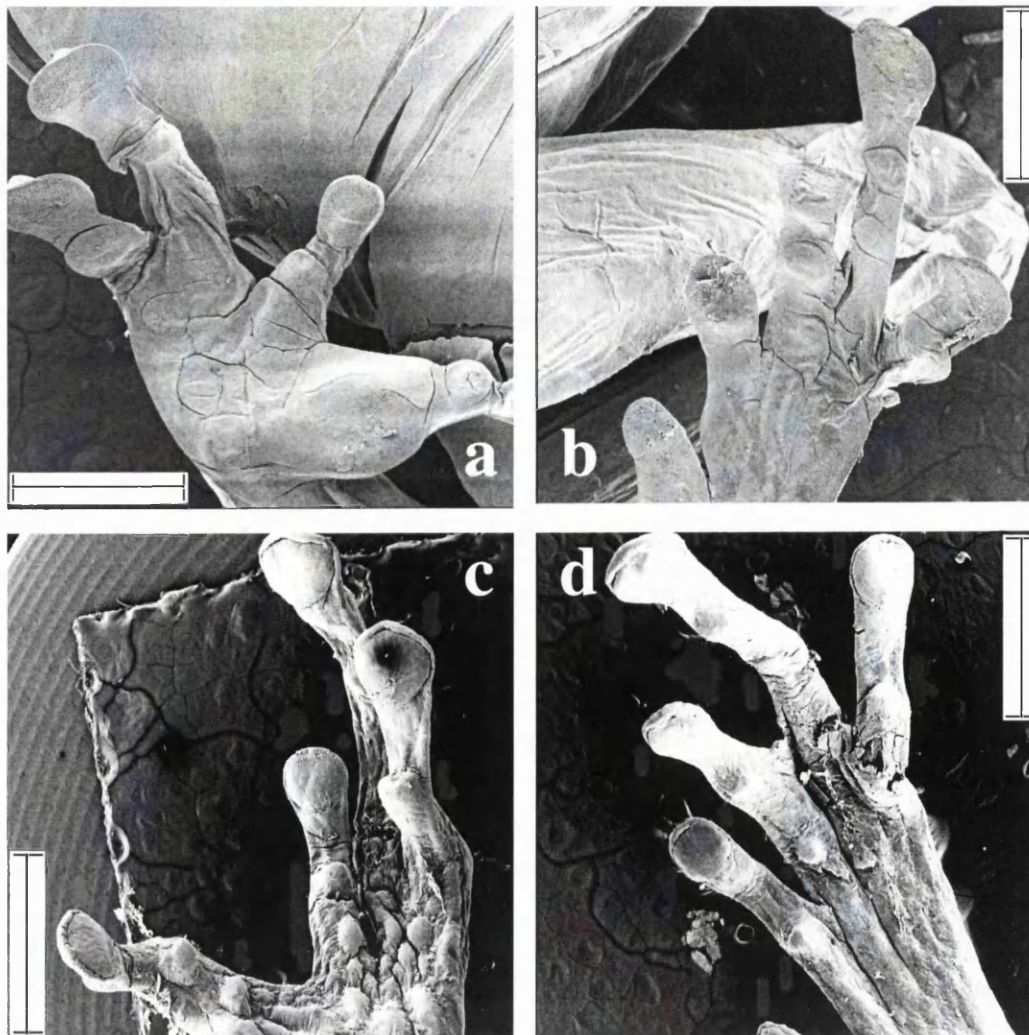


Figure 4.37: S.E.M. images of hand and foot morphology in *F. fitzgeraldi* (a) Juvenile, Scale bar = 625 μm . (b) Juvenile, Scale bar = 625 μm . (c) Adult, Scale bar = 1.25 mm (d) Adult, Scale bar = 1.25 mm.

Subarticular tubercles in adult frogs are large and conical, standing proud of the ventral surface of the toe (**Figure 4.38 a**). Cells are irregular in shape, and large ($135.49 \mu\text{m}^2 \pm 5.39$, $n = 33$). Intercellular margins are distinctly visible as shallow bare grooves through the roughened, ‘micro-villated’ apical surface of the structures (**Figure 4.38 b**) and there is a dense distribution of rounded shallow pits, similar to those seen in *Scinax rubra*, along the intercellular margins in these frogs.

Supernumerary tubercles are also larger and more developed in the adult frogs. The extent to which this is the case is most pronounced on the hands, where they are comparable in size to the subarticular tubercles (**Figure 4.37 c**). Clusters are seen at the base of the toes, with the tubercles roughly elliptical in shape and gently rounded in their elevation from the ventral surface (**Figure 4.39 a**). Cells are similar in appearance to those seen on the subarticular tubercles, though with ill-defined margins and with more compact surface microvilli, giving the surface a less ‘hairy’ appearance (**Figure 4.39 b**).

Palmar tubercles are, again, well developed in adults (**Figure 4.37 c**), with the presence of distinct compartmentalised areas on the palm of the hand. These are seen as a simple network of creases in the juvenile sample (**Figure 4.37 a**). The inner metatarsal tubercle is absent entirely in the juvenile frog, but is elongate and distinctly elevated in the adult samples (**Figure 4.40 a**). Cells are again similar in structure to those seen on the previous types of tubercle, with the trend towards less distinct cell margins and shortened surface microvilli being further pronounced in this instance (**Figure 4.40 b**).

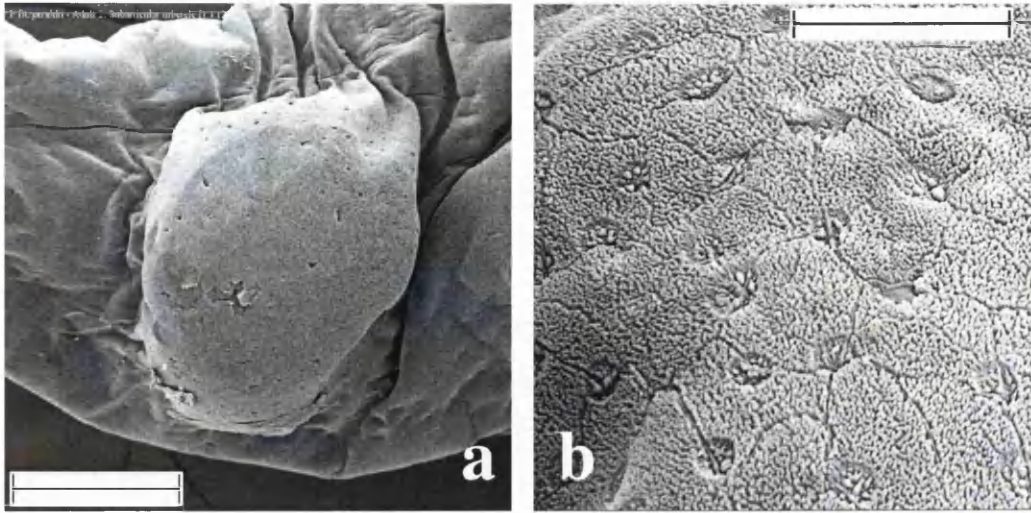


Figure 4.38: Subarticular tubercle in adult *F. fitzgeraldi* (a) Scale bar = 150 μm (b) Scale bar = 25 μm

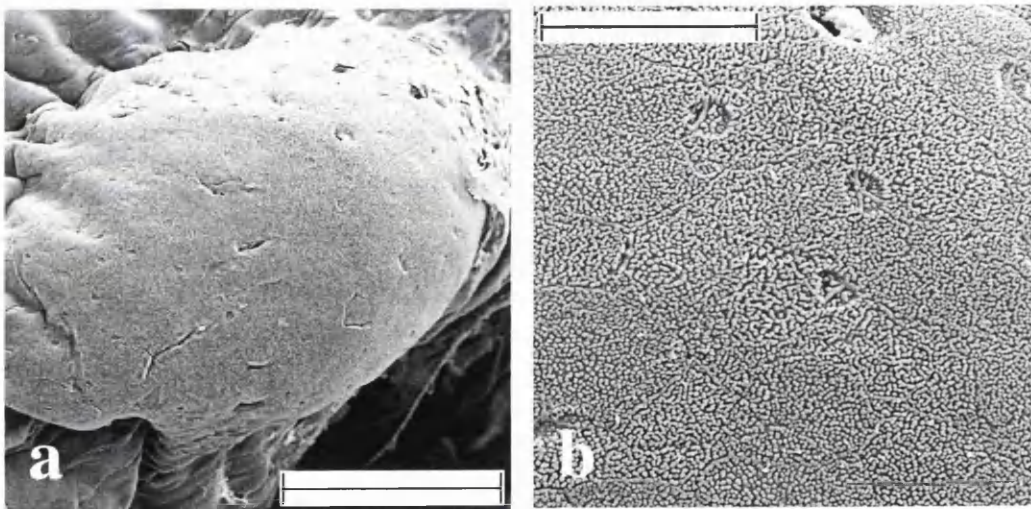


Figure 4.39: Supernumerary tubercle in adult *F. fitzgeraldi* (a) Scale bar = 100 μm (b) Scale bar = 25 μm

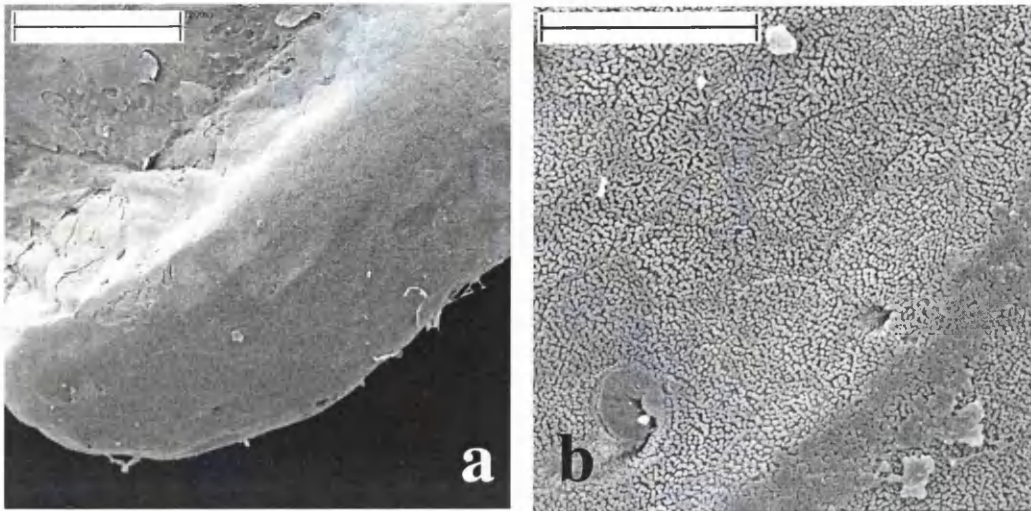


Figure 4.40: Inner metatarsal tubercle in *F. fitzgeraldi* (a) Scale bar = 150 μm (b) Scale bar = 25 μm

Hyla punctata

The system of accessory adhesive structures in *Hyla punctata* is similar between the age classes (**Figure 4.41**), though there is a tendency towards more distinct lines of supernumerary tubercles on the juvenile's front feet. Both age classes have particularly large subarticular tubercles on the first, third and fourth digits of the fore limb, (**Figure 4.41 a and c**) with the outer digits having particularly square, truncate tubercles in the juvenile sample. Subarticular tubercles are smaller and more rounded in shape on digits of the hind limb in both age classes (**Figure 4.41 b and d**).

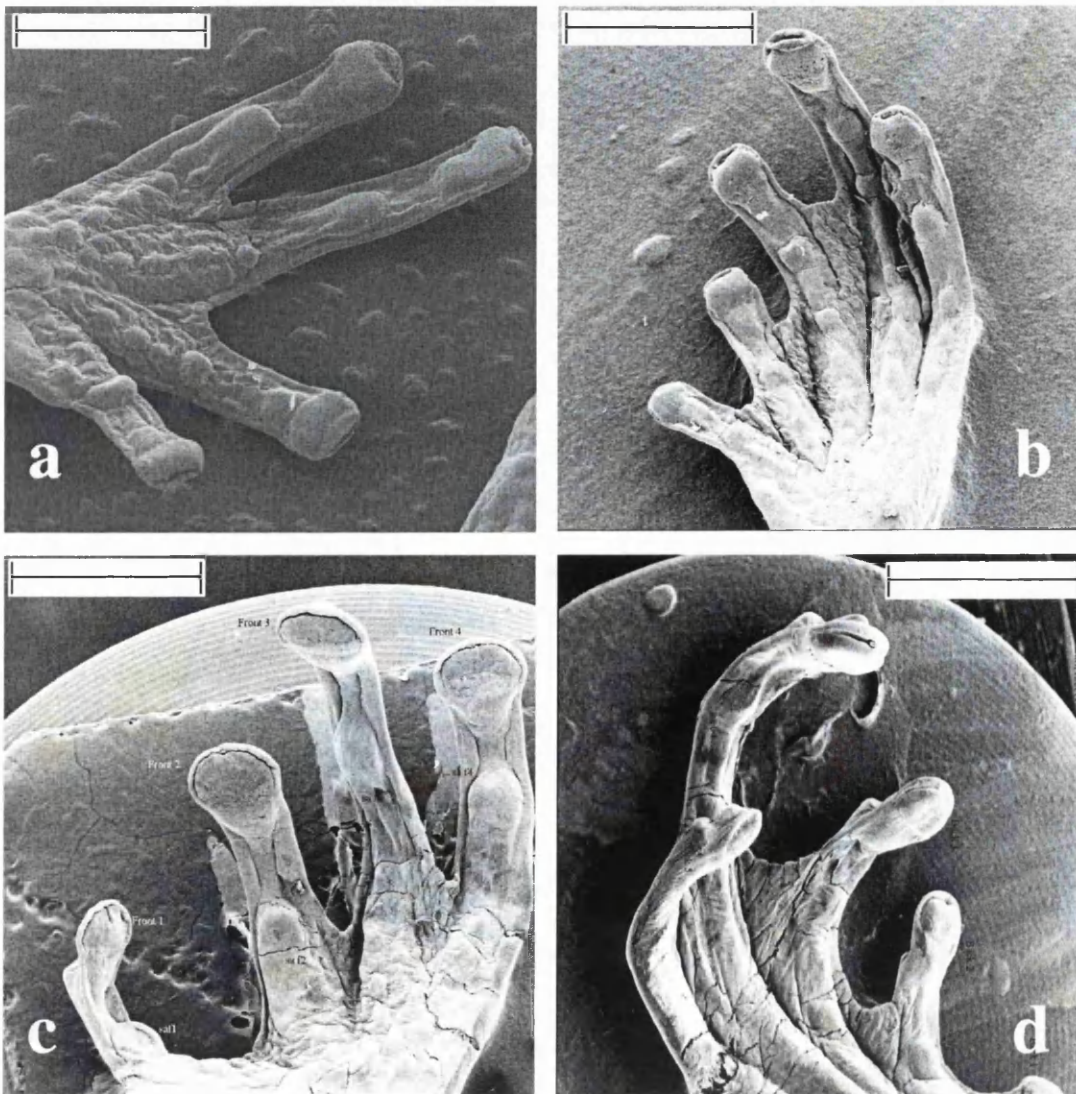


Figure 4.41: S.E.M. images of hand and foot morphology in *H. punctata* (a) Juvenile, Scale bar = 1.25 mm (b) Juvenile, Scale bar = 1.25 mm (c) Adult, Scale bar = 2.50 mm (d) Adult, Scale bar = 2.50 mm.

Subarticular tubercles are more pronounced in their elevation from the surface in the juvenile than in the adult (**Figure 4.42 a and c**), with this trend particularly pronounced in the front feet. Cells on the subarticular tubercles are, again, roughly hexagonal in shape with intercellular margins more distinct than seen in the two smaller species discussed in this chapter (**Figure 4.42 b and d**). Cells in both age classes have apices that appear to be covered with stout microvilli and on these roughened surfaces the overprinting of the margins of the previously overlying layer is distinctly visible. Furthermore, in the juvenile sample the impression of the large underlying cell nuclei is particularly pronounced (**Figure 4.42 b**).

Supernumerary tubercles are indistinct in the adult samples, but are present as gently rounded bumps on the front feet of the juvenile frog (**Figure 4.41 a**). On digits two to four these are present in lines on the proximal segments of the fingers, and are clustered at the base of the first digit (**Figure 4.43 a**). The tubercles are covered in cells with sparsely micro-villated surfaces and ill-defined margins (**Figure 4.43 b**).

Palmar tubercles are not evident in either age class, and, although there is a slight swelling in the locality of the pre-pollex (**Figure 4.41 a**), there is no evidence of specialised cells in this area at higher magnifications. In the juvenile, the equivalent region on the back foot, the inner metatarsal, has an elongate tubercle (**Figure 4.41 b**) that is covered in cells similar in structure to those found on the subarticular tubercles.

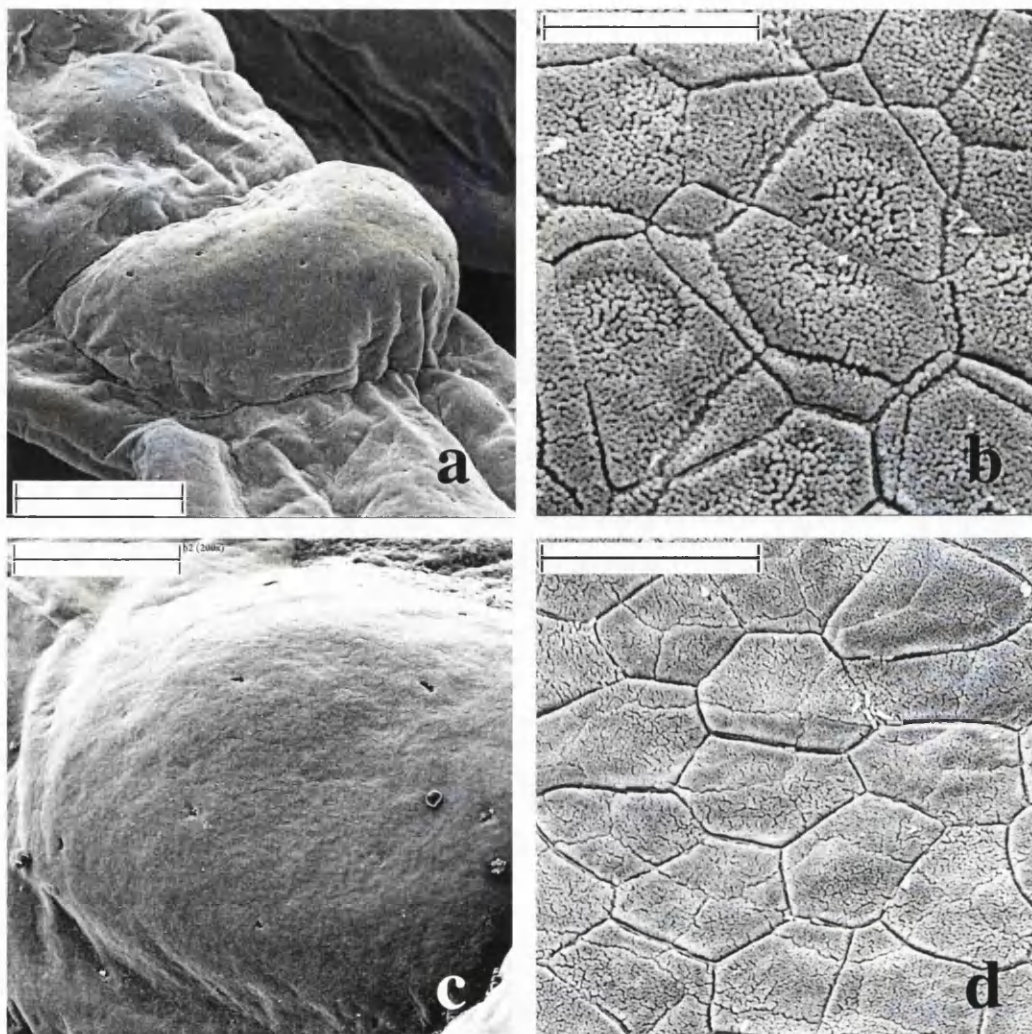


Figure 4.42: S.E.M. images of subarticular tubercles in *H. punctata*: (a) Juvenile (14.7 mm) Front 1, Scale bar = 150 μm (b) Juvenile (14.7 mm) Back 1, Scale bar = 12.5 μm . (c) Adult (34.7 mm) Back 2, Scale bar = 150 μm (d) Adult (34.7 mm) Back 2, Scale bar = 25 μm .

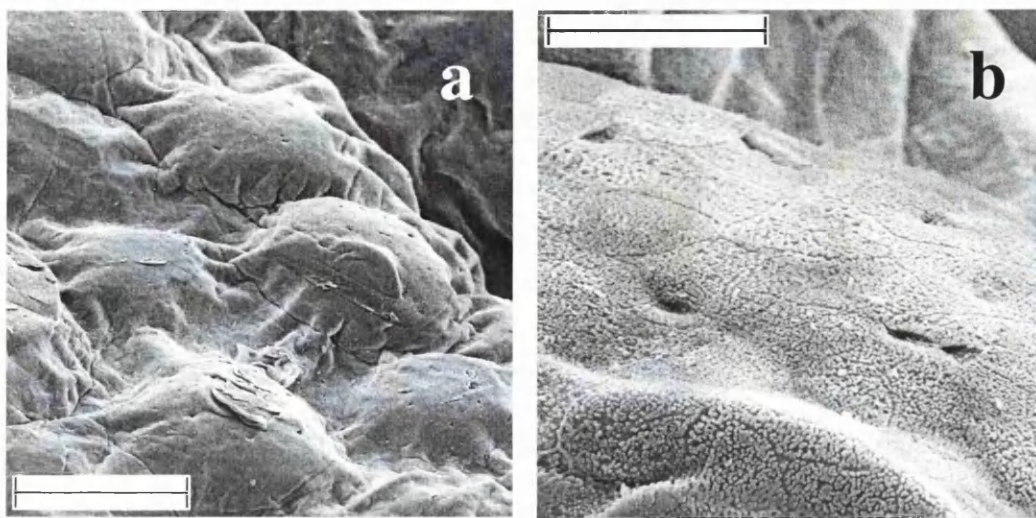


Figure 4.43: S.E.M. images of supernumerary tubercles in juvenile *H. punctata* (a) Scale bar = 150 μm (b) Scale bar = 25 μm .

4.3.5. Effects of size on toe pad morphology

Mean values for various aspects of toe pad morphology are given in **Table 4.3** for juvenile and adult frogs of the four small species of Hylid under consideration in this Chapter. Within the three species for which both juvenile and adult data are available, there is a reduction in the average cell size in the larger frogs, with this opposite to trends that would be predicted from between species effects on pad size in **Chapter 3**. This trend continues between species but is not significant, and consequently the variables that are linked to cell size, cell density and channel densities also show no significant correlative relationship with snout-vent lengths between species in these small Hylids (**Table 4.2**). There are similarly no significant relationships demonstrable between the size of the frog and either the degree of development seen in the grooves found around the pad or the general topography of the pad.

Morphological variable	Correlation with SVL			
	r	p	n	t
Cell area (μm^2)	0.52	0.08	12	-1.92
Cell density (per mm^2)	0.50	0.10	12	1.83
Channel density (mm/mm^2)	0.37	0.24	12	1.24
Pore size (μm^2)	0.36	0.34	10	1.02
Pore density (per mm^2)	0.71	0.01	11	-3.05
Pad elevation*	0.05	0.87	12	-0.16
Proximal margin*	0.16	0.61	12	0.52
Circumferal groove*	0.42	0.17	12	1.47
Lateral groove*	0.16	0.61	12	0.52
Subarticular tubercle cells	<i>0.67</i>	<i>0.06</i>	<i>8</i>	<i>-2.21</i>

Table 4.2: Correlative statistics for relationships between SVL measurements and aspects of pad morphology between species in small Hylid frogs. t-statistic for difference of line of best fit from the horizontal. Bold type indicates significant correlative relationship, italics indicates marginally insignificant result * see **Table 4.3** for score definition.

Pore size is highly variable within all of the species (**Table 4.3**), perhaps again due to differences in opening status of pores at times of sampling, as discussed in **Chapter 3.3.4**. Pore densities, although also variable, show a negative correlative relationship with SVL measurements both between species and within *S. rubra* (**Figure 4.44**). The relationship within *S. rubra* is not significantly different to that seen for the relationship between SVL and pore density across all four species ($t = 1.33$, N.S., 13 d.f.). That this trend should appear both within and between these small species may have significant implications on the frogs' adhesive abilities, for, as discussed in previous chapters, a reduction in mucus pore density with increasing size could lead to a reduced volume of mucus under the toe pad and hence better adhesion.

Trends in cell sizes found on the subarticular tubercles both between and within species are also worthy of note, with a tendency towards a reduction in average cell size between species with increasing SVL measurements (**Figure 4.45**). Although this trend is not statistically significant (by a narrow margin), reduction in cell size on these areas might be expected if these areas were responsible for additional contribution of frictional forces in larger frogs, with more potential individual sites for interlocking. Smaller cells may also allow closer contact on rough surfaces.

Species	SVL	Cell area μm^2	Cell density per mm^2	Channel density mm/mm^2	Pore area μm^2	Pores per mm^2	Scores* for				SaT cell size (μm^2)
							Pad elevation	Lateral groove	Proximal margin	Circumferal groove	
<i>H. minuscula</i>	18.40	91.52	11003	173.66	18.72	23.03	1.44	1.17	0.89	1.56	162.61
	23.00	99.62	10141	158.94	119.51	20.32	1.56	1.44	1.06	1.67	-
<i>F. fitzgeraldi</i>	7.30	116.97	8947	157.95	-	124.95	0.00	0.00	0.42	0.31	-
	15.90	115.39	8880	148.02	6.18	33.99	1.72	1.33	1.33	1.94	135.49
	18.70	86.56	11792	189.19	-	17.71	1.22	0.56	1.11	1.56	-
<i>S. rubra</i>	12.25	108.59	9512	181.39	13.41	51.77	1.83	1.81	1.33	2.13	187.04
	14.10	97.20	10568	171.56	10.25	45.75	1.50	0.56	0.61	1.56	152.20
	14.40	122.18	8274	157.26	123.81	52.61	0.67	0.72	0.78	1.00	203.78
	30.40	63.89	16111	215.72	78.99	22.85	0.50	0.17	0.21	2.07	108.95
<i>H. punctata</i>	14.70	109.52	9316	151.49	68.65	26.42	1.61	1.00	0.89	0.94	150.53
	32.70	110.70	9232	148.40	49.63	12.32	1.25	2.00	1.38	2.50	138.01
	32.80	96.77	10863	172.72	78.29	-	1.00	0.63	1.10	0.83	-

Table 4.3. Average values for aspects of toe pad morphology and subarticular (SaT) cell size in juvenile and adult frogs from four small species of Trinidadian Hyliid.

*Elevation score system: 0 = completely flat; 1 = slightly raised; 2 = rounded; 3 = globular. Groove score system: 0 = not present; 1 = shallow; 2 = defined; 3 = prominent.

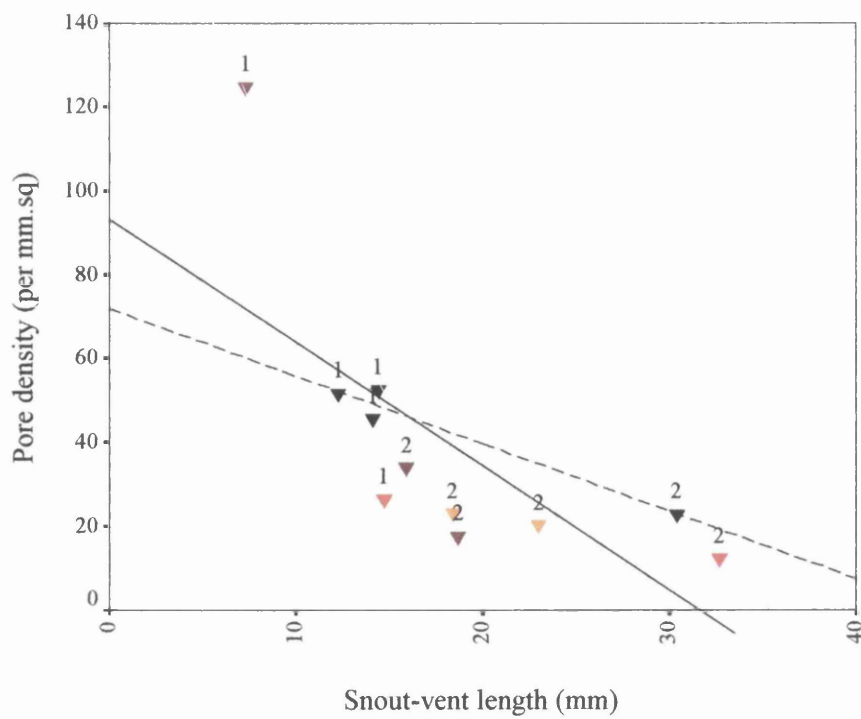


Figure 4.44: Average pore densities per toe pad vs. SVL in juvenile (1) and adult (2) frogs belonging to four small species of Hylid frog; *F. fitzgeraldi* (▼) *H. minuscula* (▼) *S. rubra* (▼) *H. punctata* (▼). Correlative relationships: All frogs; $r = 0.71$, $y = 93.32 - 2.94x$, $t = -3.05$, $p = 0.01$, $n = 11$; *S. rubra*; $r = 0.98$, $y = 71.85 - 1.61x$, $t = -6.39$, $p = 0.02$, $n = 4$.

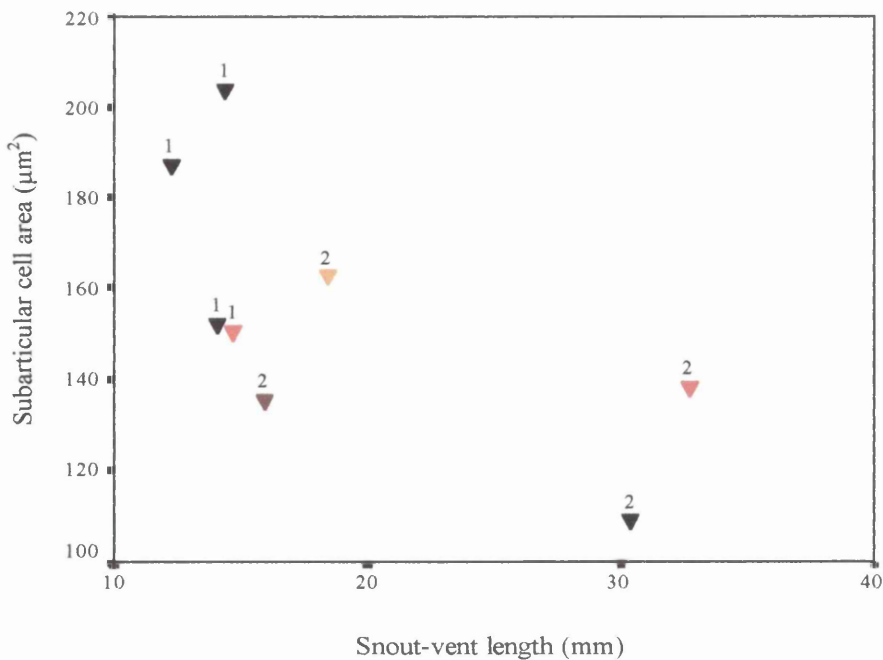


Figure 4.45: Average subarticular tubercle cell size in juvenile (1) and adult (2) frogs belonging to four small species of Hylid frog; *F. fitzgeraldi* (▼) *H. minuscula* (▼) *S. rubra* (▼) *H. punctata* (▼). Correlative relationships: All frogs, $r = 0.67$, $p = 0.06$, N.S. $n = 8$.

4.3.6. Integrating pad morphology and adhesion

Detachment angles were recorded from all frogs with toe pads that were examined using S.E.M., and adhesive forces were calculated using **Formulae 3 (Chapter 2)** for each frog (**Table 4.4**). Forces per unit area were also determined for each frog.

Species	SVL	Angle	Adhesive force (mN)	Force per mm ² (mN)
<i>H. minuscula</i>	18.40	178.40	8.16	0.46
	23.00	179.30	6.45	0.45
<i>F. fitzgeraldi</i>	7.30	173.00	0.49	0.33
	15.90	179.20	4.56	0.44
	18.70	178.10	3.54	0.57
<i>S. rubra</i>	12.25	180.00	1.96	0.51
	14.10	180.00	1.58	0.38
	14.40	154.50	2.35	0.52
	30.40	159.50	17.37	0.88
<i>H. punctata</i>	14.70	180.00	2.94	0.51
	32.70	147.30	21.98	0.73
	32.80	135.10	14.68	-

Table 4.4: Detachment angles, adhesive forces and forces per unit area calculated for frogs used in S.E.M. studies.

Considering these results with the aspects of toe pad morphology recorded from these same frogs, there are a few intraspecific trends evident though the limited data availability means that these trends should be treated with some caution. Adhesive forces within *Scinax rubra* show a positive correlation with the cell densities in the individual frogs ($r = 0.96$, $y = 0.002x - 18.03$, $t = 4.58$, $p = 0.04$, $n = 4$) and a negative correlative relationship with the average pore densities on the pads, so that greater adhesive forces are seen in frogs with a reduced density of pores on their pads ($r =$

0.98, $y = 29.21 - 0.54x$, $t = -6.20$, $p = 0.03$, $n = 4$) The degree of development of the grooves and the topography of the pad has an influence on the adhesive forces being produced in *F. fitzgeraldi*: with increasing adhesive force correlating with a rounder more elevated pad ($r = 0.999$, $y = 2.39x + 0.52$, $t = 23.35$, $p = 0.027$, $n = 3$), a better defined proximal margin ($r = 0.999$, $y = 4.45x - 1.38$, $t = 103.30$, $p = 0.006$, $n = 3$) and a more distinct circumferal groove ($r = 0.999$, $y = 2.48x - 0.28$, $t = 61.66$, $p = 0.01$, $n = 3$)

Between species, there are a number of trends in evidence between aspects of toe pad morphology and the adhesive forces measured from detachment angles recorded from frogs prior to S.E.M. studies. There is a weak correlative relationship seen between cell densities and the force per unit area of toe pad (**Table 4.5**, **Figure 4.46**). This runs counter to findings in adult frogs belonging to the genus *Hyla* where larger cell sizes were implicated with increasing adhesive forces (see **Chapter 3**). There is a trend such that a decrease in adhesive force per unit area is seen with increasing pore densities on the pad (**Table 4.5**, **Figure 4.47**). Although the trends in this are weak, similar trends seen between species in adult frogs, together with the negative correlative relationship with size seen in these small species (**Figure 4.44**) suggests that, if a larger sample were available these trends may be strengthened. The trend also follows predictions from adult frogs that, with increasing size, changes in toe pad structure will develop to maintain a thin meniscal layer beneath the pad. The lowered mucosal pore densities seen with increasing size in these small species are likely to aid in this by proportionally lower production of mucus in larger frogs.

Morphological variable	Adhesive force (mN)				Force per mm ² (mN)			
	r	p	n	t	r	p	n	t
Cell area	0.42	0.17	12	-1.48	0.58	0.06	11	-2.16
Cell density	0.45	0.14	12	1.60	0.66⁽¹⁾	0.03	11	2.65
Channel density	0.20	0.53	12	0.65	0.45	0.17	11	1.50
Pore size	0.16	0.67	10	0.45	0.35	0.35	9	1.00
Pore density	0.53	0.09	11	-1.87	0.55⁽²⁾	0.08	11	-2.00
Pad elevation	0.13	0.68	12	-0.43	0.26	0.44	11	-0.80
Proximal margin	0.08	0.80	12	0.26	0.19	0.57	11	-0.59
Circumferal groove	0.47	0.13	12	1.67	0.47	0.14	11	1.62
Lateral groove	0.20	0.53	12	0.65	0.06	0.85	11	-0.19
Subarticular cell	0.64	0.09	8	-2.03	0.63	0.09	8	-1.99

Table 4.5: Correlative statistics for relationships between adhesive forces and force per unit area and SVL in four small species of Hyliid. t-statistic for difference from the horizontal of line of best fit. Bold type denotes correlations significant to $p = 0.05$. (1) see **Figure 4.46** (2) see **Figure 4.47**

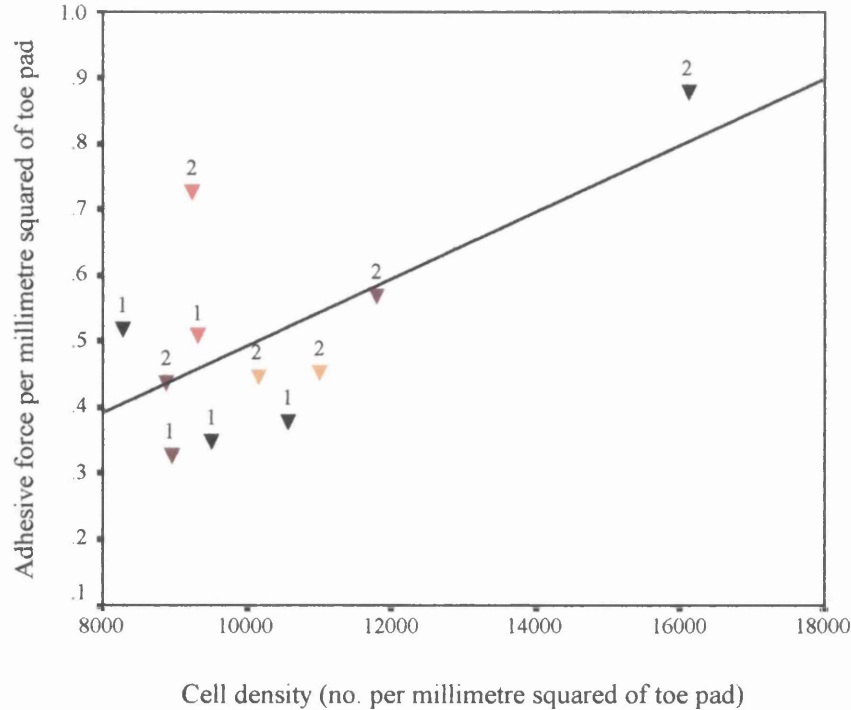


Figure 4.46: Adhesive force per mm² vs. cell densities on toe pad in juvenile (1) and adult (2) frogs belonging to four small species of Hylid frog; *F. fitzgeraldi* (▼) *H. minuscula* (▼) *S. rubra* (▼) *H. punctata* (▼). Correlative statistics: All frogs, $r = 0.66$, $y = 5.06x - 0.01$, $t = 2.65$, $p = 0.03$, $n = 11$; *S. rubra*: $r = 0.85$, $t = 2.29$, $p = 0.15$, N.S. $n = 4$; *F. fitzgeraldi*: $r = 0.88$, $t = 1.85$, $p = 0.32$, N.S. $n = 3$

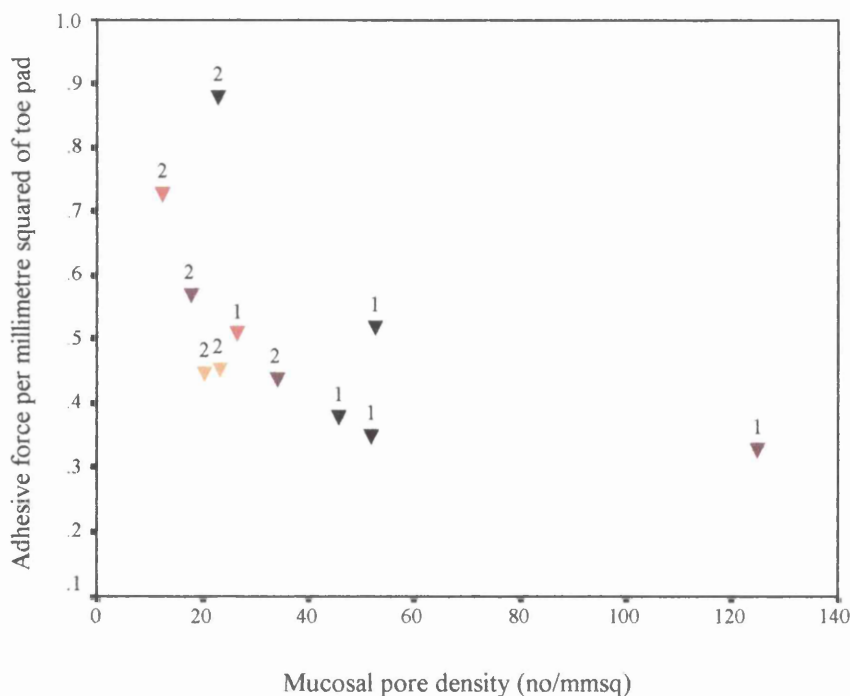


Figure 4.47: Adhesive force per mm² vs. pore densities in juvenile (1) and adult (2) frogs belonging to four small species of Hylid frog; *F. fitzgeraldi* (▼) *H. minuscula* (▼) *S. rubra* (▼) *H. punctata* (▼). Correlative relationships: All frogs, $r = 0.55$, $t = -2.00$, $p = 0.08$, N.S. $n = 11$. *S. rubra*: $r = 0.90$, $t = -2.90$, $p = 0.10$, N.S. $n = 4$; *F. fitzgeraldi*: $r = 0.91$, $t = -2.18$, $p = 0.27$, N.S. $n = 4$

4.4. Discussion

In all four of the small-sized Hylid species from which data from both age-classes was available, the ability of the frogs within a species to maintain a hold on a rotating platform was not detrimentally affected by growth, with no significant differences in the average detachments recorded in the juvenile and adult age classes. The trend towards reduced detachment angles in adult *F. fitzgeraldi* remains to be verified due to the small sample size. In this species, there is additionally the added problem that it is one of the few species in which a statistically significant difference in the adhesive abilities of the sexes has been noted (**Table A3.1**).

The high incidence of 180° angles recorded from both age-classes in all four small species suggests that it is extremely likely that limitations of the methodology are leading to an underestimate of the maximal adhesive forces that these frogs are able to produce. In spite of this, all four small Hylids are still capable of producing adhesive forces that are able to keep pace with the corresponding within species increases in weight between metamorphosis and adulthood. In all small species, toe pad area is increasing much as expected with isometric growth, as the square of the linear dimensions. How then, are these frogs able to maintain their adhesive abilities in spite of the pressures of increasing weight with growth, dependent as they are on an area-based adhesive system?

In fact, in the largest and smallest of the species; *H. minuscula* and *H. punctata* adhesive forces *are* increasing largely as would be expected for a system dominated by area-dependent forces, at a rate not significantly different to the square of the linear dimension. In *H. punctata* a high degree of variability in the adhesive forces recorded within the adult frogs means that, although the rate of adhesive force production, $(SVL)^{2.12}$, scales with equivalent toe-pad area increase $(SVL)^{2.04}$, neither is it significantly different from the reduced rate of weight increase seen in the species, $(SVL)^{2.54}$. Trends within the smaller of the two species, however, suggest that the ability within *H. minuscula* to maintain adhesive performance between age classes may be due to an extensive reduction in the increase in weight seen with growth, but as only one juvenile was available in this species, this remains to be verified.

Both *F. fitzgeraldi* and *S. rubra* show significantly greater increases in the rate of adhesive force production than the equivalent toe pad area increase can explain, as $(SVL)^{2.51}$ and $(SVL)^{2.81}$ respectively. In both species a reduced rate of weight increase is seen, though in neither case is this lowered sufficiently for the correspondent toe pad area to match it. *S. rubra* in particular has a less reduced rate of weight gain with growth than the other small species, with this trend particularly significant in view of the fact that it is this species for which the most complete continuous data set exists (t-statistics for comparison of slopes of weight increase with SVL in *S. rubra* vs.: *F. fitzgeraldi*, $t = 2.46$, $p < 0.02$, 72 d.f. vs. *H. punctata*, $t = 2.39$, $p < 0.05$, 72 d.f.).

The differences in the intraspecific growth patterns are of particular interest when the high degree of geometrical similarity between species is taken into consideration (**Table 4.6**). This suggests that, although it is an advantage to all four small species to reduce the rate of weight gain, there may be other responses within the three larger species that are additionally compensating for the pressures upon the adhesive system that reduce the necessity for this. Alternatively, it may simply be that the advantages of increased adhesion are not as great as the disadvantages that reduced weight will have on escape speed for these small species

Ratios of measured physical parameters	<i>F. fitzgeraldi</i> ¹	<i>H. microcephala</i> <i>species group</i> ^{2a}	<i>S. rubra</i> ^{2b}
Tibia: SVL	0.55	0.52	0.51
Foot: SVL	0.41	0.45	0.44
Head length: SVL	0.39	0.33	0.37
Head width: SVL	0.38	0.31	0.32

Table 4.6: Ratios of physical measurements from males of smaller species. Derived from measurements in (1) Duellman and Gray, 1983 (Trinidad and Tobago) and (2) Duellman, 2001. (a) Costa Rica (b) Ecuador.

Removing the effect of area from the adhesive forces being produced by considering the force per unit area, there is a demonstrable positive correlation within *S. rubra*, which mirrors trends in the other three species, suggesting an improvement within the adhesive mechanism that is independent of the area of the pad in contact. The tendency for an increase in the force per unit area with increasing SVL is continued across species suggesting that there is an increase in toe pad efficiency both between and within species. **Chapters 2 and 3** outline a number of ways in which the adhesive system may be being improved with

increasing SVL, through alterations of contributory factors within the wet adhesive system and through development of toe pad morphology.

There are few trends in toe pad morphology either within or between species in the variables implicated in increased adhesive force production between the adult frogs of all twelve species (**Chapter 3.4**). There is some evidence of a reduction in pore densities with an increase in SVL, both within *S. rubra* and, to a lesser degree, between species. This is of particular significance when taking into account the predictions made in **Chapter 2** with regards to the effect of this variable on the mucosal volume below the pad and consequently on the meniscal height and thus meniscal force. If higher densities of mucosal pores were to increase mucus production the increase in meniscal height that would result might well be expected to be detrimental to the frogs' sticking ability. The within-species trend towards lower pore densities in the adult frogs of these smaller species is therefore likely to be a response to the requirements of the adhesive system to maintain sticking abilities during growth from metamorphosis to adulthood.

The increase in the development of grooves that may act as mucosal channels on the pad and along the toe shows few trends between adults of all twelve species (**Chapter 3**). In *F. fitzgeraldi* however there is a significant increase both in the definition of the circumferal and proximal margins from the pad proper and in the delineation of the lateral grooves running along the ventral surface of the toe in adult frogs. An increase in the degree of development of the groove system on the toe has been implicated with greater degrees of arboreality between species in previous studies (McAllister and Channing, 1984; Green and Simon, 1986). The

dependence of *F. fitzgeraldi*'s mode of reproduction on epiphytic bromeliads (4.2.1) means that it is certainly possible that this species does become more arboreal as adults than as juvenile frogs. However, new metamorphs will certainly initially be highly arboreal as they are emergent from phytotelmata in the bromeliads in which they were placed as tadpoles and there is some evidence of specialisations of the pad in terms of modifications to the cells at the circumferal margin in juveniles (Figure 4.23 b and 4.26 a, b) that may well be a response to the hydrophobic nature of the waxes on the leaves of the bromeliads. That these modifications are not evident in adult frogs suggests that in fact it may be the juveniles that are more dependent on the microhabitats represented within the bromeliads and therefore more arboreal than the adult frogs, which are frequently found in leaf litter on the ground (Duellman and Gray, 1983).

A number of authors have suggested (Welsch *et al.* 1974; McAllister and Channing, 1984; Green and Simon, 1986) that the function of the circumferal groove is either to act as a reservoir for the excess mucus that is released on the pad or to aid in the maintenance of a thin evenly spread layer beneath the pad. If this were the case then there might be expected to be an effect on the adhesive abilities of the increasing definition of this groove and indeed, the relationship between the demarcation of the circumferal groove in *F. fitzgeraldi* and increasing adhesive force suggests that trends in the development of this area are worthy of further consideration in relation to adhesive abilities. However, the lack of a statistically significantly relationship between the delineation of the circumferal margin and size between or within species suggests that trends in the degree of development of this area in small species are not necessarily a response to the pressures of increasing

size but may be indicative of a greater dependence on adhesive ability with higher degrees of arboreality.

Although accessory adhesive areas such as the skin on the stomach, thighs and chin were excluded from contributing to the forces, through the exclusion of any angles recorded from frogs using these areas when they detached from the board, both subarticular tubercles and the region immediately below the pad were regularly in contact with the experimental substrates when angles were measured. The trend towards increased development of proximal margins and subarticular tubercles in all species, with more specialisation in the cell types seen in these regions in adult frogs in comparison to the juvenile frogs suggest that the roles of these areas is of increased importance in the adhesive abilities of larger frogs. The roughened micro-villated surfaces of the cells in these areas suggests that the accessory structures may aid in adhesion by the contribution of additional frictional or interlocking forces on rough surfaces. Furthermore, the decrease in the average subarticular tubercle cell sizes in adult frogs and the consequent increase in cell densities suggests that the frictional influence of these areas may well be enhanced in larger frogs as frictional forces directly increase with the number of sites available for interlocking (Dai *et al.* 2002). This trend suggests that the importance of these areas may well have been underestimated in previous studies on tree frog adhesion, particularly with respect to their adhesive abilities on rough surfaces such as the bark on branches and trunks of trees. The marked increase in the development of supernumerary and other additional tubercles on the hands and feet of adult *F. fitzgeraldi* suggests that the need for areas that implement adhesion on rough substrates may well be enhanced for this species.

Within all four small species frogs are able to maintain their sticking abilities to a similar degree by keeping weight increases with growth significantly lowered, with the degree to which this is the case particularly pronounced in the smallest of the four species. In *S. rubra* and *F. fitzgeraldi* where the rate of weight gain with increasing linear dimensions is least reduced from the expected, there is evidence of changes in toe pad morphology that can be linked to aspects of the wet adhesive mechanism that would increase the forces produced within the system. The fact that there is no detriment to the frogs' adhesive abilities with growth suggests that the combined effects of the reduced rate of weight gain and the changes in toe pad morphology that may facilitate a reduction in meniscal height below the pad between the age classes are sufficient to cope with the large increases in size involved between new metamorph and adult. As substantial as these increases are, the increases in weight involved between metamorphosis and adulthood in the larger size classes can be considerably higher (**Table 4.1**). The next chapter will discuss whether similar trends in allometry and toe pad morphology as those seen in these small species are also sufficient to allow medium species to maintain adhesive abilities with growth or whether further compensatory measures are necessary for the greater increase in weight involved in larger species.

Chapter 5: Adhesion in medium hyliid tree frogs.

5.1. Introduction

In **Chapter 4.1** the potential problems caused by the dependence upon an adhesive mechanism reliant upon increasing surface area, when faced with the substantial increases in weight that are involved with growth of an individual were identified. The extent of the increase in weight involved from metamorphosis can be seen to be substantially different according to the final adult size of the frog, as might be expected if the broad similarity in metamorphic size in all of the species is taken into consideration (**Table 5.1**).

Species in order of increasing SVL	Average SVL (mm)			Average weight (g)		
	Juvenile	Adult* ²	Increase in size	Juvenile	Adult* ²	Increase in size
<i>H. minuscula</i> ~	11.25	17.98	x 1.6	0.16	0.45	x 2.8
<i>F. fitzgeraldi</i> ~	7.92	18.67	x 2.4	0.06	0.52	x 8.7
<i>S. rubra</i> ~	13.38	30.23	x 2.3	0.20	2.02	x 10.1
<i>H. punctata</i> ~	14.70	33.42	x 2.3	0.30	2.43	x 8.1
<i>H. geographica</i> *	24.20	57.93	x 2.4	1.47	8.43	x 5.7
<i>H. crepitans</i> *	18.50	63.35	x 3.4	0.55	14.14	x 25.7
<i>P. trinitatis</i> *	15.30	75.90	x 4.9	0.75	21.39	x 28.5
<i>P. venulosa</i> *	19.60	74.44	x 3.8	0.39	24.79	x 63.6

Table 5.1: Species average values for snout-vent lengths and weight in juvenile and adult frogs: ~ average measurements of youngest cohort in **Chapter 4** * measurements from new metamorphs in Downie *et al.* (submitted); *² adult values from **Table 2.1**.

In the small species discussed in the previous chapter the adhesive abilities were maintained with growth through a combination of reduced weight gain with growth and an improvement of the adhesive force produced per unit area of the toe pads of adult frogs. There is some evidence that the increase in pad efficiency that this suggests in adult frogs may be effected by a reduction in mucosal pore densities and an increase in the degree of development in the circumferal grooves. Additionally there is an increase in the development of the subarticular tubercles and other accessory areas with growth that may facilitate an additional contribution of frictional forces to the overall adhesive forces being produced within the small species. The combined effects of these small adjustments to elements within the adhesive system and to morphometric considerations are sufficient to allow no significant detriment to the adult frogs' adhesive abilities, in spite of the substantial increases in weight that are involved in the development from metamorphosis (**Table 5.1**).

As substantial as these increases are, the increases in weight involved between metamorphosis and adulthood in the larger size classes are considerably higher (**Table 5.1**). This chapter will discuss whether similar trends in growth patterns and toe pad morphology, such as those seen in the smaller species, are also seen in the medium species of Trinidadian hylid, as defined in **Chapter 4.1**. If so, will these be sufficient to allow these larger species to maintain their adhesive abilities or will further adjustments to the mechanism be necessary to compensate for the greater increases in weight?

5.2. Methods

5.2.1. Experimental animals

Hyla geographica

H. geographica belongs within an eponymous species group within the genus *Hyla*, and is the most widely distributed of the three species within the group. The species group shares many characteristics with



Figure 5.1: *H. geographica*; adult male 5 (59.6 mm), dorsal and ventral views. NB: Ventral spotting is exclusive to Trinidadian frogs (Duellman, 1973) (Photos J. Smith)

the *Hyla boans* group (Duellman, 1973) particularly in terms of skull morphology and osteology. As this is the group to which *H. crepitans* belongs (Duellman, 2001), the two medium-sized species are the second most closely related in the study. However, *H. geographica* is readily distinguished from the similarly sized *H. crepitans*, with which it shares the habit of blanching during the day, by the presence of a distinctive triangular flap of skin on the heel, the calcar (Murphy, 1997). Adult frogs collected in Trinidad in 2000 and 2001 ranged between 49.7 – 59.6 mm SVL (♂) and 63.2 – 68.2 mm SVL (♀). These values are in broad agreement with those previously recorded from frogs in the locality (58 – 67mm: Murphy, 1997; Kenny, 1969), but are in the lower ranges of the maximum values seen in frogs from the South American mainland (59 – 75.5 mm; Duellman, 1973).

All adults were collected from the banks of the Damier River in the North of Trinidad (**Figure A2.1**). Male frogs were sampled from calling congregations low in the vegetation of the river bank and if silent were identified as male by the presence of a heart-shaped nuptial excrescence present on the inner wrists. Females were identified from their position in amplexant pairs and in all instances were heavily gravid upon collection. A gravid female is significantly altered in shape, carrying egg masses weighing between 70 - 110 per cent of their post-deposition body weight. It is important to note that data from gravid females are excluded from the analyses discussed here based on these allometric considerations. Adult frogs were extremely agitated in captivity and unless housed in soft-sided enclosures would injure themselves badly by throwing themselves at the glass sides of the vivarium. They are also particularly prone to desiccation and need to be misted regularly.

Tadpoles were collected at late stages from shoals in the Damier and Guanapo Rivers (**Figure A2.1**) and maintained in well-aerated aquaria with several vertical branches for emergent metamorphs to climb onto. *H. geographica* are large sized froglets at metamorphosis at around 20-21mm in SVL. They are, however, difficult to maintain in the laboratory with few surviving beyond their first few months. It seems likely that some dietary requirement of these frogs is not being met in captivity. Juveniles, released on the banks of the river from which they were collected, were seen on a number of occasions to snap at passing ants.

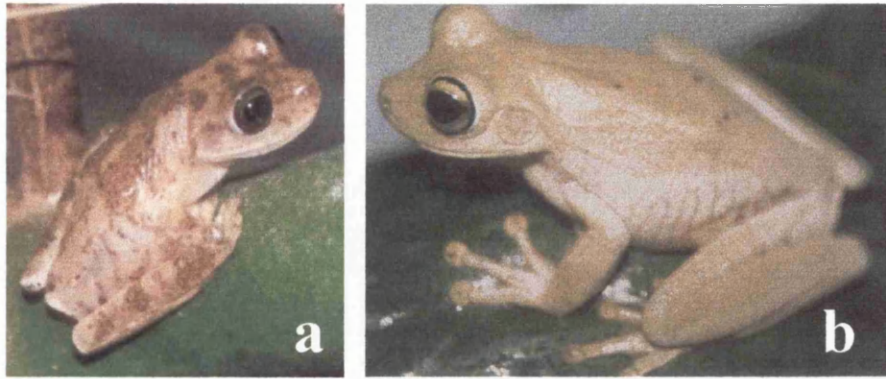
Hyla crepitans

Figure 5.2: *H. crepitans* (a) Juvenile (30mm) (b) Adult (56mm). Photo: J. Smith.

This species is one of the smaller members of the *Hyla boans* species group, with typical sizes of adults collected in Trinidad ranging between 56.5 – 64.9 mm SVL (♂) and 65.5 – 69.8 mm SVL (♀). These concur with values from the locality given in literature (61 – 73 mm: Murphy, 1997; Kenny, 1969) but are in the upper ranges of values given for this species from Central Panama where the largest male found was only 58.5 mm SVL (Duellman, 2001). Adults were sampled from calling aggregations on flooded wasteland in the Lopinot Valley, and from daytime roosts on leaves and trunks of trees and shrubs in gardens in neighbouring valleys in the Northern Range (**Figure A2.1.**). If frogs were silent upon collection, males were identifiable such by the presence of a prominent protruding prepollex (Duellman, 2001). Female frogs, sampled when gravid, produce egg masses representative of 20–25 % of their post-deposition weight when left in amplexus with male frogs in a darkened laboratory.

Tadpoles from these clutches, together with larger tadpoles sampled from the temporary breeding ponds at Lopinot and a garden pond in Port of Spain, were raised through to metamorphosis in the laboratory in Glasgow. The size of froglets at metamorphosis is around 15mm SVL (15–17mm; Murphy, 1997). Thereafter the

frogllets were fed upon a diet of fruit flies and small vitamin-dusted crickets. None survived much beyond than their first year, with maximum size achieved in this time around 35mm.

5.2.2. Measurement of sticking ability

Sticking ability in adult frogs was determined in lab conditions in Trinidad, using the methodology outlined in **Chapter 2.2.2**. Juvenile frogs were rotated at least once monthly, again according to this protocol and, as with adults, weighed and measured immediately prior to experimental use. All experiments were carried out in the room in which the frogs were kept, at temperatures comparable to typical air temperatures in Trinidad.

Species-specific notes on the behaviour of the frogs on rotation platform were utilised to make sure that detachment angles were as accurate a representation of the adhesive performance allowed by toe pad contact alone in the two medium-sized species:

Hyla geographica

On the rotation board, adult *H. geographica* tend to press themselves close to the board, maintaining a flattened pose to angles beyond 90°, and attempt to use their stomach skin up to the point when they begin to extend their legs away from their body. This skin is coarsely granular with large hexagonal tubercles on the surface reminiscent in their geometry to the toe pad cells though differing substantially in their scale (**Figure 5.3**). As the board continues to rotate to angles beyond the vertical the frogs stretch hands and feet away from the body (**Figure 5.1**), though the

extension of the back legs is not as exaggerated as in some of the larger species exhibiting limb expansion in response to tilting. Adult frogs have a propensity to get very stressed with repeated rotations, the first signs of which is a tendency to fall without adjusting the back feet at all with the front feet detaching

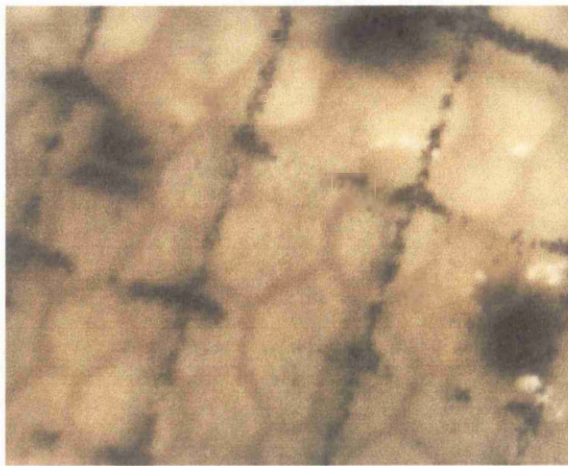


Figure 5.3: Photograph of ventral surface of adult *H. geographica* (grid = 1mm)

first; thereafter, frogs also darken considerably in colour and bring the nictating membrane over the eye. Any continued handling causes the frogs to pull their limbs towards the body and feign death, as described in Murphy (1997). Experiments were then halted and frogs placed in cool, moist, darkened conditions until their colour was restored and frogs became more active.

Hyla crepitans

Both adult and juvenile *H. crepitans* attempt, whilst being rotated, to increase the surface area of skin in contact with the platform and will stick using belly and thigh skin if allowed to. Then, as the surface continues to rotate, this skin begins to slowly peel from the surface and the front feet begin to slip. In response to this slipping, the frogs replace the front feet, spreading the front toes so that the webbing between the front toes also touches the surface, thus actively increasing the area in contact. They also alter their posture on the board by spreading their back legs wide and holding their posterior end closer to the rotation surface, thus altering their centre of gravity as their situation becomes more precarious.

5.2.3. Calculating adhesive force

Adhesive forces were calculated using the methodology outlined in **Chapter 2.2.3**.

5.2.4. Toe pad morphology

Toe pads were sampled and processed for Scanning Electron Microscopy as described in **Chapter 3.2.1**. Images captured from juvenile and adult frogs were analysed as described in **Chapter 3.2.2**.

5.2.5. Statistics

As a point of note: All statistics and graphs are generated using SPSS statistics software. This package does not have the functional capability to truncate lines of best fit to confine them to the edges of data sets and the lines of best fit on many graphs extend further than the parameters of the study can predict.

All statistical mean values are given in the format: $\bar{x} \pm 1 \text{ s.e.}$

5.3. Results

5.3.1. Morphometrics

Hyla geographica

H. geographica are large-sized froglets, being $23.28 \text{ mm SVL} \pm 0.70$ and $0.75 \text{ g} \pm 0.05$ ($n = 10$) at metamorphosis. Adults collected in Trinidad ranged in SVL size from $54.01 \pm 1.11 \text{ mm}$ in male frogs ($n = 10$) to $65.85 \pm 0.82 \text{ mm}$ in females ($n = 4$). **Figure 5.4.** shows the increase in weight with increasing linear dimensions on a log:log plot for juveniles, adults and the population as a whole. Juveniles increase in weight, as $(\text{SVL})^{2.91}$. This is not significantly different from the rate of growth that would be expected from isometric development where mass increases as linear dimensions cubed ($t = 0.14$, N.S., 19 d.f.). Adult frogs increase in weight at a slower rate – as $(\text{SVL})^{1.99}$. This is significantly less than the rate of weight increase expected through predictions from isometric growth (Difference from slope of 3: $t = 5.10$, $p < 0.01$, 11 d.f.). Combining the data from adults and juveniles together we see an overall rate of growth over the period from metamorphosis to attainment of adulthood of $(\text{SVL})^{2.48}$. This is significantly less than the expected weight increase with isometric growth, $(\text{SVL})^3$ ($t = 6.93$, $p < 0.01$, 32 d.f.).

Looking at the correlative relationship between the area of toe pad and linear dimensions on a log:log plot for juvenile and adult frogs together (**Figure 5.5**), there is a slight tendency towards a greater than expected expansion of toe pad area with growth. However, statistically, there is no significant difference of the slope of the line of best fit on the log:log plot from the expected slope of 2; $t = 0.74$, N.S., 2 d.f.

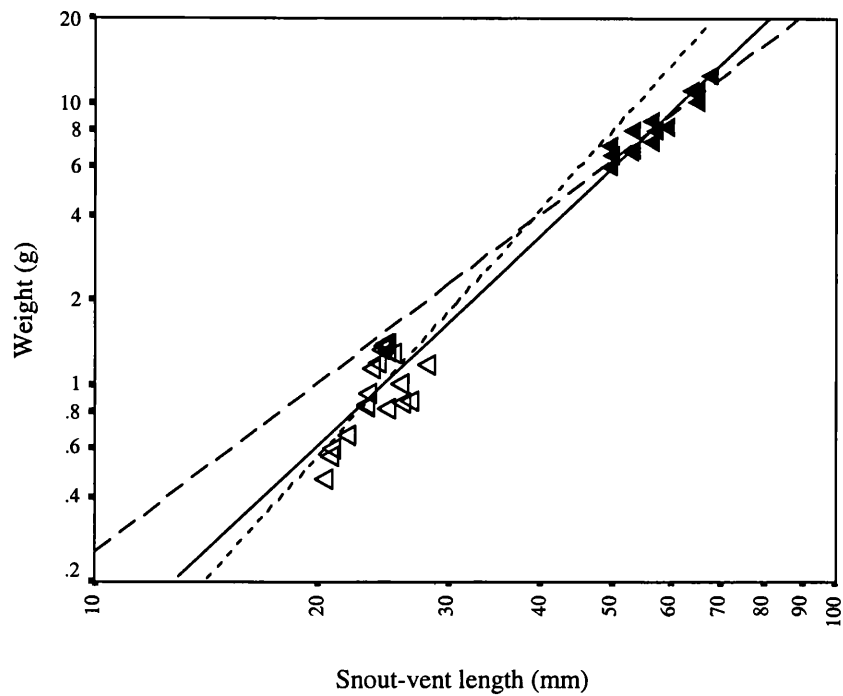


Figure 5.4: Log:log plot of weight vs. linear dimensions in juvenile (\triangle) and adult (\blacktriangle) *H. geographica*. Correlative statistics for: Juveniles $y = 2.91x - 4.04$, $r = 0.72$, $t = 4.49$, $p < 0.001$, $n = 21$; Adults ——— $y = 1.99x - 2.58$, $r = 0.95$, $t = 10.01$, $p < 0.001$, $n = 13$; Total population ——— $y = 2.48x - 3.45$, $r = 0.99$, $t = 33.23$, $p < 0.001$, $n = 34$.

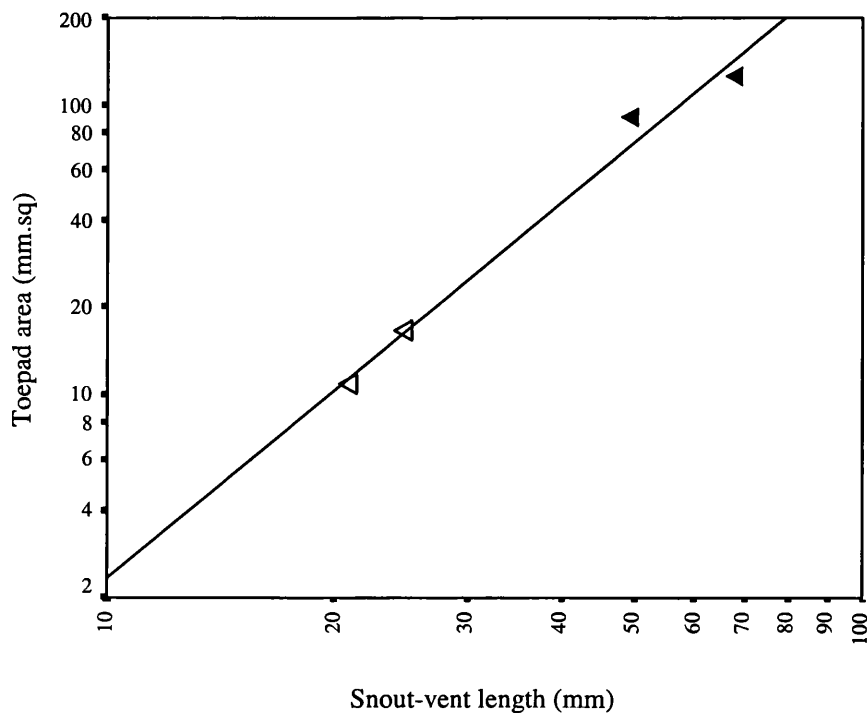


Figure 5.5: Log:log plot of toe pad area vs. linear dimensions in juvenile (\triangle) and adult (\blacktriangle) *H. geographica*. Correlative statistics: $r = 0.99$ ——— $y = 2.15x - 1.78$, $t = 11.35$, $p < 0.001$, $n = 4$.

Hyla crepitans

Size ranges of adult frogs caught in Trinidad in the summers of 2000 and 2001 averaged at $62.49 \text{ mm} \pm 0.90$ ($n = 10$) for male frogs and $67.65 \text{ mm} \pm 2.15$ ($n = 2$) for females. The size of the frogs at metamorphosis is around 15mm SVL when they are around 0.5g in weight. The juvenile frogs shown in **Figure 5.6** are *H. crepitans* sampled throughout their first year of development, in which time they have quadrupled their weight; by maturation, with typical adult weights ranging from 10-15g, they will have increased their body mass by more than twenty-fold.

If *H. crepitans* follow isometric growth patterns, on a log:log plot of weight vs. body length the expected slope of the line of best fit for such a relationship will be three, as body mass increases as the cube of the linear dimension. In fact for juvenile *H. crepitans* the slope relating to body mass increase with increasing linear dimensions is 2.51 (**Figure 5.6**); weight is therefore increasing at a significantly lesser rate than that expected with isometric growth (Difference from slope of 3: $t = 5.54$, $p < 0.01$, 101 d.f.). If the adults are included in the analysis (**Figure 5.6**), then the discrepancy between the observed and expected rates of weight increase with growth is lessened, at $(\text{SVL})^{2.69}$, but still significant ($t = 7.75$, $p < 0.01$, 113 d.f.); hence mass increase with growth in *H. crepitans* is significantly less than expected. Although weight gain in adults alone appears to be lower than predicted, increasing as $(\text{SVL})^{1.99}$, this is not statistically significantly different from the slope of three ($t = 1.61$, N.S. 10 d.f.)

Is there also a correspondent increase in toe pad area with linear dimensions at a rate greater than expected as is implied by the limited data available for the smaller of these two medium-sized species? In fact the toe pad area increase within the juveniles alone is $(\text{SVL})^{2.22}$, (**Figure 5.7**). This suggests that a trend exists for a

greater than expected increase in toe pad area, though a t-test to compare the observed slope with the expected finds no significant difference between the two ($t = 0.63$, N.S. 10 d.f.). Including the adult data in the analysis strengthens the correlative relationship between the two variables on a log:log plot (**Figure 5.7**). This time, the relationship between the two is much closer to the expected increase in pad area with the linear dimension, as $(SVL)^{2.08}$, and again is not significantly different ($t = 0.36$, N.S. 11 d.f.). Significantly, although the rate of toe pad area increase in juveniles is lower than the correspondent weight increase over the same time period, a t-test shows no statistical differences between the slopes of weight and toe pad increase vs. SVL on a log:log plot ($t = 0.81$, N.S., 111 d.f.) for these frogs. If adults are included in the correlative relationships between these physical parameters, the increase of weight does occur at a significantly greater rate than toe pad area ($t = 2.73$, $p = 0.01$, 124 d.f.).

With the morphometric trends in area and mass increase with growth, predictions about sticking abilities in both juvenile and adult frogs of these two medium sized species can now be made. The fact that the total area of the adhesive pads in contact with a surface is not increasing at a sufficient rate to match the correspondent weight increase in either species means that the area-dependent adhesive mechanism in effect (**Chapter 2**), may be expected to be detrimentally affected with growth to adult-hood. However, within juvenile *H. crepitans*, as there is no significant difference between the rate of increase in toe pad area and the rate of weight increase in the same period of growth, this suggests that there may be an ability within this particular cohort to maintain adhesive abilities to around a similar level. The poor survival rates of the *H. geographica* metamorphs made it impossible to examine whether this is also true of the other medium-sized frog in this study.

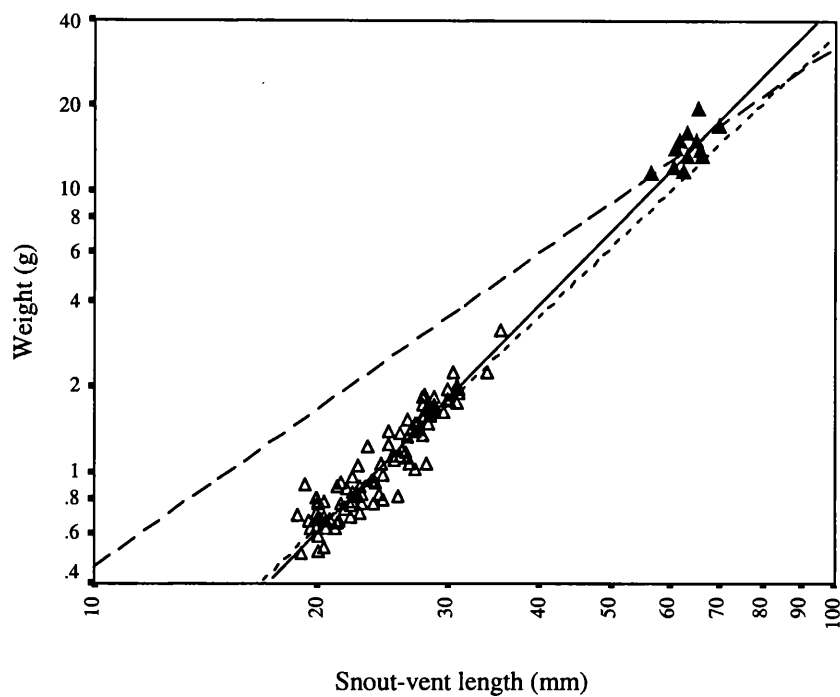


Figure 5.6: Log:log plot of weight vs. linear dimensions in juvenile (\triangle) and adult (\blacktriangle) *H. crepitans*.

Correlative statistics for: Juveniles $r = 0.94$, $y = 2.51x - 3.47$, $t = 26.68$, $p = 0.0001$, $n = 103$;
 Adults_ _ $r = 0.63$, $y = 1.85x - 2.18$, $t = 2.58$, $p = 0.02$, $n = 12$; Total population ____ $r = 0.99$, $y = 2.69x - 3.71$, $t = 63.86$, $p = 0.0001$, $n = 115$.

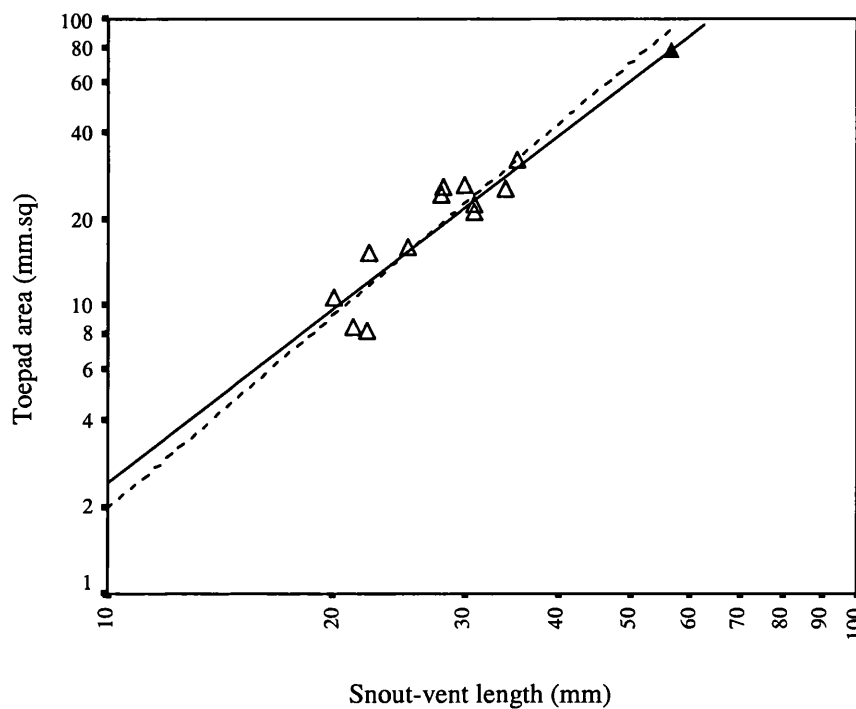


Figure 5.7: Log:log plot of toe pad area vs. linear dimensions in juvenile (\triangle) and adult (\blacktriangle) *H. crepitans*.

Correlative statistics for: Juveniles $r = 0.89$, $y = 2.22x - 1.92$, $t = 6.41$, $p = 0.0001$, $n = 12$. Total population ____ $r = 0.94$, $y = 2.08x - 1.72$, $t = 9.38$, $p = 0.0001$, $n = 13$.

With the morphometric trends in area and mass increase with growth under consideration, predictions about sticking abilities in both juvenile and adult frogs of these two medium sized species can now be examined in relation to the limitations that might be imposed. The fact that the total area of the adhesive pads in contact with a surface is not increasing at a sufficient rate to match the correspondent weight increase in either species means that the area-dependent adhesive mechanism in effect (**Chapter 2**), may be expected to be significantly detrimentally affected with growth to adult-hood. Within juvenile *H. crepitans* there is no statistically significant difference between the rate of increase in toe pad area and the rate of weight increase in the same period of growth, suggesting that there may be an ability within this particular cohort to maintain adhesive abilities to around a similar level. This may be the case in young *H. geographica* also but due to insufficient data the effect of growth within the juvenile cohort in this species is more difficult to predict.

5.3.2. Size effects on adhesion

Hyla geographica

Unusually when considering trends shown in other similar species, adult *H. geographica* have a larger average angle of detachment ($152.62^\circ \pm 4.86$, $n = 13$) than is typical in the juvenile frogs ($127.55^\circ \pm 3.24$, $n = 21$). Unequal variances ($F_{20,12} = 2.87$), due to a high variability in the angles seen in the juvenile frogs, make comparisons between these mean angles problematic, but carrying out a Mann-Whitney U test to compare medians confirms that angles of detachment in adults and juveniles are significantly different to one another ($U_{20,12} = 18$, $p < 0.05$).

There is, in fact, a significant positive correlation between the size of the frog and the angle of detachment from the surface (**Figure 5.8**). This is very unusual and it may be advisable to exercise caution in interpreting these anomalous results, taking into consideration that the juveniles, with their high laboratory mortality rate, may well be performing at a level below their natural capabilities.

Adhesive forces, calculated as discussed in **Chapter 2**, were also plotted against linear dimensions to determine the effect of growth upon adhesive abilities (**Figure 5.9**). Considering adult and juvenile data together, adhesive ability increases as $(SVL)^{2.90}$ on a log:log plot. This line of best fit (**Figure 5.9**) has a slope significantly higher than the predicted value of 2 ($t = 6.92$, $p < 0.01$, 32 df) that would occur should adhesion increase directly in proportion to an increase in the area in contact with the surface. The rate of increase in weight across the two age classes is significantly less than the increase in adhesive force ($t = 2.80$, $p < 0.01$, 64 d.f), meaning that adhesive forces are more than able to keep pace with increasing mass. This is achieved partly by better than expected increases in adhesive ability and partly by a lower than expected increase in mass. These trends are also supported when considering the juvenile data in isolation (**Figure 5.9**) since adhesive forces increase as $(SVL)^{2.43}$, not statistically significant to the rate of increase in weight in the juvenile cohort (**Figure 5.5**); $t = 0.45$, N.S., 38 d.f.). This suggests that for the juveniles alone adhesive forces are, in fact, able to keep pace with the increase in weight involved in growth and development, and that this is the case in spite of 'normal' rates of weight gain by the young frogs. In general the trends in the data examined here suggest that adhesive ability in this medium sized hylid does scale at a greater rate than would be predicted considering the mechanism of adhesion that is utilised by tree frogs.

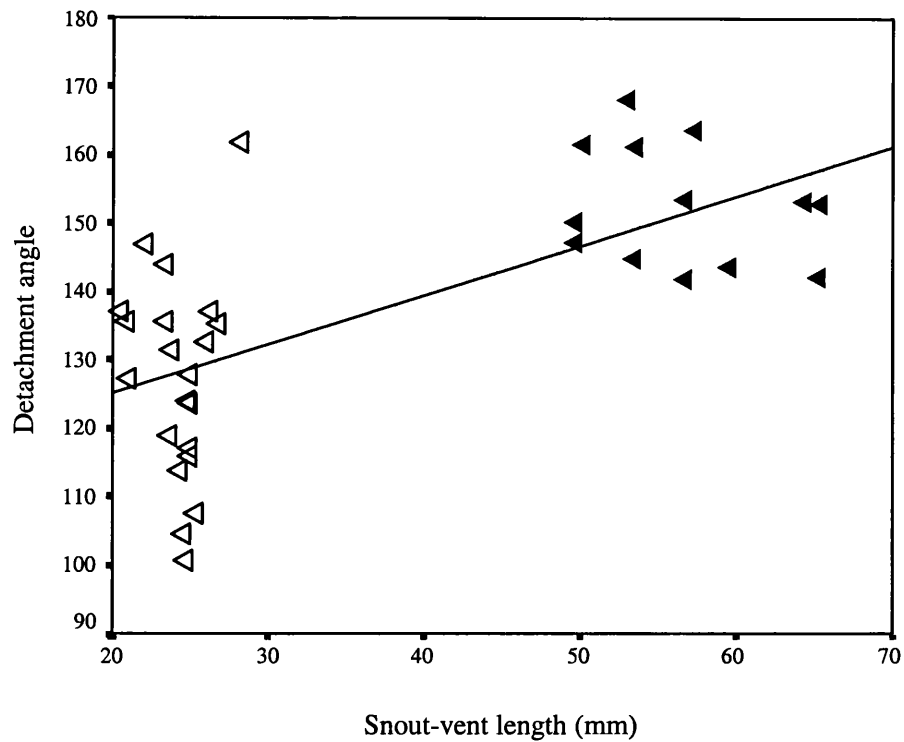


Figure 5.8: Angle of last contact in juvenile (\triangle) and adult (\blacktriangle) *H. geographica* vs. SVL. Correlative statistics for: total population: $r = 0.66$, $y = 0.72x + 110.89$, $t = 5.00$, $p < 0.01$, $n = 34$.

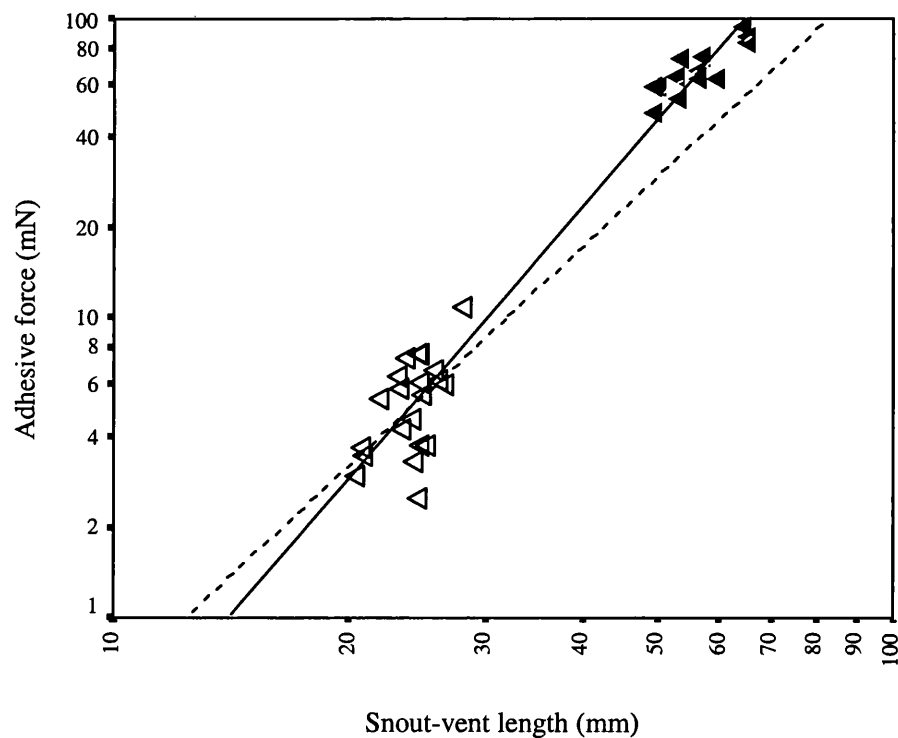


Figure 5.9: Log:log plot of adhesive force vs. linear dimensions in juvenile (\triangle) and adult (\blacktriangle) *H. geographica*. Correlative statistics for: Juveniles $r = 0.53$, $y = 2.43x - 2.65$, $t = 2.755$, $p < 0.01$, $n = 21$. ; Total population ____ $r = 0.97$, $y = 2.90x - 3.30$, $t = 23.13$, $p < 0.001$, $n = 34$.

Hyla crepitans

If the average angles of detachment within the age groups are examined for this species, there is no detrimental effect of increasing size within the juveniles considered alone. Indeed larger juveniles are often adhering to higher angles

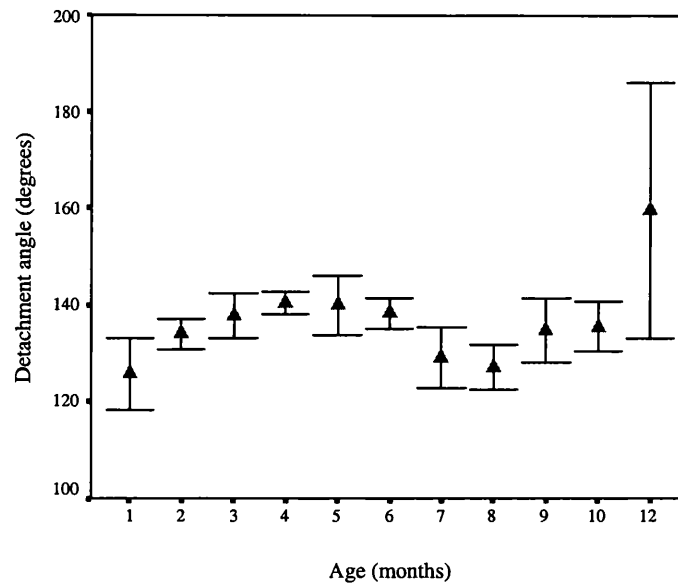


Figure 5.10: Average angles of detachment in juvenile *Hyla crepitans*. (Error bars for 95% c.i.)

than new metamorphs. The correlative relationship is weak ($r = 0.22$, $t = 2.26$, $p = 0.03$, 102 d.f.) and, if the data for juveniles are broken down into monthly age brackets (**Figure 5.10**) it can be seen that there are few differences between the first ten cohorts with a n increase in the yearling frogs. There is a higher percentage of 180° angles recorded, with full rotations making up 2.33% of the detachments recorded in comparison to 0.01% in the whole of the previous ten months. The effects of size can be seen to be significantly detrimental on frogs' sticking abilities when the angles recorded within the adults are also examined (**Figure 5.11**). The average angle of detachment in juveniles is 135.00 ± 0.94 ($n = 103$); in adults, 109.53 ± 3.49 ($n = 12$). A Levene's test ($F_{102,11} = 2.12$, $p = 0.126$) shows that the two figures are sampled from populations with similar variances and a subsequent t-test shows that there is a significant difference in the average angle of detachment in two age classes ($t = 8.48$, $p = 0.001$, 113 d.f.).

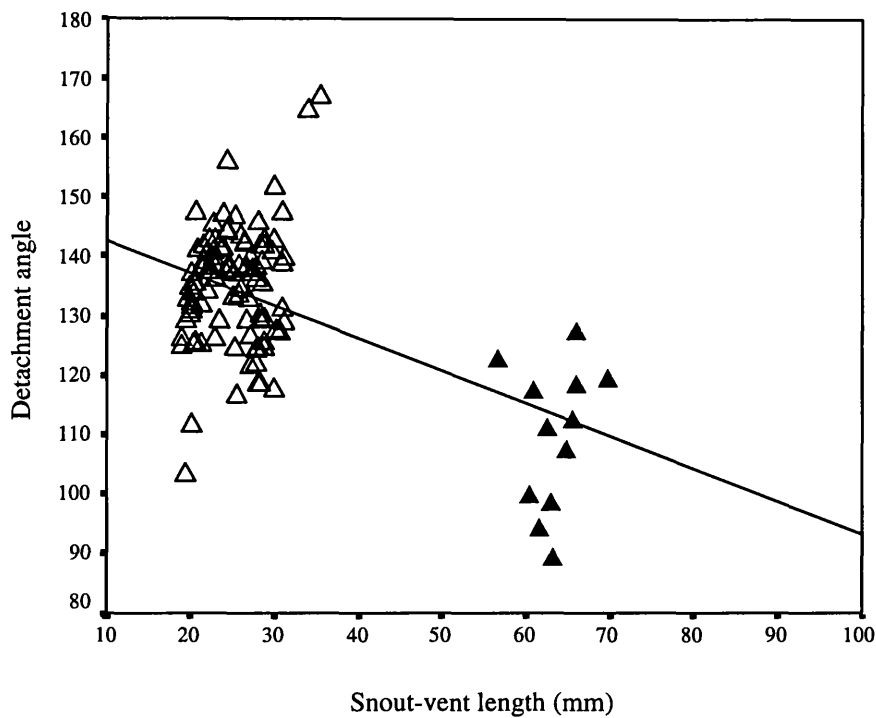


Figure 5.11: Angle of last contact in juvenile (Δ) and adult (\blacktriangle) *H. crepitans* vs. SVL. Correlative statistics: $r = 0.54$, $y = 148.23 - 0.55x$, $t = -6.88$, $n = 115$.

Translating these maximum detachment angles to adhesive forces, as described in **Chapter 2**, demonstrates the effect of size on sticking ability in these frogs. Adhesive forces can be seen to be increasing steadily with size both between the two age classes in this species (**Figure 5.12**) and within the juveniles alone. The increase in adhesive force production with increasing linear dimensions in the juveniles is occurring at a greater rate than the expected slope of two; ($t = 5.91$, $p < 0.01$, 101 d.f.). Across the whole population (**Figure 5.12 a**) the increase in adhesive force production scales as $(SVL)^{2.06}$, at a rate no different to the linear dimension squared ($t = 0.75$, N.S. 113 d.f.). This is surprising, as in other species the addition of adults to the data set has only a small effect on the eventual slope of the line. In this species, the addition of the adult data set changes the slope of the line from 2.71 to 2.06 (**Figure 5.12 a**), with the difference between these slopes being highly significant ($t = 4.51$, $p < 0.01$, 214 d.f.).

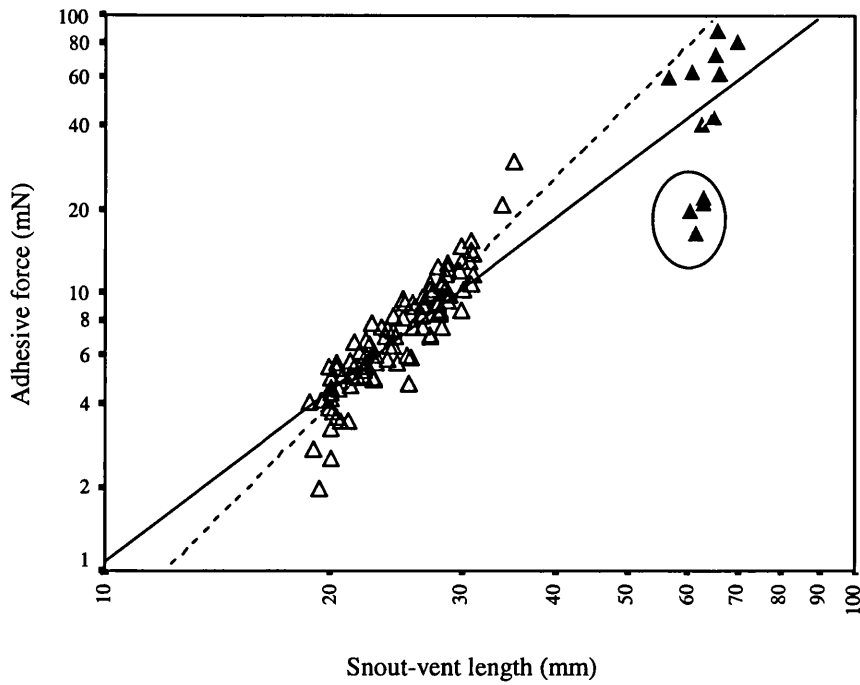


Figure 5.12a: Log:log plot of adhesive force vs. linear dimensions in juvenile (\triangle) and adult (\blacktriangle) *Hyla crepitans*. Correlative statistics for: Juveniles $r = 0.91$, $y = 2.71x - 2.92$, $T = 22.43$, $n = 103$; Total population (with encircled outliers) ____ $r = 0.93$, $y = 2.06x - 2.02$, $T = 26.17$, $n = 115$.

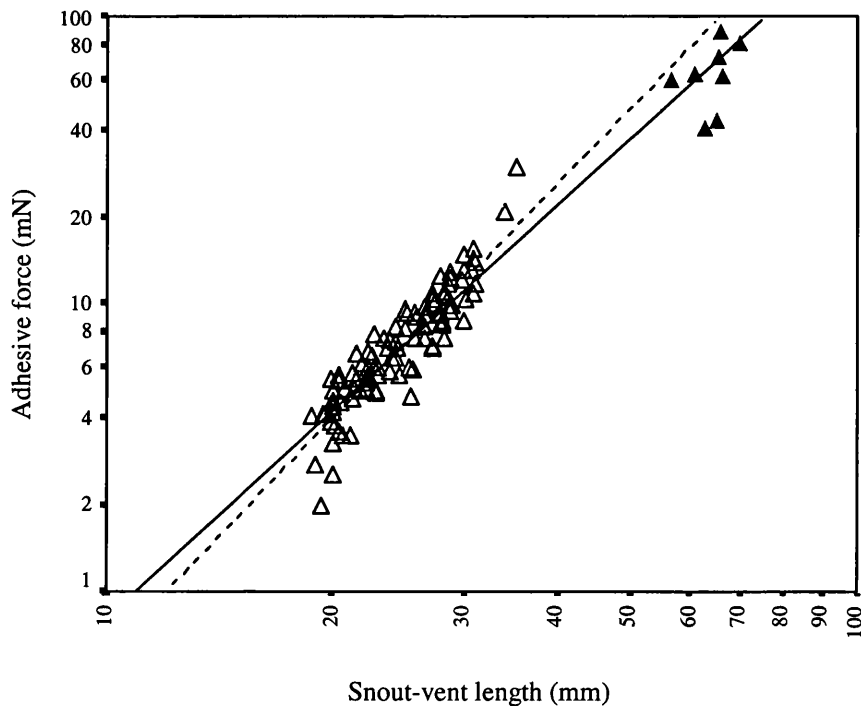


Figure 5.12b: Log:log plot of adhesive force vs. linear dimensions in juvenile (\triangle) and adult (\blacktriangle) *Hyla crepitans* with outliers removed. Correlative statistics for: Juveniles $r = 0.91$, $y = 2.71x - 2.92$, $t = 22.43$, $n = 103$; Total population ____ $r = 0.96$, $y = 2.38x - 2.47$, $t = 36.12$, $n = 111$.

The spread in the adult data is wider than seen in other species, being particularly influenced by a group of four outlying adult male frogs that consistently produced detachment angles below 90 degrees (**Figure 5.12 a**). The removal of these four ‘outliers’ has a significant effect on the strength of the correlation between the two variables, increasing the r -value from 0.93 to 0.96 and on the resulting relationship between adhesive force and linear dimensions as shown in **Figure 5.12 b**. The difference between the ‘new’ slope and the slope of the line calculated using juvenile data alone is significantly reduced ($t = 2.29$, $p = 0.05$, 210 d.f.) meaning that the addition of the adult data has, as expected, only a slight ‘damping’ effect on the rate of increase in adhesive force production with growth. The resulting relationship between adhesive force and the linear dimension, with force increasing as $(SVL)^{2.38}$, is significantly greater than expected from the actual toe pad area increase ($t = 5.29$, $p < 0.01$, 120 d.f.).

Statistical analyses of the increase in adhesive force production with increasing linear dimensions across the age classes will refer to the relationship seen in **Figure 5.12 b** as being more representative of the trends seen for this species. It seems likely then that the trend towards a greater than expected increase in adhesive force production with growth seen in *H. geographica* is supported by evidence in the larger *H. crepitans*. The extent to which adhesive force increases at a greater rate than expected is lower in *H. crepitans* than in *H. geographica* (Difference between species; $t = 3.52$, $p < 0.01$, 141 d.f.).

The lower degree of discrepancy between the observed and expected increase in weight seen in *H. crepitans* may account for the fact that this species is the first in which the increase in adhesive force production is not sufficient to match the weight

increase across the total period of growth from juvenile to adult ($t = 4.02$, $p < 0.01$, 218 d.f.), thus detrimentally affecting the maximum angle of stick (**Figure 5.11**).

Within the juvenile age class alone, mass increase is scaling at a significantly lower rate than expected and at a slightly lesser rate than seen across the population as a whole. This rate of weight increase is low enough for the increased rate of adhesive force production to cope with ($t = 1.33$, N.S. 202 d.f.) and within the juvenile cohorts alone the maximum angle of stick does not decline with increasing size. It is of some interest that the lower rate of weight increase in juveniles is not significantly different from the increase in toe pad area ($t = 0.80$, N.S., 210 d.f.) with the latter parameter increasing at a rate that is not significantly different to that expected from isometric predictions. Even though adhesive forces are not able to match weight increase between the age classes in this species adhesive force increases in the population as a whole and within the juvenile frogs alone at a rate greater than expected from predictions that these forces should scale with toe pad area.

Medium species

When frogs from both species are considered together, adhesive forces scale at a greater rate than can be explained by the effect of toe pad area in contact with a surface. By removing the effect that area has on the adhesive forces being produced, the adhesive force per unit toe pad area in the two species increases with size* (**Figure 5.13**). This leads to the speculation that there may be some element of

* These trends are present within both species when considered alone but are not statistically significant; (within species correlations, force per mm^2 vs. SVL: *H. geographica*, $r = 0.84$, $p = 0.36$, N.S. $n = 4$; *H. crepitans*: $r = 0.54$, $p = 0.06$, $t = 2.11$, $n = 13$).

change, either within the adhesive mechanism and/or at the level of toe pad structure, that is producing the increased efficiency of the adhesive system in larger frogs.

Aspects of the adhesive mechanism that are most readily changeable to allow increased adhesive abilities were identified in **Chapter 2**; physico-chemical properties of the mucosal layer and changes in the structure of the pad that may facilitate a decrease in the height of the fluid layer beneath the pad being two of the likeliest ways in which the frogs may be able to increase their adhesive abilities with increasing size. The performance of adult *H. crepitans* on different substrates suggests that adhesive ability in this species is likely to be detrimentally affected on surfaces with low surface energies, i.e. those on which the spreading tendencies of a fluid are likely to be impaired (**Figure 5.14**). This may suggest that changes in the mechanism that are suggested by the marginally non-significant trend towards a greater efficiency of toe pads in adult frogs in comparison to juveniles are not being implemented on a short-term basis.

Evidence from smaller species is that aspects of adhesion may be correlated with changes in the structure of the toe pad with growth and it is perhaps instinctive that if the function for which these specialised toe pads have evolved is to allow tree frogs a greater sticking ability then changes in the efficiency of the adhesive system are likely to be reflected in changes in the structure of the toe pad. S.E.M. studies were undertaken to determine whether this might be the case.

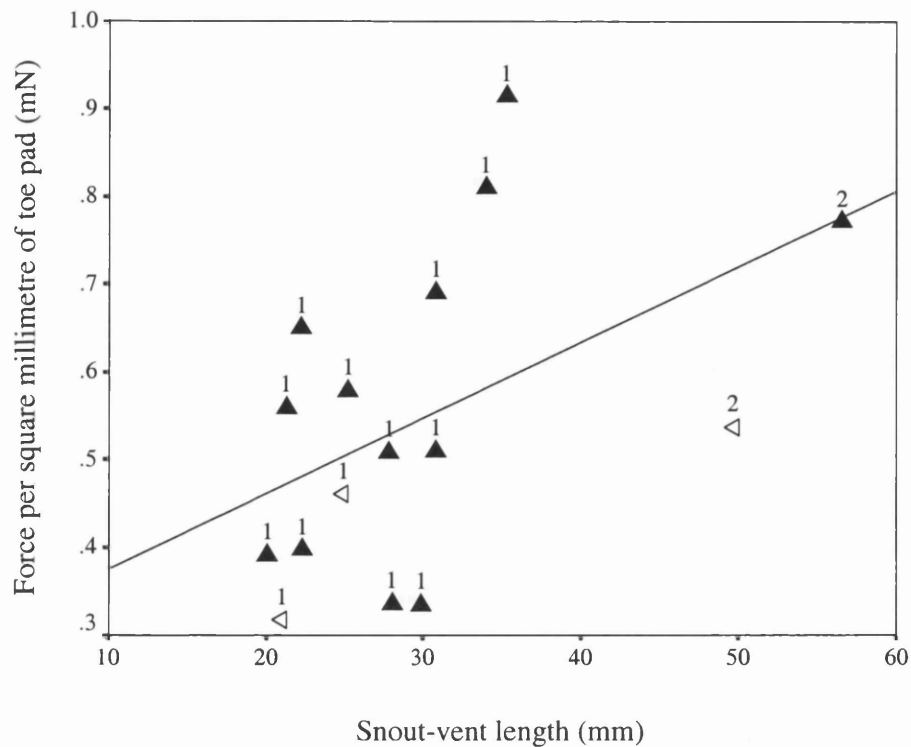


Figure 5.13: Adhesive force per mm² of toe pad vs. increasing linear dimensions in juvenile (1) and adult (2) frogs belonging to medium-sized species of Hyliid: *H. geographica* (\triangle); *H. crepitans* (\blacktriangle).

Correlative statistics, all frogs; $r = 0.49$, $y = 0.01x + 0.29$, $t = 2.10$, $p = 0.05$, $n = 16$.

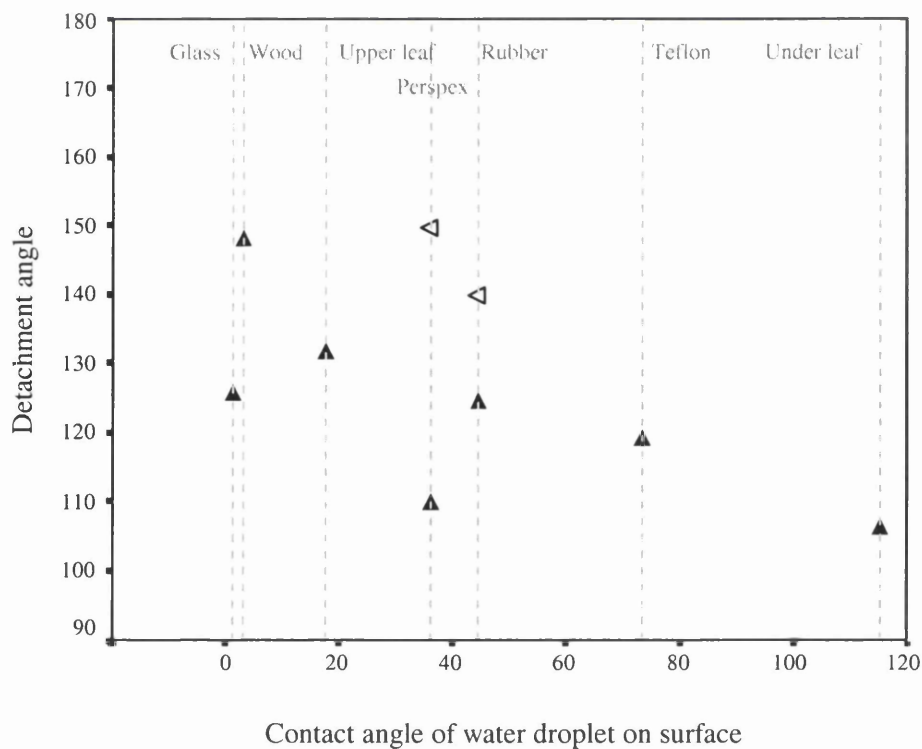


Figure 5.14: Detachment angles in adult frogs belonging to two medium-sized species of Hyliid on seven substrates of differing wettability (as defined by the contact angle of water droplet): *H. geographica* (\triangle); *H. crepitans* (\blacktriangle). Correlative statistics; All frogs, $r = 0.59$, $t = -1.97$, $p = 0.09$, N.S. $n = 9$. *H. crepitans*, $r = 0.74$, $t = -2.74$, $p = 0.06$, $n = 7$.

5.3.3. Toe pad morphology

Hyla geographica

As in the other hylid species that have been studied here, toe pad cells in *H. geographica* are columnar in nature with striated sides and hexagonal apices (**Figure 5.15 c**). Cells in juveniles and adults are structurally very similar to one another with a tendency towards a more defined surface architecture in the juveniles (**Figure 5.15 b**) though there is considerable variation in this.

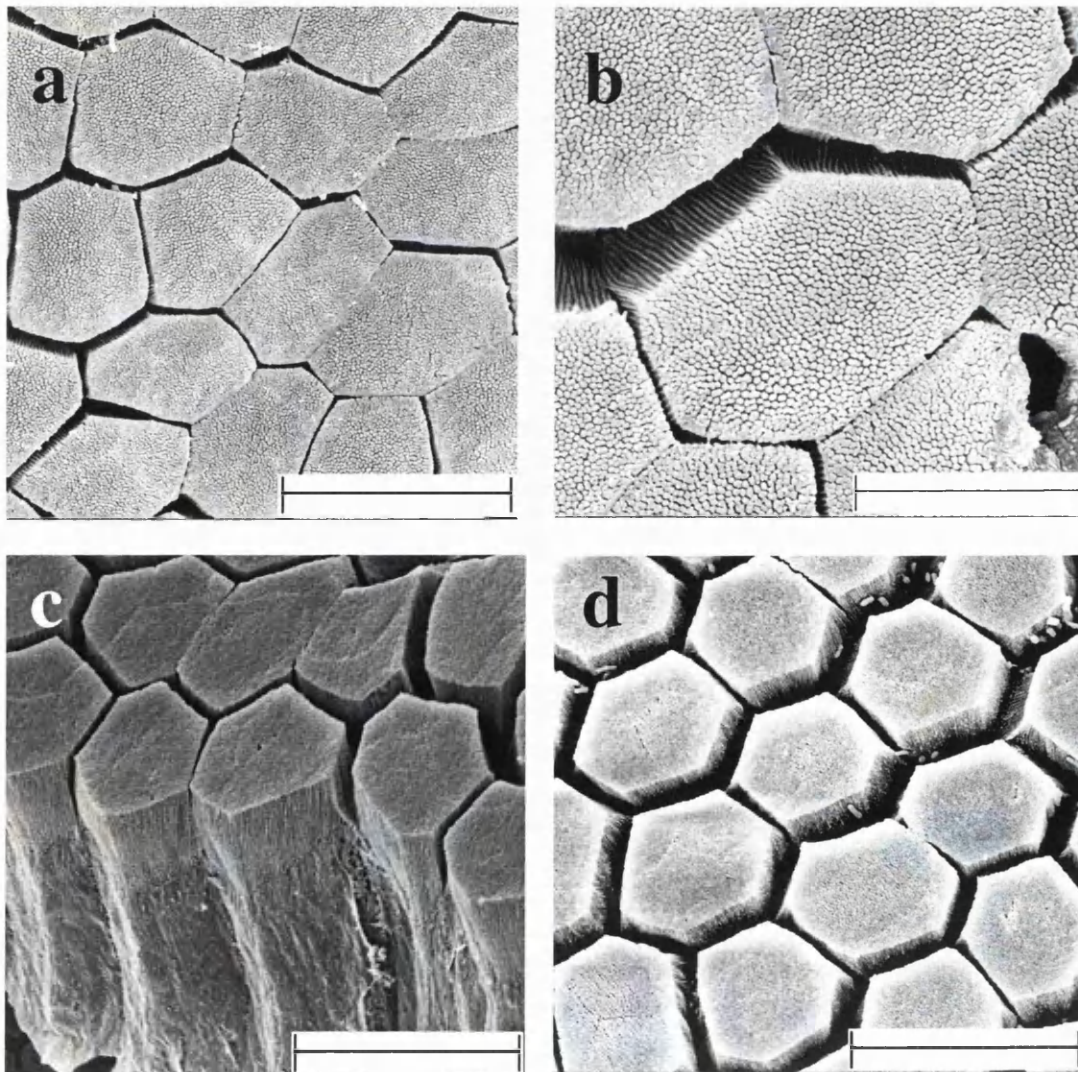


Figure 5.15: S.E.M. images of *H. geographica* toe pad cells (a) Juvenile 2 (23.3 mm) Front 3, Scale bar = 25 μm (b) Juvenile 2 (23.3 mm) Front 3, Scale bar = 12.50 μm (c) Adult (49.7 mm) Front 4, Scale bar = 25 μm (d) Adult (49.7 mm) Back 5, Scale bar = 25 μm .

There is some evidence that cell size is consistently different in the two age classes, with average cell areas for juveniles of $149.76 \mu\text{m}^2 \pm 2.52$ ($n = 272$) and in adults of 119.91 ± 2.68 ($n = 80$). Differences in variances (Levene's test statistic: $F = 23.63$, 350 d.f.) mean that non-parametric tests are necessary, and a Mann-Whitney U test performed on the data ($U_{272,80} = 5904$, $p < 0.01$) confirms the observation that the median cell size is significantly different in the two age classes.

As may be expected, one consequence of the observed cell size decrease with increasing linear dimensions, is that there is an increase in cell densities in adult frogs; juveniles have an average cell density on the toe pads of $6831.34 \text{ per mm}^2 \pm 320.41$ ($n = 33$) and adults $8538.05 \text{ per mm}^2 \pm 477.27$ ($n = 8$). The two age classes are significantly different from one another, $F_{32,7} = 1.86$, $t = 2.41$, $p < 0.05$, 39 d.f.

In both age classes, the width of the channels between the specialised columnar cells is highly variable across the toe pad, as can be seen in **Figure 5.15**. However the length of the channels is remarkably consistent, ranging from $101.06 - 132.69 \text{ mm/mm}^2$, independent of age class. There is no significant effect of size upon channel density ($r = 0.20$, $F = 1.56$, N.S., 37 d.f.) and no difference in average channel density between juveniles ($136.82 \text{ mm/mm}^2 \pm 3.76$) and adults ($145.56 \text{ mm/mm}^2 \pm 7.15$); Difference between means; $t = -1.10$, N.S. 37 d.f. This is somewhat surprising as dependent as channel length is on the total cell perimeter an increase in this would be expected with the observed increase in cell density.

Mucosal pores are Type II in the main, as defined by Green (1979) with the sides of the cells facing the pore openings being modified as compared to the normal striated cells. Examples of this type of mucosal pore are illustrated in **Figure 5.16 a** for juveniles and for adults in **Figure 5.16 c - f**. Rarely, simple Type I mucosal pores were found on the juvenile pads (**Figure 5.16 b**); these were never present in adults. In juveniles, pores are generally simple in structure; with rounded and elliptic openings onto the pad surface (**Figure 5.16 a - b**). Greater diversity in structure and levels of complexity are present in the adult mucosal pores, with three main types being seen. The commonest type has simply shaped pore openings (**Figure 5.16 c**) similar to those seen in juveniles but in most cases these are a good deal larger. The average area is $301.48 \mu\text{m}^2 \pm 39.57$ ($n = 8$) in adults as opposed to an average juvenile pore size of $55.12 \mu\text{m}^2 \pm 12.78$ ($n = 16$). The other two types of pore are more complex. Of these the commonest type opens into short grooves around 2-3 cells in length (**Figure 5.16 e**), the sides of the groove being defined as distinct from the mucosal channels by modifications to the framing cell walls. These are found most commonly at the proximal margin edge of the toe pad. Also found on some pads, more commonly in the central portion of the pad, were small pores opening into shallow depressions in the pad surface. These depressions are either circular (**Figure 5.16 d**) or highly convoluted (**Figure 5.16 f**), and were distinguished from the surrounding mucosal channels by deviations from the normal striated structures in the adjacent cell walls.

Mucosal pore numbers are low on juvenile toe pads, with pores scattered sparsely across the pad (**Figure 5.17 a**). Indeed, average mucosal pore counts for juveniles are far lower (15.25 ± 2.10 , $n = 24$) than for adults (186.83 ± 28.38 , $n = 8$). Given that adult toe pads are as much as ten times as big as the juvenile toe pads, this was not

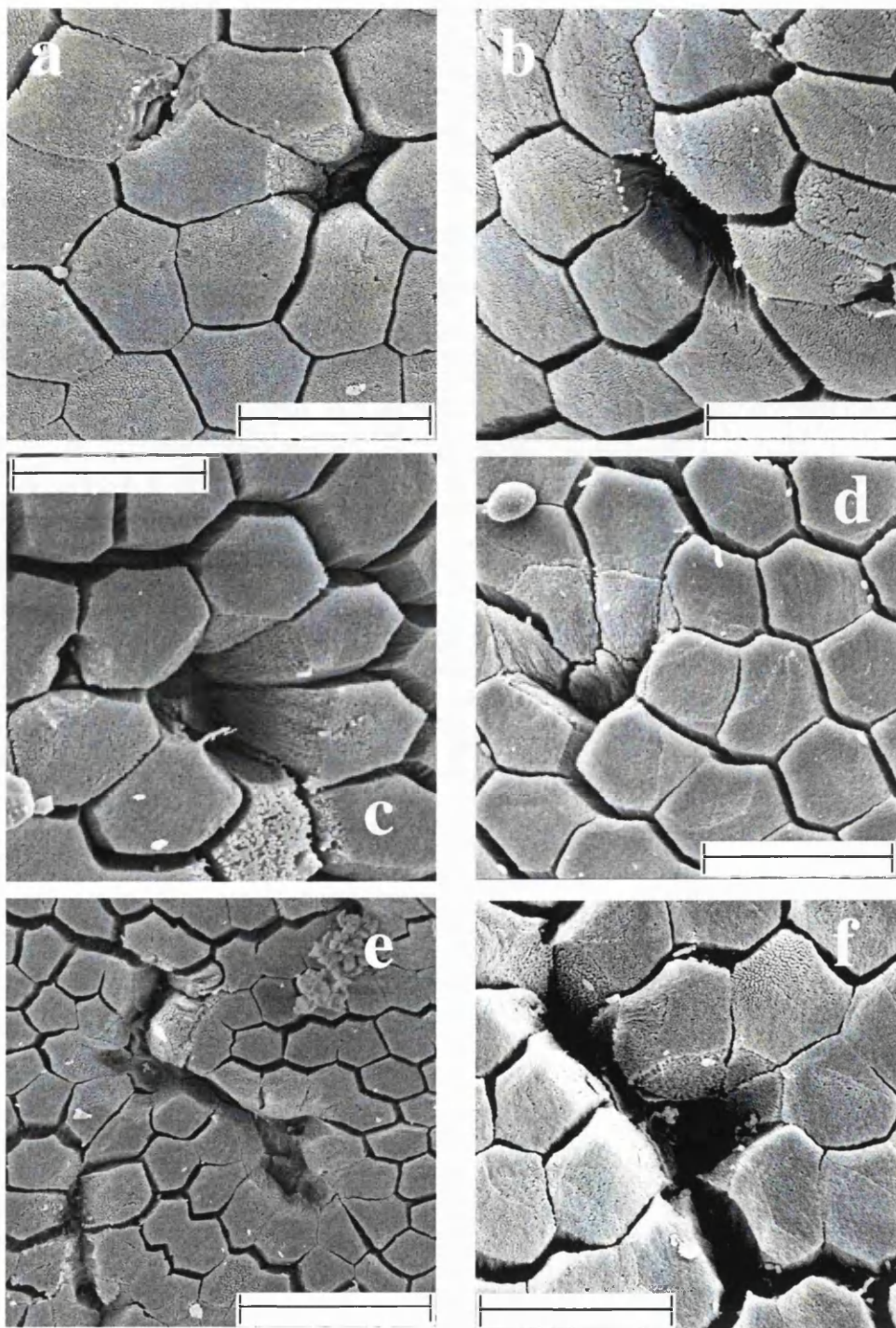


Figure 5.16. S.E.M. images of pores in *H. geographica* (a) Juvenile 3 (24.0 mm) Back 5, Scale bar = 25 μm (b) Juvenile 3 (24.0 mm) Back 5, Scale bar = 25 μm (c) Adult (49.7 mm) Front 2, Scale bar = 25 μm (d) Adult (49.7 mm) Front 3, Scale bar = 25 μm (e) Adult (49.7 mm) Front 1, Scale bar = 50 μm (f) Adult (49.7 mm) Back 3, Scale bar = 25 μm .

unexpected. By measuring toe pad areas and making pore counts on these same pads, mucosal pore density could be calculated for both juveniles and adults. Adult pore density, at 34.43 ± 6.89 ($n = 6$) per mm^2 , is significantly greater than that in juveniles, 20.60 ± 2.53 per mm^2 , $n = 15$ ($t = -2.37$, $p < 0.03$, 19 d.f.). It is important to remember that estimates of pore density obtained in this way do not take account of the fact that pore density is not uniform across the pad for either age-class. In juveniles the pores are found at the outer edges of the pad and pore density is lower in the central portion of the pad, whereas in adults the majority of the pores are centrally located (**Figure 5.17 a-b**).

A number of comparative changes in the macro-structural features of the toe pad in juveniles and adults can also be illustrated by examining **Figure 5.17**. In both adults (**Figure 5.17 b**) and juveniles (**Figure 5.17 a**) the pad area is elevated relative to the ventral surface of the toe, more pronounced in the front feet than in the back. In this species, the elevation of the toe pad is fairly shallow, this being particularly the case in the adult where the crown of the pad is almost flush with the rest of the toe.

For both age classes, the definition of the pad from the ventral surface of the toe is increased by the presence of a circumferal groove. The groove appears better defined in adults (**Figure 5.17 b**), due to the presence of a continual margin around the distal and lateral edges of the pad. The degree of development of this margin is variable in the juveniles, with some toes appearing almost emarginate (*sensu* McAllister and Channing, 1983) and others being better developed, but none with such a complete encircling ridge as that seen in the adults. The cells on these margins have varying levels of diversity in surface architecture, with the circumferal ridge in juveniles being smoother and more homogenous in nature and the dominant cell type having a

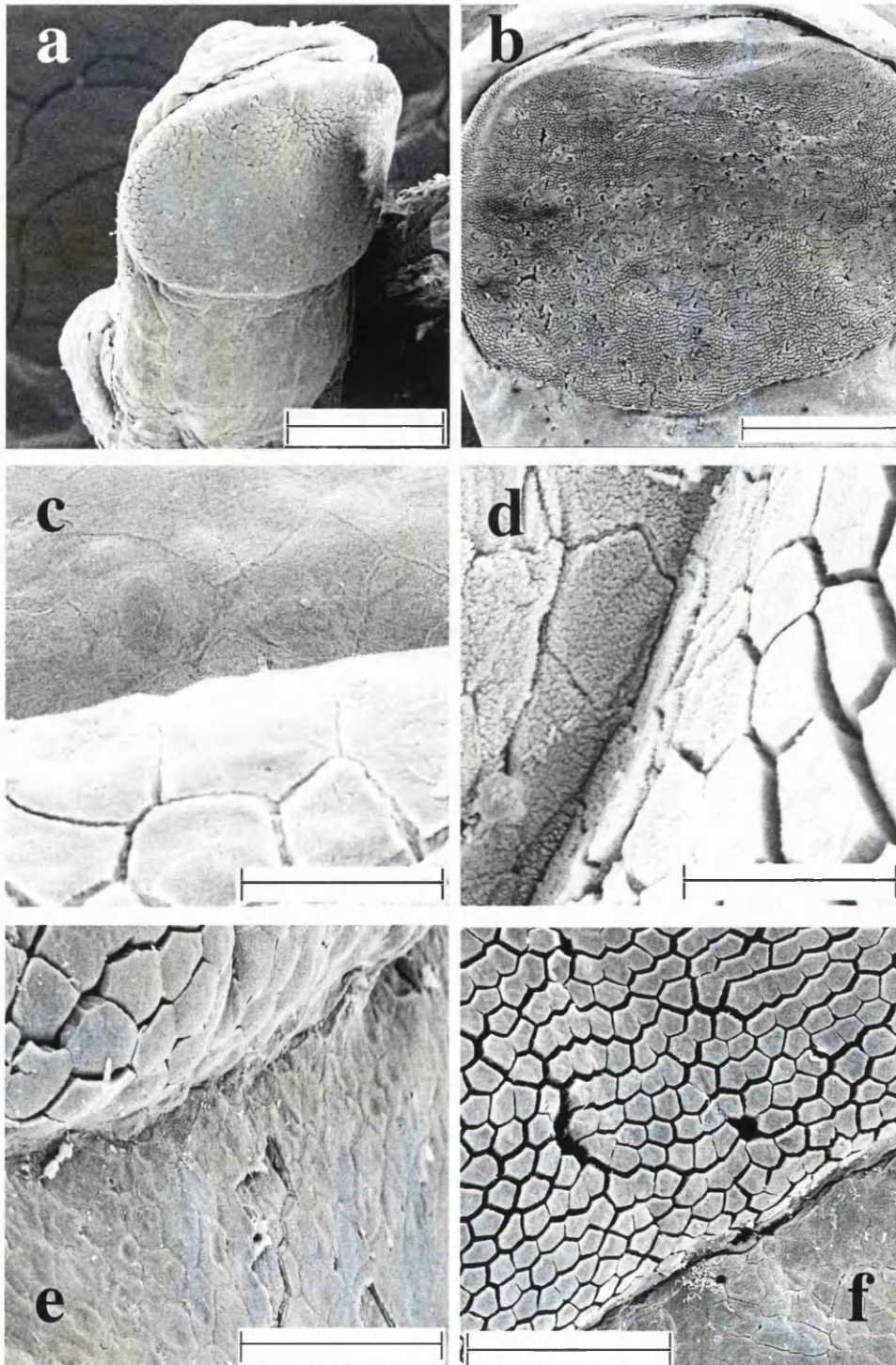


Figure 5.17: S.E.M. images of toe pads in *H. geographica* (a) Juvenile 3 (24.0 mm) Back 5, Scale bar = 300 μm (b) Adult (49.7 mm) Back 5, Scale bar = 625 μm (c) Juvenile 2 (23.3 mm) Front 4, Scale bar = 25 μm . (d) Adult (49.7 mm) Front 1, Scale bar = 25 μm . (e) Juvenile 1 (21.0 mm) Front 1, Scale bar = 50 μm (f) Adult (49.7 mm) Back 3, Scale bar = 100 μm .

convoluted surface, with indistinct, often raised cell borders (**Figure 5.17 c**). Although this surface type is also the prevalent one in the adult sample, there is some heterogeneity particularly on the inner wall of the ridge, where the cells come close to the edges of the pad in the trough of the circumferal groove (**Figure 5.17 d**). Here many cells have more villus-like spinulate structures on their surfaces and cell boundaries have become more defined and separated.

The proximal margin is defined by the transition of highly modified columnar cells characteristic of the toe pad to the relatively unmodified epidermal cells (Green, 1979). In adults the toe pad is separated from the ventral surface of the toe by a continuance of the circumferal groove (**Figure 5.17 e**), which has extended to entirely encircle the total area of specialised cells of the toe pad. Although the transitional area is obvious in juveniles due to differences in cell structure (**Figure 5.17 f**), the circumferal groove does not extend far enough to physically separate the pad from the ventral surface completely in any of the samples examined.

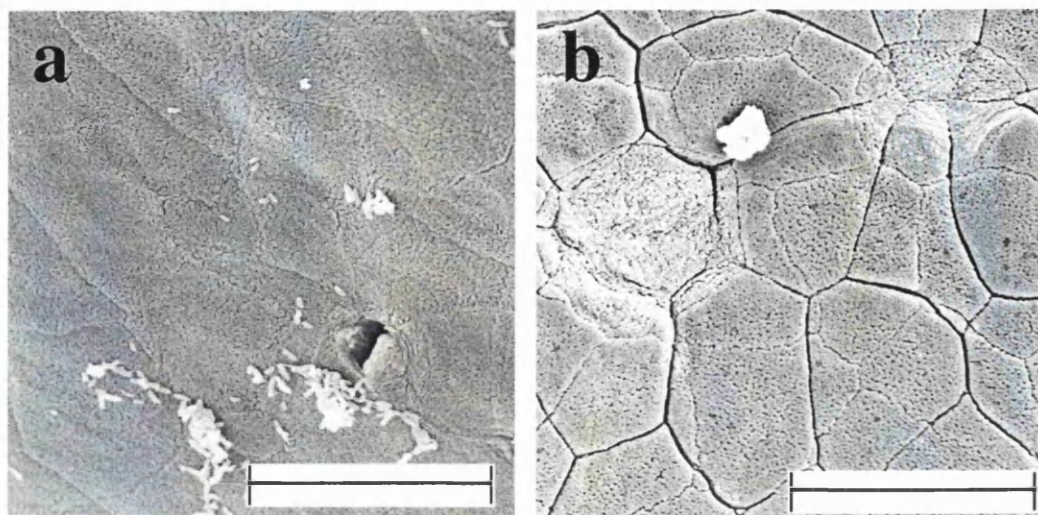


Figure 5.18: S.E.M. images of cells on proximal margin in *H.geographica* (a) Juvenile 3 (24.0 mm) Front 3 (b) Adult (49.7 mm) Back 3. Scale bars in images = 25 μ m.

In both juveniles and adults, cells below the margin are relatively large and irregular in shape compared to those on the toe pad proper (**Figure 5.18 a and b**). In juveniles, these cells have ill-defined boundaries and are structurally indistinct from ordinary squamous skin cells, though are smaller in size (**Figure 5.18 a**). In adults, the cells on this area immediately below the pad, while similar in area to those in the juveniles, are structurally distinct and more intermediary between ordinary skin cells and toe pad cells in appearance, being separated at their apical margins by narrow channels (**Figure 5.18 b**). Shallow pits at meeting cell margins are common in this region. In both age classes surface architecture of the cells is similar, with villus-like structures giving the cells a more roughly textured appearance than those found on the toe pad. This area is often also in contact with the surface when adhering under normal conditions (**Figure 2.1**)

Hyla crepitans

Toe pad cells are similar in structure to those seen in *H. geographica*, columnar in nature (**Figure 5.19 a**) with striated sides (**Figure 5.19 b**) and hexagonal apices (**Figure 5.20 a - f**). The apical areas adult frogs are larger than in juveniles; with average cell areas of $115.40 \mu\text{m}^2 \pm 3.03$ ($n = 78$) in comparison to $95.15 \mu\text{m}^2 \pm 2.19$ ($n = 162$) in juveniles, with the difference between the two age classes being statistically significant (Levene's $F_{77,163} = 0.315$, $t = -5.34$, $p < 0.001$, 238 d.f.).

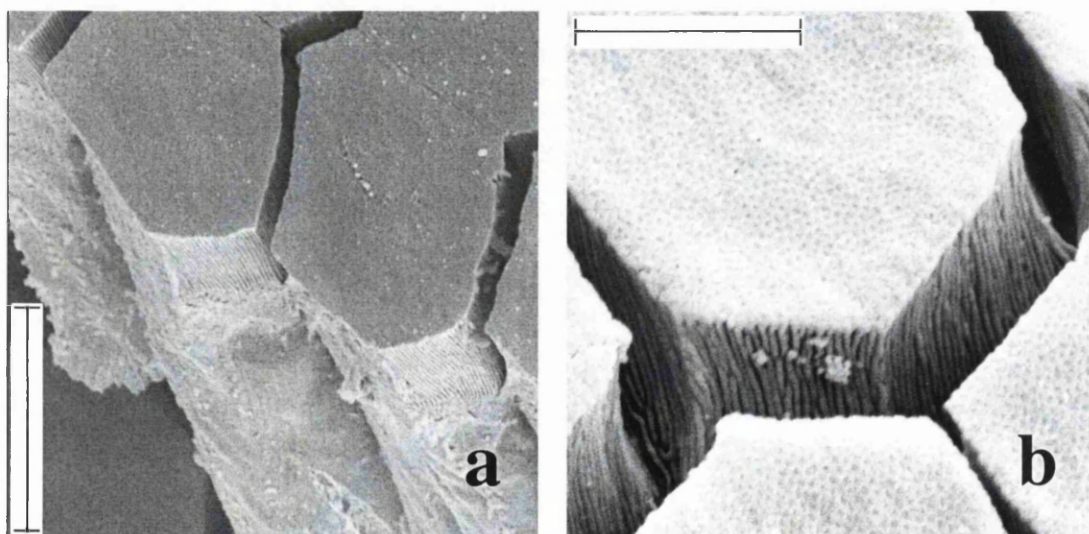


Figure 5.19: S.E.M. images of toe pad cells in *H. crepitans* (a) Juvenile (22.0 mm) Front 4, Scale bar = $12.5 \mu\text{m}$ (b) Adult (56.55 mm) Back 1, Scale bar = $6.25 \mu\text{m}$.

As a consequence of the fact that the cell size is increased, there is a tendency towards a decrease in cell density on the pads of the adult frog. Although the density in adult pads at $8992.24 \text{ per mm}^2 \pm 598.43$ ($n = 8$) is lower in value than that in the juvenile frogs, $11048.30 \text{ per mm}^2 \pm 777.62$ ($n = 17$) the densities are not statistically different to one another ($F_{16,7} = 0.92$, $t = 1.69$, $p = 0.168$, N.S. 23 d.f.) with this perhaps because of the high degree of variability seen in this parameter in both age classes.

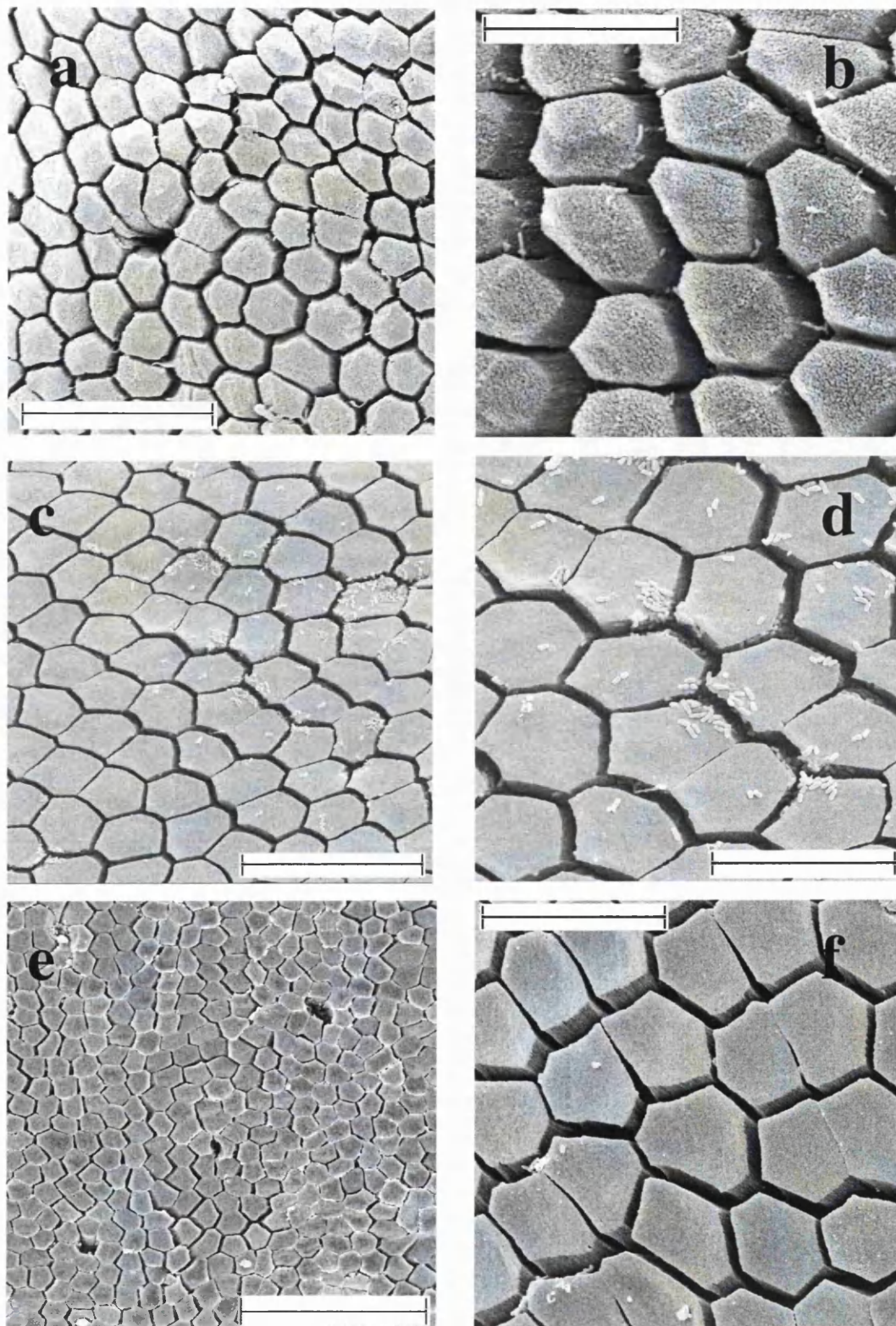


Figure 5.20: S.E.M. images of toe pad cells in *H. crepitans* (a) Juvenile (20 mm) Front 4, Scale bar = 50 μm (b) Juvenile (20 mm) Back 2, Scale bar = 25 μm . (c) Juvenile (22 mm) Front 4, Scale bar = 50 μm (d) Juvenile (22 mm) Back 2, Scale bar = 25 μm . (e) Adult (56.55 mm) Back 5, Scale bar = 100 μm (f) Adult (56.55 mm) Back 1, Scale bar = 25 μm .

The intercellular channel length, dependent as it is on the perimeter length of the cells, might also be expected to be affected by the increase in the size of the cells but, in fact, between juvenile and adults channel density is not statistically different. This is true in *H. geographica* also, indeed channel lengths measured in the smaller species fall within the range seen in *H. crepitans*, between 116.49 and 183.98 mm/mm². Average channel densities in juvenile *H. crepitans* have a value of 150.12 mm/mm² ± 4.70 (n = 17) and in adults is 131.80 mm/mm² ± 6.04 (n = 8) with no statistical difference between the two age classes: $F_{16,7} = 0.20$, $t = 0.21$, $p = 0.84$, N.S. 23 d.f. In contrast to channel length, channel width across the toe pads is highly variable (**Figure 5.20 a – f**) across a single pad.

Mucosal pores, as seen in these images (**Figure 5.20 a and e**), are all Type II pores, with the vertical sides of the cells forming the pore openings being modified from the normal striated patterns seen. In this species, the way in which the cell sculpturing forming the luminal walls is modified creates two distinct subtypes of Type II pores: those with smooth (**Figure 5.21 a and c**) and those with rough (**Figure 5.21 d**) sides.

In juveniles pores are very small and not easily detectable, a fact which is perhaps responsible for the low cell densities recorded within the juvenile frogs, with average pad densities of 34.56 pores/mm² ± 21.72 (n = 8). Mucosal pores are sparsely scattered across the pad surface (**Figure 5.23 a**), with a tendency for larger and more distinct pores on the proximal margin edge of the pads (**Figure 5.25 a and b**). The commonest type of pore seen on juvenile pads has a simple stomata-like structure, framed by two cell edges (**Figure 5.21 a**) with a typical pore opening area of around 20 μm². The cell walls that surround the lumen of the pore are smooth, the normal striations seen in the specialised columnar cells elsewhere on the pad being absent.

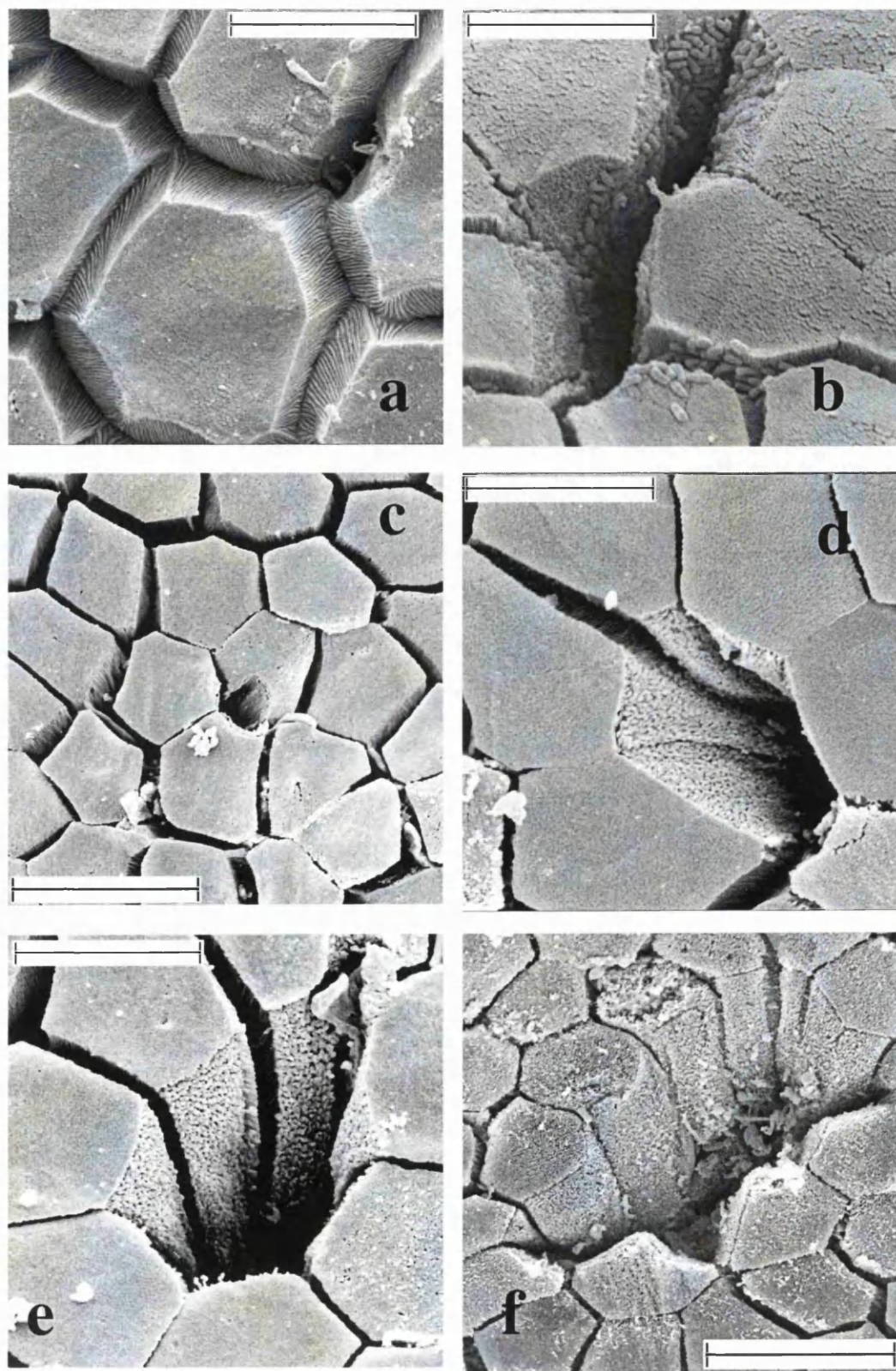


Figure 5.21: S.E.M. images of pores in *H. crepitans* (a) Juvenile (22 mm) Back 3, Scale bar = 12.50 μm (b) Juvenile (20 mm) Front 1, Scale bar = 12.50 μm (c) Adult (56.55 mm) Back 5, Scale bar = 25 μm (d) Adult (56.55 mm) Back 1, Scale bar = 12.50 μm (e) Adult (56.55 mm) Back 3, Scale bar = 12.50 μm (f) Adult (56.55 mm) Back 5, Scale bar = 25 μm .

A number of simply shaped pore openings are also seen, bordered by four to six cells in the main (**Figure 5.25 a**), and are lined by cells with roughened sides. These pores are not significantly different in structure to the simple pores seen in adult frogs. In one instance, on the proximal margin of the inner back toe of the smaller juvenile (**Figure 5.21 b**, **Figure 5.25 b**), these simple pore openings combined in a larger 'slit', common in adults, formed by adjacent polygonal shapes and bordered by nine cells with modified vertical sides.

Comparing the diversity of pore structure seen in adult *H. crepitans* with those seen in adults of its smaller relative, *H. geographica*, there are fewer types evident. A number of the small stomatal type of pore seen in juveniles are still present on adult pads (**Figure 5.21 c**) though the incidence of this type of pore is less prevalent than on juvenile pads. The majority of pores are again of the simple type with geometrical pore shapes determined by the cell number framing the opening, hexagonal (**Figure 5.21 d**) and heptagonal (**Figure 5.21 e**) being the most prevalent types of pore seen. These are sparsely distributed across the central area of the pad, with typical total pore densities of $9.44 \text{ per mm}^2 \pm 3.78$ ($n = 6$). This value is significantly reduced even in comparison to the low densities recorded from the juvenile frogs; $F_{7,5} = 10.35$, $U_{7,5} = 2.00$, $p = 0.004$. It may well be that the values derived from the adult specimen are an underestimate due to difficulties in detecting the pores which, with average sizes of $167.38 \mu\text{m}^2 (\pm 20.04, n = 17)$, are a third of the size of typical pores seen in adult *H. geographica*. At the proximal edge the simple pores become more elongate slits formed by between two and five polygonal shaped pore openings framed by nine to twelve cells (**Figure 5.21 f**).

Changes in macroscopic elements of the toe pad structure in this species can be seen in **Figure 5.22 a – d**. The pad area, as in most species, is elevated relative to the ventral surface of the toe. There is a flattening in the elevation of the pad with age (**Figure 5.22 b and d**). This feature is seen in *H. geographica* also and may well be of significance to the sticking ability of the frogs, perhaps allowing an increased and even spread of mucus below the pad in larger frogs.

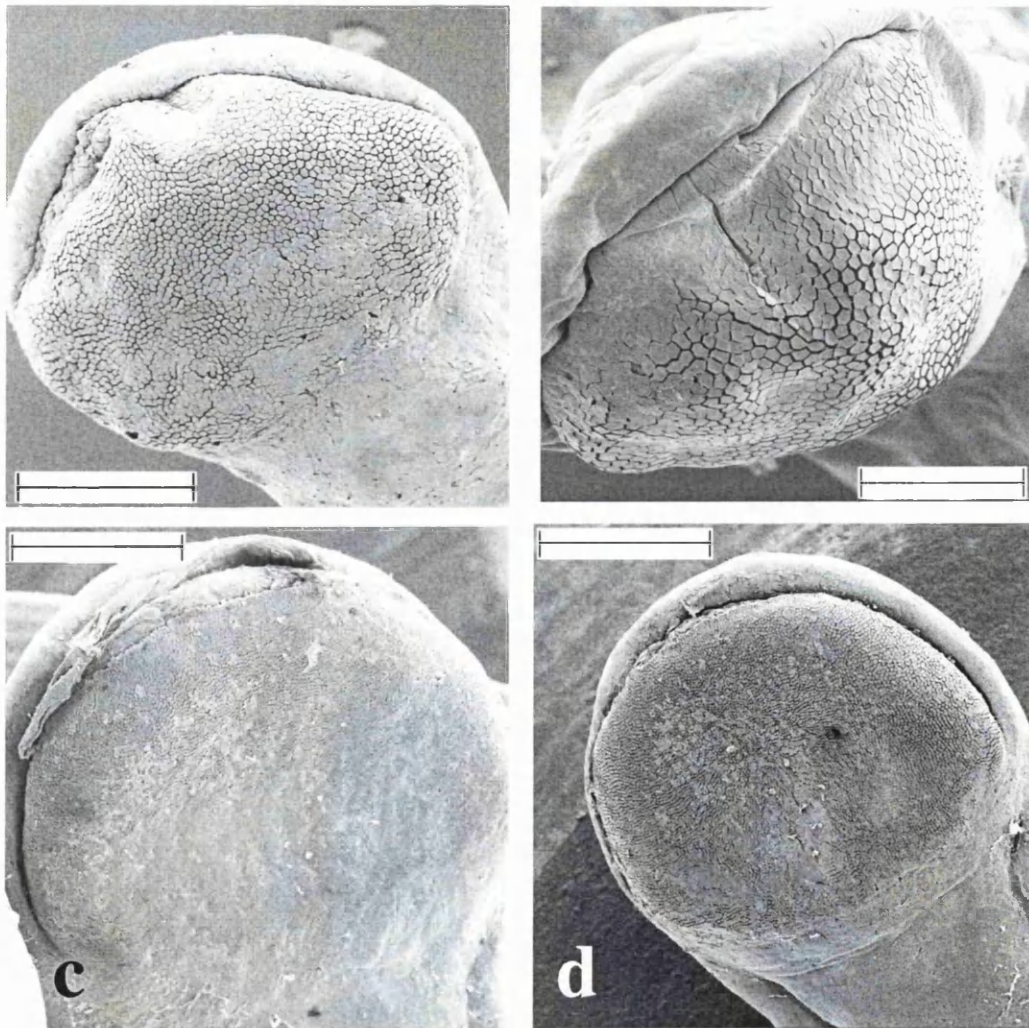


Figure 5.22: S.E.M. images of toe pads in *H. crepitans* (a) Juvenile (20 mm) Front 4, Scale bar = 300 μm (b) Juvenile (22 mm) Back 4, Scale bar = 150 μm . (c) Adult (56.55 mm) Front 1, Scale bar = 625 μm (d) Adult (56.55 mm) Back 1, Scale bar = 625 μm .

Again, as seen in *H. geographica*, there is a physical separation of the pad area from the unspecialised ventral surface of the toe at the distal edge through the presence of a circumferal groove. There is some evidence that there is an increased definition of this groove in adults in comparison to juvenile frogs (**Figure 5.22, Figure 5.24 a and b**) though the extent to which the groove encircles the pad is similar in both age classes. The margin distal to this groove has epithelial cells that vary in the definition of their surface architecture, with intercellular margins being less distinct in juveniles. Cells on this margin in adult frogs (**Figure 5.23**) have highly convoluted surface architecture with rolled cell margins.

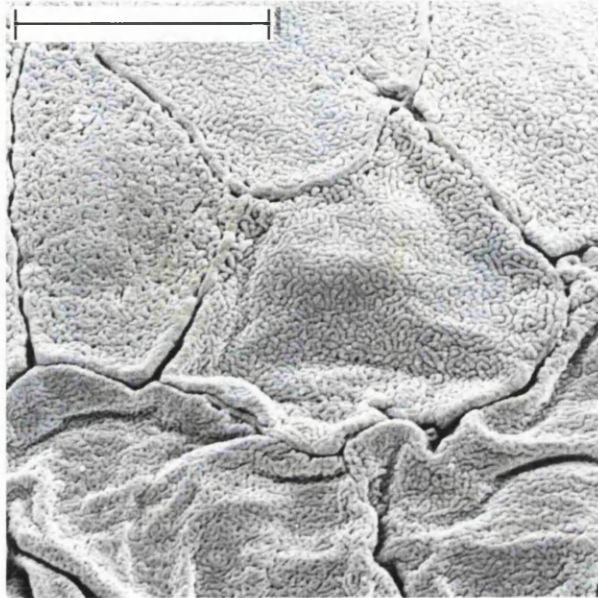


Figure 5.23: S.E.M. images of circumferal margin cells in adult *H. crepitans*. Scale bar = 12.5 μm

Cells with a very different surface architecture are also seen at the proximal margin of the pad (**Figure 5.25 d**). Here circular ‘knobs’ can be seen to cover the whole surface of the cell, with darker areas in the central portion of each circular plaque suggesting a degree of concavity at the tip of each projection. The cells are separated from one another by shallow grooves. In adult frogs, the demarcation of the pad from the ventral surface of the toe at the pad’s proximal margin is created by transition from columnar epithelium to this rougher more cuboidal cell type, rather than by the presence of any physical groove separating the two areas (**Figure 5.25 c**).

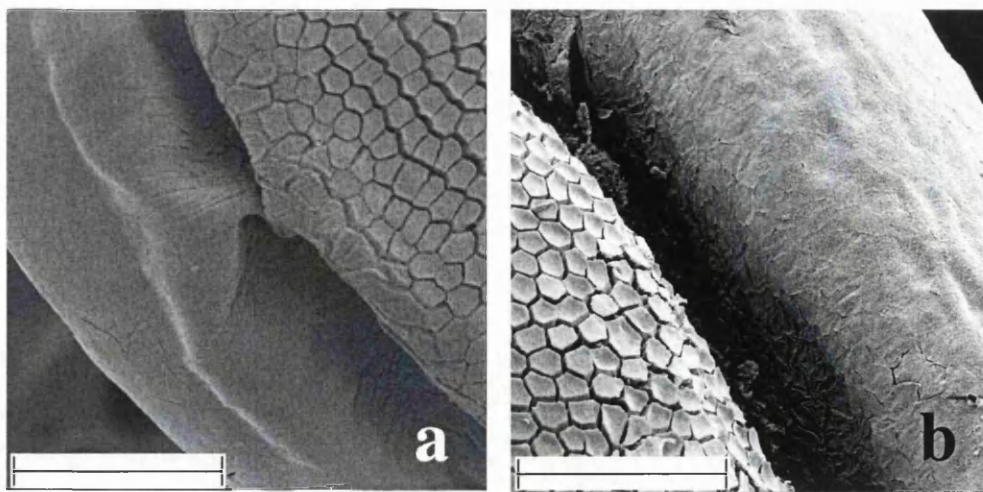


Figure 5.24: S.E.M. images of circumferential grooves and margins in *H. crepitans*. (a) Juvenile (22 mm) Front 3. (b) Adult (56.55mm) Back 2. Scale bars = 100 μm .

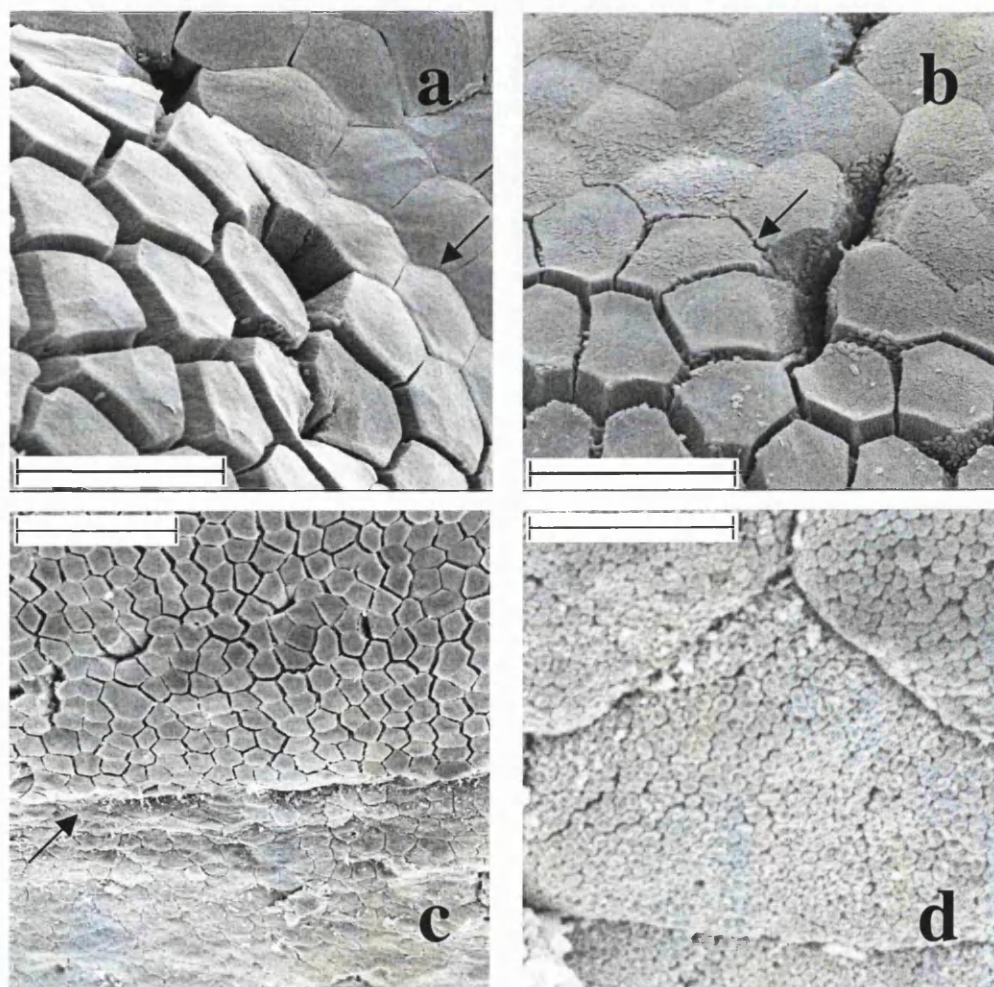


Figure 5.25: S.E.M. images of proximal margin in *H. crepitans* (a) Juvenile (22 mm) Back 1, Scale bar = 25 μm (b) Juvenile (20 mm) Front 1, Scale bar = 25 μm (c) Adult (56.55 mm) Back 1, Scale bar = 50 μm (d) Adult (56.55 mm) Back 5, Scale bar = 6.25 μm .

In juvenile frogs, the differentiation of the cells on either side of the pad margin is reduced and although the edge of the pad is demarcated by a change in the elevation (Figure 5.25 a) the change in cell type is more gradual and indistinct (Figure 5.25 b). Cells are similar to the columnar cells, with a rougher surface appearance. Cells found in this region in adult frogs are sufficiently different from the pad cells (Figure 5.25 d) to suggest that they have developed in this region by this stage in the frogs' life history and that the increased surface roughness in this area may well be functionally adaptive.

5.3.4. Accessory adhesive areas

Hyla geographica

The accessory adhesive system on the hands and feet of *H. geographica* is not particularly well developed, either in the adult or in the juvenile frogs (Figure 5.26). Subarticular tubercles are low in elevation and appear as gently swollen rounded bumps in most instances (Figure 5.26) with the subarticular tubercle on the first finger of the hand being the most developed both in adult and juvenile frogs (Figure 5.27 a and c).

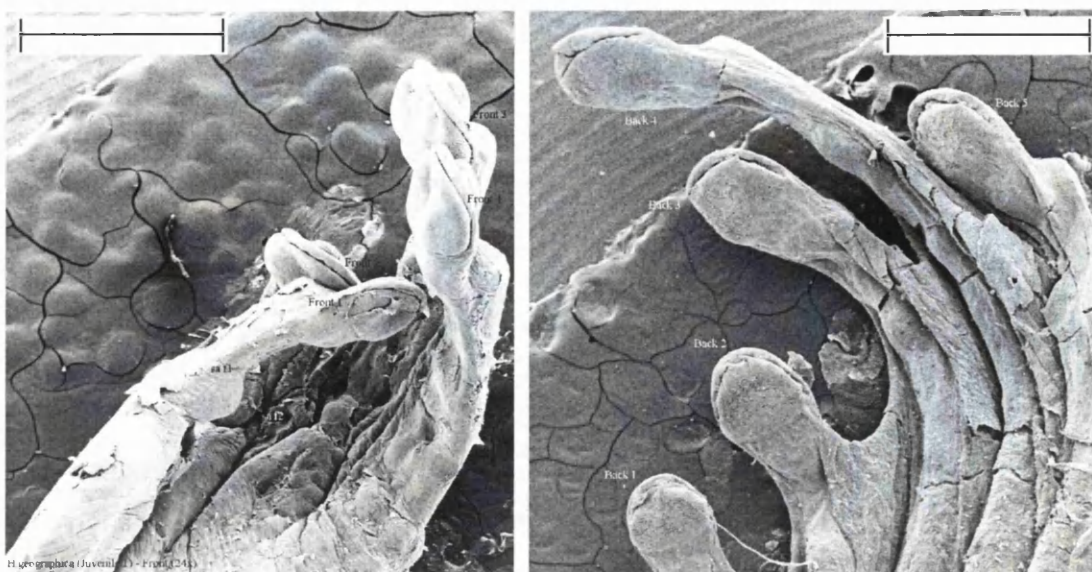


Figure 5.26: S.E.M. images of foot morphology in juvenile *H. geographica*. Scale bars = 1.25 mm.

Cells on the subarticular tubercles have irregular ill-defined margins, with this particularly the case in the juvenile frogs (**Figure 5.27 b**). Cells are roughly hexagonal in adult frogs (**Figure 5.27 d**), large ($210.75 \mu\text{m}^2 \pm 10.08$, $n = 23$) and defined by shallow margins across the surface of the tubercle. The texture of the surface is altered between the age-classes, changing in surface architecture from a micro-villated appearance in juveniles (**Figure 5.27 b**) to a compressed vermiform surface in the adults (**Figure 5.27 d**). There is little evidence of supernumerary tubercle development on the hands or feet, nor of palmar tubercles (**Figure 5.26**). Inner metatarsal tubercles are absent; the lack of development in this area being one of the diagnostic characteristics of this species (Duellman, 1973).

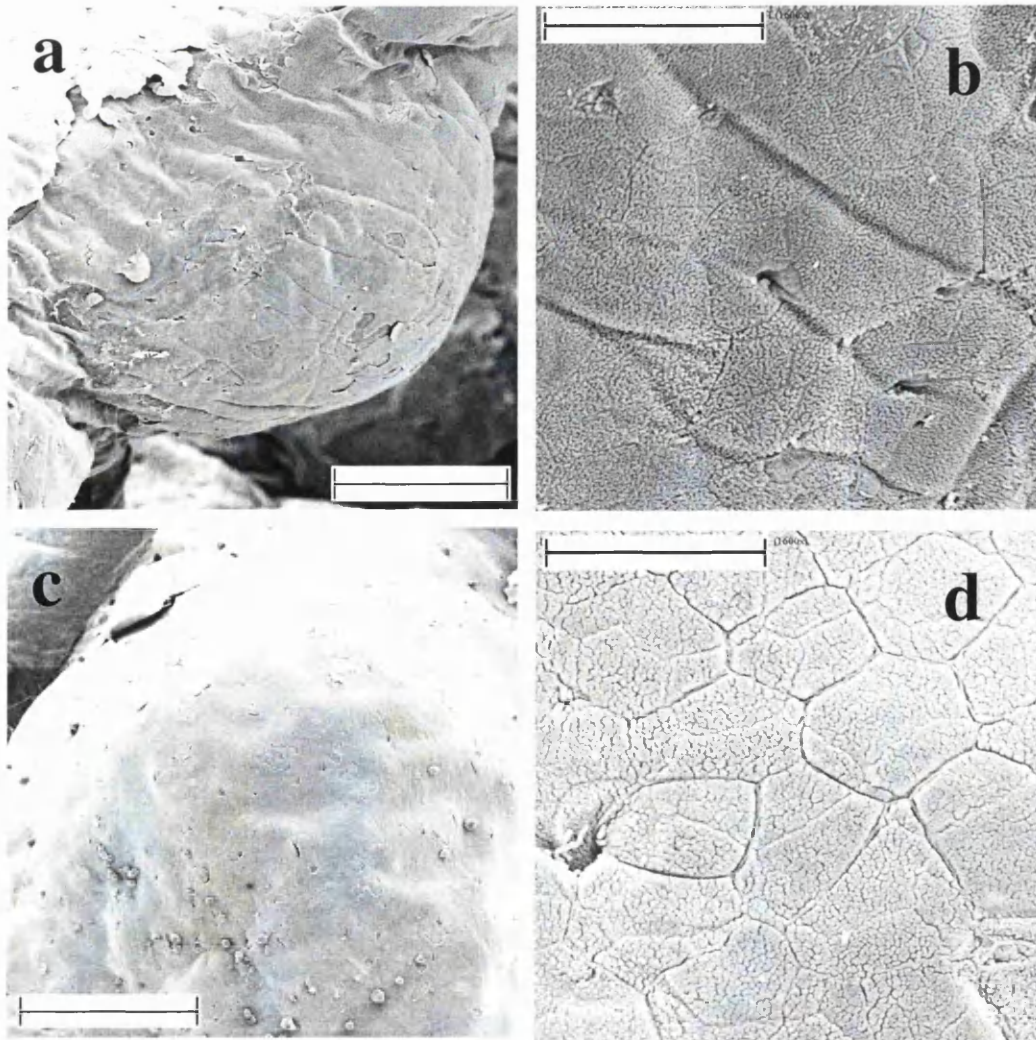


Figure 5.27: S.E.M. images of subarticular tubercles in *H. geographica* (a) Juvenile 1 (21 mm) Front 1, Scale bar = 150 μm (b) Juvenile 1 (21 mm) Front 1, Scale bar = 25 μm (c) Adult (49.7 mm) Front 1, Scale bar = 300 μm (d) Adult (49.7 mm) Front 1, Scale bar = 25 μm .

Hyla crepitans

The configuration of the tubercular system in juvenile *H. crepitans* can be seen to be broadly comparable to that described for adults by Duellman (2001), (**Figure 5.28** and **5.29**). In both age classes the subarticular tubercles are relatively large and well-developed (**Figure 5.30 a** and **c**), with few changes in the distribution of tubercles on the hands and feet between juvenile and adults. However, on a cellular level a very interesting change in the cell type found covering these tubercles has occurred (**Figure 5.30 b** and **d**) between the age classes. Cells in juveniles are much as has been seen on subarticular tubercles in all the species considered so far, being large in size ($185.48 \mu\text{m}^2 \pm 7.37$, $n = 7$) with irregular individual cell margins and a roughened surface architecture. **Figure 5.30 b** suggests that these cells are squamous in nature, much as would be seen for normal epithelial cells in frogs. However, the situation in adults is very different. For the first time in any of the species considered here, there is evidence of toe pad type cells, columnar with hexagonal apices, being found in an area other than the pad proper (**Figure 5.30 d**). Cells are not significantly different in size to those found on the pad ($100.77 \mu\text{m}^2 \pm 4.67$, $n = 36$).

There is no development of the supernumerary tubercles along the segments of the fingers in any of the samples, and no evidence of a developed palmar tubercle (**Figure 5.28**). Distinct supernumerary tubercles are seen on toes three and four of the back foot in juveniles (**Figure 5.28**) and adults (**Figure 5.29**), covered in the same kind of cells as subarticular tubercles. The inner metatarsal tubercle, positioned at an equivalent place on the first toe is prominent in the adult sample (**Figure 5.31 a**) and the cell type covering this protrusion are closer in structure to those seen on the subarticular tubercles seen in adults of other species (**Figure 5.31 b**).

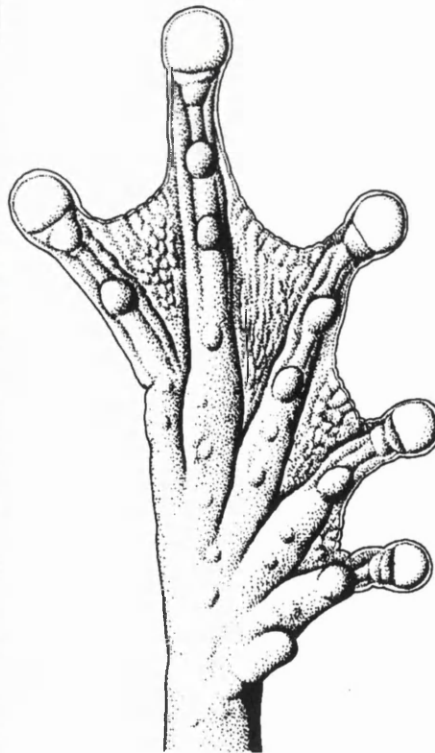
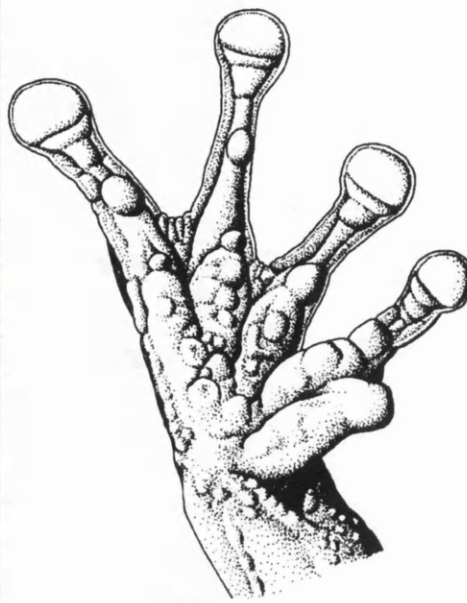
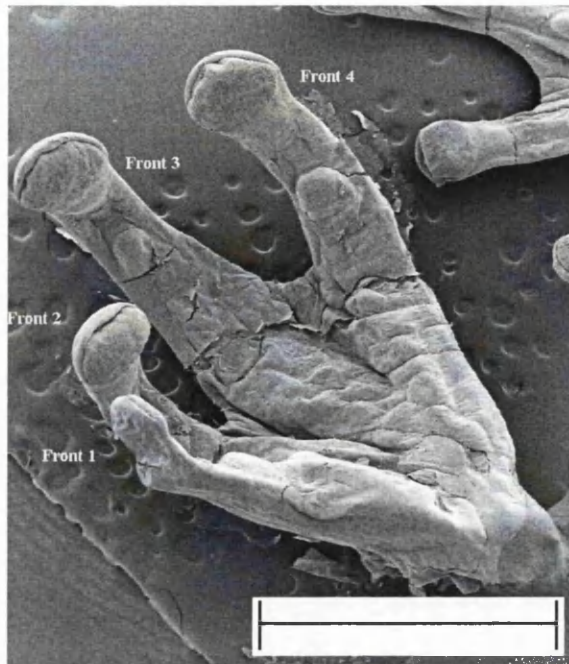


Figure 5.28: S.E.M. images of foot morphology in juvenile *H. crepitans*. Scale bar = 2.5 mm.

Figure 5.29: Hand and foot morphology in adult *H. crepitans* (from Duellman, 2001)

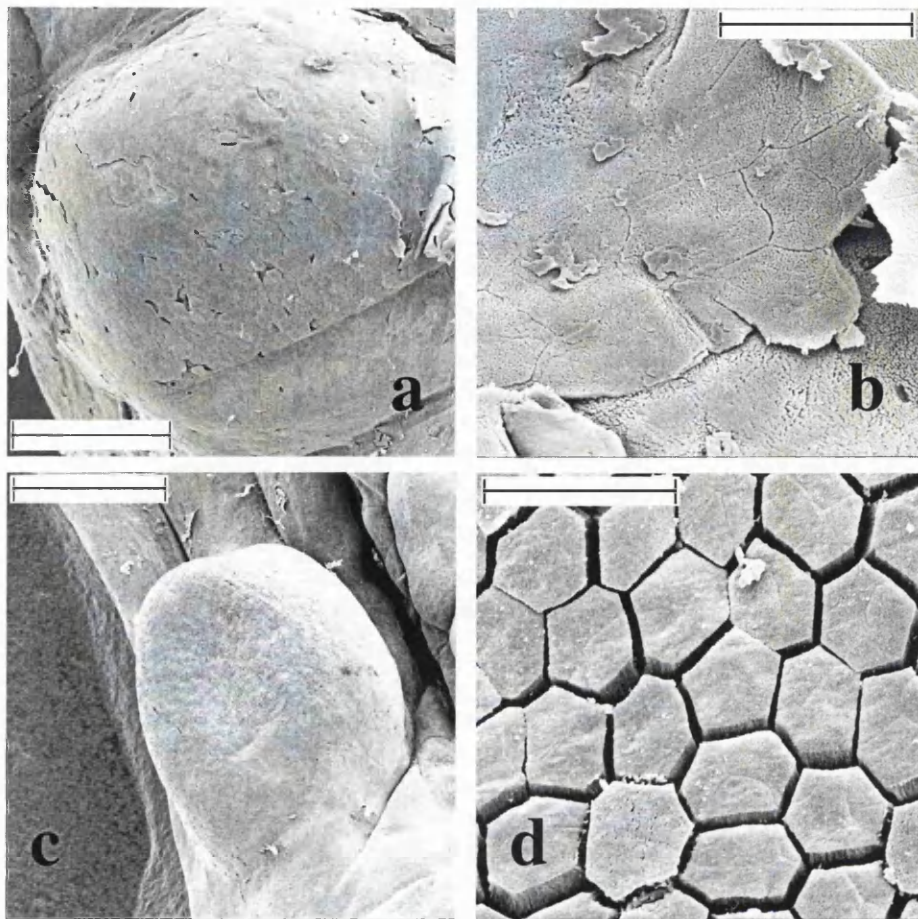


Figure 5.30: S.E.M. images of subarticular tubercles in *H. crepitans* (a) Juvenile (20 mm) Front 4, Scale bar = 150 μm (b) Juvenile (22 mm) Front 2, Scale bar = 25 μm . (c) Adult (56.55 mm) Back 1, Scale bar = 625 μm (d) Adult (56.55 mm) Back 2, Scale bar = 25 μm .

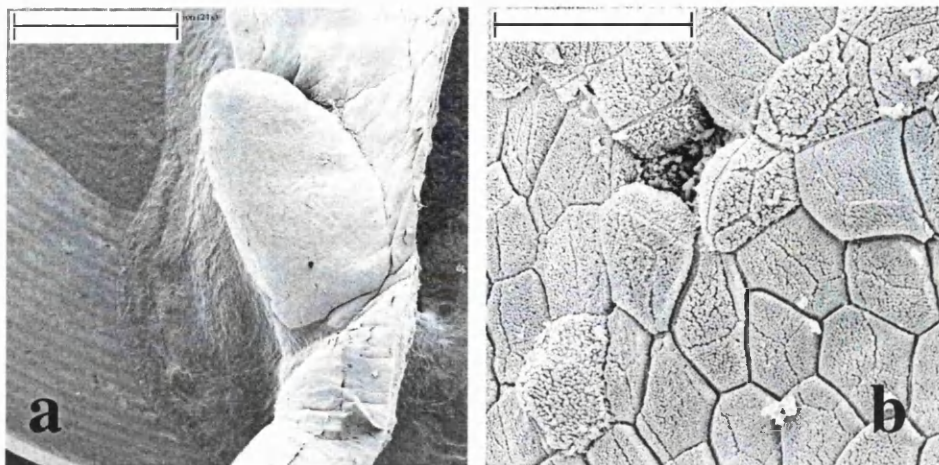


Figure 5.31: S.E.M. images of inner metatarsal tubercle in adult *H. crepitans* (a) Scale bar = 1.25 mm (b) Scale bar = 25 μm .

5.3.5. Effects of size on toe pad morphology

Mean values for various aspects of toe pad morphology are given in **Table 5.3** for juvenile and adult frogs belonging to these two medium-sized species of hylid. There are few demonstrable correlations between the linear dimension in these frogs and aspects of the toe pad morphology (**Table 5.2**) such as those seen in the smaller species in **Chapter 4** and between species in **Chapter 2**. Between species a positive relationship exists between pore size and SVL (**Figure 5.32**) and between the degree of definition of the lateral grooves along the ventral surface of the toe and SVL (**Figure 5.33**). Though the latter of these trends is statistically significant within both species (**Figure 5.33**) with the relationship between pore size and linear dimensions maintained in *H. geographica* (**Figure 5.32**).

Morphological variable	Correlation with SVL			
	r	n	p	t
Cell area (μm^2)	0.23	8	0.59	-0.57
Cell density (per mm^2)	0.08	8	0.85	0.20
Channel density (mm/mm^2)	0.25	8	0.55	0.64
Pore size (μm^2) ^a	0.83	6	0.04	3.02
Pore density (per mm^2)	0.34	5	0.57	-0.63
Pad elevation*	0.49	8	0.22	-1.37
Proximal margin*	0.48	8	0.22	1.35
Circumferal groove*	0.53	8	0.17	1.54
Lateral groove* ^b	0.84	8	0.01	3.74
Subarticular tubercle cells	0.46	3	0.69	-0.52

Table 5.2: Correlative statistics for relationships between SVL measurements and aspects of pad morphology between species in medium hylid frogs. t-statistic for difference of line of best fit from the horizontal. Bold type indicates a significant relationship. * see **Table 5.3** for score definition. ^a **Figure 4.32** ^b **Figure 4.33**.

Species	SVL	Cell area μm^2	Cell density per mm^2	Channel density mm/mm^2	Pore area μm^2	Pores per mm^2	Scores* for				SaT cell μm^2
							Pad elevation	Lateral groove	Proximal margin	Circumferal groove	
<i>H. geographica</i>	21.00	190.34	5250	128.69	61.36	27.51	1.50	0.50	2.00	2.00	-
	23.30	130.98	8269	142.88	13.97	-	1.31	0.38	0.79	0.94	-
	24.00	155.43	6471	145.79	66.24	-	1.64	0.86	2.14	1.79	-
	25.00	134.97	7415	134.94	43.36	14.55	1.50	1.06	0.89	1.83	-
	49.70	119.91	8538	145.56	301.48	34.44	1.25	2.25	2.67	2.06	210.75
<i>H. crepitans</i>	20.00	108.20	9409	141.79	-	34.55	1.78	1.00	1.42	1.67	185.48
	22.00	81.78	12892	159.49	-	-	1.69	1.00	0.63	1.38	-
	56.55	114.06	8992	148.45	167.38	9.44	1.50	1.66	1.69	2.06	100.77

Table 5.3: Average values for aspects of toe pad morphology and subarticular (SaT) cell size in juvenile and adult frogs from two medium species of Trinidadian hylid. * Elevation score system: completely flat; 1 = slightly raised; 2 = rounded; 3 = globular. Groove score system: 0 = not present; 1 = shallow; 2 = well-defined; 3 = prominent.

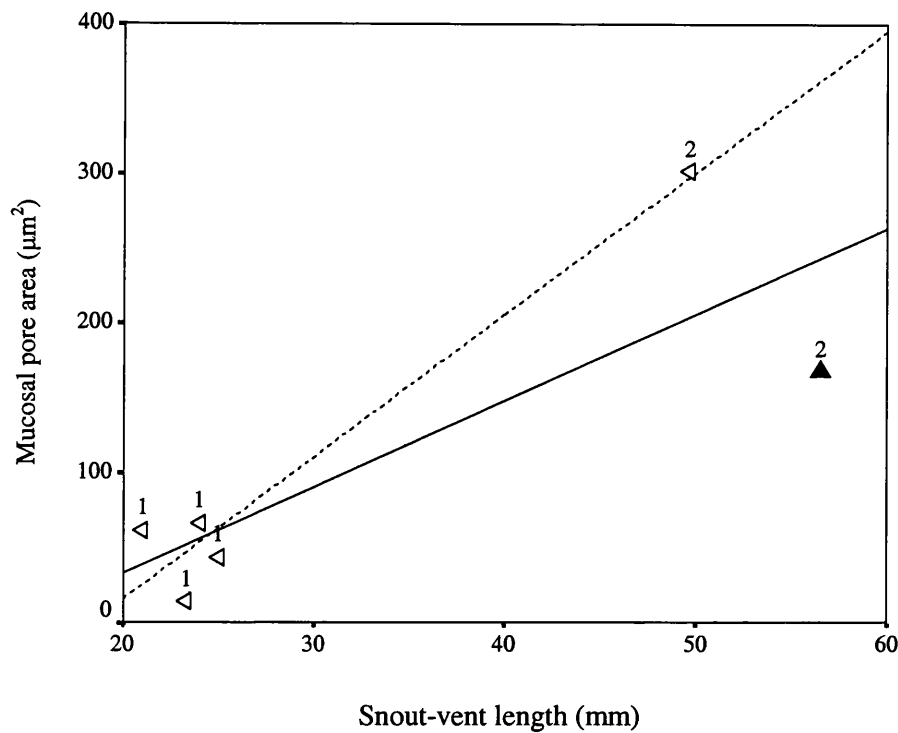


Figure 5.32: Average mucosal pore sizes vs. increasing linear dimensions in juvenile (1) and adult (2) frogs belonging to medium-sized species of hylid: *Hyla geographica* (\triangleleft); *Hyla crepitans* (\blacktriangle). Correlative statistics: All frogs, $r = 0.83$ _____ $y = 5.75x - 82.26$, $t = 3.02$, $p = 0.04$, $n = 6$; *H. geographica*, $r = 0.97$ $y = 9.48x - 173.95$, $t = 7.17$, $p = 0.006$, $n = 5$.

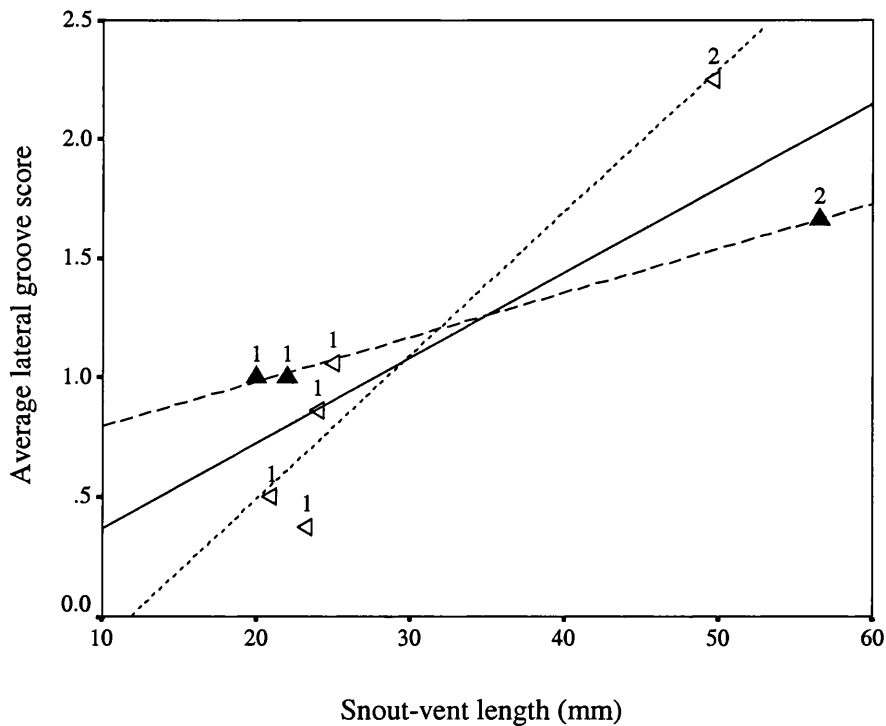


Figure 5.33: Average lateral groove score vs. increasing linear dimensions in juvenile (1) and adult (2) frogs belonging to medium-sized species of hylid: *Hyla geographica* (\triangleleft); *Hyla crepitans* (\blacktriangle). Correlative statistics: All frogs, $r = 0.84$ _____ $y = 0.04x + 0.02$, $t = 3.74$, $p = 0.01$, $n = 8$; *H. geographica*, $r = 0.96$ $y = 0.06x - 0.71$, $t = 5.66$, $p = 0.01$, $n = 5$; *H. crepitans*, $r = 0.999$ ___ $y = 0.02x + 0.61$, $t = 20.53$, $p = 0.03$, $n = 3$.

5.3.6. Integrating pad morphology and adhesion

Detachment angles were recorded from all frogs with toe pads that were examined using S.E.M. and adhesive forces and forces per unit area were calculated using for each frog (**Table 5.4**). These were then analysed with respect to the measured aspects of toe pad morphology in **Table 5.2**.

Species	SVL	Angle	Adhesive force (mN)	Force per mm ² (mN)
<i>H. geographica</i>	21.00	127.20	3.48	0.32
	23.30	144.00	6.41	-
	24.00	113.70	4.61	-
	25.00	127.70	7.61	0.46
	49.70	149.52	66.41	0.43
<i>H. crepitans</i>	20.00	136.80	4.11	0.39
	22.00	137.90	5.88	0.40
	56.55	122.30	59.03	0.77

Table 5.4: Detachment angles, adhesive forces and force per unit area calculated for frogs used in S.E.M. study.

These analyses yield few significant correlative relationships between these parameters although a positive correlation between pore size and adhesive forces between species (**Table 5.5**) and within *H. geographica* ($r = 0.98$, $y = 0.23 - 4.62$, $t = 7.76$, $p = 0.0045$, $n = 5$) runs counter to predictions that might be made from trends in smaller species. Removing the area-dependent aspect of adhesive forces by considering force per mm² of toe pad removes any significant relationship between the two variables so that the increase in pore size has no significant effect on pad efficiency (**Table 5.5**).

The relationship between the degree to which the lateral groove is defined and increasing adhesive force is also significant both between and within species (**Table 5.4**) so that higher adhesive forces are seen in frogs with better developed lateral grooves; (Lateral groove score vs. adhesive force in: *H. geographica*, $r = 0.94$, $y = 34.27x - 16.87$, $t = 4.66$, $p = 0.02$, $n = 5$; *H. crepitans*, $r = 0.999$, $y = 81.87x - 76.88$, $t = 35.25$, $p = 0.018$, $n = 3$). Again, when the area-dependent elements of adhesive force measurements are removed by considering the force per square millimetre of toe pad this correlative relationship is maintained only in *H. crepitans* (**Figure 5.34**). ($r = 0.998$, $p = 0.01$, $n = 3$.)

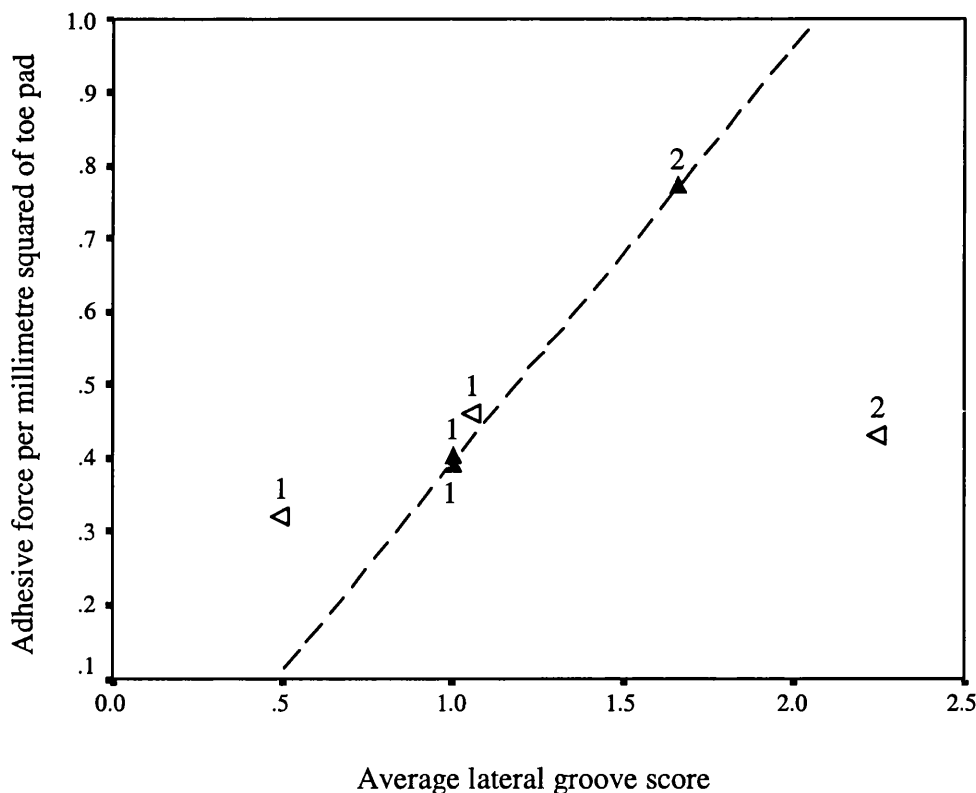


Figure 5.34: Average lateral groove score vs. adhesive force per mm^2 of toe pad in juvenile (1) and adult (2) frogs belonging to two medium-sized species of hylid: *H. geographica* (\triangle); *H. crepitans* (\blacktriangle). Correlative statistics: All frogs, $r = 0.48$, $p = 0.33$, N.S. $n = 6$.; *H. geographica*, $r = 0.60$, $p = 0.74$, $n = 3$; *H. crepitans*, $r = 0.999$, $y = 0.57 - 0.17x$, $p = 0.01$, $t = 43.31$, $n = 3$.

Morphological variable	Adhesive force				Force per mm ² (mN)			
	r	p	n	t	r	p	n	t
Cell area	0.25	0.55	8	-0.63	0.30	0.57	6	-0.63
Cell density	0.11	0.80	8	0.27	0.14	0.79	6	0.28
Channel density	0.25	0.56	8	0.62	0.33	0.53	6	0.69
Pore size	0.93	0.01	6	4.87	0.21	0.79	4	0.30
Pore density	0.13	0.83	5	-0.23	0.76	0.14	5	-2.00
Pad elevation	0.55	0.16	8	-1.58	0.16	0.76	6	-0.33
Proximal margin	0.55	0.16	8	1.61	0.02	0.97	6	0.04
Circumferal groove	0.53	0.18	8	1.53	0.37	0.47	6	0.80
Lateral groove	0.90^a	0.01	8	5.00	0.48	0.33	6	1.10
Subarticular cell	0.19	0.88	3	-0.20	0.95	0.20	3	-3.05

Table 5.5: Correlative statistics for relationships between adhesive force and forces per unit area and SVL in two medium species of hyliid. t - statistics for difference of slope of line of best fit from the horizontal. Bold type denotes correlations significant to p = 0.01. (a) **Figure 5.34**

5.4. Discussion

The two species of Trinidadian hyliid frog that fall into the medium size category as adults (50 mm < SVL < 80 mm) belong to the subfamily Hyalinae, and are thus more closely related than frogs compared within other size classes that span several genera, so that any differences in strategies to counter the effects of growth upon adhesive abilities are of particular interest, as are the differences seen in the rates of weight increase with growth.

H. geographica shows a particularly reduced rate of weight increase in adult frogs, to such a degree that weight and toe pad area are increasing with the linear dimension at similar rates, as $(\text{SVL})^2$. Rates of weight gain in adult *H. crepitans*, although reduced, are not significantly different from the expected (**Table 2.1**). Reasons for differences in these rates of weight increase may be illuminated by considering the geometrical differences between the two species, particularly in terms of the dimensions of the hind limbs (**Table 5.6**).

Ratios of measured physical parameters	<i>H. geographica</i> ¹	<i>H. crepitans</i> ²
Tibia: SVL	0.53	0.56
Foot: SVL	0.37	0.40
Head length: SVL	-	0.34
Head width: SVL	-	0.35

Table 5.6: Ratios of physical measurements from males of *H. geographica* and *H. crepitans*. Derived from (1) field notes from Trinidad, 2001 (JS) (2) Duellman, 2001; frogs from Ecuador.

Although ratios of tibia: SVL and foot length: SVL are roughly similar, there is a tendency in *H. crepitans* towards a proportionally longer hind-limb length that may indicate an increased dependence on jumping ability than is seen in *H. geographica*. Behavioural observations in *H. geographica* certainly suggest that this may be so, with frogs exhibiting a tendency to ‘play dead’ rather than actively attempting to escape when subjected to continuous handling. Further to this, it may also be that the shortening of the limbs in *H. geographica* is indicative of a more arboreal life style in this species, as this is a characteristic trend with greater degrees of arboreality (Cartmill, 1978). It is difficult to assert with any confidence that this is indeed the case as there is scarce literature about the habits of these species, though *H. crepitans* is noted to be ‘rarely in thick forest’, whereas the sites from which *H. geographica* was collected were, in both instances, on the edges of fairly thick secondary rainforest. If the shortening of limb length is indicative of increased arboreality in this species then the greater extent to which the rate of weight increase is reduced in comparison to *H. crepitans* may indicate the greater pressures to maintain adhesive ability that is likely to follow this trend due to the increased costs of dislodgement from substrates, i.e. the increased energetic cost of climbing to higher perch sites[†].

The reduced rate of weight increase in *H. geographica* is such that the extent to which the rate of increase in adhesive forces is different to the expected is sufficient to compensate for the increase in weight in the period of growth between metamorphosis and adulthood. Indeed adult frogs are capable of adhering to

[†] Hunters we met at the Damier River mentioned that they had seen these frogs ‘flying’ from trees into the river. Although the degree of hand webbing in this species is too reduced for them to be classified as ‘flying’ frogs (Emerson and Koehl, 1990) if this is a regular behaviour then this would be a further pressure upon the frogs to keep weight as reduced as possible to maximise gliding distances and to avoid injury on landing.

significantly higher angles than seen in juveniles, which may in part be explained by the substantial decrease seen in the rate of weight gain with growth in the adult age class discussed earlier. Significantly, although the total rate of weight increase across the age classes in this species is reduced to a lesser extent than this, as (SVL)^{2.48}, there is still no difference between this and the rate of increase in toe pad area in the equivalent time period ($t = 1.63$, N.S. 37 d.f.). For this species then, the increase in toe pad area as expected is enough to compensate for the weight increases with growth. While this might explain why there is no decrease in adhesive ability with growth, it does not explain how adhesive forces in this species increase at a greater rate than can be explained by toe pad area alone, as (SVL)^{2.91}.

This is also the case for the larger *H. crepitans* but in this instance the elevation in the rate of adhesive force production with growth, as (SVL)^{2.38}, is not sufficient to compensate for the only slightly reduced rate of weight gain seen in the species, (SVL)^{2.69}. With this increasing at a greater rate than the equivalent increase in pad area ($t = 2.72$, $p < 0.01$, 126 d.f.) and pad area increasing much as would be expected following isometric growth, (SVL)^{2.08}, then there is a decrease in the average maximum detachment angles recorded from adults in this species when compared to juvenile values. In spite of this, both of the medium-sized hylid species from which data from juvenile and adult frogs were available show evidence of an increase in adhesive force with growth occurring at a rate greater than can be explained by the equivalent increase in toe pad area seen in either species, which in both instances is as expected through isometric growth.

In the smaller species of frog discussed in the previous chapter, where this trend is also apparent, there is an increased efficiency of the pad implied by a greater force per unit area evident in adult frogs of the species. There are positive trends in evidence between this variable and increasing SVL in both medium-sized species separately, but in neither case is the relationship statistically significant. When data from medium-sized species are combined, there is a significant increase in the adhesive force per unit area of toe pad in the adult frogs (**Figure 5.13**) that suggests that larger frogs within the two species have more efficiently adhering pads than smaller individuals. There are a number of ways in which they may be able to achieve an increased efficiency of the adhesive mechanism; through physico-chemical changes in viscosity or by changes in the volume of the fluid layer beneath their adhesive pads. The inability to maintain adhesive abilities on surfaces with differing wettability in adult *H. crepitans* suggests that any alterations to the adhesive abilities in adult frogs of this species are not occurring on a short-term basis. If adult frogs can effect changes in the thickness or properties of the mucus then these adjustments are not sufficient to counter the detrimental effects of decreasing wettability of low surface energy substrates.

The consideration of the structure of the pad as the source for the improvements that are being seen within the adhesive system in these two species is of particular interest, taking into consideration that these two medium-sized frogs are the closest related species within a size class. This means that the differences between these two similarly sized frogs are of particular interest in view of the effects of differences in ecology as the frogs are otherwise very alike. Trends in cell size in particular warrant further consideration, especially as there is no significant difference in cell size in

adult frogs ($F_{80,78} = 0.14$; $t = 1.12$, N.S. 156 d.f.), but opposite trends in the juveniles of the two species. Juvenile *H. geographica* have significantly larger cells on the toe pad than adult frogs, whereas juvenile *H. crepitans* have significantly smaller sized cells than adults. Between adult frogs belonging to all twelve species in this study, increasing cell size was found to be positively correlated with the adhesive forces produced (**Chapter 3**). The correlation between this morphological parameter and adhesive force production has not yet been seen within any of the species considered, but if the observations of the effect of cell size on adhesive force are followed to their logical conclusion in *H. geographica* and *H. crepitans*, then the implications are that there is a need in the juvenile frogs of the smaller species to produce greater adhesive forces per unit area of the pad. The explanation for this may lie in the typical weights and snout-vent lengths of new metamorphs (**Table 5.1**), where *H. geographica* are one of the largest species at metamorphosis. Furthermore, whereas frogs within the juvenile age class in *H. crepitans* show a reduced rate of weight increase with growth, as $(SVL)^{2.51}$, *H. geographica* froglets are increasing at a higher rate, as $(SVL)^{2.91}$ thus increasing the pressure upon the adhesive system in juvenile frogs of the smaller species. However, in view of the lack of a demonstrable correlation between cell size and any aspect of the adhesive ability in either species, it is difficult to draw any firm conclusions from these trends.

In fact there are few instances of correlative relationships between the aspects of toe pad morphology and adhesive abilities in these two species, as seen in frogs in previous chapters. There is some evidence that adhesive forces increase in frogs with larger pores and with more defined lateral grooves but all three of these are highly dependent on the increasing linear dimension.

The relationship between average pore size and the increasing linear dimension in these species is surprising if taking into consideration the effect that larger pore sizes may potentially have on the volume of mucus below the pad. It is to be expected that larger pore sizes are likely to lead to greater volumes of mucus being produced below the pad and thus might be expected to have an adverse effect upon adhesive abilities. However, adhesive forces in *H. geographica* scale with increasing size at the highest rate of any species considered so far, suggesting that there are no detrimental consequences of increasing pore size upon the frogs' adhesive abilities. Indeed, if anything the within-species relationship between pore size and increasing adhesive force production in *H. geographica* suggests that, if there are any consequences of increasing pore size on sticking ability, they are positive rather than negative. If the diversity of the pore types seen in adult *H. geographica* are also considered, together with behavioural observations of the species' response to threat, this may point to a possible explanation for the increased rate of adhesive force production in the species with increased pore size. If this species is not as dependent on the ability to jump to escape predators, as is suggested by its reduced hind-limb length and tendency to feign death in response to stress, then the pressures upon the adhesive system to maintain a low viscosity mucus may be less than in other species. Whereas the need to maintain low detachment forces will still be present in order for the frog to be unimpeded during normal locomotion, it may be that the presence of a diversity of different mucosal pore types is indicative of an ability to produce mucus with differing chemical and physical properties, as in the limpets and periwinkles (Smith *et al.* 1999; Smith and Morin, 2002). However, without the means to test the surface tension and viscosity of the mucus below the pad this can only be conjecture based on behavioural and morphological observations of the species.

Adhesive forces per unit area are correlated to the degree of definition of the lateral groove in *H. crepitans* and, although a trend exists between species, the presence of the outlying adult *H. geographica* means that the relationship is not statistically significant (**Figure 5.34**). Where lateral groove development is seen in adult frogs, there is a tendency for mucosal layers to be channelled along these to the subarticular tubercle (**Figure 3.15**). This is likely to have no particular advantage for *H. geographica* as the structure of subarticular cells suggests the function of these areas is much as suggested for the smaller species in the previous chapter, allowing for an additional contribution of frictional forces to the overall adhesive force. In *H. crepitans*, however, the structure of the cells on the subarticular tubercles in adult frogs is similar to those seen on the toe pad proper, suggesting that in adults, the accessory function of these structures has changed perhaps to facilitate an increase in the total area able to produce sticking force through wet adhesion. This may well be the mechanism by which *H. crepitans* are able to produce a higher rate of force production with growth than can be explained by the equivalent increase in toe pad area alone.

Both species of medium-sized hylid increase their adhesive force production with growth at a greater rate than would be expected from interspecific studies, faster than the equivalent increase in toe pad area, which increases as expected, as approximately $(SVL)^2$, in both species. Both species show a reduced rate of weight gain with growth; in *H. geographica* the degree to which this is the case is matched by the correspondent toe pad increase. Based on morphometric considerations, there should be no need for this species to make any adjustments within an adhesive mechanism to allow the frogs to maintain sticking abilities with growth. Nevertheless adhesive abilities are increasing at a greater rate than toe pad area suggesting that

further improvements are occurring to allow this to be the case. There is some evidence that increase in pore size and an increase in the diversity of pores seen across the pad in adult *H. geographica* may allow an increase of adhesive force. There is a tendency towards an increase in pore size in adult *H. crepitans*, though the main aspect of toe pad structure in this species having an effect on adhesion is the degree of the development in the lateral grooves running along the ventral surface of the toes. The development of these is likely to facilitate the spreading of mucus along the toe towards and below the subarticular tubercles, which in this species are covered in cells that are similar in their appearance to those on the toe pad proper. This may indicate that in this species selection has favoured an increase in the area available for the production of wet adhesive forces by the development of the subarticular tubercles, though the increase involved is not enough to allow the adult frogs to maintain detachment angles to the same degree as seen in juvenile frogs. *H. crepitans*, is the first of the species considered thus far in which the effects of growth are detrimental to the sticking performance of adult frogs. If this is the case for this medium species, then there may be yet greater levels of detriment to the sticking abilities in adult frogs of the larger species, where the increase in weight involved in growth is still greater to that seen in *H. crepitans*. The following chapter will consider the effects of growth on sticking ability in relation to changes in morphometry and toe pad morphology for the three 'large' Trinidadian hylids.

Chapter 6: Adhesion in large hylid frogs

6.1. Introduction

The problems imposed upon an adhesive system predominated by area-dependent forces with growth are outlined in **Chapter 4.1**. The specific effects of growth on adhesive abilities in hylid species with adult SVL measurements below 70mm are considered in the two previous chapters. The actual increases in weight seen in these species between metamorphosis and adulthood are positively correlated to the eventual SVL measurement of the adult frogs (**Table 6.1**). If these trends continue, then the effect in the largest species can be expected to be considerably greater than the species considered in previous chapters and may thus prove problematic in terms of maintained adhesive ability with growth.

Species in order of increasing SVL	Average SVL (mm)			Average weight (g)		
	Juvenile	Adult* ²	Increase in size	Juvenile	Adult* ²	Increase in size
<i>H. minuscula</i> ~	11.25	17.98	x 1.6	0.16	0.45	x 2.8
<i>F. fitzgeraldi</i> ~	7.92	18.67	x 2.4	0.06	0.52	x 8.7
<i>S. rubra</i> ~	13.38	30.23	x 2.3	0.20	2.02	x 10.1
<i>H. punctata</i> ~	23.28	33.42	x 1.4	0.75	2.43	x 3.2
<i>H. geographica</i> ~	19.81	57.93	x 2.9	0.65	8.43	x 13.0
<i>H. crepitans</i> ~	18.50	63.35	x 3.4	0.55	14.14	x 25.7
<i>P. trinitatis</i> *	15.30	75.90	x 5.2	0.75	21.39	x 28.5
<i>P. venulosa</i> *	19.60	74.44	x 3.8	0.39	24.79	x 63.6

Table 6.1: Species average values for snout-vent lengths and weight in juvenile and adult frogs: ~ average measurements of youngest cohort in **Chapters 4** and **5** * measurements from new metamorphs in Downie *et al.* (submitted); *² adult values from **Table 2.1**.

In 'small' species (**Chapter 4**) the adhesive system is able to compensate for the increase in weight involved in the period of growth from metamorphosis to adulthood due in large part to a substantially lowered rate of weight gain with growth in the species. This together with an increased development of various aspects of toe pad morphology are sufficient to allow these frogs to maintain their sticking abilities to similar levels as juveniles and adults. The medium-sized species *H. geographica* also exhibits similar adhesive abilities in the two age classes, with this again being aided by toe pad morphology and a lower rate of weight increase than that expected through isometric growth. However, the slightly larger *H. crepitans* is not able to maintain adhesive abilities as adults to the same degree as seen in the juveniles, perhaps due to a lesser degree of development of aspects of pad morphology or due to the less substantial decrease from the expected rate of weight gain with growth to adulthood than is seen in the smaller *H. geographica*.

Literature values for *P. trinitatis* suggests that in terms of the increase in weight between new metamorph and adult there is a comparable pressure upon the adhesive system in the large species to that seen in *H. crepitans* (**Table 6.1**). If adjustments within the adhesive system for *H. crepitans* are not sufficient to allow this species to maintain its sticking abilities with growth then what are the implications for yet larger species, such as *P. venulosa*? This chapter will examine allometry with growth in the three 'large' species of Trinidadian hylid that are categorised as 'large' (**Chapter 4**) in relation to the adhesive forces that the frogs are capable of producing. S.E.M. images of toe pads from juvenile and adult frogs of these species will also be considered to determine whether any changes take place on a structural level that may facilitate adhesive abilities with growth in these large species.

6.2. Methods

6.2.1. Experimental animals

Phrynohyas venulosa

The genus *Phrynohyas* are commonly known as ‘tree toads’ (Duellman, 2001) due to the characteristic glandular appearance of their dorsal skin (**Figure 6.1**). SVL measurements in the literature for the locality range in value from 75-90 mm (Zweifel, 1964; Kenny, 1969) to 100-113 mm (Murphy, 1997). Frogs sampled in the course of this study ranged between 68.2 - 79.5 mm SVL (♂) and 88.0 - 97.6 mm SVL (♀), being closer in size to those in earlier studies.



Figure 6.1. Adult male *P. venulosa*, Simla.

Photo: J. Smith

Adult frogs were collected from breeding aggregations of up to 100 individuals gathered at ponds in secondary forest at Simla and from flooded wasteland in the Lopinot Valley (**Figure A1.1**). Calling males have everted black vocal sacs (see **Figure 6.1**) particularly diagnostic as this genus is one of only four that possess this type of laterally paired vocal sac (Yanosky *et al.* 1997). As with a number of other species in this study, males are additionally identifiable by the presence of a dark-coloured horny nuptial pad on the inner surface of the prepollex when in breeding condition (Murphy, 1997; Yanosky *et al.* 1997; Duellman, 2001). Females are considerably larger than males and when collected as gravid were found to be carrying eggs equivalent to around 50% of their post-deposition weight, with this leading to the exclusion of all females until egg masses were laid.

Wild-caught adults were processed and released as soon as possible, and should be kept in soft-sided enclosures if possible as they tend to injure themselves trying to escape from glass-sided aquariums. In spite of this amplexant pairs readily lay viable clutches in captivity, though larger tadpoles were also collected as these were more reliably raised through to metamorphosis in lab conditions. Froglets are around 15mm SVL at metamorphosis; thereafter juveniles thrive in captivity on a diet of fruit flies and crickets. Several frogs continued to grow steadily after a period of poor post-metamorphic survival at around two months in age and have achieved sizes comparable to adult frogs caught in the field within two years. As yet, none have exhibited the secondary morphological characteristics indicative of sexual maturity described for adult males of the species.

Phyllomedusa trinitatis

The genus *Phyllomedusa* belongs within a distinct subfamily of the Hylidae, the Phyllomedusinae. Frogs are characterised by a distinctive slow grasping locomotory mode, which has been variously referred to as ‘lemuroid’ (Duellman, 1968), and ‘loris-like’ (Murphy, 1997); the analogies between Phyllomedusine movement and the climbing techniques of small primates is responsible for their being commonly referred to as the ‘monkey frogs’. The subfamily is itself split into three separate species group, defined by the degree to which the hands and feet are specialised to facilitate the climbing nature of the frogs (Duellman, 2001). The group of large Phyllomedusine frogs to which *P. trinitatis* belongs is typified by the possession of fingers and toes entirely free of interdigital webbing and with a highly opposable first digit on both the hands and feet.

Literature for frogs from the locality gives typical SVL measurements of between 80 and 90 mm SVL. Adult frogs collected from breeding aggregations at temporary ponds in the Lopinot and Arima Valleys (**Figure A1.1**) are in the lower ranges of these with males measuring 68 - 78 mm SVL and females 83-89 mm SVL. Adult males are distinguishable from females by the presence of a darkened horny nuptial excrescence on the base of the pollex, similar in appearance to that described in the closely related *P. venusta* (Duellman, 2001) but omitted from previous descriptions of this species in Trinidad (Kenny, 1966; Kenny, 1969; Murphy, 1997).

If amplexant frogs (**Figure 6.2**) are transported without separating the pair then overnight the frogs will often, if supplied with plentiful fresh foliated branches and left undisturbed, produce the leaf nests typical of frogs from this genus. Tadpoles hatched from these nests maintained in laboratory conditions took as long as six months to reach metamorphosis and so larger tadpoles were also collected from breeding ponds for raising to this stage.



Figure 6.2: *P. trinitatis*, Simla. Photo: J. Smith

Froglets are relatively large at metamorphosis, at around 20mm SVL, and although the juveniles appear to feed well on crickets post-metamorphic survival is unpredictable. The maximum age attained by this species in captivity was around ten months, when froglets were around 35 mm in SVL.

Hyla boans

H. boans is a member of an eponymous species group within the subfamily Hylinæ. This group also contains *H. crepitans* and shares many characteristics with the *H. geographica* group.

SVL values from frogs of this species from mainland Central America include some of the largest recorded measurements for any known hylid (117–132 mm (Panama), Duellman, 2001).



Figure 6.3: Male *H. boans* (95.7 mm SVL) Photo: J. Smith

Whilst *H. boans* is certainly the largest sized species of tree frog in this study, adult frogs sampled in Trinidad in 2000 and 2001 were considerably smaller in size than this and smaller than found in studies by Magnusson (1999) on Brazilian frogs (107–116 mm). Indeed, with SVL values of frogs ranging between 89.0 and 100.6 mm, the study cohort are also in the lower ranges of values in the literature from the locality (100–115 mm: Kenny, 1969; Murphy, 1997). Whereas it cannot be conclusively stated that all of these frogs were definitely adult as a number were never heard to call*, the smallest of the frogs collected in the course of the study was one of the five that were calling at the time of their collection and so the observation of a trend towards body size reduction in these frogs is likely to be valid.

* Frogs collected from calling sites were generally found high in the trees and stands of bamboo at rivers at Lopinot and Arima in the Northern Range (**Figure A1.1**) with these ranging in size from 89.0 – 98.5 mm. One frog was found calling from the bank of the Turure River in the first week of June (**Figure 6.3**). Several frogs were found crossing the Arima-Blanchisseuse road on wet evenings (92.2 – 100.6 mm), and one (96.9 mm) was brought to the lab after having fallen onto a student (!).

That this smallest frog of 89.0 mm SVL is likely to be an adult male in spite of its size is all the more surprising when the consideration of the most recent studies of the species from the mainland Americas are taken into consideration (Magnusson, 1999; Duellman, 2001). Both of these have found that sexual size dimorphism is reversed in this species, with this proposed as being due to high levels of male-male aggression seen in the species in the breeding season in the Brazilian frogs (Magnusson, 1999). It is not possible to state if this reverse in the sexual size dimorphism is seen in Trinidadian frogs as the sex of the larger frogs, which were all silent on collection, was indeterminable in this instance. The enlargement of the prepollex to form a fighting 'spine' used as a diagnostic feature of the male sex in the two mainland studies was variable even in the frogs known to be calling at the time of their collection and so could not be used to confidently identify the sexes in the silent frogs. This variability in the degree of prepollex enlargement may in part be due to the fact that the majority of frogs were sampled outside of the breeding season for the species, in Trinidad's dry season, (though calling does still occur during this season).

This is also one of the main reasons for the low sample size for the juvenile frogs in the study; large tadpoles were collected from the river at Turure at the tail end of the dry season, together with algae-covered rocks from the site. These tadpoles metamorphosed at around 15 mm SVL, with this value again being slightly smaller in size to those seen in Panamanian frogs (17-18 mm: Duellman, 2001), but post-metamorphic survival is low.

6.2.2. Measurement of sticking ability

Sticking ability in adult frogs was determined in the field in Trinidad, using the methodology outlined in **Chapter 2.2.2**. Juvenile frogs were rotated at least once monthly, again according to this protocol and as with adults weighed and measured immediately prior to experimental use. All experiments are carried out in the room in which the frogs are kept, at temperatures comparable to typical air temperatures in Trinidad. Species-specific behaviour of the frogs on the rotation platform was taken into consideration to ensure that detachment angles were an accurate representation of the adhesive performance allowed by toe pad contact alone.

P. venulosa exhibit a number of behavioural counterstrategies to falling. They do use extra stomach skin, though seldom utilise additional thigh skin when allowed to adhere ‘naturally’ to the rotating board of the experimental set-up. Once adults begin to slip they will then continuously slide down the board making little effort to counter the slip with back feet detaching first, just prior to falling from the board. There were very few postural alterations noted in adults of these large frogs such as the limb extensions seen in *H. crepitans*. Young froglets often make some effort to walk around the board and sometimes adopt a position with the head bent upwards from the board, but with increasing size this effort becomes less frequent. *P. venulosa* succumb to stress far more easily than the other frogs in the study and are far more prone to appearing as if they aren’t trying to maintain a grip, so that work with the frogs is often frustrating as it involves much stopping and starting of individual trials and in many cases the abandonment of trials entirely.

This is exacerbated once juvenile frogs exceed around 1.5 – 2 g in weight when they begin to produce thick white sticky mucus from skin glands as a response to stress. This is present in adults too and has been shown to act as an anti-predator device under natural conditions (Murphy, 1997; Yanosky *et al.*, 1997; Leary, 1998) but it also known to act as an anti-experimenter device (Smith, 1951; Janzen, 1962) in that allergenic elements within the mucus can induce watering eyes, streaming noses and violent sneezing. As well as being entirely unpleasant for the handler this seems to be a traumatic event for the frogs in that it seems to take a long time for them to recover from this mucus-producing response. Attempting to resume an experiment within an hour will lead to the frogs becoming stressed very quickly, sometimes simply in response to handling.

P. trinitatis do not generally utilise additional stomach skin to aid adhesion when adult, though juveniles will tend to press their venter and thigh skin to the substrate. Once frogs of either age class begin to slip they continuously replace their front and back feet, spreading limbs and toes wide, giving the appearance of desperately clawing at the surface until they eventually fall.

As adult *H. boans* begin to slip they start to shuffle on the rotation platform at first drawing their feet beneath them. As the rotation progresses frogs spread their front toes (which are heavily webbed) and walk up the platform with their limbs extended (see **Figure 6.3**). Additional stomach skin may be utilised to a certain extent at lower angles but at angles beyond the vertical will rapidly detach from the substrate.

6.2.3. Calculating adhesive forces

Adhesive forces were calculated using methodology as outlined in **Chapter 2.2.3**.

6.2.4. Toe pad morphology

Toe pads were sampled and processed for Scanning Electron Microscopy as described in **Chapter 3.2.1**. Images captured by from juvenile and adult frogs were analysed as described in **Chapter 3.2.2**.

6.2.5. Statistics

As a point of note: All statistics and graphs are generated using SPSS statistics software. This package does not have the functional capability to truncate lines of best fit to confine them to the edges of data sets and the lines of best fit on many graphs extend further than the parameters of the study can predict.

All statistical mean values are given in the format: $\bar{x} \pm 1 \text{ s.e.}$

6.3. Results

6.3.1. Morphometrics

Phrynohyas venulosa

Juveniles of *P. venulosa* measure around 15mm SVL at metamorphosis. Frogs caught around the Lopinot Valley (**Figure A1.1**) measured between $73.32 \text{ mm} \pm 0.95$ ($\sigma_n = 11$) and $90.10 \text{ mm} \pm 0.90$ ($\phi_n = 2$). If weight increases as expected following isometry in this species; a female frog, increasing its linear dimensions by a factor of six in the period of growth from metamorphosis to maturity might be expected to experience a two-hundred-fold increase in body mass over the same period of time (i.e. $6^3 = 216$). In fact with metamorphic weights of around 0.3 – 0.4 g and maximum weights of post deposition females of around 40g the actual increase is closer to a hundred-fold, suggesting that a lower than expected rate of weight increase is occurring between metamorphosis and adulthood.

Examining the relationship between weight and the increasing linear dimension on a log:log plot we can see that this is indeed the case across the population as a whole, with weight increasing as linear dimensions to the power of 2.81 (**Figure 6.4**). While this is closer to the expected relationship between these two parameters with isometric growth than is seen in many of the smaller species, it is nevertheless, significantly lower than the expected rate of weight gain with isometric growth, as $(\text{SVL})^3$; $t = 5.76$, $p < 0.01$, 150 d.f.

* Arima Valley frogs: ϕ 87.1 ± 0.98 ($n = 3$) σ 75.1 ± 0.50 ($n = 38$)

The degree to which weight gain is reduced appears greater still when considering the adult data alone (**Figure 6.4**), with mass increasing as $(SVL)^{2.05}$. However, the reduction in weight gain with growth in this cohort is not statistically significantly different to the expected slope of 3 ($t = 2.02$, N.S. 14 d.f.). This may in large part be due to the high degree of variability in the data, and specifically to the effect that the consideration of both sexes together has on the observed relationship. Removing the female data from the analysis reduces the degree of discrepancy between the observed growth rate and that expected for isometric growth, as the linear dimension cubed; (Line of best fit for log:log relationship between weight and SVL for males alone: $y = 3.74x - 5.62$, $p < 0.01$, $n = 11$. Difference from slope of 3: $t = 0.88$, N.S. 9 d.f.). Within the juvenile age class alone, rates of weight gain with growth are less different to those expected from isometric predictions, increasing as $(SVL)^{2.95}$ (Difference from slope of 3: $t = 1.28$, N.S. 134 d.f.). This is a significantly greater rate than seen across the age classes (Difference of slopes of weight increase with the linear dimension in juveniles and for total population: $t = 2.74$, $p < 0.01$, 284 d.f.).

There is a trend towards a greater than expected rate of increase in toe pad area amongst frogs belonging to this species both across the age classes and within juveniles alone (**Figure 6.5**) increasing as $(SVL)^{2.13}$ and $(SVL)^{2.21}$ respectively. However, in neither case are these relationships statistically significantly different to the expected rate of increase in area with isometric growth, as the linear dimension squared. The difference from the expected slope of two is less significant for the juvenile frogs ($t = 1.17$, N.S. 18 d.f.) than for the population as a whole ($t = 0.93$, N.S. 22 d.f.).

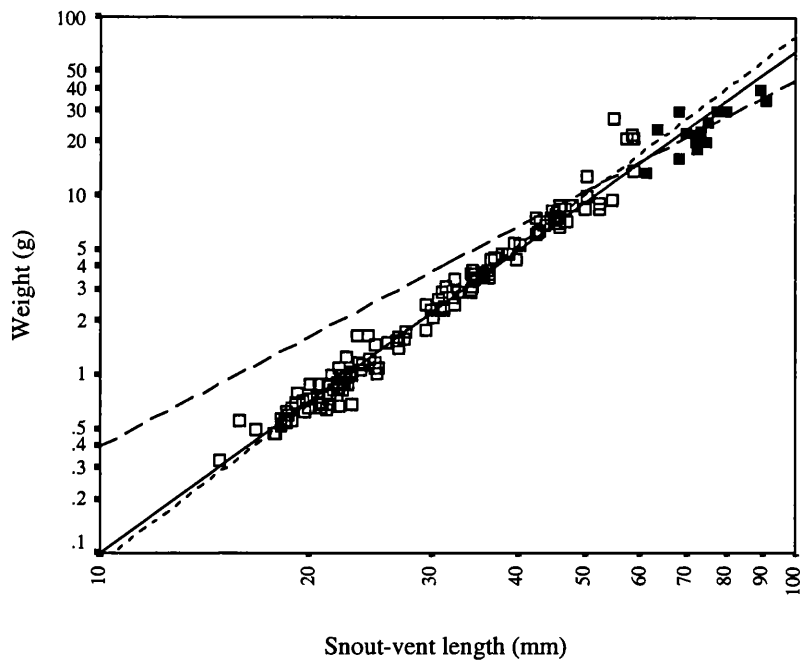


Figure 6.4: Log:log plot of weight increase with linear dimensions in juvenile (\square) and adult (\blacksquare) *P. venulosa*. Correlative statistics for: Total population ____ $r = 0.99$, $y = 2.81x - 3.81$, $t = 85.87$, $p < 0.001$, $n = 152$. Juveniles..... $r = 0.99$, $y = 2.95x - 4.00$, ($T = 75.69$), $p < 0.001$, $n = 136$. Adults _ _ _ $r = 0.76$, $y = 2.05x - 2.46$, $t = 4.41$, $p < 0.001$, $n = 16$.

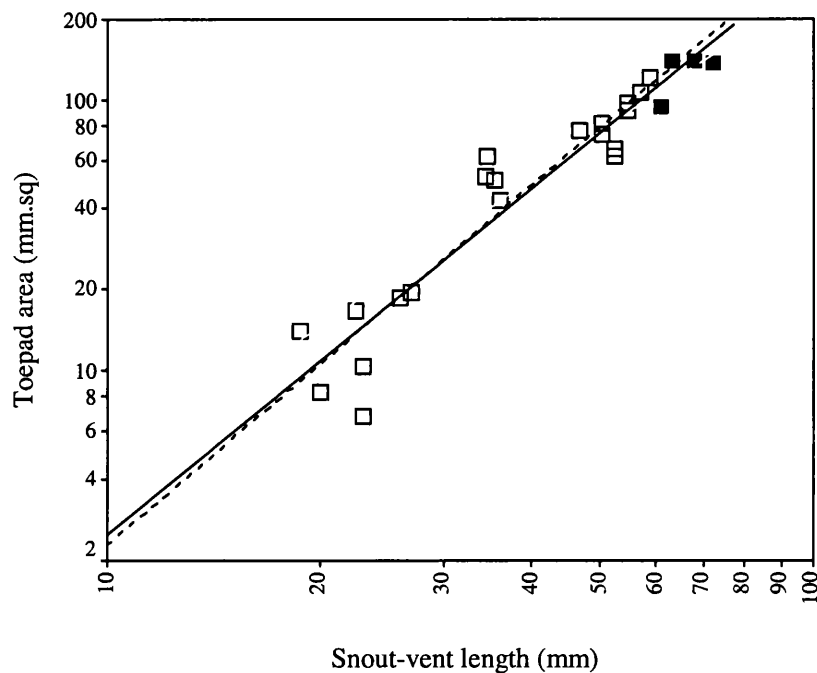


Figure 6.5: Log:log plot of toe pad area increase with linear dimensions in juvenile (\square) and adult (\blacksquare) *P. venulosa*, Correlative statistics for: Total population ____ $r = 0.95$, $y = 2.13x - 1.74$, $t = 14.87$, $p < 0.001$, $n = 24$. Juveniles..... $r = 0.94$, $y = 2.21x - 1.85$, $t = 12.12$, $p < 0.001$, $n = 20$.

Significantly then, with growth the increase in toe pad area is not sufficient to match the increase in weight involved in growth from new metamorph to adult. However, perhaps in part due to the variability seen in adult data, the difference in rates of increase in toe pad area and weight are not significantly different from one another ($t = 0.05$, N.S. 32 d.f.). The implications of these comparative rates of increase in weight and area on the adhesive abilities in these frogs, chiefly influenced as they are by area of contact, will become progressively adversely affected in the growth period from metamorph to juvenile. Additionally; it might be expected that although adults will adhere less well than the juvenile frogs, within the adult age class alone there should be no effect of size on the average adhesive abilities of the individual.

Phyllomedusa trinitatis

Phyllomedusa trinitatis metamorphose at a relatively large size, at around 20mm in snout vent length. Adults are around four times this size at maturity, with male frogs captured in the field in Trinidad averaging in size at $71.23 \text{ mm} \pm 0.85$ ($n = 12$) and females being around $86.50 \text{ mm} \pm 0.95$ ($n = 2$). If this increase in linear dimensions is accompanied by an increase in weight following predictions for isometric growth then this four-fold increase in linear dimensions will be accompanied by a sixty-four-fold increase in weight.

If the relationship between linear dimensions and weight across the age classes is considered on a log:log plot (**Figure 6.6 a**) mass can be seen to increase as $(\text{SVL})^{2.68}$, significantly less than the expected rate of 3 ($t = 10.67$, $p < 0.01$, 116 d.f.). Within the juvenile age class although weight is increasing at a rate closer to that expected, as

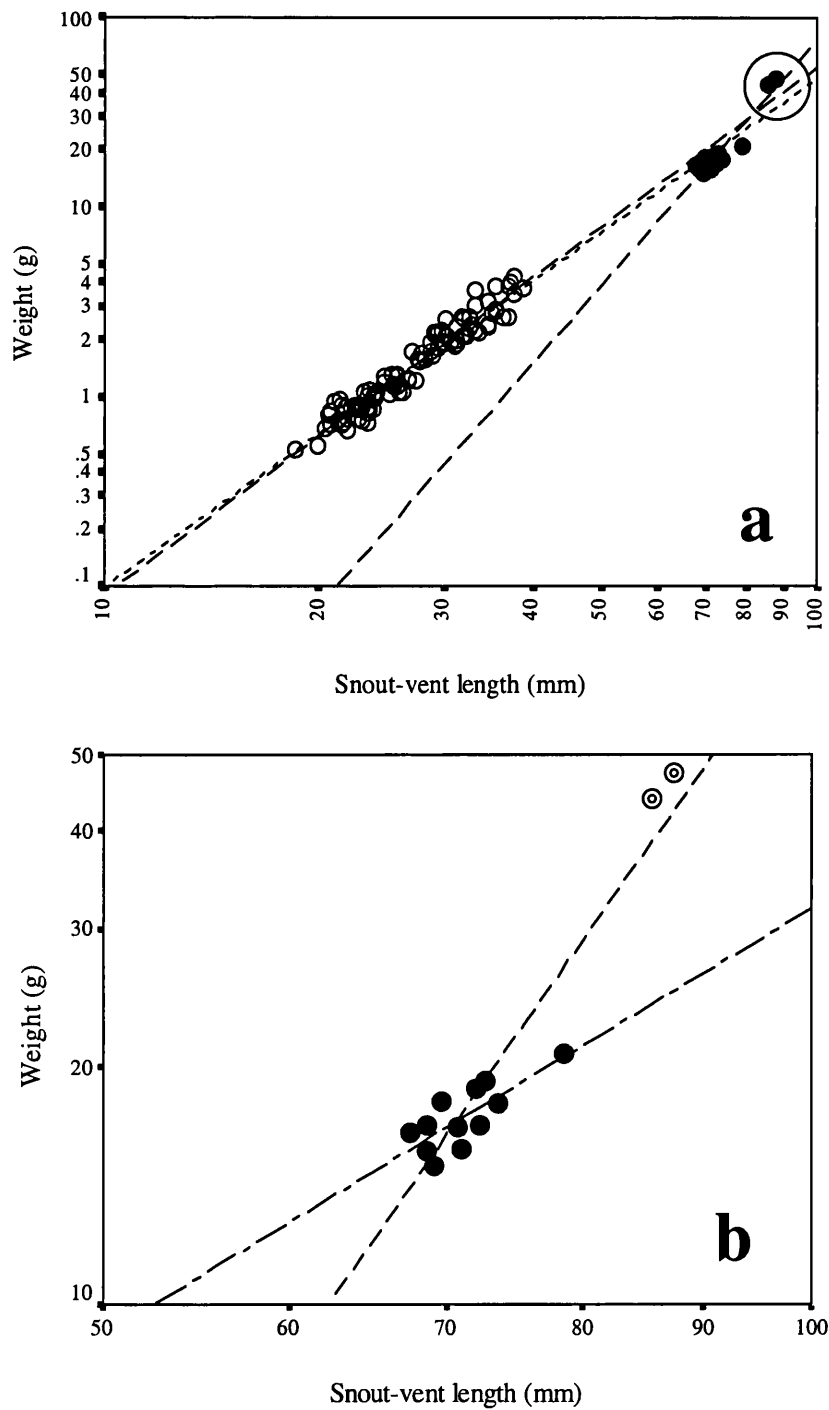


Figure 6.6: Log:log plots of weight increase with linear dimensions in (a) juvenile (○) and adult (●) *P. trinitatis*. (b) male (●) and female (⊙) adult *P. trinitatis*. Correlative statistics for: Total population — $r = 0.99$, $y = 2.68x - 3.68$, $p < 0.01$, $n = 118$; Juveniles $r = 0.97$, $y = 2.78x - 3.82$, $p < 0.01$, $n = 104$; All Adults _ _ $r = 0.94$, $y = 4.28x - 6.67$, $p < 0.01$, $n = 14$; Adult ♂ — — — $r = 0.77$, $y = 1.80x - 2.09$, $p < 0.01$, $n = 12$.

(SVL)^{2.78}, this is still less than the expected increase with isometric growth, as (SVL)³ ($t = 3.14$, $p < 0.01$, 102 d.f.). Within the adult age class alone there is an opposite trend with a greater than expected rate of weight increase if both sexes are considered together, increasing as (SVL)^{4.28} (Difference from slope of 3: $t = 2.98$, $p < 0.01$, 12 d.f.). However, the effect of the two females on the calculated line of best fit can be seen to be highly influential on the analysis (**Figure 6.6 a and b**). Removing the female data from the analysis of the relationship between weight and linear dimensions in adults gives a relationship in male frogs alone such that weight increase is occurring as (SVL)^{1.80}, significantly less than the expected (SVL)³ with isometric growth ($t = 2.55$, $p < 0.05$, 10 d.f.).

Toe pad area increase in these frogs tends towards a greater than expected rate of increase, both across the age classes and within the juveniles alone (**Figure 6.7**). The trend is not a significant one across the age classes, with area increasing as (SVL)^{2.29} rather than as the linear dimension squared ($t = 1.38$, N.S. 9 d.f.). Within the juvenile age class alone, the increase in toe pad area with growth is significantly greater than expected from isometry (Difference from slope of 2: $t = 2.33$, $p < 0.05$, 8 d.f.). Increasing at the rate it is, as (SVL)^{2.93}, the increase in toe pad area is no different to the correspondent increase in weight in juvenile frogs ($t = 0.05$, N.S. 110 d.f.).

If area dependent forces chiefly influence adhesion in these frogs, then within the juvenile age classes alone, the observed combination of reduced weight gain and proportionally high toe pad area increase will mean that sticking ability should not be detrimentally affected. Between the age classes, the increase in weight is not matched by the toe pad area increase ($t = 2.45$, $p < 0.01$, 125 d.f) and so adults will probably

show a reduced sticking ability in comparison to juvenile frogs. These predictions in terms of the average detachment angles recorded from each of these frogs and the adhesive forces calculated from these will be considered in 6.3.2.

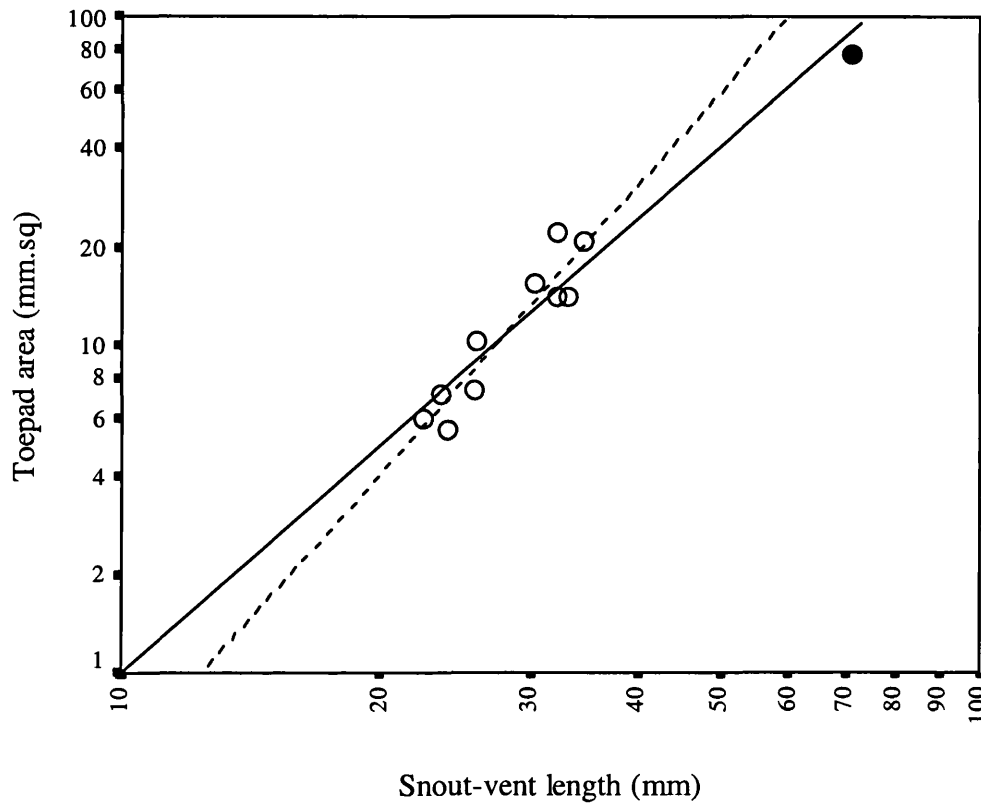


Figure 6.7: Log:log plot of toe pad area increase with linear dimensions in juvenile (○) and adult (●) *P. trinitatis*. Correlative statistics for: Total population _____ $r = 0.96$, $y = 2.29x - 2.29$, $t = 10.76$, $p < 0.01$, $n = 11$; Juveniles..... $r = 0.93$, $y = 2.93x - 3.20$, $t = 7.39$, $p < 0.01$, $n = 10$.

Hyla boans

H. boans are the largest frogs in this study, with adults collected in the field averaging $94.86 \text{ mm} \pm 1.15$ ($n = 10$) in SVL. Although frogs collected whilst calling could be diagnosed as male, sexes are otherwise difficult to determine using external characteristics (6.2.1) and so are likely to be combined in the analyses of adult data. Froglet SVL measurements are $14.59 \text{ mm} \pm 0.23$ ($n = 8$) at metamorphosis; growth

from new metamorph to adult therefore involves around a seven-fold increase in linear dimensions, which if accompanied by an increase in weight as expected through isometry will mean adults are three hundred and forty three times as heavy as the juveniles. With juveniles weighing around 0.2g and adults 50g, the actual increase in weight is around two hundred and fifty-fold, suggesting that weight gain with growth is occurring at a lesser rate than isometric predictions would suggest.

The rate of weight increase between juvenile and adult increases as $(SVL)^{2.82}$, (**Figure 6.8**), confirming the prediction that there is a lower than expected weight gain in this species ($t = 6.00$, $p < 0.01$, 16 d.f.). Within the two age classes the rates of increase in weight with linear dimensions are higher than seen across the whole population; though in neither case is this a significant difference, nor are the relationships between these variables different to the expected increase with isometry, as the linear dimension cubed (Differences from slope of 3: $t_{\text{juv}} = 1.92$, N.S. 6 d.f: $t_{\text{adult}} = 0.74$, N.S. 8 d.f.).

Although there are only limited data available for toe pad area in this species, (**Figure 6.9**), the line of best fit between these points, suggests that area is scaling as $(SVL)^{1.98}$ at a rate no different to the slope of two on a log:log plot expected through isometric growth ($t = 0.40$, N.S.).

Across the age classes, in spite of a reduced rate of weight increase with growth the toe pad area increase occurs at a significantly lesser rate ($t = 14.41$, $p < 0.01$, 14 d.f.). We might therefore expect to see a reduction in the adhesive ability of adult frogs in comparison to juveniles whereas within the new metamorphs alone, sticking ability will be likely to be unaffected by size.

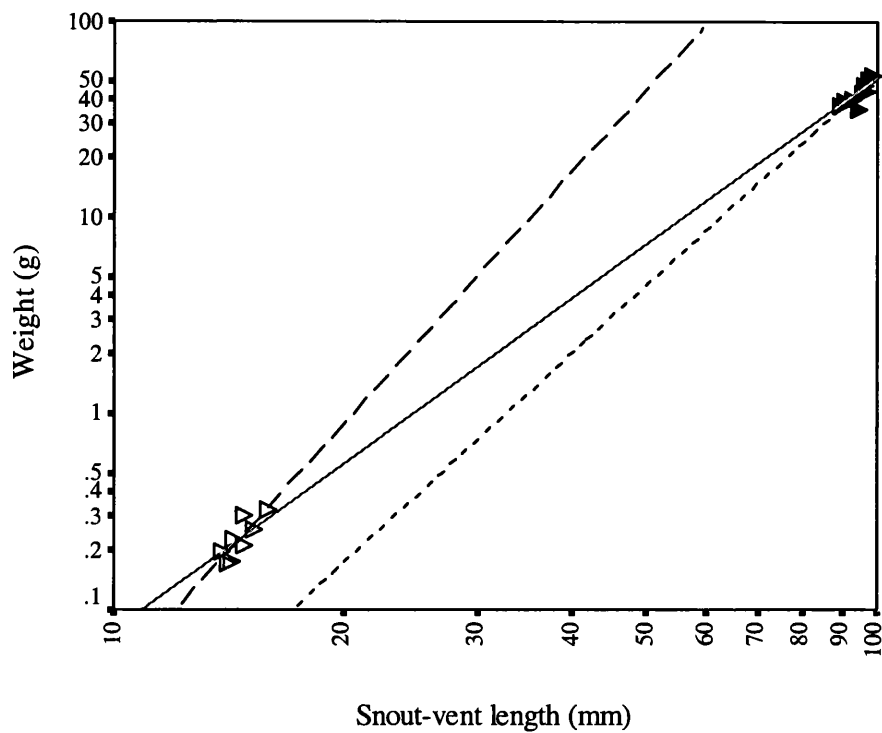


Figure 6.8: Log:log plot of increase in weight with linear dimensions in juvenile (\triangle) and adult (\blacktriangleright) *H. boans*. Correlative statistics for: Total population ____ $r = 1.00$, $y = 2.82x - 3.93$, $t = 95.06$, $p < 0.001$, $n = 18$. Juveniles..... $r = 0.83$, $y = 4.29x - 5.64$, $t = 3.59$, $p < 0.01$, $n = 8$. Adults_ _ $r = 0.86$, $y = 3.56x - 5.39$, $t = 4.71$, $p < 0.002$, $n = 10$

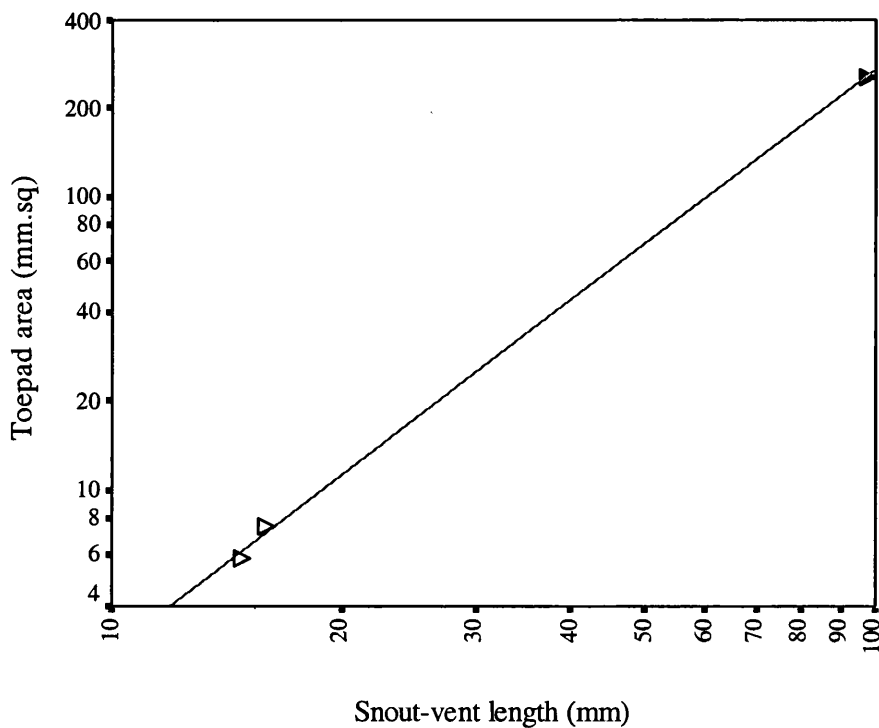


Figure 6.9: Log:log plot of increase in toe pad area with linear dimensions in juvenile (\triangle) and adult (\blacktriangleright) *H. boans*. Total population ____ $r = 0.999$, $y = 1.98x - 1.52$, $t = 37.57$, $p < 0.02$, $n = 3$.

6.3.2. Size effects on adhesion

Phrynohyas venulosa

Predictions from morphometry are borne out when the angles to which frogs belonging to the two age classes are able to adhere to the Perspex rotation platform are considered. There is a negative relationship between angle and linear dimensions across the total population and within the juveniles alone (**Figure 6.10**). This is further confirmed by comparing average angles of detachments in juveniles and adults, which at $129.02^\circ \pm 1.18$ ($n = 136$) and $121.14^\circ \pm 3.25$ ($n = 16$) respectively, are significantly different from one another ($t = 2.17$, $p = 0.03$, 150 d.f.)

Adhesive force calculated from these angles (**2.2.2**) increase with SVL at a greater rate than an adhesive system dependent on area would predict (**Figure 6.11**). This is particularly pronounced amongst the juveniles, where the adhesive forces are scaling with linear dimensions to the power of 2.72. Although this elevated rate of adhesive force production is significantly greater than the observed increase in toe pad area seen in the same frogs ($t = 2.53$, $p < 0.01$, 152 d.f.) it is not sufficient to match the increase of weight in the same growth period ($t = 2.34$, $p < 0.05$, 268 d.f.). Adding adults to the data set has no significant effect on the rate of increase in adhesive force production (Difference from slope of juveniles alone; $t = 1.16$, N.S. 284 d.f.) though the slope of the line of best fit is somewhat reduced in comparison, with adhesive forces scaling as $(SVL)^{2.58}$. The increased rate of adhesive force production is not sufficient to match the increase in weight in the same period of growth ($t = 2.66$, $p < 0.01$, 300 d.f.) but is greater than the toe pad area increase in these frogs ($t = 2.79$, $p < 0.01$, 172 d.f.).

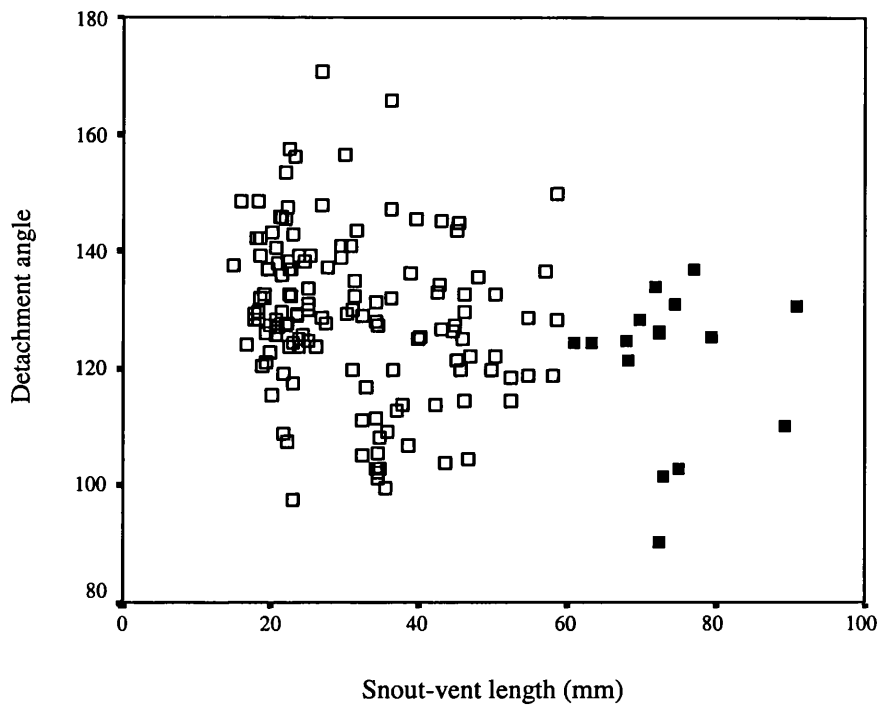


Figure 6.10: Angles of last contact in juvenile (\square) and adult (\blacksquare) *P. venulosa*. Correlative coefficients for: Total population, $r = 0.26$, $y = 135.71 - 0.21x$, $t = -3.31$, $p < 0.01$, $n = 152$; Juveniles, $r = 0.21$, $y = 137.19 - 0.26x$, $t = -2.55$, $p < 0.01$, $n = 136$; Adults, $r = 0.03$, N.S. $n = 16$.

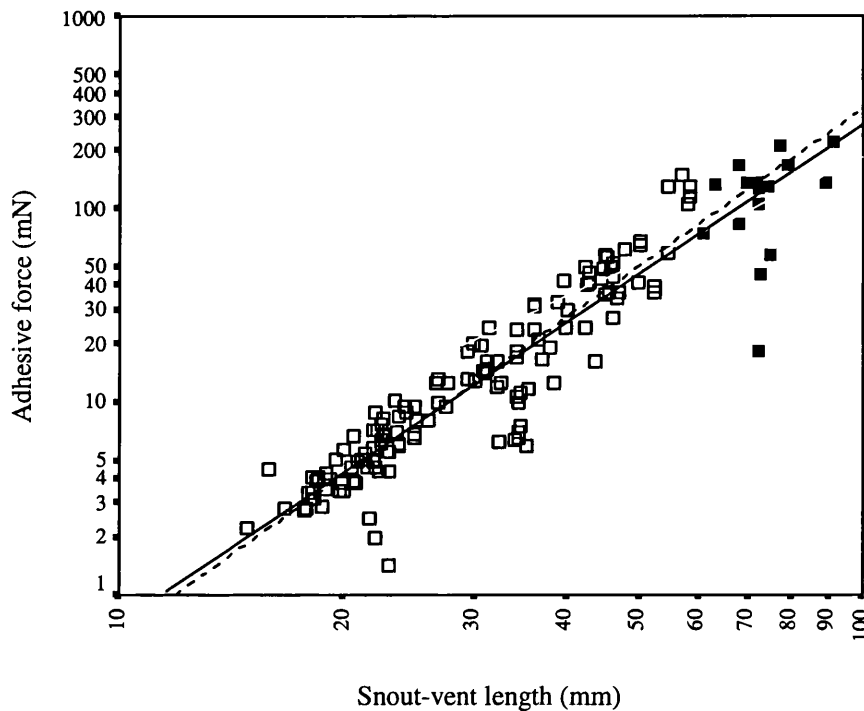


Figure 6.11: Log:log plot of adhesive force production with increasing linear dimensions in juvenile (\square) and adult (\blacksquare) *P. venulosa*. Total population____ $r = 0.94$, $y = 2.58x - 2.72$, $t = 33.02$, $p < 0.01$, $n = 152$; Juveniles..... $r = 0.93$, $y = 2.72x - 2.93$, $t = 28.68$, $p < 0.01$, $n = 136$; Adults___ $r = 0.30$, N.S. $n = 16$.

Phyllomedusa trinitatis

Both juvenile and adult *P. trinitatis* show poor sticking ability on the control platform (**Figure 6.12**); they very seldom achieve angles above 120° and there are no incidences of full rotations in either age class. There is no correlative effect of size on the angle to which frogs within either age cohort are able to maintain a grip upon the surface (**Figure 6.12**). Unusually, in view of results in other species, there is a slight increase in the angle to which the adults are able to stick in comparison to that seen in juveniles with values for the average detachment angles being $111.56^\circ \pm 2.59$ ($n = 14$) and $104.65^\circ \pm 0.85$ ($n = 104$) respectively (Difference between means: $t = -2.75$, $p = 0.007$, 116 d.f.). Subsequently there is a weak positive correlation between average detachment angle and size in this species (**Figure 6.12**).

Adhesive forces produced across the age classes increase at a rate of $(SVL)^{3.10}$, (**Figure 6.13**) significantly higher than the expected increase of linear dimensions squared that would arise in a system dependent on toe pad area ($t = 7.86$, $p < 0.01$, 116 d.f.). Furthermore, adhesive forces increase at a considerably greater rate than the actual observed increase in toe pad area, which scales much as would expected between the age classes (**6.3.1**): $t = 3.21$, $p < 0.01$, 125 d.f. The weight increase seen across the whole population is lower than isometric expectations in this species, scaling with $(SVL)^{2.68}$. The implication of this is that the rate of increase in adhesive force production is more than able to cope with the weight increase with growth from juvenile to adult, occurring across the age classes at a rate significantly higher than this ($t = 2.93$, $p < 0.01$, 232 d.f.).

Within the juvenile frogs alone (**Figure 6.13**) this is also the case, with adhesive forces increasing as $(SVL)^{3.15}$, at a rate that is not significantly different to that seen across the population as a whole ($t = 0.14$, N.S. 232 d.f.). This is significantly higher than the expected increase as linear dimensions squared that would be seen if toe pad area were increasing as predicted with isometric growth in these frogs, ($t = 3.59$, $p < 0.01$, 102 d.f.). However, within the juveniles alone, toe pad area is increasing at a rate significantly greater than these predictions, as $(SVL)^{2.93}$. So although adhesive force production is occurring at a rate that matches the weight increase ($t = 1.13$, N.S. 204 d.f.), in juveniles this can also be seen to match the correspondent disproportionate increase in toe pad area with growth in the species ($t = 1.00$, N.S. 110 d.f.).

Adhesive forces increase within the adult cohort (**Figure 6.13**) at a rate that is higher than that seen either within the juveniles or across the age classes, though the differences in the slopes of the lines of best fit are not significant. This is due in large part to the variability about the calculated line of best fit; the rate of increase in adhesive force seen in these frogs is no different to the increase in weight ($t = 0.19$, N.S. 24 d.f.) but neither is it different to the expected slope for area increase ($t = 1.59$, N.S. 24 d.f.).

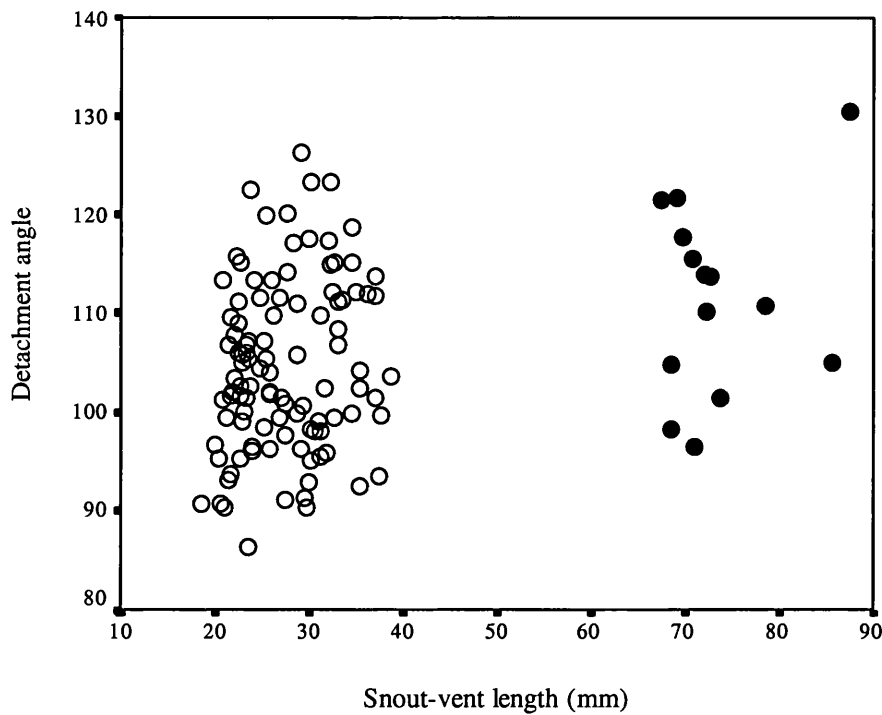


Figure 6.12: Detachment angles recorded in juvenile (○) and adult (●) *P. trinitatis*. Correlative statistics for: Total population, $r = 0.29$, $t = 3.30$, $p < 0.001$, $n = 118$; Juveniles, $r = 0.18$, $t = 1.80$, N.S. $n = 104$; Adults, $r = 0.22$, $t = 0.80$, N.S. $n = 14$.

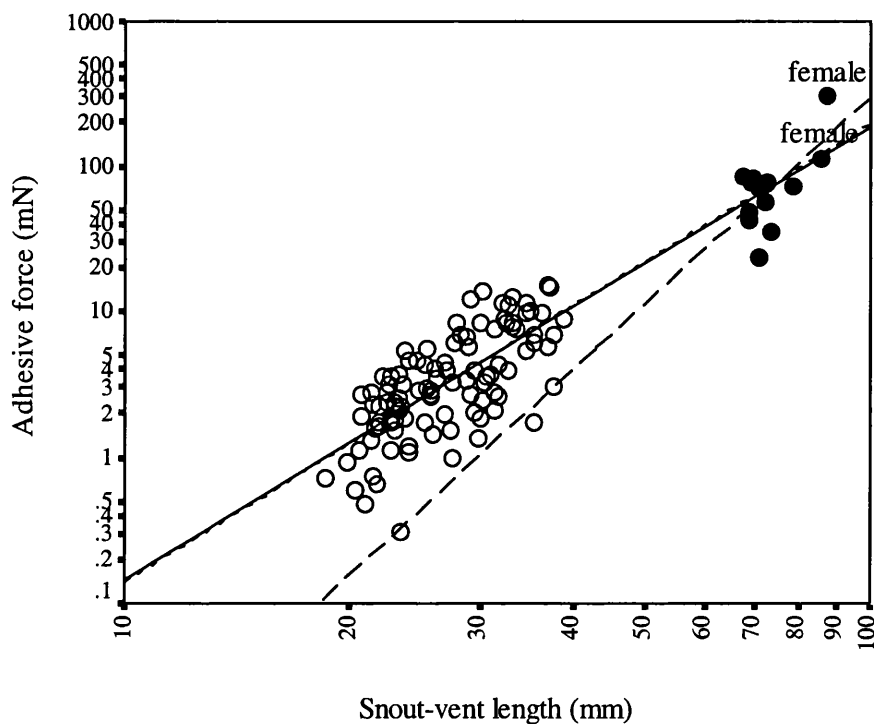


Figure 6.13: Log:log plot of adhesive force production with increasing linear dimensions in juvenile (○) and adult (●) *P. trinitatis*. Correlative statistics for: Total population ____ $r = 0.89$, $y = 3.10x - 3.94$, $t = 21.49$, $p < 0.01$, $n = 118$; Juveniles... $r = 0.70$, $y = 3.15x - 4.00$, $t = 9.96$, $p < 0.01$, $n = 104$; Adults_ _ $r = 0.63$, $y = 4.60x - 6.74$, $t = 2.83$, $p < 0.02$, $n = 14$.

Hyla boans

If we assess sticking ability by considering the average angles of detachment recorded in the two age classes (**Figure 6.14**) then it can be seen that there is a significant detriment in the ability of the adult frogs to adhere to the rotation platform. Across the population there is a negative correlative relationship between detachment angle and size (**Figure 6.14**). Average angles of detachment in the juveniles are high, at $171.02^\circ \pm 2.36$ ($n = 8$), with this in part explained by the high incidence of full rotations within the age class, with $61.30\% \pm 8.95$ ($n = 8$) of angles being 180° . Adults are never able to attain full rotations with average detachment angles of only $114.06^\circ \pm 4.51$ ($n = 10$), significantly lower than seen in juvenile frogs (Difference between means; $t = 10.04$, $p < 0.01$, 16 d.f.) The high incidence of 180-degree angles recorded in the juveniles means that the estimation of adhesive forces able to be produced in these frogs is likely to be an underestimate, due to the limitations imposed by the methodology. The slope of the line of best fit derived for the total population on a log:log plot of the adhesive forces with increasing linear dimensions is therefore likely to be steeper than that seen in **Figure 6.15**.

In spite of this, the observed increase between the two variables across the population, as $(SVL)^{2.14}$ is no different to that expected if adhesive forces are primarily influenced by area, as the linear dimension squared ($t = 0.61$, N.S. 16 d.f.) The increase in adhesive forces produced between the age classes is therefore not sufficient to match the increase in weight involved in the same time period ($t = 2.96$, $p < 0.01$, 32 d.f.).

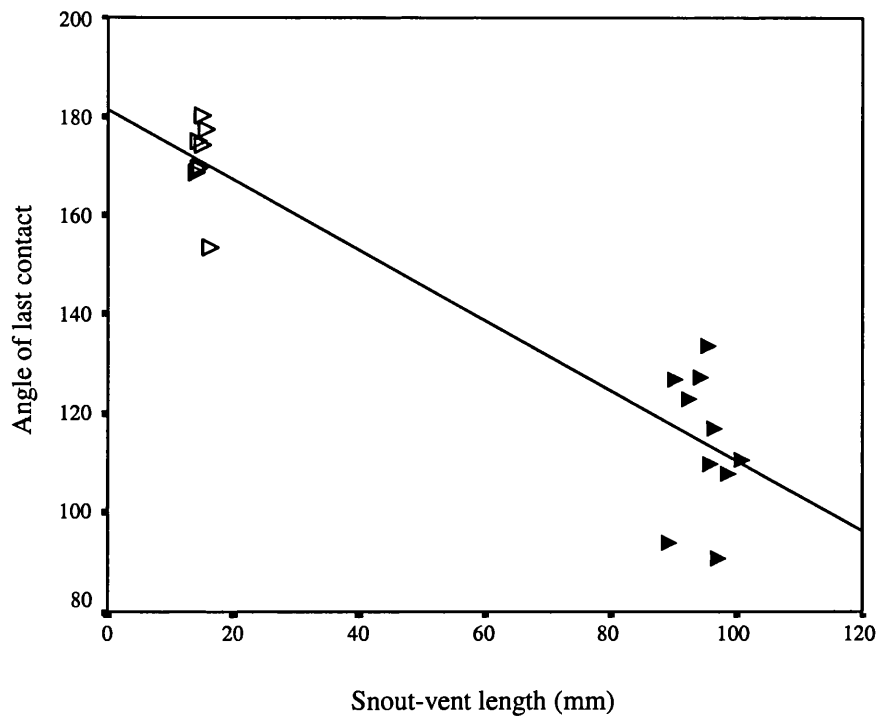


Figure 6.14: Average detachment angles recorded from juvenile (\triangle) and adult (\blacktriangle) *H. boans*.

Correlative statistics: Total population: $r = 0.93$, $y = 181.34 - 0.71x$, $t = -10.16$, $p < 0.001$, $n = 18$.

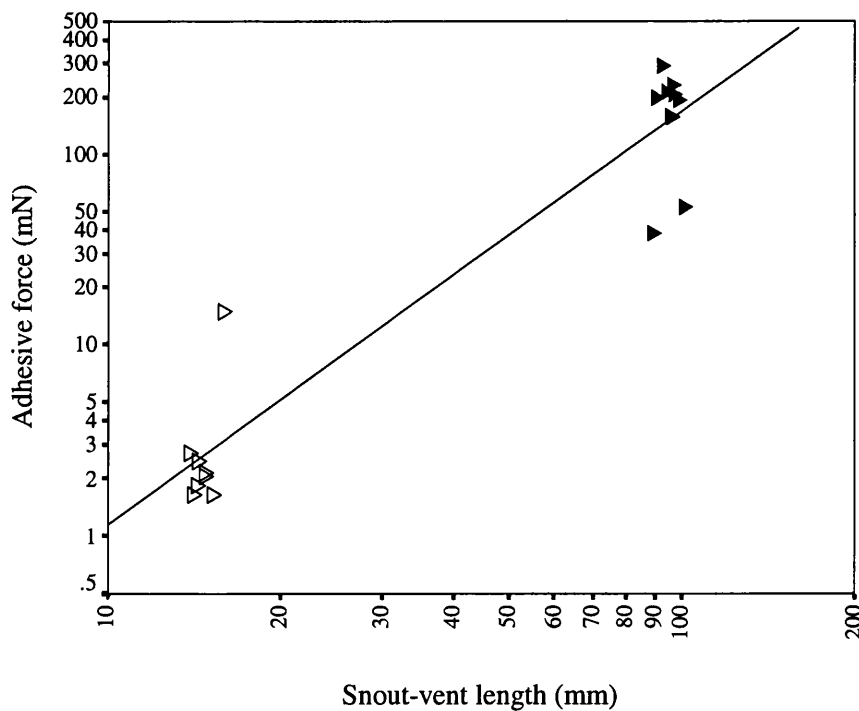


Figure 6.15: Log:log plot of adhesive force increase with linear dimensions in juvenile (\triangle) and adult (\blacktriangle) *H. boans*. Total population: $r = 0.92$, $y = 2.14x - 2.16$, $t = 9.30$, $p < 0.01$, 17 d.f. Juveniles: $r = 0.77$, $y = 3.79x - 4.08$, $t = 2.97$, 7 d.f. Adults: $r = 0.09$, N.S. 9 d.f.

There is a positive correlation between snout-vent length in the juvenile age class and adhesive force production in this species. However, there is no statistically significant difference between this slope and the predicted slope of two for area increase ($t = 1.39$, N.S. 16 d.f.), the predicted slope of three for weight increase ($t = 0.62$, N.S. 16 d.f.) or from the relationship within the population as a whole ($t = 1.27$, N.S. 22 d.f.). No relationship between the linear dimension and adhesive force exists within adults (**Figure 6.15**).

This suggests that in this largest species of frog the increase in adhesive force scaling with toe pad area is not sufficient for *H. boans* to maintain adhesive abilities with growth between metamorphosis and adulthood. This is manifest in the greater differences between the average detachment angles seen between the age classes in this largest hylid species than in any of the smaller species discussed thus far, including *P. trinitatis* and *P. venulosa*.

Large species

Within *P. venulosa* and between the large species a positive correlation exists between the force per millimetre squared of toe pad and the increasing linear dimension (**Figure 6.16**), suggesting that there is an improvement in the adhesive mechanism in effect in larger frogs in these instances.

How then might the changes in toe pad efficiency be implemented? The wet adhesive mechanism is influenced by a number of separate components; the nature of the intervening liquid layer, as yet undetermined, and the nature of the adherent surfaces. In juvenile and adult frogs tested on Perspex, the nature of the rotation platform

remains the same in all of the rotational experiments from which these values for force per unit area are derived, so changes in the system may again be facilitated by changes in the meniscal layer or in the other adherent surface – the toe pad. S.E.M. studies of the toe pad surface were undertaken to consider morphology with respect, in particular, to structural development that might reflect an increased ability to maintain lower meniscal heights and/or adjust the properties of the mucus that might explain the tendencies towards increased pad efficiency in larger frogs.

The performance of adult *P. trinitatis* on different substrates suggests that adhesive ability in this species is detrimentally affected on surfaces with low surface energies, i.e. those on which the spreading tendencies of a fluid are likely to be impaired (**Figure 6.17**). Similar trends exist in *P. venulosa* that may indicate that a reduction in adhesive ability might be expected with more data availability but in *H. boans*, which was tested on all seven substrates, no effect of decreasing surface wettability is seen. This suggests that there are quickly implementable changes to aspects of the adhesive mechanism in these species that compensate for the detrimental effect of poor wettability on a fluid-based adhesion system. As it has not been possible to test whether changes are occurring in the physico-chemical properties of the fluid in frogs adhering to these different substrates looking in particular at differences between the pads of the adults may illuminate what compensatory mechanisms might be being effected in this species.

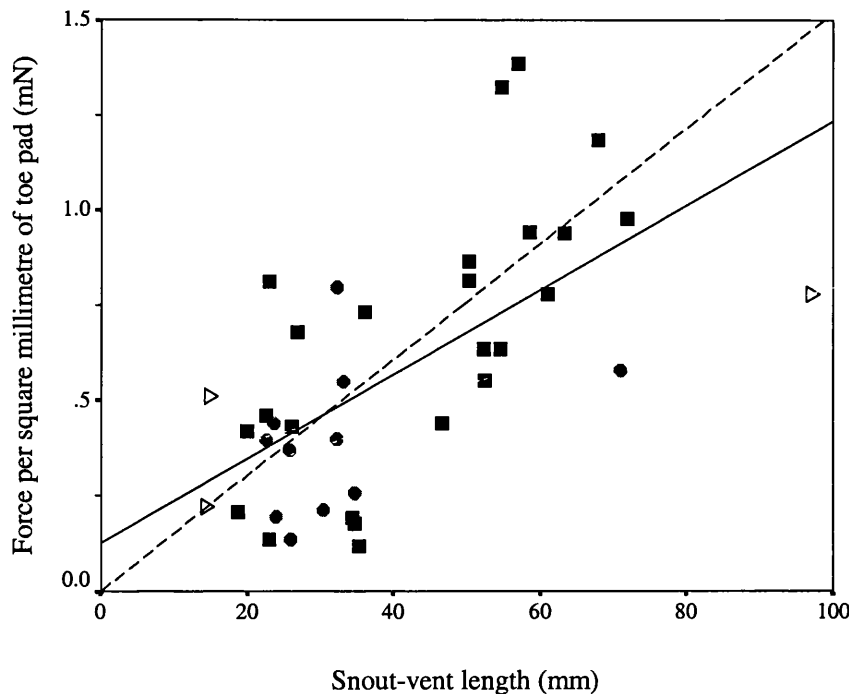


Figure 6.16: Adhesive force per square millimetre of toe pad vs. SVL in three large species of hylid frog: *P. venulosa* (■); *P. trinitatis* (●); *H. boans* (▷). Correlative statistics: All frogs, $r = 0.64$, Line of best fit $y = 0.01x + 0.13$, $t = 4.96$, $p < 0.001$, $n = 37$. Individual species: *P. venulosa*, $r = 0.69$, Line of best fit $y = 0.02x + 0.001$, $t = 4.51$, $p < 0.01$, $n = 24$; *P. trinitatis*, $r = 0.39$, N.S. $n = 11$. *H. boans*, $r = 0.86$, N.S. $n = 3$.

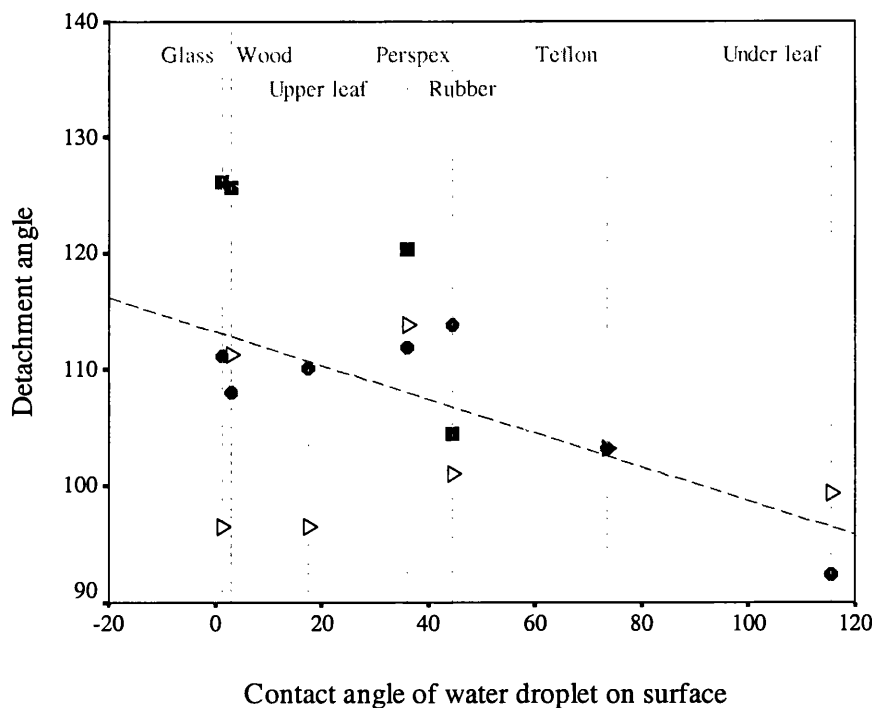


Figure 6.17: Average detachment angles recorded from adult frogs belonging to three large species of hylid frog: *P. venulosa* (■); *P. trinitatis* (●); *H. boans* (▷) on seven substrates of differing wettability (as defined by the contact angle of water droplet). Statistics: All frogs, $r = 0.53$, $t = -2.47$, $p = 0.03$, $n = 18$. Individual species: *P. venulosa*, $r = 0.86$, $t = -2.35$, $p = 0.14$, $n = 4$; *P. trinitatis*, $r = 0.82$, Line of best fit $y = 0.02x + 0.001$, $t = -3.17$, $p = 0.02$, $n = 7$; *H. boans*, $r = 0.13$, $p = 0.78$, N.S. $n = 3$.

6.3.3. Toe pad morphology

Phrynohyas venulosa

Cell structure in *P. venulosa* is no different to that seen in the other hylids (**Figure 6.18**) being columnar in nature with consistently sized cells, regularly hexagonal in shape (**Figure 6.19 b and d**). The underlying tonofilament bundles that give the sides their striated appearance are seldom exposed on the

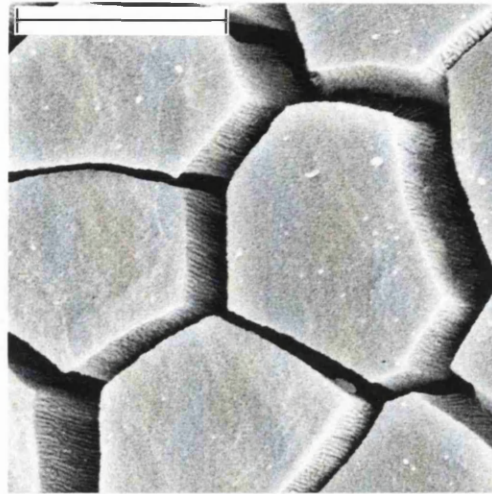


Figure 6.18: S.E.M. image of toe pad cells in juvenile *P. venulosa*. Scale bar = 12.50 μm .

apical surfaces with the cell coat being predominantly present in the samples studied here. Although the cells in adult and juvenile frogs are virtually indistinguishable in appearance, they do differ in size. Unusually, considering the results in most of the species discussed so far, cells in the adult sample ($133.23 \mu\text{m}^2 \pm 1.61$ ($n = 89$)) are significantly *larger* than those in the juveniles ($115.19 \mu\text{m}^2 \pm 1.23$ ($n = 259$)) ($F_{88,258} = 7.49$; Difference in medians: $U_{89,259} = 5289.50$, $p < 0.001$).

Consequently cell densities in adults ($7621.97 \text{ per mm}^2 \pm 213.22$, $n = 9$) are significantly lower than seen in juvenile frogs ($8901.94 \text{ per mm}^2 \pm 258.27$, $n = 26$); Difference between means: $t = 2.78$, $p < 0.01$, 33 d.f. If we consider the comparative areas taken up by mucosal pore openings in the two age classes (**Figure 6.19 c and d**) the discrepancies between the numbers of cells per mm^2 may be still greater.

Perhaps due to the lower cell densities seen in adult frogs, the average length of intercellular channel lengths per mm^2 of pad is also affected, dependent as the measurement is on the sum of the perimeter lengths. The reduced value in adult frogs, ($134.06 \text{ mm/mm}^2 \pm 4.29$, $n = 9$), is significantly lower than that seen in the juvenile samples ($152.58 \text{ mm/mm}^2 \pm 3.44$, $n = 25$); difference between means: $t = 2.94$, $p = 0.006$, 32 d.f. As in other species, the width of the intercellular channels across the pad is highly variable, with this being the case irrespective of the frog's age or size.

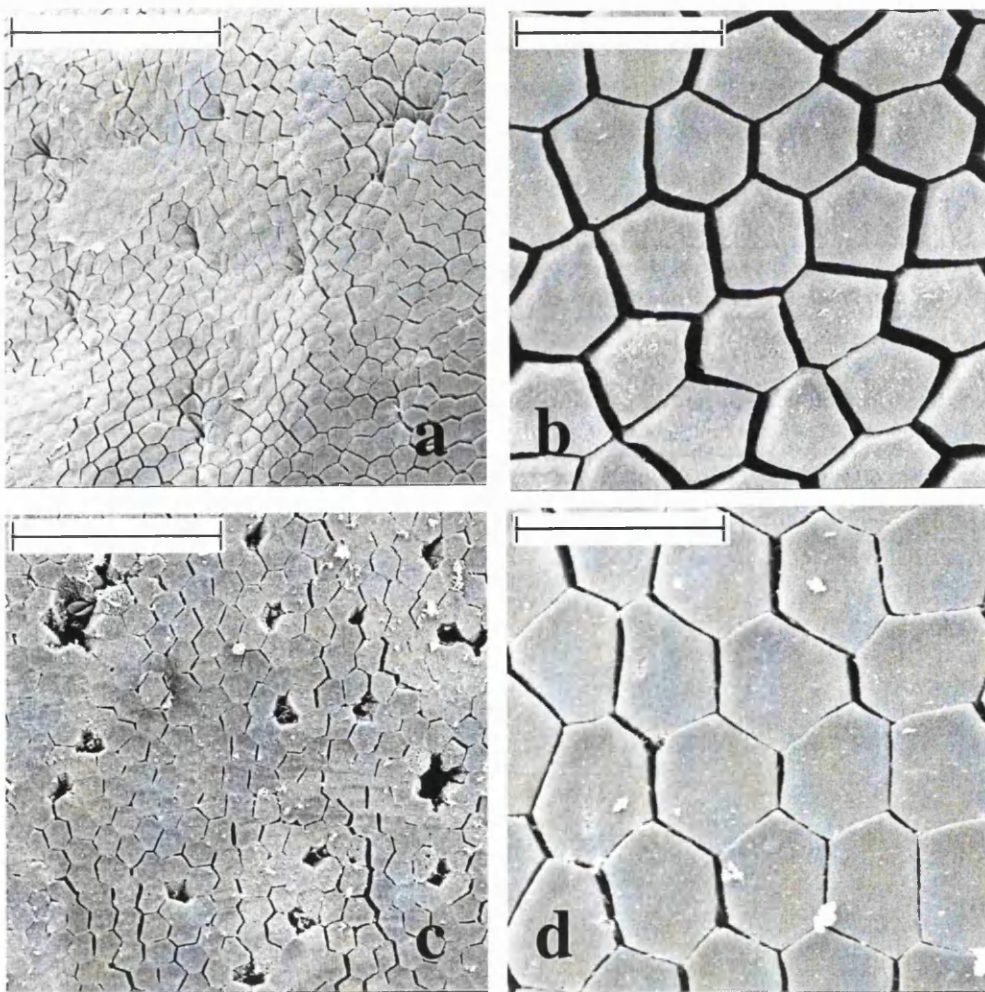


Figure 6.19: S.E.M. images of toe pad cells in *P. venulosa*: (a) Juvenile 2 (26mm) Front 1, Scale bar = $100 \mu\text{m}$ (b) Juvenile 2 (26mm) Front 3, Scale bar = $25 \mu\text{m}$. (c) Adult (72mm) Front 4, Scale bar = $100 \mu\text{m}$ (d) Adult (72mm) Back 3, Scale bar = $25 \mu\text{m}$.

Sizes of the mucosal pores in juveniles are generally small, though variable, with a mean value for the area of the pore opening of $46.04 \mu\text{m}^2 \pm 11.11$ ($n = 21$). Juveniles have both Type I and Type II pores; the former type are infrequent, rounded in shape and bordered in the main by three to four cells (**Figure 6.20 b**). A number of pores are of the stomatal type seen most frequently in the smaller species in this study, the sculpturing of the walls is not visible (**Figure 6.20 a**). The majority of pores are Type II, with modified lumen walls; in the main these have simple geometrically shaped openings framed by between five and seven cells (**Figure 6.20 c**), though hexagonal pores are the most prevalent (**Figure 6.20 d**).

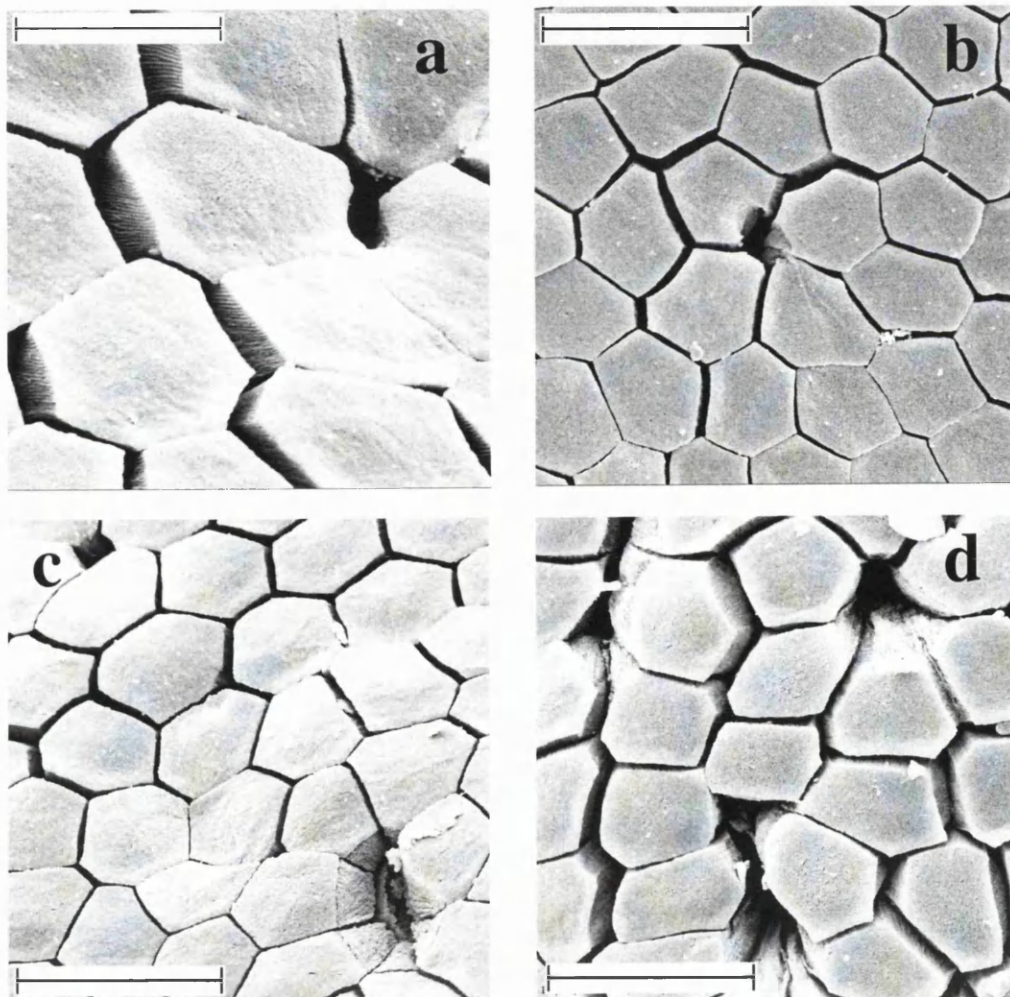


Figure 6.20: S.E.M. images of mucosal pores in juvenile *P. venulosa*: (a) Juvenile 1 (23mm) Back 3, Scale bar = $12.5 \mu\text{m}$. (b) Juvenile 2 (26mm) Back 3, Scale bar = $25 \mu\text{m}$ (c) Juvenile 1 (23mm) Front 1, Scale bar = $25 \mu\text{m}$ (d) Juvenile 1 (23mm) Back 1, Scale bar = $25 \mu\text{m}$

Average mucosal pores in adults, at $140.96 \mu\text{m}^2 \pm 19.12$ ($n = 23$) in size, are considerably greater in area than seen in juvenile frogs ($F_{22, 20} = 3.24$, $U_{21, 23} = 77.00$, $p < 0.01$). No Type I pores are evident in adults of this species; although there are some similar rounded pores present in the sample, the lumen walls of these are modified (**Figure 6.21 a**). The age classes do however share the simple geometrical Type II pores most prevalent in the juvenile samples (**Figure 6.21 a and b**) and these are again the most common in the adult sample. There are a number of pores in the adult frogs formed from combinations of simple geometrical shapes, ranging from large holes (**Figure 6.21 b and c**) to large slit-like structures apertures on the pad surface (**Figure 6.21 d**).

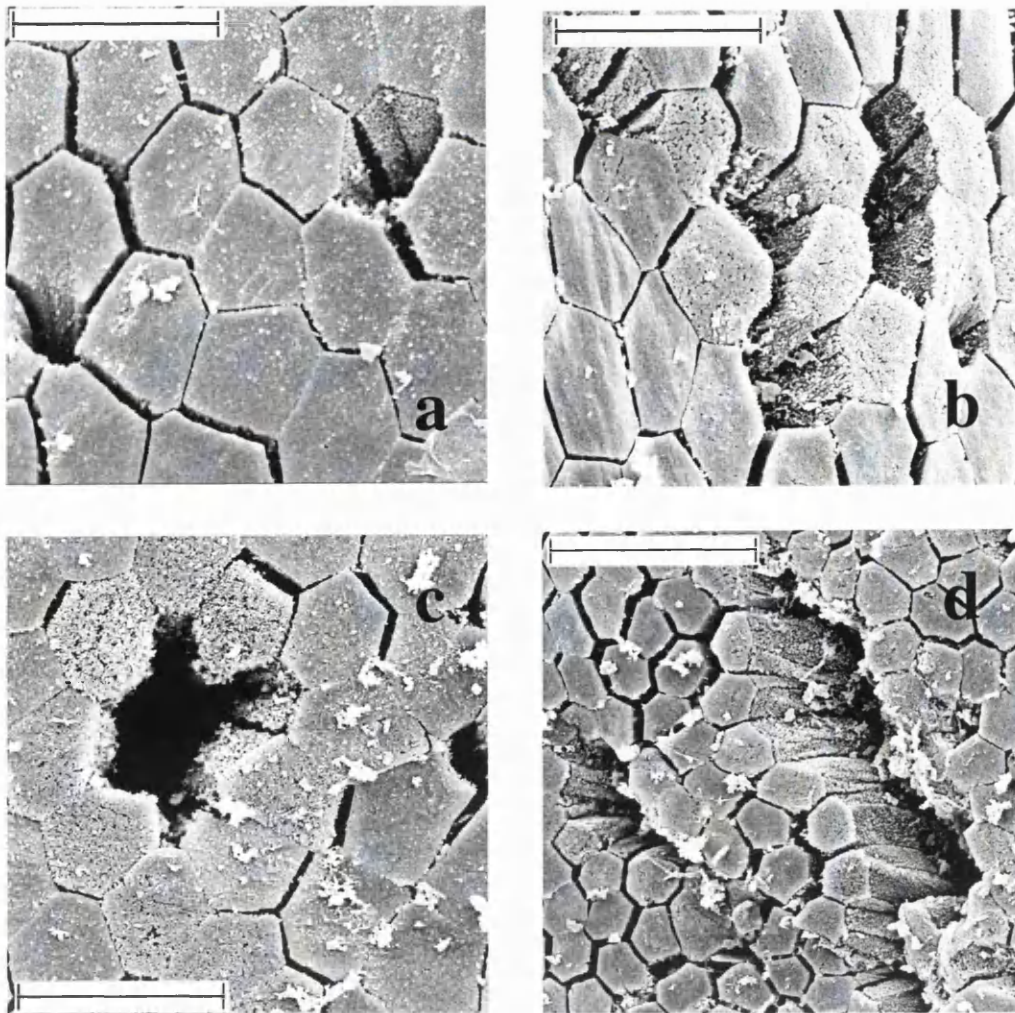


Figure 6.21: S.E.M. images of mucosal pores in adult *P. venulosa*: (a) Back 4, Scale bar = 25 μm (b) Front 2, Scale bar = 25 μm (c) Front 4, Scale bar = 25 μm (d) Front 1, Scale bar = 50 μm .

Mucosal pore counts suggest high numbers of pores on pads of adults (ca. 130 per pad) in comparison to around ten to twenty on juvenile pads. Nevertheless, the differences in pad size between the two age classes means that these counts translate to mucosal pore densities that are not effectively different. In juveniles pore densities average at $22.42 \text{ per mm}^2 \pm 2.49$ ($n = 22$); whilst the adult value is marginally lower, at $18.98 \text{ per mm}^2 \pm 2.60$ ($n = 9$), the difference in their means is not statistically significant ($(F_{8,21} = 1.26) t = 0.81, p = 0.42, \text{N.S. } 29 \text{ d.f.}$)

Pores in both juveniles and adults appear evenly distributed across the pad, though the numbers of pores on the smallest juveniles are so few as to make assessment difficult. There are further difficulties in assessing pore distributions using full pad images in adults, as the magnifications required to see the whole pad are generally too low to detect any but the very largest pore openings. These are often distributed over the lower half of the pad (**Figure 6.22 f**) towards the proximal margin.

Whole pad images do show other trends in structural development of the pads with growth in these frogs (**Figure 6.22**). As in other species, there is an evident flattening of the pad elevation between the juvenile and adult age classes accompanied by a development of the circumferal marginal area.

The circumferal groove is well developed in the adult sample (**Figure 6.24 c**) extending almost full-circle around the pad to nearly meet up with the lateral grooves running down the sides of the toe (**Figure 6.22 e**). In the juveniles, the circumferal groove is shallow and poorly developed (**Figure 6.24 a**) with the maximal extension of the groove in the smallest frog reaching a point less than half way around the pad.

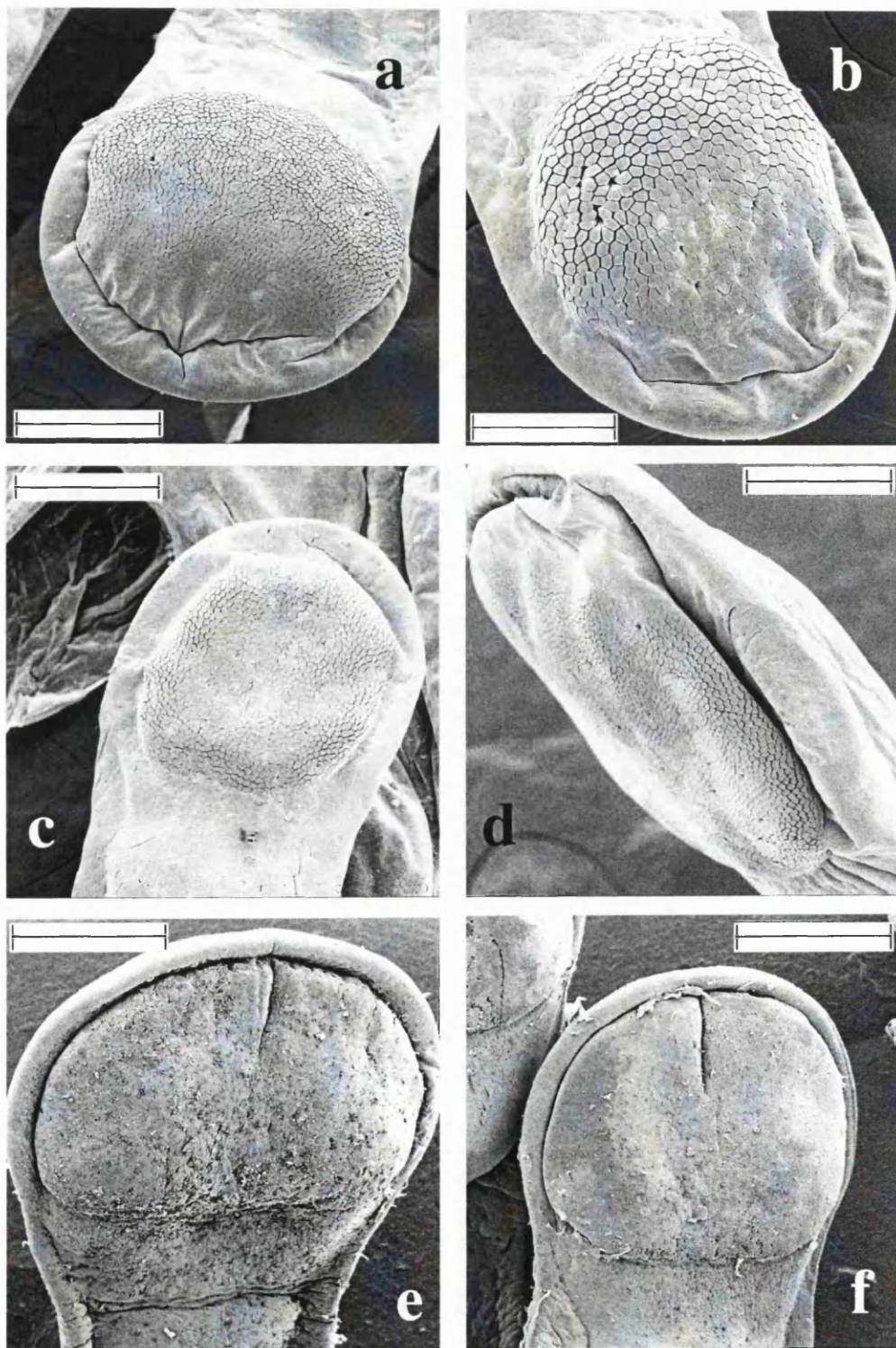


Figure 6.22: S.E.M. images of toe pads in *P. venulosa*: (a) Juvenile 1 (23mm) Front 2, Scale bar = 300 μ m (b) Juvenile 1 (23mm) Back 1, Scale bar = 150 μ m. (c) Juvenile 2 (26mm) Back 1, Scale bar = 300 μ m (d) Juvenile 2 (26mm) Back 4, Scale bar = 300 μ m (e) Adult (72mm) Front 2, Scale bar = 1.25 mm (f) Adult (72mm) Back 3, Scale bar = 1.25 mm.

Additionally, a number of toes in the adult sample have a pronounced groove running down from the circumferal margin to approximately a third of the way down the pad (**Figure 6.22 e and f**). Although it is possible that this is an artefactual result the tuck in the circumferal margin that is evident in one of the equivalent toes in the smallest juvenile (**Figure 6.22 a**) suggests that these grooves may be a characteristic feature.

Cells adjacent to the circumferal groove in adults, particularly at the distal edge of the pad, are irregular in shape and crumpled in appearance (**Figure 6.23** and **Figure 6.24 c**). It may be that this is a transitional area between cell types as there is a change from the columnar pad to squamous marginal cells. However, the absence of the cells in the juvenile sample (**Figure 6.23 a**)

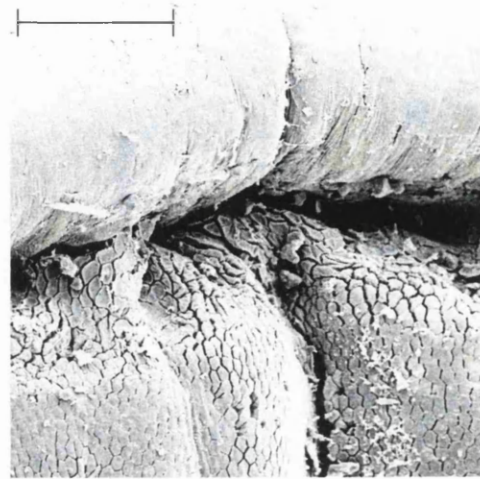


Figure 6.23: S.E.M. images of groove on toe pad in adult *P. venulosa*. Scale bar = 50 μ m.

weakens this hypothesis. It may simply be that the structure of these cells results from the inability of hexagons to tightly tessellate around the curvature of the pad as it shelves into the deepened groove seen in adults.

Cells present on the circumferal ridge are similar between the age classes, with surface architecture characterised by minute rounded knobs and convolutions (**Figure 6.24 b and d**). The definition of individual cells is less distinct in juveniles (**Figure 6.24 a and b**) than in adults, where rolled margins define the edges of the separate cells (**Figure 6.24 d**). In both age classes, large shallow pits are present on the margin which are in appearance as if one or more individual cells has been excised

from the uppermost cell layer, exposing a roughened underlying surface (**Figure 6.24 b and d**).

Whilst there were no instances of a continuance of the circumferal groove to extend below the proximal edge of the pad, the delineation of the margin in *P. venulosa* is sharp and is markedly visible on whole pad images (**Figure 6.22**). This is partially due to the change in the elevation of the pad from the ventral surface of the toe (**Figure 6.25 a and c**) and to the close juxtaposition of two distinct cell types in the two areas.

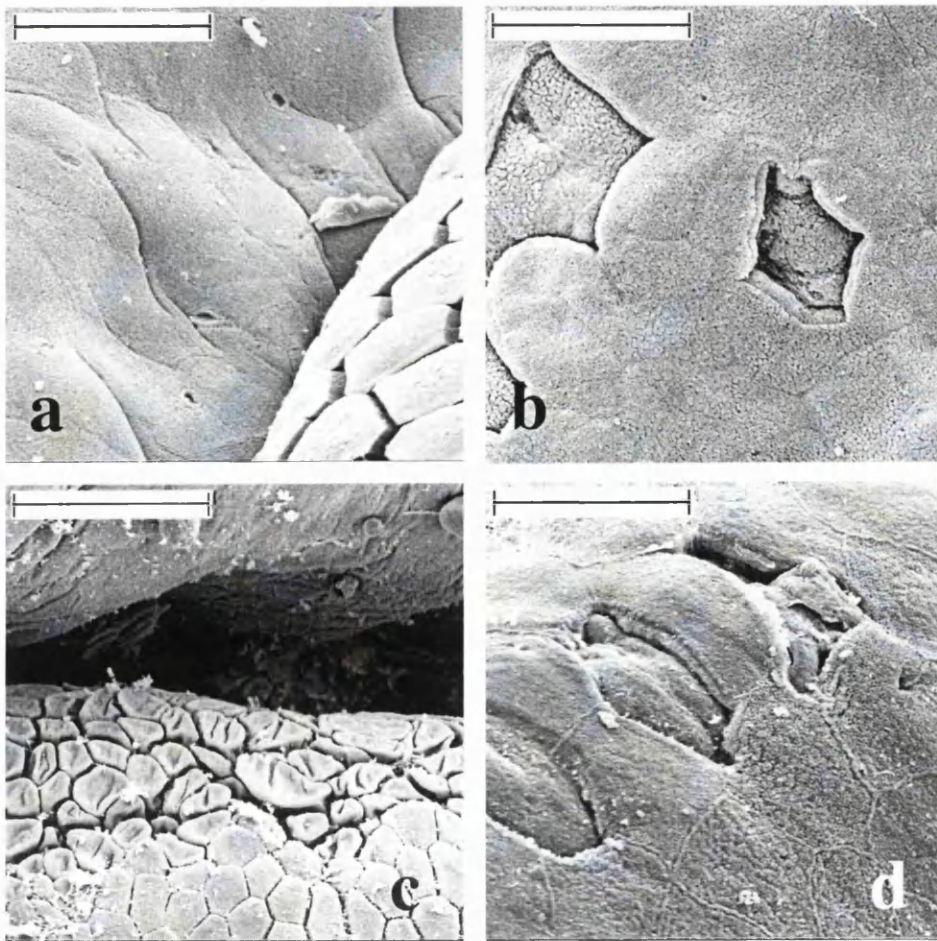


Figure 6.24: S.E.M. images of circumferal grooves and marginal cells in *P. venulosa*. (a) Juvenile 1 (23.3mm) Front 3, Scale bar = 25 μm . (b) Juvenile 2 (31mm), Scale bar = 25 μm . (c) Adult (72mm) Back 2, Scale bar = 50 μm (d) Adult (72mm) Back 2, Scale bar = 25 μm .

Sub-marginal cells in both juveniles and adults are very similar in structure (**Figure 6.25 b and d**), being roughly hexagonal though less regular in shape than the pad cells, and in general a little larger (Adults: $147.06 \mu\text{m}^2 \pm 5.26$, $n = 30$). The individual cells are separated from one another by shallow grooves with the imprints of these margins from the previously overlying layer of cells visible across the microvillated apical surfaces, with this being particularly pronounced in the adult sample.

Scattered liberally across the sub-marginal area in juvenile samples are a substantial number of shallow pits, similar in shape and size to the stomatal pores seen in the juvenile frogs, sandwiched between the edges of two neighbouring cells. These are also seen in the adult samples though more prevalent are large depressions similar in size and shape to individual sub-marginal cells.

Adult *P. venulosa* show an unusual extension in the area of distribution of the cell types found on the proximal margin. Where in other species these sub-marginal cells rarely extend below the final phalange, in this species cells run along the midline of the toe (**Figure 6.26**), at least as far as the first subarticular tubercle.

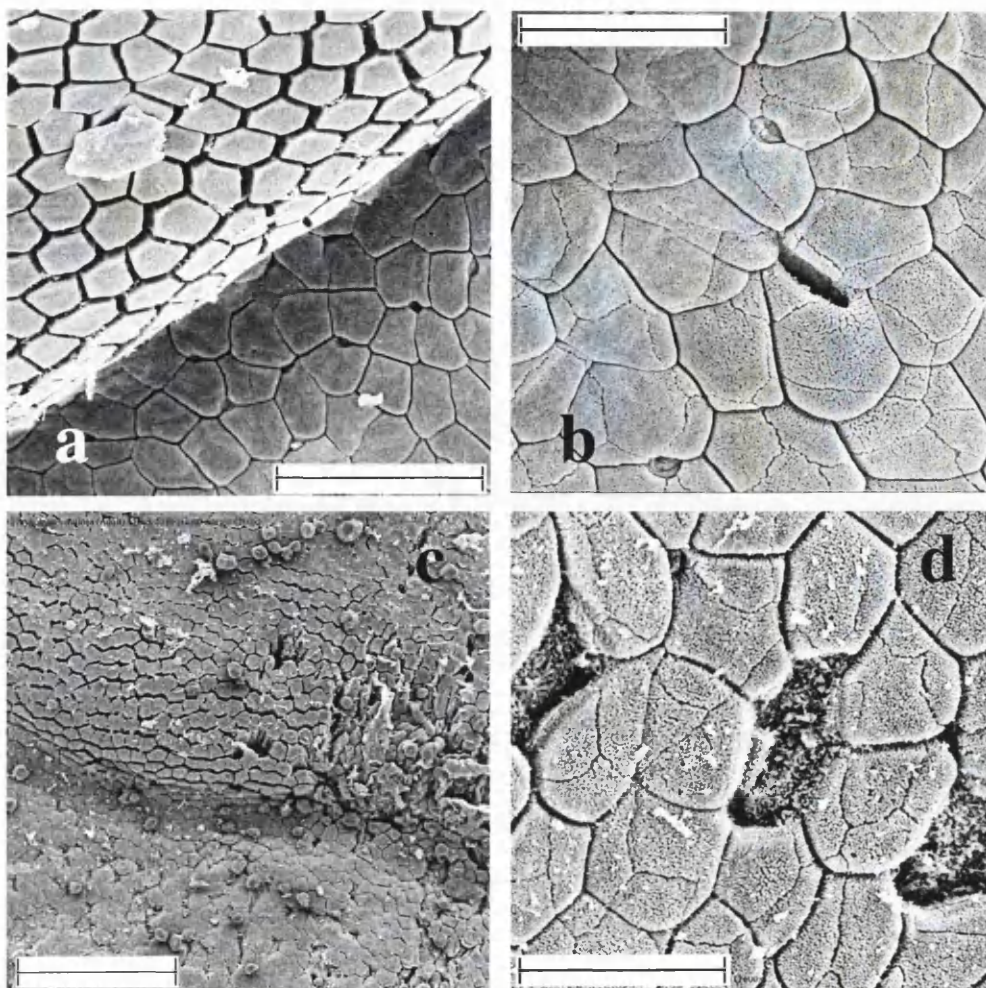


Figure 6.25: S.E.M. images of proximal margins in *P. venulosa*: (a) Juvenile 2 (26mm) Front 2, Scale bar = 50 μm (b) Juvenile 2 (26mm) Front 2, Scale bar = 25 μm . (c) Adult (72mm) Back 5, Scale bar = 150 μm (d) Adult (72mm) Front 4, Scale bar = 25 μm .

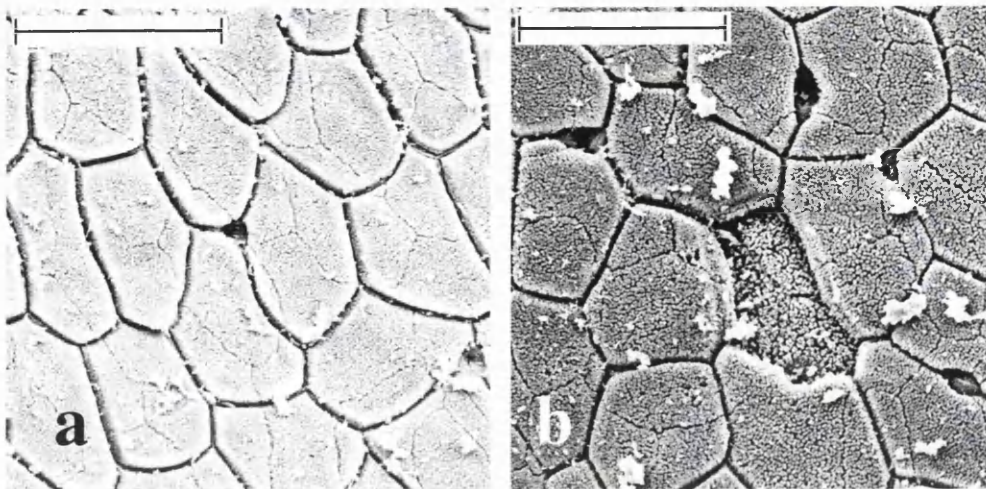


Figure 6.26: S.E.M. images of cells along mid line of ventral surface of toe in adult *P. venulosa*: (a) Front 2 (b) Front 3. Scale bars in images = 25 μm .

Images from pads in *P. trinitatis* suggest that intercellular channels in this species are shallower than in others, giving the cells a stouter appearance (**Figure 6.27**). The sides of the cells are striated, as in other species, with surface architecture in both age classes roughened. The cell coat that obscures underlying structures is less evident (**Figure 6.27 b and d**), particularly in the adult sample (**Figure 6.29 c and d**). The apices of the toe pad cells are mainly hexagonal in shape, with a criss-crossing of impressions from the previously overlying cells visible across their textured surface.

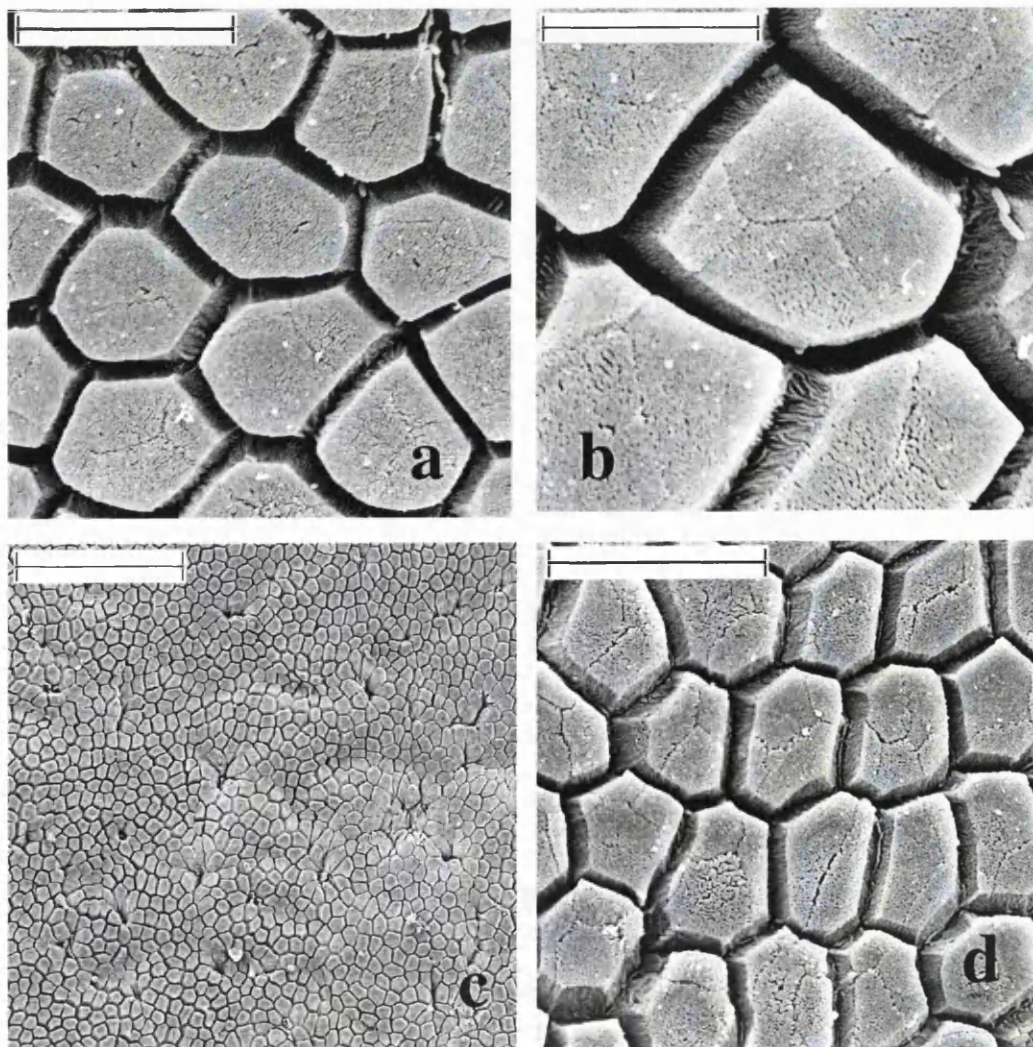


Figure 6.27: S.E.M. images of toe pad cells in *P. trinitatis*: (a) Juvenile 2 (37mm) Front 3, Scale bar = 25 μm (b) Juvenile 2 (37mm) Front 4, Scale bar = 12.50 μm. (c) Adult 2 (71mm) Back 1, Scale bar = 100 μm (d) Adult 2 (71mm) Back 1, Scale bar = 25 μm.

Cell areas in the two age classes follow the pattern seen in the majority of the species under investigation here, with a significant reduction in the sizes of cells in adult frogs. Average cell sizes in adult frogs are relatively small, at $105.00 \mu\text{m}^2 \pm 2.14$ ($n = 164$) in comparison to the average of $122.62 \mu\text{m}^2 \pm 2.75$ ($n = 150$) seen in the juvenile frogs (Difference in means ($F_{149,163} = 7.29$): $U_{150,164} = 8412.50$ $p < 0.001$).

Perhaps unsurprisingly then, the cell densities recorded from adult pads in this species are significantly greater than seen in the juvenile sample, increasing between the age classes from $8500 \text{ per mm}^2 \pm 580$ ($n_{\text{juv}} = 16$) to $9800 \text{ per mm}^2 \pm 450$ ($n_{\text{adult}} = 17$) (Difference between means ($F_{15,16} = 0.87$): $t = -1.78$, $p = 0.085$, 31 d.f.). Cell densities in adults are considerably higher than in the other large species (**Table 3.1**).

Channel widths in this species are not as variable in appearance as in other species (**Figure 6.27**) but channel densities are similar. As intercellular channel densities are influenced by the perimeters of the cells in a fixed area, and given the change in cell densities between the age classes, an increase in lengths of channels in adults is to be expected. There is a trend towards this, though the values in juveniles and adults are not actually significantly different from one another at $151.44 \text{ mm/mm}^2 \pm 4.86$ ($n = 16$) and $159.99 \text{ mm/mm}^2 \pm 2.62$ ($n = 17$) respectively (Difference between medians ($F_{15,16} = 4.21$): $U_{16,17} = 241$, $p = 0.26$, N.S.).

Mucosal pores in juvenile *P. trinitatis* are small and variable in size, averaging $47.13 \mu\text{m}^2 \pm 9.37$ ($n = 18$). Pore densities are also low at $10.92 \text{ per mm}^2 \pm 1.93$ ($n = 14$), though the distribution of the pores across the pad is not even, being more concentrated around the edges of the pad.

The majority of pores are elongate in appearance (**Figure 6.28 a - c**) particularly in the smaller sized juveniles. These vary in the degree of their development from small round-ended slits almost entirely imbedded in a single cell (**Figure 6.28 a**) to more lanceolate pores one to cell sides in length (**Figure 6.28 b and c**). A few more rounded pores are also found on pads from the smaller juveniles, at the meeting corners of four neighbouring cells. These are similar to the small round pores found in a number of species but differ in that the lumen walls appear to have pulled away from the neighbouring cells to form a smooth sided tube-like structure (**Figure 6.28 d**).

In the largest juvenile, pores similar in structure to the typical geometrical types seen in many of the species studied here are also present across the pad, framed by between four and six cells in the main. The walls of the lumen are modified in comparison to the normal striations of the cell sides, meaning that the pores belong to the Type II classification. In most cases, these modifications give the lumen walls the typically roughened and micro-villated appearance seen in many other species (**Figure 6.28 f**). However, there are also a number of instances of a less modified smoother lining to the pores, closer in appearance to the normal striations of the cell walls (**Figure 6.28 e**). In both of these cases, the modification of the walls of the lumen starts at a point a little below the crown of the neighbouring cells giving the impression of a marginal rim at the opening to the pore.

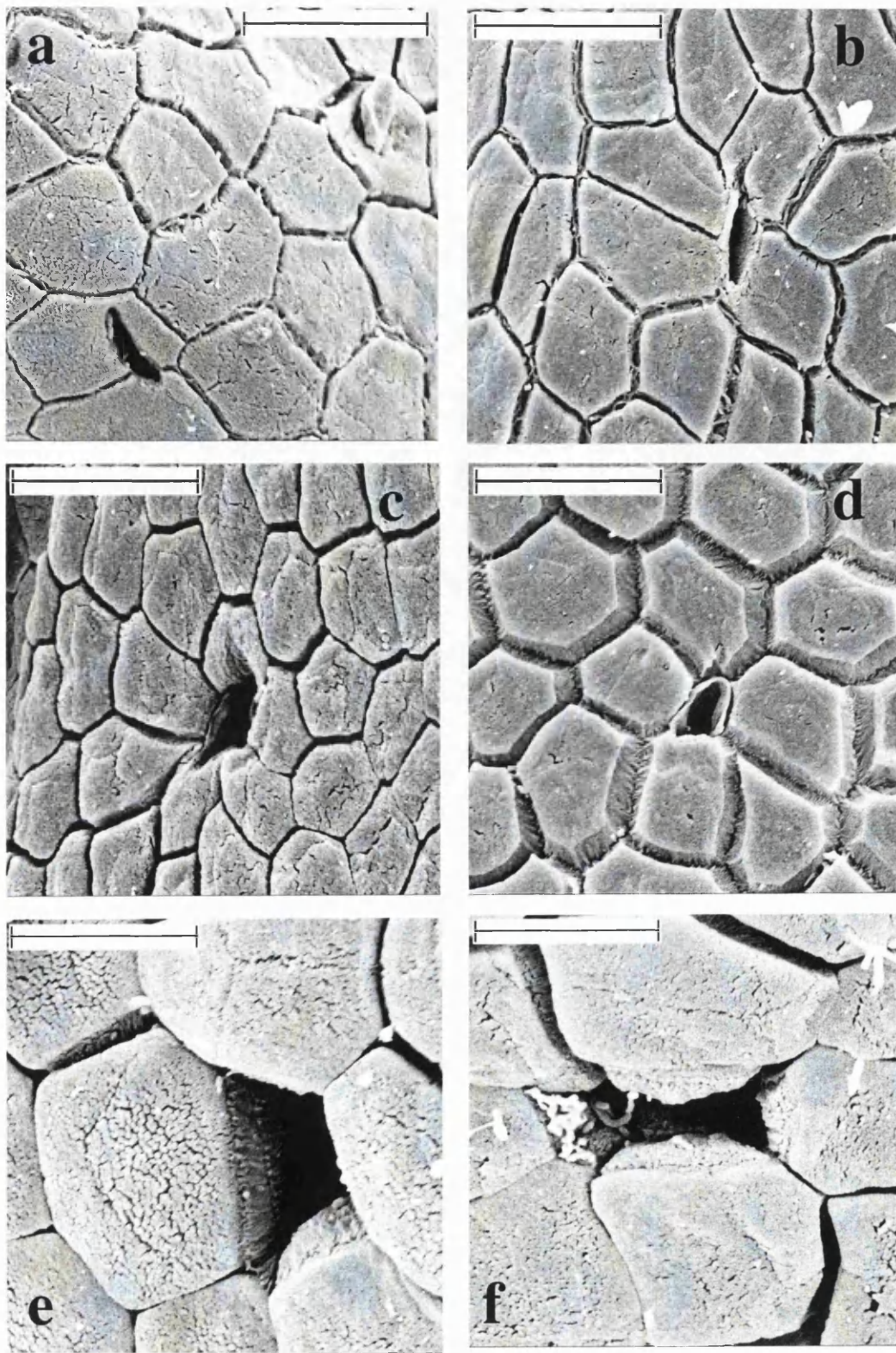


Figure 6.28: S.E.M. images of mucosal pores in juvenile *P. trinitatis*: (a) Juvenile 2 (28mm) Front 2, Scale bar = 25 μm (b) Juvenile 1 (26mm) Back 2, Scale bar = 25 μm (c) Juvenile 2 (28mm) Back 5, Scale bar = 25 μm (d) Juvenile 1, Back 1, Scale bar = 25 μm (e) Juvenile 3 (37mm) Back 1, Scale bar = 12.50 μm . (f) Juvenile 3 (37mm) Back 5, Scale bar = 12.50 μm .

Pores in adult frogs are larger in size at $92.16 \mu\text{m}^2 \pm 18.56$ ($n = 12$) than those seen in the juveniles (Difference between means ($F_{17,11} = 0.38$): $t = 2.29$, $p < 0.05$, 28 d.f.) Pore densities have significantly increased in adults at $39.70 \text{ per mm}^2 \pm 12.77$ ($n = 4$) (Difference in medians ($F_{3,13} = 14.88$): $U_{4,14} = 6.00$, $p = 0.02$), with pores mainly visible around the edges. This is because in the majority it is larger elongate pores similar in appearance to those seen in juveniles and several cell sides in length that are found around the outer edges of the pad (**Figure 6.29 a and b**). In the centre of the pad are the Type II pores dominant in other species (**Figure 6.29 c and d**), made up of either single or combined geometrical shapes and bordered by six to eight cells.

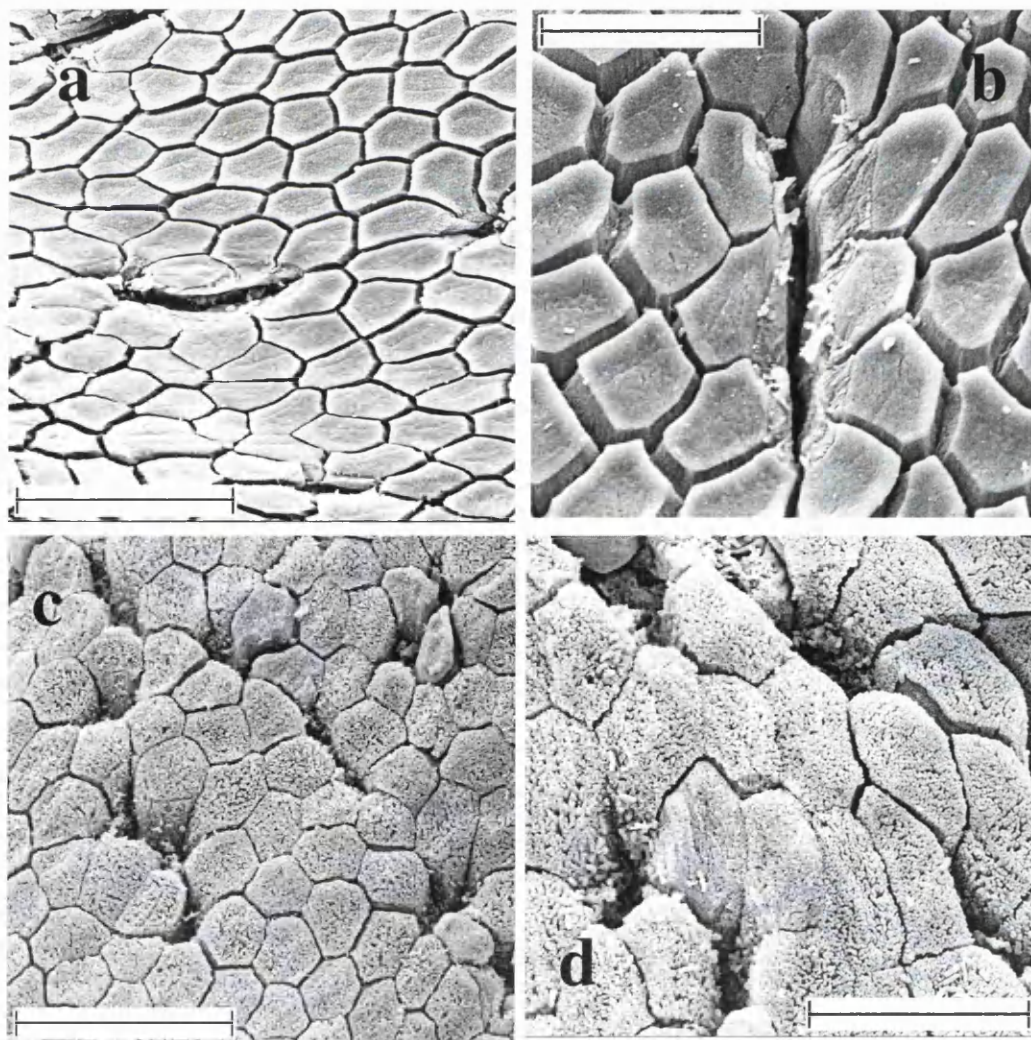


Figure 6.29: S.E.M. images of mucosal pores in adult *P. trinitatis*: (a) Adult 2 (71mm) Back 3, Scale bar = $25 \mu\text{m}$. (b) Adult 2 (71mm) Front 4, Scale bar = $50 \mu\text{m}$ (c) Adult 1 (67.6mm) Back 1, Scale bar = $50 \mu\text{m}$ (d) Adult 1 (67.6mm) Back 1, Scale bar = $25 \mu\text{m}$.

Toe tips in *P.trinitatis* are bulbous in appearance, with a far lesser degree of lateral expansion than seen in many species (**Figure 6.30**). Whereas the sub-marginal area below the proximal margin is often swollen in appearance in other species, this is extended in *P.trinitatis* to stretch well below the final phalange. The structure of the pad is less defined from the ventral surface of the toe than in other species, with very little development of the circumferal or proximal margin (**Figure 6.30 c and d**). In some instances the pad is emarginate and cells simply graduate into the dorsal skin, with no circumferal groove evident (**Figure 6.30 b**).

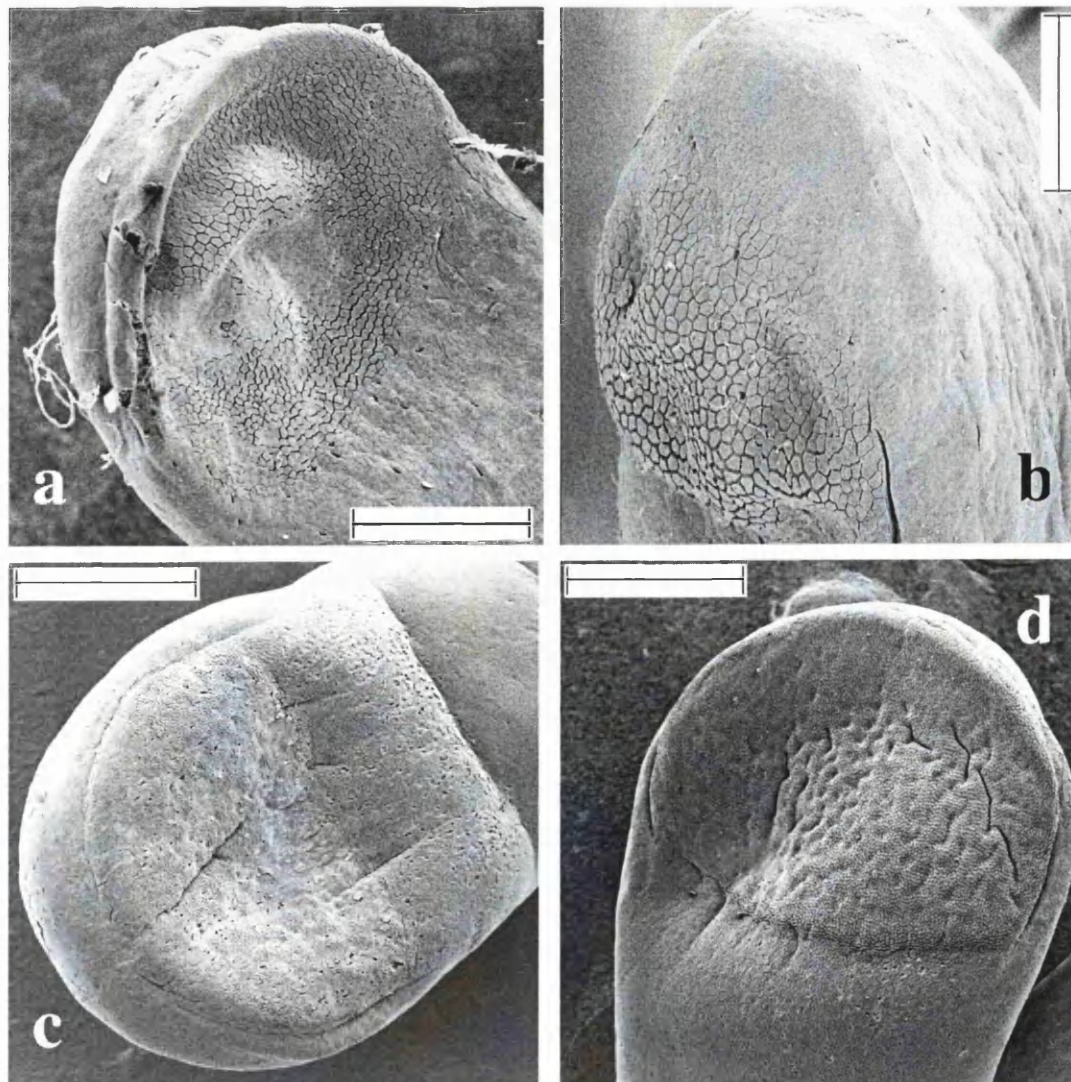


Figure 6.30: S.E.M. images of toe pads in *P. trinitatis*: (a) Juvenile (37mm) Front 2, Scale bar = 300 μ m (b) Juvenile (37mm) Back 3, Scale bar = 150 μ m. (c) Adult 2 (71mm) Front 1, Scale bar = 625 μ m. (d) Adult 2 (71mm) Back 2, Scale bar = 625 μ m.

The level of development of the circumferal margin is particularly low for the juvenile frogs (**Figure 6.31 a**). Actual grooves separating the pad from the rest of the toe as seen in other species are reduced to a shallow dent in the distal end of the toe at best. The cells on the marginal ridge show little in the way of modification, being squamous and irregular in shape. This is not the case in the adult frogs, where cells similar to those found on the proximal margin (**Figures 6.31 b** and **6.32 d**) have extended their range to cover almost the entire distal portion of the toes.

The narrow channels between these cells and the many shallow pits in the surface immediately below the pad (**Figure 6.30 a, d**) give the sub-marginal region a different textural appearance to that of the toe pad proper. This, together with shallow creases and folds caused by the juxtaposition of two cell types (**Figure 6.30** and **6.32 a, c**) is the easiest way to determine the position of what is otherwise an ill-defined proximal margin. Proximal margin cells are regular in size, cuboidal in appearance and roughly hexagonal in shape, though with more rounded edges than seen on the pad proper. Cells are a good deal larger than seen on the pad, with average apical areas of around $200\ \mu\text{m}^2$ in both age classes, and are virtually indistinguishable between the age classes (**Figure 6.32 b** and **d**). As in most species, the cell types seen below the proximal margin extend in their distribution to around the articulation point of the final phalange. However, as in the similarly sized *P. venulosa*, this is not the full extent to which specialised cells are found on the ventral surface of the toe.

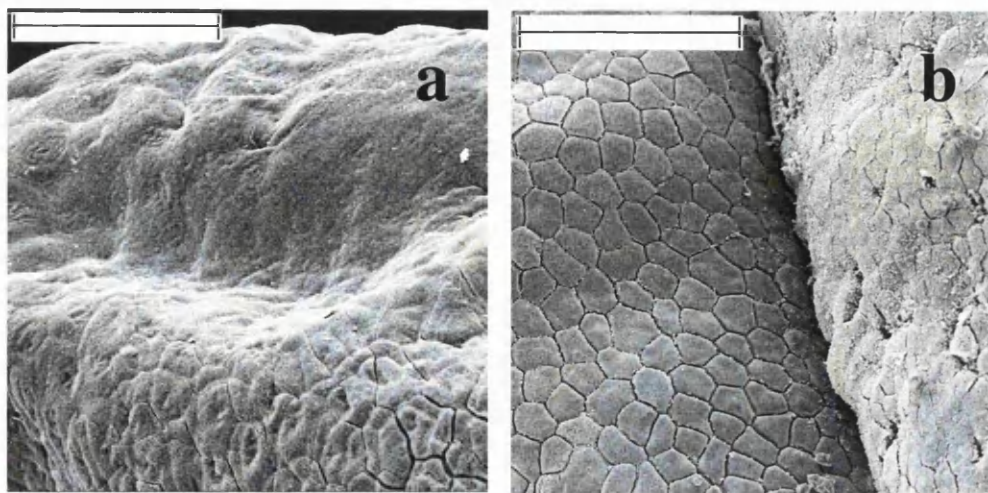


Figure 6.31: S.E.M. images of circumferential marginal areas in *P. trinitatis*: (a) Juvenile 2 (28mm) Front 4, Scale bar = 50 μm . (b) Adult 2 (71mm) Back 2, Scale bar = 100 μm .

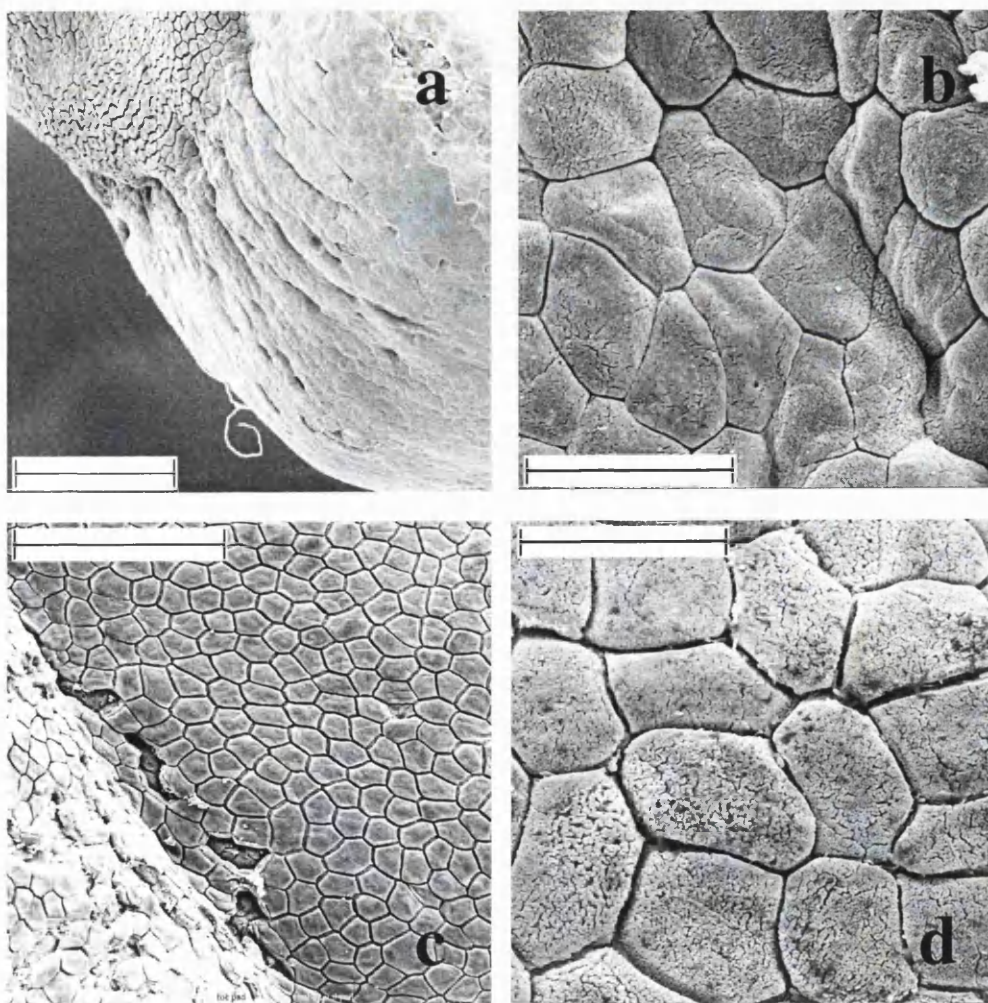


Figure 6.32: S.E.M. images of proximal margins and sub-marginal cells in *P. trinitatis*: (a) Juvenile (28mm) Front 3, Scale bar = 150 μm (b) Juvenile (28mm) Front 2, Scale bar = 25 μm . (c) Adult 1 (67.6mm) Front 1, Scale bar = 100 μm (d) Adult 1 (67.6mm) Front 2, Scale bar = 25 μm .

In this species, as in others, there is an accessory adhesive system consisting of subarticular tubercles along the length of the toes, with these being particularly large and well developed in the adult frogs (6.3.4). Between these structures and over the poorly developed lateral margins, the ventral surface of the toe is covered with cells that are significantly modified in appearance (Figure 6.33).

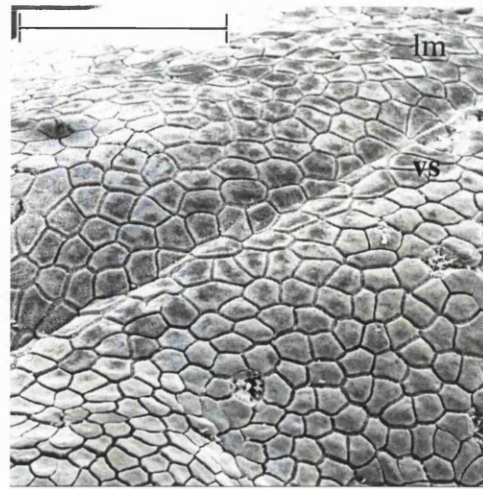


Figure 6.33: S.E.M. images of ventral surface (vs) and lateral margins (lm) of the toe in adult *P. trinitatis*. Scale bar = 10 μm .

In both age classes these are similar in structure and appearance to those seen on the surface of the subarticular tubercles (Figures 6.34 and 6.3.4). Both juveniles and adults have cell sizes on the ventral surfaces of around 200 μm^2 in area (Mean values: 241.52 ± 9.24 , $n = 4$ (Juveniles); 190.96 ± 6.32 , $n = 9$ (Adults)), though as on the toe pad proper, there is a statistically significant reduction in this variable in the adult cohort (Difference in means ($F_{4,9} = 0.01$): $t = 4.47$, $p < 0.001$, 11 d.f.).

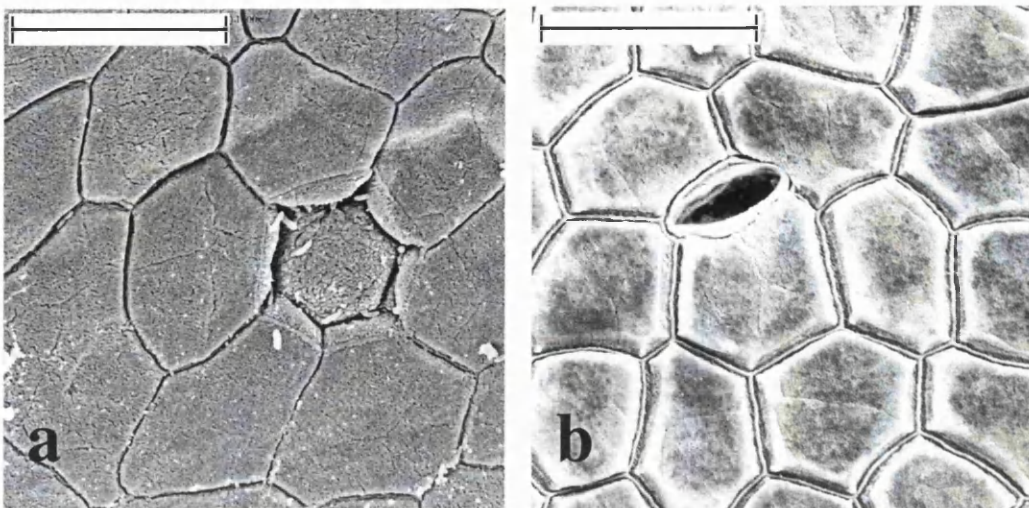


Figure 6.34: S.E.M. images of cells on ventral surface of the toe in *P. trinitatis* (a) Juvenile 3 (37mm) Front 3 (b) Adult 2 (71mm) Front 4. Scale bars = 25 μm

Hyla boans

Cells in the adult and juvenile frogs of the largest species in this study are not generally different in structure to those seen in other species, being columnar in nature with striated sides and hexagonal apices (**Figure 6.35** and **6.36**). In adult frogs, the cell coat that often obscures the underlying tonofilament bundles is generally not visible, giving the

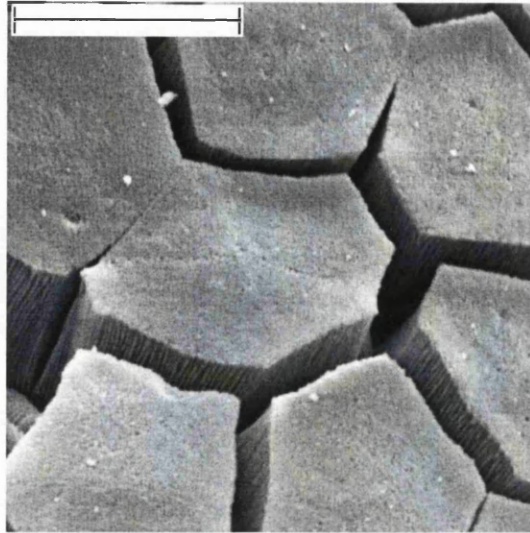


Figure 6.35: S.E.M. images of toe pad cells in juvenile *H. boans*. Scale bar = 12.5 μm .

appearance of a finely divided surface on the apices of these cells (**Figure 6.36 d**). Whole pads from the juvenile sample have a pitted appearance, with rounded depressions scattered across their surfaces (**Figure 6.39 a** and **b**). On closer examination at higher magnification these are formed by individual cells, which appear to be collapsing and pulling away from the surface of the pad (**Figure 6.36 b**).

Areas of more typical cells show that there is a significant reduction between the juvenile and adult cohorts, with respective average cell sizes of $137.39 \mu\text{m}^2 \pm 3.04$ ($n = 71$) and $118.25 \mu\text{m}^2 \pm 3.63$ ($n = 86$) ($F_{70,85} = 3.93$; $U_{71,86} = 1811$, $p < 0.001$). Consequences of this trend in the other species in which this cell size reduction with growth also occurs are an increase in cell and mucosal channel length density recorded per square millimetre of pad in adult frogs. There is little evidence of the latter of these trends in this species; though average values of channel length density are a little higher in the adult sample ($145.88 \text{ mm/mm}^2 \pm 5.28$, $n = 8$) than in juveniles ($140.24 \text{ mm/mm}^2 \pm 3.56$, $n = 8$), though this is not a statistically significant increase

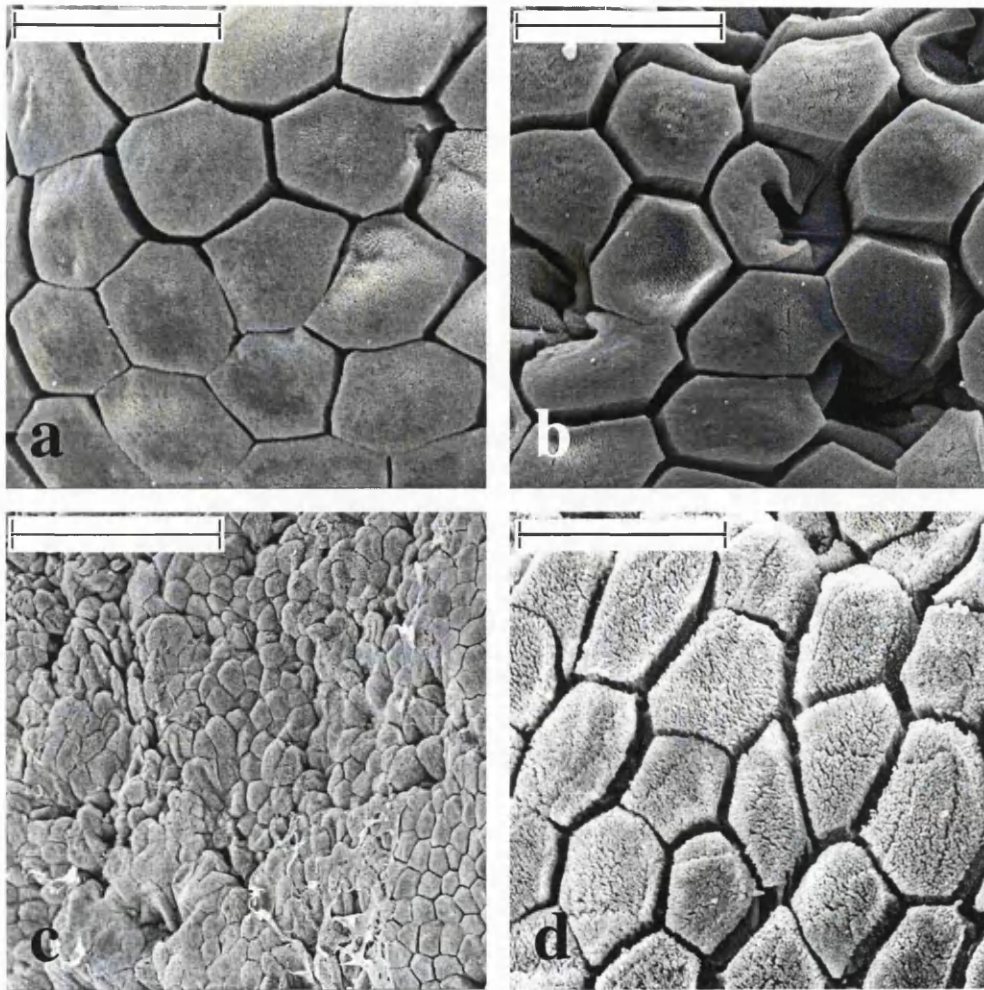


Figure 6.36: S.E.M. images of toe pad cells in *H. boans*: (a) Juvenile (14mm) Back 3, Scale bar = 25 μm . (b) Juvenile (14mm) Front 2, Scale bar = 25 μm . (c) Adult (98mm) Front 2, Scale bar = 100 μm (d) Adult (98mm) Front 1, Scale bar = 25 μm .

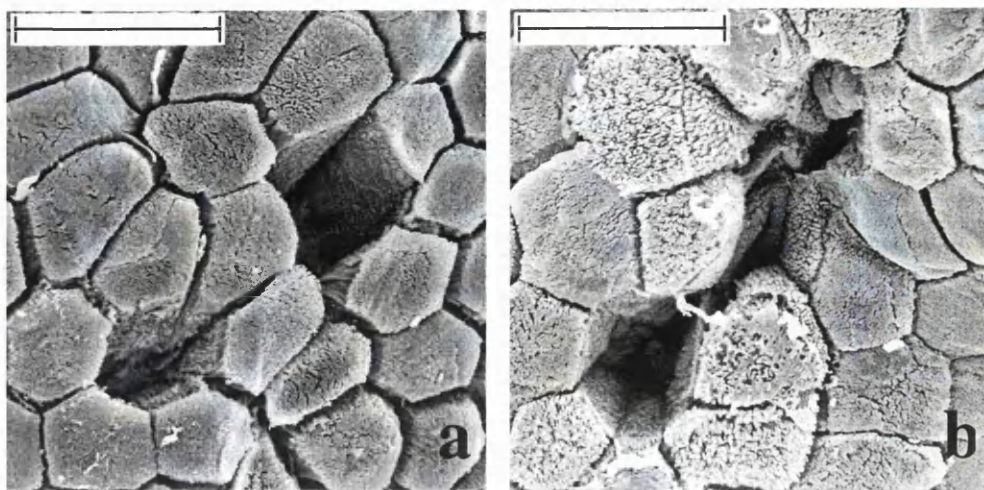


Figure 6.37: S.E.M. images of mucosal pores in *H. boans*: (a) Front 3 (b) Front 3. Scale bars = 25 μm .

($F_{7,7} = 1.43$; $t = -0.89$, N.S. 14 d.f.). Cell densities are significantly different between the age-classes ($F_{7,8} = 0.59$; $t = -2.75$, $p = 0.015$, 15 d.f.) increasing from 7265.92 per $\text{mm}^2 \pm 360.39$ ($n = 8$) in juvenile frogs to 8538.16 per $\text{mm}^2 \pm 296.54$ ($n = 9$) in adults; an increase of around a thousand cells per square millimetre of pad.

These cell densities do not take into account the area taken up by the mucosal pores over the surface of the pad, which appears fairly substantial (**Figure 6.36 c** and **6.38 c**). Although pore sizes are large and average 181.49 ± 33.06 ($n = 17$) in area, densities are in fact relatively low at around 21.03 per $\text{mm}^2 \pm 2.96$ ($n = 5$) and it is therefore unlikely that these would have a substantial effect on the cell density values seen in the adult frogs*.

Pores on the pads of adult frogs are most commonly of the geometrical Type II pores seen in other species framed by six to eight cells (**Figure 6.37 a**). A number of larger openings formed by combinations of up to four adjacent geometrical pores were also prevalent (**Figure 6.37 b**). All pores belong to the Type II classification of pore structure, with lumen walls modified in comparison to the normal striations of the pad cell sides (**Figure 6.37**). There are also a number of shallow convoluted dents in the pad surface, at the proximal edge of the pad (**Figure 6.39 b**).

Again, due to distortions of the pads sampled from this species, it is difficult to confidently ascribe any differences seen between the age classes to differences in size, though there is some evidence that trends seen in other species with large adult

* Pore size and densities were not determined in juveniles due to the deformations of the pad caused by the collapsing cells, which made it difficult to determine whether any of the depressions on the pad surface are mucus pores.

size may well be occurring in this species. Adult pads in *H. boans* appear considerably flatter in elevation than juvenile pads (**Figure 6.39**), and there is some visual evidence that the circumferal margin is more defined in the larger frogs. In adult frogs the circumferal ridge has become more ventrally positioned, lying flush with the pad surface (**Figure 6.38 c**) with a groove separating the pad from distal and lateral edges of the toe. In juveniles this groove is less defined with a number of pads appearing almost emarginate in ventral view, as a combined effect of the more rounded aspect of the pad and the 'rolled back' position of the margin (**Figure 6.38 a**).

The proximal margin is defined by a fairly abrupt change in cell types at the lower margin in the juvenile pads (**Figure 6.38 a and b**) and is fairly undeveloped with no extension of the circumferal groove to encircle the lower margins of the pad. Cells below the margins are large and irregular with ill-defined margins and are similar in appearance to those seen on the subarticular tubercles of the juvenile frogs (**6.3.5**). In the adults the proximal margin is, again, poorly defined (**Figure 6.38 b and d**) with the transition of cell types less distinct than seen in the juvenile frogs (**Figure 6.39 a**). In a few instances a shallow crease runs along the lower margin of the pad and there is vertical folds in the sub-marginal area below the pad (**Figure 6.39 a**). Cells below the pad margin appear to be a cuboidal type with indistinct margins and overlaying imprints of the previous layer similar to those seen in other species (**Figure 6.39 a**).

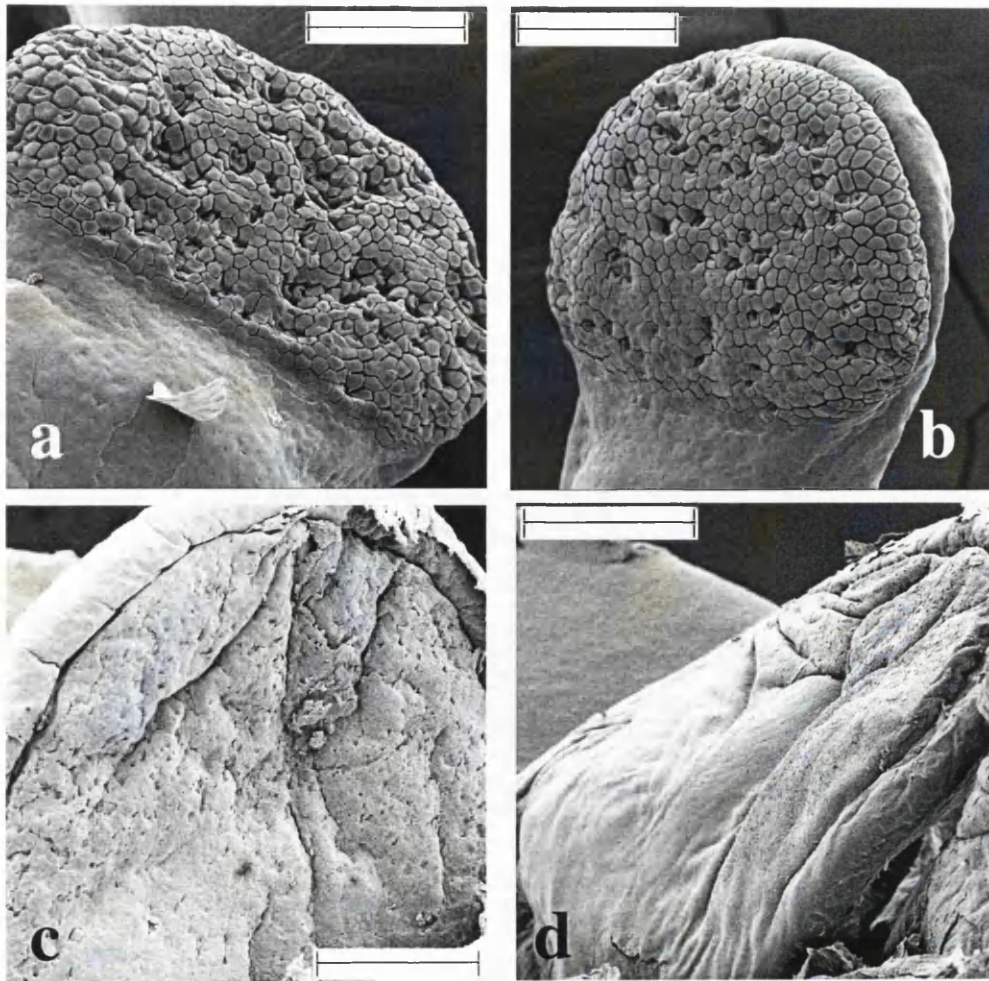


Figure 6.38: S.E.M. images of toe pad structure in *H. boans*: (a) Juvenile (14mm) Front 4, Scale bar = 150 μm . (b) Juvenile (14mm) Back 5, Scale bar = 150 μm . (c) Adult (98mm) Front 4, Scale bar = 1.25 mm (d) Adult (98mm) Back 1, Scale bar = 1.25 mm. Scale bar =

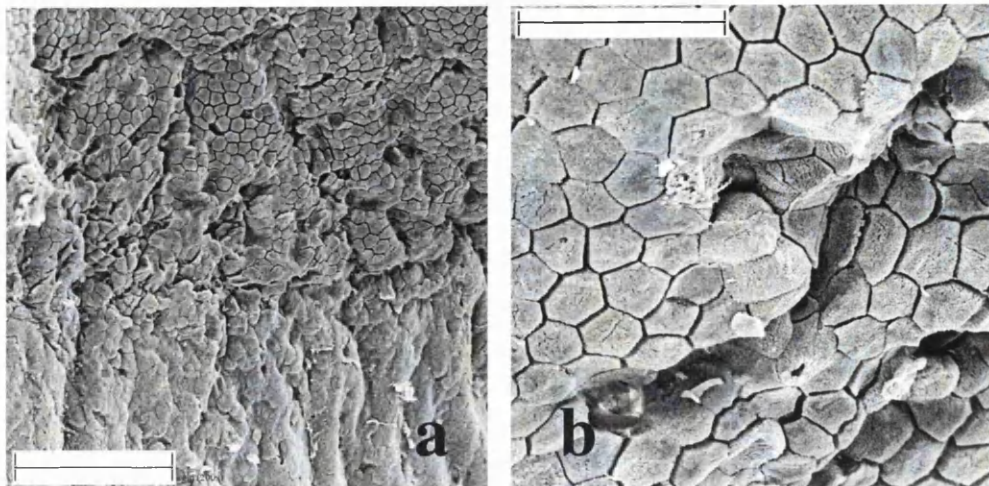


Figure 6.39: (a) S.E.M. images of proximal margin in adult *H. boans*; Front 3, Scale bar = 150 μm (b) Dimples in pad, adjacent to proximal margin; Front 3, Scale bar = 25 μm .

6.3.4. Accessory adhesive areas

The specialised toe pads are not the only areas that contribute to adhesion in these frogs. Most species exhibit behaviour on the rotation platform if allowed to adhere naturally that utilises areas of skin on the stomach, thighs and chin (see 6.2.2). Although methodology excludes the use of these areas in these frogs, examination of hand and foot morphology, suggests that there is a developed system of accessory adhesive tubercles that can be utilised: subarticular tubercles at the 'knuckle' joint; supernumerary tubercles along the digits and toes and palmar and metatarsal tubercles on the main body of the hands and feet.

Phrynohyas venulosa

The accessory tubercle system in juvenile *P. venulosa* is not as developed as described by Duellman (2001) for adult frogs (**Figure 6.40** and **6.41**). Subarticular tubercles on the hand are better developed than those on the foot, rounded in shape and projecting from the ventral surface of the fingers (**Figure 6.43 a**) whereas toe subarticular tubercles are more gently rounded bumps (**Figure 6.40**). In adults subarticular tubercles are large and conical in the main, again with this particularly being the case on the front foot. The third and fourth toes have a smaller second subarticular tubercle (**Figure 6.41** and **6.44 a**) in adult frogs, though this is absent in juveniles (**Figure 6.40**) The tubercle on the fourth digit of the hand is more flattened in the adults with an indentation on the distal edge of the tubercle (**Figure 6.43 c**), a feature that is also seen in the same tubercle in juvenile frogs (starred in **Figure 6.40**) from Trinidad. This is perhaps an example of an intraspecific variation between frogs from different localities as in Panamanian frogs this tubercle is bifid in the majority of specimens (Duellman, 2001 and **Figure 6.41**).

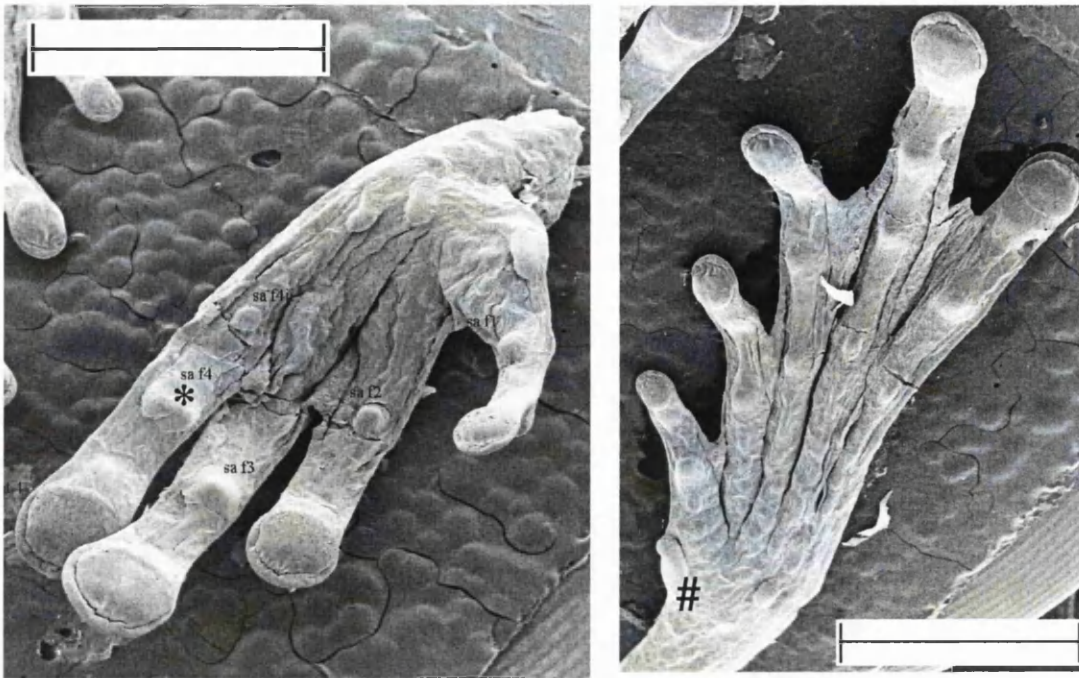


Figure 6.40: S.E.M. images of hand and foot morphology in juvenile *P. venulosa* (23.3 mm). Scale bars = 2.5 mm

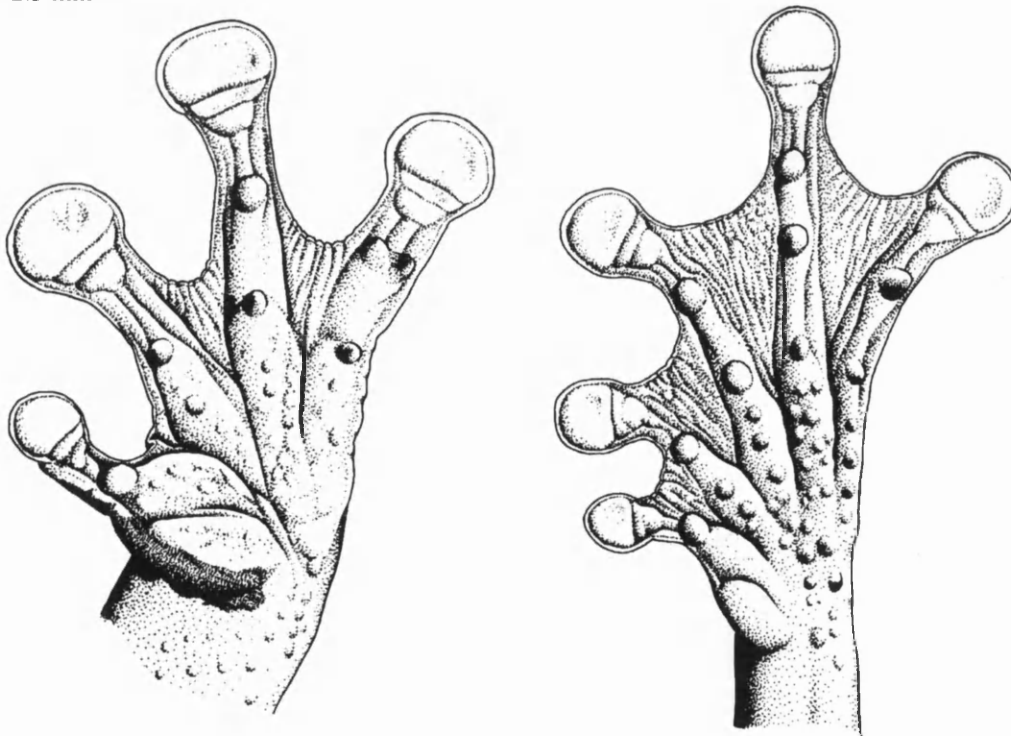


Figure 6.41: Hand and foot morphology in adult male *P. venulosa* (Duellman, 2001)

Trends seen in cell type development in the subarticular tubercles in juvenile and adult frogs are similar to *H. crepitans* (see 5.3.4). Cells on the subarticular tubercles in the juvenile frogs (**Figure 6.43 b**) are slightly larger than those found on the toe pad proper, with average areas of $147.77 \mu\text{m}^2 \pm 4.00$ ($n = 119$). They are very similar in appearance to the cuboidal, irregularly shaped roughly hexagonal cells seen on the proximal margin (**Figure 6.25 b**). In contrast, subarticular tubercles in adults, both distally and proximally (**Figure 6.43 c** and **6.44 a**) are covered in cells that are not significantly different in their appearance to the columnar type seen on the toe pad (**Figure 6.43 d** and **6.44 b**). With average sizes of $111.81 \mu\text{m}^2 \pm 3.92$ ($n = 23$) these subarticular tubercle cells are significantly smaller than on the toe pad proper ($t = 8.36$, $p < 0.01$, 109 d.f.).

Of the other possible types of tubercles that may be present in this species only the inner metatarsal is distinct in the juvenile sample (hash in **Figure 6.40**). As in adult frogs (Duellman, 2001) this is large and ovoid, projecting a little from the edge of the foot. The cells on the tubercle are similar in appearance to those seen on subarticular tubercles seen along the rest of the toes (**Figure 6.42**).

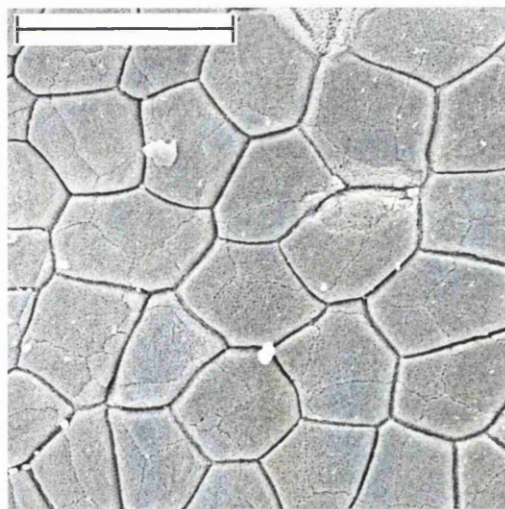


Figure 6.42: S.E.M. image of cells on the inner metatarsal. Scale bar = 25 μm .

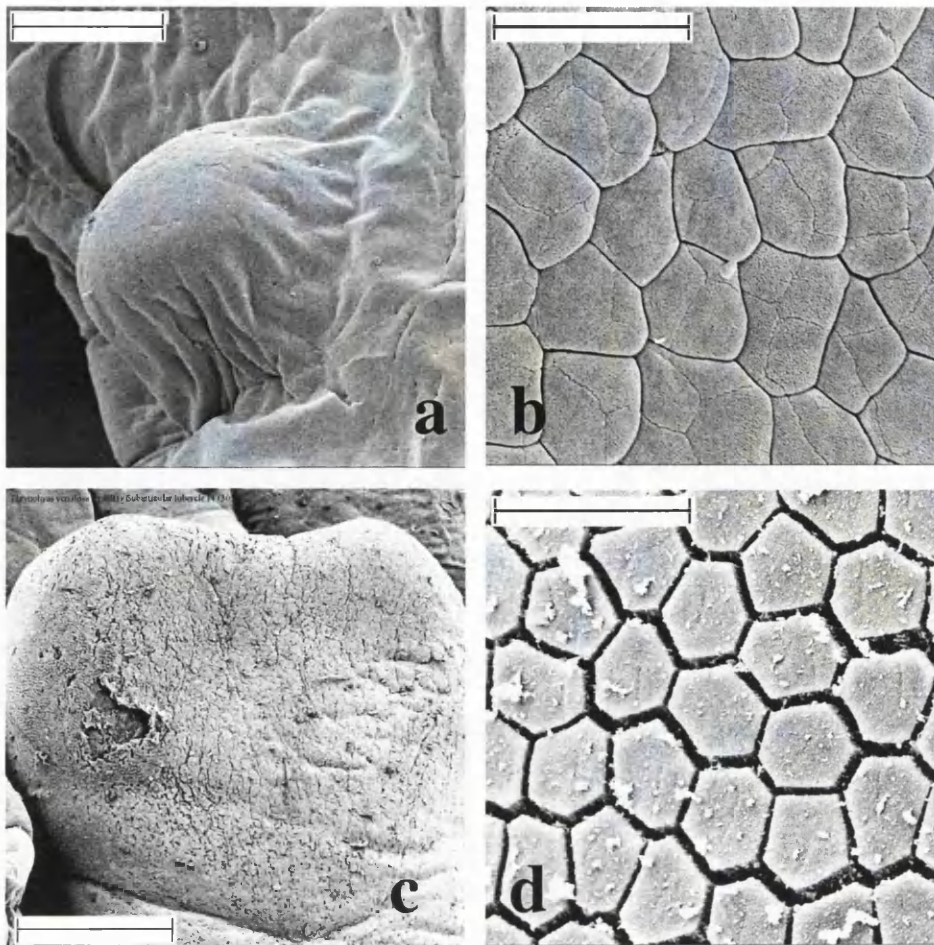


Figure 6.43: S.E.M. images of distal subarticular tubercles in *P. venulosa*: (a) Juvenile (26mm) Front 1, Scale bar = 150 μm (b) Juvenile (26mm) Front 3, Scale bar = 25 μm (c) Adult (72mm) Front 4, Scale bar = 625 μm (d) Adult, Front 4, Scale bar = 25 μm .

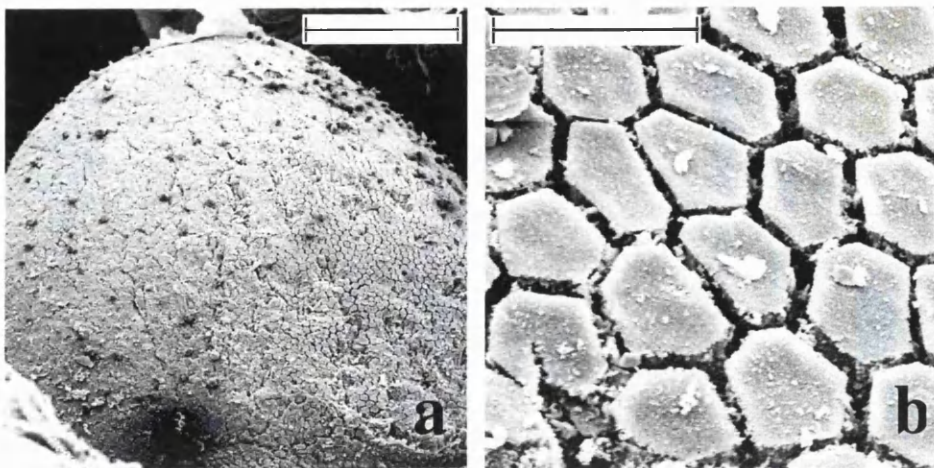


Figure 6.44: S.E.M. images of proximal subarticular tubercle (Back 4) in adult *P. venulosa* (a) Scale bar = 300 μm (b) Scale bar = 25 μm .

Phyllomedusa trinitatis

The tubercular system in juvenile *P. trinitatis* is poorly developed with the subarticular tubercles, usually the best developed structures in the accessory adhesive system, are reduced to slight swollen bumps on the joints of the toes and the fingers (**Figure 6.45**). If we assume that hand and foot morphology in closely related species within a genera are likely to be similar, studies in another member of the species group to which *P. trinitatis* belongs, *P. venusta* (Duellman, 2001) suggest that the tubercular system is better developed in adult frogs (**Figure 6.46**). Certainly, subarticular tubercles are a good deal larger in the adult frogs and more rounded (**Figure 6.47 c**) than even the most developed of these in the juveniles (**Figure 6.47 a**) and are similar in their topography to those seen in *P. venusta* (**Figure 6.46**).

Cells on the subarticular tubercles in juvenile frogs are irregularly shaped and large in juvenile frogs; $190.09 \mu\text{m}^2 \pm 7.25$ ($n = 46$), with distinct shallow grooves separating the cells at their perimeters (**Figure 6.47 b**). In adult frogs cells have become reduced in size, at around $141.3 \mu\text{m}^2 \pm 4.71$ ($n = 97$), and are more cuboidal and ‘spongy’ in appearance (**Figure 6.47 f**). Cells are more defined in shape and are largely hexagonal and heptagonal with straighter perimeter edges. Subarticular tubercles in adult frogs have shallow grooves and cell-shaped ‘spaces’ distributed across their surfaces (**Figure 6.47 e**). The sides of the cells neighbouring these trenches and gaps are modified so that the slightly inclined sides are rougher in texture to the surrounding cell surfaces (**Figure 6.47 e and f**). There is no evidence of the pad cell types being present on any of the subarticular tubercles in either adults or juveniles, which is significant in the light of the finding of these cells in other large species.

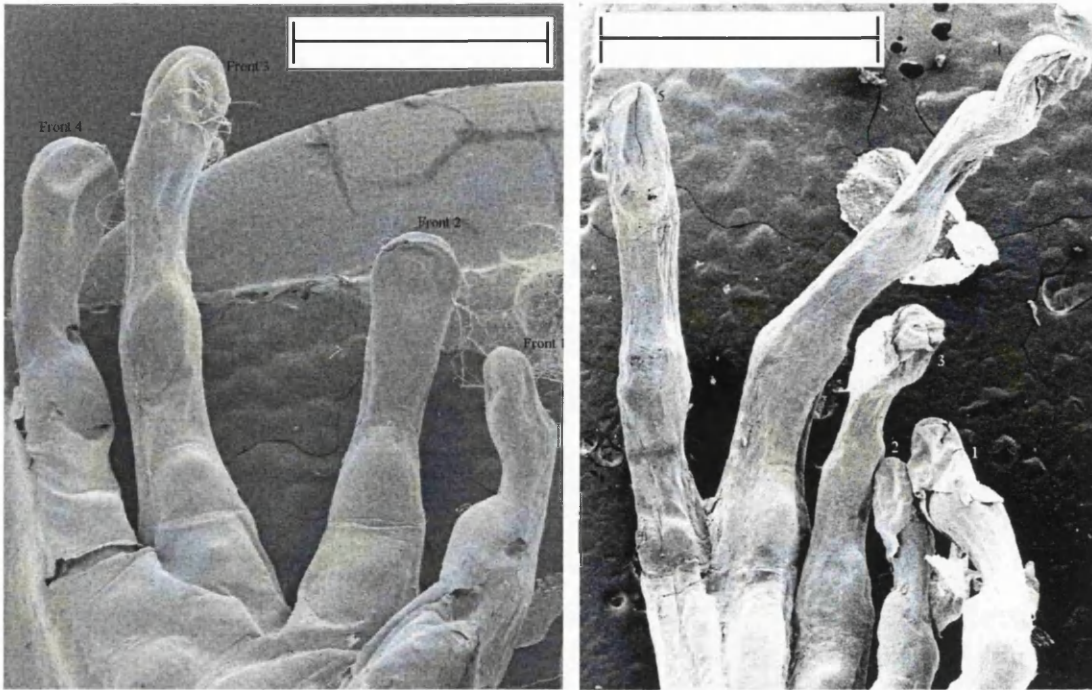


Figure 6.45: S.E.M. images of hand and foot morphology in juvenile *P. trinitatis*. Scale bar = 2.5 mm

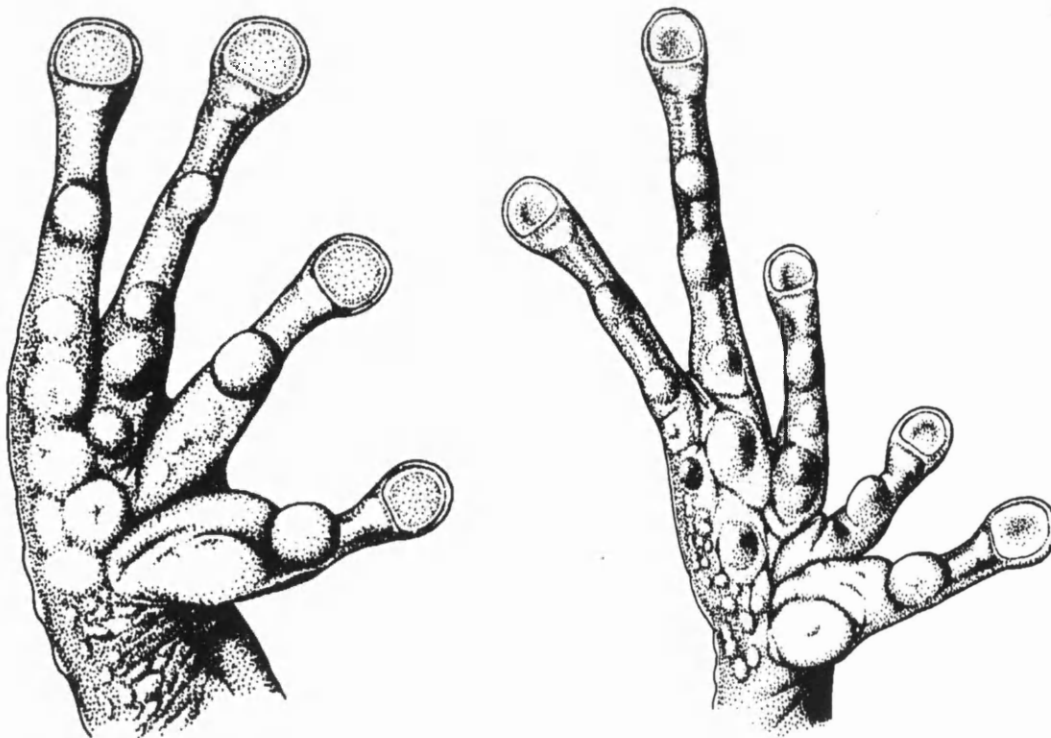


Figure 6.46: Diagram of hand and foot morphology in the closely related *P. venusta*

(Duellman, 2001)

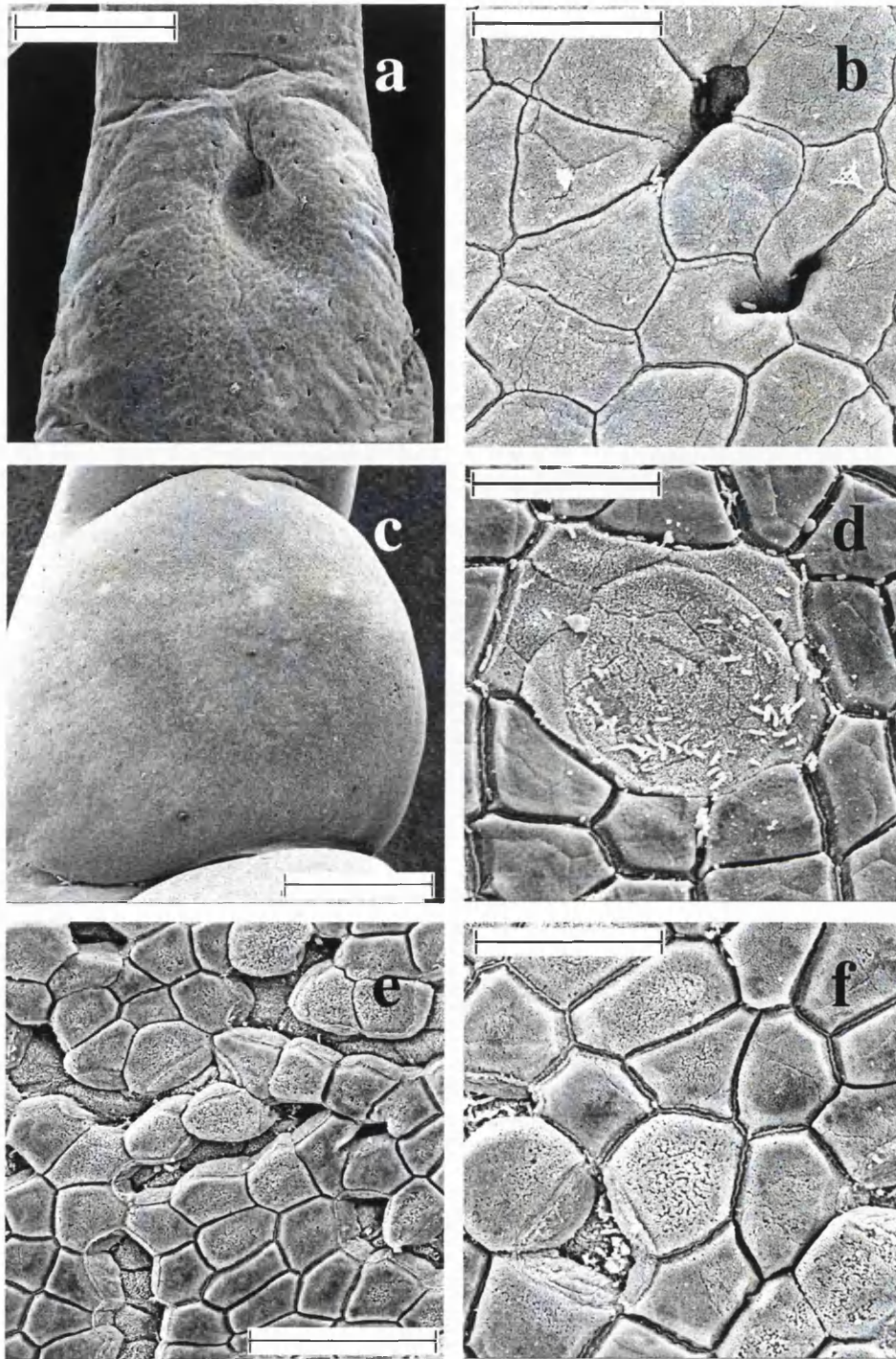


Figure 6.47: S.E.M. images of subarticular tubercles in *P. trinitatis*: (a) Juvenile 2 (28mm) Front 1, Scale bar = 300 μm (b) Juvenile 3 (37mm) Front 3, Scale bar = 25 μm . (c) Adult 1 (67.6mm) Back 1, Scale bar = 625 μm (d) Adult 1 (67.6mm) Back 1, Scale bar = 25 μm . (e) Adult 1 (67.6mm) Front 1, Scale bar = 50 μm (f) Adult 1 (67.6mm) Front 1, Scale bar = 25 μm .

Another feature of the subarticular tubercles exclusive to the adult age-class is the presence on the surfaces of distinctive rounded ‘paler’ regions (**Figure 6.47 c**). At higher magnification these can be seen to be single large concave cells that have, as yet, only been seen in this species (**Figure 6.47 d**).

These ‘bare’ patches are also visible on the swollen regions in proximal positions on the toe that form the supernumerary tubercles in the adult frogs (**Figure 6.48 c**). These are more discrete structures in juvenile frogs though are poorly developed on all but the third finger of the hand in the samples here (**Figure 6.45 and 6.48 a**). Difficulties in determining supernumerary tubercular regions in adults are in large part due to the continuance of modified cell types along almost the entire length of the toe (**Figure 6.33**). In regions where changes in elevation from the ventral surface do occur (**Figure 6.48 c**) the cells over these surfaces are not significantly different from the cell types seen in the more distally positioned subarticular tubercles (**Figure 6.48 d**), with this also being the case in juvenile frogs (**Figure 6.48 b**).

The development of tubercular region on the palm and the body of the foot in juveniles is poor and again, there is insufficient material to determine whether these are better developed in adults of the species. The swollen region at the base of the prepollex illustrated in *P. venusta* (**Figure 6.46**) is less prominent in *P. trinitatis* (**Figure 6.49 a**). Cells covering this surface are specialised and similar to those found on other tubercular regions along the toe, suggesting that this prepollical tubercle may also a part of the accessory adhesive system (**Figure 6.49 b**).

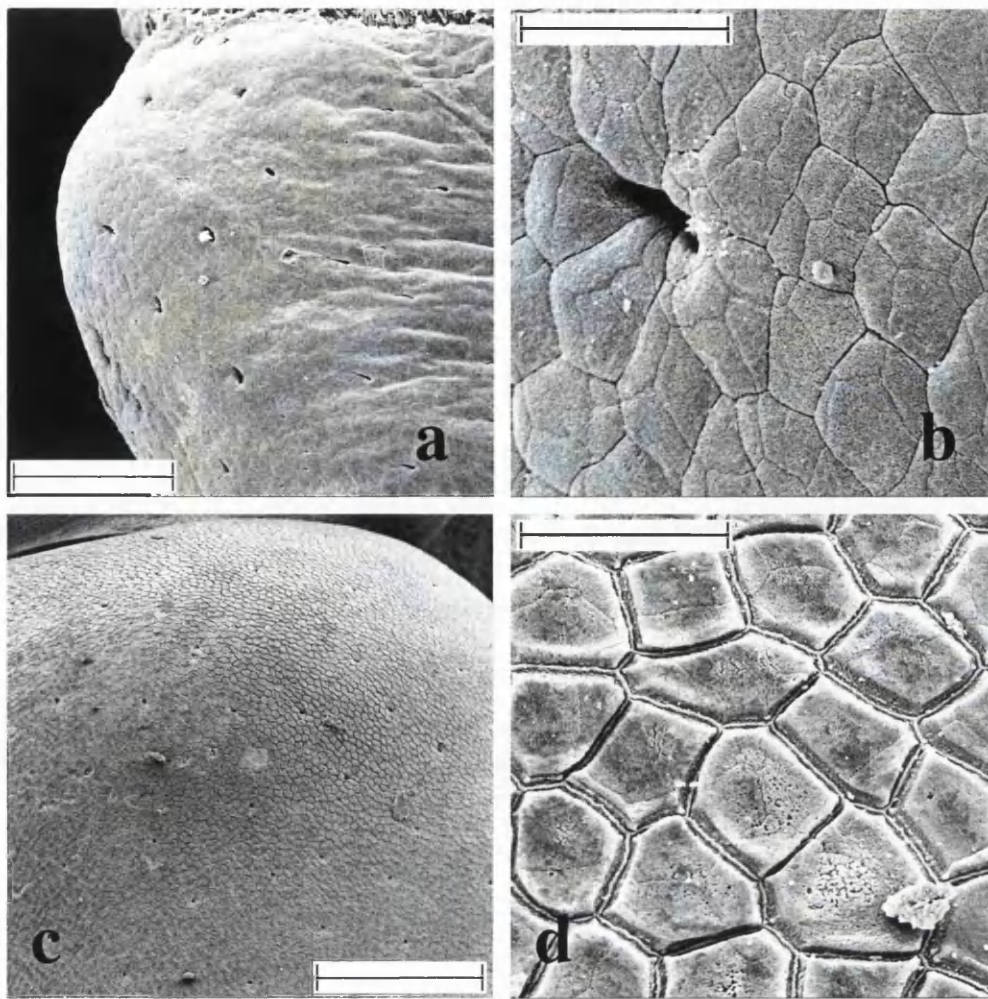


Figure 6.48: S.E.M. images of supernumerary tubercles in *P. trinitatis* (a) Juvenile (28mm) Front 3, Scale bar = 150 μm (b) Juvenile, Front 3, Scale bar = 25 μm (c) Adult 1 (67.6mm) Back 1, Scale bar = 300 μm (d) Adult 1 (67.6mm) Back 1, Scale bar = 25 μm .

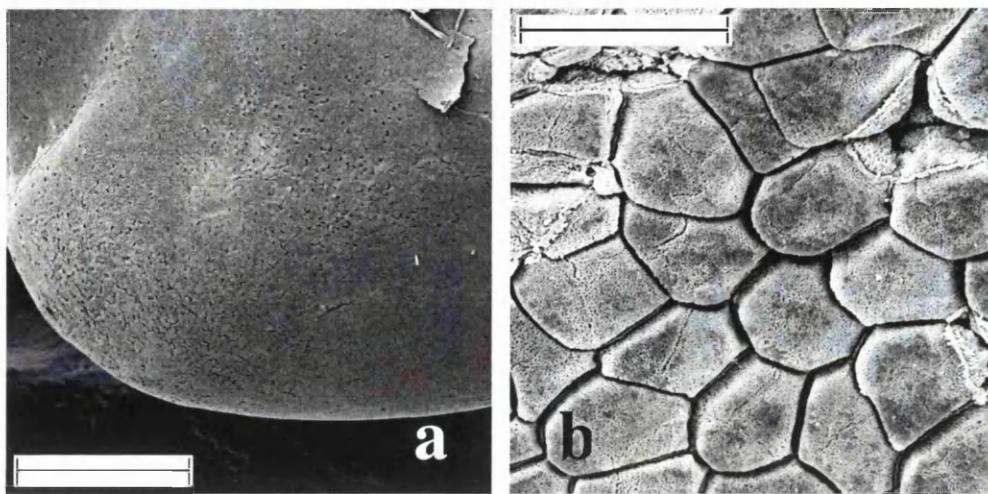


Figure 6.49: S.E.M. images of prepollex in *P. trinitatis* adult (a) Scale bar = 625 μm (b) Scale bar = 25 μm .

Hyla boans

Comparing hand and foot morphology in juveniles (**Figure 6.50**) and adult *H. boans* (**Figure 6.51**) neither age class appears to have a highly developed accessory system. The assessment of the extent of this system from adult samples in this instance is not possible, due to extensive damage to the areas below the toe pad proper, including subarticular tubercles (**Figure 6.53**). Comparisons between the age classes are based on descriptions of adults from Central America in Duellman (2001) from which the diagram of the hand and foot morphology is sourced (**Figure 6.51**).

Subarticular tubercles are small and rounded in the juvenile frogs (**Figure 6.50** and **6.52 a**), with distinctive shallow pits scattered liberally across their surface. Cells on tubercles are large and irregular in shape with ragged and indistinct intercellular margins (**Figure 6.52 b**). Whether any change in cell type in this area in adult frogs such as is seen in the closely related *H. crepitans* can only be a matter for speculation when images of the subarticular tubercles in this age-class are considered (**Figure 6.53**).

Supernumerary tubercles and palmar tubercles are described as being ‘indistinct or absent’ from adult samples in Central American frogs (Duellman, 2001). This is also the case in juvenile frogs where the most developed of the supernumerary tubercles are slight bumps at the base of the third and fourth fingers (**Figure 6.50**). The folded inner metatarsal tubercle described in adult frogs is also evident in the equivalent region of the foot in juveniles (starred in **Figure 6.50**).

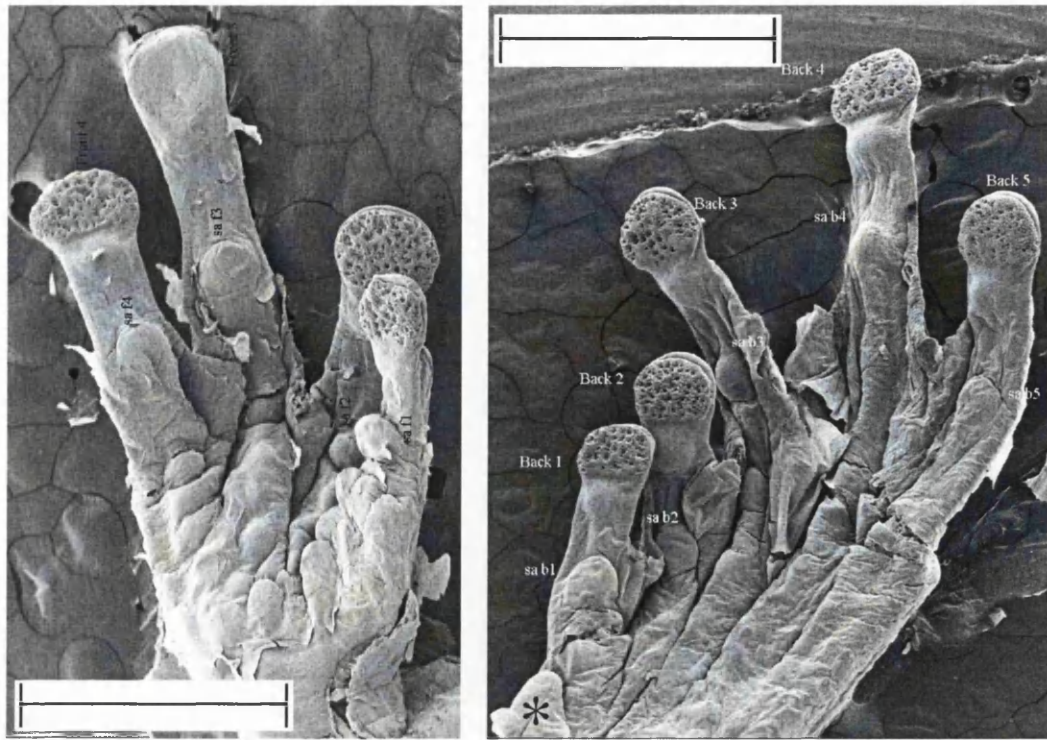


Figure 6.50: S.E.M. images of hand and foot morphology in juvenile *H. boans*. Scale bar = 1.25

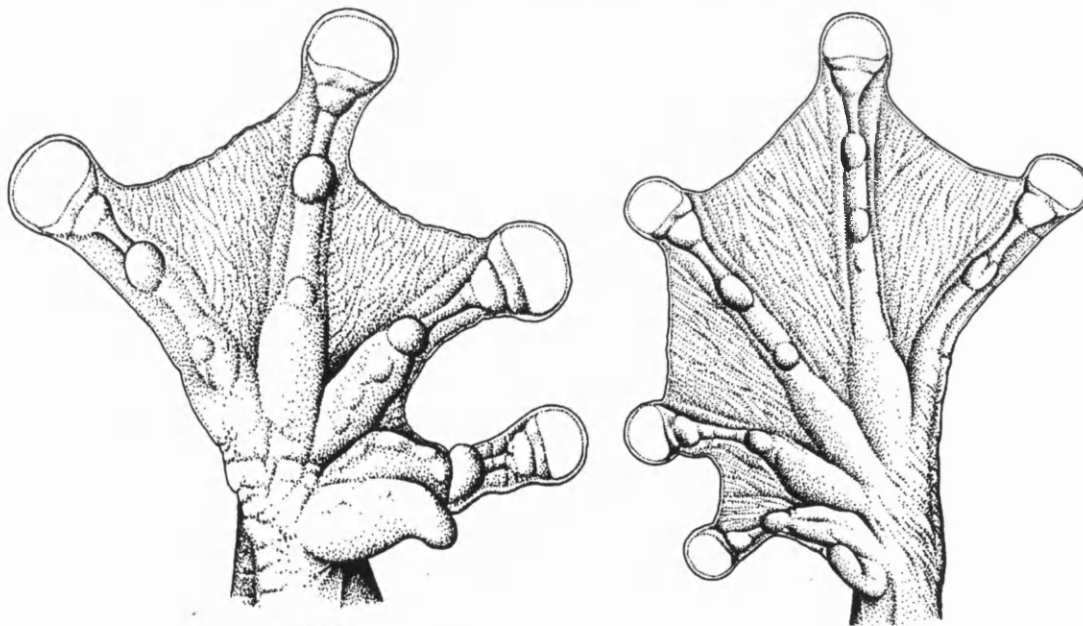


Figure 6.51: Diagram of hand and foot morphology in adult *H. boans* (Duellman, 2001)

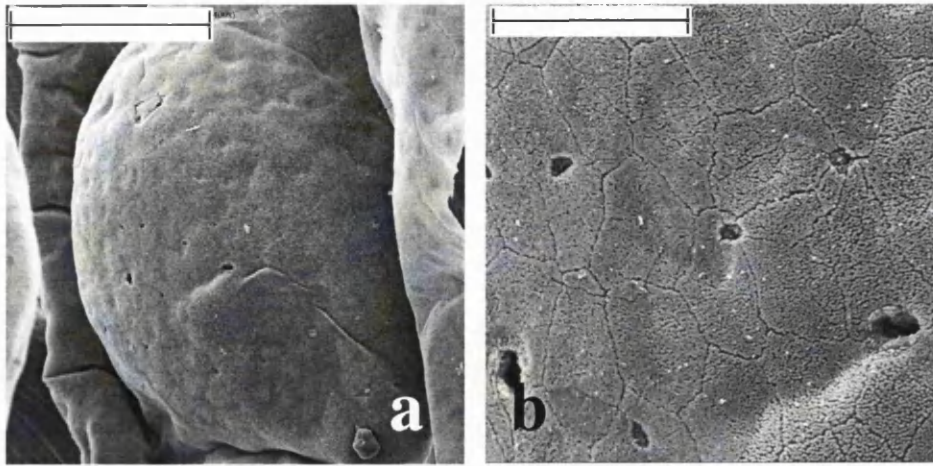


Figure 6.52: S.E.M. images of subarticular tubercles in juvenile *H. boans*: (a) Back 3, Scale bar = 150 μm (b) Back 3, Scale bar = 25 μm .

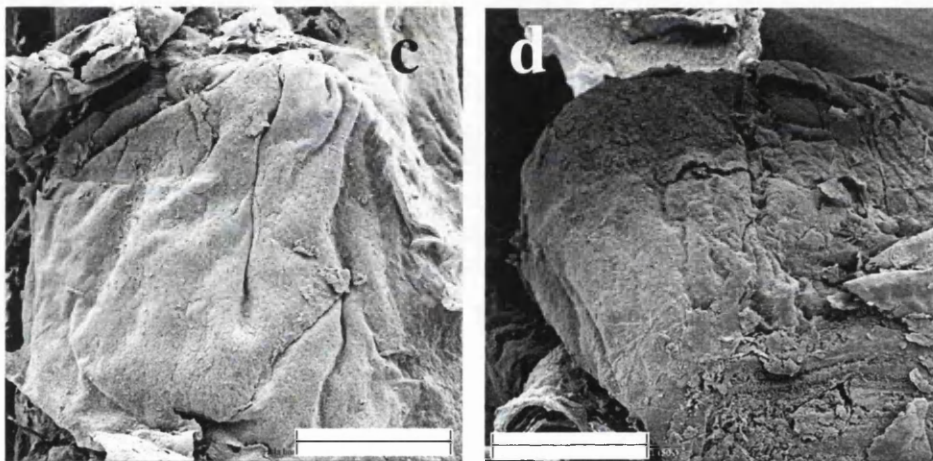


Figure 6.53: S.E.M. images of subarticular tubercles in adult *H. boans*: (a) Front 1 (b) Front 4. Scale bars = 625 μm .

6.3.4. Effects of size on toe pad morphology

Mean values for various aspects of toe pad morphology are given in **Table 6.3** for juvenile and adult frogs belonging to the three large species of hylid. There are few statistically significant correlations between these and increasing size between species though, as seen in the medium-sized species in **Chapter 5**, average mucosal pore size is positively correlated with the increasing linear dimension. This trend is retained within species in both *P. venulosa* and *P. trinitatis*, though only in the latter is this statistically significant (**Figure 6.54**).

Morphological variable	Correlation with SVL			
	r	p	n	t
Cell area (μm^2)	0.12	0.74	10	-0.35
Cell density (per mm^2)	0.30	0.40	10	0.90
Channel density (mm/mm^2)	0.06	0.87	10	0.87
Pore size (μm^2)	0.94	0.01	9	7.17
Pore density (per mm^2)	0.34	0.45	8	0.80
Pad elevation*	0.55	0.10	10	-1.87
Proximal margin*	0.51	0.13	10	-1.67
Circumferal groove*	0.04	0.92	10	0.11
Lateral groove*	0.52	0.12	10	1.73
Subarticular tubercle cells	0.24	0.57	8	-0.60

Table 6.2: Correlative statistics for relationships between SVL measurements and aspects of pad morphology between species in large hylid frogs. t-statistic for difference of line of best fit from the horizontal. Bold type indicates significant correlative relationship, * see **Table 6.3** for score definitions.

The degree of development of the grooves at the lateral margins of the toes' ventral surface is correlated with the increasing linear dimension in medium-sized species (**Chapter 5.3.5**). This trend is absent between species in this instance but is seen within species in both *P. venulosa* and *P. trinitatis* (**Figure 6.55**) However, it is noteworthy that the average score for adult *P. trinitatis* is below one (**Table 6.3**), meaning that maximally this groove is only a shallow one.

P. trinitatis also exhibits an additional within species relationship between pad structure and the linear dimension, in that there is a continual trend towards a flattening of the pad elevation with increasing size* (**Table 6.3**). This trend is of particular interest when considering the effect that the flattening of the pad may have on the adhesive abilities of larger frogs of the species adhering on a flat plane, such as that presented by the Perspex rotation platform. Although *P. trinitatis* are generally poor in terms of sticking performance, this species is one of the few in which adults are seen to maintain a grip to a significantly higher angle than juveniles. If a flatter pad in adults facilitates a more even conformation with the platform this may in part explain this observation. Whether this is the case or whether any of the other within and between species trends in pad morphology with increasing size can be explained by the effect that they may have upon the frogs' adhesive abilities, particularly in the cases where a greater than expected increase in the adhesive force production is seen, is of interest and is considered in **6.3.6**.

* Average pad elevation score vs. SVL in *P. trinitatis*: $r = 0.995$, $t = -14.63$, $p = 0.005$, $n = 4$.

Species	SVL	Cell area μm^2	Cell density per mm^2	Channel density mm/mm^2	Pore area μm^2	Pores per mm^2	Scores* for				SaT cell size (μm^2)
							Pad elevation	Lateral groove	Proximal margin	Circumferal groove	
<i>P. venulosa</i>	23.30	110.79	9166	161.39	39.65	26.75	1.89	0.72	2.17	2.06	111.81
	26.50	108.70	9473	157.71	60.82	25.09	1.44	0.89	1.78	1.61	186.28
	31.00	127.47	7963	137.53	27.93	6.67	1.28	0.94	0.56	1.28	144.96
	72.00	132.03	7622	134.06	113.76	18.98	1.44	1.50	1.28	2.28	111.81
<i>P. trinitatis</i>	28.00	102.50	1004	156.03	50.90	15.45	1.00	0.00	0.61	0.50	152.78
	37.00	142.74	7052	147.25	45.24	6.39	0.88	0.00	0.19	0.31	220.58
	67.60	92.49	11023	160.03	105.53	-	0.39	0.50	0.83	0.44	121.44
	71.00	120.21	8498	159.95	97.22	39.70	0.25	0.50	0.21	0.38	174.96
<i>H. boans</i>	14.00	137.39	7266	140.24	-	-	1.31	0.56	1.56	1.25	-
	98.00	118.25	8538	145.88	124.96	21.03	0.88	1.50	0.31	1.69	-

Table 6.3: Average values for aspects of toe pad morphology and subarticular (SaT) cell size in juvenile and adult frogs from three large species of Trinidadian hylid.

*Elevation score system: 0 = completely flat; 1 = slightly raised; 2 = rounded; 3 = globular. Groove score system: 0 = not present; 1 = shallow; 2 = defined; 3 = prominent.

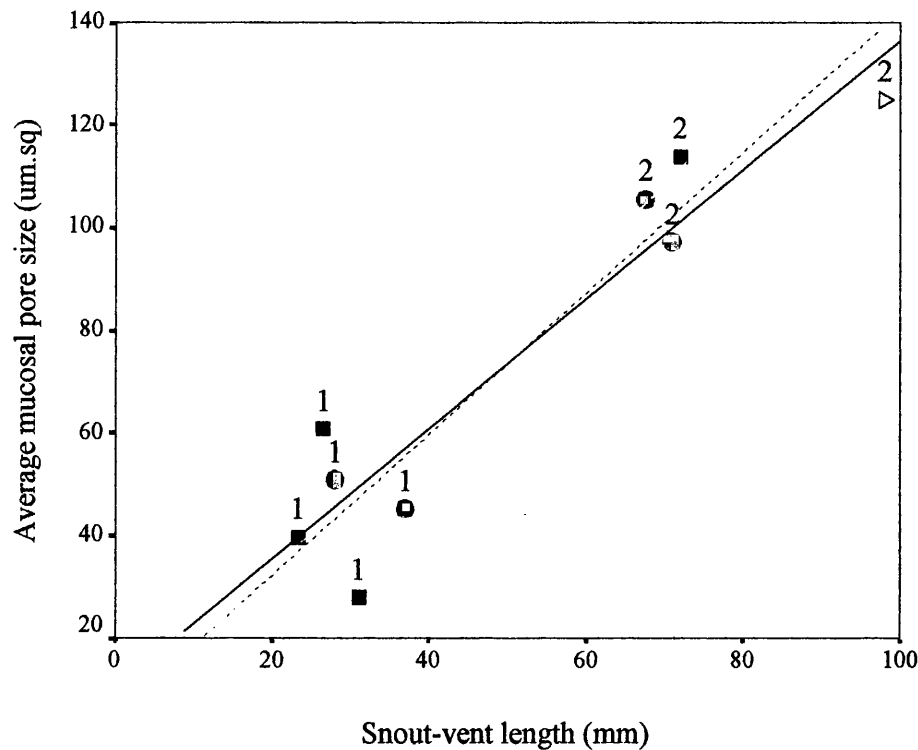


Figure 6.54: Average mucosal pore size (μm^2) vs. SVL in (1) juvenile and (2) adult frogs belonging to three large species of hyliid: *P. venulosa* (■); *P. trinitatis* (●); *H. boans* (▷). Correlative statistics: All frogs, $r = 0.94$, Line of best fit $y = 1.26x + 10.21$, $t = 7.17$, $p < 0.001$, $n = 9$. Individual species: *P. venulosa*, $r = 0.90$, N.S. $n = 4$. *P. trinitatis*, $r = 0.96$, $y = 1.37x + 4.87$, $t = 4.56$, $p = 0.05$, $n = 4$.

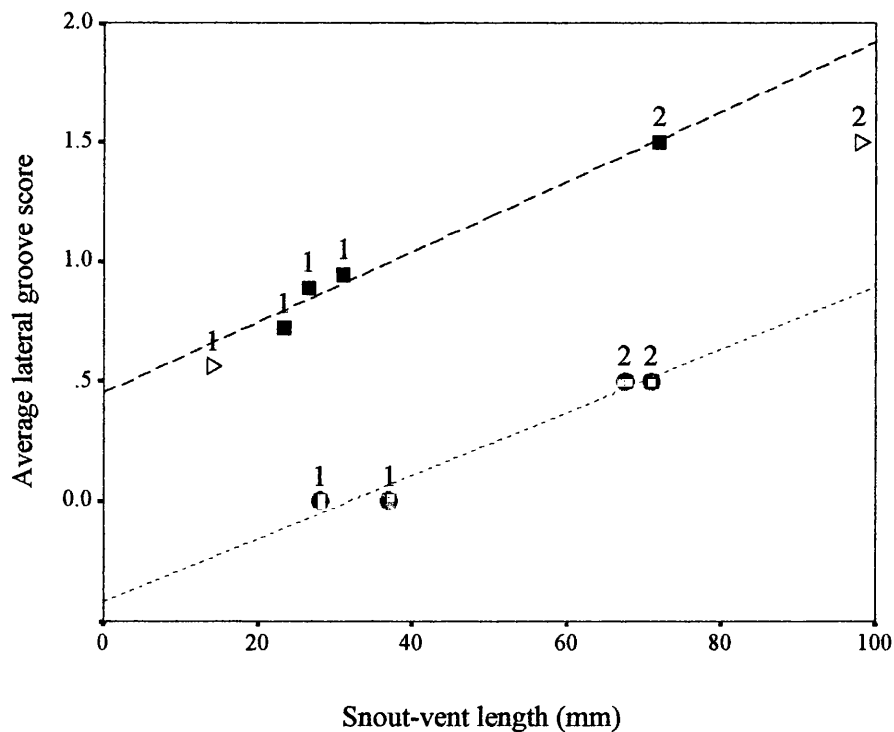


Figure 6.55: Average lateral groove score vs. SVL in (1) juvenile and (2) adult frogs belonging to three large species of hyliid: *P. venulosa* (■); *P. trinitatis* (●); *H. boans* (▷). Correlative statistics: All frogs, $r = 0.55$, N.S. $n = 10$. Individual species: *P. venulosa*, $r = 0.99$, $y = 0.01x + 0.45$, $t = 8.51$, $p = 0.01$, $n = 4$. *P. trinitatis*, $r = 0.98$, $y = 0.01x - 0.42$, $t = 7.65$, $p = 0.02$, $n = 4$.

6.3.6. Integrating pad morphology and adhesion

Detachment angles were recorded from frogs prior to the examination of their toe pads in S.E.M. studies. Adhesive forces and forces per unit area were calculated from these (as described in **Chapter 2**) for each frog (**Table 6.4**). These were then analysed with respect to aspects of toe pad morphology (**Table 6.5**).

Species	SVL	Angle	Adhesive force (mN)	Force per mm ² (mN)
<i>P. venulosa</i>	23.30	156.00	5.50	0.81
	26.50	123.60	7.96	0.43
	31.00	105.38	9.85	0.19
	72.00	133.90	134.31	0.98
<i>P. trinitatis</i>	28.00	98.30	3.27	0.21
	37.00	99.90	5.28	0.26
	67.60	105.50	55.00	-
	71.00	96.50	44.64	0.58
<i>H. boans</i>	14.00	153.70	2.72	0.36
	98.00	113.80	177.78	0.78

Table 6.4: Detachment angles, adhesive forces and forces per unit area calculated for frogs used in S.E.M. studies.

Again, as seen in the medium sized species, there are trends between these that run counter to predictions made from the between species trends in **Chapter 2**, specifically in relation to the positive correlation seen between pore size and adhesive force both between species (**Table 6.5**) and within *P. venulosa* and *P. trinitatis* (Adhesive force vs. average pore size in: *P. venulosa*, $r = 0.93$, $y = 0.56x + 38.53$, $p = 0.07$, $t = 3.59$, $n = 4$; *P. trinitatis* $r = 0.99$, $y = 1.16x + 43.42$, $p = 0.007$, $t = 12.09$, $n = 4$). The strength of the correlative relationship is reduced when considering the effect

on pad efficiency, i.e. the force per unit area, between species (**Table 6.3, Figure 6.56**) but the trend between the two parameters is still counterintuitive.

Trends are seen between the average score for lateral groove development and adhesive force both between species (**Table 6.3**) and within-species (Adhesive force vs. lateral groove score: *P. venulosa*, $r = 0.97$, $y = 0.01x + 0.81$, $p = 0.03$, $t = 5.34$, $n = 4$; *P. trinitatis*, $r = 0.99$, $y = 0.01x - 0.04$, $p = 0.01$, $t = 8.63$, $n = 4$.) The relationship between lateral groove development and adhesion is sustained when the force per unit area is considered (**Figure 6.57**). The implication of this, that there is an increasing pad efficiency facilitated by the development of the lateral groove may perhaps explain the continuous development of this feature seen in *P. trinitatis* and *P. venulosa* with the increasing linear dimension.

Force per unit area is correlated with the increasing definition of the circumferal groove around the margin of the pad, both between species and within *P. venulosa* (**Figure 6.58**). There is, however, no correspondent effect of increasing size upon the degree of development in the circumferal groove (**Table 6.2**) suggesting that the relationship between the definition of this margin and the increase in the pad efficiency is attributable to some other pressure upon the frogs' sticking ability rather than that of increasing weight with growth.

The elevation of the pad in *P. trinitatis*¹ is negatively correlated with force per unit area, supporting the prediction that the flattening of the pad seen in adults of the species (see **6.3.6**) allows the closer conformation of the pad to the surface.

¹ Adhesive force per unit area vs. pad elevation: $r = 0.999$, $t = -31.92$, $p = 0.02$, $n = 3$

Morphological variable	Adhesive force (mN)				Force per mm ² (mN)			
	r	p	n	t	r	p	n	t
Cell area	0.02	0.96	10	0.06	0.07	0.86	9	-0.18
Cell density	0.22	0.54	10	0.64	0.46	0.21	9	1.37
Channel density	0.33	0.35	10	-0.99	0.03	0.94	9	-0.09
Pore size	0.87	0.01	9	4.62	0.70	0.06	8	2.37
Pore density	0.15	0.73	8	0.36	0.51	0.20	8	1.44
Pad elevation	0.19	0.61	10	-0.54	0.23	0.56	9	0.62
Proximal margin	0.26	0.47	10	-0.76	0.32	0.40	9	0.90
Circumferal groove	0.40	0.25	10	1.23	0.71	0.03	9	2.69
Lateral groove	0.76	0.01	10	3.29	0.70	0.03	9	2.63
Subarticular cell	0.49	0.22	8	-1.36	0.63	0.13	7	-1.82

Table 6.5: Correlative statistics for relationships between adhesive force and force per unit area with SVL in three large species of hyliid. t-statistic for difference from the horizontal of line of best fit. Bold type denotes correlations significant to $p = 0.01$.

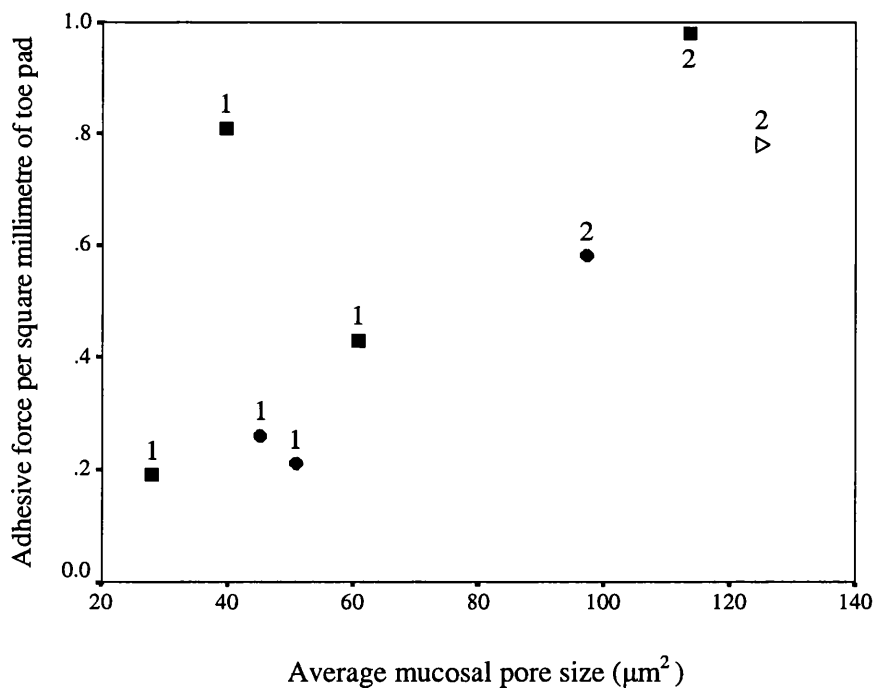


Figure 6.56: Force per unit area vs. average mucosal pore size in (1) juvenile and (2) adult frogs belonging to three large species of hyliid: *P. venulosa* (■); *P. trinitatis* (●); *H. boans* (▷).

Correlative statistics; All frogs, $r = 0.70$, ($y = 0.006x + 0.13$) $t = 2.37$, $p = 0.06$, $n = 8$;

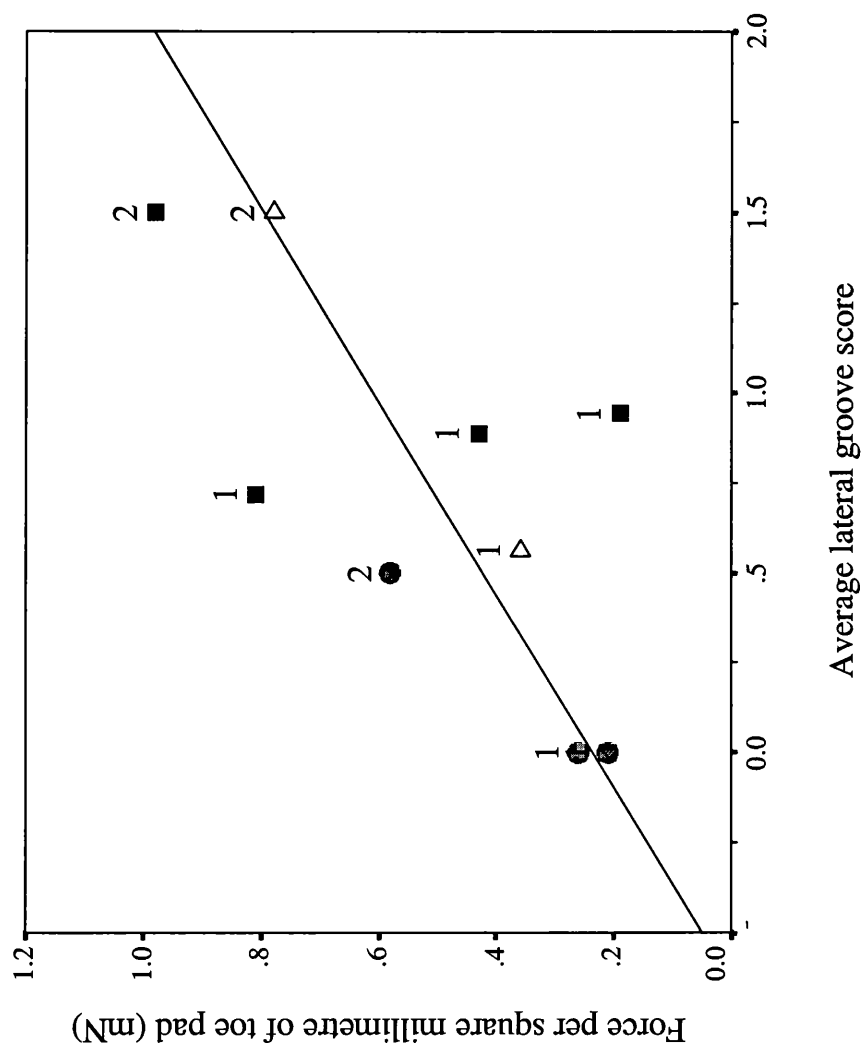


Figure 6.57: Force per square millimetre of toe pad vs. average lateral groove score in (1) juvenile and (2) adult frogs belonging to three large species of hylid: *P. venulosa* (■); *P. trinitatis* (●); *H. boans* (△). Correlative statistics: All frogs, $r = 0.70$, $y = 1.79x + 0.35$, $t = 2.69$, $p = 0.03$, $n = 9$.

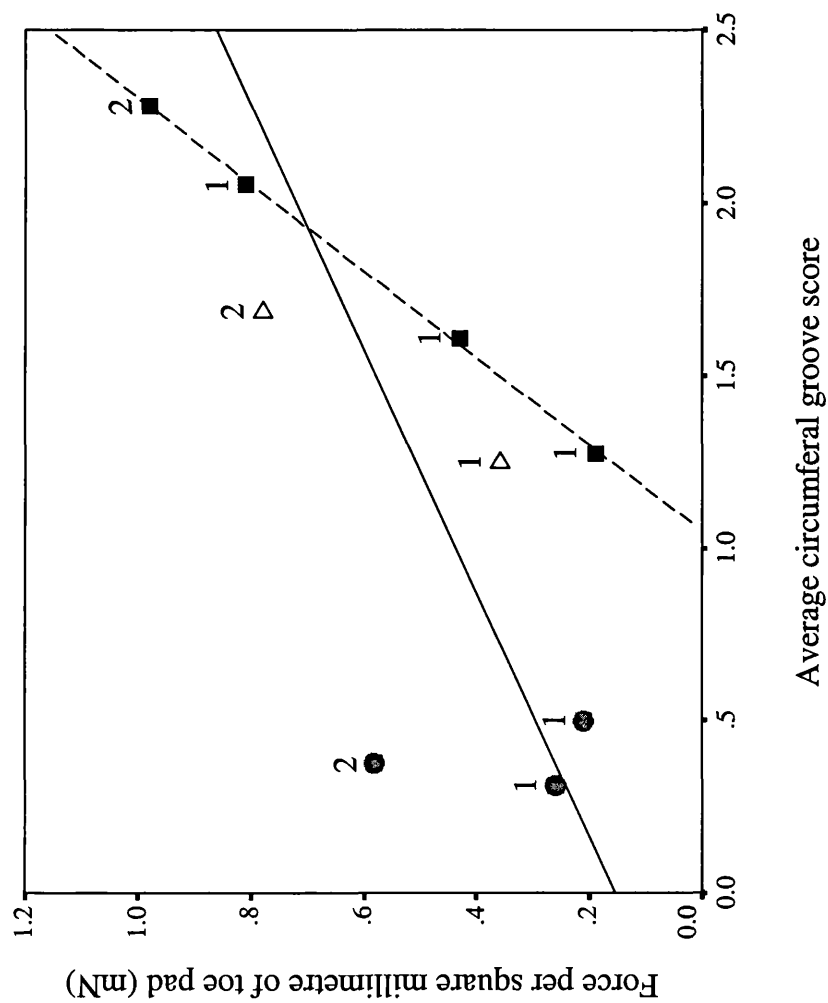


Figure 6.58: Force per square millimetre of toe pad vs. average circumferential groove score in (1) juvenile and (2) adult frogs belonging to three large species of hylid: *P. venulosa* (■); *P. trinitatis* (●); *H. boans* (△). Correlative statistics: All frogs, $r = 0.71$, $y = 1.33x + 0.05$, $t = 2.63$, $p = 0.03$, $n = 9$. Individual species: *P. venulosa*, $r = 0.999$, $y = 1.25x + 1.05$, $t = 41.64$, $p = 0.02$, $n = 4$.

6.4. Discussion

The three large species of tree frog found in Trinidad are from three different genera within two separate subfamilies within the Hylidae. The subfamily *Phyllomedusa* is thought to represent an early phyletic divergence within the Hylidae (Duellman, 1968) and differ from the Hylinae, the family to which the other hylids in this study belong, in several aspects of their behaviour and morphology. This includes, most relevantly in relation to the scope of this study, the morphology and function of their hands and feet. The Phyllomedusine genera are chiefly distinguished from other hylids by the very different way in which they move through their environment, with frogs having evolved a locomotory mode that is more dependent on grasping abilities, and which resembles those used by small primates. If, as in small primates, climbing abilities are more dependent on frictional forces (Cartmill, 1979) then this will have a significant effect on the rate of increase in adhesive force production with growth, as frictionally dependent forces would be expected to scale directly with weight. Indeed, this may well explain the rate of increase in adhesive force production with growth seen *P. trinitatis*, which is significantly higher than seen in the other large species being considered here, scaling with increasing weight to such an extent that the adhesive performance of adults is in fact significantly better than seen in juveniles of the species. In spite of this, the average angles to which both adult and juveniles are able to adhere on Perspex are lower than any of the other species considered thus far, perhaps providing evidence that the climbing abilities in these frogs is more influenced by the contribution of frictional forces than other species, as a mechanism dependent on this would be adversely affected on a smooth surface.

That behavioural differences in this species may indicate that there is a reduced dependence on wet adhesion for locomotion is all the more note-worthy when the changes in toe pad area with growth are taken into consideration. Although some larger species show trends towards a greater rate of increase in pad area than expected through isometry (as the linear dimension squared) particularly amongst the juvenile frogs, *P. trinitatis* is the only species in which the trend is significant. In juvenile *P. trinitatis* pad area is increasing at a rate no different to the equivalent increase in weight in the same growth period. This disproportionate increase in toe pad area may largely explain the greater than expected increase in adhesive forces seen in the same period but the trend does not continue across the total population so cannot explain the improvement in sticking performance seen in adults of the species.

There is, however, a trend towards a reduction in weight gain with growth seen across the total population in *P. trinitatis*. This is much as seen in most other species, where wet adhesion is likely to be the dominant mechanism by which frogs maintain sticking abilities, including the other two large hylid species under consideration in this chapter. The larger size of the adult frogs of these species might lead to an expectation that the degree to which weight gain differs from the expected will be greater than in other smaller species where the pressures of increasing size will not be as high (**Table 6.1**). That this is not the case is somewhat surprising though the explanation, as discussed for species in previous chapters, may lie in the influence of other morphological trends upon the ability of the frogs to escape predation or to otherwise function in their environment.

The comparative Tibia:SVL ratios in large species indicate that they likely to have proportionally shorter hind limbs than many of the species considered thus far (Tables 4.6, 5.6 and 6.6). This is likely to be due to the high degrees of arboreality described in the literature for all three species (Appendix 4.1) as the shortening of the limbs is beneficial to arboreal animals giving them an increased stability of locomotion when walking along branches in the trees (Cartmill, 1985). However, it is also likely to have a detrimental effect upon jumping ability in these species, particularly so in *P. trinitatis* and *P. venulosa* (Table 6.6) where the extent to which the limbs are shortened is greater than in *H. boans*.

Ratios of measured physical parameters	<i>P. venulosa</i> ¹	<i>Phyllomedusa</i> ²	<i>H. boans</i> ³
Tibia: SVL	0.48	0.47	0.51
Foot: SVL	0.40	0.35	0.44
Head length: SVL	0.30	0.35	0.35
Head width: SVL	0.31	0.34	0.35

Table 6.6: Ratios of physical measurements from male frogs of large species. Derived from (1) Duellman, 1956; frogs from Trinidad (2) Duellman, 2001; *P. venusta*, Panama (similarly sized frog in *P. trinitatis*' species group) (3) Duellman, 2001; frogs from Panama.

The reduced degree to which the rate of weight increase is lowered in *P. venulosa* may be a response to effects of shorter hind-limb length on jump distance, as heavier frogs are able to jump further (Emerson, 1978; Choi *et al.* 2000). The concurrent loss in acceleration may be of reduced importance to this species as these frogs have an additional anti-predator strategy which may reduce the degree to which it is reliant on jumping as an escape strategy, i.e. the ability to produce large amounts of highly allergenic mucus which is capable of irritating even the most persistent of predators (Leary *et al.* 1998) or biologists (Smith, 1941). This may also be the case in *P.*

trinitatis; several species of frog in the subfamily *Phyllomedusinae* are known to have an array of skin peptides that act as anti-microbial agents (Vanhoye *et al.* 2003). In the large Central American species, *Phyllomedusa bicolor*, other bioactive skin compounds include: phyllomedusine, which in humans causes severe cramping in the intestines and bowels; phyllocaerulein, which induces nausea and vomiting; phyllokinin, which acts as a vasodilator; and sauvagine which can cause severe tachycardia and stimulation of the adrenal cortex (Erspamer *et al.*, 1993)¹. If such compounds also exist in *P. trinitatis* and similar effects are induced in vertebrate predators then it is possible that these species too are able to maintain a more elevated rate of weight increase in spite of the effect it will have on jumping performance (Emerson, 1978). That there are no alternative anti-predator devices in *H. boans* may explain the less pronounced reduction in the hind limb length when compared with the other two large species, in spite of the high degree of arboreality seen in the adult frogs, so that jumping ability is maintained with increasing size.

The reduction in weight gain with growth seen in the two species from the subfamily *Hylinae*; *P. venulosa* and *H. boans*, is not sufficient for the adhesive mechanism to compensate adequately, leading to the significant decrease in the average detachment angles seen in adult frogs in both species. This is most pronounced in the largest of the species where adhesive forces increase as predicted from interspecific studies from adult frogs in **Chapter 2**, with toe pad area. In *P. venulosa*, adhesive forces do increase at a higher rate than the correspondent increase in toe pad area; though not to a sufficient extent to compensate for the weight gain, in spite of the reduction in this from the expected rate, as (SVL)³.

¹ Hence the use of these frogs in 'shamanic practices' in Central America (Erspamer *et al.*, 1993).

The suggestion that this raises of an improved efficiency within the wet adhesive system, that may allow for this greater increase in force with growth than can be explained by the equivalent toe pad area, is supported by consideration of the trends in the force per unit area with the increasing linear dimension within *P. venulosa*. It may be that if there is a reduced dependence on jumping ability for predator avoidance in this species that the limitations on the viscosity of the intervening meniscal layer will be lesser in this species and therefore this may be alterable. Although this is not determinable within the confines of the present study, the discussion of the study by Evans and Brodie (1994) on the defensive mucus in this species in **Chapter 2**, rules out the use of a viscous mucus of a similar tensile strength below the pad when considering the average adhesive forces recorded within adult frogs in comparison to that that would be possible were the viscosity of the fluid to increase.

If frogs are able to improve their adhesive abilities at a greater rate than expected, is there any evidence from looking at the structure of the specialised toe pads of changes in morphology that may aid in the reduction of the meniscal height or other meniscal properties that might have a beneficial effect on the forces that are being produced? Across-species trends exist such that larger cell size is positively correlated to adhesive force, and although in *P. venulosa* and *P. trinitatis* cell size is seen to be significantly larger in the adult frogs than in the juveniles, though no direct effect on the frogs' adhesive abilities can be demonstrated. The structuring of the cell surfaces in all three species is roughened in adults in comparison to that of the juvenile frogs, perhaps indicating that additional frictional forces in adult frogs are complementing the wet adhesive mechanism and allowing for improvement in pad efficiency within

P. venulosa and *P. trinitatis*. It may also be that this roughening is a consequence of wear and tear to the toe pad, which, if this is the case may be indicative of a need for a fairly rapid turnover in the outer cell layer in this area in large species.

Mucosal pore size increases in all three large species with increasing linear dimensions, suggesting that, counter to expectations, the mucosal layer may be increased in larger frogs. Whether the changes in the sizes and structures of the most commonly seen pore type on pads in adult frogs of these three large species is indicative of a change in the mucosal properties with growth in these frogs is, as yet, indeterminable. Mucosal pore sizes are largest in adult *H. boans*, perhaps reflecting an increased importance of the mucosal properties in this species in adhesion to those in the other large species that might allow the observation of a lack of an effect in the adhesive abilities on substrates with differing wettabilities. In *P. trinitatis* both average pore size and densities per unit area of the pad are higher in value in adult frogs that suggests the mucosal output the pad may well be increased in these frogs. The lesser tendency to escape predator threat by jumping seen in *P. trinitatis* may also indicate that the limitations on mucosal viscosity that are likely to influence the properties of the fluid involved in wet adhesion are lesser than in other species.

In species discussed in earlier chapters, there has been is some evidence of changes in pad morphology that may aid in the reduction of the meniscal height; via the increasing definition of the circumferal margin by a deepening of the circumferal groove in the 'small' species and with the development of the lateral grooves in the 'medium' species. Demonstrable relationships are seen between the degree of development of the lateral grooves and increasing frog size in large species with

average scores for lateral groove definition in large species positively correlated to the increasing linear dimension both in *P. trinitatis* and in *P. venulosa*. In *H. crepitans* (see **Chapter 5**) the increased definition of the lateral grooves corresponds with a development in the cell types seen on the subarticular tubercles in the adult frogs. Where in all species smaller in size than *H. geographica* cell structure on these accessory areas is akin to that seen on the proximal margins of the pad, with roughened micro-villated surfaces, in *H. crepitans* cells are not distinguishable visually from those seen on the pad proper. That this is also the case in *P. venulosa*, the only large species where the relationship between lateral groove development and meniscal height is maintained intraspecifically, perhaps suggests that this is another way in which the species is able to increase the contact area producing forces through wet adhesion at a proportionally higher rate than by using toe pad area alone, again suggesting that the accessory adhesive areas may play a more important contributory role in tree frog adhesion than has previously been considered. The development of the lateral groove system is likely to aid in the even spreading of mucus across the surfaces that are adhering using wet adhesion.

It is interesting to note the lack of pad cells on the subarticular tubercles of *P. trinitatis*, in the light of their presence on these structures in other similarly sized species this may indicate a lesser pressure to increase the wet adhesive abilities in these frogs relative to others. The increased tendencies to utilise branches noted in juveniles of this (**Appendix 6**) may indicate that the development of pad structure in *P. trinitatis* is more likely to favour changes in the structure that are beneficial to the grasping mode of locomotion needed to climb along branches and twigs rather than the ability to move across smooth substrates.

Both *P. venulosa* and *P. trinitatis* have increased the distribution of modified cell types along the ventral surface of the toe. Although these are not specialised to the extent of those on the pad proper, they are sufficiently different to the ordinary dorsal skin cells to suggest that they serve some function in the adhesive system. The distinct intercellular channels running between the cells may act in conjunction with the lateral grooves to aid in the even distribution of mucus to areas in contact with substrates. The cells in this region show evidence of recent sloughing of the previous layer in both species, in the imprint visible across their surfaces of the shed upper layer. This may perhaps suggest that this area is susceptible to continuous wear (Trauth and Wilhide, 1998) but as frogs regularly shed their skin after feeding, without specific information about the time that has elapsed since the last sloughing of the skin in the individuals sampled it is difficult to be certain that the visualisation of these imprints does not simply reflect the stage of moulting in the frogs.

The increasing definition of the circumferal groove, though showing a tendency towards an increasing specialisation of cell types on the marginal borders in adults, is not demonstrably linked with increasing size either within or between these large species. This suggests that the relationship between the definition of this margin and the increase in the pad efficiency is likely to be attributable to some other pressure upon the frogs' sticking ability than increasing weight with growth, perhaps an increasing degree of arboreality as suggested by Hertwig and Sinsch (1995). All three of these species are arboreal as adults, so the consideration of the interspecific differences in the development of this feature as a response to differences in the degree of arboreality is problematic.

It may well be that frogs change the degree of their arboreality at various stages of life history, in response to differences in foraging considerations between the age classes, for example. Behaviour of post-metamorphic froglets under natural conditions is generally an understudied variable, but studies on population dynamics both in *H. boans* (Duellman, 2001) and *P. venulosa* (Yanosky *et al.* 1997), found small sized individuals at substantial heights within trees; with juvenile *H. boans* sampled from heights of around 7m and new-metamorph-sized *P. venulosa* from 'high forest drift fences', suggesting that frogs are arboreal from early stages of their life histories. Behavioural studies of juvenile *P. trinitatis* with relation to the choice of substrate height were inconclusive due to strong degrees of perch fidelity seen in lab-reared individual froglets during the day (**Appendix 6**).

Results suggest that in spite of reduced weight gain with growth and changes in toe pad morphology that may facilitate increased spreading of the mucosal layer, the two large Hyalinae species are unable to increase the adhesive forces produced to allow them to maintain a grip upon the experimental substrates to the same degree as in juvenile frogs. In the only large species in which adhesive forces do manage to keep pace with increase in weight with growth, there is a tendency amongst the juvenile frogs to have a substantially increased rate of increase in toe pad area coupled with the most reduced weight gain of all three large species. Furthermore, behavioural consideration of the way in which this species moves through its environment suggests that the dependence on the area-dependent wet adhesive mechanism is likely to be much reduced.

In previous chapters, differences in the responses to the pressures upon the adhesive system have chiefly been considered in relation to the adhesive abilities under experimental conditions with some reference to aspects of species' ecology. These have suggested that the degree to which the trade-offs between the ability to maintain a grip and the effects of the response on other locomotory considerations will differ between species according to differences in anti-predator responses and degrees of arboreality. The following chapter considers the differences in the interspecific responses to the pressures imposed by growth upon the adhesive mechanism in Trinidadian hylids. These will be particularly examined in relation to differences in eventual adult size, comparative allometry and aspects of life history that may account for differences in the strengths of the responses to these pressures.

Chapter 7: General discussion

7.1. Allometry and adhesion

Many species of frog, over a wide range of taxa, possess specialised digital pads, which allow them to adhere to smooth and often vertical surfaces. The means by which the pads enhance the frogs' sticking ability has long been under dispute though recent work has led to the growing consensus that the mechanism is likely to be that of wet adhesion (Emerson and Diehl, 1980; Green, 1981a; Hanna and Barnes, 1991; Barnes, 1997; Barnes, 1999).

This study aimed to investigate the problems that this might present to tree frogs as they increase in size both on an interspecific and an intraspecific level. Emerson (1977) notes that as frogs are known to maintain a similar shape over a wide size range, they are particularly useful for the study of allometric effects; if this is true of the hylids in this study and Trinidadian frogs are geometrically similar, and growth were to occur following isometry, then weight will scale with increasing body lengths at a significantly higher rate than the equivalent to pad area. It might therefore be expected that any adhesive system dependent on toe pad area, as has been shown to be in evidence in adult frogs belonging to these species (**Chapter 2**), might be presented with a considerable challenge in terms of their ability to cope with the effects of increasing weight with growth.

At the beginning of this study it was hypothesised that there may be a number of ways in which the ability to cope with the problems of maintaining adhesion with

growth may be effected including: changes to the properties of the intervening fluid layer effecting wet adhesion, developmental changes in toe pad morphology that may enhance the functional efficiency of their ‘design’ and deviations from isometric patterns of growth that might aid in the maintenance of adhesive abilities around a similar level with growth.

Between adults belonging to the twelve species under investigation there is some evidence of the latter of these trends, with a significantly reduced rate of increase in weight from the expected should the frogs be scaling isometrically (**Figure 2.4 a**). However, the extent of this reduction between species is not sufficient for the equivalent toe pad area, which does increase following isometry (**Figure 2.4 b**), to compensate effectively for the increasing pressures upon the adhesive system imposed by increasing size and larger species are less able to maintain a sustained grip upon smooth surfaces at angles beyond the vertical than smaller ones.

This led to the question, considering the large increase in size that is involved in the period of growth from metamorphosis to adulthood, whether frogs within an individual species would be able to increase adhesive force at a sufficient rate for there not to be a detrimental effect of their increasing mass upon their sticking abilities.

Table 7.1 gives a summary of the slopes of the lines of best fit on log:log plots shown in previous chapters for the six species for which the most complete range of data from both juvenile and adult frogs exists and illustrates the relationships between snout-vent length, adhesive force, weight and toe pad area. This shows that for all the species, the increase in adhesive force with increasing linear dimension occurs at a faster rate than would be expected from the interspecific adult results (**Chapter 2**) or from previous studies on tree frog adhesion where adhesive forces scale directly with toe pad area increase (Emerson and Diehl, 1980; Green, 1981a; Hanna and Barnes, 1991; Barnes, 1997, 1999; Barnes *et al.* 2000). Furthermore, in all but the largest species, the adhesive forces scale at a sufficient rate to match the increase in weight od suggesting that tree frogs are able to adjust the mechanism in order to compensate adequately for growth effects to maintain adhesive abilities around a similar level between age classes without a significantly higher rate of increase in toe pad area.

Species	Log:log SVL vs.							Tibia: SVL ratio
	Adhesive force			Toe pad		Weight		
	Slope	vs.		Slope	vs. 2	Slope	vs. 3	
		Toe pad	Weight					
<i>F. fitzgeraldi</i>	2.51	>	=	2.07	=	2.53	<	0.55
<i>S. rubra</i>	2.69	>	=	1.53	=	2.73	<	0.51
<i>H. geographica</i>	2.90	>	>	2.15	=	2.48	<	0.53
<i>H. crepitans</i>	2.71	>	>	2.22	=	2.51	<	0.56
<i>P. trinitatis</i>	3.14	>	>	2.93	>	2.78	<	0.48
<i>P. venulosa</i>	2.72	>	<	2.13	=	2.95	<	0.47

Table 7.1: Slopes of lines of best fit for relationships between SVL and adhesive force, toe pad area and weight on log-log plots, with indications in the trends in comparative differences from slopes of relationship between other variables or from predicted slopes. Bold type denotes statistically significant differences from trends expected from previous studies on adhesion and allometric predictions.

McAllister and Channing's (1983) study of toe pad morphology in tree frogs from the family Rhacophoridae states that larger species were found to have proportionally larger pads than smaller species. As was discussed earlier, there is no evidence that such a trend exists between adult frogs of Trinidadian hylid species (**Chapter 2**). Similarly no such trend exists within the majority of the species under consideration here, with the notable exception of *P. trinitatis** (**Table 7.1**), with toe pad area increasing following predictions of isometry, as the linear dimension squared.

Alberch (1981) considers similar problems within species of arboreal salamander and hypothesises that the maximum relative size of the foot with respect to body size in these is limited by the role of the foot in locomotion. In salamanders the weight increase in the foot that would be caused by the increase in musculature required to lift the central portion of the larger sized pad will be such that the organisms will be maladapted for locomotion. Although the situation is somewhat different in tree frogs as there is no musculature within the toe pads to raise the central area there are distal extensor muscles, and it is likely that the extent to which toe pad area can increase is limited by considerations of the effect that having outsized toe pads might have on manoeuvrability and locomotion.

Whilst toe pad area increases much as would be expected following isometric predictions in all species other than *Phyllomedusa*, the rate of weight increase with growth is less than expected in all six species. The degree to which weight increase is

* The significance of this finding within this particular species is discussed in some detail in previous chapters, and is likely to be due in large part to differences in the locomotory mode utilised by these frogs.

lower than expected through isometry is lesser in the two larger species, *P. trinitatis* and *P. venulosa* (**Figure 7.1**).

There is no correlation between the degree to which the rate of weight increase is lowered and the subsequent rate of increase in adhesive force ($r = 0.22$, N.S., 5 d.f.), so it is difficult to know whether the reduction in weight increase does allow a greater degree of adhesive ability in species with proportionally lighter adults. In the similarly sized *H. crepitans* and *H. geographica* which have similar rates of weight increase, although sticking ability is quantifiably better in *H. crepitans*, there is a detrimental effect of size on this whereas in *H. geographica* both adults and juveniles attain similar maximum detachment angles. It seems likely then that in *H. geographica* the decrease in weight is not the only strategy in place to counter the adverse effects of growth upon adhesive ability.

Similarly when considering how frogs move through their environment, it is difficult to state with certainty that trends in body shape are attributable only to adhesive considerations. The strong correlation between the rate of weight and the ratio between the tibial length and SVL (**Table 7.1** and **Figure 7.2**) is of particular interest when taking into account the effect that the trends in both will have on, in particular, jumping ability. Indeed, when considering frogs moving through their environment under natural circumstances, how the whole tree frog has evolved for arboreal life must be taken into account. Many arboreal animals have relatively short limbs when compared to fossorial species; this brings the body's centre of mass closer to the support surface and thus resists overbalancing (Cartmill, 1985). This is not, however,

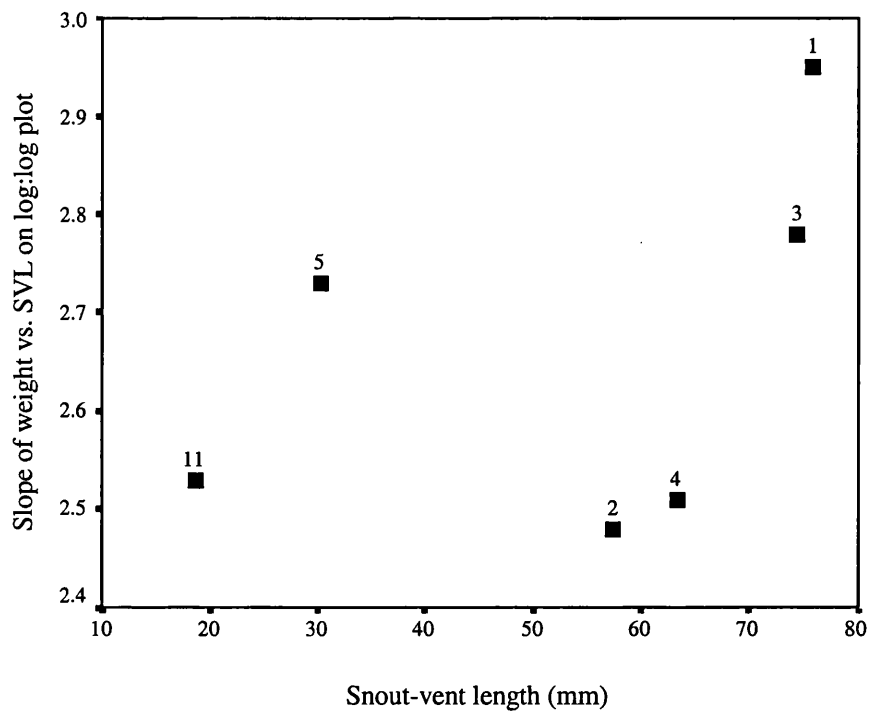


Figure 7.1: Trends in weight increase relative to snout-vent length in six hylid species. Correlative statistics: $r = 0.44$, N.S. 5 d.f. Numbers indicate species as follows: 1 = *P. venulosa*; 2 = *H. geographica*; 3 = *P. trinitatis*; 4 = *H. crepitans*; 5 = *S. rubra*; 11 = *F. fitzgeraldi*.

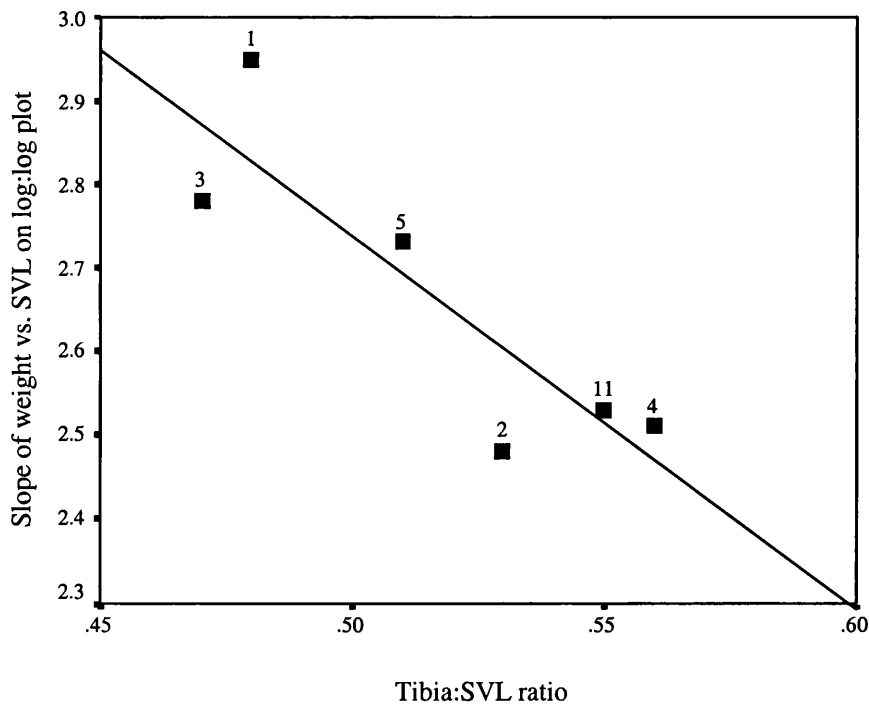


Figure 7.2: Trends in weight increase relative to the tibia to snout-vent length ratios in six hylid species. Correlative statistics: $r = 0.87$ — $y = 4.96 - 4.45x$, $t = -3.56$, $p < 0.03$, 5 d.f. Numbers indicate species as follows: 1 = *P. venulosa*; 2 = *H. geographica*; 3 = *P. trinitatis*; 4 = *H. crepitans*; 5 = *S. rubra*; 11 = *F. fitzgeraldi*.

This is not, however, a trend that is generally seen in tree frogs. It may be that the bringing of the body's centre of mass closer to the support surface is instead affected behaviourally in these animals, perhaps explaining the observation that many of the larger species of frog press their hindquarters closer towards the rotation platform when beginning to lose their grip.

The lack of shortening in the hind limbs of arboreal frogs is likely to be the result of a trade-off between the need to balance on thin branches and the need to generate a powerful jump to escape predation or to leap across gaps between trees. Most anurans are dependant to some degree on saltatorial locomotion so that their skeletal and muscular systems have become specially designed for leaping and jumping; consequently they have developed long, highly muscular hind limbs (Duellman and Trueb, 1997). Jump distance in frogs has been found to be positively correlated with hind limb length, (Rand, 1952; Stokely and Berberian, 1953; Zug, 1972; Emerson, 1978; Peplowski and Marsh, 1997;) and is generally positively correlated to mass (Emerson, 1978; Choi et. al, 2000). Jump acceleration on the other hand, is negatively correlated with body mass (Emerson, 1978; Wilson *et al.* 2000). If we assume that the tibial to snout-vent length ratio gives a measure of the degree to which the species depends upon jumping ability as an adult then the relationship between this ratio and reduced weight gain in these species and increasing hind limb length may reflect a need to keep maintain jumping ability with growth, with respect to both distance and speed. It may also be that these frogs are keeping their body weight down to maintain their adhesive abilities as they grow, but the inability to separate the influence that body shape has on both jumping performance and

adhesion again highlights the problem of examining allometric trends in isolation, as body shape is rarely likely to be affected by a single factor.

Looking at the design of the toe pads may be more informative; as the convergent evolution of such similar structures in the range of families in which the pads are seen suggests that pads are functionally adaptive. Furthermore, the prevalence in species that inhabit environments in which they are likely to be susceptible to dislodgement effects, in the stream frogs (Öhler, 1995) and in the tree frogs (Green, 1979) suggests that the driving force behind their convergent evolution may be adhesive ability. There are however, small changes in various aspects of toe pad structure between species, and it is important to understand what the influences of such variations on adhesion are, particularly if any future studies aim to scale up (or scale down) the toe pad ‘design’ for biomimetic applications, such as has been proposed for wet weather tyres (Barnes *et al.*, 2002).

7.2. Adhesion and toe pad morphology

Toe pad morphology in the twelve species of Trinidadian hylid investigated is very similar to those described in climbing frogs in several previous studies (Ernst, 1973a; Green, 1979; Emerson and Diehl, 1980; McAllister and Channing, 1983; Green and Simon, 1986; Hertwig and Sinsch, 1995; Öhler, 1995; Ba-Omar *et al.* 2000). There are variations in the details of a number of pad features, such as extra-pad grooves and elevations, which perhaps reflect slight differences in the evolutionary lineages of the different species or differences in ecology and behaviour between species, particularly with respect to the degree of arboreality that the frogs typically exhibit.

Variations also exist in the mucosal pore structures between species that may suggest that there are changes in the nature of the secretory mucus that forms the adhesive layer (see 7.3). One aspect of the structure that does remain remarkably similar, both between these species and when compared with other species that have been considered in previous studies, is the shape and structure of the columnar cells that cover the surface of the pad. The high degree of convergence in evolution that this suggests implies that the specialised structure of these cells is likely to be critical to the functionality of the pads. The function of the separated apices and intercellular channels in facilitating the spread of mucus (Emerson and Diehl, 1979; Öhler, 1995) and in allowing the individual cells to find their closest mating with the substrate upon which the pads are placed has been discussed in previous studies (Green and Carson, 1988), but relatively few considerations have been made of the effects of the size and shape of the cell apices that are actually in contact with the surface on the adhesive function of the pad. Green's (1981) study of adhesion in the *H. versicolor* complex found a 5% increase in the adhesive forces recorded from the tetraploid *H. versicolor* in comparison to the diploid *H. chrysocelis*. These species are 'virtually identical' in all respects other than cell size, which are considerably larger in *H. versicolor* due to its greater degree of ploidy (1.46x larger in the case of the toe pad cells; Green, 1980). Although Green (1981) dismisses the link between larger cell size and increased adhesive ability in the tetraploid species as being due to either: 'a limited amount of suction by the cells'; 'experimental error' or 'an effect' due to tiling efficiency of differently sized cells, positive correlations between adhesive force and cell size in the adult frogs belonging to species within the genus *Hyla* in this study (**Figure 3.11**) suggests that this trend perhaps warrants further investigation.

7.2.1. Cell size

There is some evidence from adult frogs that within species belonging to the genus *Hyla* of a trend towards an increase in cell size with increasing snout-vent length (**Figure 3.4**) with a positive correlative relationship between cell size and force per unit area of toe pad in these same frogs (**Figure 3.11**). However, if we extend the parameters of this study to include species and families in previous studies of toe pad morphology (**Table 7.2**: values from Ernst, 1973a; Green, 1979; McAllister and Channing 1983) there is no demonstrable correlation between cell size and snout-vent length either within or between the separate families of arboreal frogs considered to date (Cell vs. SVL: All frogs, $r = 0.23$, $t = -1.18$, $p = 0.25$, $n = 26$; Rhacophorids, $r = 0.19$, $t = -0.19$, $p = 0.88$, $n = 3$; Hyperoliids, $r = 0.31$, $t = 0.80$, $p = 0.45$, $n = 8$; Hylids, $r = 0.15$, $t = 0.53$, $p = 0.60$, $n = 15$).

Green (1980) also considered the relationship between SVL and cell size within two species of the *Hyla versicolor* complex and found that there was no effect of the increasing linear dimension on the average cell area on the toe pad. Trends in toe pad cell size with growth within the hylids considered here are inconclusive for all eight of the species for which S.E.M. data is available for both juvenile and adult frogs but differ according to the size classification of the adult frogs. Small species and the smaller of the two medium species exhibit a tendency towards a decrease in cell size with growth that runs counter to the predictions that might be made from trends between species (**Table 4.3; 5.3**). The implications of these trends in cell size for adhesion in species belonging to separate size classes are discussed in earlier chapters.

Family	Species	SVL (mm)	Cell area (μm^2)	Approximate cell density (per mm^2)
Rhacophoriidae	<i>Kassina maculata</i> ¹	60	66	15150
	<i>Chiromantis xerampelina</i> ¹	60	135	7400
	<i>Leptopelis natalensis</i> ¹	65	89	11250
Hyperoliidae	<i>Hyperolius pusillus</i> ¹	18	136	7350
	<i>Hyperolius nasutus</i> ¹	22	163	6100
	<i>Hyperolius marmoratus</i> ¹	25	123	8200
	<i>Hyperolius pickersgilli</i> ¹	26	150	6650
	<i>Hyperolius tuberlinguis</i> ¹	30	144	6950
	<i>Hyperolius argus</i> ¹	31	167	6000
	<i>Hyperolius semidiscus</i> ¹	35	124	8100
	<i>Hyperolius horstocki</i> ¹	43	172	5800
Hylidae	<i>Flectonotus fitzgeraldi</i>	17	117	8600
	<i>Hyla minuscula</i>	23	97	10350
	<i>Hyla microcephala</i>	20	66	15200
	<i>Hyla minuta</i>	21	102	9800
	<i>Scinax rubra</i>	30	72	13800
	<i>Hyla punctata</i>	33	106	9400
	<i>Sphaenorhynchus lacteus</i>	39	136	7350
	<i>Hyla versicolor</i> ²	42	144	6950
	<i>Hyla chrysocelis</i> ²	41	98	10150
	<i>Hyla geographica</i>	50	119	8400
	<i>Hyla crepitans</i>	57	114	8800
	<i>Hyla cinerea</i> ³	60	80	12500
	<i>Phrynohyas venulosa</i>	72	132	7600
	<i>Phyllomedusa trinitatis</i>	68	92	10900
	<i>Hyla boans</i>	98	101	1000

Table 7.2: Cell sizes and densities from twenty-six species of ‘tree frog’ in order of increasing SVL within families. 1. SVL values from Schiotz, (1999); Morphology data from McAllister and Channing, (1983). 2. SVL values from Behler and King, (1997); Morphology data from Green, (1979, 1980). 3. SVL values from Conant and Collins, (1998); Morphology data from Ernst, (1973a). All other data from adult frogs in this study.

Trends in cell size during growth are of particular interest when considering their possible implications for improvements to adhesive ability. For instance, a positive correlation is seen between adhesive force per unit area of toe pad and increasing cell size between adult frogs belonging to the genus *Hyla* discussed in **Chapter 3.4**. However, when the species are considered separately there are no demonstrable effects of cell size on adhesive force within any species when juvenile data are also considered. Furthermore, the addition of data from juvenile frogs removes any relationship between the two parameters between species within the hylid genera ($r = 0.12$, $t = -0.75$, N.S. $n = 16$), and no relationship can be demonstrated when all twelve species are considered together ($r = 0.14$, $t = -0.73$, N.S. $n = 30$).

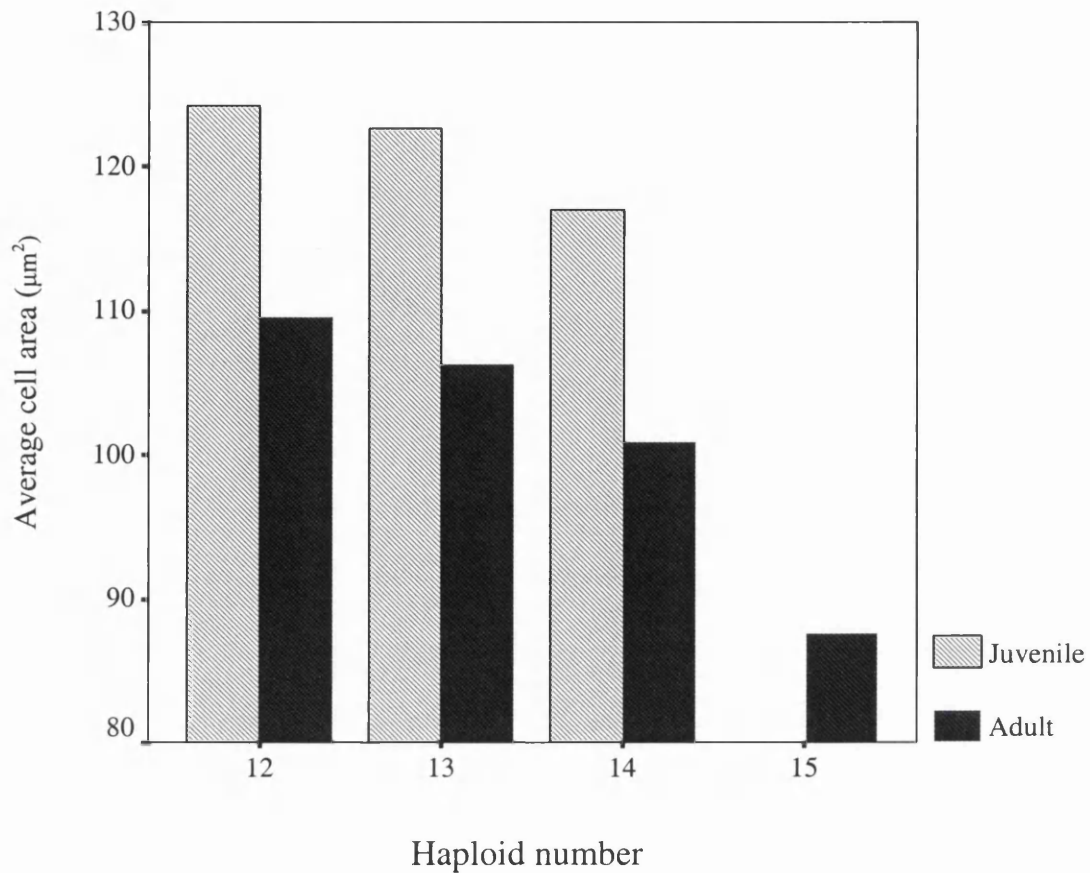
The only demonstrable factor yet proved to influence cell size in any of the previous studies of toe pads in tree frogs is seen in Green's 1980 study of frogs of the *Hyla versicolor* complex. In this study, he demonstrates that there is a positive correlation between the degree of ploidy within frogs of the *Hyla versicolor* complex and the average cell size seen on their toe pads. Polyploidy in amphibians is seen in many genera, and is prevalent in several species groups within the genus *Phyllomedusa* (Haddad *et al.* 1994). Levels of ploidy are unknown in these frogs but differences between cell size in adult *P. trinitatis* in this study (ca. $105 \mu\text{m}^2$) and in the Ba-Omar *et al* (2000) study of the same species (ca. $120 \mu\text{m}^2$) do not suggest differences in polyploidy levels in this case.

Haploid numbers are different in the species in this study (**Table 7.3**). Using literature values for haploid numbers in these species (Gregory, 2001) there is a trend such that smaller cells are seen in species with higher haploid number (**Figure 7.3** and **Table 7.4**). Though statistically these trends are non-significant the presence of similar patterns in cell size with haploid number both within adult frogs and between age classes make these trends worthy of note, particularly if we consider differences in trends seen in cell size in the three separate size classes in relation to aspects of adhesion.

Species	Haploid no
<i>Hyla minuscula</i>	15
<i>Flectonotus sp.</i>	14
<i>Hyla minuta</i>	15
<i>Hyla microcephala</i>	15
<i>Scinax rubra</i>	12
<i>Hyla geographica</i>	12
<i>Hyla crepitans</i>	12
<i>Phyllomedusa sp.</i>	13
<i>Phrynohyas venulosa</i>	12
<i>Hyla boans</i>	12

Table 7.3: Typical haploid numbers in study species and closely related species groups. All values from Gregory, (2001).

In large frogs and in the larger of the two medium sized frogs, there is no effect of cell size on the adhesive force per unit area generated across the toe pad (**Table 5.5, 6.5**), but neither is there any marked variation in the haploid numbers of the species within these size classes which might affect cell size. As discussed earlier, all species of frog belonging to the smaller size classes within the Trinidadian Hylids (**Table 4.3**) exhibit a tendency towards a decrease in cell size with the increasing linear dimension although in none of these instances is a correlative relationship demonstrable. At the same time, between frogs of the smallest species there is also a trend suggesting that increasing adhesive forces are correlated to smaller cell size (**Table 4.5**), and there is a higher degree of variation in haploid number. If these trends hold true with larger sample sizes and smaller cell sizes do promote increasing



Haploid no	Age classes								
	Juvenile			Adult			Combined		
	mean	s.e.	n	mean	s.e.	n	mean	s.e.	n
12 (5 sp)	124.16	7.66	13	109.63	11.82	5	120.12	6.44	18
13 (1 sp)	122.62	20.12	2	106.35	13.86	2	114.49	11.03	4
14 (1 sp)	116.97	-	1	100.98	14.42	2	106.31	9.88	3
15 (3 sp)	-	-	-	87.68	7.48	4	-	-	-

Figure 7.3 and Table 7.4 : Trends in average cell size in species according to haploid number. ANOVA statistics: Juveniles, $F_{2,13} = 0.03$, $p = 0.97$, N.S., 15 d.f.; Adults, $F_{3,9} = 0.80$, $p = 0.58$, N.S. 12 d.f.; Combined age classes, $F_{3,25} = 1.96$, $p = 0.15$, 28 d.f. (Species combined in each haploid group as indicated in Table 7.3).

adhesive force per unit area of pad in these species, then this might be a driving force for increasing haploid number in smaller species. There is some evidence of a trend within the frogs of the *Hyla microcephala* species group, which have a haploid number of fifteen, that larger cell size is detrimental to the force per unit area (Correlative statistics for linear regression for force per mm^2 vs. cell area in frogs with haploid number of 15: $r = 0.95$, $y = 0.95 - 0.005x$, $t = -4.32$, $p < 0.05$, $n = 4$).

There is a low level of arboreality seen in the smaller species (with the notable exception of *Flectonotus fitzgeraldi*), which generally tend to favour lower level vegetation and are frequently found in swampy grassland and in open disturbed habitats. One feature of the shrubs and grasses prevalent in these habitats is that the perches that these provide within the frogs' environment are likely to be smaller in diameter than those encountered by more arboreal frogs*. If the tendencies to encounter smooth flat planes, on which wet adhesion will be most efficient, are lessened for these smaller species then it may be that the advantages that smaller cell size will bring to the adhesive abilities in terms of increased frictional and interlocking contributions on rough substrates and small diameter perches, will outweigh the detrimental effect on the wet adhesive mechanism. There is some evidence from ten of the species under consideration here that an increase in initial slip angle, which is influenced to a large degree by the frogs' ability to withstand shear force, is facilitated by a decrease in the average cell size on the toe pads of

* Glossip and Losos' study of the ecological correlates of numbers of subdigital lamellae on the feet of anoles found that lizards that utilise smaller perch diameters have more lamellae on their feet. The similarities between the findings of this study and my own are noteworthy, but key differences in adhesive mechanisms utilised by lizards and tree frogs suggest that the parallels may be due to the greater degree of conformation to the substrates that the increased number of smaller adhesive elements will facilitate in both groups.

adult frogs (**Figure 7.4 a**). Detachment angles in the same frogs, on the other hand, are independent of toe pad cell size (**Figure 7.4 b**).

There is a trend towards increasing cell size with arboreality that might support this theory (**Appendix 4**), considering the species' average cell area values according to the degree of arboreality typical for adult frogs. If the cell areas from adults of all twelve species are pooled and then compared then this trend is strengthened, and a demonstrable difference in cell size exists according to the degree of arboreality typical of the species (**Figure 7.5** and **Table 7.5**: ANOVA statistics for comparison of means: $F_{2,1492} = 28.73$, $p < 0.01$). However, if the trends in cell number with haploid number between species in this study are accurate then it may be that the smaller cell size seen in the semi-arboreal frogs is due to the prevalence of species with large haploid number amongst this group. To remove this effect the species were also considered separately according to typical haploid numbers given in literature (Gregory, 2001). This strengthens the difference between the means according to the degrees of arboreality seen in species that share a haploid number of twelve (**Table 7.5**: ANOVA statistics for comparison of means: $F_{2,401} = 152.83$, $p < 0.01$).

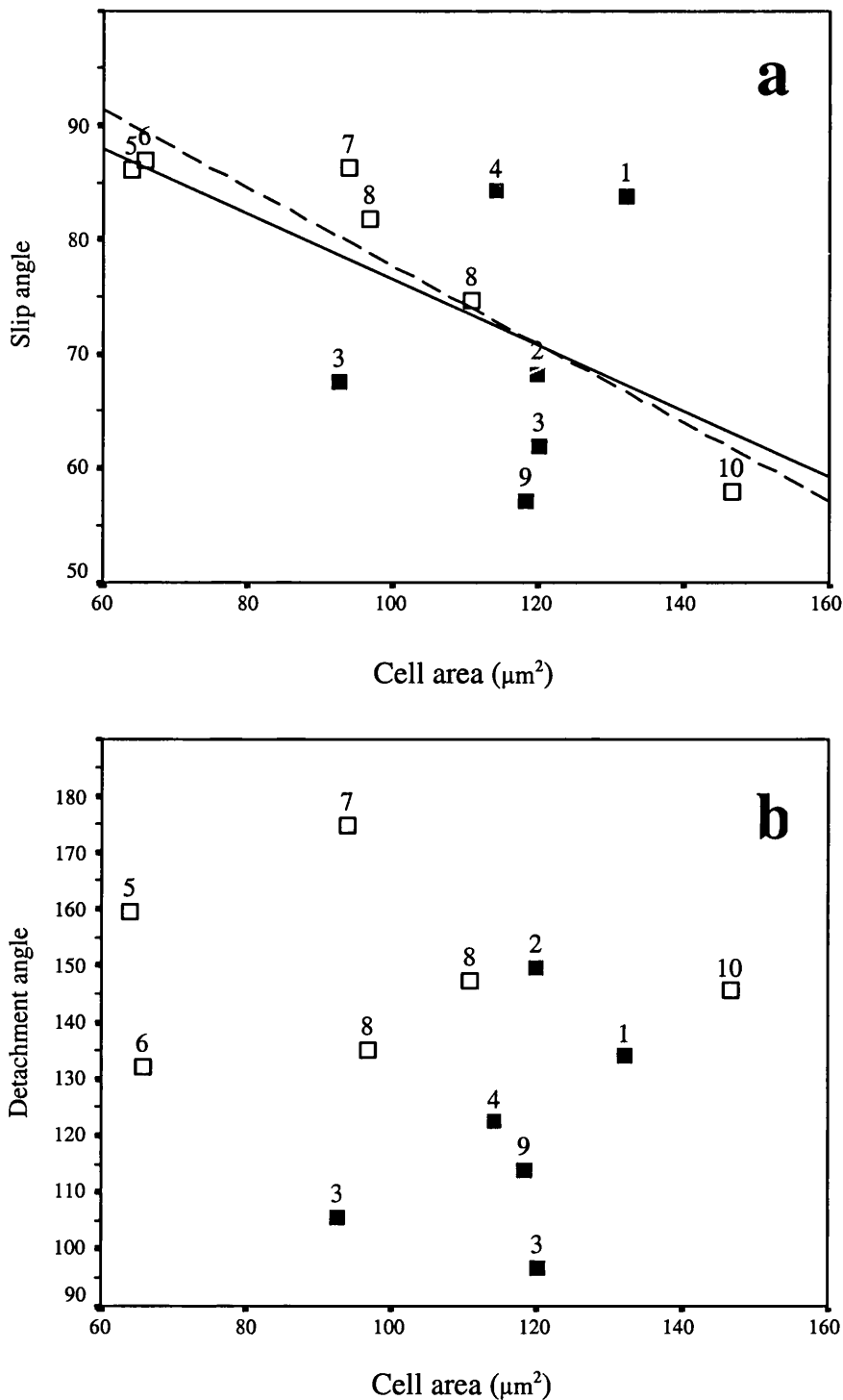
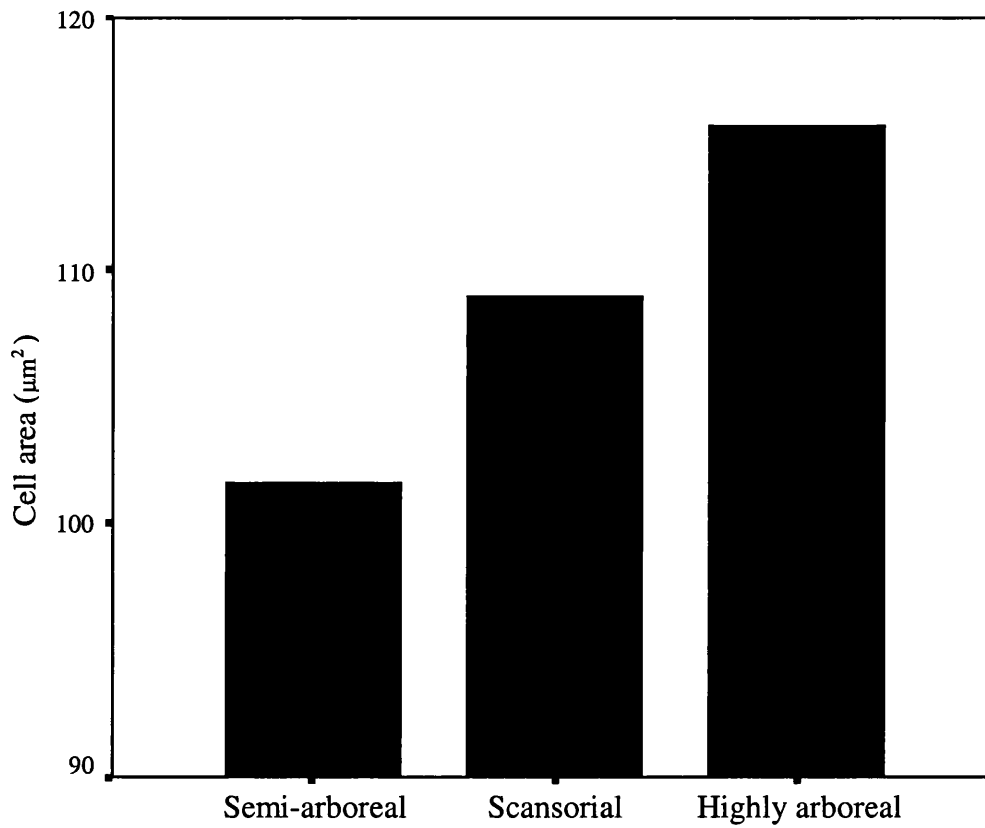


Figure 7.4: (a) Slip angles and (b) Detachment angles vs. average cell size in adult Hylids sampled for S.E.M. analysis according to size class; small (\square), medium (\blacksquare) and large (\blacksquare). Correlative statistics for: (a) All frogs, — $r = 0.61$, $y = 105.19 - 0.29x$, $t = -2.45$, $p = 0.03$, $n = 12$; Small species, --- $r = 0.93$, $y = 111.83 - 0.34x$, $t = -5.08$, $p < 0.01$, $n = 6$; Large species $r = 0.37$, N.S. $n = 3$. (b) All frogs, $r = 0.30$, $t = -1.76$, $p = 0.09$, $n = 12$; Small species, $r = 0.04$, N.S., $n = 6$; Large species, $r = 0.56$, N.S. $n = 3$. Species numbered as follows: 1 = *P. venulosa*; 2 = *H. geographica*; 3 = *P. trinitatis*; 4 = *H. crepitans*; 5 = *S. rubra*; 6 = *H. microcephala*; 7 = *H. minuta*; 8 = *H. punctata*; 9 = *H. boans*; 10 = *S. lacteus*.



Arboreality	All species			Haploid no = 12		
	Cell area (µm ²)	s.e.	n	Cell area (µm ²)	s.e.	n
Semi-arboreal	101.70	1.08	818	65.60	1.95	70
Scansorial	109.07	1.47	337	117.68	2.02	158
Highly arboreal	115.78	1.58	340	125.82	2.05	176

Figure 7.5 and Table 7.5: Average cell areas from adult frogs sampled from twelve species of Trinidadian Hylid according to degrees of arboreality and trends within species with a shared haploid number. See **Appendix 4** for definitions of classifications of arboreality.

If the trends seen in cell size in adult frogs are the result of an evolutionary trade-off between the advantages that different cell sizes will confer on the types of substrates most commonly encountered in the course of normal behaviour in each species then it is important to future studies that habitat choices and the typical degrees of arboreality seen in new metamorphs and juveniles are more fully understood.

7.2.2. Cell shape

One aspect of the toe pad structure that is highly notable in the degree of convergence that exists both between species and families of frogs that exhibit enhanced adhesive ability is seen in the geometric nature of the

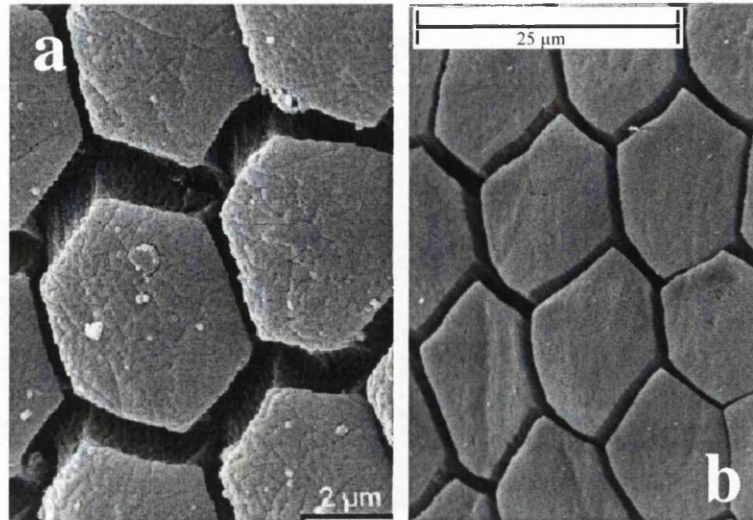


Figure 7.6: Hexagonal cells on the pads of (a) the green bush cricket, *T. viridissima* (Gorb and Scherge, 2000) (b) the Hylid tree frog, *P. trinitatis*.

cells that cover the surface of the pads. The prevalence of the hexagonal shape of the cells on the pads of tree frogs is attributed in a number of studies to the need for an even spreading of the fluid layer involved in wet adhesion, facilitated by the channels formed between the closely tiling regular shapes (Öhler, 1997; Green, 1979; Ernst 1973a). Hexagonal cells are seen on the smooth adhesive pads of the green bush cricket, *Tettigonia viridissima*, though these are smaller in size than seen in the Hylid frogs (**Figure 7.6**). It seems likely, given the independent evolution in both vertebrate and invertebrate adhesive pads that the hexagonal shape of the cells on the attachment structures in both animals is in some way key to the adhesive abilities of the pads in both species. Cells elsewhere on the epidermis of these frogs are large and irregular in shape and are significantly different in appearance to those on the toe pads (**Figure 7.7**).

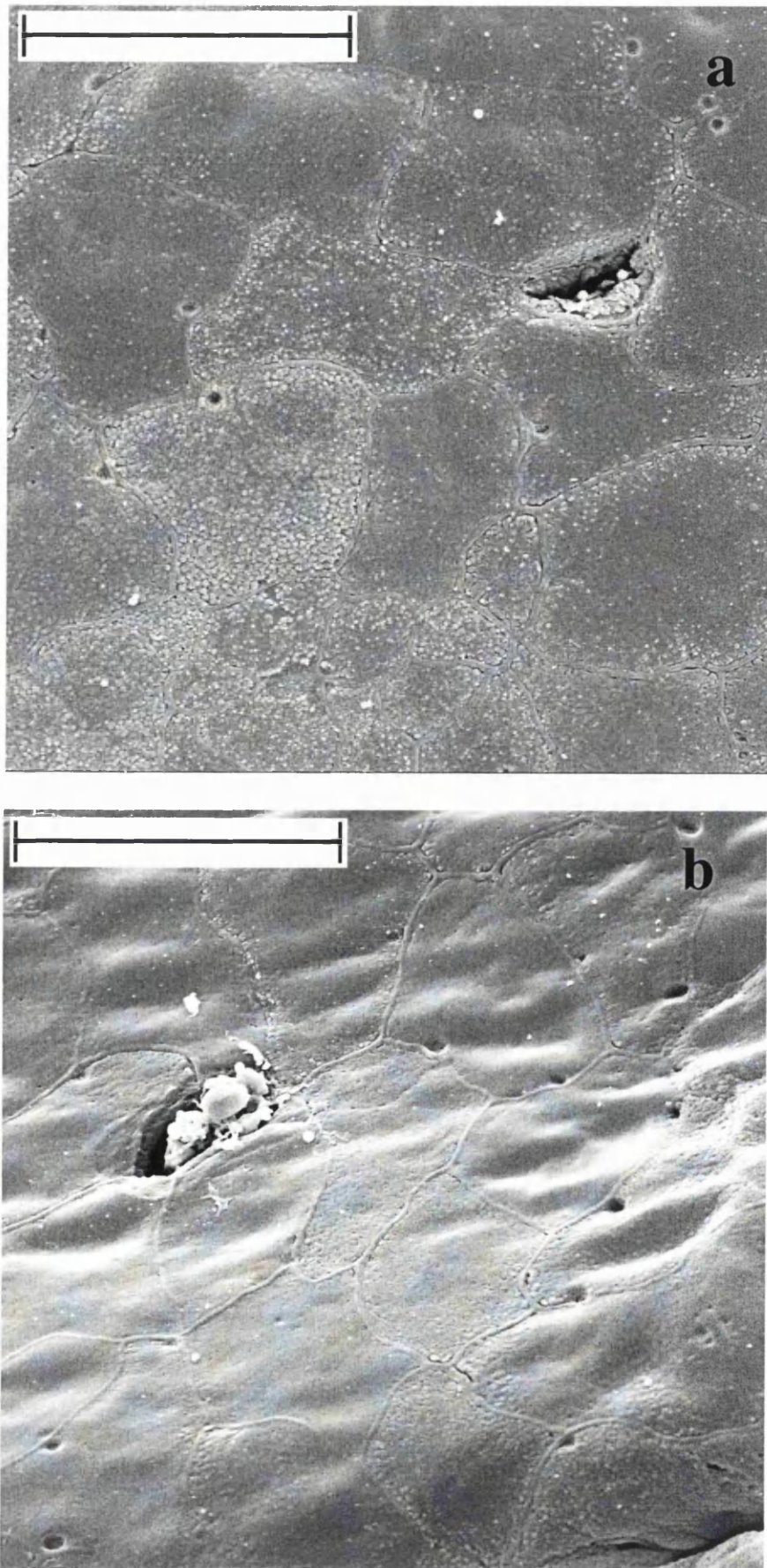


Figure 7.7: S.E.M. images of epidermal cells on the (a) stomach and (b) thighs of juvenile *F. fitzgeraldi* (Scale bars = 25 μ m).

Where a mosaic of rounded, similarly sized cylindrical elements are placed closely together on a planar surface it has long been noted that the density of objects within a space is optimised by adopting hexagonal patterns (Kepler's conjecture, 1611), with the structures following formations known as hexagonal close-packing (Conway and Sloane, 1993). This has led to the repeated evolution of the hexagonal shape and hexagonal configurations in the natural world, particularly where the need for similarly sized cells has driven the evolution of a structure; consider the cells of the honeycombs and nests of bees and wasps (**Figure 7.8 a**), the facets of the insects' compound eye (**Figure 7.8 b**) and the mosaic distribution of the cells on the human retina (**Figure 7.8 c**).

These structures, considered in relation to the adhesive pads of tree frogs, may have very different functions but all share a degree of commonality in that the evolution of their structure has been driven in part by the need for the efficient close packing of roughly equally sized cells with as few inter-unitary spaces as possible for their maximal functionality. In the case of the cells of the honeycomb, large spaces between individual larval cells will increase the cost of building the comb in terms of the amount of wax/paper required. However, reducing the intercellular spaces by evolving one single large unit is also not desirable: in bees this will reduce the

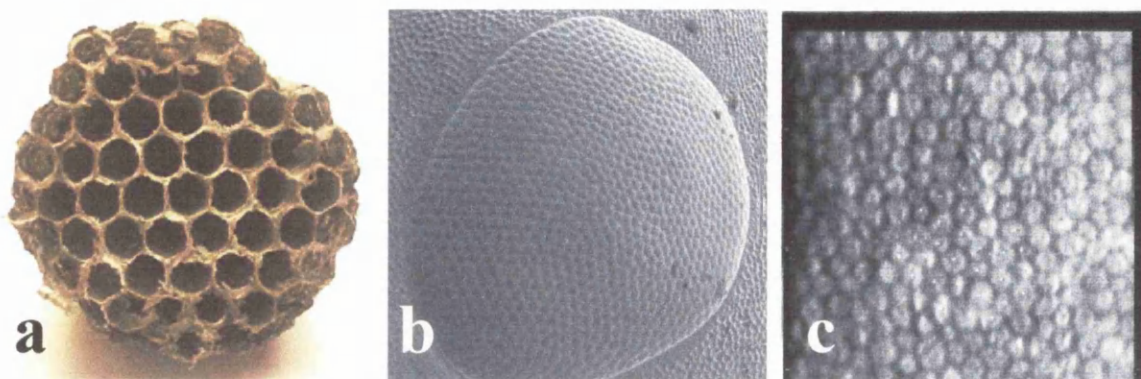


Figure 7.8: Images illustrating the hexagonal elements found in (a) bee honeycomb (Weisstein, 2003) (b) the compound eye of an ant (R.Passey, 2003) (c) the human retina (Konan Inc.Co.)

productivity of the colony and in eyes this would reduce the degree of resolution and the detail perceptible in the field of vision. The need to reduce intercellular spaces whilst maintaining a high number of individual units can also be inferred for the structure of the cells seen on the adhesive toe pads in tree frogs. The functionality of the adhesive mechanism in several species of Hylid has been demonstrated to be significantly affected by the contact area between the pad and the substrate, though the unpredictability of the substrates encountered by a frog in the course of its movement through its environment may suggest that there is an additional need for a high degree of flexibility of the pad. The evolution of regular units has arisen in large part from the need to maximise the actual area of contact between the cell apices and substrata whilst still maintaining a degree of ability to deform to uneven surfaces. If the hexagonal shape has been proved to be the most efficient in terms of maximising the number of units in an area whilst remaining stable and resistant to area-altering deformation forces due to the obtuse angles of the apices then why are other cell shapes prevalent on the adhesive pads of the species of tree frog (see **Figures 3.10, 4.15, 4.22.**) under consideration in this thesis?

The prevalence of irregularly shaped units in other examples of hexagonally organised structures, such as in the compound eye of insects (**Figure 7.9**) and on the human retina (**Figure 7.10**), suggests that they may in some way be

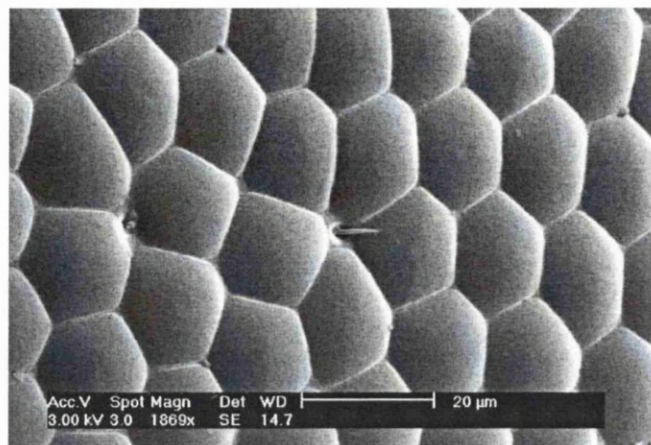


Figure 7.9: S.E.M. showing irregularly shaped cells on the compound eye of an ant. (Image: R.Passey, 2003)

due to the consideration of tiling efficiency of hexagons on surfaces which exhibit a natural degree of curvature. Whilst the efficiency of hexagonal packing in relation to the maximal density of individual units is high on a flat plane, it is in fact impossible to completely tessellate a spherical object, or indeed any volume, using only regular hexagonal units (McCollum, 2000).

The reasons for this are illuminated if considering the maximum number of various regular polygons that can come together at a vertex before forming a flat plane, when the total of the adjacent angles equal 360° . For example, in the case of an equilateral triangle with angles of 60° at each corner, the maximum number of triangles that can meet at a vertex before the formation of a flat plane results is six. The minimum order of vertex for the enclosure of any three-dimensional space by polygonal shapes is, by definition, three. These facts limit the formation of polyhedra with regular triangular facets to instances where there are three, four or five-fold vertices; these structures are represented by the tetrahedron, octahedron and dodecahedron respectively. In the case of the regular hexagon, with its six equal 120° angles, the maximum number of hexagons that can come together at a vertex before a flat plane is formed is three, so that the minimum requirement for the formation of a three-dimensional regular polyhedron is not fulfilled (Calkins, 2003).

Gaussian theory states that to enclose a spherical volume by folding a flat surface one must remove wedges with angles totalling 720° at evenly distributed points across the planar surface, followed by a joining of the two sides of the wedge to form a cone at each of the points of removal (McCollum, 2000). Removing twelve 'wedges' of 60° from a surface tiled by hexagons converts twelve hexagons to

pentagons, creating an integral number of equally sized ‘spacers’ which allow the formation of a closed structure (Feynmann, 2002). The effects of this can be illustrated by the case of recently discovered spherical forms of carbon, the fullerenes, which are only present as closed units through the interposition of pentagonal shaped units within the hexagonal networks typical of carbon forms (Kroto *et al.* 1985). Without the presence of irregular cell types on tree frog toes there could be no curvature, a feature that has been identified as key in determining a pad’s frictional characteristics in the case of primates and other climbing mammals (Cartmill, 1979; Hamrick, 1998; Haffner, 1998). This might be expected to be particularly relevant to species with a high degree of climbing behaviour (Cartmill, 1985) and may explain the prevalence of irregular cell shapes seen on the surface of the pad noted in *P. trinitatis* (Chapter 6.3.3) and *F. fitzgeraldi* (Chapter 4.3.3), both of which have been noted to be highly arboreal in their habits (Table A5.1).

Whilst the presence of irregular cell types on various points of the surface of the toe pads appears to be random, the superficial similarity of the distribution of irregular units to those seen on the human retina is of some interest (Figure 7.10). Analysis of patterns in the distribution of irregular cells on the human retina has shown that the

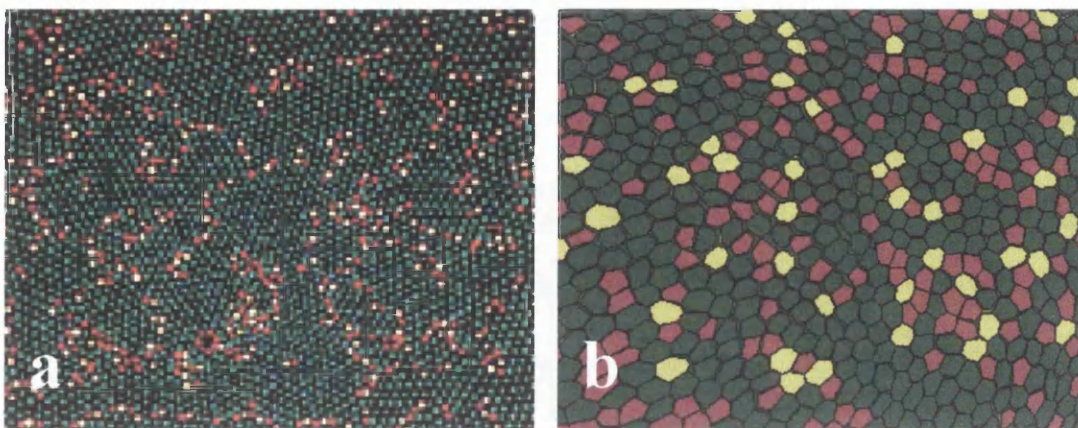


Figure 7.10: Patterns in distribution of cells across (a) the human retina (Ahnelt, 2003) and on (b) the toe pad of *H. crepitans*. Colours indicate the number of neighbouring cells as follows: Green = six; Red < six; Yellow > six.

positions of the non-hexagonal units are not random and in fact delineate different 'iso-orientation areas', sites of reorganisation in the hexagonal mosaic in respect to the angular orientation of the cones (Pum *et al.* 1990; Anhelt, 2003). If there were no disturbances in the geometry of the cell type then such a rearrangement in the orientation of the hexagonal units would not be possible. It may be that the irregular cell shapes seen across the surface of the toe pads in tree frogs function in a similar way by allowing the cells to be angled at slightly different orientations to the horizontal when the toe is not in contact with any surface so that when the pad is deformed elastically on contact with a surface there is a maximal area of apical contact. The development of epidermal ridges on the fingertips of small primates is implicated in tendencies to forage on small diameter branches, allowing the pad to contact the substrate on several planes and thus increasing the stability of the hands and feet on small diameter branches (Scherge and Gorb, 2001). If the distribution of the irregular cell types across the pads of tree frogs is indicative of differentiated regions in terms of the orientation of the cells to the horizontal then it might again be expected that frogs with more arboreal lifestyles will tend to have a greater incidence of irregular cell types.

If these cell types are implicated in the ability of the pad to conform closely to substrates then it will be important to understand the function of the different cell shapes seen across the pad with respect to the deformability of the pad and to determine whether any patterns do exist in the seemingly random distributions in irregular cell types.

7.2.3. Pad curvature

In adult frogs of the twelve Trinidadian species under consideration here, pad curvature shows a tendency towards flattening in the highly arboreal species* and a tendency towards an elevated pad profile in the ‘scansorial’ frogs (**Figure 7.11**). The flattening of the pads in highly arboreal species runs counter to predictions from studies on primates discussed earlier. Although not statistically significant (ANOVA: $F_{2,9} = 1.36$, $p = 0.31$), these trends are of some interest. Scansorial species tend to shelter in low vegetation during inactive diurnal periods and become more highly arboreal when nocturnally active, climbing to heights of over two metres on a regular basis (Green and Simon, 1986). If pad curvature is considered with respect to the amount of climbing that is undertaken in order to move between habitats this may explain the higher average scores for pad elevation seen in scansorial species.

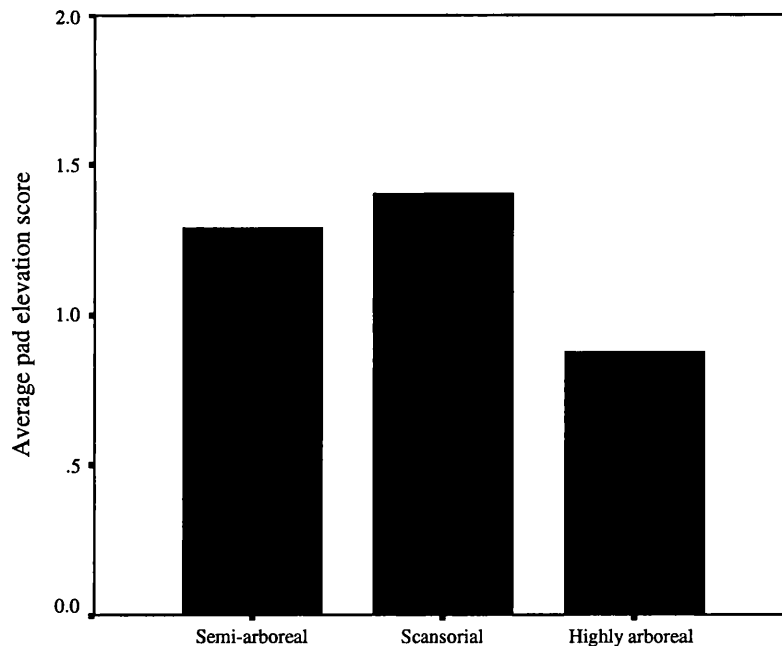


Figure 7.11: Bar chart illustrating trends in average pad elevation in adult frogs belonging to twelve species of Trinidadian Hylid according to special degrees of arboreality.

* see **Appendix 5** for classification of arboreality in different species

As additional frictional components to the adhesive mechanism are likely to be most desirable in species that regularly have a need to climb along branches and trunks of trees, it is perhaps surprising that the species that exhibit the highest degree of arboreality as adults have the flattest pads. The reasons for this may be illuminated by consideration of the frogs where the most extreme degree of flatness in the pad topography is seen, in the newly metamorphosed *Flectonotus fitzgeraldi* (**Figure 4.25 a**). As discussed in **Chapter 4.1** and **4.4**, this species is closely associated with epiphytic bromeliads at various points in the life history, particularly the early stages. Such plants have very smooth leaves and the lack of surface irregularities on the substrata that these represent will make any additional contribution of frictional forces minimally useful. As adults, these frogs are often found active on the ground during the day (Duellman and Gray, 1983; field notes, JS) and the pad is considerably more distinctly raised from the ventral surface of the pad. If highly arboreal frogs encounter smooth leaf surfaces often whilst moving through the environment then the tendency seen towards a higher degree of flattening may have arisen as a trade-off between any advantages conferred by the additional frictional components that increased curvature may promote and the effect that this will have on wet adhesive abilities. The flattening of the pad seen in arboreal species, together with the progressive flattening seen between species with increasing linear dimensions (**Figure 7.12**), may suggest that the advantages that might be conferred by increasing pad curvature in terms of the increased frictional contributions are not as great as those conferred by keeping meniscal heights to a minimum. However, there is little evidence that pad elevation has any effect on the average angle of initial slip, a comparative estimate of the ability to withstand shear force (**Figure 7.13**). Similarly, the average frictional coefficients (see **Table 7.6** later) calculated for each

species (Barnes *et al.* 2002) show no dependence on the relative elevation of the pad ($r = 0.06$, N.S., $n = 10$).

It may be the case that additional frictional and interlocking components that may aid adhesion whilst climbing in arboreal frogs, such as *Phyllomedusa trinitatis*, are supplied instead by contributions of other structures such as the subarticular tubercles, which are particularly well defined and rounded in this species (**Figure 6.47**). Changes in the cellular architecture in both the proximal margin and on the subarticular tubercles in these arboreal species may also indicate that these are involved in the increase of frictional contributions to the overall adhesive forces seen in a number of species.

There are, it must be noted, a number of problems in drawing any firm conclusions from estimates of pad curvature using scores for elevation from the ventral surface in toes prepared for S.E.M. as the drying procedures involved in processing are likely to have significant effects on the shape of the toe pad in all of the species. It is of some importance to determine both what the curvature of the pad is under normal active conditions and the biomechanical properties of the cellular elements of the toe pad in order to understand the degree of deformability that is inherent within the pad structure.

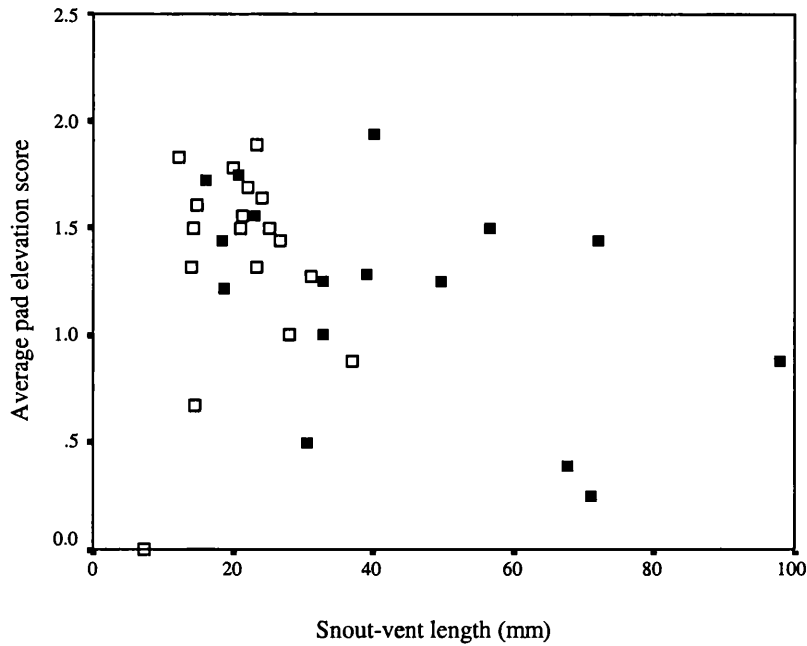


Figure 7.12: Average pad elevation scores in juvenile (□) and adult (■) frogs belonging to twelve species of Hylid vs. snout-vent length. Correlation statistics: Total population, $r = 0.32$, $y = 1.52 - 0.01x$, $t = -1.92$, $p = 0.06$, $n = 34$; Juveniles, $r = 0.15$, N.S. $n = 18$; Adults, $r = 0.48$, $y = 1.63 - 0.01x$, $t = -2.03$, $p = 0.06$, $n = 16$.

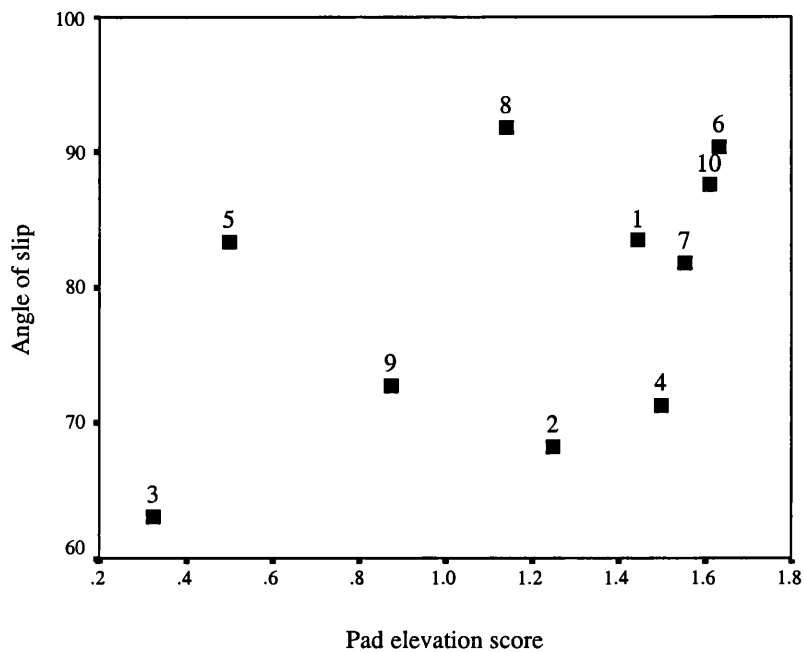


Figure 7.13: Average values for angle of slip on Perspex vs. score for pad elevation in adults from ten species of Hylid frog. Correlative statistics; $r = 0.48$, $p = 0.15$, $n = 10$. Numbers indicate species as follows: 1. *P. venulosa*, 2. *H. geographica*, 3. *P. trinitatis*, 4. *H. crepitans*, 5. *S. rubra*, 6. *H. microcephala*, 7. *H. minuta*, 8. *H. punctata*, 9. *H. boans*, 10. *S. lacteus*,

7.2.4. Extra-accessory areas

One important aspect of the adhesive abilities of hylid frogs that would benefit from some further study is highlighted by the observations that, during natural adhesive behaviour, both juvenile and adult frogs regularly utilised accessory areas of skin on the stomach, thighs and subarticular tubercles. Whilst the forces recorded from frogs adhering in this study excluded all instances where excess skin was in contact with the substrate, the subarticular tubercles further down the toe and areas around the pad on the proximal edge and the circumferal margins were often in contact in the later phases of rotation. The subarticular tubercles in many species, particularly in larger species, are particularly well developed (**Chapter 6.3.4.**), suggesting that there may be an increased function for these areas in larger species in adhesion or in climbing. If, as suggested earlier, the roughened surfaces of the cells in these areas seen in smaller species (**Figure 7.14 a**) are increasing the contribution of frictional components, then these forces will not be recorded in the overall forces from the methodology used here as on surfaces orientated at angles above 90° frictional forces will not be significant, requiring as they do an application of a force normal to the surface. In the case of adult frogs from the larger species of hylid in this study, in which the cells on the subarticular tubercles are not significantly different to those seen on the pads (**Figure 7.14 b**), the increase in the development may provide a means by which these frogs are able to increase the area of contact at a higher rate than the increase in toe pad area alone can allow for. Changes in surface architecture of the cells on the subarticular tubercles and in the development of the lateral grooves that lead to these structures between juveniles and adults of the larger species are likely to be indicative of an increased importance of these areas to the adhesive abilities in these frogs (**Figure 7.14 c and d**).

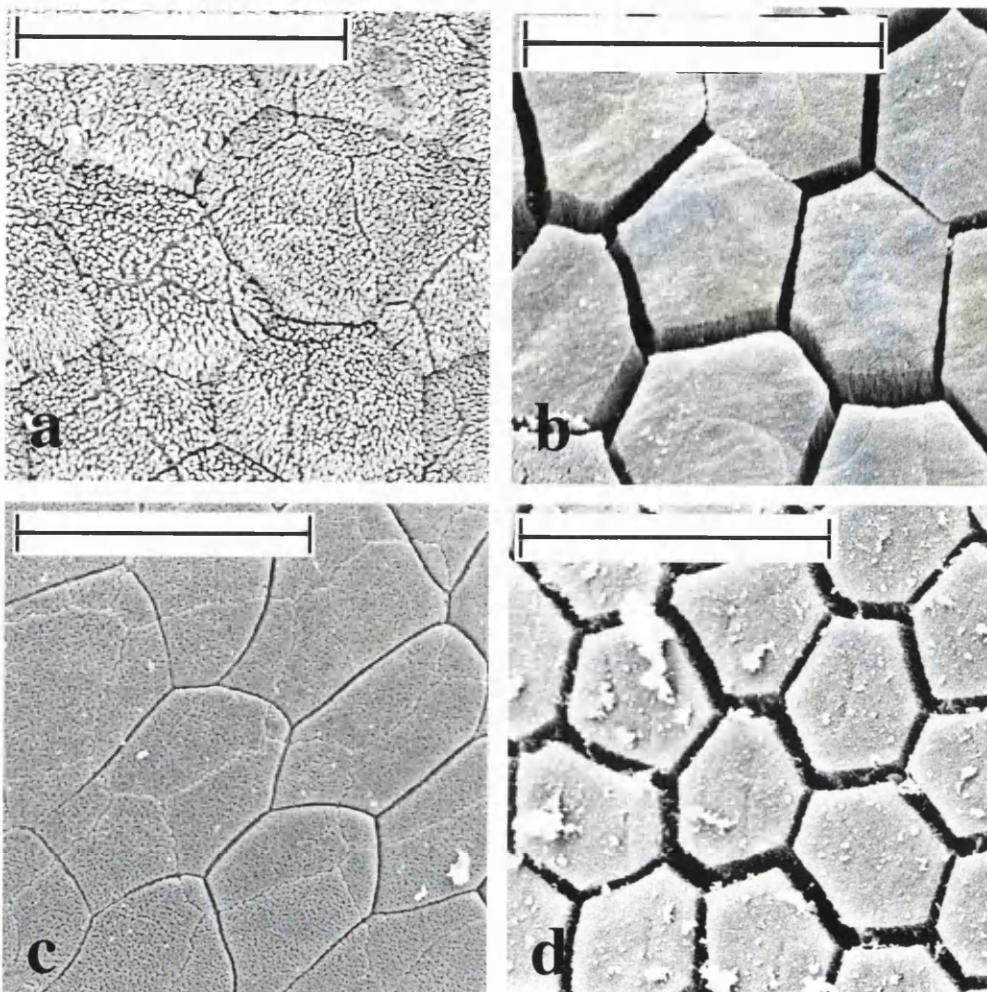


Figure 7.14: S.E.M. images of Subarticular tubercle cells in (a) Adult *H. punctata* (b) Adult *H. crepitans*. (c) Juvenile *P. venulosa* (d) Adult *P. venulosa*. Scale bars = 25 μm.

There is a range in the architecture of cells seen in other areas that may be in contact with substrates during adhesion, with the most diverse ranges in structures seen on the distal edges of the circumferal margin; where cell surfaces are covered in patterns of knobbed projections (**Figure 7.15 a**); convoluted ridges (**Figure 7.15 b and c**) and with micro-pores (**Figure 7.15 d**). The significance in the variation in surface architecture found in cells outside of the toe pad is not known but Green and Simon (1986) who also found a range of surface architectural types in similar areas of the toe in microhylid frogs proposed that they may act to enable the spread and holding of the mucus to the skin surface. Patterns of micro-ridges are seen in the epidermal cells of teleost fish where they are believed to fulfil this function (Sperry and Wassersug, 1976). The presence of a structural architecture that controls the spread of the mucus to confine it to a fixed area at the margins of the pad would certainly be useful for an animal adhering through capillary adhesion, as this is likely to be highly dependent on the maintenance of a stable air-water interface at the meniscal boundary. Structures that aid in the conformation of the edges of adhesive structures are seen in fish (Hora, 1923) and tadpoles (Gradwell, 1973; Daugherty and Sheldon, 1982) that live in torrential streams. Octopus suckers have chitinous ridges round the edges of their tentacular suckers which aid in interlocking on substrates in their environment to maintain a close conformation at the edges of the suction cup (Kier and Smith, 1990). If the microridges and other textured surfaces of the cells at the pad margins function in a similar way then they may allow the edges of the pad to closely conform to the substrates in conditions in which the meniscal boundary may be compromised.

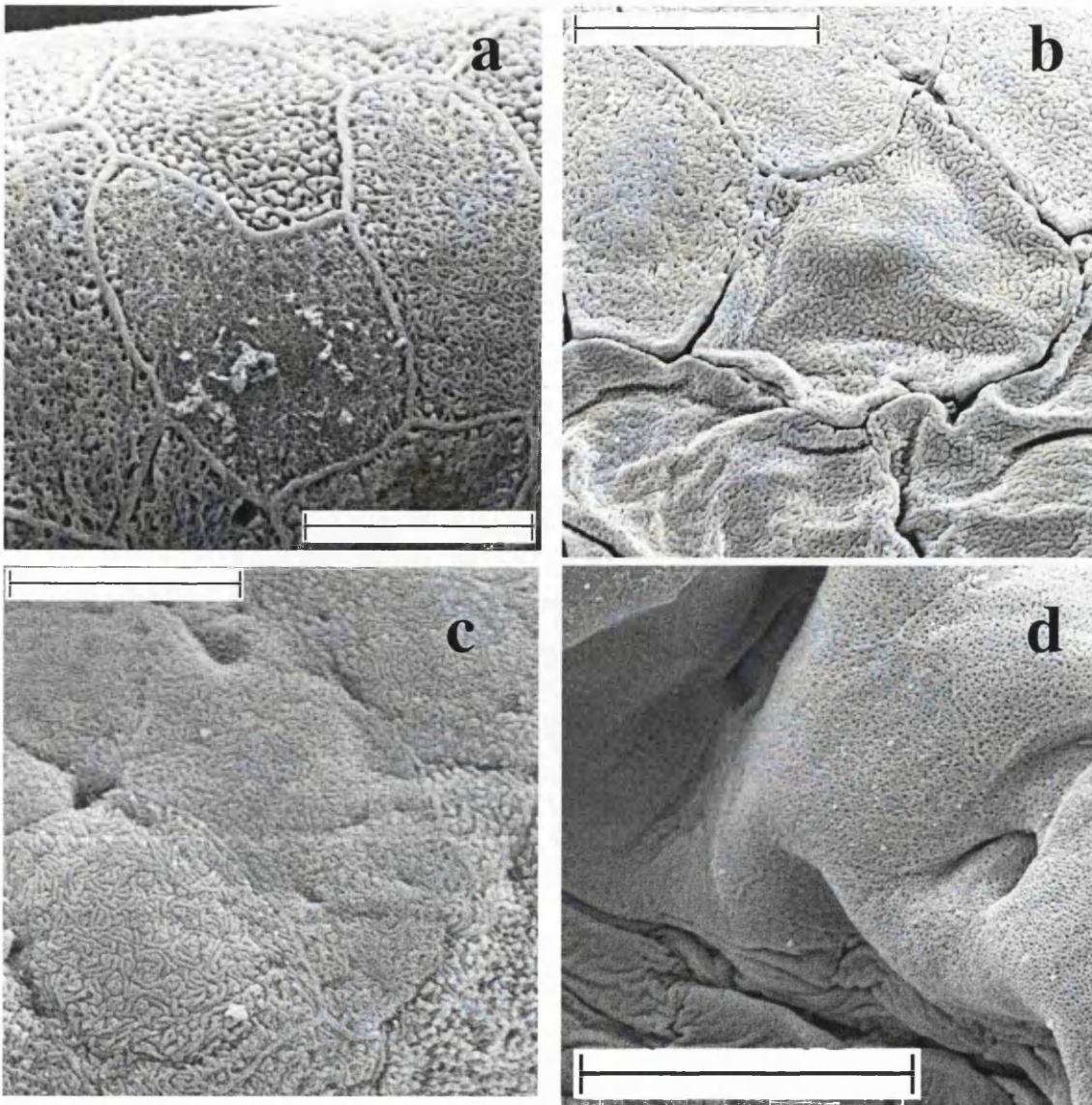


Figure 7.15: Cells on the circumferential groove in (a) Juvenile *S. rubra*, Scale bar = 25 μm . (b) Adult *H. crepitans*, Scale bar = 25 μm . (c) Juvenile *H. punctata*, Scale bar = 25 μm . (d) Adult *F. fitzgeraldi*. Scale bar = 12.5 μm .

Mason (2001), in his study of the effects of water flow on adhesion in the Cuban tree frog, *Osteopilus septentrionalis* found that frogs are able to largely exclude excess water from beneath the pad at low rates of water flow across the substrates, although a faint encroachment at the margins of the pad did occur at the leading edge of the pad which may conflict with the idea that this circumferal margin is acting as a physical barrier to the flow of water to below the pad (**Figure 7.16**). It may be then that the sculpturing of the cells on the margin acts to channel excess fluid into the circumferal

groove and thereafter to the lateral grooves to direct the flow of water away from the surface of the toe pad, thus minimising the adverse affects that water flow might have on the adhesive abilities of the frogs. Under natural conditions this might

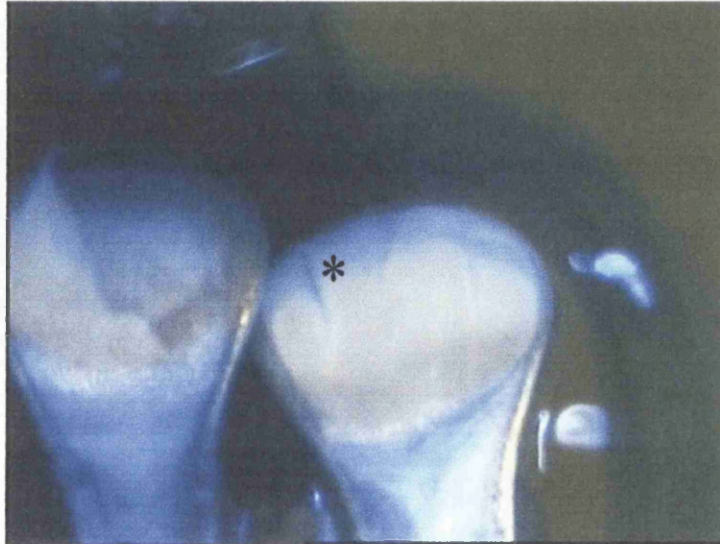


Figure 7.16: Toe pads of adult *O. septentrionalis* adhering to Perspex surface oriented at 90° with water, stained with vegetable dye, flowing over the surface at a rate of 150ml min⁻¹. * Note the lines of encroachment at the distal edge of the pad – this is a species that has distinct grooves on the surface of the pad.

prove of particular importance to Trinidadian species of tree frog as, with seasonal regularity, heavy rains inundate the substrates within their environment. The threat of dislodgement from wet surfaces might be particularly costly to more highly arboreal frogs, as they will have further to climb back to perches and this may explain the greater degree of development in the circumferal groove noted with increasing arboreality in some species (McAllister and Channing, 1983; Green and Simon, 1986).

At higher rates of flow, Mason (2001) noted that as flow rates increased, *O. septentrionalis* attempted to actively increase the surface area in contact by pressing the ventral skin close to the substrate; this is a behaviour seen in several of the species in this study though at the point of detachment from the rotation platform this skin is rarely still in contact. In some species, in particular *H. punctata* and *S. lacteus*, frogs were able to adhere to angles well beyond 90° using only the ventral epidermis when allowed to, and it may be of some interest to look more closely at this area in species which regularly utilise it in adhesion under natural conditions. Rosenberg and Warburg's (1995) study on the European tree frog, *Hyla arborea*, found that the ventral epidermis is covered by 'tubercles with deep grooves between them' covered in turn by a network of micro-ridges (**Figure 7.17**). Goniakowska-Witalinska and Kubiczek's (1998) S.E.M. study of the same species similarly found that whilst the dorsal skin is smooth, the ventral skin has folds and grooves across the surface. As such structuring may well provide an additional frictional contribution to a sliding frog when this skin is in contact, it may be that these are evolved to some degree for adhesive function, though the degree to which this is the case is likely to be limited by the fact that the ventral epidermis is often implicated in water absorption and osmoregulation in amphibians (Toledo and Jared, 1993).

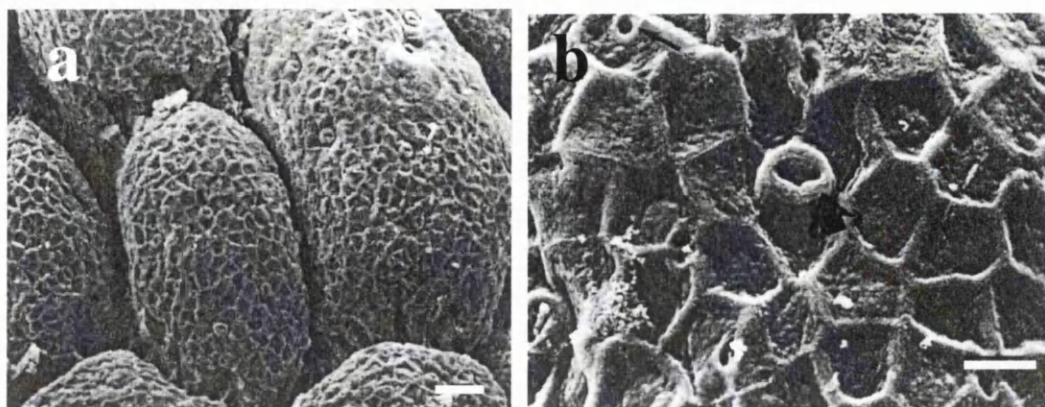


Figure 7.17: S.E.M. images of ventral epidermis cells of the European tree frog *H. arborea*, images from Rosenberg and Warburg (1995) (a) Scale bar = 20 μm (b) Scale bar = 10 μm .

7.3. Adhesion and mucosal properties

As was discussed in earlier chapters the resistance to separation in the meniscus in a wet adhesive mechanism is itself a product of two component forces, capillarity (F_C) and Stefan adhesion (F_{SA}):

Capillary adhesion is classically demonstrated by the movement of a liquid up a capillary tube due to forces generated at the air-water interface, the meniscus. In wet adhesion, the air-liquid interface occurs around the edge of the contact area of the two objects. Through its tendency to move outwards, there is a lowering of the pressure within the liquid that draws the two surfaces together.

Stefan adhesion is functional when two surfaces with a liquid between them are pulled apart when liquid is also present outside the joint; surrounding liquid must flow into the gap created by attempts to pull the surfaces apart and this produces adhesive force which will increase with the viscosity of the intervening liquid, but will eventually decline to zero. F_C and F_{SA} are thus affected by the properties of the liquid in different ways, with F_C chiefly dependent on the surface tension and F_{SA} on viscosity (see **Formula 7.1**).

Data from adult frogs across the twelve species (**Chapter 2**) corroborate the assertions of previous studies that the most influential forces within the wet adhesion mechanism are likely to be capillary forces, increasing as they do directly with the increase in toe pad area (Emerson and Diehl, 1980; Green, 1981a; Hanna and Barnes, 1991; Barnes, 1997; Barnes, 2000).

Trends seen in most species when also considering data from juvenile frogs are a little more problematic, with adhesive forces increasing at a greater than expected rate should capillary adhesion dominate, directly with toe pad area, but at a lesser rate than that expected through Stefan adhesion, as toe pad area squared (**Formula 7.1**).

$$(7.1) \quad F_{\text{total}} = F_{\text{SA}} + F_{\text{c}} \longrightarrow \frac{2\pi r^2 \gamma}{h} + \frac{3\pi r^4 \eta}{2h^3} \longrightarrow \frac{2(\text{area})\gamma}{h} + \frac{(\text{area})^2 \eta v}{2h^3}$$

Where: r = radius; η = viscosity; γ = surface tension; h = meniscal height, v = speed of separation of two surfaces.

If this formula has area dependent elements substituted by values for a theoretical pad of one millimetre squared then the following formula shows the relative contribution of component forces to the overall adhesive force per unit area:

$$(7.2) \quad F_{\text{mm}}^2 = \frac{2\gamma}{h} + \frac{\eta v}{2h^3}$$

Where: η = viscosity; γ = surface tension; h = meniscal height, v = speed of separation of two surfaces.

In previous chapters it has been demonstrated that the force per unit area of the pad for the majority of the species in this study increases with the linear dimension. If it is assumed that the speed of the separation of the pad from the surface is constant in all species, as detachment is not an active process but a passive peeling from the substrate as the frogs are acted upon by gravity (Hanna and Barnes, 1991), then this would suggest that there is a change elsewhere within the mechanism that is responsible for the changing adhesive force with growth. The two areas that are most likely to effect this change are the properties of the mucosal layer, either in terms of its viscosity or surface tension and/or in the height of the meniscus formed below the pad.

According to the simplified formulae for Stefan adhesion and capillary adhesion (**Formula 7.2**) the rate of change in the adhesive forces will be affected by an increase in meniscal height to a greater degree in the former model of wet adhesion than in capillary adhesion (**Figure 7.18**). One notable area illustrated in this graph is bounded by the curve for $y = 2h^3$ and that of $y = h$. The crossing points of these two curves show the values of h for which the values of $2h^3$ are lower than the value of h . In the case of the adhesive force per unit area, where this unit is considered in terms of mN/mm^2 of toe pad and values of η and γ are also considered in terms of mN/mm then the implications are, that for meniscal heights of between 0 and 0.7 mm, Stefan adhesion will produce higher forces within a wet adhesive mechanism than surface tension. If we consider the values for an adhesive system dependent on a fluid with a viscosity similar to that calculated from *Litoria caerulea* ($1.38 \times 10^{-3} \text{ mN}/\text{mm}^2$), and with a surface tension similar to that of water ($7.3 \times 10^{-2} \text{ mN}/\text{mm}$)*, plotting the force that might be generated per unit area for a range of meniscal heights for a wet adhesive mechanism dependent either on viscosity (**Figure 7.19**: red line) or capillarity (**Figure 7.19**: blue line), confirms that, even for the low viscosity of the fluid in this instance, frogs would be able to increase their adhesive abilities to a far greater extent by utilising a mechanism dependent on Stefan adhesion (**Figure 7.19**). However, if we consider the range of meniscal heights expected beneath the pad for both models that would produce the range of the observed adhesive forces per unit area in the species in this study, then the values for meniscal height that would produce observed force in a system dependent on surface tension are orders of magnitude greater than suggested from either fluorescence microscopy (Riehle and Barnes, in prep.) or interference microscopy (Federle *et al.* in prep.).

* Assuming a fairly rapid speed of separation, for simplicity's sake, of 1 mm/s.

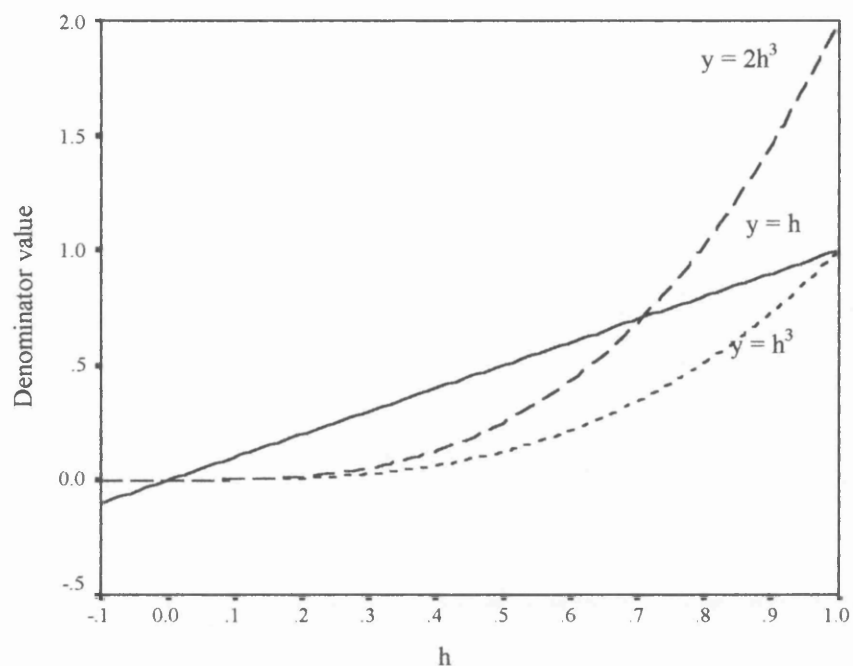


Figure 7.18: Relationships between theoretical values for h and the effect on the denominator factor of capillary adhesion ($y = h$) and Stefan adhesion ($y = 2h^3$)

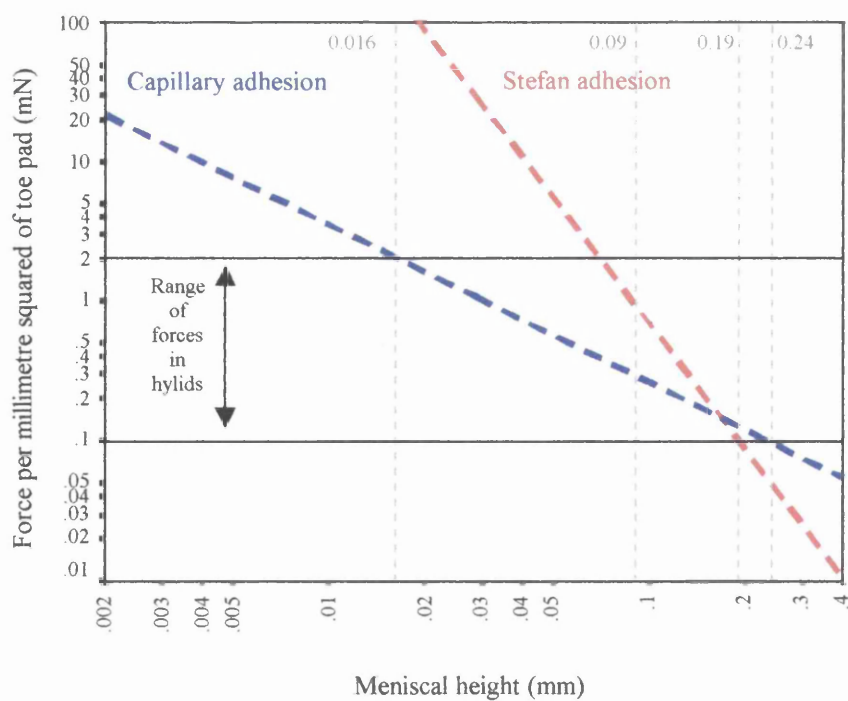


Figure 7.19: Log:log plot of theoretical forces produced by different models of adhesion for a range of meniscal heights. --- Stefan adhesion --- Capillary adhesion.

Even for a mucus with a low viscosity similar to water, at the range of meniscal heights predicted from recent studies this model predicts that Stefan adhesive forces should dominate. As adhesive forces scale with area in adult frogs it clearly doesn't in this case so it seems that this simple model of wet adhesion is, again, not sophisticated enough to take into account the effect of factors such as the curvature and deformability of the pad or the presence of intercellular channels across the pad surface on both models of adhesion. The effects of the dense networks of narrow intercellular channels across the surface on the ability of a fluid, even with the relatively low viscosity of water, to flow into them as the pad is moved away from the surface are likely to particularly adversely affect Stefan adhesion but it seems likely that there will be at least some contribution of viscosity to the overall forces recorded from tree frogs.

If meniscal heights predicted from fluorescence microscopy of between 0.5 to 5 μm are within the correct range, then findings in Roberts (1971), where frictional forces generated in thin water films were found to be dependent on the liquid's viscosity at thicknesses above 7 nm, will have significant implications and it is likely then that viscosity will play a significant function in the ability of frogs to resist shear force. Differences in the angles of initial slip, occurring at angles below 90° where shear forces are more influential, might reflect differences between species in terms of the viscosity of the fluid beneath the pads. However, friction is strongly dependent on weight and comparing interspecific differences in the angle of initial slip does not take into account differences between species in terms of their weight (**Figure 2.5a**). Barnes *et al.* (2002) consider the coefficient of friction (μ) as a comparative variable between species; this is a dimensionless parameter and gives a relationship between

shear and normal contact force and is used to quantify grip in engineering, calculated using the relative angles of slip and fall in this instance as follows:

$$(7.3) \quad \mu = \frac{\sin \theta_1}{\cos \theta_1 - \cos \theta_2}$$

Where: θ_1 = angle at which the frog first slips on platform; θ_2 = angle that frog falls from platform.

If we consider the coefficients of friction* calculated from adult frogs adhering on Perspex for the species in this study (**Table 7.6**) in relation to the size of the frog then there is a significant effect of the increasing linear dimension on this dimensionless value, perhaps indicating that there is an increase in the viscosity of the intervening layer in larger species in comparison to smaller ones (**Figure 7.20**). On an intraspecific level, there are no significant trends in frictional coefficients according to the wettability of the substrate for the majority of species with the one notable exception being *S. lacteus* (**Figure 7.21**). This may suggest that there is an adhesive mechanism more influenced by viscosity in *S. lacteus*, though the lack of any correlations between size and adhesive force in adult frogs within any of the species (**Chapter 2**) means that it is difficult to determine whether this might be the case. As discussed earlier (**Chapter 3.4**) the habitat in which this species is found, combined with its distinctive physical attributes may indicate a more aquatic lifestyle in these frogs in comparison to the other more typical ‘tree frogs’ in the study. This

* These are high values: frictional coefficients between tyre and rough surfaces are seldom higher than 1 (Barnes *et al.* 2002). If the initial observations of the adhering pads of live tree frogs under interference microscopy are correct then meniscal heights are an order of magnitude lower than predictions from fluorescence microscopy and are closer to 1 nm (W.Federle, pers. comm.) then this may explain in part the high frictional coefficients: for liquid films below 7 nm in thickness, friction forces increase strongly due to the formation of dry contact or to solid-like molecular ordering of the liquid at zones where the film becomes thinner than around 10 monolayers (Federle *et al.*, 2003).

would have a significant effect on sticking abilities if the frog were to be entirely dependent on an adhesive mechanism dependent on surface tension as capillarity is only functional when the intervening liquid is not present outside the adhesive joint. Stefan adhesion, on the other hand, is functional when liquid is present both at the surface interface and around it so may be more useful to a species that lives in a habitat in which the substrates that it encounters are regularly inundated or underwater.

Species in order of increasing size	Frictional coefficients of frogs on materials (in order of decreasing wettability)						
	Glass	Wood	Upper leaf	Perspex	Rubber	Teflon	Under leaf
<i>H. microcephala</i>	1.04	1.02	1.00	1.22	1.00	1.27	1.54
<i>H. minuta</i>	1.00	1.13	1.02	1.00	1.00	1.00	1.15
<i>S. rubra</i>	1.00	1.00	1.00	1.00	1.02	1.00	0.99
<i>H. punctata</i>	1.00	1.00	1.74	1.05	1.05	1.29	1.38
<i>S. lacteus</i>	0.95	1.09	1.00	1.19	1.03	1.11	1.42
<i>H. geographica</i>	-	-	-	1.34	1.35	-	-
<i>H. crepitans</i>	1.09	1.09	1.04	1.49	1.18	0.96	1.32
<i>P. venulosa</i>	1.06	1.85	-	1.48	2.77	-	-
<i>P. trinitatis</i>	0.95	1.71	1.04	1.07	1.18	1.02	1.27
<i>H. boans</i>	1.66	2.21	2.29	1.98	1.88	1.40	1.99

Table 7.6: Frictional coefficients for ten species on different substrates (values from Barnes *et al.* 2002)

The possibility that there might be interspecific differences in terms of the mucosal properties in response to differences in ecology has been discussed in some detail in previous chapters, particularly with reference to the effect on jumping ability. It has been demonstrated that there is a significantly detrimental effect of high viscosity mucus on jumping ability in the Cuban tree frog, *Osteopilus septentrionalis* (W.J.P. Barnes *et al.*, unpublished data).

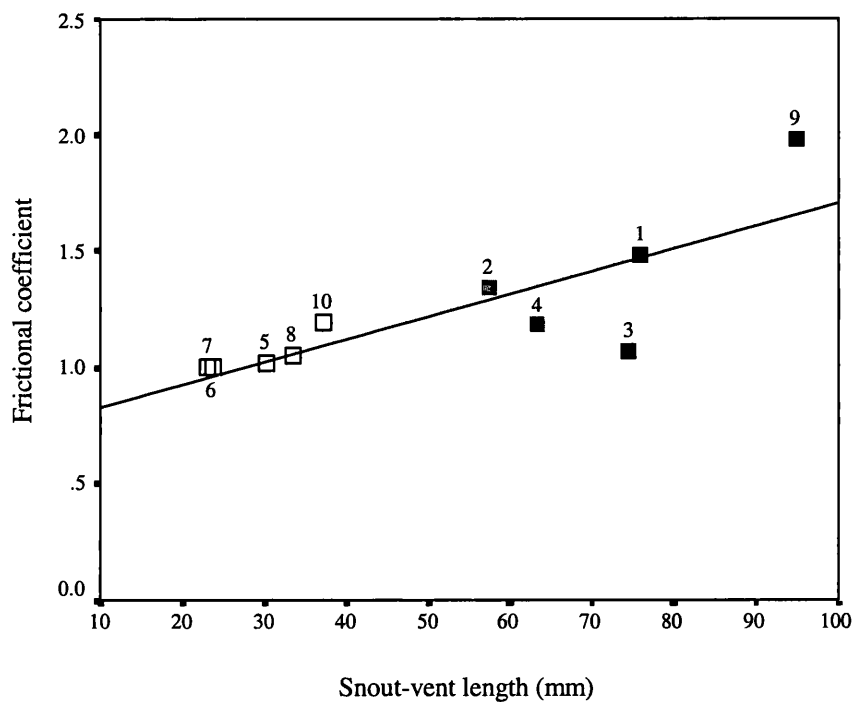


Figure 7.20: Frictional coefficients vs SVL in ten species of hyliid from three size classes: (□ small ■ medium and ■ large). Correlative statistics for total population: $r = 0.81$, $y = 0.01x + 0.73$, $t = 3.84$, $p = 0.01$, 9 d.f. Numbers denote species as follows: 1 = *P. venulosa*, 2 = *H. geographica*, 3 = *P. trinitatis*, 4 = *H. crepitans*, 5 = *S. rubra*, 6 = *H. microcephala*, 7 = *H. minuta*, 8 = *H. punctata*, 9 = *H. boans*, 10 = *S. lacteus*.

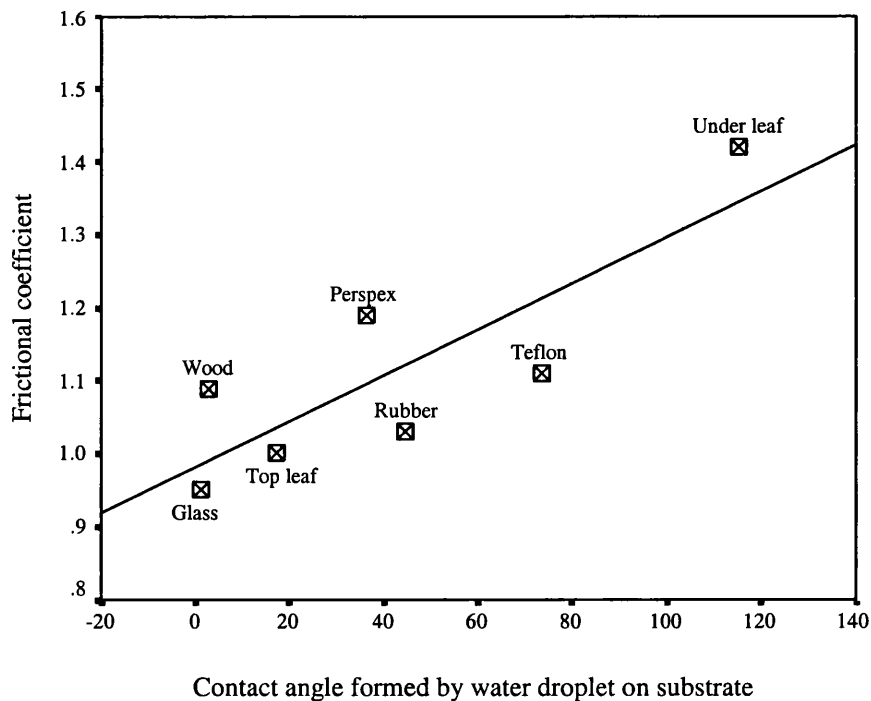


Figure 7.21: Frictional coefficient calculated from angles recorded from *S. lacteus* on seven different substrates of differing wettability. Correlative statistics: $r = 0.83$, $y = 0.003x + 0.98$, $t = 3.31$, $p = 0.02$, 6 d.f.

However, different species are likely to have differing degrees of dependence on jumping as an escape strategy: for example, *H. geographica* ‘play dead’ in response to perceived predation threat (Murphy, 1997; field notes, JMS) and *P. venulosa* ‘gum up’ the mouths/beaks of potential predators (Leary and Razafindratsita, 1998), and so although there are likely to at least be some limitations to the extent to which the viscosity of the mucus can be altered, this may be less so for these species. As discussed in earlier chapters, the tendencies of *P. trinitatis* to escape predation threat by jumping are also lesser than in the other species and this is thus one of the most likely candidates for the use of viscous mucus in adhesion. To determine whether or not the limitations to the use of Stefan adhesion in these species is due to considerations of the effects on escape behaviour, and to more completely understand the evolutionary significance of the need for an efficient adhesive mechanism in arboreal frogs, it is important to ascertain typical viscosities of the mucous layer for all of the species under consideration at different stages of their life histories.

Scherge and Gorb (2001) outline the conditions that an ideal adhesive should fulfil, including (a) a high molecular weight to promote better cohesion (b) the presence of bulky molecular side chains and cross-linking to prevent crystallisation, improve cohesion and retard degradation (c) a zero contact angle indicative of a tendency to spontaneously spread along an adherent surface (d) a low initial viscosity to facilitate diffusion into any depressions on the surface. Mucus produced in the skin of many species of frog contains long-chain, high molecular weight polymers and Emerson and Diehl (1981) suggest this means the fluid is likely to have a viscous nature and should act as a good wet adhesive due to its cohesive strength. This observation is,

however, based on studies of the property of mucus secreted from dorsal skin glands; no physico-chemical analyses of the mucus produced by the glands on the toes has yet been undertaken beyond the use of histological staining to determine that it is a mucopolysaccharide complex (Noble and Jaekle, 1928; Ernst, 1973a). On a recent collaboration with Dr. W. Federle at the University of Würzburg, the viscous nature of mucus sampled from the pads of White's tree frog, *Litoria caerulea*, was investigated by holding a protein-coated polystyrene sphere in solution using optical tweezers with a position-sensing detector and a lock-in amplifier to measure the displacement magnitude and phase responses of the sphere driven sinusoidally to determine viscous drag (following protocol of Valentine *et al.* 1996). Analyses are still underway to determine a quantitative value for the viscosity of the mucus beneath the pads of this species, but preliminary observations of the images suggests that the viscous properties of the mucus in this species, are much as predicted from models of adhesion assuming the mucus has properties similar to water, being equivalent to 1.38 times that of water (W.Baumgartner, pers. comm.). It is difficult however to state conclusively that this will be the case for all species of frog under investigation; *Litoria caerulea*, although a hylid, originates from Australia and is subject to very different environmental, seasonal and ecological conditions to the Trinidadian frogs in this study.

The ways in which frogs might be able to control properties within the functional mucosal layer are relatively simple if we consider the solutions seen in other organisms, in particular the gastropods and a number of marine invertebrates, that are able to make physio-chemical changes within the fluid secretions that effect adhesion (Smith *et al.* 2002). These are considered below in relation to the changes in

viscosity in the mucus and the alteration in the tenacity that this causes, so although the majority of this discussion will focus on factors that alter the viscosity, it should be taken into consideration that the factors that influence viscosity are also likely to have some effect on surface tension.

Evidence from periwinkles and limpets suggests that the addition of specific proteins to the mucus can increase the adhesive potential and thus the tenacity of the adhering gastropod (Smith *et al.*, 1999; Smith and Morin, 2002). Studies of the relative contents of mucopolysaccharides and proteins in the dorsal secretions sampled from a number of species of frog, suggest that protein content is highly variable in skin mucus (Dapson, 1970; Delfino *et al.* 1998; Shepherd *et al.* 1998). This may be in part due to the fact that the secretory epidermal glands of Hylid frogs produce a range of products from secretory epidermal glands including waterproofing waxes, antimicrobial peptides and toxins (Blaylock *et al.* 1976; Ferroni, 2000; Vanhoye *et al.* 2003). Histological staining of the mucous glands of the toe pads in both Hylid and Rhacophorid tree frogs shows proteins are present (Ernst, 1973b; Hertwig and Sinsch, 1995) and if the variability in protein content seen in epidermal mucus secretions of frogs is also demonstrable within the toe pad mucus then this may provide a simple way in which these frogs may be able to alter the properties of the mucus as they grow or in adults when additional pressures are placed on the adhesive system, such as the weight gain during gravidity in female frogs.

Another interesting factor raised through observations the pads of *Litoria caerulea* using interference microscopy was the presence of small rod-shaped ‘particulates’ within the mucus that appeared to be moving independently of it’s flow. The size of these, together with S.E.M. samples from frogs in this study, in which bacterial cells were observed clustered within the lumen of mucosal pores (**Figure 7.22 a**) and in the intercellular channels (**Figure 7.22 b**), suggests that bacteria may be present within the mucous layer of adhering tree frogs. If this is a commonplace occurrence, then there would be implications for the adhesive function; as the viscosity of a mucous secretion is strongly influenced by bacterial presence. Particularly significant in the presence of bacterial colonies is the production of extracellular DNA; because of its very high molecular weight, DNA solutions, even at low concentrations, can have a significant effect on viscoelasticity (Fung, 1981). However, increasing concentration of DNA in solution also lowers the surface tension of the fluid (Ohsie, 2001), which might be expected to be detrimental to the tree frogs adhesive mechanism.

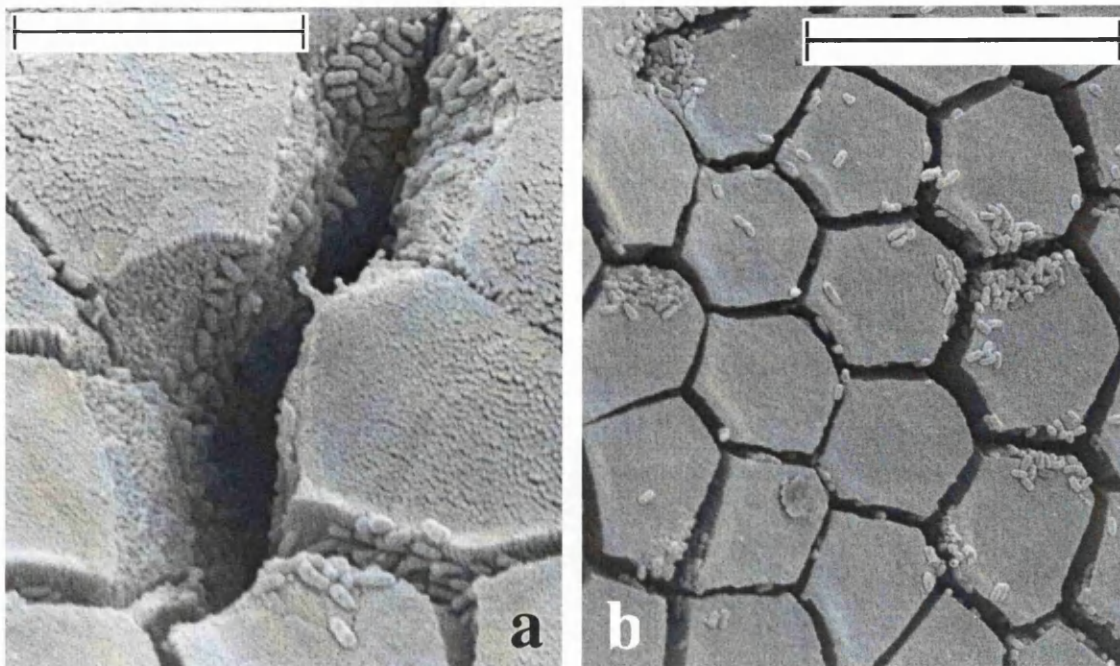


Figure 7.22 S.E.M. images showing bacterial clusters around the mucous pores and intercellular channels on the toe pads of two juvenile *Hyla crepitans* (a) Scale bar = 12.50 μm (b) Scale bar = 25 μm

Perhaps the most familiar example of the effects of bacteria on mucosal viscosity to many of us is the effect of bacterial infections on the consistency of bronchial mucus, one of the major indicators of the onset of a chest infection being the presence of thickened mucus. Other medical examples include changes in viscosity of salivary fluid in bulimics and in the pancreatic juices during pancreatitis. Typical saliva has a mean viscosity of around 4 mPas (around four times the viscosity of water) but increases to 7.4 mPas in bulimic patients, due in part to the increased presence of gut flora in the mouth (and partly to cross-link formation with increased acidification). Pancreatic 'juice' produced by a healthy pancreas has a mean viscosity of 1.61 mPas with this increasing to 5.8 mPas in patients with chronic pancreatitis (Freitas, 1999)*.

Studies mucosal properties of the banana slug *Arioliomax colombianus* (Deyrup-Olsen *et al.* 1983, 1988; Deyrup-Olsen and Jindrova, 1996; Verdugo *et al.* 1996) discovered that mucus is produced in epithelial glands in membrane-bounded granules that rupture to release mucins, with the thickness of mucus being controlled by the degree to which this occurs. Deyrup-Olsen and Jindrova (1996) found that the presence of certain bacterially produced lipopolysaccharides also initiated granule rupture, thus affecting the viscosity of the mucus. In this instance the thickening of the mucus is for protective antibacterial purposes but if similar responses were typical to mucous granules then the presence of bacteria on the toe pads of the frogs may effect the viscosity of the mucus secreted by the pads.

* One of the best-studied cases in medicine is the case of cystic fibrosis, in which the mucus in the lungs becomes excessively thickened and has high values for both viscosity and surface tension (3.80×10^7 mPa and 0.10 mN/mm respectively) and which is characterised by the defective transport of the chloride ion (DeNeuville *et al.* 1997). Luchtel *et al.* (1991) found that the rupturing of mucous granules in *A. colombianus* is, in part, controlled by the presence of chloride ions, with this being one of the first direct demonstrated links between thickening mucus and the chloride ion.

Many species of hyliid are able to produce anti-bacterial secretions with which they suppress the growth of microbial colonies (Vanhoye *et al.* 2003). The fact that there appear to be free-living bacteria within the mucus of at least one species of tree frog in life suggests that these are not necessarily detrimental to the frogs. Future physico-chemical analyses of the mucosal properties might benefit from consideration of whether or not bacteria are prevalent, and if this is the case, where might these originate within the frog's environment? If bacterial presence is commonplace it may be of some interest to determine whether there is a stage within the life history that this becomes the case.

The adhesive properties of the mucus may also be changed over time through a progressive alteration in the water content. Dehydration of mucus is implicated in the abilities of a number of marine prosobranchs to increase their tenacity with time after attachment (Smith, 2002). The tenacity of the periwinkle *Lottia irrorata* changes from roughly 12 kPa when moving to thousands of kilopascals when glued down with this facilitated by and increase in mucosal stiffness of roughly six orders of magnitude as it changes water content from full hydration to full dehydration (Smith, 2002). Looking at the adhering pads of live frogs on a glass coverslip using interference microscopy, preliminary observations suggest that there is a progressive increase in the contact area of the apical part of the cells over time and a decrease in the amount of visible liquid beneath the pad (**Figure 7.23**). If this were effected by an absorption or drainage of the watery components of the mucus then this may be useful to frogs when resting for prolonged periods during the day. However, the substrates that the frogs do choose to rest upon during diurnal conditions are likely to be more dynamic in terms of the factors that will influence dehydration than is a

glass cover slip in experimental conditions. Consider the behaviour of juvenile *H. crepitans* in laboratory conditions (**Appendix 6**); in diurnal conditions most frogs rarely move and when stationary approximately half are resting at angles of over 90° from the horizontal. The majority of frogs sleeping at such angles are found on leaves and of these 80% are on the non-waxy undersides of these leaves. This is significant as the underside of a transpiring leaf is likely to provide a humid microhabitat (Ramsay *et al.* 1938) which this will not favour dehydration as mechanism by which to increase their tenacity in non-mobile conditions.

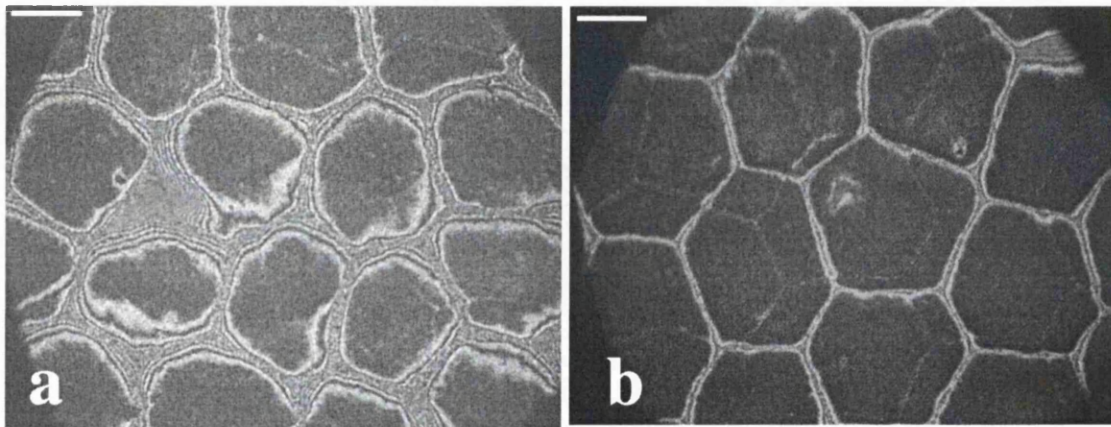


Figure 7.23 Cell apices of *Litoria caerulea* in close contact at (a) beginning and (b) end of hour long interference microscopy experiment. Scale bars = 10 μm

Juvenile *H. crepitans* also exhibit a tendency to select the undersides of leaves at higher temperatures (see **Appendix 6**). If it were significantly cooler in the microhabitat beneath a transpiring leaf compared to the top surface then this may indicate that there is a higher dependency on viscosity in adhesion during rest as this decreases much more strongly with temperature than surface tension (Federle *et al.* 2002) and such microhabitat selection would help to minimise the adverse effects of temperature. The high prevalence of resting angles over 90° belies the theory that viscosity is involved in these resting frogs. Whilst utilising a high viscosity fluid may

give the frogs a strong degree of resistance to the rapid detachment force of a sudden gust of wind, due to the time dependent degradation of Stefan adhesion forces, it is likely to present a poor defence against the continuous relentless pull of gravity on the mass of the frog. A more likely explanation of the tendencies to favour the undersides of leaves seen in these juvenile *H. crepitans* is that this microhabitat selection is a behavioural hydroregulative strategy; the use of microhabitat selection is well documented as a water conservation strategy in a number of species of frog (Hillyard, 1999) and there is some evidence that tree frogs resting on the underside of leaves exhibit a lowered degree of water loss than those on waxy upper side or on non-biological surfaces (J.R. Downie, *pers. comm.*).

The need for hydroregulation in tree frogs is another factor that may limit the extent to which the properties of mucus may be altered. In all species of frogs the mucous layer is implicated in various aspects of osmoregulation and respiration (Duellman and Trueb, 1997). Properties of the mucous layer that will facilitate functionality in these variables are likely to conflict with changes that will improve cohesive strength in the fluid layer. In fact in the many organisms that produce mucus, ranging from simple coelenterates to mammals, the functions of the material are many-fold; being implicated in adhesion, feeding and as a protective coat on the surface of integument and mucosa (Verdugo *et al.* 1987). In amphibians the epidermal mucosal layer is particularly important in terms of the protection that the combined chemical and physical barrier that the mucous layer provides against fungal and bacterial infections, both in terms of the antimicrobial content and its thickness (Ferroni, 2000). The properties of the mucous layer covering the epidermis are also believed to have been key in the ability of the amphibia to live out of the water and there is

evidence that mucus aids in hydroregulation and resistance to drought (Toledo and Jared, 1993; Rosenburg and Warburg, 1994; Christian and Parry, 1997; Linsenmair *et al.* 1999). Considering the importance of mucus in amphibians to perform a variety of other functions including: hydroregulation, protection from microbial and fungal infection, respiration and as an anti-predator device, it may be that properties of the mucus and the evolution of the wet adhesive mechanism, rather than being driven only by the need for an efficient mechanism to withstand dislodgement, is limited by the dependence of tree frogs on mucus for these other functions. The properties of the mucus involved in adhesion are, as yet, largely unknown and this is a major gap in our current understanding of differences between species and between age classes.

7.4: Conclusions

This study has been concerned with the functional morphology of the toe pads in tree frogs with reference to the abilities that the frogs have to adhere to smooth surfaces, and related these to differences in ecology, allometric growth and development. Studies that consider the influence of an organism's phenotype on its fitness have often focused on locomotion or feeding ability (Zani, 2000). However, the functional relationships between morphology and adhesion may be particularly illuminating in that the evolution of specialised adhesive structures has facilitated niche expansion for many organisms. Specifically in this case, adhesive ability has allowed many species of hyliid to exploit the abundant food sources available in arboreal habitats.

At the beginning of this study the problems presented by utilising a wet adhesive mechanism in relation to increasing size both within and between species of hyliid were discussed and a number of questions posed (**Chapter 2.1**). To answer these

questions, patterns in growth and scaling, adhesive force and toe pad morphology in both adult and juveniles from a range of size classes were examined:

Adhesive forces produced by adult frogs belonging to twelve species scale in direct relation to the contact area of the specialised toe pads. This is as expected from previous studies suggesting capillarity is the dominant contributory mechanism in adhesion in tree frogs (Barnes, 2000; Hanna and Barnes, 1991; Emerson and Diehl, 1980). However, fluorescence and interference microscopy suggest a mucosal depth at which, even for a low viscosity fluid such as water, the contribution of Stefan adhesion forces will be significant (**Figure 7.19**)*.

Between species, toe pad area scales as expected through isometry, as the linear dimension squared and although mass increases between the smallest and largest species at a lesser rate than isometry predicts, the degree to which this is the case is not matched by pad area. With the adhesive mechanism scaling with area, large species are therefore less able than small species to adhere to angles beyond the vertical on smooth test surfaces.

In spite of this, there is some evidence, in terms of the force per unit area, that large species have toe pads that are more efficient than those of small species. Between species there are differences in features of toe pad morphology that appear to have a direct effect on the adhesive efficiency of the pad. For example, there are increases in the development of grooves defining the separation of the pad from the ventral

* Stefan adhesion is time dependent and so will not be present in a static system but may be a significant contributory factor in adhesion in the sliding phase of resistance to falling and may perhaps help to explain the high coefficients of friction seen in most species in this study.

surface of the toe in large species that correlate to increased pad efficiency, perhaps aiding adhesion by maintaining meniscal boundaries. However, there are ecological differences between species in the study that makes it difficult to attribute differences in pad morphology directly to the effect on adhesion.

Within species there is some evidence that adult frogs are able to maintain adhesive ability on a range of substrata with low surface energies where wet adhesion might be expected to be significantly impeded. Although the angles to which they are able to maintain a grip are generally reduced frogs are still able to cling to angles significantly beyond the vertical, suggesting that there may be accessory adhesive mechanisms in effect. The presence of tubercles with roughened surfaces found along the length of the toe in many species may suggest a complementary function of these areas. Furthermore, considering the magnitude of the distance between pad and substrate suggested by fluorescence and interference microscopy there is a potential for additional contribution to adhesion by rubber friction and intermolecular bonding.

Within species, as frogs increase in size from juvenile to adult, there is evidence that adhesive forces increase at a greater rate than can be explained by contact area of toe pads alone in most species. The degree to which this is the case differs according to the size class of the frog, with small species more able than large species to maintain adhesion on smooth surfaces to a similar degree in juvenile and adult frogs. Indeed there is little, if any, significant detrimental effect of growth on the maximum angle to which most of the small species of frog can adhere. This is aided in part by a reduction in the rate of weight increase with growth from that expected following isometric predictions, with this trend being particularly marked in large species.

Within most species, as between species, toe pad area shows little evidence of a deviation from the rate of increase expected in the period of growth from metamorphosis to adulthood, scaling as the linear dimension squared. Adult frogs from the larger species in this study tended to have pads that were marginally proportionally larger than in juveniles. This in itself is not sufficient to explain the higher than expected increase in adhesive force with growth in smaller species, nor the increase in adhesive efficiency in the toe pads seen in all species here.

Within species, as on an interspecific level, there is evidence of change in toe morphology seen between small and large frogs that can be correlated to aspects of adhesive function. These are, in the main, centred on the increasing delineation of the grooves defining the edges of the pad and on the increasing development of the extra-accessory structures of the toe but differ between species according to ecological and life history considerations. Of particular significance in large species is the extension of the distribution of the specialised columnar epithelium typical of toe pads to include the subarticular tubercles, as this is likely to further increase the area available for wet adhesion.

Preliminary observations suggest that the fluid that facilitates wet adhesion in tree frogs is a thin, watery mucus produced by glands found across the toe pad, comparable in its viscosity to water and in the order of between 1-10 μm in depth. **Figures 7.18 and 7.19** show that the simple model of wet adhesion based on two flat rigid smooth surfaces held together by a thin layer of fluid used in previous studies (Barnes, 2000; Hanna and Barnes, 1991; Emerson and Diehl, 1980) is not sophisticated enough to describe the tree frog adhesive mechanism accurately. There

are a number of features of tree frog toe pads that this model does not take into account that might be expected to have an effect on wet adhesion and which need to be quantified in order that a more sophisticated model can be developed:

1. Tree frog toe pads are, in general, not flat; most have at least some degree of curvature. This means that the depth of the meniscus is likely to vary across the area of contact. Any future model of adhesion in tree frogs would benefit from the examination of the effect of differing degrees of curvature on sticking ability.
2. Tree frog toe pads are not rigid plates, but are deformable. It is important that the degree of deformability possible, as influenced by intracellular structure and material properties of the cell layers covering the surface of the pad is determined by future consideration of the adhesive mechanism in tree frogs. This is of particular importance in view of findings in insects that adhesion is strongly dependent on the material properties of the adhesive pads cells particularly in allowing a contribution of rubber friction to the adhesive forces produced by the animals (Gorb *et al.* 2000; Federle *et al.* 2001, 2002).
3. Tree frog toe pads are also not continuous planes, but are divided across their surface by a network of micrometric channels. The effects of such subdivisions on the relationship between force and area in wet adhesive mechanisms effected by viscous and non-viscous fluids has not been investigated previously. It is of some importance that the effects of the channels that criss-cross the surface are investigated to develop a more accurate model of adhesion. Together with this, a consideration of the effects of variations in the size and shape of toe pad cells

contributing to the total contact area on force production and resistance to shear would be beneficial.

4. This model assumes fixed mucosal properties. In fact, the mucosal layer is likely to be variable according to a number of factors[#] and it is important for future studies to attempt to understand the range of this variability under natural conditions for the frogs and the effects on adhesive ability. The more accurate quantification of, in particular, the depth and physical properties of the fluid layer is essential for the understanding of the tree frog adhesive mechanism.

Overall, this study suggests that the adhesive mechanism that tree frogs rely upon to allow them to exploit the arboreal environment, whilst it is dominated by wet adhesion, is adaptable enough to allow frogs to cope to varying degrees with pressures placed upon the system by increasing size and substrate variability. The ability of frogs to maintain adhesion with growth is facilitated to some extent by alterations to the rates of growth that might be expected following isometric predictions. Furthermore, morphological studies suggest that the design of the pad is an important factor in the ability of frogs to adjust their adhesive abilities to compensate for increasing size, with evidence that alterations in structure correlate to increased pad efficiency both within and between species. However, as certain structural features are also known to differ according to the ecology of the species it is important for future studies that the specific influence of features such as cell size and shape, mucosal pore density, groove development and subarticular tubercles are better understood. It seems likely too that changes within the fluid layer effecting wet

adhesion might play a role in adhesive adaptability and properties such as the viscosity, surface tension and volumes of the mucus found below the pad are unknown parameters within the tree frog adhesive mechanism at present.

The applications of the ability of tree frogs to adhere well in the presence of a fluid layer has already been considered with respect to wet weather tyre technology, based on the tread-like pattern of the hexagonal cells paving the pad (Barnes *et al.* 2002). There are many other possible biomimetic applications of the tree frog toe pad in situations that may require an enhanced ability to resist detachment and shear under wet conditions (shoes for rock-climbing and gloves for goal keeping being only two of the most obvious). If the biomimetic potential of the tree frog toe pad 'design' is to be realised then the relative importance of factors such as; the shape and size of the pad cells, the mechanical properties of the pad and properties of the fluid layer, must be better understood and quantified in future studies.

[#] (i.e. the degree of hydration of the frog, time, humidity and temperature of the external environment, dilution effects of rain, mucopolysaccharide content)

APPENDICES

APPENDIX 1: Literature values for adhesion forces recorded from a variety of organisms

	Species	Tenacity (mN/mm ²)	Principal mechanism	Adhesive organ	Reference
Insect	<i>Tettigonia viridissima</i>	2	Friction	Tarsal arolia	Jiao <i>et al</i> (2000)
	<i>Oecophylla smaragdina</i>	124	Wet adhesion	Tarsal arolia	Federle <i>et al</i> (2001)
	<i>Hemisphaerota cyanea</i>	25	Friction	Bristled tarsi	Eisner and Aneshansley (2000)
	<i>Megoura vicae</i>	2	Wet adhesion	Pulvilli	Lees and Hardie (1988)
	<i>Calliphora vomitoria</i>	7	“	Pulvilli	Walker <i>et al.</i> (1985)
Barnacle	<i>Semibalanus balanoides</i>	98	Gluing	Antennules	Flammang (1996)
Anenome	<i>Metridium senile</i>	100	“	Muscular foot	Flammang (1996)
	<i>Actinia equina</i>	20	“	Muscular foot	Flammang (1996)
Echinoderms	<i>Asterias vulgata</i>	170	Suction	Podia	Flammang (1996)
	<i>Holothuroidea species</i>	30-135	Gluing	Cuvieran tubules	Flammang <i>et al.</i> (2002)
Cephalopod	<i>Octopus vulgaris</i>	168	“	Tentacular suckers	Smith (1991)
	<i>Oegopsida sp.</i>	830	“	Tentacular suckers	Smith (1996)

	Species	Tenacity (mN/mm ²)	Principal mechanism	Adhesive organ	Reference
Gastropod	<i>Patella vulgata</i>	40-680	Suction	Muscular foot	Denny (2000)
	<i>Patella argenvillei</i>	676	“	Muscular foot	Davenport and Thorsteinssen (1990)
	<i>Lottia gigantea</i>	120	“	Muscular foot	Denny and Blanchette (2000)
	<i>Lottia gigantea</i>	40	“	Muscular foot	Miller (1974)
	<i>Ariolimax columbianus</i>	2	Adhesive mucus	Muscular foot	Denny and Gosline (1980)
Fish	<i>Cyclopterus lumpus</i>	100	“	Ventral sucker	Davenport and Thorsteinssen (1990)
Salamander	<i>Bolitoglossa mexicana</i>	11	“	Muscular foot	Alberch (1991)
Lizards	<i>Anolis carolinensis</i>	50	Van der Waal's intermolecular bonding	Lamellar setae	Irschick <i>et al</i> (1996)
	<i>Anolis sagrei</i>	61	“	Lamellar setae	Irschick <i>et al</i> (1996)
	<i>Anolis leachi</i>	81	“	Lamellar setae	Irschick <i>et al</i> (1996)
	<i>Anolis grahami</i>	70	“	Lamellar setae	Irschick <i>et al</i> (1996)

	Species	Tenacity (mN/mm ²)	Principal mechanism	Adhesive organ	Reference
Lizards cont...	<i>Gekko gecko</i>	1	“	Lamellar setae	Aurtumn <i>et al</i> (2000)
	<i>Hemidactylus frenatus</i>	40	“	Lamellar setae	Irschick <i>et al</i> (1996)
	<i>Hemidactylus turcicus</i>	37	“	Lamellar setae	Irschick <i>et al</i> (1996)
	<i>Gehyra oceanica</i>	38	Van der Waal's intermolecular bonding	Lamellar setae	Irschick <i>et al</i> (1996)
	<i>Gehyra. mutilata</i>	44	“	Lamellar setae	Irschick <i>et al</i> (1996)
	<i>Lepidodactylus lugubris</i>	74	“	Lamellar setae	Irschick <i>et al</i> (1996)
	<i>Prasinohaema virens</i>	21	“	Lamellar setae	Irschick <i>et al</i> (1996)
	<i>Prasinohaema. prehensicauda</i>	9	“	Lamellar setae	Irschick <i>et al</i> (1996)
	<i>Prasinohaema flavipes</i>	15	“	Lamellar setae	Irschick <i>et al</i> (1996)
	<i>Lipinia leptosoma</i>	22	“	Lamellar setae	Irschick <i>et al</i> (1996)

APPENDIX 2: Maps of study and collection sites



Figure A2.1: Collection sites in Northern range, species and age cohorts sampled: **Light Blue:** Mt St Benedicts – *H. crepitans* (t,a) **Orange:** Sunset Drive, flooded wasteland on Lopinot Road – *H. crepitans* (t,a) *P. venulosa* (t,a) *H. microcephala* (a) *H. minuta* (a) *P. trinitatis* (t,a) **Brown:** Arouca River: *H. boans* (a) *H. punctata* (t,a, j) **Green:** Damier River: *H. boans* (a) *H. geographica* (t,a,j) **Yellow:** Morne Bleu: *F. fitzgeraldi* (t,a,j) **Dark blue:** Simla Research Station: *P. trinitatis* (t,a) *P. venulosa* (t,a) *H. minuta* (a) *H. crepitans* (a,j) *S. rubra* (t,a) *H. boans* (a) **Pink:** Lampost 69, Arima-Blanchisseuse Rd. *H. minuta* (a) *H. microcephala* (t, a) *S. rubra* (a) *P. trinitatis* (a) *H. boans* (a) **Maroon:** Guanapo River: *H. geographica* (t, j) *H. boans* (t) **Purple:** Ture River: *H. boans* (a, t). (tadpoles = t, adults = a, juveniles = j).

APPENDIX 2: Maps of study and collection sites



Figure A2.2: Collection and study sites on Southwest Peninsula: **Green:** Swampy cow pasture at forest edge; *S. lacteus* (t, a) *Hyla minuscula* (a) **Blue:** Roadside swamp: *H. punctata* (a) *H. minuscula* (a) **Orange:** Drainage ditch in coconut plantation, Pelican Drive: *H. minuscula* (a, j) *S. lacteus* (a) (as point of interest: 2 *P. trinitatis* seen in thorny tangles in swampy area to the East of Bonasse) (tadpoles = t, adults = a, juveniles = j).



Figure A2.3: Collection site on east coast. **Orange dot** = *S. rubra* (t, a) (tadpoles = t, adults = a).

APPENDIX 3: Sex effects on adhesion in adult frogs

T-tests were carried out on average values of last contact on the rotation board (**Table A3.1**). For the majority of species no difference exists between sexes or between females in gravid state and post-deposition females in the average angle of dislodgement from the rotation platform.

Table A3.2 shows results from 16 individual females belonging to eight species that were available in both gravid and post-deposition states whilst still in captivity. In spite of an increase in weight of as much as half of their normal body weight whilst carrying egg masses most frogs are not significantly affected by their gravidity. Though there is a trend towards there being a negative effect of the gravid state on a frogs ability to maintain a hold on the rotation platform, a paired t-test analysis of the data reveals that this is non-significant ($t = 1.50$, N.S. 14 d.f.).

Examining the relationships between adhesive forces and SVL in the two sexes and in gravid females suggests that there are differences in the adhesive forces being produced. In both males and females the slope of the line of best fit does not deviate from the expected slope should the main adhesive mechanism be chiefly dependent on surface area (**Table A3.3**) increasing at a rate approximate to $(SVL)^2$. The rates of increase in adhesive forces with linear dimensions in the two sexes are not significantly different from one another ($t = 0.19$, N.S., 14d.f.). In gravid females, however, not only does adhesive force increase with linear dimensions at a greater rate than expected, as $(SVL)^{2.51}$, the slope of the line of best fit is also significantly different to that seen in the post-deposition females ($t = 2.30$, $p < 0.05$, 14 d.f.).

Species	Average angle of fall			T-statistics		
	♂	♀	g♀	♀ vs ♂	g♀ vs ♂	g♀ vs ♀
<i>F. fitzgeraldi</i>	178.65	166.60	158.20	15.48	26.28	-
<i>H. minuscula</i>	179.25	179.20	176.10	0.05	2.04	0.78
<i>H. minuta</i>	155.24	171.84	168.30	2.89	2.08	1.41
<i>H. microcephala</i>	145.70	142.40	140.40	0.05	0.29	0.09
<i>H. geographica</i>	153.57	139.40	134.40	1.81	3.71	0.46
<i>H. crepitans</i>	104.73	119.15	133.90	2.30	3.11	1.54
<i>P. trinitatis</i>	110.53	115.50	117.75	0.58	0.98	0.13
<i>P. venulosa</i>	120.33	120.50	132.07	0.02	1.29	1.25

Table A3.1: Sex-dependent species averages for angle of dislodgement and comparative statistics.

Bold type indicates significant difference at $p < 0.05$.

Species	SVL	% age Body mass = eggs	Average fall angle		Diff.	t
			Post-dep	Gravid		
<i>F. fitzgeraldi</i>	21.4	35.24	166.60	158.20	-	1.05
<i>H. minuscula</i>	22.8	23.95	180.00	180.00	=	-
<i>H. minuscula</i>	23.0	29.79	178.40	172.20	-	1.61
<i>H. minuta</i>	23.7	39.52	168.60	163.70	-	0.72
<i>H. minuta</i>	23.9	7.56	168.20	170.80	+	0.32
<i>H. minuta</i>	24.7	16.30	178.00	172.80	-	1.23
<i>H. minuta</i>	25.0	12.03	170.50	165.20	-	0.64
<i>H. minuta</i>	26.0	20.10	170.80	175.20	+	0.95
<i>H. microcephala</i>	25.0	19.41	166.20	156.70	-	1.45
<i>H. microcephala</i>	25.0	16.54	177.90	124.10	-	17.84
<i>H. geographica</i>	64.4	47.53	153.20	141.90	-	2.24
<i>H. geographica</i>	65.3	28.26	142.30	130.10	-	1.93
<i>H. geographica</i>	65.5	52.36	152.90	136.70	-	3.48
<i>H. crepitans</i>	69.8	32.24	119.20	143.60	+	5.55
<i>P. venulosa</i>	91.0	45.97	130.80	136.90	+	1.39

Table A3.2: Fall angles in individual gravid and post-deposition females with comparative statistics.

Bold type indicates significant difference at $p < 0.05$.

	Slope of adhesive force vs. SVL	t-statistic for difference from slope of :		
		2	Toe pad vs. SVL	Weight vs, SVL
Male	2.12	0.64	1.53	2.97
Female	2.17	1.63	2.68	3.45
Gravid female	2.51	4.64	4.08	2.37

Table A3.3: Slopes of lines of best fit for adhesive force vs. SVL on log-log plot in different sexes and t-statistics for comparisons of slopes. Bold type indicates significant difference at $p < 0.05$.

APPENDIX 4: Species average values for slip and detachment angles on different materials

Species	Material	Angle of slip		Detachment angle		Adhesive force (mN)		N
		Mean	s.e.	Mean	s.e.	Mean	s.e.	
<i>H. minuta</i>	Glass	88.56	4.35	140.32	8.46	5.00	0.53	10
	Wood	101.15	1.89	146.05	6.24	5.45	0.29	10
	Top leaf	107.18	2.00	156.15	2.80	5.84	0.17	10
	Rubber	97.31	1.62	153.65	4.91	5.61	0.32	11
	Perspex	81.78	2.18	157.35	3.78	7.79	0.56	22
	Teflon	95.42	4.44	153.57	6.23	5.81	0.42	10
	Under leaf	61.53	4.88	111.93	7.12	2.53	0.52	4
<i>H. microcephala</i>	Glass	92.03	3.29	151.24	6.18	5.77	0.51	9
	Wood	120.35	5.32	155.19	5.87	5.14	0.29	6
	Top leaf	93.02	5.00	153.76	3.94	4.66	0.28	5
	Rubber	98.42	6.83	157.24	5.22	6.25	0.68	9
	Perspex	90.36	3.28	144.33	6.83	6.17	0.74	12
	Teflon	95.18	8.62	132.78	6.30	3.52	0.46	5
	Under leaf	76.55	3.54	113.93	5.61	2.57	0.47	4
<i>S. rubra</i>	Glass	93.83	5.05	159.46	5.74	17.27	1.53	9
	Wood	116.99	7.06	169.01	6.35	17.18	1.43	9
	Top leaf	93.08	4.35	160.11	5.74	16.11	1.19	9
	Rubber	89.53	3.60	154.24	6.79	15.52	1.64	8
	Perspex	83.30	3.62	151.64	4.49	16.50	1.08	10
	Teflon	82.91	1.50	145.70	8.03	14.21	1.80	8
	Under leaf	82.23	5.38	160.33	11.04	14.71	1.99	3
<i>H. punctata</i>	Glass	88.93	2.94	153.93	6.84	18.25	1.56	10
	Wood	138.97	4.71	178.20	0.93	20.06	0.57	9
	Top leaf	100.23	3.43	126.71	3.64	12.07	0.91	10
	Rubber	96.08	4.27	146.09	6.55	16.48	1.66	10
	Perspex	91.82	6.05	143.21	5.26	17.48	1.38	12
	Teflon	97.89	5.85	141.33	9.67	14.20	2.22	8
	Under leaf	88.23	7.38	132.45	11.02	12.64	3.10	4

Table A4.4: Mean values and s.e. for slip angle, detachment angle and adhesive forces on seven substrates in eight species of tree frog. Cont. over...

<i>S. lacteus</i>	Glass	84.77	5.41	155.30	2.52	30.78	1.65	10
	Wood	125.97	2.67	157.95	2.34	31.13	1.17	10
	Top leaf	96.62	6.26	151.81	2.98	28.89	1.54	10
	Rubber	115.03	3.95	158.40	3.52	31.25	1.94	10
	Perspex	87.50	4.90	143.90	2.44	27.93	1.62	12
	Teflon	106.00	4.92	154.03	3.14	30.24	1.53	10
	Under leaf	88.63	7.32	123.08	4.30	20.04	2.56	4
<i>H. crepitans</i>	Glass	71.81	2.17	125.60	2.56	75.49	5.94	11
	Wood	110.06	4.66	147.68	7.66	103.51	10.06	10
	Top leaf	74.34	2.02	131.38	2.93	81.60	4.90	10
	Rubber	77.033	1.95	125.73	4.06	78.85	8.83	9
	Perspex	71.25	2.08	109.53	3.49	47.34	7.58	12
	Teflon	64.60	1.83	118.99	3.75	59.33	7.43	10
	Under leaf	65.00	.	107.20	.	54.92	.	1
<i>P. trinitatis</i>	Glass	56.333	2.29	110.96	2.37	62.21	6.50	9
	Wood	77.97	2.20	110.18	3.35	66.17	7.98	9
	Top leaf	60.77	2.79	109.00	2.83	61.72	7.42	9
	Rubber	75.12	2.92	115.62	3.05	72.53	7.34	10
	Perspex	59.72	6.84	101.68	4.32	44.64	10.14	9
	Teflon	62.31	2.66	111.56	2.59	82.45	17.83	14
	Under leaf	56.40	3.61	89.833	4.27	31.93	6.15	3
<i>H. boans</i>	Glass	63.13	1.51	96.53	8.74	84.48	60.57	3
	Wood	88.43	1.74	111.30	0.75	176.55	19.36	3
	Top leaf	74.35	8.05	96.45	12.05	99.37	73.43	2
	Rubber	76.93	11.07	101.03	5.21	110.98	45.98	3
	Perspex	72.67	9.19	113.80	4.67	170.09	26.87	10
	Teflon	67.57	6.80	103.17	5.49	115.32	49.45	3
	Under leaf	71.20	3.50	99.35	3.65	114.27	29.98	2

Table A4.4 cont....: Mean values and s.e. for slip angle, detachment angle and adhesive forces on seven substrates in eight species of tree frog.

APPENDIX 5: Arboreality and toe pad morphology

The twelve species of frogs were defined as being ‘arboreal’ ‘semi-arboreal’ or ‘scansorial’ according to the protocol of Green and Simon (1986) and Burton (1998) and using information in literature about lifestyles of each species in conjunction with personal observations from the field. Therefore in **Table A5.1**: Arboreal = found in woody trees at least at 5 m; Scansorial = terrestrial by day but climbing to vegetation of between 2-3 m at night; Semi-arboreal = terrestrial by day and climb to less than 1m at night. There are no statistically significant differences in species’ toe pad morphology according to their degrees of arboreality for any factor other than the development of the proximal margin (**Table A5.2**), though there is no demonstrable correlation between the degree of development of any of the extra-pad grooves and margins and the degree of arboreality, as might have been expected from previous studies (Welsch *et al.* 1974; Green and Simon, 1986; Hertwig and Sinsch, 1995). There are, however, a number of interesting trends when considering the toe pad variables in relation to the degree of arboreality evident in **Table A5.2** with reference to correlations between pad morphology and adhesive ability discussed in **Chapter 3.4**. Increased adhesive forces per square millimetre of the toe pad are seen in species of frog with increasing cell size leading to decreased cell and channel densities (**Figures 3.11 – 3.13**). This is of particular interest when considering the trends in these variables in the most arboreal species in comparison with those in scansorial and semi-arboreal species: in all cases they follow those seen in conjunction with an increase in adhesive ability (**Figure A5.1 – A5.3**).

Species	Category*	Notes from literature	Reference
<i>Hyla minuscula</i>	Semi-arboreal	A savanna and forest-edge frog calling from emergent vegetation along the margins of ponds swamps and rice paddies 10 –150 cm from the ground.	Murphy (1997)
<i>Flectonotus fitzgeraldi</i>	Scansorial	An arboreal crepuscular forest frog	Murphy (1997)
		Terrestrial by day and arboreal by night	Duellman and Gray (1983)
<i>Hyla microcephala</i>	Semi-arboreal	Cutover forests, second growth and pastureland. Calling males perch on grasses or reeds in or at edges of water.	Duellman (2001)
		Males call from emergent grasses and sedges in flooded areas between 0.05 – 1m above the water	Murphy (1997)
<i>Hyla minuta</i>	Semi-arboreal	0-2m high perches	Schwartz (1986)
		A small bush dwelling tree frog	Kenny (1969)
		Forest and forest-edge species inhabiting vegetation at the margins of forest ponds.	Murphy (1997)
<i>Scinax rubra</i>	Semi-arboreal	Bush-dwelling scrubby open areas	Kenny (1969)
		Call from bushes and herbs at the edge of small rain pools	Pombal <i>et. al</i> (1995)
		Calling from bushes up to 2m	Murphy (1997)
<i>Hyla punctata</i>	Semi-arboreal	Grasses, bushes and almost always over slowly moving water	Kenny (1969)
		A savannah dwelling frog. Grass and sedges 10-30cm above substrate.	Murphy (1997)
<i>Sphaenorhynchus lacteus</i>	Semi-arboreal	Low bushes over water in permanent or semi-permanent water, at the edges of forest clearings but frequently in open swampy country	Kenny (1969)
		Reported from low bushes over water at the edge of forest clearings and in swampy terrain	Murphy (1997)
<i>Hyla geographica</i>	Scansorial	Habitat variable, most frequently found in low bushes at edges of mountain streams.	Kenny (1969)
		A savanna and forest-edge frog associated with streams.	Murphy (1997)
<i>Hyla crepitans</i>	Scansorial	Habitat variable, commonly found on the ground, in bushes and in trees always in fairly open country, rarely in thick forest.	Kenny (1969)
		Savanna and forest edge frog. Open country, gallery forest	Murphy (1997)
<i>Phrynohyas venulosa</i>	Arboreal	Arboreal	Kenny (1969)
		Collected in December from high forest drift fences	Yanosky (1997)
		Refuges in trees	Duellman (2001)
<i>Phyllomedusa trinitatis</i>	Arboreal	Lowland arboreal frog inhabiting secondary forest	Murphy (1997)
		More arboreal than other species of Hylid	Duellman (1968)
<i>Hyla boans</i>	Arboreal	Call at a mean height of 229cm (s = 187, n = 220, 0-750)	Magnusson (1999)
		Highly arboreal, as high as 7m above ground.	Duellman (2001)

Table A5.1: Classification of arboreality in twelve study species

	Degree of arboreality									ANOVA statistics			
	Arboreal			Scansorial			Semi-arboreal			F	p	d.f.	
	Mean	s.e.	n	Mean	s.e.	n	Mean	s.e.	n				
Toe pad cell area (μm^2)	118.83	8.15	3	112.26	5.55	3	99.89	10.75	6	0.89	0.45	2	
Cell density/mm ²	8664.93	641.88	3	9288.91	539.93	3	11117.88	11221.78	6	1.32	0.32	2	
Channels mm/mm ²	146.64	7.50	3	154.20	7.25	3	168.89	10.97	6	1.17	0.35	2	
Pore density/mm ²	26.57	6.59	3	23.06	7.30	3	19.31	3.77	6	0.49	0.63	2	
Sat cells (μm^2)	126.55	14.75	3	149.00	32.46	3	146.72	7.58	5	0.32	0.74	2	
Circumferal groove score	1.63	0.68	3	1.96	0.10	3	1.92	0.08	6	0.31	0.74	2	
Lateral groove score	1.00	0.50	3	1.62	0.38	3	1.50	0.30	6	0.61	0.57	2	
Proximal margin score	0.72	0.29	3	1.97	0.53	3	0.93	0.15	6	4.44	0.05	2	
Pad elevation score	0.88	0.32	3	1.41	0.08	3	1.30	0.18	6	1.36	0.31	2	

Table A5.2: Mean values for aspects of toe pad morphology in species according to the degree of arboreality and ANOVA statistics. Bold type indicates significant differences

APPENDIX 2: Maps of study and collection sites

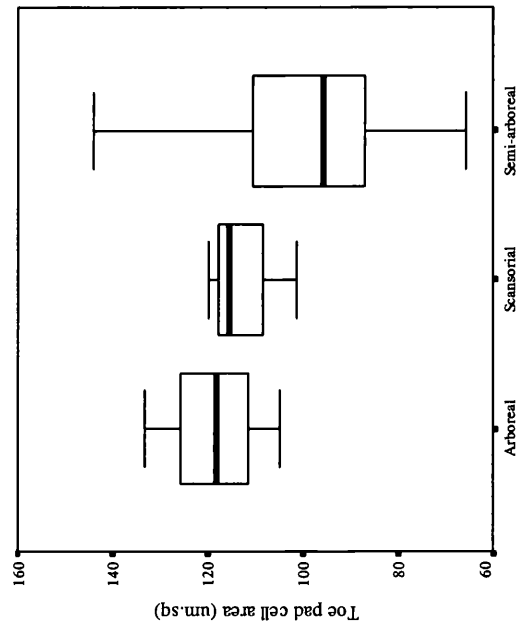


Figure A5.1: Medians and ranges of toe pad cell size according to degree of arboreality in Trinidadian Hylids. Median values: Arboreal, 118.25 μm^2 ; Scansorial, 115.40 μm^2 ; Semi-arboreal, 95.88 μm^2 .

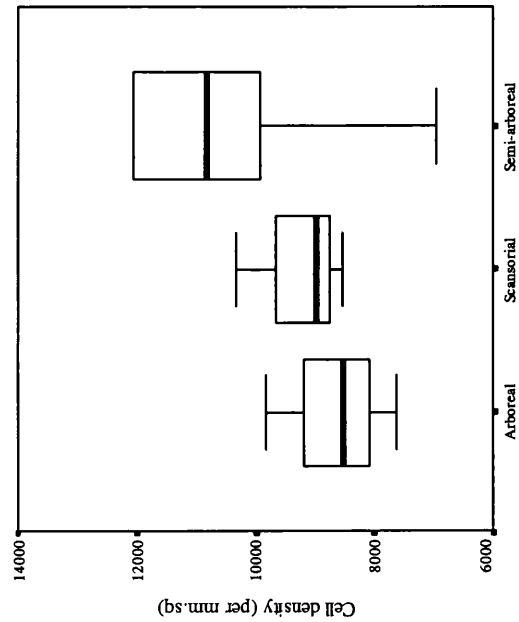


Figure A5.2: Medians and ranges of cell densities on toe pads according to degree of arboreality in Trinidadian Hylids. Median values: Arboreal, 8538.16/ mm^2 ; Scansorial, 8992/ mm^2 ; Semi-arboreal, 10821.82/ mm^2 .

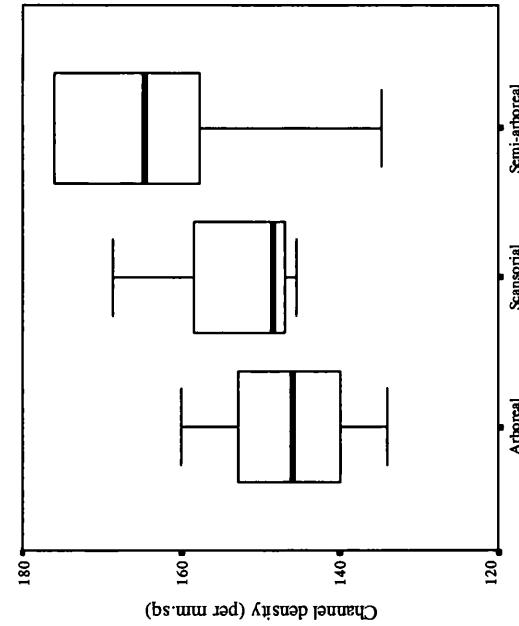


Figure A5.3: Medians and ranges of channel densities on toe pads according to degree of arboreality in Trinidadian Hylids. Median values: Arboreal, 145.88 mm/mm^2 ; Scansorial, 148.45 mm/mm^2 ; Semi-arboreal, 164.59 mm/mm^2 .

APPENDIX 6: Behavioural observations of juvenile frogs

A6.1. Methods

Enclosures: Hyla crepitans (Glasgow).

Juvenile *H. crepitans* were maintained in a vivarium with dimensions of 129cm (height) x 91cm (length) x 31 cm (breadth). The base of the tank had a covering of gravel, gradually sloping from around 1cm in depth to 10 cm with half of the base being covered in water. The water was aerated using a pump and air-stone to prevent stagnation and to help maintain humidity levels. The vivarium was planted with two species of plant; *Scindapsis*, to form a low-growing carpet of small leafed foliage over the gravel base and *Monstera*, which has large leaves and gives the choice of a high perch site to the frogs. The tank was misted daily with fresh water and the frogs fed with small crickets every two days. On each day frogs were monitored over the course of several hours and notes made hourly on their positions (see **Table A6.1**).

Enclosures: Hyla geographica & Phyllomedusa trinitatis (Trinidad)

Frogllets raised from tadpoles were placed in mosquito netting enclosures of around a cubic metre constructed in the grounds of accommodation at the University of the West Indies and at Simla Research Station. Frogs were provided with a water source in the form of a large washbasin set into the ground to form an artificial 'pond'. The enclosures contained a range of vegetation, of varying heights and leaf size. Whilst observations were being carried out the tops of the enclosures were left open to allow flying insects access and every two days small insects caught in sweep-nets in adjacent grassland were added to the enclosures. Behavioural observations were made for both enclosures and air temperature, humidity and weather notes made each hour.

29.02.00	Species	ID	Colour	Substrate	Leaf side	Cover?	Angle	Height (cm)	Horizontal distance from water (cm)	Activity
1400hrs	H.crepitans	1	olive green	dark monstera leaf	underside	hidden	60	14	0	sleeping
28degC	H.crepitans	2	pale green	light* scindapsis leaf	upperside	exposed	50	13	18	sleeping
48%humid	H.crepitans	3	yellow green	light scindapsis leaf	upperside	exposed	40	15	22	sleeping
	H.crepitans	4	olive green	fruit fly containers	n/a	hidden	0	4.5	13	moving
	H.crepitans	5	pale green	aerial root (med dia)	n/a	exposed	0	18	15	moving
	H.crepitans	6	olive green	dark monstera leaf	n/a	hidden	90	29	0	sitting alert
	H.crepitans	7	yellow green	dark monstera leaf	upperside	exposed	90	39	0	sleeping
	H.crepitans	8	olive green	monstera branch	upperside	exposed	90	45	0	sleeping
	H.crepitans	9	yellow green	tank side (Perspex)	n/a	exposed	90	50	9	sleeping
	H.crepitans	10	yellow green	dark monstera leaf	upperside	hidden	50	57	0	sleeping
	H.crepitans	11	pale green	dark monstera leaf	upperside	hidden	60	65	0	sleeping
	H.crepitans	12	pale green	light monstera leaf	underside	hidden	120	77	12	sleeping
	H.crepitans	13	yellow green	dark monstera leaf	underside	exposed	20	89	40	sleeping
	H.crepitans	14	yellow green	dark monstera leaf	upperside	hidden	10	88	40	sleeping

Table A6.1: Typical data sheet for one hours observation of tank of *Hyla crepitans* juveniles in laboratory conditions. Leaf types defined as light and dark by degree of variegation of leaves, *light = 50%+variegation; ** dark = 50%-variegation.

A6.2. Results

Looking at the percentages of frogs recorded in different activity categories, (**Figure A.6.1**), it is evident that juvenile *P.trinitatis* are not recorded at angles beyond 90° in the course of their natural behaviour. Both *H. geographica* and *H. crepitans* are regularly recorded at orientations beyond the vertical on substrates within their environment, with the greater percentage of these observations in sleeping frogs. This suggests that the use of adhesion in these frogs is most commonly utilised to aid in attachment to substrates when resting. The usefulness of a wet adhesive system that would promote sticking abilities on smooth substrata can be illustrated when considering the substrate preferences in frogs from all three species (**Figure A6.2**). In all three species, frogs exhibit a tendency to choose leaves as resting surfaces within their enclosure, though this tendency is lesser in *P. trinitatis*, which exhibits the highest incidence of branch use whilst sleeping (**Figure A6.2 c**).

Of the frogs that are found sleeping on leaves, there is a distinct preference in all three species for the upperside of the leaves (**Table A.6.1**). *H. geographica* froglets exhibit a greater tendency to rest at angles beyond the vertical when on leaves, independent of the side that they are found on, though the degree to which this is the case is most pronounced on the underside of leaves. In *H. crepitans* this is only the case in the third of frogs seen resting on the underside of the leaves (**Table A6.1**), which is not surprising as by being the undersides of the leaves these surfaces are likely to be at orientations tending towards 180°. Nevertheless the significance of this is of some interest if the environmental conditions that are being experienced by the frogs in the different enclosures are considered (**Figure A6.3**).

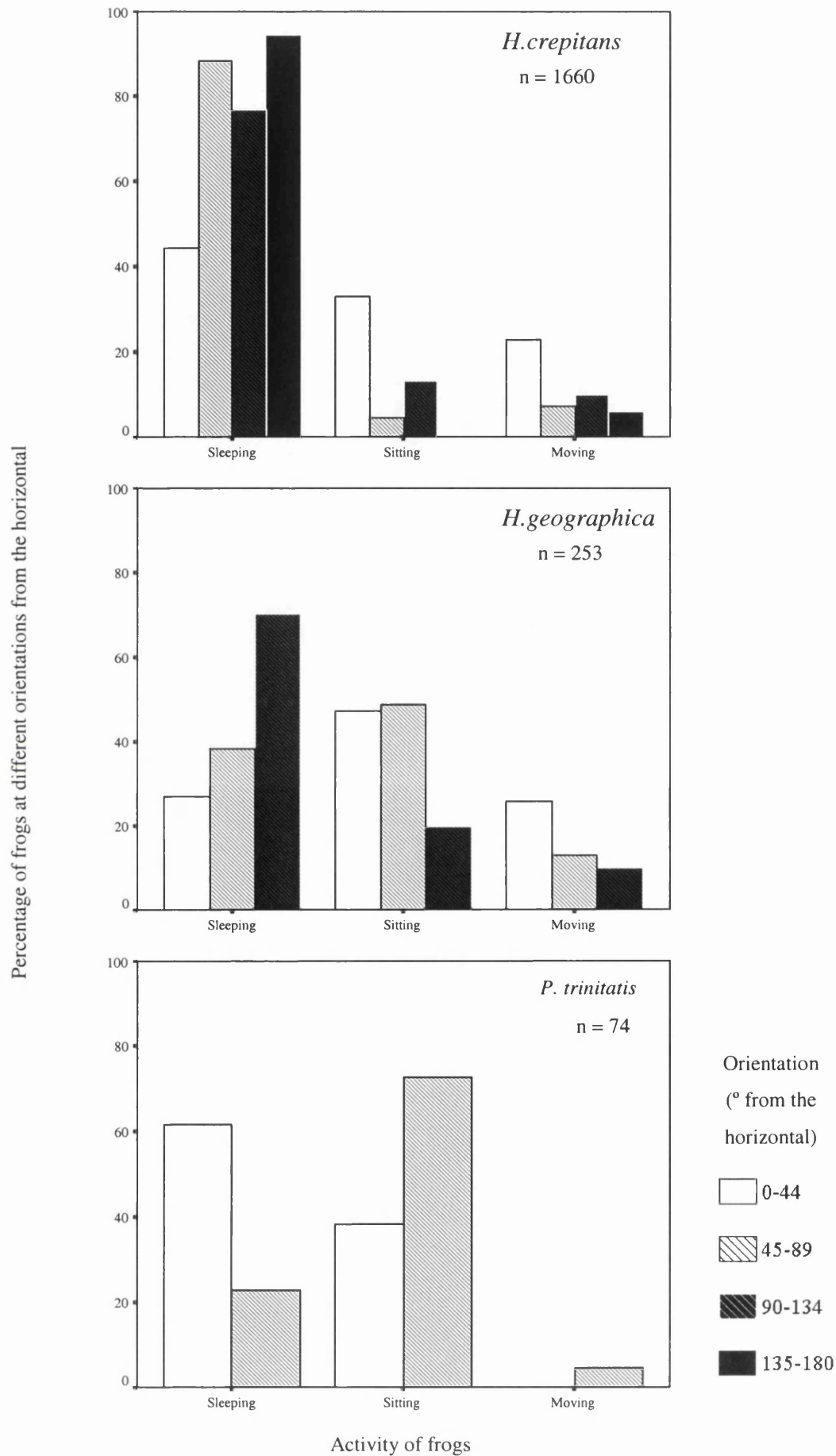


Figure A6.1: Bar charts illustrating distribution of activity observations from both day and night time observations of juvenile frogs from three different species of hyliid according to their orientation from the horizontal.

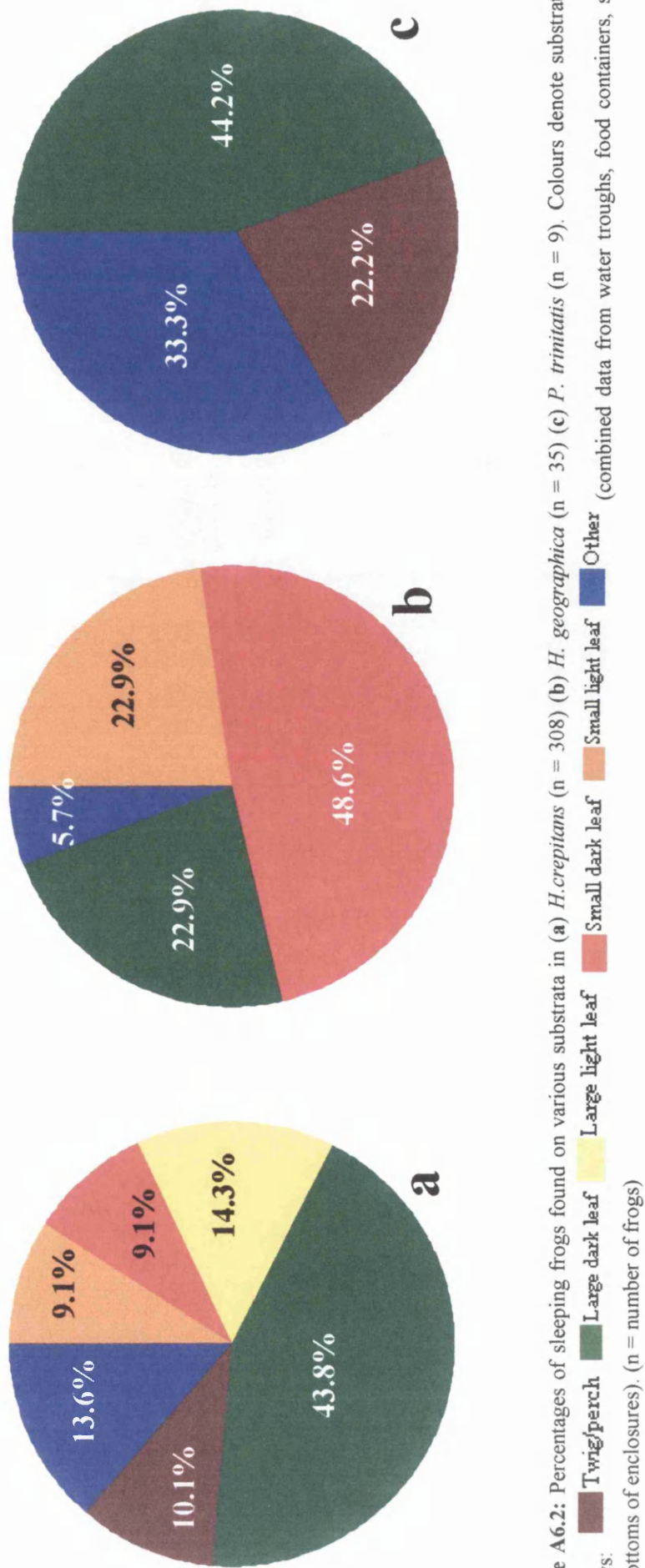


Figure A6.2: Percentages of sleeping frogs found on various substrata in (a) *H. crepitans* (n = 308) (b) *H. geographica* (n = 35) (c) *P. trinitatis* (n = 9). Colours denote substrata as follows: **Large dark leaf** (dark green) **Small dark leaf** (dark blue) **Small light leaf** (light blue) **Large light leaf** (yellow) **Other** (red) (combined data from water troughs, food containers, sides and bottoms of enclosures). (n = number of frogs)

Species	Number of frogs observed on leaf ...									
	Upper side					Under side				
	0-44	45-89	90-134	135-180	Total	0-44	45-89	90-134	135-180	Total
<i>H. crepitans</i>	77	64	24	1	166	5	4	56	5	70
<i>H. geographica</i>	8	4	16	-	28	1	-	6	-	7
<i>P. trinitatis</i>	3	1	-	-	4	-	-	-	-	-

Table A6.1: Numbers of sleeping juvenile frogs from three species of hylid observed on uppersides and undersides of leaves with respect to their orientation from the horizontal.

Figure A6.3 shows that there is a significant effect of increasing temperature on the angle relative to the horizontal seen in juvenile *H.crepitans* resting on leaf surfaces during sleep. Also of some significance is the finding that the incidences of froglets utilising the undersides of leaves are all recorded at higher temperatures during the day and that high temperatures are negatively correlated with percentage humidity (**Figure A6.4**). This is particularly interesting as there is some evidence that tree frogs resting on the underside of leaves exhibit a lower degree of water loss than those on waxy upper sides or on non-biological surfaces (J.R. Downie pers.comm) and microhabitat selection is well documented as a water conservation strategy in a number of species of frog (Hillyard, 1999).

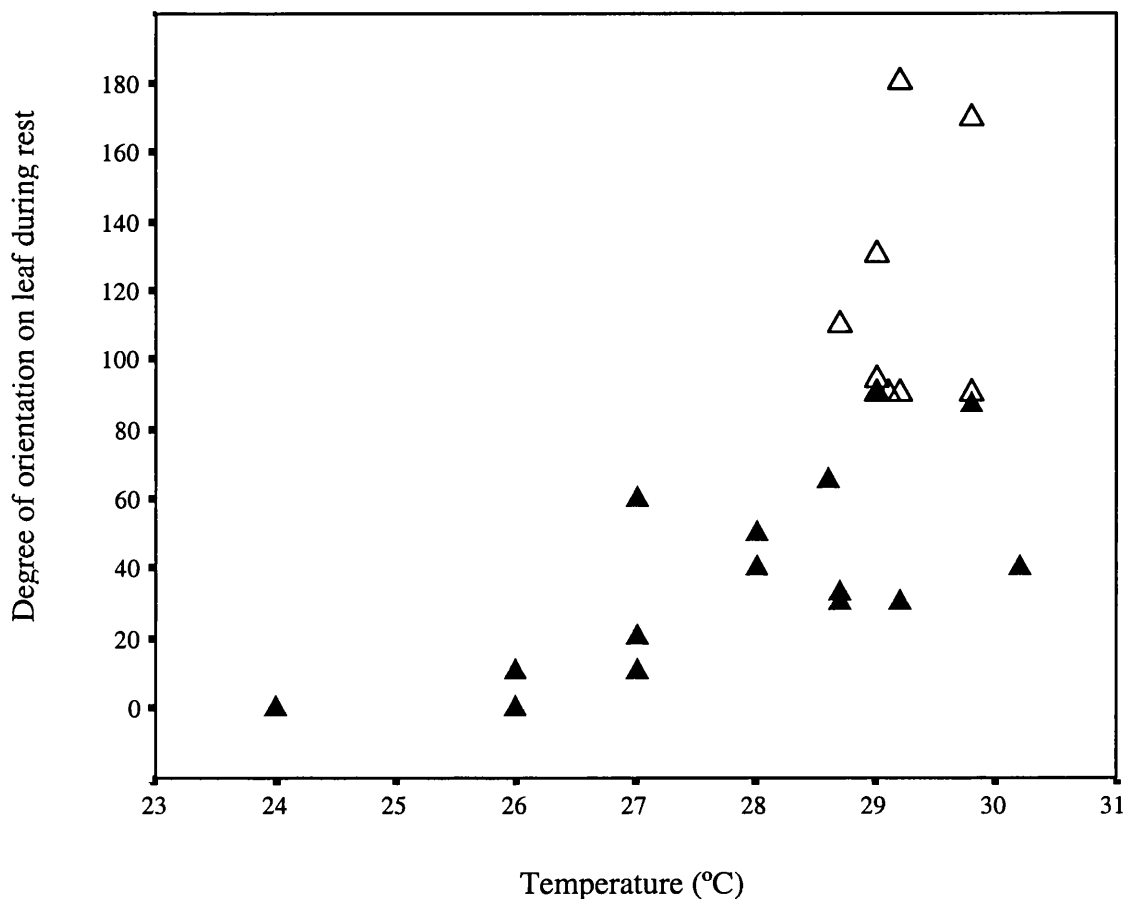


Figure A6.3: Degree of orientation from horizontal of sleeping juvenile *H.crepitans* on leaf surfaces relative to increasing temperature. Correlative statistics; $r = 0.66$, $t = 4.48$, $p < 0.001$, $n = 28$. ▲ Upper side △ Under side

Temperatures in Trinidad are, on average, higher than those in lab conditions in Glasgow and humidity is lower (**Table A6.2**) so *H. geographica* and *P. trinitatis* are likely to be subject to more drying conditions than are juveniles in laboratory enclosures in Glasgow. This makes the lack of any correlative relationship between humidity/temperature and the tendency to utilise undersides of leaves in the frogs in Trinidad is therefore somewhat surprising if the function is osmoregulative. The reason that such a trend is not in evidence in the case of *P. trinitatis*, may be due to characteristics of skin structure. *P. trinitatis*, like all Phyllomedusines, has a waterproof coating of waxes and lipids over the skin which allows the frogs to withstand unusually dehydrating conditions (McClanahan & Shoemaker, 1987). This is not, however, the case in *H. geographica*.

H. geographica show a strong tendency towards a decrease in perch height during the day with increasing temperature (**Figure A6.5**), which is not seen in *H. crepitans*. Indeed, if anything the trend in *H. crepitans* is opposite, with juveniles selecting higher perches with temperature, though the correlative relationship is weak (**Figure A6.5**). This is significant to considerations of water balance as height is a measure of the distance from the water containers that comprise half of the enclosure floor. *H. geographica* froglets show a lesser ability to adhere on smooth surfaces than do *H. crepitans* (**Chapter 5**), so it may be that they are unable to utilise the under-surfaces of leaves as humid refuges in increasing temperature. Instead, it may be that *H. geographica* select lower perches in the enclosure, closer to the water surfaces where it is likely there are some differences in humidity. At both the Damier River and at Guanapo where the tadpoles of this species were collected, juvenile froglets were regularly found on low shrubs overhanging the riverbanks.

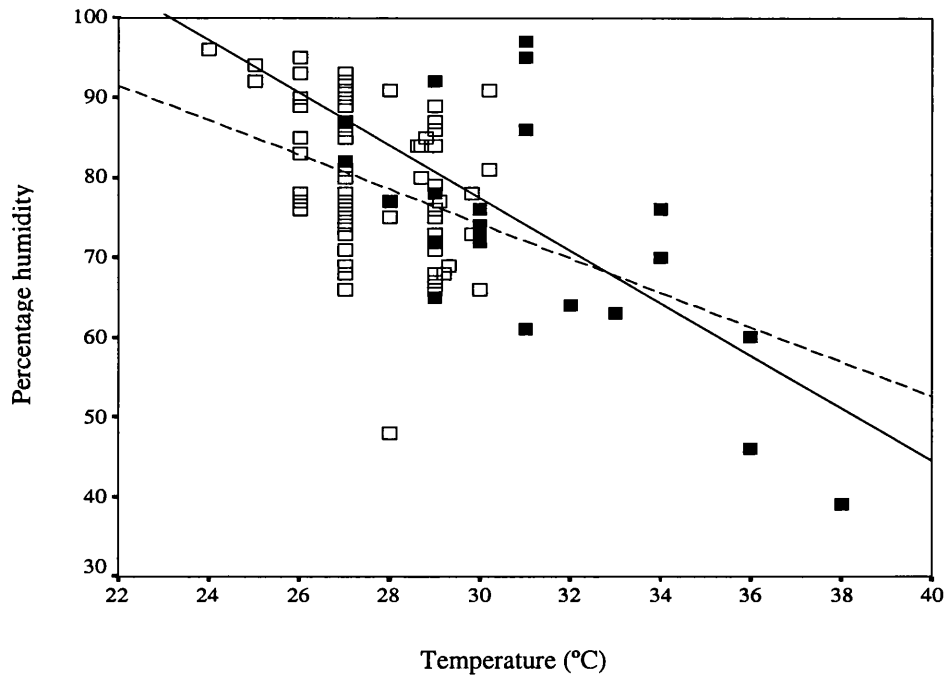


Figure A6.4: Daytime temperatures vs. humidity in enclosures in Glasgow (□) and Trinidad (■).

Correlative statistics for: Glasgow, $r = 0.32$, $--- y = 139.00x - 2.16x$, $t = -3.10$, $p < 0.003$, $n = 82$; Trinidad: $r = 0.64$, $— y = 176.07 - 3.29x$, $t = -3.91$, $p < 0.001$, $n = 23$. t-statistic for difference between slopes of lines of best fit = 1.04, N.S. 103 d.f.

Site	Percentage humidity		Temperature (°C)		n
	Mean	s.e.	Mean	s.e.	
Trinidad	73.83	2.96	31.08	0.58	24
Glasgow	79.66	1.01	27.48	0.15	82

Table A6.2: Average daytime humidity and temperature readings in enclosures in Trinidad and Glasgow. Statistical differences are performed on medians due to differences in variances: Humidity (Levene's test $F_{82,24} = 26.05$) Mann-Whitney $U_{81,23} = 730$, $p = 0.05$; Temperature (Levene's test $F_{82,24} = 14.76$) Mann-Whitney $U_{81,23} = 199$, $p < 0.01$.

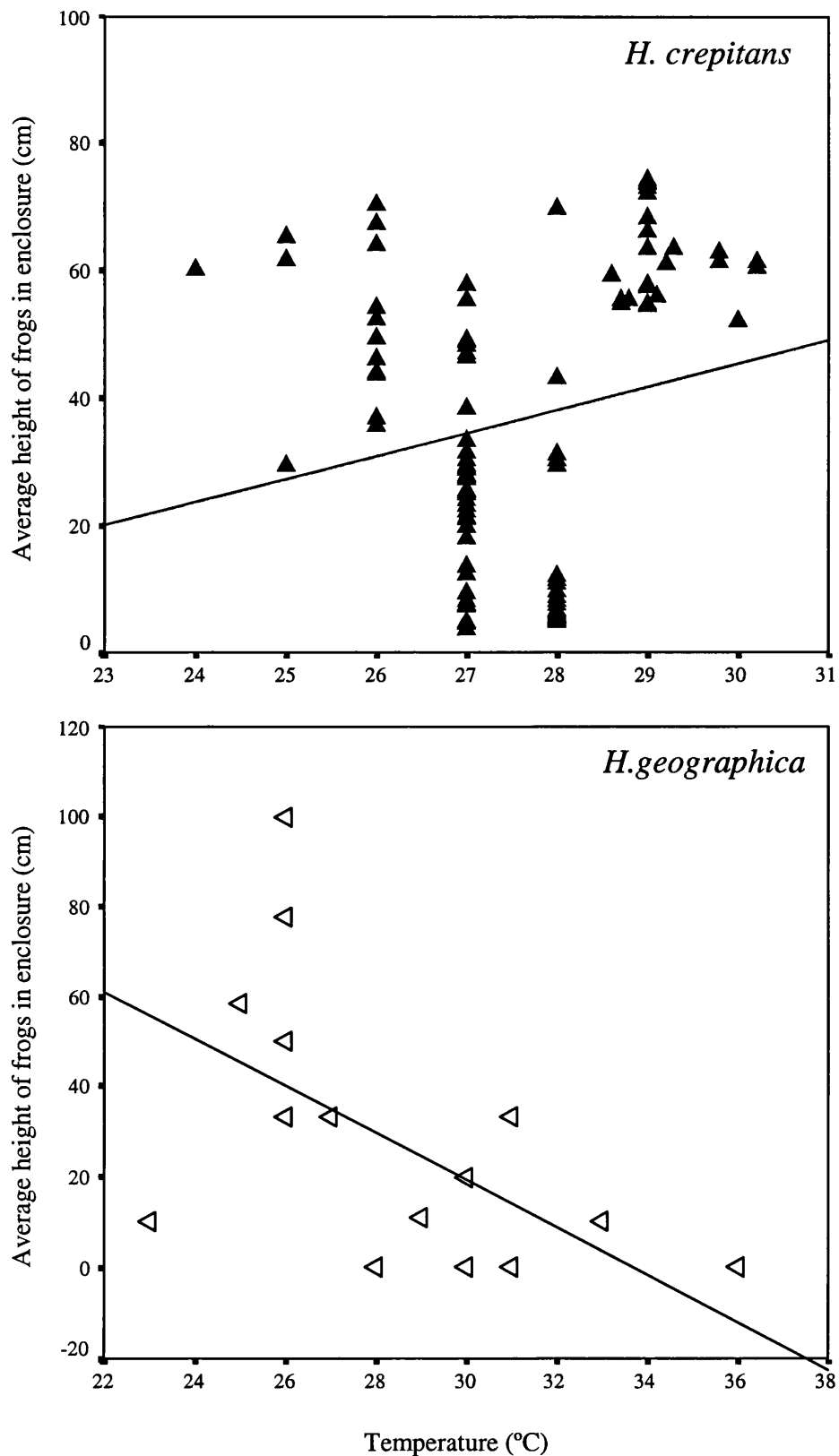


Figure A6.5: Temperature effects on average perch heights in groups of *H. geographica* and *H. crepitans* within enclosures in Glasgow and Trinidad. Correlative statistics: *H. crepitans*, $r = 0.18$, $y = 3.61x - 62.84$, $t = 2.02$, $p < 0.05$, $n = 118$; *H. geographica*, $r = 0.57$, $y = 175.86 - 5.22x$, $t = -2.68$, $p < 0.02$, $n = 16$.

As adults, *H. crepitans* are remarkable in their habit of basking in the open (Murphy, 1997; Kenny, 1979) undergoing spectacular changes of colour from dark-orangey brown during the night when they are active to an ashy white during the day. There is no

Colour	Distance from ground		
	Average	s.e.	n
White/green	71.29	1.89	107
Yellow/green	48.37	3.58	82
Olive/green	48.09	4.17	45
Blue/green	24.50	-	1

Table A6.3: Average distances from the ground in juvenile *H. crepitans* sleeping on leaves according to skin colour.

literature about similar behaviour in juveniles, but there is a tendency in lighter coloured frogs towards higher perch heights (**Table A6.3:** ANOVA: $F_{235,3} = 15.38$, $p < 0.001$).

If *H. crepitans* do utilise higher perches with increasing temperature and are thermoregulating by ‘basking’ and osmoregulating by selecting the undersides of leaves at these heights the finding in earlier chapters that the juveniles of this species exhibit higher angles of detachment on the rotation platforms in comparison to the other two species (**Chapters 5 and 6**) may be a significant clue as to the function of adhesion in this species. Increased ability to adhere to smooth surfaces at angles beyond the vertical may allow frogs to hydoregulate without the need to move lower down and closer to water sources (*H. geographica*) or to develop skin waxes (*P. trinitatis*) both of which may well be costly in terms of resource allocation. To test these theories it will be of interest to determine the amounts of water produced by transpiring leaves and whether these amounts would be significant enough to create a choice effect on the frogs in the period of time that they spend ‘sleeping’ on the leaves during the day.

There are however, a number of problems involved with captivity studies of behaviour in these juvenile tree frogs. In all of these instances due to restrictions in availability of froglets, statistical analyses have had to assume that observations of frogs on different days are independent from one another on a day to basis: on a single day if a frog was recorded in the same position from hour to hour then only the original observation of that frog was considered in the analyses but on a daily basis it may well be that individual frogs have a preference for particular perch sites. Certainly, juvenile *P. trinitatis* in laboratory conditions had such high levels of perch fidelity that behavioural studies of these frogs in Glasgow yielded little variation in substrate preferences, being found perched on the same twig day after day; adult *P. trinitatis* visiting breeding ponds also appear to exhibit some degree of site fidelity (Johnson, 2001). The assumption that observations of the same individuals from day to day are independent is, therefore, somewhat questionable and a degree of pseudoreplication cannot be excluded from the consideration of the results. Analysis also assumes that the decision of one individual is uninfluenced by the decision of others, which in the case where twenty individual froglets in an enclosure of a cubic metre are competing for water and food is unlikely to be the case. Furthermore, laboratory conditions and enclosures are unlikely to provide the complexity of choices that are available to a young frog under natural conditions, particularly with respect to weather. Whilst the findings here point the way towards some questions that should be answered to illuminate aspects of the function of adhesion in tree frogs, it is essential that in the future some way of assessing more natural behaviour is found in order to gain a better understanding of the interrelationships between environmental factors, substrate choice and adhesion.

References

- Ahnelt, P.K. (1998) The photoreceptor mosaic. *Eye*, 12: 531-540.
- Ahnelt, P.K. (2003) Organization of the foveal cone mosaic. *Internet source* <http://www.univie.ac.at/Vergl-Physiologie/doc/ret-fovea.html>. Accessed June 2003.
- Aiken, R.B. and Khan, A. (1992) The adhesive strength of the palettes of a boreal water beetle, *Dytiscus alaskanus*. *Canadian Journal of Zoology* 70 (7): 1321-1324.
- Alberch, B. (1981) Convergence and parallelism in foot evolution in the Neotropical salamander genus *Bolitoglossa* I. Function. *Evolution* 35: 84-100.
- Attenborough, D. (2002) The life of mammals. *BBC Books, U.K.*
- Attygalle, A.B.; Aneshanley, D.J.; Meinwald, J. and Eisner, T. (2000) Defence by foot adhesion in a Chrysomelid beetle (*Hemisphaerota cyanea*): characterization of the adhesive oil. *Zoology - Analysis of Complex Systems* 103: 1-6.
- Autumn, K. and Peattie, A. (2002) Mechanisms of adhesion in geckos. *Integrative and Comparative Biology* 42: 1081–1090.
- Autumn, K.; Liang, Y.A.; Hsleh, S.T.; Zesch, W.; Chan, W.P.; Kenny, T.W.; Fearing, R. and Full, R.J. (2000) Adhesive force of a single gecko foot-hair. *Nature* 405: 681-684.
- Baier, R.E. and Taylor, A (1970) Surface properties influencing biological adhesion. In *Adhesion in biological systems* R.S. Manley (ed.) Academic Press, New York p 15-48.
- Baier, R.E.; Shafrin, E.G. and Zhisman W.A. (1968) Adhesion: mechanisms that assist or impede it. *Science* 162: 1360-1368.

- Ba-Omar, T.A.; Downie, J.R. and Barnes, W.J.P. (2000) Development of adhesive toe-pads in the tree frog (*Phyllomedusa trinitatis*). *Journal of Zoology* 250: 267-282.
- Barnes, W.J.P. (1997) Mechanisms of adhesion in tree frogs: an allometric study. *Journal of Morphology* 232: 232.
- Barnes, W.J.P. (1999) Tree frogs and tire technology. *Tire Technology International* March: 42-46.
- Barnes, W.J.P.; Smith, J.; Oines, C. and Mundl, R. (2002) Bionics and wet grip. *Tire Technology International* December 2002: 56-60.
- Bauer, A.M. (1998) Morphology of the adhesive tail-tips of carphodactylid geckos (Reptilia; Diplodactylidae). *Journal of Morphology* 235: 41-58.
- Bausch, C. (2001) Measurements of components of wet adhesion on the toe pads of the tree frog *Phrynosoma macleayi*. *Unpublished honours project* 75 pp.
- Behler, J. and King, F.W. (1997) National Audubon Society Field Guide to North American Reptiles and Amphibians. *Chanticleer Press Inc., New York*. 404-405.
- Berra, T.M. and Humphrey, J.D. (2002) Gross anatomy and histology of the hook and skin of forehead brooding male nursery fish, *Kurtus gulliveri*, from northern Australia. *Environmental Biology of Fishes* 65 (3): 263-270.
- Betz, O. (2002). Performance and adaptive value of tarsal morphology in rove beetles of the genus *Stenus* (Coleoptera, Staphylinidae). *Journal of Experimental Biology* 205 (8): 1097-1113.
- Betz, O. (2003) Structure of the tarsi in some *Stenus* species (Coleoptera, Staphylinidae): External morphology, ultrastructure, and tarsal secretion. *Journal of Morphology* 255 (1): 24-43.

- Beutel, R.G. and Gorb, S.N. (2001) Ultrastructure of attachment specializations of hexapods, (Arthropoda): evolutionary patterns inferred from a revised ordinal phylogeny. *Journal of Zoological Systematics and Evolutionary Research* 39 (4) 177-207
- Blacker, R.W. (1983) Pelagic records of the lumpsucker, *Cyclopterus lumpus*. *Journal of Fish Biology* 23: 405-417.
- Blaylock, L.A.; Ruibal, R. and Platt-Aloia, K. (1976) Skin structure and wiping behaviour of phyllomedusine frogs. *Copeia* 1976: 283-295.
- Bourne, G.R. (1992) Lekking behaviour in the Neotropical frog *Ololygon rubra*. *Behavioural Ecology and Sociobiology* 31: 173-180.
- Buchanan, B.W. and Taylor, R.C. (1996) Lightening the load: Micturition enhances jumping performance of squirrel tree frogs. *Journal of Herpetology* 30(3): 410-413.
- Buchmann, K.; Lindenstrom, T. (2002) Interactions between monogenean parasites and their fish hosts. *International Journal for Parasitology* 32: 309-319.
- Budgett, H.M. (1911) The adherence of flat surfaces. *Proceedings of the Royal Society* A86: 25-35.
- Burton, T.C. (1996) Adaptation and evolution in the hand muscles of Australo-Papuan hylid frogs (Anura: Hylidae: Pelodryadinae). *Australian Journal of Zoology* 44: 611-623.
- Burton, T.C. (1998) Are the Distal Extensor Muscles of the Fingers of Anurans an Adaptation to Arboreality? *Journal of Herpetology* 32 (4): 611-617.
- Caldwell, J.P. (1989) Structure and behaviour of *Hyla geographica* tadpole schools, with comments on classification of group behaviour in tadpoles. *Copeia* 1989: 938-950.

- Calkins, K.G. (2003) A Review of Basic Geometry. <http://www.andrews.edu/~calkins/math/webtexts>. Last accessed July 2003.
- Callow M.E. and Callow J.A. (2002) Marine biofouling: a sticky problem. *The Biologist* 49: 10-14.
- Cartmill, M (1979) The volar skin of primates: its frictional characteristics and their functional significance. *American Journal of Physical Anthropology* 50: 497-510.
- Cartmill, M. (1985) Climbing. in *Functional Vertebrate Morphology* (Ed. Hildebrand et al.) *Harvard University Press, London*. p 73-88.
- Choi, I-H.; Shim, J.H.; Lee, Y.S. and Ricklefs, R.E. (2000) Scaling of jumping performance in anuran amphibians. *Journal of Herpetology* 34 (2): 222-227.
- Christian, K. and D. Parry (1997). Reduced rates of water loss and chemical properties of skin secretions of the frogs *Litoria caerulea* and *Cyclorana australis*. *Australian Journal of Zoology* 45(1): 13-20.
- Conant, R., and J. T. Collins. (1998) A Field Guide to Reptiles and Amphibians. Eastern and Central North America. *Third Edition, Expanded*. *Houghton Mifflin Company, Boston*. 616 pp.
- Conway, J. H. and Sloane, N.J.A. (1993) Sphere packings, lattices, and groups. *2nd ed. New York: Springer-Verlag*.
- Dai, Z.D.; Gorb, S.N. and Schwarz, U. (2002) Roughness-dependent friction force of the tarsal claw system in the beetle *Pachnoda marginata* (Coleoptera, Scarabaeidae). *Journal of Experimental Biology*. 205 (16): 2479-2488.
- Dapson, R. W. (1970) Histochemistry of mucus in the skin of the frog, *Rana pipiens*. *Anatomical Records* 166: 615-626.

- Daugherty, C.H. and Sheldon, A.L. (1982) Age-specific movement patterns of the frog *Ascaphus truei*. *Herpetologica* 38(4): 461-468.
- Davenport, J. and Thorsteinsson, V. (1990) Sucker action in the lumpsucker *Cyclopterus lumpus*, L. *Sarsia* 75 (1): 33-42.
- Delfino, G., Alvarez, B.B. and Brizzi, R.R. (1998) Serous cutaneous glands of Argentine *Phyllomedusa wagleri* 1830 (Anura: Hylidae): Secretory polymorphism and adaptive plasticity. *Tropical Zoology* 11(2): 333-351.
- DeNeuille, E.; Perrot-Minot, C.; Pennaforte, F.; Roussey, M.; Zahm, J-M.; Clavel, C.; Puchelle, E. and de Bentzmann, S. (1997) Revisited physicochemical and transport properties of respiratory Mucus in genotyped cystic fibrosis patients. *American Journal of Respiratory Critical Care Medicine* 156 (1): 166-172.
- Denny, M.W. (1993) Air and water: the biology and physics of life's media. *Princeton University Press, Princeton*.
- Denny, M.W. (2000) Limits to optimisation: Fluid dynamics, adhesive strength and the evolution of shape in limpet shells. *Journal of Experimental Biology* 203: 2603-2622.
- Denny, M.W. (1984) Mechanical properties of pedal mucus and their consequences for gastropod structure and performance. *American Zoologist* 24: 23-36.
- Denny, M.W. and Gosline, J.M. (1980) The physical properties of the pedal mucus of the terrestrial slug, *Ariolimax columbianus*. *Journal of Experimental Biology* 88: 375-393.
- Deyrup-Olsen, I. and Jindrova, H. (1996) Product release by mucous granules of land slugs: *Ariolimax columbianus* as a model species. *Journal of Experimental Zoology* 276 (6): 387-393.

- Deyrup-Olsen, I.; Luchtel, D. L. and Martin, A. W. (1983) Components of mucus of terrestrial slugs (Gastropoda). *American Journal of Physiology* 245(3): 448-452.
- Deyrup-Olsen, I.; Luchtel, D. L. and Martin, A. W. (1988). Mucus secretion by the skin of the land slug, *Ariolimax columbianus*. *Journal of General Physiology* 92(6): A37-A38.
- Dixon A.F.G.; Croghan, P.C. and Gowing R.P. (1990) The mechanism by which aphids adhere to smooth surfaces. *Journal of Experimental Biology* 152: 243-253.
- Dorst, J. and Dandelot, P. (1980) A field guide to the larger mammals of Africa. 4th Edition. *William Collins Sons and Co. Glasgow, U.K.*
- Downie, J.R.; Smith, J.M. and Bryce, R. (2003) Metamorphosis in anurans: an understudied variable. (Submitted)
- Duellman, W. and Trueb, L. (1997) Biology of amphibians. 2nd Edition. *John Hopkins University Press. Baltimore, U.S.A.*
- Duellman, W.E. (1968) The genera of Phyllomedusine Frogs (Anura: Hylidae) *University of Kansas Museum of Natural History* 18 (1): 1-10.
- Duellman, W.E. (1973) Frogs of the *Hyla geographica* group. *Copeia* 3: 515-533.
- Duellman, W.E. (2001) Hylid Frogs of Middle America. (First edition). *Society for the Study of Amphibians and Reptiles. Publications of the Natural History Museum of the University of Kansas, U.S.A.*
- Duellman, W.E. (1956) The frogs of the hylid genus, *Phrynohyas* Fitzinger 1843. *Miscellaneous Publications of the Museum of Zoology of the University of Michigan* 96: 1-47.

- Duellman, W.E. and Gray, P. (1983) Developmental biology and systematics of the egg-brooding hylid frogs, genera *Flectonotus* and *Fritziana*. *Herpetologica* 39: 333-359.
- Eigenbrode, S.D. and Jetter, R. (2002) Attachment to plant surface waxes by an insect predator, *H. convergens*. *Integrative and Comparative Biology* 42: 1091–1099.
- Eisner, T. and Aneshansley, D.J. (2000) Defence by foot adhesion in a beetle (*Hemisphaerota cyanea*). *Proceedings of the National Academy of Sciences of the United States of America* 97 (12): 6568-6573.
- Ellem, G.K.; Furst, J.E. and Zimmerman, K.D. (2002) Shell clamping behaviour in the limpet *Cellana tramoserica*. *Journal of Experimental Biology* 205: 539-547.
- Emerson, S.B. (1978) Allometry and jumping in frogs: Helping the twain to meet. *Evolution* 32: 551-564.
- Emerson, S.B. and Diehl, D. (1980) Toe pad morphology and mechanisms of sticking in frogs. *Biological Journal of the Linnean Society* 13: 199-216.
- Emerson, S.B. and Koehl, M.A.R. (1990) The interaction of behavioural and morphological change in the evolution of a novel locomotor type: 'flying' frogs. *Evolution* 44: 1931-1946.
- EngNet® (2003) Units converter. *Internet source* <http://www.engnet.co.uk/> last accessed September 2003.
- Ernst, V.V. (1973a). The digital pads of the tree frog, *Hyla cinerea*. I. The epidermis. *Tissue and Cell* 5(1): 83-96.
- Ernst, V.V. (1973b). The digital pads of the tree frog, *Hyla cinerea*. II The mucous glands. *Tissue and Cell* 5(1): 97-104.

- Erspamer, V.; Falconieri-Erspamer, G; Severini, C.; Potenza, R.L.; Barra, D.; Mignogna, G. and Bianchi, A. (1993). Pharmacological studies of "sapo" from the frog *Phyllomedusa bicolor* skin: A drug used by the Peruvian Matses Indians in shamanic hunting practices. *Toxicon* 31: 1099-1111.
- Evans, C.M. and Brodie, E.D. (1994). Adhesive strength of amphibian skin secretions. *Journal of Herpetology* 28 (4): 499-502.
- Federle, W.; Brainerd, E.L.; McMahon, T.A. and Holldobler, B. (2001). Biomechanics of the movable pretarsal adhesive organ in ants and bees. *Proceedings of the National Academy of Sciences of the United States of America* 98(11): 6215-6220.
- Federle, W.; Maschwitz, U.; Fiala, B.; Riederer, M. and Holldobler, B. (1997) Slippery ant-plants and skilful climbers: selection and protection of specific ant partners by epicuticular wax blooms in *Macaranga* (Euphorbiaceae). *Oecologia* 112: 217-214.
- Federle, W.; Riehle, M.; Curtis, A. S. G. and Full, R. J. An (2002) An integrative study of insect adhesion: Mechanics and wet adhesion of pretarsal pads in ants. *Integrative and Comparative Biology* 42: 1100–1106.
- Federle, W.; Rohrseitz, K. and Holldobler, B. (2000) Attachment forces of ants measured with a centrifuge: better 'wax-runners' have a poorer attachment to a smooth surface. *Journal of Experimental Biology* 203: 505-512.
- Ferroni, S.E.N. (2000) A review on the occurrence of bioactive compounds in amphibian skin secretion. *Toxicon* 38 (4): 500-501.
- Feynman, R. P. (2002) The hidden fiveness in spheres. *Internet source* http://www.iitk.ac.in/infocell/Archive/dirnov2/science_fiveness.html. Last accessed July 2003.

- Flammang, P.; Ribesse, J. and Jangoux, M. (2002) Biomechanics of adhesion in sea cucumber Cuverian tubules (*Echinodermata, Holothuroidea*). *Integrative and Comparative Biology* 42 (6): 1107-1115.
- Flammang, P; Dermeulenaere, S. and Jangoux, M. (1994) The role of podial secretions in adhesion in two species of sea stars. *Biological Bulletins* 187 (1): 35-47.
- Fowler, J.; Cohen, L. and Jarvis, P. (1998) Practical statistics for Field Biology (2nd Edition). *John Wiley and Sons, U.K.*
- Frantsevich, L. and S. Gorb (2002). Arcus as a tensegrity structure in the arolium of wasps (Hymenoptera : Vespidae). *Zoology* 105(3): 225-237.
- Freitas, R.A. (1999) Nanomedicine, Volume I: Basic capabilities. *Internet source* <http://www.nanomedicine.com/NMI/8.2.3.html>. Last accessed August 2003.
- Fung, Y.C. (1981) Biomechanics: Mechanical properties of living tissues. *Springer-Verlag Berlin Heidelberg New York*.
- Gao, C. (1997) Theory of menisci and its applications. *Applied Physics Letters* 71: 1801-1803.
- Gillett, J.P. and Wigglesworth, V.B. (1932) The climbing apparatus of an insect, *Rhodnius prolixus*, (Hemiptera; Reduviidae). *Proceedings of the Royal Society Series (B)* 111: 364-375.
- Glossip, D. and Losos, J.B. (1997) Ecological correlates of number of sub digital lamellae in anoles. *Herpetologica* 53: 192-199.
- Goin *et al.* (1968) DNA and the evolution of the vertebrates. *American Midland Naturalist* 80(2): 289-298. <http://www.genomesize.com/amphibians.htm>. Last accessed July 2003.

- Goniakowska-Witalinska, L. and Kubiczek, U. (1998) The structure of the skin of the tree frog (*Hyla arborea arborea* L.). *Annals of Anatomy-Anatomischer Anzeiger* 180(3): 237-246.
- Gorb, E.V. and Gorb, S.N. (2002) Attachment ability of the beetle *Chrysolina fastuosa* on various plant surfaces. *Entomologia experimentalis et applicata*. 105 (1): 13 – 28.
- Gorb, SN (2001) Structural design and biomechanics of attachment devices in insects. *American Zoologist* 41 (6) 1459
- Gorb, S and Scherge, M (2000) Biological microtribology: anisotropy in frictional forces of orthopteran attachment pads reflects the ultrastructure of a highly deformable material. *Proceedings of the Royal Society Series B*. 267 (1449): 1239-1244.
- Gorb, S. N.; Beutel R. G.; Gorb, E. V.; Jiao, Y.; Kastner, V.; Niederegger, S.; Popov, V. L.; Scherge, M.; Schwarz, U. and Votsch, W. (2002) Structural design and biomechanics of friction-based releasable attachment devices in insects. *Integrative and Comparative Biology* 42 (6): 1127-1139.
- Gorb, S.; Gorb, E. and Kastner, V. (2001) Scale effects on the attachment pads and friction forces in Syrphid flies (Diptera, Syrphidae). *Journal of Experimental Biology* 204: 1421-1431.
- Gorb, S.N. (1998) The design of the fly adhesive pad: distal tenent setae are adapted to the delivery of an adhesive secretion. *Proceedings of the Royal Society of London: Series B*. 265 (1398): 747-752.
- Gosner, H.L. (1962) A simplified table for staging anuran embryos and larvae with notes on identification. *Herpetologica* 16: 183-190.
- Gradwell, N. (1973) On the functional morphology of suction and gill irrigation in the tadpole of *Ascaphus* and notes on hibernation. *Herpetologica* 29: 84-93.

- Green, D.M. (1979) Tree frog toe pads: comparative surface morphology using scanning electron microscopy. *Canadian Journal of Zoology* 57: 2033-2046.
- Green, D.M. (1980) Size differences in adhesive toe-pad cells of tree frogs of the diploid-polyploid *Hyla versicolor* complex. *Journal of Herpetology* 14: 15-19.
- Green, D.M. (1981a) Adhesion and the toe-pads of tree frogs. *Copeia* 1981: 790-796.
- Green, D.M. and Alberch, P. (1981b) Interdigital webbing and skin morphology in the Neotropical salamander genus *Bolitoglossa*. *Journal of Morphology* 170: 273-282.
- Green, D.M. and Barber, D.L. (1988) The ventral adhesive disc of the clingfish, *Gobiesox maeandricus*: integumental structure and adhesive mechanisms. *Canadian Journal of Zoology* 66: 1610-1619.
- Green, D.M. and Carson, J. (1988) The adhesion of tree frog toe pads to glass: a cryogenic examination of a capillary adhesion system. *Journal of Natural History* 22: 131-135.
- Green, D.M. and Simon, P. (1986) Digital microstructure in ecologically diverse microhylid frogs genera *Cophixalus* and *Sphenophryne* (Amphibia: Anura) from Papua New Guinea. *Australian Journal of Zoology* 34: 135-145.
- Gregory, T.R. (2001). Animal Genome Size Database. Internet source <http://www.genomesize.com>. Last accessed August 2003.
- Grenon, J.F. and Walker, G. (1981) The tenacity of the limpet, *Patella vulgata* L., an experimental approach. *Journal of Experimental Marine Biology and Ecology* 54: 277-308.
- Haddad, C.F.B. (1991) Satellite behaviour in the neotropical tree frog *Hyla minuta*. *Journal of Herpetology* 25 (2): 226-229.

- Haddad, C.F.B.; Pombal, J.P. and Batistic, R.F. (1994) Natural hybridization between diploid and tetraploid species of leaf-frogs, Genus *Phyllomedusa* (Amphibia). *Journal of Herpetology* 28: 425-430.
- Häffner, M. (1998) A comparison of the gross morphology and micro-anatomy of the foot pads in two fossorial and two climbing rodents (Mammalia). *Journal of Zoology* 244: 287-294.
- Hamrick, M.W. (1998) Functional and adaptive significance of primate pads and claws: Evidence from New World anthropoids. *American Journal of Physical Anthropology* 106(2): 113-127.
- Hamrick, M.W. (2001) Morphological diversity in digital skin microstructure of didelphid marsupials. *Journal of Anatomy* 198 (6): 683-688.
- Hamwood T.E., Cribb B.W., Halliday J.A., Kearn G.C. and Whittington I.D. (2002) Preliminary characterisation and extraction of anterior adhesive secretion in monogenean (Platyhelminth) parasites. *Folia Parasitologica* 49 (1): 39-49.
- Hanna, G. and Barnes, W.J.P. (1991) Adhesion and detachment of the toe pads of tree frogs. *Journal of Experimental Biology* 155: 103-125.
- Hermans, C.O. (1983) The duo-gland adhesive system. *Oceanography and Marine Biology* 21: 283-339.
- Herrel, A.; Meyers, J.J.; Aerts, P. and Nishikawa, K.C. (2000) The mechanics of prey prehension in chameleons. *Journal of Experimental Biology* 203 (21): 3255-3263.
- Hertwig, I. and Sinsch, U. (1995) Comparative toe pad morphology in marsupial frogs (genus *Gastrotheca*): arboreal versus ground-dwelling species. *Copeia* 1: 38-47.
- Hiller, U. (1975) Comparative studies on the functional morphology of two gekkonid lizards. *Journal of the Bombay Natural History Society* 73: 278-282.

- Hillyard, S.D. (1999) Behavioural, molecular and integrative mechanisms of amphibian osmoregulation. *Journal of Experimental Zoology* 283: 662-674.
- Holmes S.P.; Cherrill A. and Davies M.S. (2002) The surface characteristics of pedal mucus: a potential aid to the settlement of marine organisms? *Journal of the Marine Biological Association* 82(1): 131-139.
- Hora, S.L. (1923) The adhesive apparatus on the toes of certain geckos and treefrogs. *Journal of the Asiatic Society of Bengal* 19: 137-145.
- Hora, S.L. (1930) Ecology, bionomics and evolution of the torrential fauna with special reference to the organs of attachment. *Philosophical Transactions of the Royal Society of London Series B* 218: 171-282.
- Inger, R.F. (1967) The development of a phylogeny of frogs. *Evolution*. 21: 369-384.
- Irschick, D.J., Austin, C.C., Petren, K., Fisher, R.N., Losos, J.B. and Ellers, O. (1996) A comparative analysis of clinging ability among pad-bearing lizards. *Biological Journal of the Linnean Society* 59: 21-35.
- Jagota, A. and Bennison, S.J. (2002) Mechanics of adhesion through a fibrillar microstructure. *Integrative and Comparative Biology* 42: 1140-1145.
- Janzen, D.H. (1962) Injury caused by toxic secretions of *Phrynohyas spilomma* Cope. *Copeia* 1962: 651.
- Jiao, Y; Gorb, S. and Scherge, M. (2000) Adhesion measured on the attachment pads of *Tettigonia viridissima* (Orthoptera; Insecta). *Journal of Experimental Biology* 203 (12): 1887-1895.
- Johnson, R. (2001). Investigating courtship/mating behaviour in *Phyllomedusa trinitatis*. Unpublished honours project.

- Kenmuir, D. and Williams, R. (1985) Bundu series: Wild mammals. 4th edition. *Longman, Zimbabwe*.
- Kenny, J.S. (1966) Nest building in *Phyllomedusa trinitatis* Mertens. *Caribbean Journal of Science* 6: 1-2.
- Kenny, J.S. (1969) The Amphibia of Trinidad. *Studies on the fauna of Curacao and other Caribbean islands* 103: 1-77.
- Kenny, J.S. (1977) The Amphibia of Trinidad: an addendum. *Studies on the fauna of Curacao and other Caribbean islands* 169: 92-95.
- Kier, W.M. and Smith, A.M. (1990) The morphology and mechanics of octopus suckers. *Biological Bulletins* 178 (2): 126-136.
- Kurabuchi, S. (1994) Fine structures on the surface of nuptial pads of male hylid and rhacophorid frogs. *Journal of Morphology* 219: 173-182.
- Kurabuchi, S. (1993) Fine structure of nuptial pad surface of male ranid frogs. *Tissue Cell* 25: 589-598.
- Lauff, R.F.; Russell, A.P. and Bauer, A.M. (1993) Topography of the digital sensilla of the tokay gecko, *Gekko gecko* (Reptilia, Gekkonidae), and their potential role in locomotion. *Canadian Journal of Zoology* 71: 2462-2472.
- Leary, C.J. and Razafindratsita, V.R. (1998) Attempted predation on a hylid frog, *Phrynohyas venulosa*, by an indigo snake, *Drymarchon corais*, and the response of conspecific frogs to distress calls. *Amphibia-Reptilia* 19: 442-446.
- Lees, A.M. and Hardie J. (1988) The organs of adhesion in the aphid *Megoura viciae*. *Journal of Experimental Biology* 136: 209-228.

- Linsenmair, K.E.; Rosenberg, M. and Warburg, M.R. (1999) Unusual cell ultrastructure in ventral epidermis of the African reed frog *Hyperolius viridiflavus*, (Anura; Hyperoliidae). *Anatomical Embryology* 200: 607-614.
- Losos, J.B. and Irschick, D.J. (1996) The effect of perch diameter on escape behaviour of anolis lizards: laboratory predictions and field tests. *Animal Behaviour* 51: 593-602.
- Luchtel, D. L.; I. Deyrup-Olsen, and Martin, A. W. (1991). Ultrastructure and lysis of mucin-containing granules in epidermal secretions of the terrestrial slug *Ariolimax columbianus* (Mollusca, Gastropoda, Pulmonata). *Cell and Tissue Research* 266(2): 375-383.
- Lutz, B. (1960) Fighting and an incipient notion of territoriality in male tree frogs. *Copeia* 1960: 61-63.
- Mack, D.R.; Neumann, A.W.; Policova, Z. and Sherman, P.M. (1994) Surface hydrophobicity properties of rabbit stomach in vitro. *Paediatric Research* 35: 209-213.
- Macrini, T.E.; Irschick, D.J. and Losos, J.B. (2003) Ecomorphological differences in toe pad characteristics between mainland and island anoles. *Journal of Herpetology* 37 (1): 52-58.
- Maderson, PFA (1964) Keratinized epidermal derivatives as an aid to climbing in lizards. *Nature* 203: 780-781.
- Magnusson, W.E.; Lima, A.P.; Hero, J.; de Araujo, M.C. (1999) The rise and fall of a population of *Hyla boans*: Reproduction in a neotropical gladiator frog. *Journal of Herpetology* 33(4): 647-656.
- Mason, G. J. C. (2001) Accessory adhesion mechanisms in the Cuban tree frog, *Osteopilus septentrionalis*. *Unpublished honours project*. 61 pp.

- Mattison, C. (1992) Frogs and toads of the world (2nd Edition). *Blandford Press, London*.
- McAllister A. and Channing (1983) Comparisons of toe pads of some Southern African climbing frogs. *South African Journal of Zoology* 18: 110-114.
- McCollum, J.M. (2000) Honeycombing the icosahedron and icosahedroning the sphere. *Proceedings of the Second Annual Forest Inventory and Analysis Symposium* 25-31.
- Mendelson, J.R.; Da Silva, H.R. and Maglia, A.M. (2000) Phylogenetic relationships among marsupial frog genera (Anura: Hylidae: Hemiphractinae) on evidence from morphology and natural history. *Zoological Journal of the Linnaean Society* 128: 125-148.
- Miller, S.L. (1974) Adaptive design of locomotion and foot form in prosobranch gastropods. *Journal of Experimental Marine Biology and Ecology* 14: 99-156.
- Muntz, W.R.A. and Wentworth, S.L. (1995) Structure of the adhesive surface of the digital tentacles of *Nautilus pompilius*. *Journal of the Marine Biological Association* 75: 747-750.
- Murphy, J.C. (1997) Amphibians and reptiles of Trinidad and Tobago. *Krieger Publishing, Florida*.
- Nachtigall, W (1974) Biological mechanisms of attachment. The comparative morphology and bioengineering of organs for linkage, suction and adhesion. *Springer-Verlag Berlin Heidelberg New York*.
- Niederegger, S.; Gorb, S. and Jiao, Y. (2002) Contact behaviour of tenent setae in attachment pads of the blowfly *Calliphora vicina* (Diptera, Calliphoridae). *Journal of Comparative Physiology A* 187: 961-970.

- Noble, G.K. and Jaeckle, M.E. (1928) The digital pads of the tree frogs. A study of the phylogenesis of an adaptive structure. *Journal of Morphology and Physiology* 45: 259-292.
- Ober, K. A. (2003). Arboreality and morphological evolution in ground beetles (Carabidae : Harpalinae): Testing the taxon pulse model. *Evolution* 57(6): 1343-1358.
- Ohler, A. (1995) Digital pad morphology in torrent-living Ranid frogs. *Asiatic Herpetological Research* 6: 85-96.
- Olmo, E. and Morescalchi, A. (1978) Genome and cell size in frogs: a comparison with salamanders. *Experientia* 34: 44-46 in Green (1980).
- Pellicer, J.; Garcia-Morales, V.; Guanter, L.; Hernandez, M.J. and Dolz, M. (2002) On the experimental values of the water surface tension used in some textbooks. *American Journal of Physics* 70 (7): 705-709.
- Peplowski, M.M. and Marsh, R.L. (1997) Work and output in the hindlimb muscles of Cuban tree frogs *Osteopilus septentrionalis* during jumping. *The Journal of Experimental Biology* 200: 2861-2870.
- Pombal, J.P.; Haddad, C.F.B. and Kasahara, S. (1997) A new species of *Scinax* (Anura: Hylidae) from South-Eastern Brazil, with comments on the Genus. *Journal of Herpetology* 29(1): 1-61.
- Pounds, JA (1991) Habitat structure and morphological patterns in arboreal vertebrates. *Habitat Structure: The Physical Arrangement of Objects in Space*. 109-119.
- Pum, D.; Ahnelt, P.K. and Grasl, M. (1990) Iso-orientation areas in the human foveal cone mosaic. *Journal of Visual Neuroscience*. 5:511-523.

- Ramsay, J.A.; Butler, C.G. and Sang, J.H. (1938) The humidity gradient at the surface of a transpiring leaf. *Journal of Experimental Biology* 88: 91-107.
- Raviv, U.; Laurat, P. and Klein, J. (2001) Fluidity of water confined to subnanometre films *Nature* 413: 51-54.
- Richards, C.M.; Carlson, B.M.; Connelly, T.G.; Rogers, S.L. and Ashcraft, E. (1978) A scanning electron microscopic study of differentiation of the digital pad in regenerating digits of the Kenyan reed frog, *Hyperolius viridiflavus ferniquei*. *Journal of Morphology* 153: 387-396.
- Riskin, D.K. and Fenton, M.B. (2001) Sticking ability and locomotion in Spix's disk-winged bat, *Thyroptera tricolor* (Microchiroptera: Thyropteridae). *Canadian Journal of Zoology* 79: 2261–2267.
- Rivero, J.A. (1969) A new name for *Sphaenorhynchus aurantiacus* (Daudin) (Amphibia, Salientia). *Copeia* 4: 700-703.
- Roberts (1971) The shear of thin liquid films. *Journal of Physics D: Applied Physics* 4: 433-440.
- Rosenberg, H.I. and Rose, R. (1999) Volar adhesive pads of the feathertail glider, *Acrobates pygmaeus* (Marsupalia; Acrobatidae). *Canadian Journal of Zoology* 77: 233-348.
- Rosenburg, M. and Warburg, M.R. (1994) Changes in structure and function of ventral epidermis in *Hyla arborea savignii* Aud. (Anura; Hylidae) throughout metamorphosis. *Acta Zoologica* 76: 217-227.
- Roth, LM; Willis ER (1952) Tarsal structure and the climbing ability of cockroaches. *Journal of Experimental Biology* 119: 483-517.

- Rovner, J.S. (1978) Adhesive hairs in spiders: behavioural functions and hydraulically mediated movement. *Symposium of the Zoological Society of London* 42: 99-108.
- Rudman, W.B. (2001). How sea slugs move. *Sea Slug Forum* <http://www.seaslugforum.net/locomotion.html>. Last accessed June 2003.
- Ruibal, R. and Ernst, V. (1965) The structure of the digital setae of lizards. *Journal of Morphology* 117: 271-294.
- Russell, A.P. (2002) Integrative functional morphology of the Gekkotan adhesive system (*Reptilia: Gekkota*). *Integrative and Comparative Biology* 42 (6): 1154-1163.
- Russell, A.P. (1975) A contribution to the functional analysis of the foot of the Tokay, *Gekko gekko*. *Journal of Zoology* 176: 437-476.
- Russell, A.P. (1979) Parallelism and integrated design in the foot structure of Gekkonine and Diplodactyline geckos. *Copeia* 1: 1-19.
- Russell, A.P. and Bels, V. (2001) Digital hyperextension in *Anolis sagrei*. *Herpetologica* 57(1): 58-65.
- Savage, Jay M. and W. Ronald Heyer. (1967) Variation and distribution in the tree-frog genus *Phyllomedusa*. *Beitraumlge zur Neotropischen Fauna*. 5 (2): 111-131.
- Scherge, M. and Gorb, S. (2001) Biological Micro and Nanotribology: Nature's Solutions. *Springer-Verlag Berlin Heidelberg New York*
- Schiotz, A. (1999) Tree frogs of Africa. *Edition Chimania, Frankfurt am Main*.
- Schmidt-Nielsen, K. (1993) Scaling: Why is animal size so important? *Cambridge University Press, U.K.*

- Schwartz, J.J. (1986) Male calling behaviour and female choice in *Hyla microcephala*. *Ethology* 73: 116-127.
- Semlitsch, R.D.; Pickle, J.; Parris, M.J. and Sage, R.D. (1999) Jumping performance and short-term repeatability of newly metamorphosed hybrid and parental leopard frogs (*Rana sphenoccephala* and *blairi*). *Canadian Journal of Zoology* 77: 748-754.
- Shepherd, B.A.; McDowell, W.T and Matan, J. (1998) Skin glands of *Hyla japonica*. *Journal of Herpetology* 32(4): 598-601.
- Shine, R. (1979) Sexual selection and sexual dimorphism in the Amphibia. *Copeia* 1979: 297-139.
- Smith, A.M. (1991a) Negative pressure generated by octopus suckers: a study of the tensile strength of water in nature *Journal of Experimental Biology* 157: 257-271.
- Smith, A.M. (1991b) The role of suction in the adhesion of limpets. *Journal of Experimental Biology* 161: 151-169.
- Smith, A.M. (1992) Alternation between attachment mechanisms by limpets in the field. *Journal of Experimental Marine Biology and Ecology* 160 (2): 205-220.
- Smith, A.M. (1996) Cephalopod sucker design and the physical limits to negative pressure. *Journal of Experimental Biology* 199 (4): 949-958.
- Smith, A.M. (2002) The structure and function of adhesive gels from invertebrates. *Integrative and Comparative Biology* 42: 1164-1171.
- Smith, A.M. and Morin, M.C. (2002) Biochemical differences between trail mucus and adhesive mucus from marsh periwinkle snails. *Biological Bulletin* 203: 338-346.
- Smith, A.M., Quick, T. J. and St. Peter, R. L. (1999) Differences in the composition of adhesive and non-adhesive mucus from the limpet *Lottia limatula*. *Biological Bulletin* 196: 34-44.

- Smith, H.M. (1941) Snakes, frogs and bromelias. *Chicago Naturalist* 4: 35-43.
- Sperry, D.G. and Wassersug, R.J. (1976) A proposed function for microridges on epithelial cells. *Anatomical Records* 185: 253-258.
- Stork, N.E. (1980a) A scanning electron microscope study of tarsal adhesive setae in the Coleoptera. *Zoological Journal of the Linnean Society* 68: 173-306.
- Stork, N.E. (1980b) Experimental analysis of adhesion of *Chrysolina polita* on a variety of surfaces. *Journal of Experimental Biology* 88: 91-107.
- Stork, N.E. (1983a) The adherence of beetle tarsal setae to glass. *Journal of Natural History* 17: 583-597.
- Stork, N.E. (1983b) A comparison of the adhesive setae on the feet of lizards and arthropods. *Journal of Natural History* 17: 829-835.
- Stumpf, P. and Welsch, U. (2002) Cutaneous eccrine glands of the foot pads of the rock hyrax (*Procavia capensis*, Hyracoidea, Mammalia). *Cells Tissues Organs* 171(2-3): 215-226.
- Thewissen, J.G.M. and Etnier, S.A. (1995) Adhesive devices on the thumbs of vespertilionid bats (Chiroptera). *Journal of Mammalogy* 76 (3): 925-936.
- Thomas, L.A. and Hermans, C.O. (1985) Adhesive interactions between the tube feet of a starfish, *Leptasterias hexactis* and substrata. *Biological Bulletins of the Marine Biology Lab, Woods Hole*. 169: 675-688.
- Toledo, R. C. and C. Jared (1993) Cutaneous adaptations to water-balance in amphibians. *Comparative Biochemistry and Physiology A* 105(4): 593-608.
- Tomlinson, K. (1995) The development of toe pads and adhesion in juvenile tree frogs. *Unpublished honours project*.

Transtronics, Inc. (2001). Viscosity. <http://xtronics.com/reference/viscosity.html>. Last accessed August 2003.

Trauth, S. E. and Willhide, J.D. (1998) Toe tip morphology in six species of salamanders, genus *Ambystoma* (Caudata: Ambystomatidae), from Arkansas using scanning electron microscope. *Arkansas Academy Of Science Proceedings*. 42: 86-88.

Valentine, M.T.; Dewalt, L.E. and Ou-Yang, H.D. (1996) Forces on a colloidal particle in a polymer solution: a study using optical tweezers. *Journal of Physics: Condensed Matter* 8: 9477–9482.

Vanhoye, D.; Bruston, F.; Nicolas, P. and Amiche, M. (2003) Antimicrobial peptides from hyliid and ranin frogs originated from a 150-million-year-old ancestral precursor with a conserved signal peptide but a hypermutable antimicrobial domain. *European Journal of Biochemistry* 270(9): 2068.

Verdugo, P.; Deyrup-Olsen, I.; Aitken, M.; Villalon, M. and Johnson, D. (1987) Molecular mechanism of mucin secretion: I. The role of intragranular charge shielding. *Journal of Dental Research* 66: 506-508.

Vickery, M.S. and McClintock, J.B. (2000) Comparative morphology of tube feet among the Asteroidea: Phylogenetic implications. *American Zoologist* 40 (3): 355-364.

Viney, C. (2002) http://www.rsc.org/lap/educatio/eic/2002/viney_jan02.htm *Internet source*.

Vogel, S. (1988) Life's devices: The physical world of animals and plants. *Princeton Uni Press, Princeton*.

- von Boletzky, S. and Roeleveld, M.A.C. (2000) "Ventral adhesion" to hard substrates: A thigmotactic response in sepiid cuttlefish (Mollusca, Cephalopoda). *Vie et Milieu -Life and Environment* 50(1): 59-64.
- Votsch, W.; Nicholson, G.;Muller, R.; Stierhof, Y-D.; Gorb, S.; Schwarz, U. (2002) Chemical composition of the attachment pad secretion of the locust *Locusta migratoria*. *Insect Biochemistry and Molecular Biology* 32: 1605-1613.
- Walker, G.; Yule A.B. and Ratcliffe J (1985) The adhesive organ of the blowfly, *Calliphora vomitoria*: a functional approach (Diptera: Calliphoridae). *Journal of Zoology (London)* 205: 297-307.
- Watanabe, T. and Yamaguchi I. (1991) Studies on wetting phenomena on plant surfaces 1. Evaluation of wettability of plant leaf surfaces. *Journal of Pest Science* 16: 491-498.
- Watkins, T.B. (1997) The effect of metamorphosis on the repeatability of maximal locomotor performance in the performance in the Pacific tree frog *Hyla regilla*. *Journal of Experimental Biology* 200: 2663-2668.
- Weisstein, E.W. (2003) World of maths. *Internet source*: <http://mathworld.wolfram.com/HexagonalClosePacking.html>. Last accessed July 2003.
- Wells, K.D. and Taigen, T.I. (1989) Calling energetics of a neotropical tree frog, *Hyla microcephala*. *Behavioural Ecology and Sociobiology* 25: 13-22.
- Welsch, U.; Storch, V. and Fuchs, W. (1974) The fine structure of the digital pads of Rhacophorid tree frogs. *Cell Tissue Research* 148: 407-416.
- Weygoldt P. and Silva S.P.C.S. (1991) Observations on mating, oviposition, egg sac formation and development in the egg brooding frog, *Fritziana goeldii*. *Amphibia-Reptilia* 12: 67-80.

Whittington, I.D.; Cribb, B.W.; Hamwood, T.E. and Halliday, J.A. (2000) Host-specificity of monogenean (Platyhelminth) parasites: a role for anterior adhesive areas? *International Journal for Parasitology* 30: 305-320.

Williams, E.E. and Peterson, J.A. (1982) Convergent and alternative designs in the digital adhesive pads of scincid lizards. *Science* 215: 1509-1511.

Wilson, RS; Franklin, CE and James, RS (2000) Allometric scaling relationships of jumping performance in the striped marsh frog *Limnodynastes peronii*. *Journal of Experimental Biology* 203 (12): 1937-1946.

Yanosky, R.; Mercolli, C. and Dixon, J.R. (1997) Field ecology and population estimates for the veined tree frog (*Phrynohyas venulosa*) on the Eastern Chaco of Argentina. *Texas Journal of Science* 49(1): 41-48.

Zani, P.A. (2000) The comparative evolution of lizard claw and toe morphology and clinging performance. *Journal of Evolutionary Biology* 13: 316-325.

Zhu, L. (1999) Strength and stability of a meniscus in a slider-disc interface. *IEEE Transactions on Magnetics* 35(5): 2415-2417.

Zug, G. (1972) Anuran locomotion: Structure and function. I. Preliminary observations on the relation between jumping and osteometrics of the appendicular and postaxial skeleton. *Copeia* 1972: 613 – 614.

Zweifel, R.G. (1964) Life history of *Phrynohyas venulosa* (Salientia: Hylidae) in Panama. *Copeia*. 1964: 201-208.